

XXII International Conference on Chemical Thermodynamics in Russia

**June 19-23, 2019
Saint Petersburg, Russia**

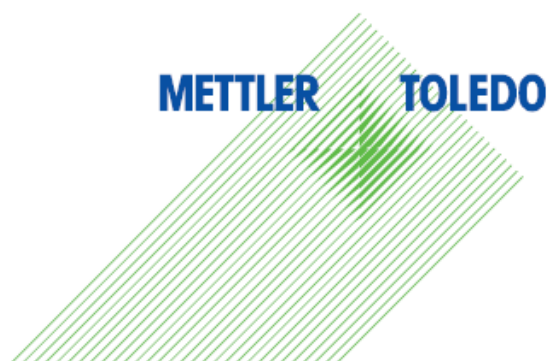


RCCT-2019

BOOK OF ABSTRACTS

**Saint Petersburg State University
Ministry of Science and Higher Education
Kurnakov Institute of General and Inorganic Chemistry of the Russian Academy
of Sciences
Russian Academy of Sciences
The Mendeleev Russian Chemical Society
Interregional Innovative Development Center (INNO-MIR) LLC**

SPONSORS



METTLER TOLEDO



project 19-03-20022



CONTACTS

e-mail: rcct2019@spbu.ru

<http://rcct2019.spbu.ru>

ISBN: 987-5-9676-1076-9

CONTENTS

Committees	V
Preface	VII
Conference Timetable	IX
Scientific Program	XV
Abstracts	1
Oral Program	3
Poster Session I	125
Poster Session II	191
Poster Session III	265
Author Index	335

Organizing Committee

Chair

Anatoly I. Rusanov, St. Petersburg

Vice-Chairmen

Alexey I. Victorov, St. Petersburg

Konstantin S. Gavrichev, Moscow

Members

Gleb A. Abakumov, Nizhni Novgorod

Andrey S. Alikhanyan, Moscow

Mikhail F. Churbanov, Nizhni Novgorod

Vladimir A. Durov, Moscow

Vladimir P. Fedin, Novosibirsk

Pavel P. Fedorov, Moscow

Nikolay V. Gelfond, Novosibirsk

Alexey A. Goryunkov, Moscow

Viktor V. Gusarov, St. Petersburg

Alexander B. Kaplun, Novosibirsk

Michael G. Kiselev, Ivanovo

Alexander V. Knyazev, Nizhni Novgorod

Oskar I. Koifman, Ivanovo

Arkady M. Kolker, Ivanovo

Oleg L. Kuskov, Moscow

Nikolay T. Kuznetsov, Moscow

Sergei I. Lopatin, St. Petersburg

Valery V. Lunin, Moscow

Andrey K. Lyashchenko, Moscow

Vladimir M. Novotortsev Moscow

Oleg V. Mikhailov, Kazan

Valentin N. Parmon, Novosibirsk

Andrey A. Pimerzin, Samara

Alexander K. Shchekin, St. Petersburg

Natalia N. Smirnova, Nizhni Novgorod

Boris N. Solomonov, Kazan

Valentina L. Stolyarova, St. Petersburg

Sergey V. Stankus, Novosibirsk

Alexander M. Toikka, St. Petersburg

Aslan Yu. Tsivadze, Moscow

Irina A. Uspenskaya, Moscow

Andrey B. Yaroslavtsev, Moscow

Anatoliy G. Zakharov, Ivanovo

Ludmila N. Zelenina, Novosibirsk

Kseniya V. Zherikova, Novosibirsk

Irina A. Zvereva, St. Petersburg

International Scientific Committee

Gabriele Sadowski, Dortmund, Germany

Andrei Rotaru, Bucharest, Romania

Juan Z. Dávalos, Madrid, Spain

Edward Maginn, Notre Dame, USA

Kenneth Kroenlein, Boulder, USA

Christoph Schick, Rostock, Germany

Sergey P. Verevkin, Rostock, Germany

Deresh Ramjugernath, Durban, South Africa

Li-Xian Sun, Guilin, China

Vahur Oja, Tallinn, Estonia

Fabrice Mutelet, Nancy, France

James S. Chickos, Missouri, USA

Manuel J. Monte, Porto, Portugal

Stefano Vecchio Cipriotti, Roma, Italy

John M. Simmie, Galway, Ireland

Local Organizing Committee

Alexey I. Victorov (Vice-Chair)

Alexander K. Shchekin

Valentina L. Stolyarova

Sergei V. Lopatin

Sergei M. Shugurov

Konstantin N. Mikhelson

Alexander M. Toikka

Boris A. Noskov

Aleksandr A. Vanin

Vladimir V. Sizov

Anastasia A. Sizova

Irina A. Zvereva

Alexandra D. Golikova

Evgenia A. Safonova (Scientific Secretary)

Igor V. Prikhodko (Scientific Secretary)

Igor Yu. Gotlib

Ksenia A. Emelianova

Alina S. Koneva

Ilya V. Kopanichuk

Olga Yu. Kurapova

Anastasia V. Penkova

Maria A. Toikka

Artemiy A. Samarov

Mikhail A. Voznesenskyi

Alexei G. Bykov

PREFACE

**XXII International Conference on Chemical Thermodynamics in Russia, RCCT-2019
June 19-23, 2019, St.Petersburg, Russia: Abstracts.** – St.Petersburg: Petropolis PH. Ltd,
2019. - 382 p.

ISBN 978-5-9676-1076-9

This book contains the scientific program and the abstracts of presentations at the XXII International Conference on Chemical Thermodynamics in Russia (RCCT-2019). The conferences on chemical thermodynamics are among the largest conferences held in Russia since 1961. Until 1977 a conference of this series was called "All-Union Conference on Calorimetry" and later, until 1992, "All-Union Conference on Calorimetry and Chemical Thermodynamics". After a long break the tradition of holding these conferences was revived in St.Petersburg (2002). Today the RCCT International Conferences are organized every two years by large Russian scientific centers that have included Moscow (2005, 2013), Ivanovo (2007), Kazan (2009), Samara (2011), Nizhny Novgorod (2015) and Novosibirsk (2017). Every RCCT is a unique and important scientific event both for Russian and international thermodynamic communities. The conference traditionally covers all aspects of chemical thermodynamics from fundamentals to applications, including multidisciplinary approaches and related fields of science.

RCCT2019 takes place in the year declared "The International Year of Periodic Table of Chemical Elements" that marks the 150th anniversary of the publication of Mendeleev's Periodic Table of Chemical Elements in 1869; you can see the original Mendeleev's lifetime Periodic Table right at its birthplace in one of the meeting rooms of RCCT2019. Our conference brings together around 300 scientists from 22 different countries; many of them are young researches, including undergraduate and graduate students. Two junior poster awards have been established by the organizers for the best poster presentations: the RCCT-2019 junior poster award "Excellence in Chemical Thermodynamics" and "Mikhail M. Schultz award", a special award dedicated to 100 years from the birthday of Acad. Mikhail M. Schultz.

The scientific program of RCCT2019 includes plenary and invited lectures, 3 parallel sessions of oral presentations and 3 poster sessions. These contributions reflect the latest trends in Chemical Thermodynamics, including the development and application of theory, new experimental techniques and computer simulation for a variety of different systems.

It is our pleasure to thank all the participants of RCCT2019 and to welcome you in St.Petersburg. We only hope that the treacherous St.Petersburg's weather will not prevent us from enjoying the beauty of our city and its magnificent "white" nights.

On behalf of the organizers,

Alexey Victorov, RCCT2019 Vice-chair

CONFERENCE TIMETABLE

WEDNESDAY, 19.06.2019

17.00 – 19.30	Arrivals Registration (<u>Ceremony Hall, main building</u>)
19.30	Welcome reception

THURSDAY, 20.06.2019

09.00 – 09.15	Opening (<u>Ceremony Hall, main building</u>)		
Plenary session (<u>Ceremony Hall, main building</u>) Chair: Sadowski G., Coutinho J.			
09.15 – 9.50	Sadowski G. (p. 4)		
9.50 – 10.25	Coutinho J. (p. 5)		
10.25 – 11.00	Anisimov M. (p. 6)		
11.00 – 11.30	Coffee break		
	Section 2: Thermodynamics of Liquids, Fluid Mixtures, and Phase Equilibria (<u>Ceremony Hall, main building</u>) Chair: Anisimov M., Kleiber M.,	Section 1: Development of General Methods and Tools of Chemical Thermodynamics: New Experimental Techniques, Theory and Computer Simulation (<u>Room 133, main building</u>) Chair: Yagofarov M., Kiselev M.	Section 5: Thermodynamics of Functional Materials and Engineered Self- Assembly (<u>Mendeleev Center building</u>) Chair: Markarian Sh., Bykov A.
11.30 – 11.50	Nikitin E. (p. 8)	Schawe J. (p. 16)	Bykov A. (p. 24)
11.50 – 12.10	Khodov I. (p. 9)	Nagrimanov R. (p. 17)	Schick C. (p. 25)
12.10 – 12.30	Chuev G.N. (p. 10)	Yagofarov M. (p. 18)	Antina L (p. 26)
12.30 – 12.50	Shilov I. (p. 11)	Chua Y. (p. 19)	Emelianova K. (p. 27)
12.50 – 13.10	Kleiber M. (p. 12)	Schick C. (p. 20)	Markarian Sh. (p. 28)
13.10 – 13.30	Polishuk I. (p. 13)	Toikka A (p. 21)	Kuznetsov V (p. 29)
13.30 – 13.50	Davydov A. (p. 14)	Asadov M. (p. 22)	Milyaeva O. (p. 30)
13.50 – 15.30	Lunch		
Plenary session (<u>Ceremony Hall, main building</u>) Chair: Ciach A., Brilliantov N.			
15.30 – 16.05	Kiselev M. (p. 32)		
16.05 – 16.40	Idrissi A. (p. 33)		
16.40 – 17.00	Schawe J.E.K. (p. 34)		
17.00 – 18.30	Poster Session 1 (p. 125)		
20.00 – 23.00	Gala Dinner (Grand Duke's Palace, next to the Hermitage)		

FRIDAY, 21.06.2019

Plenary session (Ceremony Hall, main building) Chair: Victorov A., Shchekin A.			
09.00 – 09.35	Budkov Yu. (p. 36)		
09.35 – 10.10	Ciach A. (p. 37)		
10.10 – 10.45	Brilliantov N. (p. 38)		
10.45 – 11.15	Coffee break		
	Section 2: Thermodynamics of Liquids, Fluid Mixtures, and Phase Equilibria (Ceremony Hall, main building) Chair: Banerjee T., Sineva S.	Section 4: Thermodynamics of Interfacial and Confined Phenomena (Room 90, main building) Chair: Barannikov V., Idrissi A.	Section 5: Thermodynamics of Functional Materials and Engineered Self- Assembly (Mendeleev Center building) Chair: Marczak W, Sizova A.
11.15 – 11.35	Vorozhtcov V. (p. 40)	Shchekin A. (p. 48)	Amashaev R. (p. 56)
11.35 – 11.55	Sineva S. (p. 41)	Barannikov V. (p. 49)	Sizova A. (p. 57)
11.55 – 12.15	Shner N. (p. 42)	Kopanichuk I. (p. 50)	Asabina E. (p. 58)
12.15 – 12.35	Banerjee T. (p. 43)	Akimenko S. (p. 51)	Marczak W. (p. 59)
12.35 – 12.55	Nikfarjam S. (p. 44)	Sizov V. (p. 52)	Mosyagina S. (p. 60)
12.55 – 13.15	Rychkov D. (p. 45)	Baidakov V. (p. 53)	Vasileva A. (p. 61)
13.15 – 13.35	Alekseeva O. (p. 46)	Samsonov V. (p. 54)	Voznesenskiy M. (p. 62)
13.35 – 15.00	Lunch		
	Section 2: Thermodynamics of Liquids, Fluid Mixtures, and Phase Equilibria (Ceremony Hall, main building) Chair: Pimerzin A., Gabrielyan L.	Section 1: Development of General Methods and Tools of Chemical Thermodynamics: New Experimental Techniques, Theory and Computer Simulation (Room 90, main building) Chair: Cicciooli A., Ustinov E.	Section 5: Thermodynamics of Functional Materials and Engineered Self- Assembly (Mendeleev Center building) Chair: Kurapova O., Zherikova K.
15.00 – 15.20	Pimerzin A. (p. 64)	Medvedev N. (p. 72)	Gavrichev K. (p. 80)
15.20 – 15.40	Gabrielyan L. (p. 65)	Ustinov E. (p. 73)	Zherikova K. (p. 81)
15.40 – 16.00	Miroshnichenko E. (p. 66)	Ukhov S. (p. 74)	Lozanov V. (p. 82)
16.00 – 16.20	Cherkasov D. (p. 67)	Varfolomeev M. (p. 75)	Zavrzhnov A. (p. 83)
16.20 – 16.40	Oparin R. (p. 68)	Khvan A. (p. 76)	Kurapova O. (p. 84)
16.40 – 17.00	Sineva M. (p. 69)	Cicciooli A. (p. 77)	Mikhailov O. (p. 85)
17.00 – 19.00	Poster Session 2 (p. 191)		

SATURDAY, 22.06.2019

Plenary session (Ceremony Hall, main building) Chair: Neau E., Smirnova I.			
09.00 – 09.35	Monte M. (p. 88)		
09.35 – 10.10	Smirnova I. (p. 89)		
10.10 – 10.45	Skorb E. (p. 90)		
10.45 – 11.15	Coffee break		
	Section 2: Thermodynamics of Liquids, Fluid Mixtures, and Phase Equilibria (Ceremony Hall, main building) Chair: Smirnova I., Skorb E.	Section 4: Thermodynamics of Interfacial and Confined Phenomena (Room 90, main building) Chair: Gor G., Noskov B.	Section 3: Thermochemistry and Databases (Mendeleev Center building) Chair: Verevkin S., Vecchio Cipriotti S.
11.15 – 11.35	Orekhov M. (p. 92)	Noskov B. (p. 100)	Zelenina L. (p. 108)
11.35 – 11.55	Fomin Yu. (p. 93)	Kolesnikov A. (p. 101)	Dávalos J. (p. 109)
11.55 – 12.15	Brazhkin V. (p. 94)	Tavares F.W. (p. 102)	Samosudova Ya. (p. 110)
12.15 – 12.35	Toikka M. (p. 95)	Lasich M. (p. 103)	Verevkin S. (p. 111)
12.35 – 12.55	Smotrov M. (p. 96)	Tsiok E. (p. 104)	Vecchio Cipriotti S. (p. 112)
12.55 – 13.15	Adamova T. (p. 97)	Talyzin I. (p. 105)	Morozov I. (p. 113)
13.15 – 13.35	Abdulagatov I. (p. 98)	Baidakov V. (p. 106)	Miroshnichenko E. (p. 114)
13.35 – 15.00	Lunch		
	Special session “100 Years from Birthday of Acad. Mikhail M. Schultz” (Ceremony Hall, main building) Chair: Toikka A, Stolyarova V.		
15.00 – 15.35	Rusanov A.I. (p. 116)		
15.35 – 16.10	Toikka A. (p. 117)		
16.10 – 16.45	Stolyarova V. (p. 118)		
16.45 – 18.45	Poster Session 3 (p. 265)		

SUNDAY, 23.06.2019

Plenary session (Ceremony Hall, main building) Chair: Gor G., Gavrichev K.	
09.00 – 09.35	Jacobson N. (p. 120)
09.35 – 10.10	Kramarenko E. (p. 121)
10.10 – 10.45	Gor G. (p. 122)
10.45 – 11.15	Coffee break
11.15 – 11.50	Vishnyakov A (p. 123)
11.50 – 12.25	Samsonov V. (p. 124)

12.25 – 12.40	Solomonov B.N. Presentation of the 23th RCCT
12.40 – 13.00	Conference Closure
13.10 – 14.40	Lunch
	Departure

Sectional talks: 20 min (15 min for talk + 5 min for questions)

Plenary talks: 35 min (30 min for talk + 5 min for questions)

SCIENTIFIC PROGRAM

THURSDAY, 20.06.2019

PLENARY SESSION

Chair persons: Sadowski G., Coutinho J.

<i>Thermodynamics and Kinetics of Biochemical and Chemical Reactions</i> <u>Sadowski G.</u>	4
<i>DES – Do they exist? And Why Should You be Concerned About it...</i> <u>Coutinho J.A.P.</u>	5
<i>Thermodynamics of Fluid Polyamorphism</i> <u>Anisimov M.A.</u>	6

SECTION 2: Thermodynamics of Liquids, Fluid Mixtures, and Phase Equilibria

Chair persons: Anisimov M., Kleiber M.

<i>Critical Properties, Heat Capacities, and Thermal Diffusivities of Levulinic Acid and its n-Alkyl Esters</i> <u>Nikitin E.D., Popov A.P., Bogatishcheva N.S. and Faizullin M.Z.</u>	8
<i>Screening of Conformational Diversity of Molecules of Biologically Active Compounds Based on Nuclear Overhauser Effect Spectroscopy</i> <u>Khodov I.A, Efimov S.V., Kiselev M.G.</u>	9
<i>Site Density Models of Inhomogeneous Classical Molecular Liquids</i> <u>Chuev G.N., Fedotova M.V.</u>	10
<i>Permittivity and Activity Coefficients in Aqueous Solutions of Electrolytes: Insights from the Extended Debye-Hückel Theory</i> <u>Shilov I.Yu., Lyashchenko A.K.</u>	11
<i>An Azeotrope in the Desert</i> <u>Kleiber M.</u>	12
<i>Implementation of CP-PC-SAFT EoS for Predicting Thermodynamic Properties of 1-Alkyl-3-methylimidazolium bis(trifluoromethylsulfonyl)imide Ionic Liquids and Phase Equilibria in their Binary Systems without Fitting Adjustable Parameters</i> <u>Polishuk I.</u>	13
<i>Calculation of the Contribution of Polarization Interactions in the Energy of Alkali Halide Melts by the Method of Thermodynamic Perturbation Theory</i> <u>Davydov A.G., Tkachev N.K.</u>	14

SECTION 1: Development of General Methods and Tools of Chemical Thermodynamics: New Experimental Techniques, Theory and Computer Simulation

Chair persons: Yagofarov M., Kiselev M.

<i>Transformations in Glasses and Nano-structured Materials Measured by Fast Differential Scanning Calorimetry</i> <u>Schawe J.</u>	16
<i>Improving the Method of Solution Calorimetry for Evaluation of The Enthalpies of</i>	

<i>Phase Transitions and Condensed State Enthalpies of Formation</i> <u>Nagrimanov R.</u> , Samatov A.A., Zaitsau Dz. H., Verevkin S.P., Solomonov B.N.	17
<i>On the Ways of the Fusion Enthalpy Determination below the Melting Temperature</i> <u>Yagofarov M.I.</u> , Solomonov B. N.	18
<i>Direct Determination of the Thermodynamic Properties of Melting for Amino Acids</i> <u>Chua Y.Z.</u> , Abdelaziz A., Zaitsau D., Held C., Do H.T., Schick C.	19
<i>Determination of the Sublimation Vapor Pressure of Thermally Labile Compounds with Fast Scanning Calorimetry</i> Abdelaziz A., Zaitsau D.H., Verevkin S.P., <u>Schick C.</u>	20
<i>Alternative Forms of Conditions of Thermodynamic Stability</i> <u>Toikka A.M.</u> , Gromov D.V.	21
<i>Nonequilibrium Thermodynamics of Oxidative Recovery Reactions Vanadium Containing Titanomagnetite Concentrates</i> Mammadov A.N., Sharifova U.N., Qasimova A.M., Samedzade Q.M., <u>Asadov M.M.</u>	22

SECTION 5: Thermodynamics of Functional Materials and Engineered Self-Assembly

Chair persons: Markarian Sh., Bykov A.

<i>Relaxation Processes in Monolayer of Pulmonary Surfactant</i> <u>Bykov A.G.</u> , Loglio G., Miller R., Milyaeva O.Y., Noskov B.A.	24
<i>Tammann's Nuclei Development Approach in Crystallization of Macromolecules</i> <u>Schick C.</u> , Andrianov R., Mukhametzyanov T., Androsch R.	25
<i>The Influence of Structural Factors on The Spectral Properties and Prospects of Application of Bis(BODIPY) Luminophors</i> <u>Antina L.A.</u> , Ksenofontov A.A., Kalyagin A.A., Antina E.V., Berezin M.B., Dyshin A.A.	26
<i>Molecular Thermodynamic Modeling of Stomatosomes and Flat Perforated Bilayers in Surfactant Mixtures</i> <u>Emelianova K.A.</u> , Sorina P.O., Victorov A.I.	27
<i>Effect of Dialkylsulfoxides on the Thermal Denaturation of DNA</i> <u>Markarian S.A.</u>	28
<i>Effect of Acidity and Chloride Addition on Phase Equilibria in Aqueous Two-Phase System Peg-1500-Sodium Sulfate</i> <u>Kuznetsov V.N.</u> , Milevskii N.A., Kabanova E.G.	29
<i>Polydopamine Films: the Dynamic Surface Rheology Study</i> <u>Milyaeva O.Yu.</u>	30

PLENARY SESSION

Chair persons: Ciach A., Brilliantov N.

<i>Possibility of Pressure Crossover Prediction by Classical DFT for Sparingly Dissolved Compounds in Supercritical Carbon Dioxide</i> <u>Kiselev M.G.</u> , Budkov Y.A., Ivlev D.V., Kolesnikov A., Kalikin N.N.	32
<i>Mixing two Neat Liquids in Computer Simulation: Free Energy Calculation and Local</i>	

Structure Analysis	
Jedlovsky P., Fábán B., Kiss B., Szőri M., and Idrissi A.	33
Innovations in Thermal Analysis – the New Flash DSC+	
Flachsmann B., <u>Schawe J.E.K.</u>	34

FRIDAY, 21.06.2019

PLENARY SESSION

Chair persons: Victorov A., Shchekin A.

<i>Modified Poisson-Boltzmann Equations with Explicit Account of Polarizable Impurities in the Context of Electric Double Layer Theory</i>	
<u>Budkov Y.A.</u> , Kolesnikov A.L., Kiselev M.G.	36
<i>Theory for Systems with Spontaneous Inhomogeneities on a Mesoscopic Length Scale</i>	
<u>Ciach A.</u>	37
<i>Conformational Control of Polyelectrolyte Chains by Electric Field: from Field-Operated Collapse to Nano-Actuators</i>	
<u>Brilliantov N.V.</u>	38

SECTION 2: Thermodynamics of Liquids, Fluid Mixtures, and Phase Equilibria

Chair persons: Banerjee T., Sineva S.

<i>Comparison of Thermodynamic Properties in the Gd₂O₃-ZrO₂-HfO₂, Sm₂O₃-ZrO₂-HfO₂ and Sm₂O₃-Y₂O₃-HfO₂ Systems at High Temperatures</i>	
Stolyarova V.L., <u>Vorozhtcov V.A.</u> , Lopatin S.I.	40
<i>Experimental Study of the Slag/Matte/Spinel/Gas Equilibria in the</i>	
<u>Sineva S.</u> , Shichin D., Shevchenko M., Hayes P.C., Jak E.	41
<i>Liquid-Liquid Equilibria for Separation of Alcohols from Esters Using Deep Eutectic Solvents Based on Choline Chloride: Experimental and PC-SAFT Modeling</i>	
Samarov A., Prikhodko I. <u>Shner N.</u> , Sadowski G., Held C., Toikka A.	42
<i>A Priori Prediction of Liquid-Liquid-Liquid Equilibria Using COSMO-SAC Model</i>	
<u>Banerjee T.</u> , Kundu D., Bairagya P.	43
<i>Nature of Mesoscopic Aggregates in Lysozyme Solutions</i>	
<u>Nikfarjam S.</u> , Anisimov M., Woehl T.J.	44
<i>Current Experimental and Theoretical Concepts for High-Pressure Phase Transition Studies in Molecular Crystals</i>	
<u>Rychkov D.A.</u>	45
<i>Modifications of Differential Adiabatic Scanning Microcalorimetry Method for Melting of Multilamellar DMPC Membranes</i>	
<u>Alekseeva O.M.</u> , Kremetsova A.V., Kim Yu.A.	46

SECTION 4: Thermodynamics of Interfacial and Confined Phenomena

Chair persons: Barannikov V. , Idrissi A.

Thermodynamic Model of Solubilization in Direct Nonionic Micelle

<u>Shchekin A.K.</u>	48
<i>Thermochemical and Structural Description of Interaction Between Dipeptides and Anionic Micelles</i>	
<u>Barannikov V.P.</u> , Kurbatova M.S., Badelin V.G.....	49
<i>Solubilization of Organic Compounds in AOT Reverse Micelles by Molecular Dynamics Simulations</i>	
<u>Kopanichuk I.V.</u> , Burovaya E.S., Vanin A.A.	50
<i>Multi-Orientational Models of Planar Ordering of Functional Organic Molecules on Solid Surfaces: Thermodynamics and Monte Carlo Simulation</i>	
<u>Akimenko S.S.</u> , Gorbunov V.A., Ustinov E.A.	51
<i>Surfactant Effects on the Molecular Mobility in Confined Decane/Water Mixtures: A Systematic Computational Study</i>	
<u>Sizov V.V.</u> , Kopanichuk I.V., Berezhnaya A.S., Sizova A.A., Brodskaya E.N.....	52
<i>Interfacial Free Energy at a Curved Liquid–Crystal Interface: Molecular Dynamics Simulation</i>	
<u>Baidakov V.G.</u> , Protsenko K.R.....	53
<i>Molecular Dynamic Approaches to Prediction of Size Dependences of Thermodynamic Properties of Metal Nanoparticles</i>	
<u>Samsonov V.M.</u> , Talyzin I.V., Vasiliev S.A., Kartoshkin A. Yu.....	54

SECTION 5: Thermodynamics of Functional Materials and Engineered Self-Assembly

Chair persons: Marczak W, Sizova A.

<i>Synthesis and Antibacterial Properties of Nitrogen or Carbon Doped Titanium Oxide Thin Films</i>	
<u>Abdulagatov A.I.</u> , Ashurbekova Kr.N., Ashurbekova Ka.N., <u>Amashaev R.R.</u> , Maksumova A.M., Aliev A., Rabadanov M.Kh., Abdulagatov I.M.	56
<i>Separation of Gas Mixtures by Adsorption in CMK-5 and CMK-3: Effects of Adsorbent Topology</i>	
<u>Sizova A.A.</u> , Ivanova E.A., Sizov V.V., Brodskaya E.N.	57
<i>Thermal Expansion of the Phosphates with Kosnarite and Langbeinite Type Structures</i>	
<u>Asabina E.A.</u> , Pet'kov V.I., Shipilov A.S., Alekseev A.A., Mayorov P.A., Glukhova I.O.	58
<i>Surface Pressure Model for Particle Layers on Liquids</i>	
<u>Marczak W.</u> , Rogalski M., Modaressi A., Rogalska E.	59
<i>Thermal Properties of Zr(IV) and Y(III) Complexes with Dipivaloylmethane</i>	
<u>Mosyagina S.A.</u> , Zherikova K.V., Igumenov I.K., Kuratieva N.V.....	60
<i>Additional Criteria of High-Entropy Alloys Formation</i>	
<u>Vasileva A.</u> , Sineva S., Starykh R.....	61
<i>Computer Simulation of Self-Assembly of Spatial Networks in Solutions of Branching Aggregates</i>	
<u>Voznesenskiy M.</u> , Petrov A., Vorotsov-Velyaminov P., Victorov A.	62

SECTION 2: Thermodynamics of Liquids, Fluid Mixtures, and Phase Equilibria

Chair persons: Pimerzin A., Gabrielyan L.

<i>Liquid Organic Hydrogen Carriers (LOHC): Thermodynamics of Hydrogenation-Dehydrogenation of Polycyclic Aromatic Hydrocarbons and Nitrogen-Containing Heterocycles</i>	
<u>Pimerzin A.A., Verevkin S.P.</u>	64
<i>Dielectric Relaxation and Field-Cyclinc ¹H NMR Relaxometry Studies of Dimethylsulfoxide/Glycerol Mixtures at Low Temperatures</i>	
<u>Gabrielyan L.S., Markarian S.A., Flämig M., Rössler E.A.</u>	65
<i>Thermodynamics of Perluoroorganic Compounds and the Additive Scheme of Calculation of Vaporization Enthalpies</i>	
<u>Pashchenko L.L., Druzhinina A.I., Miroshnichenko E.A.</u>	66
<i>Influence of Salts on the Phase Behavior of Ternary Liquid Systems with a Closed Delamination Field</i>	
<u>Cherkasov D.G., Smotrov M.P., Il'in K.K.</u>	67
<i>Conformational Equilibrium and Polymorphism of Mefenamic Acid in Supercritical Carbon Dioxide</i>	
<u>Oparin R.D., Krestyaninov M.A., Idrissi A., Kiselev M.G.</u>	68
<i>Joint Approximation of Enthalpy Increments and Heat Capacity Data for Substances in the Condensed State</i>	
<u>Sineva M.A., Aristova N.M., Belov G.V., Lavrinenko Ya., Morozov I.V.</u>	69

SECTION 1: Development of General Methods and Tools of Chemical Thermodynamics: New Experimental Techniques, Theory and Computer Simulation

Chair persons: Ciccioli A., Ustinov E.

<i>Driving Forces of the Clustering in Solutions</i>	
<u>Medvedev N.N.</u>	72
<i>Thermodynamics of Melting/Freezing Transition in Molecular Layers from a Monte Carlo Simulation: a Direct Evaluation of the Chemical Potential</i>	
<u>Ustinov E.A.</u>	73
<i>Application of the Specific Ion Interaction Theory for Investigation of Indium (III) Complexation</i>	
<u>Ukhov S.A.</u>	74
<i>A Promising Hybrid Methane Hydrate Inhibition on the Basis of Polyurethane for Hydrate Management Risk: Thermochemistry, Kinetics and Phase Behavior</i>	
<u>Varfolomeev M.A., Farhadian A.</u>	75
<i>Transformation from 2nd to 3rd Generation of Critically Assessed Thermodynamic Data for the Elements</i>	
<u>Khvan A.V., Dinsdale A.T.</u>	76
<i>Vaporization Thermodynamics of Tetramethylammonium Iodide Revisited: a Multitechnique Investigation</i>	
<u>Brunetti B., Ciccioli A., Latini A., Panetta R., Patterson E.V., Vecchio Cipriotti S.</u>	77

SECTION 5: Thermodynamics of Functional Materials and Engineered Self-Assembly

Chair persons: Kurapova O., Zherikova K.

<i>High-Temperature Thermodynamic Properties and Thermal Expansion of Some RE Tantalates for TBC Materials</i>	
<u>Gavrichev K.S.</u> , Guskov V.N., Ryumin M.A., Tyrin A.V., Khoroshilov A.V., Ashmarin A.A...	80
<i>In a Search for Enhanced Secondary Electron Emission: is there any Component Interactions in MgO-RuO₂ System?</i>	
<u>Zherikova K.V.</u> , Vikulova E.S., Vasilyeva I.G., Zabuslaev S.V.	81
<i>Formation of Refractory Hafnium- and Tantalum-Containing Compounds on Silicon Carbide Support by the Reactive Chemical Vapor Deposition</i>	
<u>Lozanov V.V.</u> , Baklanova N.I.	82
<i>The Identification and Stabilization of New Phases in Ga – S and In – S Systems</i>	
<u>Zavrzhnov A.Y.</u> , Nekrylov I.N., Brezhnev N.Y., Malygina E.V., Kosyakov A.V., Sidey V.I., Volkov V.V.	83
<i>The Thermodynamic Approaches for Zirconia Based Precursors and Ceramics Investigation</i>	
<u>Kurapova O.Y.</u> , Shugurov S.M., Lopatin S.I., Vasil'eva E.A., Konakov V.G.	84
<i>Thermodynamics of Al₂M₃ Metalclusters (M= 3d-Element) According to Quantum-Chemical Calculation by DFT Method</i>	
<u>Mikhailov O.V.</u> , Chachkov D.V.	85

SATURDAY, 22.06.2019

PLENARY SESSION

Chair persons: Neau E., Smirnova I.

<i>Estimation of Thermodynamic Properties of Substituted Benzenes Related to their Environmental Mobility</i>	
<u>Monte M.J.S.</u> , Almeida A.R.R.P.	88
<i>Phase Equilibria in Reactive Biocatalytic Processes</i>	
<u>Smirnova I.</u>	89
<i>Mesoscopic Non-Equilibrium Organic Periodic Self-Assembly</i>	
<u>Koltsov S.</u> and <u>Skorb E.V.</u>	90

SECTION 2: Thermodynamics of Liquids, Fluid Mixtures, and Phase Equilibria

Chair persons: Smirnova I., Skorb E.

<i>Effect of Fluctuations on Diffusivity in Liquid Solutions</i>	
<u>Norman G.E.</u> , <u>Orekhov M.A.</u>	92
<i>Anomalous Behavior of Dispersion Curves in Water-Like Systems and Water</i>	
<u>Fomin Yu.D.</u> , <u>Tsiok E. N.</u> , <u>Ryzhov V. N.</u> and <u>Brazhkin V. V.</u>	93
<i>Precise Experimental Study of Water Thermodynamics up to the Record Pressures 12 kbar</i>	

<u>Brazhkin V.V., Dzhavadov L.N., Fomin Yu.D., Tsiok E.N., Ryzhov V.N.</u>	94
<i>Thermodynamic Peculiarities and Phase Diagrams of Biofuel Systems</i>	
<u>Toikka M.A., Golikova A.D., Pulyalina A.Yu.</u>	95
<i>Topological Transformation of the Phase Diagrams of Ternary Systems Salt + Water + Organic Solvent, Including a Binary Liquid System with a Closed Binodal Curve</i>	
<u>Smotrov M.P., Cherkasov D.G., and Il'in K.K.</u>	96
<i>Visual Studies of Methane Hydrate Formation on the Water – Oil Boundaries</i>	
<u>Adamova T.P., Stoporev A.S., Manakov A.Yu.</u>	97
<i>PVT and Phase Transition Properties of Binary Mixture of n-Hexane+IL in the Critical and Supercritical Regions</i>	
<u>Abdulagatov I.M., Rasulov S.M., Isaev I.A., Orakova S.M.</u>	98

SECTION 4: Thermodynamics of Interfacial and Confined Phenomena

Chair persons: Gor G., Noskov B.

<i>Dynamic Surface Elasticity of Protein/Surfactant Solutions</i>	
<u>Noskov B.A., Lin S.-Y., Milyaeva O.Y., Krycki M.M.</u>	100
<i>Deformation Induced by Fluid Adsorption: Enhanced Flexibility and Pore Size Distribution</i>	
<u>Kolesnikov A.L., Budkov Yu.A., Möllmer J., Adolphs J., Georgi N., Hofmann J.</u>	101
<i>Thermodynamic Modeling of Confined Fluid: From Incompressible to Compressible Matrices</i>	
<u>Sermoud V. de M., Barbosa G.D., Segtovich I.S.V., Barreto Jr. A.G., Tavares F.W.</u>	102
<i>Limitations of the Single-Site Approach to Describing Adsorption in Structure-I Clathrate Hydrates</i>	
<u>Lasich M., Tumba K.</u>	103
<i>Influence of Confinement on Melting of Two-Dimensional Core-Softened System</i>	
<u>Tsiok E.N., Fomin Yu.D., Ryzhov V.N.</u>	104
<i>Whether the Heat Capacity of Nanoparticles can be Negative?</i>	
<u>Talyzin I.V., Samsonov V.M.</u>	105
<i>Nucleation in Superheated Solutions of Simple Liquids</i>	
<u>Baidakov V.G., Kaverin A.M.</u>	106

SECTION 3: Thermochemistry and Databases

Chair persons: Verevkin S., Vecchio Cipriotti S.

<i>Thermodynamic Study of α-, β-, γ-Cyclodextrin Hydrates Dehydration Processes</i>	
<u>Zelenina L.N., Chusova T.P., Rodionova T.V.</u>	108
<i>Thermochemical Properties of Halogen-Containing Organic Compounds with Influence on Atmospheric Chemistry: a Computational Study</i>	
<u>Dávalos J.Z., Notario R., Cuevas C.A., Oliva J.M., Saiz-Lopez A.</u>	109
<i>Calorimetric Investigation of Carbosilane and Carbosilanecyclesiloxane Dendrimers of Versatile Structure</i>	
<u>Samosudova Ya.S., Markin A.V., Smirnova N.N., Sologubov S.S., Sarmini Yu.A.</u>	110

<i>Milestone Thermodynamics of the Renewable Fuels and Hydrogen Storage</i> <u>Verevkin S.P., Pimerzin A.A.</u>	111
<i>Thermodynamic Study of Tetramethylammonium Iodide. Thermal Behavior, Molar Isobaric Heat Capacities and Thermodynamic Functions</i> <u>Brunetti B., Ciccioli A., Latini A., Vecchio Cipriotti S.</u>	112
<i>Development of the IVTANTHERMO-Online Thermodynamic Database for Pure Substances</i> <u>Morozov I.V., Belov G.V., Dyachkov S.A., Levashov P.R., Minakov D.V.</u>	113
<i>Thermochemistry of Polycyclic Hydrocarbons. Energy Characteristics of Bonds and Radical's Reorganization</i> <u>Miroshnichenko E.A., Kon'kova T.S., Pashchenko L.L.</u>	114

SPECIAL SESSION: 100 Years from Birthday of Acad. Mikhail M. Schultz

Chair persons: Toikka A., Stolyarova V.

<i>M.M. Schultz and Thermodynamics: First Steps, but what were Significant!</i> <u>Rusanov A.I.</u>	116
<i>Mikhail Mikhailovich Shultz and his Thermodynamic Investigations</i> <u>Toikka A.M.</u>	117
<i>Developing of Thermodynamic Approach to Study of Oxide Systems and Materials by Academician M.M. Shultz</i> <u>Stolyarova V.L.</u>	118

SUNDAY, 23.06.2019

PLENARY SESSION

Chair persons: Gor G., Gavrichev K.

<i>Thermochemistry of Water Vapor/Refractory Oxide Reactions at Elevated Temperatures</i> <u>Jacobson N.S., Myers D.L., Bauschlicher Jr. C.W., Opila E.J.</u>	120
<i>Microphase Separation in Polyelectrolytes</i> <u>Kramarenko E.Yu., Rumyantsev A.M., Gavrilov A.A.</u>	121
<i>Compressibility of Confined Simple Fluid from an Equation of State and Molecular Simulation</i> <u>Dobrzanski C.D., Corrente N., Gor G.Y.</u>	122
<i>Critical Condition of Macromolecule Adsorption: Application for Size-Independent Separations</i> <u>Vishnyakov A.V., Santo K.P., Rasmussen R., Neimark A.V., Brun E.</u>	123
<i>On Size Dependence of Surface Tension and Surface Energy</i> <u>Samsonov V.M., Sdobnyakov N.Yu., Talyzin I.V., Bazulev A.N., Vasilyev S.A.</u>	124

POSTER SESSION I

THURSDAY, 20.06.2019

PI-1. <i>New Study of Viscosity for the Binary System n-Alkane + 1-Alkanol</i> Castelo S., Gayol A., <u>Mato M.M.</u> , Legido J.L.	126
PI-2. <i>Surface Tension of the Ternary System Diethyl Carbonate + p-Xylene + n-Decane</i> Gayol A., Casás L., <u>Mato M.M.</u> , Legido J.L.	127
PI-3. <i>Thermal Properties of Mixtures of Montmorillonite with Water</i> Rosino J., <u>Tobar J.L.</u> , Gómez C.P., Mato M.M., Mourelle M.L., Legido J.L.	128
PI-4. <i>Measurement of Binary Vapour-Liquid Equilibrium for High Relative Volatility Systems</i> <u>Narasigadu C.</u> , Moodley K., Raal J.D.	129
PI-5. <i>Internal Pressure in Water + 1,3-Dimethylurea Mixtures</i> <u>Egorov G.I.</u> , Makarov D.M.	130
PI-6. <i>Effect pressure on the Intermolecular Interactions of N-Methylacetamide with Water</i> Makarov D.M., <u>Egorov G.I.</u> , Kolker A.M.	131
PI-7. <i>Experimental Determination of (p, ρ, T) Data of Liquid Toluene and n-Tetradecane in a Wide Range of State Parameters</i> <u>Shchamialiou A.P.</u> , Samuilov V.S., Holubeva N.V., Paddubski A.G., Drăgoescu D., Sîrbu F.	132
PI-8. <i>Determination of Thermodynamic Properties of Liquid Toluene and n-Tetradecane in a Wide Range of Temperatures and Pressures Based on Dissimilar Initial Data</i> <u>Shchamialiou A.P.</u> , Samuilov V.S., Holubeva N.V., Drăgoescu D., Sîrbu F.	133
PI-9. <i>Volumetric and Caloric Properties of Liquid Cesium–Bismuth Alloys</i> <u>Stankus S.V.</u> , Khairulin R.A., Abdullaev R.N., Savchenko I.V., Yatsuk O.S.	134
PI-10. <i>Chemical Interaction in the Na,Rb F,I,CrO₄ Quaternary Reciprocal System</i> <u>Babenko A.V.</u> , Egorova E.M., Garkushin I.K.	135
PI-11. <i>Thermodynamical Properties of L-Carnosine on Solid and Liquid Phase</i> <u>Kuritsyna A.A.</u> , Tyunina V.V., Mezhevoi I.N., Tyunina E. Yu., Badelin V.G.	136
PI-12. <i>Phase Equilibrium and Structure of Acrylic Blocks and Gradient Copolymers</i> <u>Nikulova U.V.</u> , Chalykh A.E., Khasbiullin R.R., Gerasimov V.K.	137
PI-13. <i>The Influence of Solute-Solute and Solute-Solvent Correlations on Urea-Urea and Tetramethylurea-Tetramethylurea Pair Interactions in Water</i> <u>Kustov A.V.</u> , Antonova O.A., Smirnova N.L., Kruchin S.O., Ivanov E.V., Makarov V.V.	138
PI-14. <i>Thermodynamics of Solution of 3,5-Diamino-1,2,4-Triazole and 3,5-Diamino-1-Phenyl-1,2,4-Triazole in Water</i> <u>Kustov A.V.</u> , Kudayrova T.V., Antonova O.A., Smirnova N.L.	139
PI-15. <i>Enthalpic Parameters of Pair Interactions between Urea and Tetramethylurea Molecules in Ethanediol at 298 - 318 K</i> <u>Batov D.V.</u> , Smirnova N.L., Kustov A.V., Antonova O.A.	140
PI-16. <i>Heat Capacity and Structural Changes Associated with Solvation of Polar and Apolar Groups in Water and Ethylene Glycol</i> Krest'yaninov M.A., Kustov A.V., <u>Batov D.V.</u> , Ivanov E.V., Makarov V.V.	141
PI-17. <i>Extractive Crystallization of Sodium Chloride in the Ternary System Sodium Chloride–Water–Diisopropylamine</i> <u>Danilina V.V.</u> , Cherkasov D.G.	142

PI-18. Vapor Pressure of Dipropylene Glycol Methyl Ether and Vapor-Liquid Equilibria of its Aqueous Mixture: Experimental Measurements by The Static Method and Modeling Development <i>Dimitrov O., Neau E., Raspo I., Guichardon P., Dergal F., Mokbel I., Jose J., Testa A.</i>	143
PI-19. Synthesis of the Compounds with High Partial Pressure of Arsenic <i>Kostyanko A.A., Sineva S.I., Starykh R.V.</i>	144
PI-20. Repeatings of DMPC Multilamellar Membranes Meltings Dramatically Change the Thermodynamic Parametrs Registered by Differential Adiabatic Scanning Microcalorimetry Method <i>Alekseeva O.M., Krementsova A.V., Kim Yu.A.</i>	145
PI-21. Features of the Association of Biocompatible Ionic Liquids: the Case of Holin-Based Amino Acid Ionic Liquids <i>Fedotova M.V., Kruchinin S.E. Chuev G.N.</i>	146
PI-22. Phase Solubility Digrams of the 4-Aminobenzoic Acid Cocystal <i>Drozd K.V., Manin A.N.</i>	147
PI-23. Ion-Dipole Interactions During the Complex Formation of d-Metal Ions with Some Organic Derivatives of Hydrazine <i>Amerkhanova Sh.K., Shlyapov R., Uali A.S.</i>	148
PI-24. TPT-Modeling of the Liquidus Surface in Molten Alkali Metal Halides with the Inclusion of the Ion Polarization Effect <i>Davydov A.G., Tkachev N.K.</i>	149
PI-25. Liquid Organic Hydrogen Carriers. Chemical Equilibrium of Hydrogenation Reactions of Condensed Aromatic Hydrocarbons <i>Vostrikov S.V., Konnova M.E., Pimerzin A.I.A., Martynenko E.A., Verevkin S.P., Pimerzin A.A.</i>	150
PI-26. Liquid Organic Hydrogen Carriers. Chemical Equilibrium of Hydrogenation Reactions of Some N-Heterocycles <i>Konnova M.E., Vostrikov S.V., Chernova M.M., Verevkin S.P., Pimerzin A.A.</i>	151
PI-27. Modeling of Thermodynamic Characteristics for Polysubstituted Crystals with a M-Type Hexaferrites Structure <i>Zaitseva O.V., Zhivulin D.E., Chernukha A.S., Galkina D.P., Vakhitova E.R.</i>	152
PI-28. Calorimetric Study of Binding of Substituted Benzoic Acids to Bovine Serum Albumin <i>Khaibrakhmanova D.R., Nikiforova A.A., Sedov I.A.</i>	153
PI-29. Asymptotically Exact Equation for Describing Phonon Heat Capacity of Solids in a Wide Temperature Range <i>Bespyatov M.A., Naumov V.N.</i>	154
PI-30. The Two-Parameter Equilibrium Constant for Gas Reactions <i>Vitvitskiy A.I.</i>	155
PI-31. Approaches to the Equilibrium Composition Calculations for the Conversion of Diesel Fuel <i>Uskov S.I., Potemkin D.I., Snytnikov P.V., Belyaev V.D., Sobyandin V.A.</i>	156
PI-32. Investigation of Evaporation of HfCx and ZrCx Near and Above Melting Point <i>Frolov A.M., Sheindlin M.A., Falyakhov T.M., Petukhov S.V.</i>	157

PI-33. <i>Solubility of Drug Compounds in Supercritical Carbon Dioxide. Molecular Dynamics Simulation</i> <i>Ivlev D.V., Kalikin N.N., Kiselev M.G.</i>	158
PI-34. <i>Classical DFT Based Method of the Solubility Estimation of Sparingly Soluble Compounds in SC CO₂</i> <i>Budkov Y.A., Kalikin N.N., Kolesnikov A.L., Ivlev D.V., Kiselev M.G.</i>	159
PI-35. <i>Thermovap – Calculation Program of Vaporization Enthalpy and Heat Capacity Organic Compounds</i> <i>Krasnykh E.L., Kazakov A.K., Portnova S.V.</i>	160
PI-36. <i>The Use of Density Functional Theory in the Calculation of Structural, Energetic and Thermodynamic Characteristics of Triethylammonium - Based Protic Ionic Liquids</i> <i>Fedorova I.V., Krestyaninov M.A., Safonova L.P.</i>	161
PI-37. <i>Solubility of Caffeine in the Binary Solvent Carbon Tetrachloride – Methanol</i> <i>Golubev V.A., Kiselev M.G.</i>	162
PI-38. <i>On the Possibility of Realization of Labile States</i> <i>Fedorov P.P.</i>	163
PI-39. <i>A New Equation of State for Solids Based on Linear Combination of Planck-Einstein Functions</i> <i>Perevoshchikov A.V., Kovalenko N.A., Uspenskaya I.A.</i>	164
PI-40. <i>Derivation of Effective Intermolecular Potential for Water via Molecular Modeling</i> <i>Volkov N.A., Shchekin A.K.</i>	165
PI-41. <i>Colloidal Aggregation of Asphaltenes Studied with Brownian Dynamics and Monte Carlo Simulations</i> <i>Taherkhani F., Vishnyakov A., Kolattukudy P. Santo</i>	166
PI-42. <i>Approximation of Thermodynamic Properties by Expanded Einstein Model: Possibilities and Problems</i> <i>Babkina T.S., Ivanov A., Konstantinova N.M., Uspenskaya I.A.</i>	167
PI-43. <i>A New Method to Calculate the Change in Ion Solvation Energy at Ion Transfer Between Two Nonlocal Dielectric Media Possessing Different Correlation Lengths</i> <i>Rubashkin A.A., Iserovich P., Vorotyntsev M.A.</i>	168
PI-44. <i>Thermodynamic Properties of Thulium Orthovanadate: a Low-Temperature Heat Capacity Study</i> <i>Kondrat'eva O.N., Ryumin M.A., Morozova E.A., Gavrichev K.S.</i>	169
PI-45. <i>Novel Bodipy Sensors for the Hydrocortisone Spectral Detection in Organic Media</i> <i>Antina E.V., Ksenofontov A.A., Antina L.A., Berezin M.B., Guseva G.B.</i>	170
PI-46. <i>Computer Simulation of Polyvinylpyrrolidone (PVP) Adsorption on Cellulose Nanocrystals (CNC) and The PVP-Assisted CNC Self-Assembly</i> <i>Surov O.V., Voronova M.I., Gurina D.L., Zakharov A.G.</i>	171
PI-47. <i>Pharmaceutical Cocrystals of Flurbiprofen: Thermodynamic and Structural Aspects</i> <i>Surov A.O., Voronin A.P.</i>	172
PI-48. <i>Congruent Sublimation of an Organic Cocrystal: Experimental Data on Sublimation Thermodynamics and Calculated Lattice Energies</i> <i>Voronin A.P., Boycov D.E., Vasilyev N.A., Surov A.O., Manin A.N.</i>	173

PI-49. <i>Thermodynamic Aspects of the Formation of Composites Based on Protein with the Ability to Inhalation Administration</i> <u>Boldyrev A.E., Gerasimov A.V.</u>	174
PI-50. <i>Sorption of Water by Carbon Fibers</i> <u>Petrova T.F., Chalykh A.E., Aliev A.D., Antipov Y.V.</u>	175
PI-51. <i>Heat Capacity and Thermodynamic Functions of Praseodyme Orthoniobate</i> <u>Tyurin A.V., Nikiforova G.E., Ryumin M.A., Khoroshilov A.V., Gavrichev K.S</u>	176
PI-52. <i>Effects of Spatial Bonds Grids of Acrylic Copolymers on their Adhesion Properties</i> <u>Shapagin A.V., Shokurova N.A., Chalykh A.E.</u>	177
PI-53. <i>Thermodynamic Modeling of the Behavior of A²B⁶ Compounds in a Wide Range of Temperatures and Pressures</i> <u>Ilinykh N.I., Kovalev L.E.</u>	178
PI-54. <i>Thermodynamic Modeling of the Equilibrium Composition and Thermodynamic Characteristics of SiC</i> <u>Ilinykh N.I., Verchovtsev A.Ju.</u>	179
PI-55. <i>Thermodynamic Aspects of Structure Formation in Oil Dispersed Systems During Transportation</i> <u>Boytsova A., Kondrasheva N.</u>	180
PI-56. <i>Thermal Expansion of Complex Phosphates, Containing Copper, Iron and Zirconium</i> <u>Glukhova I.O., Asabina E.A., Pet'kov V.I.</u>	181
PI-57. <i>Thermodynamic Properties of the NZP Compounds M²⁺Ti₄P₆O₂₄ (M – Ni, Zn)</i> <u>Glukhova I.O., Asabina E.A., Pet'kov V.I., Smirnova N.N., Markin A.V.</u>	182
PI-58. <i>Vaporization and Thermodynamics of the Ceramics Based on the Y₂O₃-ZrO₂-HfO₂ system</i> <u>Vorozhtcov V.A., Stolyarova V.L., Lopatin S.I., Karachevtsev F.N.</u>	183
PI-59. <i>Thermodynamic Properties of Diatomic Argon Compounds</i> <u>Maltsev M.A., Morozov I.V., Osina E.L.</u>	184
PI-60. <i>Phase Transitions in n-Butanol-Propionic Acid-n-Butyl Propionate-Water System at 333.15 K</i> <u>Skvortsova I., Toikka M.</u>	185
PI-61. <i>Thermodynamic Solubility of Two Different Dihydropyridine Compounds in Various Alcohols at 298.15-328.15 K</i> <u>Lava D., Parmar D. and Baluja S.</u>	186
PI-62. <i>The Influence of Rare-Earth Elements on Glass-Forming Ability of Al-Ni-Co-Rem Amorphous Alloys</i> <u>Rusanov B.A., Sidorov V.E., Svec Sr. P., Svec P., Janickovic D., Moroz A.I.</u>	187
PI-63. <i>Partitioning Behavior of L-Tryptophan in Aqueous-Salt Biphasic Systems Formed by Aminoacid Alkylimidazolium Ionic Liquids</i> <u>Korchak P.A., Safonova E.A.</u>	188
PI-64. <i>How Strong are Intramolecular Interactions in Nitrobenzaldehydes?</i> <u>Siewert R., Verevkin S.P.</u>	189

POSTER SESSION 2

FRIDAY, 21.06.2019

PII-1. <i>The Modified SIT Conception for Evaluation of Ionic Equilibria in Concentrated Mixed Electrolytes Solutions</i> <u>Ukhov S.A.</u>	192
PII-2. <i>A New Quartz Crystal Microbalance (QCM) to Determine Sublimation and Vaporization Enthalpies</i> <u>Brunetti B., Ciccioli A., Magi M., Vecchio Cipriotti S.</u>	193
PII-3. <i>Stability of Nanoclusters of Methane and Carbon Dioxide Hydrates: Effects of Particle Size</i> <u>Sizova A.A., Sizov V.V., Brodskaya E.N.</u>	194
PII-4. <i>New Units of Solutions Concentration</i> <u>Kadtsyn E.D., Anikeenko A.V., Medvedev N.N.</u>	195
PII-5. <i>Thermodynamic Properties of Pure Vanadium</i> <u>Lineva V.I., Sineva M.A., Morozov I.V., Belov G.V.</u>	196
PII-6. <i>Molecular Dynamics Study of Melting of Alkali Halides Mixtures</i> <u>Kobelev M.A., Zakiryaynov D.O., Tkachev N.K.</u>	197
PII-7. <i>A Quantum Chemical Simulation of the Interaction Between (α-ALA)₂ Dipeptide Zwitterion and the Dimer of Sodium Dodecyl Sulphate as Model of Micelle Fragment</i> <u>Kurbatova M.S., Barannikov V.P., Giricheva N.I.</u>	198
PII-8. <i>KEV: a Free Software for Solving the Direct and Inverse Problems of Chemical Equilibria</i> <u>Gamov G.A., Meshkov A.N.</u>	199
PII-9. <i>Molecular Simulations of Liquid Hydrocarbon Mixtures Viscosity</i> <u>Pisarev V.V., Kondratyuk N.D.</u>	200
PII-10. <i>Thermal Behaviour of the Polystyrene Films Filled with Bentonite</i> <u>Alekseeva O.V., Noskov A.V., Guseynov S.S.</u>	201
PII-11. <i>Quantum Chemical Calculation of Thermodynamic Properties of Diethyl Sulfone</i> <u>Gabrielyan L.S., Papanyan Z.K., Mkhitaryan A.S.</u>	202
PII-12. <i>Thermodynamic Properties of the Tl₉TmTe₆ and TlTmTe₂ Compounds</i> <u>Mekhdiyeva I.F., Imamaliyeva S.Z., Sultanova S.Q., Babanly M.B.</u>	203
PII-13. <i>Thermodynamic Investigation of the PbX-AgSbX₂ (X-Se, Te) Systems Using Two Modifications of the EMF Method</i> <u>L.F.Mashadiyeva L.F., Mansimova Sh.H., Babanly D.M., Shukurova G.M., Babanly M.B.</u>	204
PII-14. <i>Study of Hydrogen Reaction with Tio.₉Zro.₁Mn₁₃Vo.₆ by Calorimetric Method</i> <u>Anikina E., Verbetsky V.</u>	205
PII-15. <i>Simultaneous Measurements of The Temperature and Specific Volume Derivatives of Internal Energy of Benzene in the Critical and Supercritical Regions</i> <u>Abdulagatov I.M., Rasulov S.M., Isaev I.A., Orakova S.M.</u>	206
PII-16. <i>Temperature Heat Capacity of Pb_{10-x}Nd_x(GeO₄)_{2+ x}(VO₄)_{4- x} (x = 0, 1, 2, 3) Apatites in the Range 320–1000 K</i>	

<u>Denisova L.T., Galiakhmetova N.A.</u>	207
PII-17. <i>Anomalies in Thermodynamic Parameters of the Li_2CO_3-Na_2CO_3-K_2CO_3 - Nanopowder MgO Heterogeneous System</i>	
<u>Zakiryanova I.D., Korzun I.V.</u>	208
PII-18. <i>Structure and Phase Behavior of Iron(III) Schiff Base Complex with 3,6-Di-Tert-Butyl-Carbazole Moieties</i>	
<u>Kolker A.M., Chervonova U.V., Alexandrov A.I., Gruzdev M.S., Ksenofontov A.A., Pashkova T.V.</u>	209
PII-19. <i>Thermodynamic Assessment of High-Entropy Crystalline Phase with the Magnetotlumbite Structure</i>	
<u>Vinnik D.A., Trofimov E.A., Zhivulin V.E., Zaitseva O.V., Gudkova S.A., Starikov A.Yu., Kirsanova A.A., Zherebtsov D.A.</u>	210
PII-20. <i>Thermal Properties of Iridium (I) Volatile Complexes with Cyclooctadiene-1,5 and (O,N)-Coordinated Ligands</i>	
<u>Karakovskaya K.I., Vikulova E.S., Zelenina L.N., Sysoev S.V., Morozova N.B.</u>	211
PII-21. <i>First Example of Large Anisotropic Plasticity of Organic Crystal Preserved at Cryogenic Temperatures. Structure-Property Relation</i>	
<u>Nguyen T.T., Arkhipov S.G., Losev E.A., Rychkov D.A.</u>	212
PII-22. <i>Thermodynamic Issues of L-Valinium Hydrogen Maleate: Crystallographic and Computational Insight</i>	
<u>Arkhipov S.G., Rychkov D.A.</u>	213
PII-23. <i>Resonant Active Sites in Catalytic Ammonia Synthesis over Metal Alloys and Clusters</i>	
<u>Cholach A.R., Bryliakova A.A.</u>	214
PII-24. <i>Molecular Brushes Based on Polyimide and Polymethyl Methacrylate as Compatibilizers of Epoxy-Thermoplastic Mixtures</i>	
<u>Chalykh A.E., Stepanenko V.Y., Budylin N.Y., Shcherbina A.A., Meleshko T.K., Yakimanskij A.V.</u>	215
PII-25. <i>The Effect of the Latrepirdine on the Structure of Microsomal and Synaptosomal Membranes</i>	
<u>Gerasimov N.Yu., Nevrova O.V., Kasparov V.V., Kovarskii A.L., Goloshchapov A.N., Burlakova E.B.</u>	216
PII-26. <i>Research of the Experimental Alzheimer`S Disease to Search for the Treatment</i>	
<u>Gerasimov N.Yu., Nevrova O.V., Krivandin A.V., Goloshchapov A.N., Burlakova E.B.</u>	217
PII-27. <i>Disjoining Pressure in a Thin Spherical Liquid Film within Molecular and Mechanical Approaches</i>	
<u>Lebedeva T.S., Shchekin A.K., Suh D.</u>	218
PII-28. <i>Dynamic Surface Properties of Heptadecafluoro-1-Nonanol Solutions</i>	
<u>Akentieva A.V., Noskov B.A., Lin S.-Y.</u>	219
PII-29. <i>Dynamic Surface Properties of Fullerenol Solutions</i>	
<u>Timoshen K.A., Noskov B.A., Akentieva A.V., Chirkov N.S., Lin S.-Y., Sedov V.P., Borisenkova A.A., Dubovsky I.M., Lebedev V.T.</u>	220
PII-30. <i>Dynamic Surface Properties of DNA/Polyelectrolyte Aqueous Solutions</i>	
<u>Chirkov N.S., Noskov B.A., Lin S.-Y.</u>	221

PII-31. <i>Theory for Charge Distribution in Ionic Liquids Near a Charged Wall</i> <u>Ciach A.</u>	222
PII-32. <i>Surfactant Adsorption in Porous Media: Adsorption Equilibria and Self-Assembly</i> <u>Faria B.F., Vishnyakov A.</u>	223
PII-33. <i>Impact of L(+)-Arabinose on Micellar Structure of Aqueous Solutions of Nonionic Surfactant Triton X-114 in a Mean Concentration Range</i> <u>Levashova E.Y., Koneva A.S., Safonova E.A.</u>	224
PII-34. <i>Seawater Nanodroplets Under Atmospheric Conditions. A Molecular Dynamics Simulation Study</i> <u>Egorov A.V., Brodskaya E.N., Laaksonen A.</u>	225
PII-35. <i>Thermodynamic Modeling of Fluid Systems Based on Baku Oil</i> <u>Ramazanova E.E., Asadov M.M., Aliyev E.N.</u>	226
PII-36. <i>Thermodynamics and Dielectric Properties of As₂S₃-As₂Se₃-InSe</i> <u>Asadov M.M., Mustafaeva S.N., Lukichev V.F.</u>	227
PII-37. <i>Thermodynamic and Transport Properties of Choline Chloride + Urea as a Deep Eutectic Solvent and its Binary Mixtures with Molecular Liquids</i> <u>Agieienko V. N., Buchner R.</u>	228
PII-38. <i>Termophysical Properties of CoFeSiBNb Alloy in Crystalline and Liquid States</i> <u>Sidorov V.E., Rusanov B.A., Mikhailov V.A., Son L.D.</u>	229
PII-39. <i>On Application of the CP-PC-SAFT Model for Estimation of Sound Speed in Synthetic and Natural Oil-Gas Mixtures</i> <u>Prikhodko I., Samarov A., Toikka A.</u>	230
PII-40. <i>Liquid-Liquid Equilibria for Separation of Alcohols from Esters Using Deep Eutectic Solvents Based on Choline Chloride</i> <u>Samarov A., Prikhodko I., Liubichev D., Toikka A.</u>	231
PII-41. <i>Evaluation of Thermal Stability Duration (Useful Life) of Organic Heat-Carriers</i> <u>Dzhapparov T.A-G., Bazaev A.R., Bazaev E.A., Bagavudinova D.G., Medzhidova F.Kh.</u>	232
PII-42. <i>Urea and Tetramethylurea Solutions in Ethylene Glycol: a Comparative Analysis of Temperature-Dependent Volumetric Solvation Characteristics and Interaction Parameters</i> <u>Ivanov E.V., Lebedeva E. Yu., Kustov A.V., Ivanova N.G.</u>	233
PII-43. <i>Standard Thermodynamic Properties in Water for Equimolecular Co-Crystal of Cis- and Trans- Coordinated Dimethylglycolurils at Temperatures from 278.15 K to 318.15 K and at the Ambient Pressure</i> <u>Ivanov E.V., Lebedeva E. Yu., Batov D.V., Baranov V.V., Kravchenko A.N.3, Ivanova N.G.</u>	234
PII-44. <i>Thermodynamic Properties of Dimethylsulfone-Dimethylsulfoxide-Water Ternary System</i> <u>Ghazoyan H.H., Markarian S.A.</u>	235
PII-45. <i>Thermodynamic Evaluation of Chemical and Electrochemical Oxidation of V – Si System</i> <u>Nikolaychuk P. A.</u>	236
PII-46. <i>Thermal Conductivity and Thermal Diffusivity of Cerium in the Temperature Range 293 - 1773 K</i>	

<u>Savchenko I.V., Samoshkin D.A., Stankus S.V.</u>	237
PII-47. <i>Excess Enthalpies of Hydroxy-Containing Esters by Capillary Gas Chromatography</i> <u>Portnova S.V., Krasnykh E.L.</u>	238
PII-48. <i>The Determination of the Characteristics of Sorption, Vapor Pressure and Enthalpy of Vaporization of Esters of Neopentylglycol</i> <u>Lukina O.D., Krasnykh E.L., Portnova S.V.</u>	239
PII-49. <i>Vapor Pressure and Enthalpy of Vaporization of Pentaerythritol Esters</i> <u>Emel'yanov V.V., Krasnykh E.L., Levanova S.V.</u>	240
PII-50. <i>Stability of Solid Phases of Ytterbium Oxide and Oxychloride in Molten Alkali Metal Chlorides</i> <u>Nikolaeva E.V., Zakir'yanova I.D., Sosnovtseva T.V.</u>	241
PII-51. <i>Solubility of Gadolinium Oxide in Molten GdCl₃ - KCl System</i> <u>Nikolaeva E.V., Zakir'yanova I.D., Korzun I.V.</u>	242
PII-52. <i>Phase Equilibria in Oxide-Chloride Systems Gd₂O₃ - GdCl₃ AND Gd₂O₃ - GdCl₃ - KCl</i> <u>Korzun I.V., Nikolaeva E.V., Zakir'yanova I.D.,</u>	243
PII-53. <i>Modifications of Ethanol, Toluol and Water at Equilibrium System Liquid - Perfect Gas</i> <u>Vitvitskiy A.I.</u>	244
PII-54. <i>The Study of Phase Equilibria in the Fe-Cu-As, Fe-As-S, Cu-As-S Systems</i> <u>Trofimov E.A., Starykh R.V., Sineva S.I., Zaitseva O.V., Galkina D.P.</u>	245
PII-55. <i>Study of Phase Equilibria at the Fe-As-S Ternary System</i> <u>Starykh R., Ilatovskaia M., Kostyanko A., Trofimov E.A., Samoiloa O., Sineva S.</u>	246
PII-56. <i>Thermophysical Properties of Ionic Liquids at Wide Range of State Parameters</i> <u>Safarov J.T., Guluzade A.N., Hassel E.P.</u>	247
PII-57. <i>Vapor Pressure of 1-Butyl-3-Methylimidazolium Trifluoromethanesulfonate and Methanol Solution over Wide Range of Temperature</i> <u>Safarov J.T., Guluzade A.N., Hassel E.P.</u>	248
PII-58. <i>Molecular Models for Phase Equilibria of Alkanes with Air Components and Combustion Products</i> <u>Vishnyakov A.V., Santo K.P., Rasmussen R., Neimark A.V., Brun E.</u>	249
PII-59. <i>Determination of Separatric Manifold Structure of Five-Component System Phase Diagram</i> <u>Frolkova A.V., Makhnarilova E.G.</u>	250
PII-60. <i>The Properties of Separatric Manifold as Poincare Integral Invariant</i> <u>Frolkova A.K., Frolkova A.V.</u>	251
PII-61. <i>Liquid ⇌ Gas Phase Transitions Water+Aliphatic Alcohol Binary Mixtures</i> <u>Osmanova B.K., Bazaev A.R., Bazaev E.A.</u>	252
PII-62. <i>Liquid-Liquid Equilibrium of Ternary System Cyclohexene + Water + N,N-Dimethylacetamide</i> <u>Zhuchkov V.I., A. Malyugin A., Frolkova A.V., Frolkova A.K.</u>	253
PII-63. <i>Determination of Critical Parameters of the Mixture [xH₂O+(1-x)C₇H₁₆] (x = 0.053</i>	

<i>Molar Fractions) by the Method of Pressure Measurement</i>	
<i>Nazarevich D.A., Mirskaya V.A., Ibaov N.V.</i>	254
PII-64. <i>Experimental Assessment of the Ionic Liquids Selectivity for Extractive Distillation of Binary Mixtures</i>	
<i>Raeva V.M., Zhuchkov V.I., Ryzhkin D.A.</i>	255
PII-65. <i>Experimental Investigation of the Liquidus Surface Projection of The Cu-Pd-Sn Ternary System</i>	
<i>Khartsyzov G., Sineva S., Starykh R., Kareva M., Kuznetsov V.</i>	256
PII-66. <i>Fast Methods of Debye-Hückel Limiting Slopes Calculation Based on $\ln p_{ws}$ Equation of State of Water</i>	
<i>Voskov A.L., N.A. Kovalenko N.A.</i>	257
PII-67. <i>Solubility and the Structure of Equilibrium Crystal Solvates in Systems $MX_2 - S_1 - S_2$ ($M = Cd, Cu; X = Cl, Br, I; S_1, S_2 =$ Dimethylsulfoxide, N,N-Dimethylacetamide, 1,4-Dioxane) at 298 K</i>	
<i>Tolmachev M.V., Bogachev N.A., Skripkin M. Yu.</i>	258
PII-68. <i>Volumetric Properties of Double-Charged Ions in N-Methylacetamide Solutions over the Temperature Range from 308.15 to 328.15 K at Ambient Pressure</i>	
<i>Dyshin A.A., Kiselev M.G.</i>	259
PII-69. <i>Liquid \rightleftharpoons Gas Phase Transitions of 1-Propanol – n-Hexane Binary and Water – 1-Propanol – n-Hexane Ternary Mixtures</i>	
<i>Bazaev A.R., Bazaev E.A., Osmanova B.K., Dzhapparov T.A-G.</i>	260
PII-70. <i>Experimental Study of Azeotropy in the n-Heptane-Water Binary System</i>	
<i>Ibaov N.V., Mirskaya V.A., Nazarevich D.A.</i>	261
PII-71. <i>Complex Approach to Acetamide-Water System Investigation</i>	
<i>Krestyaninov M.A., Dyshin A.A., Ivlev D.V., Kolker A.M.</i>	262
PII-72. <i>Quantum-Chemical, Molecular Dynamics and IR Spectroscopic Study of Hydrogen-Bonded Clusters of N-Methylacetamide-Water Mixture</i>	
<i>Krestyaninov M.A., Ivlev D.V., Dyshin A.A., Kolker A.M.</i>	263
PII-73. <i>Influence of the Initial Composition of the Powders on the Phase Composition of the Surface Layer Formed in the Conditions of Electron Beam Surfacing</i>	
<i>Kryukova O.N., Knyazeva A.G.</i>	264

POSTER SESSION 3

SATURDAY, 22.06.2019

PIII-1. <i>Electrophysical and Transport Properties of $Me(La, Sm)_2WO_7$ ($Me = Sr, Ba$)</i>	
<i>Taimassova Sh.T., Gogol D.B., Bissenqaliyeva M.R., Balbekova B.K.</i>	266
PIII-2. <i>Effect of the rGO (Reduced Graphene Oxide) Addition on Conductivity and Microstructure of Ceramics $ZrO_2 - Y_2O_3$ Sintered Using Different Techniques</i>	
<i>Glukharev A.G., Temnikova M.S., Glumov O.V. and Konakov V.G.</i>	267
PIII-3. <i>Structure and Conductivity of 9CaO-91ZrO₂ Ceramics, Obtained from Freeze-Dried Powder With Cryoprotectant Addition</i>	
<i>Grega M.E., Kurapova O. Yu., Nikiforova K.V., Konakov V.G.</i>	268

PIII-4. <i>On the Thermal Behavior of Ammonium Fluorometallates</i> <u>Laptash N.M.</u>	269
PIII-5. <i>Sublimation Thermodynamics of Pyridinedicarboxylic Acids</i> <u>Drozd K.V., Manin A.N., Perlovich G.L.</u>	270
PIII-6. <i>Vapor Pressure and Vaporization Enthalpies of Glycolic Acid Esters</i> <u>Yamshchikova Y.F., Portnova S.V., Krasnykh E.L.</u>	271
PIII-7. <i>Thermodynamic Parameters of Formation Reactions for Binary and Ternary Complexes of Zinc(II), Cobalt(II), Nickel(II), Copper(II) Ions with Some Aminocarbonic Ligands</i> <u>Gridchin S.N., Pyreu D.F.</u>	272
PIII-8. <i>Thermodynamic Study of Ammonium Sulfamate</i> <u>Tiflova L.A., Druzhinina A.I., Kosova D.A., Uspenskaya I.A., Monayenkova A.S.</u>	273
PIII-9. <i>Dicyclopropyldinitromethane and Tricyclopropylmethane: Standard Enthalpies of Formation in Condensed and Gas States</i> <u>Tiflova L.A., Lukyanova V.A., Pimenova S.M., Ilin D.Y., Druzhinina A.I., Dorofeeva O.V.</u> .	274
PIII-10. <i>Thermodynamic Functions of Lanthanide Orthotantalates at 10-330 K</i> <u>Gagarin P.G., Guskov V.N., Gavrichev K.S., Sazonov E.G.</u>	275
PIII-11. <i>Low-Temperature Heat Capacity of Pd(C₅HF₆O₂)₂</i> <u>Bespyatov M.A., Gelfond N.V., Morozova N.B.</u>	276
PIII-12. <i>Phonon Density of States and Zero-Point Energy of Eu(C₁₁H₁₉O₂)₃</i> <u>Musikhin A.E., Bespyatov M.A.</u>	277
PIII-13. <i>Thermodynamic Characteristics and Phonon Density of States of Barium Tungstate Based on the Low-Temperature Heat Capacity</i> <u>Musikhin A.E., Naumov V.N.</u>	278
PIII-14. <i>Thermodynamics of Evaporation Processes of Yttrium Trichloride and Tribromide</i> <u>Osina E.L., Gorokhov L.N., Osin S.B.</u>	279
PIII-15. <i>Study of Thermochemical Properties of Various Porphyrin Ligands</i> <u>Lazarev N.M., Petrov B.I., Makarov S.G.</u>	280
PIII-16. <i>Thermodynamic Properties of Ir(C₅H₇O₂)(C₈H₁₂)</i> <u>Kuzin T.M., Bespyatov M.A., Pischur D.P., Gelfond N.V.</u>	281
PIII-17. <i>Thermochromism and Anomaly in the Heat Capacity of Dimeric Tris(2,2,6,6-Tetramethyl-3,5-Heptanedionato) Europium</i> <u>Bespyatov M.A., Cherniaikin I.S., Kuzin T.M., Stabnikov P.A.</u>	282
PIII-18. <i>Influence of N-Methyl Substitution in the Glycine Molecule on its Enthalpic Dissolution Characteristics in Mixed Aqueous - Organic Solvents at T=298.15 K</i> <u>Smirnov V.I., Badelin V.G.</u>	283
PIII-19. <i>Influence of The Properties of Organic Solvents and the Composition of Water-Organic Mixtures on Thermochemical Characteristics of L-Glutamine Dissolution at T=298.15 K</i> <u>Smirnov V.I., Badelin V.G.</u>	284
PIII-20. <i>The Evaluation of Originated Carbon-Paste Electrode Modified by Animal Waste Products Applicability for the Study of Thermodynamic Characteristics of Complex</i>	

<i>Formation Processes</i>	
<u>Amerkhanova Sh.K., Shlyapov R., Uali A.S.</u>	285
PIII-21. <i>Thermodynamic Properties of Crystalline Phosphate $\text{BiFe}_2(\text{PO}_4)_3$ in the Range from $T \rightarrow 0$ to 670 K</i>	
<u>Pet'kov V.I., Lavrenov D.A., Smirnova N.N., Markin A.V., Asabina E.A.</u>	286
PIII-22. <i>Thermal Stability of Oxychlorides LnOCl ($\text{Ln} = \text{Gd}, \text{Yb}$)</i>	
<u>Zakir'yanova I.D., Korzun I.V.</u>	287
PIII-23. <i>Thermodynamic Properties of 4'-Cyclohexylacetophenone</i>	
<u>Blokhin A.V., Kantsiava V.V., Kilchytskaya Y.V., Tarazanov S.V.</u>	288
PIII-24. <i>Thermodynamic Parameters of Methyl 3,5-di-tert-Butylbenzoate</i>	
<u>Blokhin A.V., Kantsiava V.V., Neviadzimtsau A.V., Tarazanov S.V.</u>	289
PIII-25. <i>Thermodynamic Properties of L-Menthol</i>	
<u>Yurkshtovich Y.N., Blokhin A.V., Neviadzimtsau A.V.</u>	290
PIII-26. <i>Thermodynamic Characteristics of Energy-Intensive Jet Fuels with Stacked-Cup Multiwall Carbon Nanotubes (MCNTs)</i>	
<u>Karpushenkava L.S., Kabo G.J., Blokhin A.V., Seradzenka S.U.</u>	291
PIII-27. <i>Thermodynamics and Crystal Growth of Lithium Tungstate Doped by Molybdenum</i>	
<u>Grigorieva V.D., Shlegel V.N., Matskevich N.I.</u>	292
PIII-28. <i>Low-Temperature Heat Capacity of $\text{Cu}(\text{C}_{11}\text{H}_{19}\text{O}_2)_2$</i>	
<u>Cherniaikin I.S., Bespyatov M.A., Stabnikov P.A., Dorovskikh S.I., Morozova N.B., Gelfond N.V.</u>	293
PIII-29. <i>Thermochemistry of Compounds Formed from Guaiacyl Lignin Fragment</i>	
<u>Maksimuk Y.V., Krouk V.S1, Ponomarev D.A., Antonava Z.A.</u>	294
PIII-30. <i>The Thermal Decomposition of Lanthanide (III) Chloride Hydrates</i>	
<u>Korzun I.V., Zakir'yanova I.D. and Salulev A.B.</u>	295
PIII-31. <i>High-Temperature Heat Capacity of $\text{LnInGe}_2\text{O}_7$ ($\text{Ln} = \text{Tb} - \text{Lu}$)</i>	
<u>Irtuygo L.A., Kudashova N.G., Denisov V.M.</u>	296
PIII-32. <i>Synthesis and Thermodynamic Properties of the Titanates $\text{R}_2\text{Ti}_2\text{O}_7$ ($\text{R} = \text{Gd}, \text{Lu}$)</i>	
<u>Golubeva E.O., Chunilina L.G.</u>	297
PIII-33. <i>Vaporization Enthalpies of Mono- and Dibromoalkanes</i>	
<u>Samatov A.A., Nagrimanov R.N., Solomonov B.N.</u>	298
PIII-34. <i>Metal Acetylacetonates: Thermochemistry and Structure-Property Relationships</i>	
<u>Makarenko A.M., Zherikova K.V.</u>	299
PIII-35. <i>Thermodynamic Properties of $\text{CeO}_2\text{-ZrO}_2$ and $\text{CeO}_2\text{-Y}_2\text{O}_3$ Systems</i>	
<u>Lopatin S.I., Shugurov S.M., Vasil'eva E.A., Kurapova O.Yu., Konakov V.G.</u>	300
PIII-36. <i>Thermodynamic Analysis of The Possibility of NO_2 to NO Reforming</i>	
<u>Nikiforova K.V., Konakov V.G.</u>	301
PIII-37. <i>Excess Enthalpies in the Chemically Equilibrium System Ethanol + Acetic Acid + Ethyl Acetate + Water</i>	
<u>Golikova A.D., Tsvetov N.S., Toikka M.A., Toikka A.M.</u>	302
PIII-38. <i>Thermodynamic Properties of Cation-Ordered Layered Perovskite-Like Oxides</i>	

	<i>K₂Nd₂Ti₃O₁₀ and its Protonated Forms</i>	
	<i>Sankovich A.M., Myshkovskaia T.D., Smirnova N.N., Markin A.V., Zvereva I.A.</i>	303
PIII-39.	<i>Calorimetric Study of Hyperbranched Polyphenylene Pyridine-Containing Polymers in the Range from T → 0 to 680 K</i>	
	<i>Smirnova N.N., Markin A.V., Sologubov S.S., Serkova E.S., Kuchkina N.V., Shifrina Z.B.</i>	304
PIII-40.	<i>Benchmark Properties of 2-, 3- and 4-Nitrotoluene: Evaluation of Thermochemical Data with Complementary Experimental and Computational Methods</i>	
	<i>Bikelytė G., Härtel M., Stierstorfer J., Klapötke T.M., A. Pimerzin A., Verevkin S.P.</i>	305
PIII-41.	<i>Recent Developments on The Energetics of Morpholine Derivatives</i>	
	<i>Ribeiro da Silva M.D.M.C., Silva C.A.O., Freitas V.L.S.</i>	306
PIII-42.	<i>Physical Characterization of a Novel Electrolyte Based in Ionic Liquid MPPyrr-TFSI + dMSO + Li-TFSI</i>	
	<i>Cabeza O., Segade L., García-Garabal S., Domínguez-Pérez M., Ausín D., Rilo E., Varela L.M.</i>	307
PIII-43.	<i>The Influence of Crystalline Structure and Surface Characteristics of Different TiO₂ Nanoforms on Human Serum Albumin Thermal Denaturation: a Differential Scanning Calorimetry Study</i>	
	<i>Gheorghe D.</i>	308
PIII-44.	<i>Thermodynamic Parameters of the Protein Interaction with SiO₂ Nanoparticles</i>	
	<i>Botea-Petcu A., Precupas A., Gheorghe D., Sandu R., Popa V.T., Tanasescu S.</i>	309
PIII-45.	<i>Salting-Out of Isobutyric Acid From Aqueous Solutions with Sodium Chloride</i>	
	<i>Il'in K.K., Kapustina D.V., Kurskiy V.F.</i>	310
PIII-46.	<i>Definition of Subtypes of Three Component System Diagrams, Containing Binary Biazeotropic Constituents and Not Having a Ternary Azeotropes</i>	
	<i>Chelyuskina T.V., Polkovnichenko A.V., Modurova D.D.</i>	311
PIII-47.	<i>Mutual Transformations of $\alpha=1$ Lines Diagrams of Butyl Butyrate - Butyric Acid - γ-Butyrolactone System</i>	
	<i>Polkovnichenko A.V., Chelyuskina T.V.</i>	312
PIII-48.	<i>Determination of Mean Ionic Activity Coefficients in the Li₂CO₃ - H₂O System at 25 °C and P_{CO₂}=1 Atm</i>	
	<i>Gorbachev A.V., Mamontov M.N.</i>	313
PIII-49.	<i>The Viscosity Predictions for Branched Alkanes at Pressures up to 1 GPa Using Molecular Dynamics</i>	
	<i>Kondratyuk N.D., Pisarev V.V.</i>	314
PIII-50.	<i>Thermodynamic Modeling and Experimental Investigations in the System Formed by Water, Nitric Acid, Neodymium Nitrate, o-Xylene and D2EHPA</i>	
	<i>Kovalenko N.A., Kurdakova S.V., Arkhipin A.S., Maksimov A.I., Uspenskaya I.A.</i>	315
PIII-51.	<i>The Conformational Equilibrium of Mefenamic Acid in DMSO: Thermodynamic or Kinetic Origin?</i>	
	<i>Belov K.V., Khodov I.A., Kiselev M.G., Efimov S.V., Batista de Carvalho L.A.E.</i>	316
PIII-52.	<i>Thermodynamic Models of the H₂O – HNO₃ – UO₂(NO₃)₂ and H₂O – HNO₃ – Th(NO₃)₄ systems</i>	
	<i>Maliutin A.S., Kovalenko N.A.</i>	317

P111-53. <i>Extinction and Saturated Vapor Pressure of Indium Monochloride</i> <i>Malygina E.N., Zavrazhnov A. Y., Kosyakov A. V., Naumov A. V.</i>	318
P111-54. <i>Phase Equilibria in ZrO₂ and 4Y₂O₃-96ZrO₂ Precursors (mol.%), Obtained by Cryochemical Method</i> <i>Lomakina T.E., Kurapova O. Yu., Konakov V.G.</i>	319
P111-55. <i>Inverse Solidus Surface Projection of the Cu-Co-Ni Ternary System</i> <i>Novozhilova O., Sineva S., Starykh R.</i>	320
P111-56. <i>Revisiting the Heat-Capacity Anomaly in Supercooled Water by High-Resolution Adiabatic Calorimetry</i> <i>Voronov V.P., Podnek V.E., Anisimov M. A.</i>	321
P111-57. <i>Prediction of Solubility of Polymers Using Polystyrene-Polysiloxane System as an Example</i> <i>Poteryaev A.A., Chalykh A.E.</i>	322
P111-58. <i>Melting Scenarios and Unusual Crystal Structures in Two-Dimensional Core-Softened Systems</i> <i>Ryzhov V.N., Fomin Yu.D., Tareyeva E.E., Tsiok E.N.</i>	323
P111-59. <i>Calculation of the Thermodynamic Properties of Natural Gas Using a Limited Number of Experimental Parameters</i> <i>Samarov A., Toikka M., Golikova A., Farzaneh-Gord M., Toikka A.</i>	324
P111-60. <i>Phase Diagram of the Ternary System n-Dodekan-n-Eykozan-Cyclododecane</i> <i>Shamitov A.A., Garkushin I.K., Kolyado A.V.</i>	325
P111-61. <i>Calculation of the Thermodynamic Parameters of the Fe-Ni-Co-Cu-Cr-Al-Mn Multicomponent Metallic System</i> <i>Vladimirov E.S., Starykh R.V., Sineva S.I., Vasil'eva A.A.</i>	326
P111-62. <i>Thermodynamics of Ion Exchange Process for Titanium(IV) Hydrophosphates</i> <i>Ivanenko V.I., Maslova M.V.</i>	327
P111-63. <i>Phase Relations in the Fe-Cu-As System</i> <i>Ilatovskaia M., Novoghilova O., Samoilova O., Sineva S., Starykh R.</i>	328
P111-64. <i>How are Structures, Properties and Crystallisations Conditions Interrelated? New Solid Forms of Metacetamol as a Case Study</i> <i>Zemtsova V.M., Rychkov D.A., Pulham C.R., Boldyreva E. V.</i>	329
P111-65. <i>The Structure of Ionic and Neutral Liquids of the Similar Molecules</i> <i>Shelepova E.A., Paschek D., Ludwig R., Medvedev N.N.</i>	330
P111-66. <i>Melting Temperature Calculation Through the Simulation of Coexisting Phases</i> <i>Zakiryanov D.O., Kobelev M.A., Tkachev N.K.</i>	331
P111-67. <i>Solubility of hydroxyapatite. New Approaches and Results</i> <i>Kuranov G., Mikhelson K., Puzyk A.</i>	332
P111-68. <i>Influence of Freezing and Annealing Protocols on Phases Formed in The Tert-Butanol – Water System</i> <i>Ogienko A.G., Stoporev A.S., Ogienko A.A., Yunoshev A.S., Adamova T.P., Manakov A. Yu., Boldyreva E. V.</i>	333
P111-69. <i>Quasi-Chemical Approach – Novel Powerful Tool to Study Supramolecular</i>	

*Organization, Macroscopic Equilibrium and Non-Equilibrium Properties of Non-Ideal
Liquid Systems. Polyamorphism of Liquid Mixtures*

Durov V.A...... 334

ABSTRACTS

THURSDAY, 20.06.2019

PLENARY SESSION

Thermodynamics and Kinetics of Biochemical and Chemical Reactions

Sadowski G.

TU Dortmund University, Germany, Dortmund

gabriele.sadowski@tu-dortmund.de

Solvents are widely used in chemical industry to facilitate a broad variety of applications. It is well-known that they may strongly influence reaction equilibrium (yield) as well as reaction kinetics.

The key property for describing reaction equilibria is the thermodynamic equilibrium constant K_a which is directly related to the equilibrium concentrations of reactants and products (K_x) and their activity coefficients (K_γ).

$$K_a = K_x \cdot K_\gamma = \prod_i x_i^{\nu_i} \cdot \prod_i \gamma_i^{\nu_i}$$

The equilibrium constant K_a only depends on temperature but neither depends on reactant concentrations nor on solvents. In contrast, K_γ is often strongly influenced by solvents and reactant concentrations and that's why also K_x (and therewith the yield) depends on these properties. Once K_a is known, a thermodynamic model for determining the activity coefficients of reactants and products allows for successfully **predicting** the influence of solvents on the equilibrium concentrations. This will be demonstrated for various chemical and biochemical reactions for which the yield is strongly influenced by reactant concentration/solvents. It will be shown that the predicted effects always were in almost quantitative agreement with the experimental data.

For reactions in which the catalyst is not affected by the solvent(s), also the solvent influence on the reaction kinetics (e.g. for reaction $A+B \rightarrow C+D$) can be predicted using the solvent-independent (intrinsic) rate constant k^* and the reactant activity coefficients γ_A and γ_B according to:

$$r = k^* \cdot x_A \gamma_A \cdot x_B \gamma_B.$$

This will also be shown for various examples.

Thus, using thermodynamic modeling allows for predicting the solvent influence on chemical and biological reactions and therewith drastically reduces the experimental effort for selecting the best-suitable solvent for a reaction of interest.

DES – Do They Exist? And Why Should You Be Concerned About it...

Coutinho J.A.P.

CICECO- Aveiro Institute of Materials, Department of Chemistry, University of Aveiro, 3810-193 Aveiro, Portugal

jcoutinho@ua.pt

After years of ionic liquids fad a new star seems to shine bright on thermodynamicists sky: Deep Eutectic Solvents (DES). Proposed more than a decade ago by Abbott and co-workers they seem to have been overshadowed by the ionic liquids for a long time, but as expectations about ionic liquids floundered they found a surprising new interest from the scientific community as cheaper and greener ionic liquid derivatives. Admittedly a number of interesting applications have been reported but the understanding about DES and its nature seems to be shrouded in myths that often hurt the sensibility of a thermodynamicist.

Having been working with ionic liquids for a long time and being forced to face the DES torrent our research group felt compelled to study them not just from an applied point of view but in an attempt to understand the nature of these mixtures, for mixtures they are, and to use the concepts of macroscopic thermodynamics, along with some tools of molecular simulation, to reach for an understanding of the nature of these mixtures.

This lecture will be about our findings that failed to identify DES where everybody reported they were, finding DES where nobody had look for them, and attempting at demystifying many ideas wrong assumptions that are widespread in the literature. Using solid liquid phase diagrams of these mixtures, that are surprisingly scarce in the literature, and the concepts of non-ideality, we will poke into the very nature of the liquid phase of a wide number of systems reported as DES to show that most are nothing else than ideal eutectic mixtures, and that some basic thermodynamic knowledge can prevent you to be a victim of the DES craze.

Thermodynamics of Fluid Polyamorphism

Anisimov M.A.

Department of Chemical & Biomolecular Engineering and Institute for Physical Science & Technology, University of Maryland, College Park, U.S.A.

anisimov@umd.edu

For most pure materials (at a given temperature and pressure), molecules are arranged in a single noncrystalline or amorphous structure that is liquid, gas, or solid. Conventional theory adequately predicts the thermodynamic properties of such materials, which are well understood. In contrast to this simple picture, there is increasing evidence that many pure fluids exist in several alternative structures, resulting in the phenomenon known as “fluid polyamorphism.” It has been hypothesized that even water may exhibit this behavior at very low temperatures. Our recent research¹ contributes to better understanding of this phenomenon by developing a unified theoretical framework that is capable of making robust predictions for the thermodynamic properties of different polyamorphic fluids.

We use the theory of phase transitions and the concept of two competing interconvertible amorphous structures to develop a generic phenomenological approach, which is independent of the underlying molecular origin of the phenomenon and provides new physical insights. It succeeds in unifying all, apparently unrelated, cases of fluid polyamorphism with and without phase separation, from the liquid-liquid transition in supercooled water and silicon to superfluid helium and polymerized sulfur. Our approach generically describes the phase behavior and thermodynamic anomalies typically observed in polyamorphic materials, including liquid-vapor and liquid-liquid transitions, as well as stretched metastable liquid states under negative pressures.

Our results mark a paradigm shift that significantly broadens fluid polyamorphism from its original narrow scope to a cross-disciplinary field that addresses a wide class of systems and phenomena with interconversion of alternative molecular or supramolecular states.

1. M. A. Anisimov, M. Duška, F. Caupin, L. E. Amrhein, A. Rosenbaum, and R. J. Sadus, “*Thermodynamics of Fluid Polyamorphism*,” *Phys. Rev. X*, **8**, 011004 (2018).

THURSDAY, 20.06.2019

**SECTION 2:: Thermodynamics of Liquids, Fluid
Mixtures, and Phase Equilibria**

Critical Properties, Heat Capacities, and Thermal Diffusivities of Levulinic Acid and its *n*-Alkyl Esters

Nikitin E.D., Popov A.P., Bogatishcheva N.S. and Faizullin M.Z.

Institute of Thermal Physics, Ural Branch of RAS, Russia

e-nikitin@mail.ru

Levulinic (4-oxopentanoic) acid is considered as one of the most important platform chemicals in the process of conversion of biomass into valuable fuels and fuel additives. Levulinic acid esters have characteristics that allow using them as oxygenate additives for diesel and gasoline fuels and as cold flow improvers in biodiesel. Besides, these esters are widely used as solvents and plasticizers. The paper presents the results of measuring the critical temperatures T_c , critical pressures P_c , molar heat capacities $C_{p,m}$, and thermal diffusivities a of levulinic acid, methyl-, ethyl-, propyl-, and butyl levulinates. The samples of the compound studied were purchased from Sigma-Aldrich and have purities better than 98 mol.%.

The measurements of the critical properties have been made by the pulse-heating method developed by the authors and recognized in Russia as a “standard state method” (GSSSD 163-2010) [1]. Heat capacity has been measured with the help of a differential scanning calorimeter DSC 204 F1 Phoenix (Netzsch); thermal diffusivity has experimentally been determined by the laser flash technique using LFA 457 MicroFlash (Netzsch). The measurements of heat capacity and thermal diffusivity have been performed in the temperature range from 303.15 to 373.15 K. The relative combined expanded uncertainties at 0.95 level of confidence are $U_r(T_c)=0.015$, $U_r(p_c)=0.04$ for levulinic acid, $U_r(T_c)=0.01$, $U_r(p_c)=0.03$ for the esters, $U_r(C_{p,m})=0.02$ and $U_r(a)=0.05$ for all the compounds studied. Equations for the dependence of molar heat capacities and thermal diffusivities of the compounds studied on temperature have been obtained.

The thermophysical properties of levulinic acid and its esters measured in this work have been compared with the values obtained by various methods. The methods of Lydersen, Wilson/Jasperson, and Constantinou/Gani [2] have been used to calculate the critical properties. Heat capacities have been estimated by the group contribution methods of Dvorkin et al. [3] and Kolska et al. [4]. Thermal diffusivities $a = \lambda / (\rho C_p)$ have been calculated in the following way. The values of heat capacity C_p have been taken in accordance with this work, the densities ρ have been taken from [5,6], and the thermal conductivities have been calculated using the methods of Latini et al. and Sastri et al. [2].

Acknowledgements. The study was supported by the Complex Program for Basic Research of the Ural Branch of the Russian Academy of Sciences N 18-2-2-13.

- [1] E.D. Nikitin, A.P. Popov, Y.G. Yatluk, V.A. Simakina, *J. Chem. Eng. Data*, 2010, 55, 178.
- [2] B.E. Poling, J.M. Prausnitz, J.P. O’Connell, *The Properties of Gases and Liquids*, 2000, McGraw-Hill, New York.
- [3] P.L. Dvorkin, G.L. Ryzhova, Y. A. Lebedev, *Bull. Acad. Sci. USSR, Div. Chem. Sci.*, 1984, 33, 982.
- [4] Z. Kolska, J. Kukul, M. Zábranský, V. Růžička, *Ind. Eng. Chem. Res.*, 2008, 47, 2075.
- [5] L. Lomba, B. Giner, I. Bandrés, C. Lafuente, R. Pino, *Green Chem.*, 2011, 13, 2062.
- [6] L. Lomba, C. Lafuente, M. García-Mardones, I. Gascón, B. Giner, *J. Chem. Thermodyn.*, 2013, 65, 34.

Screening of Conformational Diversity of Molecules of Biologically Active Compounds Based on Nuclear Overhauser Effect Spectroscopy

Khodov I.A.^{1,2}, *Efimov S.V.*², *Kiselev M.G.*¹

¹G.A. Krestov Institute of Solution Chemistry, Russian Academy of Sciences, Russia;

²Institute of Physics, Kazan Federal University, Russia

Ilya.Khodov@gmail.com

Depending on conditions, crystallization of polymorphs from solution can be either kinetically or thermodynamically controlled. In the latter case, the obtained polymorph is independent of the nature of the solvent. It was shown [1] that even in cases when the choice of the solvent seems to be crucial, this can be in fact a minor factor related to the concentration achieved in the chosen solvent rather than a specific effect of solvent–solute interaction. Therefore, it is necessary to determine solubility curves and the width of the metastable zone in order to control the crystallization process of a polymorph. A very important factor, however, is very rarely taken into account today: namely, the influence of a molecule's conformational state on the crystallization process. Spatial structures of the molecule was shown to be a key factor in the nucleation, regarding both kinetics [2,3] and thermodynamics of the process [4]. In this work we propose a method of screening of the conformational state depending on the pressure and temperature, based on nuclear Overhauser effect spectroscopy. This approach can provide unique information on structural characteristics of small molecules in subcritical and supercritical states.

Acknowledgments The work was supported by Russian Foundation for Basic Research (project nos. 18-29-06008, 18-03-00255 and 17-03-00459), by the Ministry of Education and Science of the Russian Federation, project no. RFMEFI61618X0097, by the Basic Research Program of Ministry of Education and Science, project no. 01201260481.

[1] T. Threlfall *Organic Process Research and Development*, 2000, 4, 384.

[2] I.A. Khodov, S.V. Efimov, M.Y. Nikiforov, V.V. Klochkov, and N. Georgi, *Journal of Pharmaceutical Sciences*, 2014, 103, 392.

[3] I.A. Khodov, S.V. Efimov, M.G. Kiselev, L.A.E. Batista De Carvalho, and V.V. Klochkov, *Journal of Molecular Structure*, 2016, 1113, 191.

[4] C. Bhugra, M.J. Pikal, *Journal of Pharmaceutical Sciences*, 2008, 97, 1329.

Site Density Models of Inhomogeneous Classical Molecular Liquids

Chuev G.N.¹, Fedotova M.V.²

¹Institute of Theoretical and Experimental Biophysics of the Russian Academy of Science,
Pushchino, Moscow Region, 142290, Russia;

²G.A. Krestov Institute of Solution Chemistry of the Russian Academy of Sciences,
Akademicheskaya St., 1, Ivanovo, 153045, Russia

genchuev@rambler.ru

Density based description could provide a useful framework for statistical mechanics description of liquid systems. This has resulted in the development of density functional theory (DFT) for simple liquids. Extension to molecular liquids, however, proved to be quite challenging. Unlike the atomic case the "particles" that comprise the liquid now had the distinct internal structure. An elegant solution has been proposed by Chandler by introducing site density representation, i.e. density of individual atoms in the molecule. This has provided a simple way to convey the presence of the internal structure and incorporate atomistic potentials that are used in explicit simulations. The idea has led to the development of reference interaction site model (RISM). Beglov and Roux provided extension to inhomogeneous 3D case (3DRISM), which has been used extensively for the evaluation of structural and thermodynamic properties of various solutes in molecular liquids. The appealing feature of site density approach is order of magnitude improvement in the computational efficiency compared to molecular dynamics. However, there are numerous examples indicating significant discrepancies between 3DRISM and experimental data or simulations, including some troubling unphysical results. The origin of these problems is still not well understood which hampers the ability to expand the scope of current application beyond SPC-like water models.

Building on the original idea of Chandler, we have developed a systematic framework for the analysis of inhomogeneous molecular liquids using site density as the underlying collective variable.¹ Our approach is based on the same effective action techniques that were used in the past to systematically analyze the Kohn–Sham variant of electronic structure DFT. The main remaining challenge here is how to deal with the presence of intrinsically different interaction scales - a feature fundamental to molecular liquid systems. As a result, the non-interacting reference system would have had a difficult time accommodating the disparity of still localized intra-molecular interactions and extended features of inter-molecular correlations in molecular liquids.

Our solution to this problem consisted of using a molecular gas reference system containing all the intra-molecular correlations in the system. This system was represented by an expression using one-point Mayer cluster expansion. The resulting approach referred to us as cluster site density functional theory (CSDFT) has an appealing physical interpretation as an expansion in terms of density fluctuations that sets up a natural hierarchy of progressively complicated representations of the molecule ('bonds', 'angles', etc). This expression proved particularly useful in the context of the implicit site density representation, setting up a self-consistent density equation that provides a clean separation intra-molecular and inter-molecular scales. Unlike most of the existing approaches, no assumption of rigid molecules is required, and the framework naturally accommodates previous methods as particular limiting cases. We have employed the CSDFT in a numerical code and applied to investigate various solutes solvated in normal water and supercritical liquid nitrogen and carbon dioxide. The obtained results indicate the critical importance of proper treatment of inter-molecular interactions. The framework presented in this work is all but a starting point in further explorations.

[1] M. Valiev, G. N. Chuev, *J. Stat. Mech.* 2018, 093201.

Permittivity and Activity Coefficients in Aqueous Solutions of Electrolytes: Insights from the Extended Debye-Hückel Theory

*Shilov I.Yu.*¹, *Lyashchenko A.K.*²

¹Department of Chemistry, Lomonosov Moscow State University, Moscow, Russia;

²Kurnakov Institute of General and Inorganic Chemistry, Moscow, Russia

ignatshilov@mail.ru

The extended Debye-Hückel (EDH) theory [1-3] which allows for concentration variation of electrolyte solution static permittivity is employed to predict activity coefficients in aqueous electrolyte solutions at ambient conditions. The salts with various stoichiometries (1:1, 2:1, 1:2, 3:1 and 3:2) are considered, including alkali chlorides, alkali iodides, MgCl₂, AlCl₃ and Al₂(SO₄)₃. The calculations are performed without parameter adjustments. The model calculations show in general case a semiquantitative agreement with experimental data, reproducing the nonmonotonic concentration dependence of activity coefficients. In the series of alkali chlorides and iodides the correct ordering of activity coefficients for the salts with different cations is reproduced. In case of some systems a quantitative agreement is observed in the concentration range up to 7 mol/kg. The role of solvation and ion pairing in performance of EDH theory is discussed.

Acknowledgements The financial support of RFBR (grant N 19-03-00033) is gratefully acknowledged.

[1] I.Yu. Shilov and A.K. Lyashchenko, *J. Phys. Chem. B*, 2015, 119, 10087.

[2] I.Yu. Shilov and A.K. Lyashchenko, *J. Mol. Liq.*, 2017, 240, 172.

[3] I.Yu. Shilov and A.K. Lyashchenko, *J. Sol. Chem.*, 2019, in press.

An Azeotrope in the Desert

Kleiber M.

Thyssenkrupp Industrial Solutions AG, Germany

michael.kleiber@thyssenkrupp.com

The separation of the azeotropic binary system tetrahydrofurane / water is a very elegant application of phase equilibrium thermodynamics. Due to the strong pressure dependence of the azeotropic composition, a simple pressure swing distillation is possible, without introduction of an additional selective agent into the process. This technique was applied in a project on the Arabian peninsula.

While the general results were quite as expected, it turned out to be not possible to keep the specification for the tetrahydrofurane, which was obviously contradictory to thermodynamics. The presentation describes the way how to find out where the errors occurred. Not only thermodynamics but also analytics, sampling, column hydrodynamics, distillation column control, chemistry, meteorology, and, last but not least, Arabian culture had to be taken into account.

Rigorous application of thermodynamics and the knowledge of its capabilities and limitations was finally decisive to come to a solution and avoid unreasonable modifications of the plant.

Implementation of CP-PC-SAFT EoS for Predicting Thermodynamic Properties of 1-Alkyl-3-methylimidazolium bis(trifluoromethylsulfonyl)imide Ionic Liquids and Phase Equilibria in their Binary Systems without Fitting Adjustable Parameters

Polishuk I.

Department of Chemical Engineering, Biotechnology and Materials, Ariel University,
40700, Ariel, Israel.

polishuk@ariel.ac.il

In this presentation a simple molecular weight-based correlations for the CP-PC-SAFT¹ parameters for [C_nmim][NTf₂] ionic liquids are presented. These correlations allow a nearly precise modeling of densities including the elevated pressures and up to ~400 K and truthful predictions of the isobaric heat capacities, sound velocities and compressibilities. The available data reveal that solubility of gases is directly related to their critical temperatures. As the critical temperatures increase, the gas-IL systems become more symmetric and the solubility increases. The intrinsic robustness of CP-PC-SAFT along with obeying the pure compound critical temperatures attach this model by a capability to truthfully predict VLE in [C_nmim][NTf₂]-systems of various gases, such as CO, O₂, CH₄, Kr, N₂O, H₂S, SO₂, R134a, R1234ze(E) and CO₂ without previous consideration of any mixture data and adjusting binary parameters. Predictions of LLE in the [C_nmim][NTf₂] – 1-alkanols systems with $k_{12} = 0$ are also considered.

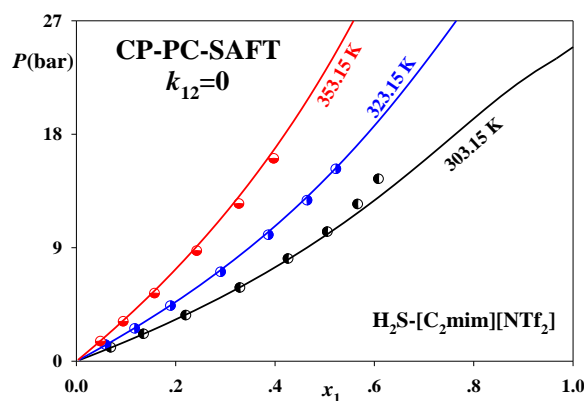


Figure 1. Solubility of H₂S in [C₂mim][NTf₂] ILs. Points – experimental data² – points. Lines – data predicted by CP-PC-SAFT with $k_{12} = 0$.

References

- (1) Polishuk, I. Standardized Critical Point-Based Numerical Solution of Statistical Association Fluid Theory Parameters: The Perturbed Chain-Statistical Association Fluid Theory Equation of State Revisited. *Ind. Eng. Chem. Res.* **2014**, *53*, 14127.
- (2) Sakhaeinia, H.; Jalili, A. H.; Taghikhani, V.; Safekordi, A. A. Solubility of H₂S in Ionic Liquids 1-Ethyl-3-methylimidazolium Hexafluorophosphate ([emim][PF₆]) and 1-Ethyl-3-methylimidazolium Bis(trifluoromethyl)sulfonylimide ([emim][Tf₂N]). *J. Chem. Eng. Data* 2010, *55*, 5839.

Calculation of the Contribution of Polarization Interactions in the Energy of Alkali Halide Melts by the Method of Thermodynamic Perturbation Theory

Davydov A.G., Tkachev N.K.

Institute of High Temperature Electrochemistry UB RAS, Russia

A.Davydov@ihite.uran.ru

The calculation of the thermodynamic properties (energy, entropy, etc.) of liquids is one of the important tasks of present theoretical chemistry, since many other properties of liquids can be calculated on this basis, including the description of the interfacial boundary between a liquid and solid. At the same time, the theoretical description of the properties of the liquid state is more complex, since in this case there is no long-range order structure.

One of the interesting directions of such research is the description of the properties of molten salts, where in addition to the forces of excluded volume and electrostatic interactions, the effect of reciprocal polarization of cations and anions must also be taken into account. The most developed approaches to this problem are related to molecular dynamic modeling and quantum-chemical calculations. However, a model for taking into account the polarization of ions in these systems using the statistical theory was not previously proposed.

The most difficult task here is to consider the latter type of interactions, namely, polarization effects. The ion charge induces dipole moments on neighboring ions, consequently, they will not only interact with each other, but they also will induce dipole moments on other ions. However, the excluded volume forces and electrostatic interactions define the structure of the melt, thus polarization effects can be considered as an addition to the energy of the system, which is relatively low in magnitude. In this case, it is convenient to take into account polarization interactions of ions of the molten salt in the framework of thermodynamic perturbation theory:

$$\beta f = \frac{F}{Nk_B T} = \beta f_0 + \frac{\beta \rho}{4\pi^2} \sum_{i,j} \sqrt{x_i x_j} \int_0^{\infty} \varphi_{ij}^1(k) \cdot g_{ij}^0(k) k^2 dk,$$

where k_B is Boltzmann's constant, T is the temperature, x_i is the mole fractions of i -th ion species, ρ is the numerical density, f is the full free energy of the system per atom, f_0 is the free energy of the reference system per atom, $\varphi_{ij}^1(k)$ is the perturbing addition of polarization interactions to the pair potential of the reference system in the inverse Fourier space, $g_{ij}^0(k)$ is the pair distribution function of the reference system in the inverse Fourier space.

Herewith, the model of charged hard spheres can be used for alkali-halide melts as the reference system (denoted by the zero indexes). The advantage of applying such reference system is the existence of exact solution for the model of charged hard spheres within the framework of the mean spherical approximation.

The results of calculations of the energy and other thermodynamic characteristics for molten alkali metal halides within the framework of the proposed approach of thermodynamic perturbation theory will present in the report, and the comparison of the calculated results with experimental data available in the literature will also be given.

Acknowledgements The reported study was funded by RFBR according to the research project № 18-03-00606

THURSDAY, 20.06.2019

**SECTION 1: Development of General Methods and Tools
of Chemical Thermodynamics: New Experimental
Techniques, Theory and Computer Simulation**

Transformations in Glasses and Nano-structured Materials Measured by Fast Differential Scanning Calorimetry

Schawe J.

Mettler-Toledo GmbH, Nänikon, Switzerland

juergen.schawe@mt.com

Fast differential scanning calorimetry (FDSC) is a non-adiabatically chip calorimetry technique. The commercial available Flash DSC 2+ enables typical heating and cooling rates in the order of 40,000 K/s in a temperature range between -100 °C up to 1000 °C.

This technique is used to study the kinetics in silicate glasses, the formation of differently structured glasses and non-isothermal nucleating processes in bulk metallic glass alloys. Depending on the thermal history and the heating conditions monotropic polymorphic phases can be formed which can be transformed into the more stable phase on different pathways. Furthermore, we discuss a method to distinguish between heterogeneous and homogeneous nucleation processes.

Improving the Method of Solution Calorimetry for Evaluation of The Enthalpies of Phase Transitions and Condensed State Enthalpies of Formation

Nagrimanov R.N.¹, Samatov A.A.¹, Zaitsau Dz. H.¹, Verevkin S.P.², Solomonov B.N.¹

¹Department of Physical Chemistry, Kazan Federal University, Russia;

²Department of Physical Chemistry, University of Rostock, Germany

Rnagrimanov@gmail.com

Aliphatic compounds can be perceived as a “milestone” of the whole organic chemistry. They are applied in the most branches of chemical industry, synthesis of pharmaceuticals, and oil industry. However, the profound investigation of thermochemical properties of aliphatic compounds especially enthalpies of phase transitions and enthalpies of transfer from condensed to the gas phase is hindered by the need to address a wide range of possible isomers as aliphatic tails tend to form cycles or branch.

The classical approaches for determination of enthalpies of vaporization/sublimation as direct calorimetric technique or methods based on vapor pressure determination provide only limited possibilities in case of aliphatic compounds [1]. The aliphatic compounds with long alkyl chain and biomolecules often possess very low vapor pressure. Due to this fact, an average measurement temperature is shifted to the higher range leading to the thermal stability issue.

The present study is aimed at finding and testing a unified media which can be applied for linear and cyclic alkanes as an athermal solvent with the solution enthalpy close to zero. The second objective of our work is to extend the range of thermochemical properties which can be estimated with the solution calorimetry.

In the present work, *n*-heptane was used as a solvent with the zero-thermal effect of solution enthalpy for normal and cyclic alkanes. For alkanes in *n*-heptane, no obvious dependence of the solution enthalpy on alkyl chain length was found with the absolute values of the solution enthalpy being below the uncertainty of determination.

For aliphatic and aromatic compounds, the linear correlation between solvation enthalpy in *n*-heptane and molar refraction of these solutions was observed. Using evaluated linear fitting and the experimental values of solution enthalpies, the formation enthalpies in the condensed state for some classes of organic compounds were determined. The gas phase enthalpies of formation were computed at DLPNO-CCSD(T)/def2-QZVP level of theory. Evaluated values of enthalpies of formation in condensed state at 298.15 K are in good agreement with literature data within 5 %.

Acknowledgements This work has been performed according to Grant No. 14.Y26.31.0019 from Ministry of Education and Science of Russian Federation.

[1] Verevkin, S.P. Pure component phase changes liquid and gas. R.D. Weir, T. De Loos (Eds.), Measurement of the Thermodynamic Properties of Multiple Phases, Elsevier, 2005.

On the Ways of the Fusion Enthalpy Determination below the Melting Temperature

Yagofarov M.I., Solomonov B.N.

Kazan Federal University, Department of Physical Chemistry, Russian Federation

mikhailyago@gmail.com

Fusion enthalpy is one of the key values in thermal analysis. Both fusion enthalpy values at the melting temperature and below this are of interest in chemical thermodynamics. However, its temperature dependence, which is related to the difference of the heat capacities of the liquid and crystal, is generally unavailable due to fast crystallization of liquids below the melting point. A direct way to overcome crystallization of liquids below T_m while measuring the heat capacity is increasing the scanning rates. In the present work the methodology for determination of the heat capacity of deeply supercooled low-molecular-weight organic compounds by fast scanning calorimetry was developed.

Solution calorimetry can be used as an indirect source of information about the fusion enthalpy value at 298.15 K. In the present work the relationship between the fusion enthalpies of aromatic compounds at the melting temperature and the solution enthalpies in benzene at 298.15 K was studied according to Eq. (1):

$$\begin{aligned} \Delta_{\text{soln}} H^{A_i/C_6H_6}(\text{cr}, 298.15 \text{ K}) - \Delta_{\text{soln}} H^{A_i/C_6H_6}(\text{l}, 298.15 \text{ K}) = \\ = \Delta_{\text{cr}}^1 H^{A_i}(T_m) + \int_{T_m}^{298.15} [C_p^{A_i}(\text{l}, T) - C_p^{A_i}(\text{cr}, T)] dT \end{aligned} \quad (1)$$

Where $\Delta_{\text{soln}} H^{A_i/C_6H_6}$ is the enthalpy of solution of compound A_i in benzene, $\Delta_{\text{cr}}^1 H^{A_i}(T_m)$ is the enthalpy of fusion at the melting temperature and $\int_{T_m}^{298.15} [C_p^{A_i}(\text{l}, T) - C_p^{A_i}(\text{cr}, T)] dT$ is a thermal adjustment of the fusion enthalpy to 298.15 K calculated according to Kirchhoff's law.

Analysis of Eq. (1) allowed estimating the $\int_{T_m}^{298.15} [C_p^{A_i}(\text{l}, T) - C_p^{A_i}(\text{cr}, T)] dT$ values for the compounds which cannot be supercooled without crystallization at the currently available cooling rates. It was found that the linear extrapolation of the liquid state heat capacity temperature dependence between 298.15 K and T_m led to the $\int_{T_m}^{298.15} [C_p^{A_i}(\text{l}, T) - C_p^{A_i}(\text{cr}, T)] dT$ agreeing with the difference between $\Delta_{\text{cr}}^1 H^{A_i}(T_m)$ and $\Delta_{\text{soln}} H^{A_i/C_6H_6}$ for 30 compounds. Linearity of $C_p^{A_i}(\text{l}, 298.15 \text{ K} < T < T_m)$ was directly confirmed by fast scanning calorimetry for 5 compounds.

Acknowledgements This work has been supported by Grant No. 14.Y26.31.0019 from Ministry of Education and Science of Russian Federation.

[1] M.I. Yagofarov, R.N. Nagrimanov, B.N. Solomonov, *J. Mol. Liq.* 2018, 256, 58.

[2] M.I. Yagofarov, S.E. Lapuk, T.A. Mukhametzyanov, M.A. Ziganshin, C. Schick, B.N. Solomonov, *Thermochim. Acta*, 2018, 668, 96.

Direct Determination of the Thermodynamic Properties of Melting for Amino Acids

Chua Y.Z.¹, Abdelaziz A.², Zaitsau D.², Held C.², Do H.T.², Schick C.¹

¹University of Rostock, Institute of Physics, Germany;

²University of Rostock, Institute of Chemistry, Germany; ³TU Dortmund University, Department of Biochemical and Chemical Engineering, Germany

yeong.chua@uni-rostock.de

The properties of melting are used for the prediction of solubility of solid compounds. Unfortunately, by using the conventional DSC or adiabatic calorimetry direct determination of the melting enthalpy and melting temperature is often not possible for biological compounds due to the decomposition during the measurement. The apparent activation energy of decomposition is at least one order of magnitude smaller than that of melting. This allows shifting of the decomposition process to higher temperature without seriously disturbing the melting by applying very high heating rates. High scanning rates up to $2 \cdot 10^4 \text{ K} \cdot \text{s}^{-1}$ are utilized with fast-scanning calorimeter Mettler Toledo Flash DSC1, which employs thin film chip sensors with sub $\mu\text{J} \cdot \text{K}^{-1}$ addenda heat capacities. With the help of this technique the melting parameters for a series of amino acids, as well as dipeptides and tripeptides were successfully determined, which the melting temperature of samples (extrapolated to zero heating rate) were determined. The ultra-fast cooling of the melted samples allows the studied compounds to retain in the liquid state and to determine for the first time its glass transition temperatures. The determined glass transition temperatures agree with the Beaman-Kauzmann rule ($T_g \approx 2/3 T_{\text{fus}}$). The correlation between the melting properties of the amino acids, dipeptides and tripeptides with their molecular structures were investigated. The results for melting properties are in reasonable agreement with the simulated PC-SAFT values.

Acknowledgements The financial support of German Research Foundation (DFG CH1922/1-1).

Determination of the Sublimation Vapor Pressure of Thermally Labile Compounds with Fast Scanning Calorimetry

Abdelaziz A.^{1,2}, Zaitsau D.H.^{2,3}, Verevkin S.P.^{2,3}, Schick C.^{1,2,4}

¹Universität Rostock, Institute of Physics, Albert-Einstein-Str. 23-24, 18059 Rostock, Germany

²Universität Rostock, CALOR, Albert-Einstein-Str. 25, 18059 Rostock, Germany

³Universität Rostock, Institute of Chemistry, Dr-Lorenz-Weg 2, 18059 Rostock, Germany

⁴Kazan Federal University, 18 Kremlyovskaya Street, Kazan 420008, Russian Federation

amir.abdelaziz@uni-rostock.de

The determination of vapor pressure and corresponding enthalpy of sublimation lay within focus of many scientific fields and industrial applications. These values directly connected to the intermolecular forces in crystal state, provides the lattice energy and change in ordering by going from crystal to gas phase. In the present study, the fast scanning calorimetry was successfully applied for determination of vapor pressure and enthalpies of sublimation of low volatile organic substances.

In many cases, investigation of thermally labile systems e.g. biomolecules are accomplished with low thermal stability of them and application of classic techniques often fails by determining the decomposition rate of the system. Our technique is based on the determination of the mass loss rate of the sample from the experimental total heat capacity and preliminary determined specific heat capacity of the compound under study. Sublimation of the sample is carried out during repeated isotherms of pre-defined duration and at selected temperatures. Sample is heated to needed temperatures using high heating rates accessible by this technique, which allows reaching the sublimation temperatures without any mass loss during the heating time. From the other side in the proposed technique, the surface to volume ratio of the sample is so high, that sublimation mass loss rate is incomparably higher than decomposition rate. Thus, the sample of a few nano-grams sublimes without any thermal degradation.

Alternative Forms of Conditions of Thermodynamic Stability

Toikka A.M., Gromov D.V.

Saint Petersburg State University, Russia

a.toikka@spbu.ru

The study of thermodynamic stability is one of the main tasks of traditional chemical and non-equilibrium thermodynamics. The stability conditions allow determining the possible values of thermodynamic properties and their changes at the influence of various external forces. The limits of stability determine the disposition of spinodal in thermodynamic space; this statement is of special importance for the tasks of material science. In the lecture the different approaches to the analysis of the thermodynamic stability of multicomponent heterogeneous systems are considered.

The general base of our analysis is a system of thermodynamic inequalities and chains of inequalities for non-reacting and reacting systems under different external conditions. Previously the traditional approach to the analysis of thermodynamic stability will be discussed. Thereafter other variants of formulations of stability conditions will be presented, e.g. some forms of Le Châtelier – Braun principle is considered as an alternative approach. The possibility is discussed to describe different types of physicochemical processes on the base of the generalized concept of affinity. Respective thermodynamic relationships could be considered as special cases of theorems of moderation.

The main point of presentation will be various transformations of the stability matrix that are variants of mathematical formulations of stability conditions. The general form of the stability matrix could be built with the second derivatives of a generalized thermodynamic potential. Such approach gives the opportunity to present stability conditions by the second variations of any thermodynamic potential and demonstrates the equivalence of the use of these potentials (Gibbs and Helmholtz energy, enthalpy, etc.) for estimation stability (some results had been also presented in [1]). It should be mention that in spite the equivalence of thermodynamic potentials is a well-known fact, the discussion of the possibility to apply stability conditions presented by different potentials often meets misunderstanding.

Considering the variants of transformation of the stability matrix, we obtained a new result concerning transformation of the stability matrix that was indicated by Gibbs [2]: the reduction of the stability matrix due to the replacement of variables. As a result the stability matrix presents a product of derivatives. Such transformation has been clearly described in [2] but our approach gives a new view on the properties of stability matrix and opportunities of application of this form of stability conditions (e.g. as equation of spinodal).

The possibility is discussed to use the stability criteria for the characterisation of the non-equilibrium process. Inequalities for the second derivatives of thermodynamic potentials give an opportunity to compare the changes of thermodynamic parameters in equilibrium and non-equilibrium processes. Processes in homogeneous and heterogeneous systems are discussed, including the processes accompanied by the generation of new phases. The interpretation is given for the so-called jumps in the values of the second derivatives of the thermodynamic potentials.

Acknowledgement. This research was supported by the Russian Foundation for Basic Research (grant 19-03-00375).

[1] A. Toikka, in book *Mathematical Chemistry*, 2010, Chapter 11, 509-535. Nova Science Publishers, Inc., NY, USA.

[2] J.W. Gibbs, *The Collected Works. V. 1. Thermodynamics*, 1931. Longmans, Green and Co., NY, London, Toronto.

Nonequilibrium Thermodynamics of Oxidative Recovery Reactions Vanadium Containing Titanomagnetite Concentrates

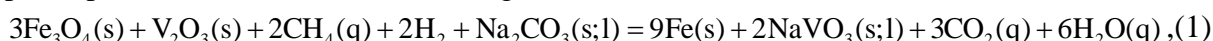
Mammadov A.N.,¹ Sharifova U.N.,¹ Qasimova A.M.,¹ Samedzade Q.M.,¹ Asadov M.M.^{1,2}

¹Nagiyev Institute of Catalysis and Inorganic Chemistry ANAS, Baku, Azerbaijan;

²"Geotechnological Problems of Oil, Gas and Chemistry" SRI. Azerbaijan

asif.mammadov.47@mail.ru

Due to the depletion of reserves of rich magnetite ores, research is developing on the technology of processing titanium-magnetite ores to produce iron, titanium, chromium and vanadium. In [1] a thermodynamic analysis of the reactions of direct reduction of magnetite with methane to free iron and oxidation of vanadium oxide (3) to vanadium oxide (4) and vanadium oxide (5) in granules with fluxed soda vanadist titanomagnetite concentrates was carried out. In this work, equilibrium and non-equilibrium thermodynamic conditions for the reduction of magnetite using a mixture of natural gas and hydrogen are determined. The total oxidation reactions of vanadium oxide (3) and the reduction of magnetite with the participation of soda have the following form:



Titanium dioxide TiO_2 , not involved in the redox process, is not included in the reaction equation. To determine the temperature dependences of the Gibbs free energy of the reaction in the temperature range 500-1400K, the following equation was used:

$$\Delta G_T = \Delta H_{298}^0 - T\Delta S_{298}^0 - \Delta C_{p,298}^0 T[\ln(T/298) + 298/T - 1] - nRT[x\ln x + (1-x)\ln(1-x)] + RT \sum v_i \ln P_i, (2)$$

ΔG_T , ΔH_{298}^0 , ΔS_{298}^0 - free energies, standard enthalpies and entropies of reaction (1), ΔC_{298}^0 - total change in heat capacity of substances, v_i - stoichiometric coefficients, P_i - partial pressures of components in a non-equilibrium state. The fourth term in eq. (2) is the free energy of formation of solid solutions due to the replacement of V^{3+} ions in the Fe_3O_4 crystal cell of Fe^{3+} .

From Fig. 1 it follows that if in a non-equilibrium flow regime with the removal of gaseous products, reaction (1) shifts towards 1145 K in the right direction, then under standard conditions this only happens at 1270 K.

Acknowledgements This work was supported by a grant from the Foundation for the Development of Science of the President of Azerbaijan EIF / MQM / Science and Education-1-2016-1 (26).

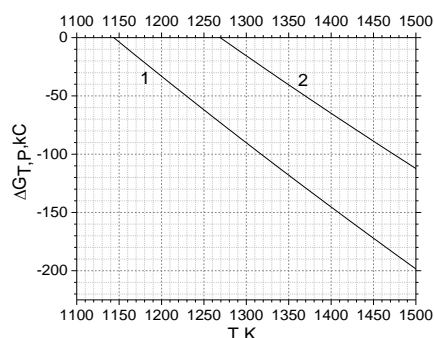


Figure 1. Temperature dependence of the Gibbs energy of reaction (1): 1- in the flow regime of the gas mixture (non-equilibrium state); 2-equilibrium state.

[1] Asif Mammadov, Gunel Pashazade, Afarida Gasymova, Ulviya Sharifova, *Chem. Chem. Technol.*, 2019,N.3

[2] U.N. Sharifova, A.N. Mamedov, A.M. Gasymova, Q.M. Samedzade, *Fundamental'nye issledovaniya*, 2018,N.6, 35 (In Russian).

THURSDAY, 20.06.2019

**SECTION 5: Thermodynamics of Functional Materials
and Engineered Self-Assembly**

Relaxation Processes in Monolayer of Pulmonary Surfactant

Bykov A.G.¹, Loglio G.², Miller R.³, Milyaeva O.Y.¹, Noskov B.A.¹

¹Saint-Petersburg State University, Russian Federation,

²CNR–Istituto per l'Energetica e le Interfasi, Italy,

³MPI fur Kolloid und Grenzflächenforschung, Germany

ag-bikov@mail.ru

The surface elasticity characterizes a dynamic response of monolayer to surface dilation in particular of monolayers of pulmonary surfactant. However, measurements of the dynamic surface elasticity in the systems with extremely low values of the surface tensions a serious experimental problem. It has been shown recently that a modified stress decomposition method can be used for the determination of the dynamic surface elasticity from a non-linear response of highly compressed monolayers [1, 2].

It was shown in this work that the application of the modified stress decomposition method to spread monolayers of DPPC and adsorbed layers of pulmonary surfactants (Curosurf) allowed determination of dilational surface elasticity at extremely low values of surface tension (up to 1 mN/m) [3]. The dilational surface elasticity for these systems was determined at different concentrations of pulmonary surfactants and at different frequencies of surface area oscillations. It was also shown, that the characteristic time of relaxation processes in the surface layer of pulmonary surfactant solutions strongly depended on the temperature due to the transition from liquidlike to solidlike monolayers.

Acknowledgements The work was financially supported by the Russian Science Foundation (project No. 17-73-10171).

[1] A.G. Bykov, L. Liggieri, B.A. Noskov, P. Pandolfini, F. Ravera, G. Loglio, *Adv. Colloid and Interface Science*, 2015, 222, 110.

[2] A.G. Bykov, G. Loglio, F. Ravera, L. Liggieri, R. Miller, B.A. Noskov, *Col. Surf. A*, 2018, 532, 238.

[3] A.G. Bykov, B.A. Noskov, *Colloid Journal*, 2018, 5, 467.

Tammann's Nuclei Development Approach in Crystallization of Macromolecules

Schick C.^{1,2}, Andrianov R.², Mukhametzyanov T.², Androsch R.³

¹Institute of Physics and Competence Center CALOR, University of Rostock, Albert-Einstein-Str. 23-24, 18051 Rostock, Germany

²Kazan Federal University, 18 Kremlyovskaya street, Kazan 420008, Russian Federation

³Center of Engineering Sciences, Martin Luther University Halle-Wittenberg, 06099 Halle/Saale, Germany

Christoph.schick@uni-rostock.de

Poly(lactic acid) has been cooled from the molten state to obtain glasses free of crystals and homogeneous crystal nuclei. The kinetics of enthalpy relaxation and the formation of homogeneous crystal nuclei have then been analyzed using fast scanning chip calorimetry [1]. Formation of homogeneous crystal nuclei in the glassy state requires the completion of the relaxation of the glass [1,2]. Once formed crystal nuclei accelerate crystallization at the growth stage up to unexpected high temperatures [3]. Furthermore, the data show that the slower formation of homogeneous crystal nuclei in random L/D lactide copolymers is not caused by different chain segment mobility in the glassy state but by the segregation of chain defects in this very early stage of the crystallization process [4].

Acknowledgements The financial support from the Ministry of Education and Science of the Russian Federation, grant 14.Y26.31.0019, is acknowledged.

References

- [1] E. Zhuravlev, et al., *Polymer* **52** 1983 (2011).
- [2] R. Androsch, et al., *Europ. Polym. J.* **53** 100 (2014).
- [3] E. Zhuravlev, et al., *Crystal Growth & Design* **15** 786 (2015).
- [4] R. Androsch, and C. Schick, *J. Phys. Chem. B* **120** 4522 (2016).

The Influence of Structural Factors on the Spectral Properties and Prospects of Application of Bis(BODIPY) Luminophors

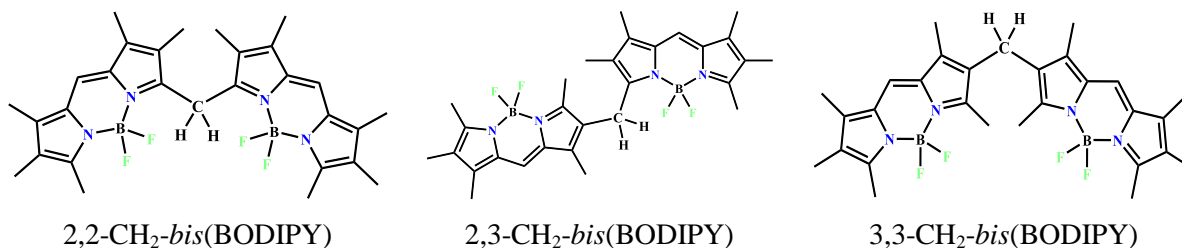
Antina L.A., Ksenofontov A.A, Kalyagin A.A., Antina E.V., Berezin M.B., Dyshin A.A.

G.A. Krestov Institute of Solution Chemistry of the Russian Academy of Sciences, Russia

lyubov.antina@mail.ru

BF₂-*bis*(dipyrromethene) complexes (BODIPY) are promising luminophors for practical application in various industries: laser technology, biochemistry and medicine. Therefore, the design and research of new BODIPY-structures with a set of optimal properties for specific practical tasks are extremely relevant. The key task is to establish the relationship of the BODIPY dyes spectral characteristics and chemical activity with their molecular structure and the nature of the solvate medium. To date, the oligomeric analogs with two or more BODIPY domains are of particular interest.

The synthesis and spectral properties of three new dimeric *bis*(BODIPY)s are presented in this report. They are formed by two fragments of methylated BF₂-dipyrromethene complexes (BODIPY), which are connected by the methylene bridge to the 2,2'-, 2,3'- or 3,3'-positions of proximal pyrroles. Their spectral properties were studied in various nature solvents and polymer films. All synthesized luminophores show a high fluorescence characteristics sensitivity to the media nature. The fluorescence quantum yield (ϕ) values change from 99% in nonpolar and aromatic solvents to 1% in polar proton-donor, electron-donor medium. It is not typical for the most known BODIPY.



A thorough quantum-chemical analysis of the structural, conformational and spectral characteristics of 2,2-, 2,3- and 3,3-CH₂-*bis*(BODIPY)s was carried out. The results showed that the (BODIPY)s have conformational invariance. The electronic absorption and fluorescence spectra of 2,2-CH₂-*bis*(BODIPY) are differ from others *bis*(BODIPY) by the presence of additional absorption and emission bands. It is caused by the presence in the solutions of equilibrium mixture of two stable 2,2-CH₂-*bis*(BODIPY) conformations with different spectral characteristics.

The results of the first studies on the preparation of *bis*(BODIPY)s supramolecular complexes with steroid hormones (hydrocortisol and analogues) are presented in the report.

The first data on the preparation of new phosphor materials based on single-walled carbon nanotubes and *bis*(BODIPY)s with the extended range of the absorption and emission spectra (from the visible to the infrared) are discussed.

Acknowledgements The financial support of Russian Foundation for Basic Research (RFBR), project no. 18-29-06008 mk (composites with carbon nanotubes); Russian Foundation for Basic Research (RFBR), project no. 18-33-20218 mol_a_ved (synthesis)

Molecular Thermodynamic Modeling of Stomatosomes and Flat Perforated Bilayers in Surfactant Mixtures

Emelianova K.A., Sorina P.O., Victorov A.I.

St. Petersburg State University, Russia

noctua94@gmail.com

Holes in bilayers are common in nature: pores are formed in cell membranes providing ionic transport or leading to necrosis [1]. Perforated bilayer structures spontaneously self-assemble in a diversity of amphiphilic solutions including lipids, block-copolymers, surfactants and their mixtures [1 – 4]. Although perforated unilamellar vesicles are promising in micellar catalysis, drug delivery and oil recovery, there is still no explicit theory of pore formation in bilayers. Moreover, in dilute amphiphilic solutions, where perforated bilayer structures are known to occur, there are often several types of coexisting aggregates which are energetically close to each other. A reliable theory is yet awaited for predicting the preferable aggregate morphology that responds to minute changes in temperature, solution salinity or pH.

Here we extend a classical molecular thermodynamic model [5, 6] to perforated vesicles using our previous results for flat perforated lamellae [7] in aqueous salt mixed surfactant solution. We provide a mechanism of formation of a pore with toroidal rim in unilamellar vesicles and determine experimental conditions (salinity, ratio of components and temperature) which are necessary to its stabilization. The dependence on surfactant molecular parameters is described by the model. The obtained theoretical results are in agreement with available experimental data for cationic mixture [3].

Acknowledgements The financial support of Russian Foundation for Basic Research (project # 18-03-00698)

[1] P. Zavala-Rivera, K. Channon, V. Nguyen et al. *Nature Materials*, 2012, 11, 53.

[2] M. Almgren. *Soft Matter*, 2010, 6, 1383.

[3] L.M. Bergström, S. Skoglund, K. Edwards et al. *Langmuir*, 2014, 30, 3928.

[4] H.V. Berlepsch, B.N.S. Thota, M. Wyszogrodzka et al. *Soft Matter*, 2008, 25, 5256.

[5] Self -Assembly: From Surfactants to Nanoparticles, Ed. Nagarajan R., 2019, Wiley&Sons, 353 P.

[6] P.K. Yuet, D. Blankshtein, *Langmuir*, 12, 1996, 3802.

[7] K.A. Emelianova, A.I. Victorov, *PCCP*, 20, 2018, 27924.

Effect of Dialkylsulfoxides on the Thermal Denaturation of DNA

Markarian S.A.

Department of Chemistry, Yerevan State University, 0025 Yerevan, Armenia

shmarkar@ysu.am

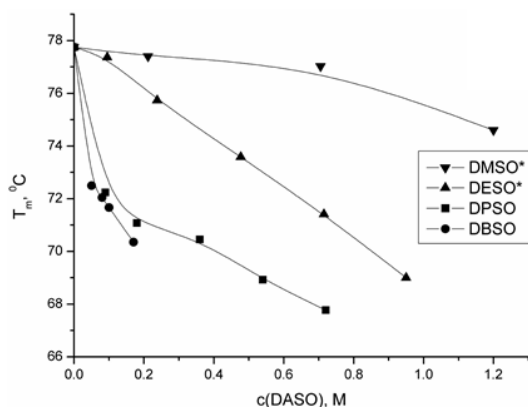
In our earlier works it was shown that not only dimethylsulphoxide (DMSO), but also the other nearest homologues such as diethylsulphoxide (DESO), dipropylsulfoxide (DPSO) and dibutylsulfoxide (DBSO) have biomedical significance, in some cases even are more pronounced compare with DMSO [1,2].

DNA thermal denaturation has been investigated in aqueous solutions of DMSO, DESO, DPSO and DBSO using UV-vis spectroscopy and density measurements. It is suggested that, on the one hand, the structural change of entire solutions and, on the other hand, a direct interaction of DESO with DNA are responsible for the observed peculiar behavior. The results obtained were compared with those of DMSO, also known from literature.

The dependence of the melting temperature of DNA (T_m) as a function of sulfoxide concentration is presented in figure:

It is concluded that the lowering of the transition enthalpy (Table) with increasing length of the carbon chain of the dialkylsulfoxides due to significance contribution of hydrophobic interactions.

The melting temperatures, T_m and van't Hoff enthalpies, of DNA denaturation in the presence of DASO



The melting temperature of DNA as a function of sulfoxide concentration

	C_{DASO} , M	T_m , °C	$\Delta H_{\text{vH}} = 6RT_m^2 \left(\frac{\partial \alpha}{\partial T} \right)_{T=T_m}$ kJ/mol
DMSO	0.7	71.77	451.1
	2.1	59.80	293.1
DESO	0.7	67.83	336.4
	2.0	55.90	280.8
DPSO	0.18	71.08	455.1
	0.72	67.77	347.8
DBSO	0.10	71.67	314.4
	0.17	70.35	268.9

- [1] S. Markarian, A. Asatryan, K. Grigoryan, H. Sargsyan, *Biopolymers*, 2006, 82, 1.
 [2] M. Aznauryan, S. Markarian, *J. Solution Chem.*, 2010, 39, 43.

Effect of Acidity and Chloride Addition on Phase Equilibria in Aqueous Two-Phase System Peg-1500-Sodium Sulfate

Kuznetsov V.N.¹, Milevskii N.A.², Kabanova E.G.¹

¹Chemical Department, Moscow Lomonosov State University, Russia;

²High Chemical College, D. Mendeleev University of Chemical Technology, Russia.

vnk@general.chem.msu.ru

The aqueous two-phase systems (ATPS) are widely used for the separation and concentration of both organic substances and metals. These systems are of interest in terms of potential applications for extraction of platinum group metals. That is carried out at high acidity in the presence of chloride ions. The influence of acidity and of the concentration of Cl^- ions on phase equilibria in ATPS water–[polyethyleneglycole with $M = 1500$ (PEG-1500)]– Na_2SO_4 is studied at 25 °C.

Position of the binodal line was determined using turbidimetric titration of stock solution of PEG by solution of Na_2SO_4 or *vice versa*. Both solutions contained identical concentrations of acid (HCl or H_2SO_4) and of NaCl. Some tie-lines were determined using refractometric and physico-chemical analyses of compositions of coexisting phases.

Correlation of the binodal data was performed by empirical formula suggested by Merchuk *et al.* [1] using mas.% of PEG-1500 and of Na_2SO_4 as working coordinates, whereas HCl (H_2SO_4) and NaCl are considered as extra components (in addition to water) of the solvent with fixed concentrations. The example of the correlation is presented on Fig. 1.

The increase of the concentration of sodium chloride widens the heterogeneous region in ATPS studied. The same effect was reported for the water–PEG-8000–sodium sulphate system at $\text{pH} = 7$ [2]. The effect of acidity on phase equilibria in ATPS is reverse: the addition of HCl increases the mutual solubility of the PEG and Na_2SO_4 .

The influence of concentration of HCl proved to be much stronger than that of concentration of Cl^- ions. Replacement of HCl with an equivalent amount of H_2SO_4 weakens the influence of acidity on the position of binodale line.

For the thermodynamic analysis of the data obtained (including the position of the tie-lines) the modified Pitzer model [3] was tested.

Acknowledgements. The paper was prepared as part of the project of the Russian Foundation for Basic Research 18-03-01171.

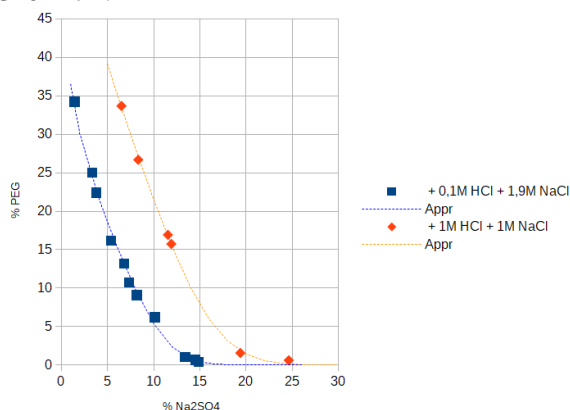


Figure 1. Dependence of binodal on $C(\text{HCl})$ at fixed $C(\text{Cl}^-) = 2 \text{ mol l}^{-1}$.

[1] J. Merchuk, B. Andrews, J. Asenio, *J. Chromatogr. B*, 1998, **711**, 285.

[2] L.A. Ferreira, J.A. Teixeira, L.M. Mikheeva. *J. Chromatogr. A*, 2011, **1218**, 5031.

[3] Y.-T. Wu, D.-Q. Lin, Z.-Q. Zhu, L.-H. Mei, *Fluid Phase Equilibria*, 1996, **124**, 67.

Polydopamine Films: the Dynamic Surface Rheology Study

Milyaeva O.Yu.

Department of Colloid Chemistry, St. Petersburg State University, St. Petersburg, Russia

o.milyaeva@spbu.ru

Poly(dopamine) has attracted interest recently as a universal surface modification agent in a broad range of biotechnological, electrochemical and nanotechnological applications [1]. One of the most common way of the polydopamine synthesis is dopamine oxidation in its solution. Dopamine hydrochloride is easily oxidized and undergoes spontaneous polymerization in a slightly alkaline environment. Oxygen from the air acts as an oxidant. The reaction proceeds spontaneously under mild conditions. Polymerization leads to changes of the solution color from almost colorless through light brown to dark brown. The polymer film is formed on the surface and polymer grains are formed in the bulk. The dynamic surface properties of polymer film at the air-water interface during formation were studied by the dilatational surface rheology, ellipsometry and Brewster angle microscopy (BAM). The dynamic surface elasticity was measured as function of time and concentration by the oscillation ring method. It was shown that there is a significant increase of the elasticity for solutions with concentration from 0.75 g/l to 2 g/l. The highest values of the dynamic surface elasticity (~ 60 mN/m) were obtained for solutions with concentration of 1 g/l. These values are comparable with those for solutions of globular proteins [2] indicating that the film consists of separate domains. The high surface elasticity is due to the interactions of relatively rigid domains of the polymer film. This assumption is proved by BAM images (fig.1). One can see different steps of the growth of the film: first. The heterogeneity of the film increases gradually at the approach to equilibrium. The higher the initial concentration is, faster the polymerization takes place and the thicker film is formed. The dynamic surface elasticity decreases for dopamine solutions of 2 g/l and 5 g/l. For these solutions the thickness of the polymer film reaches about 80 nm. In this case the film could break under its own weight. The cracks in the film lead to impairment of mechanical properties of the layer.

Acknowledgements. The financial support of Russian Science Foundation (project № 18-73-00108) is acknowledged.

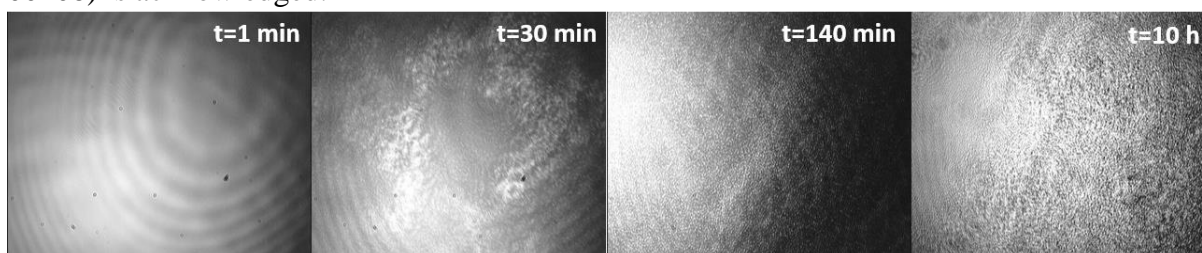


Figure 1. BAM images of polydopamine film formation from dopamine hydrochloride solution.

[1] Y. Liu, K. Ai, L. Lu, *Chem. Rev.*, 2014, 114, 5057.

[2] B.A. Noskov, *Curr. Opin. Colloid Interface Sci.*, 2010, 15, 229.

THURSDAY, 20.06.2019

PLENARY SESSION

Possibility of Pressure Crossover Prediction by Classical DFT for Sparingly Dissolved Compounds in Supercritical Carbon Dioxide

Kiselev M.G.¹, Budkov Y.A.^{1,2}, Ivlev D.V.¹, Kolesnikov A.³, Kalikin N.N.¹

¹Institute of Solution Chemistry of the RAS, Russia,

²Tikhonov Moscow Institute of Electronics and Mathematics, School of Applied Mathematics,
National Research University Higher School of Economics, Russia,

³Institut für Nichtklassische Chemie e.V., Germany

mgk@isc-ras.ru

Keywords: solubility, supercritical carbon dioxide

A new method of solubility calculations, applied for sparingly dissolved compounds in supercritical carbon dioxide will be introduced in this report. The method is based on determination of solubility contributions along of thermodynamic path consisting of sublimation and solvation processes. The contribution of sublimation process takes from experiment, while the free energy of solvation calculates from the classical density functional theory based on the fundamental measure theory. The parameterization of potential was performed using the procedure of Weeks-Chandler-Anderson, where Lennard-Jones parameters were obtained from thermodynamics data of solute critical point. As one could expect, the solubility values as calculated from that methodology are underestimated as far as Coulomb interactions does not account within classical DFT, however that underestimation is not significant. On the other hand, the prediction of pressure crossover is very close those obtained from experiment. Therefore, the introduced methodology might be a good instrument for prediction of solubility of sparingly dissolved compounds in scCO₂ near the critical point. There are two advantages of DFT method for calculation of solvation free energy. First, the classical DFT does not claim extended computer calculations, thus one can easily calculate solvation free energy over wide region of phase diagram. Second, the pressure crossover prediction as it is obtained from DFT calculations is pretty close to experiment and MD simulation. It is found to be, that within the region of pressure crossover, the solute partial isothermal compressibility is negative and crossing zero at points of lower and upper crossovers. This observation may give a clue for understanding of physical mechanism of the pressure crossover phenomenon.

Mixing two Neat Liquids in Computer Simulation: Free Energy Calculation and Local Structure Analysis

Jedlovsky P.¹, Fábán B.,² Kiss B.,³ Szóri M.,³ and Idrissi A.⁴

¹Department of Chemistry, Eszterházy Károly University, Leányka u. 6, H-3300 Eger, Hungary, email: jedlovsky.pal@uni-eszterhazy.hu

²Department of Inorganic and Analytical Chemistry, Budapest University of Technology and Economics, Szt Gellért tér 3, H-1111 Budapest, Hungary

³Institute of Chemistry, University of Miskolc, Egyetemváros A/2, H-3515 Miskolc, Hungary

⁴LASIR, University of Lille, Faculty of Sciences and Technologies, 59655 Villeneuve d'Ascq Cedex, France

abdenacer.idrissi@univ-lille.fr

The free energy of mixing two components is a key physical-chemical quantity, because its sign determines whether the components mix or demix at a given molar ratio. In cases when the mixing of the two components in computer simulation is accompanied by a slight increase of the free energy, demixing might not visibly occur on the simulation time and length scales. [1] Detection of such demixing is also hindered by the use of periodic boundary conditions. Further, besides the qualitative description of the mixing of the components, good reproduction of the experimental free energy of mixing in computer simulation is a prerequisite of the accurate description of the microscopic structure (e.g., in terms of self-association) of the mixture. On the other hand, the calculation of the free energy of mixing is computationally rather costly, because the Helmholtz free energy is related to the entire phase space on the canonical ensemble, and hence it cannot simply be calculated by sampling its lowest energy domains. To calculate the free energy of mixing we proposed the following thermodynamic path. [2] First, the neat components are brought to the ideal gas state. The change of the Helmholtz free energy in this step can be calculated by the method of thermodynamic integration. [3] In the second step, the two neat components are mixed in the ideal gas state. The change of the Helmholtz free energy in this step can simply be given as the corresponding change of the ideal mixing. Finally, in the third step the mixture is brought back from the ideal gas to the liquid state; the change of the thermodynamic quantities accompanying this step can be calculated just as in the first step.

In this talk the technical issues of such calculations are discussed, and its application is presented for several systems in which the free energy of mixing, resulted from a subtle interplay of the energetic and entropic terms, deviates only slightly from zero. Examples are shown for mixtures in which the miscibility is energy- or entropy-driven, and where the mixing is close to ideal. Consequences of the origin (i.e., energetic vs. entropic) of the miscibility on the local structure is discussed; it is shown that microheterogeneous structure occurs in cases of entropy-driven miscibility, when the energetic factor acts against the mixing of the two components. The free energy results are complemented with local structure analysis data, obtained from Voronoi polyhedra analysis; the use of the Voronoi method in characterizing the local structure of these binary mixtures and its relation with the origin of their miscibility is also demonstrated.

REFERENCES

- [1] P. Jedlovsky, A. Idrissi, and G. Jancsó, "Can existing models qualitatively describe the mixing behavior of acetone-water mixtures?" *J. Chem. Phys.* 130, 124516-1-7 (2009)
- [2] M. Darvas, G. Jancsó, and P. Jedlovsky "Free Energy of Mixing of Pyridine and Its Methyl-Substituted Derivatives with Water, As Seen from Computer Simulations.", *J. Phys. Chem. B* 113, 7615-7620 (2009).
- [3] M. Mezei and D. L. Beveridge, "Free Energy Simulations." *Ann. Acad. Sci. NY* 482, 1-23 (1986).

Innovations in Thermal Analysis – the New Flash DSC 2+

Flachsmann B., Schawe J.E.K.

Mettler Toledo GmbH, Heuwinkelstr. 3, 8606 Nänikon, Switzerland

beat.flachsmann@mt.com

Keywords: Innovations, Flash DSC 2+, STAR^e-software

METTLER TOLEDO is a global manufacturer and marketer of precision instruments for use in laboratory, industrial and food retailing applications. The products and services are available worldwide in over one hundred countries. With more than 10,000 employees, most of them in sales, service and development, Mettler Toledo guarantees customers unique products and support of very high quality.

Thermal analysis has played an important role in METTLER TOLEDO since the early 1960s. The first commercially available TGA/DTA System, the TA1 was available in 1964. Since the beginning, we have offered innovative Thermal Analysis solutions, products, services and software.

Introducing the Flash DSC 1 in 2011, fast scanning calorimetry was revolutionized. In 2018, the new Flash DSC 2 + which allows an even higher temperature range (-95 to 1000 °C) and faster scanning rates (6 to 50,000 K/s) than the Flash DSC 1, was introduced. New measurement possibilities of this instrument will be shown.

Thermal analysis STAR^e-software provides unrivalled flexibility and unlimited evaluation possibilities for example with the reference library, quality control or data integrity software options. The reference library option allows to organize and store any type of sample information in a centralized location and three different search functions to identify thermal analysis data. Using the quality control option, it is possible to create a statistic template, perform a statistic evaluation and make a trend analysis. The latest software option data integrity allows to easily organize data for different users and define user rights.

References

1. L J.E.K. Schawe, The revolutionary Flash DSC 1: maximum performance for metastable materials UserCom 32

FRIDAY, 21.06.2019

PLENARY SESSION

Modified Poisson-Boltzmann Equations with Explicit Account of Polarizable Impurities in the Context of Electric Double Layer Theory

Budkov Y.A.^{1,2}, *Kolesnikov A.L.*³, *Kiselev M.G.*²

¹National Research University Higher School of Economics, School of Applied Mathematics, Moscow, Russia;

²G.A. Krestov Institute of Solution Chemistry of the Russian Academy of Science, Ivanovo, Russia

³Institut für Nichtklassische Chemie e.V. (INC), Leipzig, Germany

ybudkov@hse.ru

The Poisson-Boltzmann (PB) equation is the simplest and very efficient tool for describing distribution of charged particles near the macroscopic charged surfaces in many areas, such as electrochemistry, chemical engineering, biophysics, *etc* [1]. Firstly, the mean-field PB theory itself does not allow us to take into account the effects of the ionic correlations that are very important for medium and high concentrated electrolyte solutions. Secondly, considering the solvent as a continuous dielectric medium makes it impossible to study the effects of the solvent molecular structure. These two factors have motivated the researchers to improve the PB equation in the last two decades [2]. In present report a review our recent theoretical results [3 – 5] on the formulation of the modified PB equations for electrolyte solutions and ionic liquids with a small additives of polarizable molecules (impurities) will be presented. Application of the obtained self-consistent field equations to the theory of electric double layer will be demonstrated. The effects of polarizability and permanent dipole moment of impurity molecules and their concentration in the bulk on the differential capacitance of electric double layer will be discussed and analyzed.

[1] Jacob N. Israelachvili, *Intermolecular and surface forces*, 2011 Academic Press.

[2] Naji A., Kanduc M., Forsman J., Podgornik R. *J. Chem. Phys.*, 2013, 139, 150901

[3] Budkov Yu.A., Kolesnikov A.L., Kiselev M.G *EPL*, 2015, 111, 28002

[4] Budkov Yu.A., Kolesnikov A.L., Kiselev M.G *J. Chem. Phys.*, 2016, 144, 184703

[5] Budkov Yu.A., et al. *Electrochim. Acta* 2018, 284, 346

Theory for Systems with Spontaneous Inhomogeneities on a Mesoscopic Length Scale

Ciach A.

Institute of Physical Chemistry, Polish Academy of Sciences, 01-224 Warszawa, Poland

aciach@ichf.edu.pl

The low-T part of the phase diagram in self-assembling systems is correctly predicted by the known versions of the density functional theory (DFT). The high-T part obtained in DFT, however, does not agree with simulations even on the qualitative level (Fig.1). In this work a new version of the DFT is developed. The contribution to the grand thermodynamic potential associated with mesoscopic fluctuations is explicitly taken into account. The expression for this contribution is obtained by the methods known from the Brazovskii field theory. In addition, we develop a simplified version of the theory valid for weakly ordered phases, i.e. for the high -T part of the phase diagram. The simplified theory is verified by a comparison with the results of simulations for a particular version of the short-range attraction long-range repulsion (SALR) interaction potential. Except from the fact that in our theory the ordered phases are stable at lower T than in simulations, a good agreement for the high-T part of the phase diagram is obtained for the range of density that was considered in simulations. In addition, the equation of state and compressibility isotherms are presented. Finally, the physical interpretation of the fluctuation-contribution to the grand potential is discussed in detail.

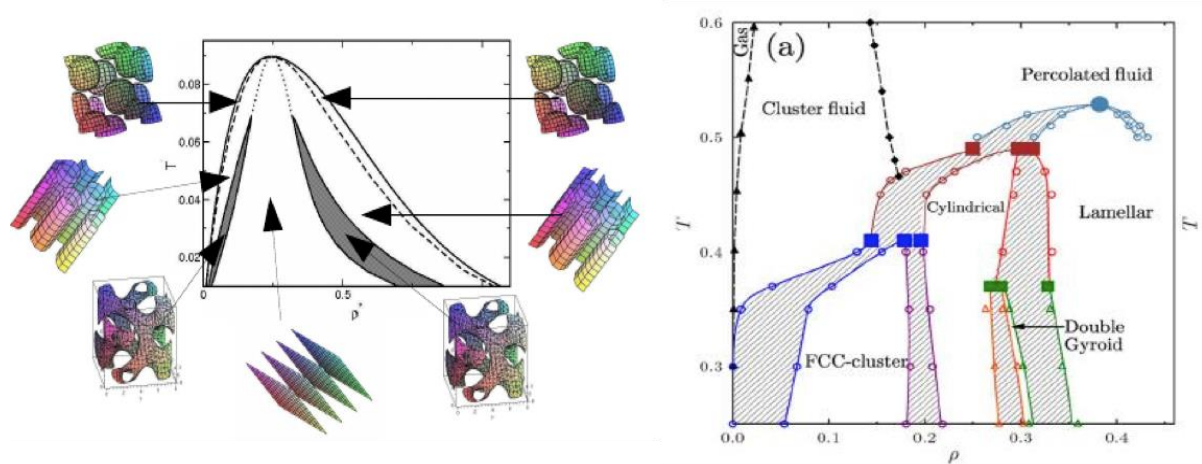


Fig.1 . Density-temperature phase diagram of the SALR system obtained in mean-field approximation (left) and in simulations (right). Cartoons surrounding the right figure represent the stable structures. Inside the surfaces, the droplets or bubbles are present for low or high average density, respectively.

Conformational Control of Polyelectrolyte Chains by Electric Field: from Field-Operated Collapse to Nano-Actuators

Brilliantov N.V.^{1,2}

¹Department of Mathematics, University of Leicester, Leicester LE1 7RH, United Kingdom;

²Skolkovo Institute of Science and Technology, Moscow, Russia

nb144@leicester.ac.uk

Conformation behaviour of a single polyelectrolyte (PE) chain in external electric field is studied theoretically and numerically. We investigate the globular-stretched conformational transition of a chain, induced by the field and the dependence on the field of the dimension of a chain under an external load. We start from salt-free dilute polyelectrolyte solutions and analyse the dependence of the gyration radius of a chain on the strength of electrostatic interactions, counterion charge and properties of the solvent without an external field [1]. We find the parameters of the field-free electrostatic collapse of a PE chain. Then we consider the action of the external field on the collapsed state of the chain and analyse the dependence of the threshold electric field that causes the globular-stretched transition on the systems parameters. Next, a setup based on a polyelectrolyte chain, grafted on a charged plane, under an action of external mechanical force is studied; the force acts at the non-grafted chain end [2, 3]. We investigate the conformation behaviour of the chain in response to the external field, the magnitude of the external force and properties of the solvent, including concentration of salt ions. Two different systems are analysed – with a constant external force and with a force, arising in a deformable target body, linked to the polyelectrolyte chain. In the latter case the magnitude of the force is determined by the elastic properties of the target body. Our theoretical findings are in a good agreement with the results of Molecular Dynamics simulations. Possible applications of the setup for polyelectrolyte-based nano-devices (nano-actuators, nano-mixers, nano-pumps, etc.), operated by an external electric field is discussed [4].

[1] A.M. Tom, S. Vemparala, R. Rajesh, and N.V. Brilliantov, *Phys. Rev. Lett.*, 2016, 117, 147801; *Soft Matter*, 2017, 13, 1862.

[2] N.V. Brilliantov, Yu. A. Budkov and C. Seidel, *Faraday Discussion*, 2017, 199, 487.

[3] N.V. Brilliantov, Yu. A. Budkov and C. Seidel, *Phys. Rev. E*, 2016, 93, 032505.

[4] C. Seidel, Yu. A. Budkov and N.V. Brilliantov, *J. Nanoengineering and Nanosystems*, 2013, 227, 142

FRIDAY, 21.06.2019

**SECTION 2:: Thermodynamics of Liquids, Fluid
Mixtures, and Phase Equilibria**

Comparison of Thermodynamic Properties in the Gd_2O_3 - ZrO_2 - HfO_2 , Sm_2O_3 - ZrO_2 - HfO_2 and Sm_2O_3 - Y_2O_3 - HfO_2 Systems at High Temperatures

Stolyarova V.L., Vorozhtcov V.A., Lopatin S.I.

Saint Petersburg State University, Russia

v.stolyarova@spbu.ru

Study of ternary systems containing hafnia is urgent for development of aircraft and aerospace engineering, which requires increase of performance capacities of the materials used at high temperatures. The Gd_2O_3 - ZrO_2 - HfO_2 , Sm_2O_3 - ZrO_2 - HfO_2 and Sm_2O_3 - Y_2O_3 - HfO_2 systems are promising for production of a wide spectrum of refractory ceramics, such as thermal barrier coatings and casting molds for gas turbine engine blades, since substitution of zirconia by hafnia in traditionally applied ZrO_2 -based materials allows their working temperature ranges to be increased significantly. However, at high temperatures of synthesis or application of refractory materials vaporization of the volatile components may take place. This may lead to alteration of physicochemical properties of high temperature ceramics during exploitation, which justifies the importance of study of vaporization properties and thermodynamic properties in the systems under consideration.

The comparison of thermodynamic properties in the Gd_2O_3 - ZrO_2 - HfO_2 , Sm_2O_3 - ZrO_2 - HfO_2 and Sm_2O_3 - Y_2O_3 - HfO_2 systems as well as the corresponding earlier obtained data in the Gd_2O_3 - Y_2O_3 - HfO_2 and La_2O_3 - Y_2O_3 - HfO_2 systems [1, 2] found by high temperature mass spectrometric method. It was done for the samples with the same molar relative ratio of Gd_2O_3 (Sm_2O_3 , La_2O_3): ZrO_2 (Y_2O_3): HfO_2 . The vaporization processes and thermodynamic properties of the ceramics based on the Gd_2O_3 - ZrO_2 - HfO_2 , Sm_2O_3 - ZrO_2 - HfO_2 and Sm_2O_3 - Y_2O_3 - HfO_2 systems were studied by the high temperature mass spectrometric method as described earlier in the case of the Gd_2O_3 - Y_2O_3 - HfO_2 system [1]. Identification of the gaseous phase and determination of partial pressures of vapor species in these systems were carried out for the first time at high temperatures. Consideration of the vapor phase-condensed phase equilibria for the samples under study led to determination of the thermodynamic properties in the Gd_2O_3 - ZrO_2 - HfO_2 , Sm_2O_3 - ZrO_2 - HfO_2 and Sm_2O_3 - Y_2O_3 - HfO_2 systems, such as the component activities, excess Gibbs energies and Gibbs energies of mixing. Thermodynamic data found in these systems were discussed using acid-base concept of vaporization of oxide systems considered in details in [3]. This approach allows to predict and to identify the ternary hafnia-containing system as the most suitable for development of refractory materials [4]. The results obtained in the present study enable one to choose the optimal compositions of ceramics for production of thermal barrier coatings with enhanced performance capacities, to find the least volatile concentration ranges in the systems studied for development of synthetic and application routes of the refractory materials and to derive the comprehensive thermodynamic description of the systems using various model approaches.

Acknowledgements The financial support of the present study was carried out by the Russian Foundation for Basic Research according to Project No. 19-03-00721.

[1] E.N. Kablov, et al., *Rapid Commun. Mass Spectrom.*, 2017, 31, 1137.

[2] E.N. Kablov, V.L. Stolyarova, S.I. Lopatin, V.A. Vorozhtcov, O.B. Fabrichnaya, M.O. Ilatovskaya and F.N. Karachevtsev, *Rapid Commun. Mass Spectrom.*, 2018, 32, 686.

[3] V.L. Stolyarova and G.A. Semenov, *Mass spectrometric study of the vaporization of oxide systems*, 1994, 494, Wiley&Sons, Chichester, Great Britain.

[4] V.L. Stolyarova, V.A. Vorozhtcov and S.I. Lopatin, *Trudy Kolyskogo Nauchnogo Tcentra RAN*, 2018, 9, 104

Experimental Study of the Slag/Matte/Spinel/Gas Equilibria in the “Cu₂O”-“FeO”-SiO₂-S-Al₂O₃-MgO-CaO System

Sineva S.^{1,2}, Shichin D.¹, Shevchenko M.¹, Hayes P.C.¹, Jak E.¹

¹PYROSEARCH, The University of Queensland, Brisbane, QLD, 4072, Australia;
²LLC Gipronickel Institute, Laboratory of Pyrometallurgy, St. Petersburg, 195220, Russia

svetlana.sinyova@gmail.com

Optimization of the metallurgical primary and recycling operations needs accurate and reliable information on high temperature chemistry of increasingly complex slag/matte/metal/gas systems. The lack of data and reliable models exists due to difficulties in high temperature experiments and thermodynamic modeling. The authors of the project are continuously developing the integrated experimental and modeling research program for non-ferrous smelting and recycling systems. This program allows accurate determination of phase equilibria in complex systems at high temperatures and different gas atmospheres. Experimental and modeling studies are focused on the phase equilibria in “Cu₂O”-“FeO”-SiO₂-S multicomponent system with Al₂O₃, MgO and CaO slagging elements. The experiments involve high temperature equilibration in controlled gas atmospheres, rapid quenching and direct measurement of equilibrium phase compositions with quantitative microanalytical techniques including electron probe X-ray microanalysis and Laser Ablation ICP-MS. The thermodynamic modelling is undertaken using computer package FactSage with the quasi-chemical model for the liquid slag phase and other advanced models.

The current research is devoted to the improvement of the precision and accuracy of the results, obtained with the applying of experimental technique. Significant advances have been achieved through continuous developments of experimental methodologies [1 – 3]. Systematic analysis of all experimental steps including preparation of the initial mixture, achievement of equilibrium at desired conditions, quenching, EPMA uncertainties, etc. is done. Systematic analysis enables to identify a number of possible sources of uncertainties and to develop the ways to mitigate those shortcomings.

Achievement of equilibrium is the most important and common uncertainty in the phase equilibria studies. The key four-test approach is applied to ensure the achievement of equilibrium state. It will be discussed in details during the conference.

The equilibration/quenching/microanalysis approach will be discussed applying to phase equilibria in the “Cu₂O”-“FeO”-SiO₂-S-Al₂O₃-MgO-CaO system at different conditions.

[1] E.Jak, Integrated experimental and thermodynamic modelling research methodology for copper and other metallurgical slags, Keynote Invited Lecture, MOLTEN 12, The 9th int. conf. on molten slags, fluxes and salts, Beijing, China, May 2012, paper w77

[2] A. Fallah-Mehrjardi T. Hidayat., P.C. Hayes, E. Jak. Experimental Investigation of Gas/Slag/Matte/ Tridymite equilibria in the Cu-Fe-O-S-Si system in Controlled Atmospheres: Development of Technique, Metall. Mater. Trans. B, 48 (6), 3002-3012 (2017)

[3] T. Hidayat, A. Fallah-Mehrjardi, P.C. Hayes, E. Jak, Experimental Investigation of Gas/Slag/Matte/Spinel Equilibria in the Cu-Fe-O-S-Si System at T=1250 °C and P(SO₂)=0.25 atm, Metall. Mater. Trans. B, 49(4), 1732-1739 (2018)

Liquid-Liquid Equilibria for Separation of Alcohols from Esters Using Deep Eutectic Solvents Based on Choline Chloride: Experimental and PC-SAFT Modeling

Samarov A.¹, Prikhodko I.¹, Shner N.¹, Sadowski G.², Held C.², Toikka A.¹

¹Saint Petersburg State University, Russia;

²Technical University of Dortmund, Germany

n.kuzmintseva@mail.ru

In recent years, more attention is paid to the issues of «green chemistry». One of new potentially environment-friendly solvents is deep eutectic solvents (DESs). DES is a mixture consisting of a hydrogen bond donor and a hydrogen bond acceptor. Upon mixing, it forms a liquid with a substantially lower melting point than the individual components. DES has several advantages over traditional ionic liquids (ILs): the ease of preparation and availability of relatively inexpensive components. This allows production of DES at relatively low cost compared to conventional ILs and further allows large-scale applications. The systems including DESs reveal complex intermolecular interactions, where hydrogen-bonding and/or polar interactions play an important role and still remain challenging for thermodynamic models elaborated for chemical engineering applications. Promising results in modeling of systems containing different DESs have been already obtained using original Perturbed-Chain Statistical Associating Fluid Theory (PC-SAFT) equation of state (EoS) [1-3]. PC-SAFT is popular among chemical engineers due to its capabilities to describe various types of phase diagrams for miscellaneous mixtures including non-polar, polar and associating substances.

In the present paper, we consider, first, the ability of DESs on the basis of choline chloride and glutaric acid for the separation of mixtures of alcohols with acetic and propionic acids esters: ethyl acetate, *n*-propyl acetate, *n*-butyl acetate, ethyl propionate, *n*-propyl propionate and *n*-butyl propionate. Second, PC-SAFT was applied to model liquid-liquid equilibria (LLE) of these systems using the “pseudo-pure component” approach (it means that a DES is assumed as a pseudo-pure compound, and its pure-component PC-SAFT parameters are determined by fitting to pure DES density data).

Choline chloride-based DES was tested for the separation of azeotropic mixtures of ethanol–ethyl acetate, *n*-propanol–*n*-propyl acetate, *n*-butanol–*n*-butyl acetate, ethanol–ethyl propionate, *n*-propanol–*n*-propyl propionate, and *n*-butanol–*n*-butyl propionate via liquid–liquid extraction. The mixture of choline chloride with glutaric acid with a molar ratio of 1:1 was used. Experimental data of LLE were obtained at temperature 313.15 K and atmospheric pressure. Liquid–liquid tie-lines for studied systems were determined and analyzed. The extraction performance of DES was characterized with distribution coefficients and values of selectivity respectively to alcohol. PC-SAFT modeling showed a very good agreement with the experimental data for the pseudo-ternary systems. This is promising as the selectivity values are sensitive properties. In sum, PC-SAFT is a suitable model for describing the phase behavior of complex mixtures containing DES.

Acknowledgements. The financial support of Russian Foundation for Basic Research (research grant No. 16-33-60128 mol_a_dk), Saint Petersburg State University (grant “COLLAB 2018”), and TU Dortmund (grant from DFG RESOLV EXC 1069) is gratefully acknowledged.

[1] J. Gross, G. Sadowski, *Ind. Eng. Chem. Res.*, 2001, 40, 1244.

[2] J. Gross, G. Sadowski, *Ind. Eng. Chem. Res.*, 2002, 41, 5510.

[3] S.P. Verevkin, A.Yu. Sazonova, A.K. Frolkova, D.H. Zaitsau, I.V. Prikhodko, C. Held, *Ind. Eng. Chem. Res.*, 2015, 54, 3498.

A Priori Prediction of Liquid-Liquid-Liquid Equilibria Using COSMO-SAC Model

Banerjee T.¹, Kundu D.¹, Bairagya P.²

¹Department of Chemical Engineering, Indian Institute of Technology Guwahati, India; ²Department of Chemical Engineering, Jadavpur University, India

tamalb@iitg.ac.in

Three phase liquid equilibria is frequently encountered in microextraction, triphasic catalysis processes. However, the multicomponent, multiphase equilibria depends on the nature of compounds and the size of the phase region. Herein, we have predicted the liquid-liquid-liquid equilibria (LLLE) of 6 ionic liquid (IL) containing systems and 7 aqueous-organic systems (hereby, non-IL) employing quantum chemical based Conductor like Screening Model Segment Activity Coefficient (COSMO-SAC). The modified Rachford-Rice algorithm was used, assuming the triphasic systems into two biphasic liquid-liquid equilibrium which were simultaneously solved iteratively to predict the mole fractions in all three phases. An average root mean square deviation (RMSD, in %) of 13% was obtained for IL systems whereas 8% was calculated for non-IL systems. The RMSD of top phase are 15.7% and 15.5% for the IL and non-IL systems respectively. However, in the middle phase, 7.8% and 5.3% RMSD were obtained in IL and non-IL systems respectively. The RMSD further drops down to 3.8% and 2.2% for IL and non-IL systems respectively for the bottom phase.

Nature of Mesoscopic Aggregates in Lysozyme Solutions

*Nikfarjam S.*¹, *Anisimov M.*, *Woehl T.J.*²

¹University of Maryland, College Park, United States; ²Professor2

shnikfar@umd.edu

Understanding of protein stability, folding and aggregation in solutions is important for a better control of the behavior of proteins *in vivo*, and in protein-based therapeutics. Lysozyme is known to form mesoscopic aggregates at high concentrations, while the origin and thermodynamic state of these aggregates remain debatable^{1,2}. In order to elucidate the thermodynamic nature of this phenomenon, we have investigated the effects of filtration and temperature on the size and amount of the mesoscopic aggregates in concentrated solutions of lysozyme (> 30 mg/mL).

It has been known that mesoscopic protein aggregates (~100 nm size) form in concentrated lysozyme solutions. Their formation was previously attributed to self-assembly, with the aggregates being in equilibrium with protein monomers, resembling micellization. In this work, we use dynamic light scattering (DLS), small angle x-ray scattering (SAXS), and size exclusion chromatography (SEC) experiments to obtain the size and relative population of the mesoscopic aggregates and test the self-assembly hypothesis.

We have shown that systematic filtration through 20 nm filter completely removes the aggregates from solution. The aggregates do not reform, indicating that they are not a result of lysozyme self-assembly. Without filtration, the relative number of lysozyme monomers decreases with increase of the temperature, indicating the formation of more aggregates. SEC is used to search for the presence of lysozyme dimers, which have been hypothesized to be the source of mesoscopic aggregates³. SEC did not detect dimers in solutions of filtered or unfiltered lysozyme solutions. Our results suggest that the mesoscopic aggregates in lysozyme solutions are not formed by self-assembly but are due to some impurities present in commercial lysozyme, such as other protein molecules or misfolded lysozyme, introduced during purification or lyophilization processes.

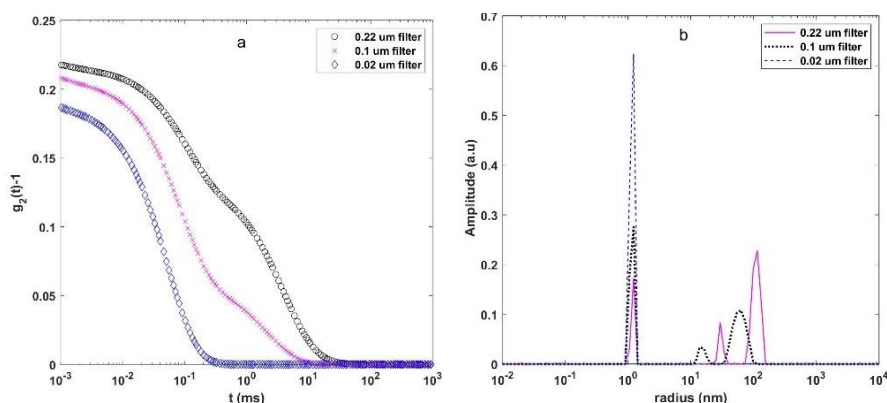


Figure 1. (a): DLS correlation functions (g_2) and (b) the size distribution in a solution of 60 mg/mL lysozyme filtered through a 0.02, 0.1, and 0.22 μm pore size filters (blue, pink, and black, respectively), in a 20 mM HEPES sodium buffer with pH = 7.8.

[1] Pan, W., Vekilov, P. G., Lubchenko, V. "Origin of Anomalous Mesoscopic Phases in Protein Solutions," *J. Phys. Chem. B*, **114**, 7620 (2010).

[2] M. S. Safari, M. C. Byington, J. C. Conrad, and P. G. Vekilov, "Polymorphism of Lysozyme Condensates," *J. Phys. Chem. B*, **121**, 39, 9091 (2017).

[3] P. G. Vekilov *et al.*, "Weakly-bound Dimers that Underlie the Crystal Nucleation Precursors in Lysozyme Solutions," *bioRxiv*, p. 275222, March 2018.

Current Experimental and Theoretical Concepts for High-Pressure Phase Transition Studies in Molecular Crystals

Rychkov D.A.^{1,2}

¹Institute of Solid State Chemistry and Mechanochemistry SB RAS, Russia;

²Novosibirsk State University, Russia

rychkov.dennis@gmail.com

Change of intensive thermodynamic parameters, such as pressure and temperature, is well-known method for studying the nature of selected systems. Molecular crystals are not an exception, being widely studied for many of years. High-pressure research of amino acids, pharmaceutical materials and other bioactive molecules revealed new properties of these systems: new polymorphs¹, hydrates and solvates formation², charge transfer, etc. Nevertheless, main techniques used in such studies are quite limited: single-crystal X-Ray diffraction, IR- and Raman spectroscopy (both for pressure and temperature changes) and thermal analysis (low and high-temperature studies only) and rarely computational methods. Even more surprising is that most of studies in last decade are limited to simple crystallography research, paying attention only to space group changes and mutual positions of molecules, their functional groups or even atom positions. Traditional crystallographic concepts, such as motives, synthons, H-bonded networks are of great importance for scrupulous examination of system changes at high-pressure, but still unable to generalize phase transition reasons, mechanisms or produce theory for predicting these changes³. Thus, thermodynamic parameters should be considered for such systems, paying specific attention not to structural changes, but *thermodynamic* changes of whole unit cell and energies of particular molecular interactions.

In this work an overview of traditional methods for high-pressure researches, including experimental and theoretical methods is presented. Traditional concepts, described above, are contrasted to new ideas and methods (mostly computational) which allow to reveal true reasons for phase transitions in molecular crystals at pressure. Old data is revisited with new methods, showing how calculation of thermodynamic parameters deepen an understanding of high-pressure changes in molecular systems. As a closing word a couple of examples of comprehensive works are provided, showing new trends in highlighted field^{3,4}.

Acknowledgements This work is performed with financial support of RSCF 18-73-00154 grant.

[1] S. A. Moggach, Simon Parsons, Peter A. Wood, *Crystallography Reviews*, 2008, 14 (2), 143-184.

[2] N. A. Tumanov, E. V. Boldyreva, B. A. Kolesov, A. V. Kurnosov, R. Quesada Cabrera, *Journal Acta Crystallographica Section B: Structural Science*, 2010, 66 (4), 458-471.

[3] E. V. Boldyreva, *Acta Crystallographica Section A: Foundations of Crystallography*, 2007, A64, 218-231.

[4] D. A. Rychkov, J. Stare, E. V. Boldyreva, *Physical Chemistry Chemical Physics*, 2017, 19 (9), 6671-6676.

[5] S. Hunter, T. Sutinen, S. F. Parker, C. A. Morrison, D. M. Williamson, S. Thompson, P. J. Gould, C. R. Pulham, *Journal of Physical Chemistry C*, 2013, 117 (16), 8062-8071.

Modifications of Differential Adiabatic Scanning Microcalorimetry Method for Melting of Multilamellar DMPC Membranes

Alekseeva O.M.¹, Kremntsova A.V.¹, Kim Yu.A.²

¹ Emanuel Institute of Biochemical Physics RAS, Moscow, Russia;

² Institute of Cell Biophysics, RAS., Moscow region, Pushchino, Russia

olgavek@yandex.ru

The actions of different rates of DMPC melting (1 grad/min; 0,5 grad/min; 0,25 grad/min, 0,125 grad/min) to microdomains level of membranes organizations at bilayers of multilamellar liposomes formed from synthetic phospholipid dimyristoilphosphatidylcholine were investigated by DSC. This modification of DSC parameters influenced to enthalpy; cooperativity; Tmax of DMPC melting (Figure 1). The changing of thermodynamic properties of DMPC melting indicates that the organization of bilayers at multilamellar liposomes was changed greatly at microdomain's levels. If 100% is the value of parameters at the rate of DMPC melting 1 grad/min., that the enthalpy decreased to the 80%/ But Tmax and 1/cooperativity (the value of half-width on half-altitude of main transition is reciprocal quantity for cooperativity) of main phase transition were changed negligible. This phenomenon indicates that the main phase transition at bilayers DMPC microdomain structure was disrupted when rates of DMPC melting was decreased greatly. The main phase transition was not shown as a big peak at thermodynamic curves under the 0,125 grad/min rate melting. Phospholipid at all thickness of multilamellar liposomes were melting slowly without clear phase transition jumps.

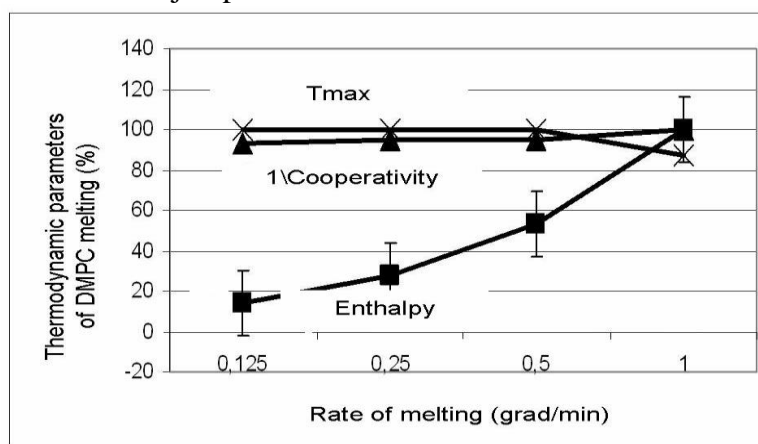


Figure 1. The curves of influences of different rates of DMPC melting (1 grad/min; 0,5 grad/min; 0,25 grad/min, 0,125 grad/min) to the thermodynamic parameters enthalpy; 1/cooperativity; Tmax. 100% - is the value of parameters at the rate of DMPC melting 1 grad/min.

These phenomenon of DMPC melting was mirrored the temperature changing at animals body. Our experimental model is very simple, but it may be used for investigation of variation phase transitions at lipid components at biological membranes. At animal cells there are many organelles which have the multilamellar structure, or between organelles the multilamellar structure were formed. Variations of temperature changing are take place at animals too. By this similar investigations were actually.

FRIDAY, 21.06.2019

**SECTION 4: Thermodynamics of Interfacial and
Confined Phenomena**

Thermodynamic Model of Solubilization in Direct Nonionic Micelle

Shchekin A.K.

St. Petersburg State University, Russia, Department of Statistical Physics

akshch@list.ru

Addition of hydrophobic admixture to surfactant solution with polar solvent and direct micelles leads (due to the hydrophobic effect) to redistribution of the molecules of this additive in micellar cores. This phenomenon is called solubilization and is the mostly widely used in applications of micellar solution. In particular, micellar solubilization gives a possibility to dissolve hydrophobic drugs in aqueous environments and transport them with micelles. This report gives a new insight into constructing an analytical molecular thermodynamic model for solubilization in nonionic spherical micelles. The basic part of such model is finding a minimal work of formation a nonionic micelle as a function of the aggregation number of surfactant molecules and the number of solubilized molecules. There are two analytical models for minimal work of formation of spherical surfactant aggregates as a function of the surfactant aggregation number which are called the ‘droplet’ and ‘quasi-droplet’ models [1-3]. It should be noted that there is a lack of similar models for the case of direct nano- and microemulsions. Here we extend the droplet model for pure micelles to include the dependence on the number of solubilized molecules in the spherical micellar core. Such a model can be directly incorporated in kinetic analysis of processes in micellar solutions described in [4].

Let n_1 and n_2 be the aggregation number of surfactant monomers the number of molecules of a hydrophobic admixture in the aggregate. A relation between the hydrophobic core radius R of the aggregate and the numbers n_1 and n_2 can be written as $4\pi R^3/3 = v(n_c + 1)n_1 + v_2 n_2$, where v and v_2 are the volumes of a single segment of the hydrocarbon chain of the surfactant monomer and respectively the admixture molecule, n_c is the total number of segments in the hydrocarbon chain. The minimal work $W(n_1, n_2)$ of formation of such aggregate as a function of n_1 and n_2 has a form

$$\begin{aligned} \frac{W(n_1, n_2)}{k_B T} = & -n_c B n_1 - B_2 n_2 - (n_1 - 1) \ln \left[\frac{4\pi \lambda^3 c_1}{3n_1} (n_1 + \alpha n_2) \right] - n_2 \ln \left[\frac{4\pi \lambda^3 c_2}{3n_2} (n_1 + \alpha n_2) \right] + \\ & + \frac{4\pi \gamma_0 \lambda^{2/3}}{k_B T} (n_1 + \alpha n_2)^{2/3} + \frac{q^2 \delta}{8\pi \epsilon_0 \epsilon k_B T \lambda^{2/3}} \frac{n_1^2}{(n_1 + \alpha n_2)^{2/3}}. \end{aligned}$$

Here B and B_2 are positive constants of hydrophobic contribution per hydrocarbon segment and respectively per admixture molecule, k_B is Boltzmann’s constant and T is the solution temperature, $\alpha \equiv v_2/v(n_c + 1)$, $\lambda \equiv [(3v/4\pi)(n_c + 1)]^{1/3}$, c_1 and c_2 are the solution concentrations of the surfactant and admixture, γ_0 is the surface tension of hydrocarbon segments, last term represents the contribution of the electric double layer, q is the electric charge of a dipole of hydrophilic part of surfactant monomer, δ is the length of the dipole of the hydrophilic part.

Acknowledgements This work was supported by the Fund for the Promotion of Joint International Research (Fostering Joint International Research (B)) of KAKENHI (Grants-in-Aid for Scientific Research).

[1] A.I. Rusanov, F.M. Kuni, A.P. Grinin, A.K. Shchekin, *Colloid J.*, 2002, 64, 605.

[2] A.I. Rusanov, A.P. Grinin, F.M. Kuni, A.K. Shchekin, *Russ. J. Gen. Chem.*, 2002, 72, 607.

[3] A.P. Grinin, A.I. Rusanov, F.M. Kuni, A.K. Shchekin, *Colloid J.*, 2003, 65, 145.

[4] A.K. Shchekin, L.Ts. Adzhemyan, I.A. Babintsev, N.A. Volkov, *Colloid J.*, 2018, 80, 107.

Thermochemical and Structural Description of Interaction Between Dipeptides and Anionic Micelles

Barannikov V.P., Kurbatova M.S., Badelin V.G.

G.A.Krestov Institute of Solution Chemistry of RAS, Russia

vpb@isc-ras.ru

The interaction of micellar assemblies with biologically active substances of different classes attracts interest due to its numerous applications in biosciences, foods, cosmetics, drug delivery, detergency and biotechnological processes. There are a number of works in which the change of physicochemical properties of micellar solutions (CMC, volume, viscosity, refractive index, conductivity) is recorded in dependence on concentration of a surfactant and amino acids or peptide additives. The mechanism of interactions of organic substances with the micellar assemblies is explored in lesser degree. The distinctive feature of our approach is the keeping of surfactant concentration constant in the experimental investigation to segregate the interaction processes from micellar assembly reorganization induced by the concentration variation.

The obtained values of enthalpy of transfer of zwitterion alanine dipeptides from water into aqueous SDS micellar solution have been discussed as thermochemical characteristics of interaction of the peptides with micelles. The interaction of α -Ala- α -Ala, α -Ala-Val, α -Ala-NIn with SDS micelles is an endothermic process over the whole range of dipeptide concentrations. The positive values of $\Delta_{tr}H^m$ increase with the increase in dipeptide content up to peptide/surfactant mole ratio of 0.2. The approximate constancy of transfer enthalpy indicates that the level of saturation of SDS micelles interaction with peptide zwitterions has been achieved. The effect of hydrophobicity and structure branching of zwitterion peptides on effectiveness of binding with anionic micelles has been analyzed. The obtained data indicate that strengthening of the hydrophobic properties of the side chain of peptides in the series: β -Ala- β -Ala < α -Ala- α -Ala < α -AlaVal < α -AlaNIn initiates the weakening of the intermolecular interactions of peptides with micellar SDS in the same order. The interaction between β -Ala- β -Ala and SDS micelles is characterized by a weak endothermic effect when small amount of the peptide is added while at higher concentrations the interaction is accompanied by exothermic effect. More favorable enthalpy of interaction with micelles may be attributed to chain structure and weaker hydrophobic properties of β -Ala- β -Ala. The absence of steric hindrances causes dispersion interaction with SDS molecules to become stronger and giving the chance for zwitterion of β -Ala- β -Ala to penetrate into micelle pore. Conversely, interaction with α -Ala- α -Ala, α -Ala-Val, α -Ala-NIn is followed by steric hindrances due to its branched structure. The hydrophobic side groups strengthen the water structure in the peptide hydration shell. The latter fact increases the endothermic contribution of peptide desolvation to the enthalpy of its interaction with SDS micelles. Tendencies of changing in the average size and ζ -potential of SDS micelles at the interaction with dipeptides, as well as change of chemical shifts of H atoms for aliphatic and peptide groups of α -L-Ala- α -L-Ala, β -Ala- β -Ala, α -DL-Ala- α -DL-NIn in SDS micellar solution permit to indicate some essential features of peptide/micelle interaction mechanism. The data indicated a considerable effect of ion – zwitterion electrostatic and hydrophobic – hydrophobic interactions, which are accompanied by deformation of HNCO peptide group. Quantum chemical simulation of α -L-Ala- α -L-Ala and β -Ala- β -Ala complexes with SDS dimer as model of anion micelle fragment has been carried out by making use of DFT method including hybrid exchange-correlation Becke functional B97-D with Grimme dispersion correction. Optimized configurations of complexes of the zwitterion peptides with SDS dimer are stabilized by electrostatic interactions and hydrogen bonds of (H₂)N-H...O(S). Data showed the preference localization of α -L-Ala- α -L-Ala among the charged groups of SDS dimer. Localization of β -Ala- β -Ala among the charged groups and in the dimer pore gives complexes with closely spaced energy values. This fact presumes that both complexes are able to exist in a water solution.

The study was financially supported by the RFBR (grant No. 18-03-01032-a).

Solubilization of Organic Compounds in AOT Reverse Micelles by Molecular Dynamics Simulations

Kopanichuk I.V., Burovaya E.S., Vanin A.A.

St. Petersburg State University, St. Petersburg, Russia

i.kopanichuk@spbu.ru

Computer simulations of the derivatives of pyridine and benzene distribution in AOTNa/water reverse micelles in n-decane has been performed. All solubilized compounds except benzene are polar and have different numbers of donors/acceptors forming hydrogen bonds. The most probable positions of molecules relative to a reverse micelle depend fundamentally on the number of their hydroxyl groups. Pyridine and benzene molecules are likely located in the nonpolar medium, other molecules are preferably distributed between the different parts of the reverse micelle. The number and arrangement of hydrophilic groups in the structure of a molecule have stronger effect on the ability to solubilization in the reverse micelles than the polarity of a molecule. The effect of presence of reverse micelles in the system has been also studied. The distribution coefficients of molecules in the water-decane-AOTNa system with and the water-decane system. It has been found that the water-decane interfacial potential is more significant for the solubilization than the interfacial potential of the reverse micelle.

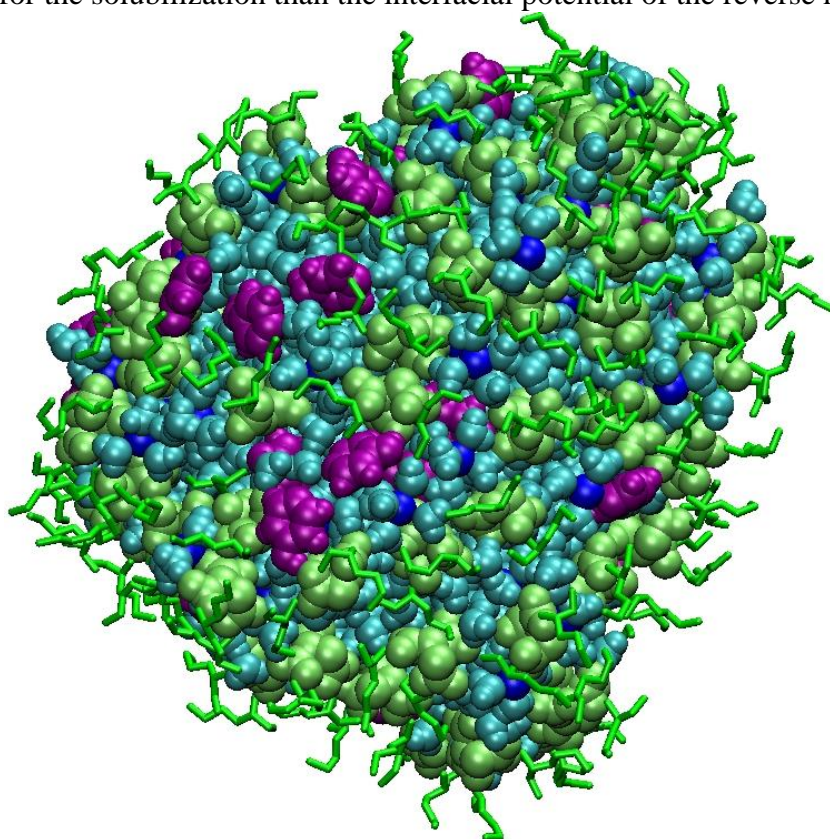


Figure 1. 32 pyridin-4-ol molecules (purple) solubilized within AOTNa reverse micelle.

Acknowledgements

This work was supported by the grant of RSCF № 16-13-10042.

Multi-Orientational Models of Planar Ordering of Functional Organic Molecules on Solid Surfaces: Thermodynamics and Monte Carlo Simulation

*Akimenko S.S.*¹, *Gorbunov V.A.*¹, *Ustinov E.A.*²

¹Omsk State Technical University, Russian Federation;

²Toffe Institute, Russian Federation

akimenkosergey@mail.ru

Liquid-crystal, crystal-crystal and orientational phase transitions in two-dimensional molecular layers on solid surfaces have attracted much attention for a long time. Their thermodynamic description and prediction of phase transition parameters represent a fundamental importance. Even in such a simple adsorption system as nitrogen on the graphite surface an orientational phase transition is observed at low temperatures [1-3]. Using special techniques (kinetic algorithm, simulation in an elongated cell, etc.) for a Monte-Carlo simulation allows one to perform a complete thermodynamic analysis of various adsorption systems. From this viewpoint, self-assembled molecular layers and supramolecular nanostructures consisting of complex organic molecules on the solid surface are of great interest. However, a theoretical study of self-assembly and phase transitions in the adsorption layers of complex functional organic molecules encounters serious difficulties because of increasing algorithmic complexities and computational cost of simulations.

We propose an alternative approach that allows us to take into account a detailed chemical structure of the molecules. It is assumed to make a preliminary calculation of the intermolecular interaction energy at a given distance between the molecules for all their possible mutual orientations with a certain increment of corresponding angles (Fig. 1). Further, the obtained potential is used in the Monte Carlo simulation. Thus, within the framework of the Monte Carlo method, it becomes possible to simulate the self-assembly of the molecular layer and equilibrium phase transitions using various molecular-mechanical and quantum-mechanical potentials. In this presentation, the proposed approach was applied to the adsorption layer of trimesic acid. We have performed the Monte-Carlo simulation of the molecular layer and made an attempt to generalize the simulation data in the form of thermodynamically consistent regression equations of state.

Acknowledgements The financial support of the Russian Foundation for Basic Research, project no. 17-03-00091a.

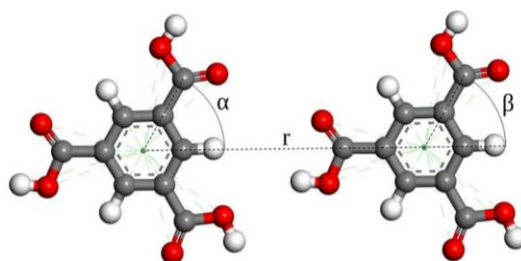


Figure 1. Pair configuration of two trimesic acid molecules and forcefield parameters.

[1] M. Golebiowska, L. Firlej, B. Kuchta, R. Fabianski, *J. Chem. Phys.*, 2009, 130, 204703.

[2] E. A. Ustinov, *Carbon*, 2016, 100, 52.

[3] E. A. Ustinov, V. A. Gorbunov, S. S. Akimenko, *J. Phys. Chem. C*, 2018, 122, 2897.

Surfactant Effects on the Molecular Mobility in Confined Decane/Water Mixtures: A Systematic Computational Study

Sizov V.V., Kopanichuk I.V., Berezhnaya A.S., Sizova A.A., Brodskaya E.N.

St. Petersburg State University, St. Petersburg, Russia

sizovvv@mail.ru

In the present work molecular dynamics simulations are used to study the molecular mobility of water and hydrocarbon confined in slit-like mesopores with hydrophilic or hydrophobic walls in the presence of surfactants. Since the mobility of water and hydrocarbon molecules in confinement is strongly affected by the local structure of the fluid, it can be enhanced by a surfactant either via stabilization of planar liquid layers favoring smooth diffusion or via destabilization of spherical or cylindrical aggregates, which hinder the motion of molecules. Alternatively, surfactants can destabilize the layer of liquid (water at hydrophilic surfaces or hydrocarbon at hydrophobic surfaces) adsorbed at the pore wall, though this mechanism is less probable for strongly hydrophilic or hydrophobic surfaces.

In order to fine-tune the balance of hydrophilic and lyophilic properties for optimal surfactant performance, a systematic computational study of a series of polyethylene oxide alkyl ethers (C_nE_m) was carried out. The results obtained for various C_nE_m species were compared with several widely used surfactants, both ionic and nonionic.

Molecular dynamics simulations were performed in the NVT ensemble at 298 K. Basic cells with dimensions of up to 20x20x8 nm were used with three-dimensional periodic boundary conditions. The simulation length was at least 15 ns with 5 ns for equilibration and 10 ns for data collection. The description of intermolecular interactions was largely based on GROMOS96 53a6 force field; the partial charges for C_nE_m were obtained from quantum chemical calculations. The shape of aggregates and localization of surfactant molecules were determined directly from molecular dynamics trajectories. Structure of the liquid in the pore was described by local density profiles, which were evaluated separately for water and decane. Mobility of decane and water molecules was quantified by lateral self-diffusion coefficients, which were evaluated from the dependence of mean-square displacements on time. The diffusion coefficients in the presence of surfactants were compared to the data obtained for confined decane/water reference system, thus allowing one to observe the positive or negative effect of surfactant on mobility of liquid molecules. The results for the C_nE_m series were utilized to construct a surfactant efficiency scale, which can be used as a reference in further studies of surfactant effects on molecular mobility in confined water/hydrocarbon mixtures.

Acknowledgements. This work was supported by the Russian Foundation for Basic Research (project No.18-03-01238-a). Calculations were partially performed using the facilities of the Computational Resource Center (Science Park, St.Petersburg State University).

Interfacial Free Energy at a Curved Liquid–Crystal Interface: Molecular Dynamics Simulation

Baidakov V.G., Protsenko K.R.

Institute of Thermal Physics, Ural Branch of the Russian Academy of Sciences, Russia

baidakov@itp.uran.ru

The interfacial free energy is one of the main parameters determining the work of formation of a new-phase nucleus. On a curved interface this parameter, at a constant temperature, depends on the radius of curvature of the dividing surface or the pressure in the system. The effective value of γ_e at a crystal nucleus – liquid interface may be obtained in the framework of classical nucleation theory from data on the nucleation rate in a supercooled liquid.

The kinetics of spontaneous crystallization of a supercooled Lennard-Jones liquid has been investigated by us in molecular dynamics (MD) experiments. The homogeneous nucleation rate J was determined by the methods of mean lifetime ($J = 10^{31}–10^{35} \text{ s}^{-1}\text{m}^{-3}$), forward flux sampling ($J = 10^{26}–10^{31} \text{ s}^{-1}\text{m}^{-3}$) and nucleus seeding ($J = 10^{-4}–10^{14} \text{ s}^{-1}\text{m}^{-3}$). The nucleus size diffusion coefficient, the Zeldovich nonequilibrium factor and the interfacial free energy at a plane crystal – liquid interface γ_∞ have also been determined in the framework of MD simulation. Calculations of J were made in a wide range of temperatures and pressures along isobars and isotherms. The maximum temperature value was equal to $0.7T_c$, where T_c is the temperature at the critical point, and the minimum to $0.5T_t$, where T_t is the temperature at the triple point. The data obtained were used to determine the value of γ_e from classical nucleation theory.

Figure 1 presents the dependence of the interfacial free energy of critical crystal nuclei on the curvature of the surface of tension ($1/R$) along isotherms (open symbols) and isobars (solid symbols). All quantities are given in dimensionless form. The reduction units are parameters of the Lennard-Jones potential and the particle mass.

The asymptotic of γ_e at $1/R \rightarrow 0$ and $1/R \rightarrow \infty$ are discussed for temperatures $T > T_K$, where T_K is the temperature at the endpoint of the melting line, and also for temperatures below T_K , when in a metastable liquid there is neither a spinodal nor a phase-equilibrium line.

Acknowledgements The financial support of the Russian Science Foundation (project No. 18-19-00276).

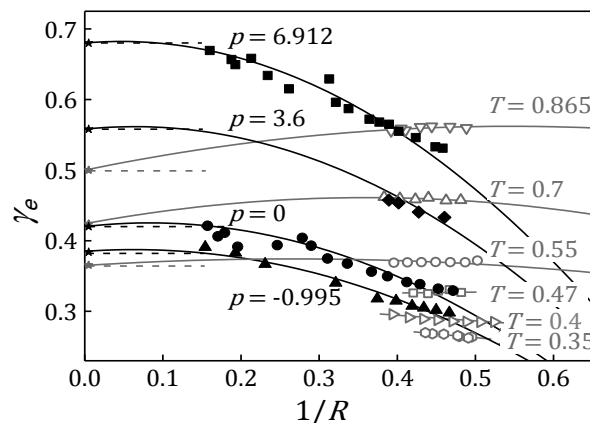


Figure 1. Dependence of the effective interfacial free energy of crystal nuclei on the curvature of the surface of tension.

Molecular Dynamic Approaches to Prediction of Size Dependences of Thermodynamic Properties of Metal Nanoparticles

Samsonov V.M., Talyzin I.V., Vasiliev S.A., Kartoshkin A.Yu.

Tver State University, Russia

samsonoff@inbox.ru

Basic results of atomistic simulation correspond to current and final configurations of simulated objects. Then, using potentials of the interatomic interaction, these configurations make it possible to evaluate the potential (cohesive) term into the internal energy equal by modulus to the binding energy E of the object. In turn, when the binding energy is known, characteristic functions of the simulated ensemble of nanoparticles (NPs) may be found though relationships between E and thermodynamic properties of NPs are not always quite trivial and may be treated as an important problem not entirely solved up now. In development of our former papers [1, 2] we have used the well-known program LAMMPS and the embedded atom method to predict and analyze size dependences of the melting T_m and T_c crystallization temperatures of metal NPs, enthalpies of melting ΔH_m , evaporation ΔH_{ev} and sublimation ΔH_{sub} as well as of the entropy of melting. The temperatures and heats of the above phase transition have been found with respect to the melting-crystallization hysteresis, i.e. in non-equilibrium conditions and by means of relaxation of NPs at fixed temperatures. Corresponding properties, found by the second way ($T_m^{(eq)}$, $\Delta H_m^{(eq)}$, $\Delta H_{ev}^{(eq)}$, $\Delta H_{sub}^{(eq)}$), are interpreted as equilibrium ones. As one can see in Figure 1, our MD size dependence of the equilibrium melting temperature $T_m^{(eq)}$ agrees with the available experimental data [3-5].

Acknowledgements Financial support of RFBR (grant No 18-03-00132) and Ministry of Science and Higher Education of RF (project No 3.5506.2017/BP) is an acknowledged.

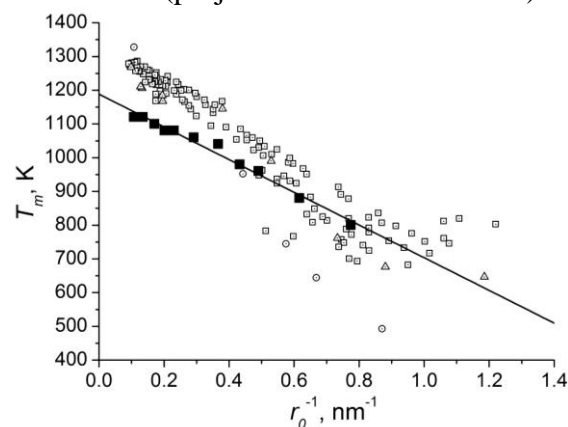


Figure 1. Comparison of our MD size dependence of the equilibrium melting point of Au nanoparticles (solid line and dots ■) with available experimental data: □ [3], ○ [4] and Δ [5].
[1] N.Yu. Sdobnyakov, et al., *Computational Materials Science*, 2018, 153, 153.
[2] V.M. Samsonov, et al., *J. Therm. Anal. Calorim.*, 2018, 133, 1207.
[3] Ph. Buffat, J.P. Borel, *Phys. Rev. A.*, 1976, 13, 2287.
[4] T Castro, R. Reifengerger, *Phys. Rev. B.*, 1990, 42, 8548.
[5] K. Dick, T. Dhanasekaran, Zh. Zhang, D. Meisel, *J. Am. Chem. Soc.*, 2002, 124, 2312.

FRIDAY, 21.06.2019

**SECTION 5: Thermodynamics of Functional Materials
and Engineered Self-Assembly**

Synthesis and Antibacterial Properties of Nitrogen or Carbon Doped Titanium Oxide Thin Films

Abdulagatov A.I.¹, Ashurbekova Kr.N.,¹ Ashurbekova Ka.N.¹, Amashaev R.R.¹, Maksumova A.M.¹, Aliev A.², Rabadanov M.Kh.¹, Abdulagatov I.M.^{1,2}

¹Dagestan State University, Russia;

²Dagestan State Medical University, Ecological Medicine Research Institute, Makhachkala, Dagestan, Russia

amashaev007@gmail.com

According to an analysis firms, antibacterial coatings market in 2024 will exceed US \$ 7.4 billion [1]. US Centers for Disease Control and Prevention, allocated in 2016 fourteen million dollars in grants to the thirty-four research teams to create a protective coating against antibiotic resistant bacteria [2]. There is also a rising interest in antibacterial coating from the food industry. The development of simple, inexpensive and effective antibacterial coatings is very important since the damage from harmful and stable microorganisms has become a serious social problem. The use of photocatalytic effect on nanoscale TiO₂ is conceptually simple and promising technology to mitigate bacterial contamination. However, the band gap of titanium dioxide is 3.0-3.2 eV, which means that it can be excited by UV radiation with a wavelength < 380 nm, which is only 5% of the solar spectrum. One way to overcome this problem is to dope TiO₂ with carbon or nitrogen. This allows engineering a material with a band gap less than 3.0 eV, which would support the photoactivity in low light conditions. Over the years, numerous methods were developed to obtain nitrogen or carbon doped coatings. In this work atomic and molecular layer deposition (ALD and MLD) techniques were used to synthesize photoactive thin (<10nm) films. If ALD allows to deposit only inorganic coatings, using MLD one can deposit organic and hybrid organic-inorganic thin films. Unique features of these techniques as follows – atomic level thickness and composition control; high-level of film uniformity when deposited on membranes and nanoparticles. In ALD and MLD films deposited via sequential surface chemistry reactions. For this study, antibacterial ALD TiO_xN_y coatings were deposited using TiCl₄ and hydrazine (N₂H₄) chemistry. Carbon doped TiO_xC_y films were synthesized by pyrolysis of MLD titanium alcoxide thin films.

In this presentation, we will show our findings for photocatalytic distraction of stems of *E. Coli* and *Staph. Aureus* bacteria under exposure to artificial UV and ambient light sources for various TiO_xN_y and TiO_xC_y films.

[1] Antimicrobial Coatings Market Research Report by Global Market Insights, I., <https://www.gminsights.com/pressrelease/antimicrobial-coatings-market>.

[2] CDC funds 34 innovative projects to combat antibiotic resistance.

<http://www.cdc.gov/media/releases/2016/p1006-cdc-antibiotic-resistance-research.html>.

Separation of Gas Mixtures by Adsorption in CMK-5 and CMK-3: Effects of Adsorbent Topology

Sizova A.A., Ivanova E.A., Sizov V.V., Brodskaya E.N.

St. Petersburg State University, Russia

shapovalovaaa@mail.ru

Separation and purification of gas mixtures by adsorption in porous solids is recognized as a potentially promising technique. Mesoporous carbons can be used as adsorbents due to a number of important advantages, such as controllable structure and surface chemistry, which enables one to optimize the material for efficient separation of a given mixture. On the molecular level the effects of material topology on the thermodynamic and transport properties can be studied by molecular simulation.

In this work the adsorption and diffusion of CO_2/N_2 and CO_2/CH_4 mixtures in mesoporous carbonaceous CMK-5 and CMK-3 materials were investigated. Molecular simulations were performed using Monte Carlo and molecular dynamics methods in grand canonical and canonical ensembles, respectively, at 298 K and various pressures. Both adsorptive and kinetic total selectivities were evaluated for each material, as well as local selectivities for various parts of the adsorbents. The role of the mesopores, which present in CMK-5, but not in CMK-3, was determined. The detailed explanation of the selectivity dependence on pressure was presented in terms of solid-fluid interactions and fluid density distribution relative to the adsorbent surface.

Acknowledgements. This work was supported by the Russian Foundation for Basic Research (grant no. 19-03-01051 A).

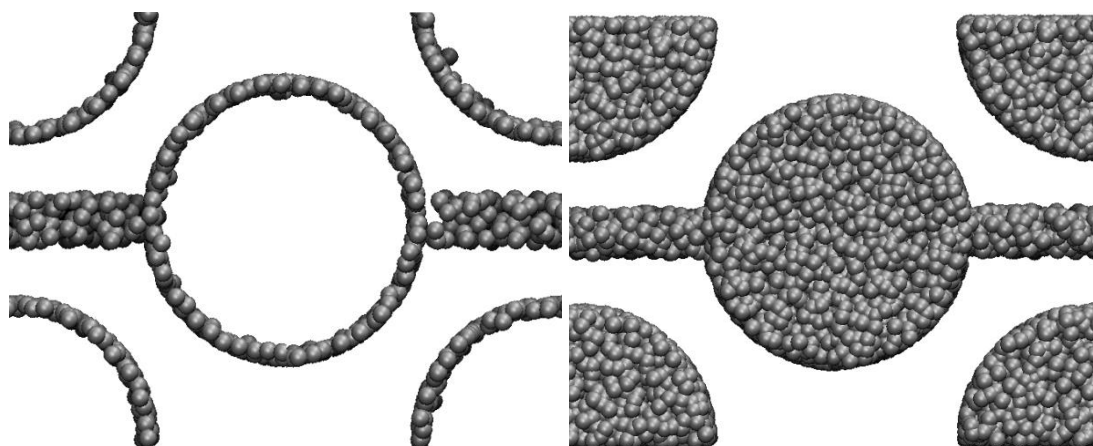


Figure 1. Structures of CMK-5 (left) and CMK-3 (right) materials.

Thermal Expansion of the Phosphates with Kosnarite and Langbeinite Type Structures

Asabina E.A., Pet'kov V.I., Shipilov A.S., Alekseev A.A., Mayorov P.A., Glukhova I.O.

Lobachevsky University, Nizhni Novgorod, Russia

elena.asabina@inbox.ru

Inorganic compounds of the framework structure, belonging to the kosnarite ($\text{KZr}_2(\text{PO}_4)_3$, related to NASICON) and langbeinite ($\text{K}_2\text{Mg}_2(\text{SO}_4)_3$) types, are considered as functional ceramics due to their high ionic conductivity, catalytic activity and stability to the action of high temperatures, aggressive media, radiation damage [1]. Both structures are based on the framework of octahedral and tetrahedral fragments. These types differ in the fragments' orientation and, therefore, size and amount of the framework cavities. The kosnarite type is more flexible to isomorphic substitutions, while the langbeinite one seems to be preferred for the compounds with large cation in the cavities and small in the framework sites. Thermal shocks resistance of these materials is strongly associated with their low thermal expansion. For practical applications, it is of interest to investigate the possibility to control thermal behavior of the materials by changing their chemical composition.

In the present study, the complex and mixed phosphates of the framework structure were characterized by high-temperature X-ray diffraction. The following compounds were chosen for the investigation: $\text{M}^{\text{I}}\text{M}_2^{\text{IV}}(\text{PO}_4)_3$, $\text{M}_{0.5}^{\text{II}}\text{M}_2^{\text{IV}}(\text{PO}_4)_3$, $\text{M}^{\text{I}}\text{Zr}_2(\text{TO}_4)_x(\text{PO}_4)_{3-x}$ (M^{I} – Li, Na, K, Rb, Cs; M^{II} – Mg, Ca, Cd, Sr, Pb, Ba; M^{IV} – Ti, Zr; T – As, V), $\text{K}_{1-x}\text{Rb}_x\text{Ti}_2(\text{PO}_4)_3$, $\text{K}_{2-x}\text{Rb}_x\text{Mg}_{0.5}\text{Zr}_{1.5}(\text{PO}_4)_3$, $\text{KPbMgTi}(\text{PO}_4)_3$, $\text{K}_{5/3}\text{MgTi}_{4/3}(\text{PO}_4)_3$, $\text{K}_{5/3}\text{MgZr}_{4/3}(\text{PO}_4)_3$.

The samples were synthesized by sol-gel method. Their phase and chemical compositions, crystal structures were studied by X-ray diffraction (Shimadzu XRD-6000), electron microscopy (JEOL JSM 7600F) and microprobe analysis, IR spectroscopy (Shimadzu FTIR-8400S). The data of adiabatic and differential scanning calorimetry showed that the compounds don't undergo phase transitions below room temperature. For thermal expansion study, X-ray diffraction patterns of the samples were collected within the temperature interval 25–800°C.

From the obtained results, langbeinite type compounds (cubic symmetry) can be suitable as isotropic expanding ceramics, whereas kosnarite type ones (hexagonal symmetry) exhibited anisotropy. However, both structural families had representatives with near-zero expansion.

The compounds $\text{M}^{\text{I}}\text{M}_2^{\text{IV}}(\text{PO}_4)_3$, $\text{M}_{0.5}^{\text{II}}\text{M}_2^{\text{IV}}(\text{PO}_4)_3$, $\text{M}^{\text{I}}\text{Zr}_2(\text{TO}_4)_x(\text{PO}_4)_{3-x}$ (M^{I} – Li, Na, K, Rb, Cs; M^{II} – Mg, Ca, Cd, Sr, Pb, Ba; M^{IV} – Ti, Zr; T – As, V), $\text{K}_{1-x}\text{Rb}_x\text{Ti}_2(\text{PO}_4)_3$ crystallized in the kosnarite structure. Most of these materials demonstrated the thermal behavior of the unit cell with $\alpha_a < \alpha_c$. The composition dependencies of the thermal expansion coefficients showed difference of the series in the behavior of their anisotropy and volume expansion. The lowest anisotropy and linear coefficients were observed in the case of $\text{CsZr}_2(\text{AsO}_4)_3$, $\text{CsZr}_2(\text{AsO}_4)_{1.5}(\text{PO}_4)_{1.5}$, $\text{CsZr}_2(\text{VO}_4)_{0.2}(\text{PO}_4)_{2.8}$ and $\text{K}_{0.5}\text{Rb}_{0.5}\text{Ti}_2(\text{PO}_4)_3$.

The structural deformations during the heating of the langbeinite-type phosphates $\text{K}_{2-x}\text{Rb}_x\text{Mg}_{0.5}\text{Zr}_{1.5}(\text{PO}_4)_3$, $\text{KPbMgTi}(\text{PO}_4)_3$, $\text{K}_{5/3}\text{MgTi}_{4/3}(\text{PO}_4)_3$, $\text{K}_{5/3}\text{MgZr}_{4/3}(\text{PO}_4)_3$ strongly depended on the nature and occupancies of the cations in the framework cavities. Among them, the solid solutions $\text{K}_{2-x}\text{Rb}_x\text{Mg}_{0.5}\text{Zr}_{1.5}(\text{PO}_4)_3$ were characterized by the minimal expansion.

The results of the investigation may be useful in predicting the thermal behavior of new functional ceramics based on the phosphates with framework structures.

Acknowledgements The financial support of RFBR, project 18-29-12063.

[1] V.I. Pet'kov, S.S. Shipilov, A.S. Dmitrienko, A.A. Alekseev, *J. Ind. Eng. Chem.*, 2018, 57, 236.

Surface Pressure Model for Particle Layers on Liquids

Marczak W.¹, Rogalski M.², Modaressi A.², Rogalska E.²

¹Jan Długosz University of Częstochowa, Poland; ²University of Lorraine, France

w.marczak@ujd.edu.pl

In properties of a film formed by insoluble particles on a liquid subphase, interactions between the particles themselves and those with the subphase are manifested. The surface elasticity can be characterized by the “surface modulus”, defined by analogy to well-known bulk modulus as:

$$Y \equiv -A(\partial\Pi/\partial A)_T, \quad (1)$$

where $\Pi = \gamma_0 - \gamma$ is the surface pressure, A is the surface area, γ is the surface tension, and subscript “0” denotes pure subphase. A decrease of the surface area due to the film compression results in the particles aggregation. As the contacts between particles may occur only in certain sites on the particle surface, dependent on its shape, a two-state approach can be applied: $F \rightarrow C$, where F and C denote the “free” and “contacting” sites, respectively.

Assuming that the fraction of contacting sites x_C is proportional to the surface pressure Π , one obtains the following formula:

$$x_C = \Pi / \Pi_L, \quad (2)$$

where Π_L is the maximum surface pressure, *i.e.* that for the uniform layer of the particles. As Y depends on the number of the sites capable of changing their state, and $x_F + x_C = 1$, then:

$$Y = kx_Fx_C = k\Pi/\Pi_L(1 - \Pi/\Pi_L), \quad (3)$$

where $k = \text{const}$. The $\Pi(A)$ function which fulfills the eqs. 1 and 3 is the surface pressure isotherm for the monomolecular particle layer:

$$\Pi = \Pi_L / [1 + (A/A_L)^\varphi], \quad (4)$$

where $\varphi = k/\Pi_L$, and A_L is the surface area at which $\Pi = 0.5 \Pi_L$.

The model can be readily extended to multilayer systems:

$$\Pi = \sum_i \Pi_{L,i} / [1 + (A/A_{L,i})^{\varphi_i}], \quad (5)$$

where i denotes the layer. An example of two-layers model curve fitted to experimental data is reported in Fig. 1. The model was successfully applied to layers of glass beads, violanthrone-78, anthracene and asphaltenes on water subphase [1].

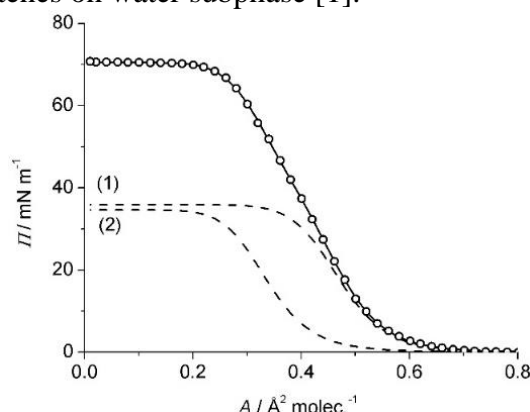


Figure 1. Surface pressure of anthracene film on water. Points – experimental results, solid line – fitted eq. 5, broken lines – surface pressure for two consecutive layers [1] W. Marczak, M. Rogalski, A. Modaressi and E. Rogalska, *Colloids Surf. A: Physicochem. Eng. Aspects*, 2016, 489, 128.

Thermal Properties of Zr(IV) and Y(III) Complexes with Dipivaloylmethane

Mosyagina S.A.^{1,2}, *Zherikova K.V.*², *Igumenov I.K.*², *Kuratieva N.V.*²

¹Novosibirsk State University, Russia;

²Nikolaev Institute of Inorganic Chemistry, Russia

s.mosiagina@g.nsu.ru

Metal β -diketonates and their derivatives are one of the most demanded compounds in a world of MOCVD (metal organic chemical vapor deposition). Due to their physicochemical (especially thermal) properties, they are used as MOCVD precursors to obtain different functional films and coatings (fuel cells, high-k dielectric, optic and optoelectronic coatings in microelectronics etc.). However, the industry development inevitably involves new areas the MOCVD method to be applied. A search for improved features of Thermal Barrier Coatings (TBCs) of gas turbine results in MOCVD consideration as an alternative perspective technological method.

Yttria-stabilized zirconia (YSZ) layers are actively used as a ceramic part of TBCs. For creating thick multicomponent coatings using the MOCVD method, it is necessary to properly organize the deposition zone, ensuring the constancy of the gas phase composition and the high growth rate, which the processes of sublimation/vaporization of the precursors used are responsible for. Moreover, from the technological point of view, i.e. in order to reduce the number of controlled parameters, one-source delivery system for the precursor vapors transportation is required. In this case, the information on thermal properties and possible mutual influences in mixtures is needed. The objects of this part of our investigation were zirconium(IV) and yttrium(III) dipivaloylmethanates and their mixtures. Phase and thermal behavior in condensed phase was investigated by XRD, thermogravimetry (TG) and differential-thermal analysis (DTA). Thermodynamics and kinetics of mixture sublimation/vaporization processes were studied by transpiration method. Also test MOCVD experiments were carried out with mixtures of $Zr(dpm)_4 - Y(dpm)_3$ for obtaining thick YSZ coatings with high growth rate.

In case of co-deposition several precursors in one deposition process, it is preferable to use a compound with a common ligand in order to avoid exchange reactions in the gas phase. But as for dopant precursor complementary for zirconium(IV) dipivaloylmethanate, $Y(dpm)_3$ has a tendency toward aggregation in order to saturate its coordination number higher than six forming adducts, for example, with water molecule. Also the polymerization processes of $Y(dpm)_3$ has shown to occur in gaseous phase in enclosed space [1]. For the stabilization of condensed and, consequently, gas phase neutral bidentate ligands were introduced into the $Y(dpm)_3$ complex. As a result, new (perhaps, more appropriate for MOCVD) mixed ligand complexes of yttrium(III) with dipivaloylmethanate and neutral N,N-, O,N-ligands (N,N-dimethylethylenediamine, N,N,N',N'-tetramethylpropanediamine, 2,2-dimethyl-1,3-propanediamine, ethanolamine, 2-methylethanolamine, N,N-dimethylethanolamine, 2-pyridineethanol, 1,3-phenantroline, pyrazine) were synthesized, purified, characterized and investigated by using X-ray structural diffraction and TG/DTA and tensimetric methods.

Acknowledgements The financial support of RFBR № 18-08-01105 A

[1] L. Zelenina, T. Chusova, K. Zherikova, etc., *Journal of Thermal Analysis and Calorimetry*, 2018, 133, 1157 – 1165.

Additional Criteria of High-Entropy Alloys Formation

Vasileva A.¹, Sineva S.², Starykh R.³

¹Saint-Petersburg Mining University, Russia; ²University of Queensland, Australia; ³LLC Gipronickel Institute, Russia

fml0914@gmail.com

The subject of the research is thermodynamic and experimental study of multicomponent metallic systems, as promising materials for synthesis of high entropy alloys (HEAs). These of alloys attract many scientists all around the world, as they can exhibit unusual properties due to unique thermodynamic characteristic and structure. Consequently, they are extensively studied nowadays.

By now several well-known criteria have been developed for determination of high-entropy alloys. HEAs are multicomponent alloys based on 5 or more elements, with content of each of them from 5 to 35 at.% [1, 2]. Also HEAs are characterised by high entropy of mixing (≥ 13.381 J/mol $\approx 1,61R$), sluggish diffusion and crystal structure of unordered solid solution [3, 4]. Additionally, there are some empirical parameters proposed in accordance with the Hume-Rothery rules, which make it possible to predict the formation of the single-phase solid solution structure in alloys (and, certainly, HEA) [3]. One of the main ones are: ΔS_{mix} , ΔH_{mix} , δ , Ω , $\Delta\chi$.

The authors of present work have suggested the existence of another important factor, which plays a significant role in the formation of HEAs. In particular, it is appearance of an exothermic effect during the synthesis of alloys from simple elementary substances (metals). Within the framework of this study 7 multicomponent systems were chosen: the first is Ag-Cr-Mn-Ti-Co-Au-Cu-Fe-Ni-Rh-Pt-Pd system with 12 components, and the next six systems are formed by gradual removal of one of the constituent components from the initial system (Ag, Cr, Mn, Ti, Co, Au, respectively). For study of these multicomponent systems several experimental methods of analysis were used, namely: differential thermal analysis (DTA), scanning electron microscopy (SEM), electron probe microanalysis (EPMA) and measurements of microhardness by Vickers method.

As a result of research it was found that for systems with number of components more than eight severe exothermic effect was registered during the initial heating of the powder mixture of pure metals. On the contrary, during the secondary heating of an already formed sample, the indicated exothermic effect is not observed. The phase compositions of these alloys showed multicomponent solid solutions structures with close to equimolar ratio of components. Moreover, measurement of microhardness detected abrupt change of discussed property, proving formation of HEAs. Since the presence of a reliable theoretical basis is important in almost any field of research, the direction, covered by this work, is highly efficient and is an urgent actual issue.

[1] Yang X., Zhang Y. // *Materials Chemistry and Physics*, 233-238, 2012.

[2] J.W. Yeh, et al. Chang. // *Advanced Engineering Materials*, Volume 6, Issue 5, 299-303, 2004.

[3] Yiming Tan, et al. // *Journal of Alloys and Compounds*, Volume 742, 430-441, 2018.

[4] Y. Zhang, Y. J. Zhou., Vols. 561-565, 1337-1339, 2007.

Computer Simulation of Self-Assembly of Spatial Networks in Solutions of Branching Aggregates

Voznesenskiy M., Petrov A., Vorotsov-Velyaminov P., Victorov A.

St-Petersburg State University, Russia

mikhail.voznesenskiy@gmail.com

Spatial networks may self-assemble in a diversity of systems, including solutions of wormlike surfactant micelles and polymer physical gels. Network-forming systems find numerous applications that range from tissue engineering and drug delivery to self-healing coatings and production of oil. Formation and breakup of a network has a strong impact on viscoelasticity and other important properties of the system. Among the key issues are the mechanism and conditions of self-assembly into a network, and the effect of the molecular architecture of the building units on the network's structure.

We developed a coarse grain model of micellar network in the framework of Brownian Dynamics and Monte Carlo methods. A structural unit of the model is a soft sphere. Spheres move within a cell with periodic boundary conditions as Brownian particles. If two spheres come close together, they can form a bond. An existing bond might break. Either way it's a Monte-Carlo process, which is repeated after a number of Brownian dynamics steps. The number of bonds per sphere is not allowed to exceed 3. In this way we obtain a percolating living network with dangling ends and junctions. Slip boundary conditions are applied to the simulation cell in order to simulate a bulk shear flow and to study changes in the network structure under the influence of shear flow.

A very similar model was developed for a network of associative polymers. A polymer chain is composed from soft spherical monomers and cannot be broken. Some of monomers of the chain are assigned as stickers and can form an associative bond with other stickers. One sticker might form only one associative bond. Again, we obtain a percolating living network. We examine a network structure depending on association energy, number of stickers per chain and solution concentration.

Acknowledgements Authors thank the Russian Foundation for Basic Research (project # 18-03-00698a) for financial support.

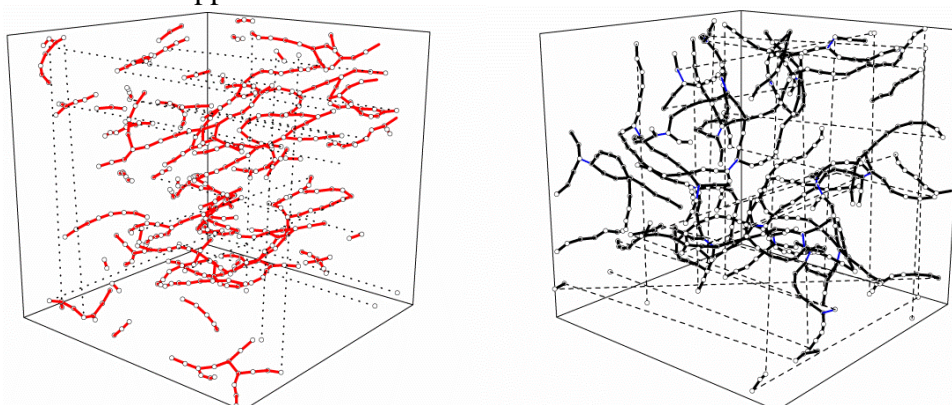


Figure 1. On the left: micellar network under shear flow along x-axis. On the right: associative polymer network.

[1] A.I. Victorov, M.A. Voznesenskiy, E.A. Safonova, *Russ. Chem. Rev.* 2015, 84, 693–711.

[2] I.Yu. Gotlib, et al., *J. Phys. Chem. B* 2016, 120, 7234–7243.

FRIDAY, 21.06.2019

**SECTION 2:: Thermodynamics of Liquids, Fluid
Mixtures, and Phase Equilibria**

Liquid Organic Hydrogen Carriers (LOHC): Thermodynamics of Hydrogenation-Dehydrogenation of Polycyclic Aromatic Hydrocarbons and Nitrogen-Containing Heterocycles

Pimerzin A.A.¹, Verevkin S.P.^{1,2}

¹ Samara State Technical University, Samara, Russia;

²Institute of Chemistry, University of Rostock, Germany

pimerzin.aa@samgtu.ru

The rapid development of renewable energy creates serious prerequisites for the gradual replacement of traditional energy sources by renewable energy. Prospects for the use of alternative energy sources are directly related to the search for efficient ways to accumulate, store and release renewable energy. A successful solution to this problem dictates the use of a new energy source - hydrogen. One of the most effective technologies for the storage and subsequent use of renewable energy is the use of organic compounds that can accumulate hydrogen, forming chemical bonds with it. At the same time, the release of hydrogen is achieved due to the reverse dehydrogenation reaction with the formation of the original organic essential fluid. Thus, the "accumulation - release of hydrogen" cycle, realized with the help of LOHC can be repeated many times.

Aromatics and nitrogen-containing heterocycles have been shown to be the promising LOHC. As a rule, chemical reactions of hydrogenation-dehydrogenation (HYD-DEH) for these classes of compounds are reversible and occur in the presence of catalysts. Obviously, the choice of preferred LOHC samples should be based on a thermodynamic analysis of a system consisting of two forms of organic substrates – saturated and unsaturated with hydrogen.

This paper summarizes the results of our own thermodynamic studies of HYD-DEH reactions of aromatic hydrocarbons and nitrogen-containing heterocycles made in the laboratory of promising technologies of the Samara State Technical University and literature data from this field. Information on the chemical equilibrium of HYD-DEH reactions is compared with reliable thermochemical information and theoretical calculations using composite quantum-chemical methods. A good consistency of the results obtained from all three sources is shown. Approaches have been developed for reliable prediction of chemical equilibrium and thermodynamic characteristics of reactions HYD-DEH of unexplored compounds of interest as promising LOHCs. The results are discussed in terms of the concept of "structure-property" relationships.

Acknowledgments

This research was supported by the Government of Russian Federation (decree №220 of 9 April 2010) agreement №14.Z50.31.0038.

Dielectric Relaxation and Field-Cycling ^1H NMR Relaxometry Studies of Dimethylsulfoxide/Glycerol Mixtures at Low Temperatures

Gabrielyan L.S.¹, Markarian S.A.¹, Flämig M.², Rössler E.A.²

¹ Department of Chemistry, Yerevan State University, 0025 Yerevan, Armenia;

² Nordbayerisches NMR-Zentrum, University of Bayreuth, D-95444 Bayreuth, Germany

lgabriel@ysu.am

The dynamics of pure molecular liquids and their mixtures was extensively investigated in the last decades particularly when being strongly super-cooled and approaching the glass transition temperature T_g . In the present work, dielectric as well as proton field-cycling (FC) NMR spectra of mixtures of glycerol and dimethyl sulfoxide (DMSO) at high viscosities over a large concentration range are presented. A number of solvents are known to protect living cells against freezing including glycerol, ethylene glycol and DMSO. Glycerol is one of the most studied glass formers, and it is known, that compared with glycerol, DMSO is considerably more permeable across membranes.

The relaxation dynamics of DMSO/glycerol binary mixtures is studied by dielectric relaxation spectroscopy (by means a high resolution Alpha-A analyzer from Novocontrol Technologies) in the whole concentration range for the frequencies between 10^{-2} and 10^7 Hz and wide temperature range from 90 to 323 K. The FC NMR technique provides the frequency dependence ($10^4 - 3 \cdot 10^7$ Hz) of the spin-lattice relaxation rate which is transformed to the susceptibility representation and thus allows directly comparing NMR and dielectric spectroscopy results. The permittivity spectra in these mixtures reveal a single relaxation process, which is described by a Cole-Davidson function (Fig. 1). The temperature dependence of relaxation times follows the Vogel-Fulcher-Tammann law. The concentration dependences of various parameters, such as static dielectric permittivity, glass transition temperature, fragility etc. are also obtained. It is shown, that the spectral shape does not change with temperature as well as with concentration. Thus, mixing of the two liquids leads to a change of $\tau(T)$, only. It appears that although DMSO is an aprotic liquid the molecule is continuously incorporated in the hydrogen network of glycerol without changing the overall nature of the hydrogen bond network structure.

Acknowledgements This work was partially supported by the RA MES State Committee of Science, in the frame of the research project N 18T-1D086.

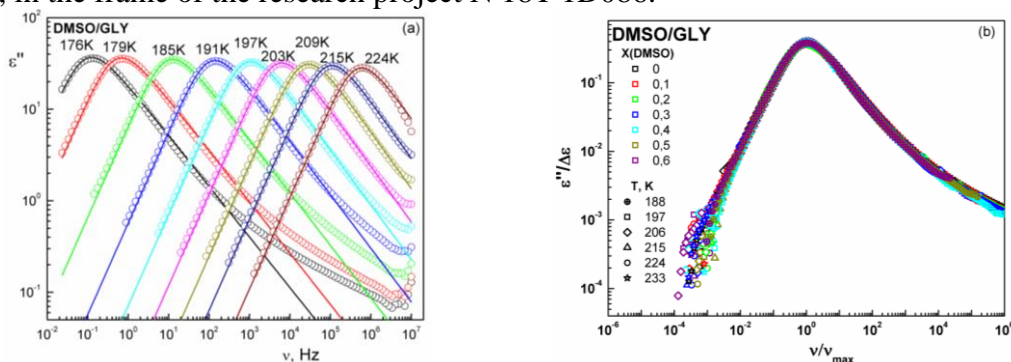


Figure 1. (a) Dielectric loss spectra of DMSO/glycerol mixture ($X_{\text{DMSO}}=0.5$) at various temperatures, (b) dielectric loss spectra as master-curve ($\epsilon''/\Delta\epsilon - (\nu/\nu_{\text{max}})$) at various concentrations ($0 \leq x_{\text{DMSO}} \leq 0.6$) and temperatures (188-233 K).

[1] L.S. Gabrielyan, S.A. Markarian, M. Flämig, E. Rössler, *J. Phys. Chem.*, 2019, to be submitted.

Thermodynamics of Perfluoroorganic Compounds and the Additive Scheme of Calculation of Vaporization Enthalpies

Pashchenko L.L.¹, Druzhinina A.I.¹, Miroshnichenko E.A.²

¹Department of Chemistry, Lomonosov Moscow State University, Moscow, Russia;

²Semenov Institute of Chemical Physics, Russian Academy of Science, Moscow, Russia

lara.paschenko@gmail.com

Perfluoroorganic compounds (PFOC) are promising as components of aqueous emulsions artificial hemoconcealer, currently used in medical practice. In this work the temperature dependence of the saturation vapor pressure, p_s , of perfluorooctylbromide, $C_8F_{17}Br$, was determined by comparative ebulliometry over the moderate “atmospheric” pressure range from 8.4 to 101.6 kPa. The apparatus has been used for the determinations of the vapor pressure in the temperature range from 298 to 461 K. Temperature(T) measurements are carried out by means of platinum resistance thermometers ($R \sim 100 \Omega$) at 20 fixed pressures maintained automatically by a mercury-contact manometer. The total errors of the temperature - pressure measurements were evaluated as $S_T = \leq 1 \cdot 10^{-2} K$ and $S_p = 13 \div 26 Pa$, respectively. The experimental values ($p_s(T)$) were fitted by the semi-empirical equation, was derived by integration of the Clausius - Clapeyron equation. The standard vaporization enthalpies, $\Delta_{vap}H^0$ of PFOC were estimated by micro calorimeters Wadso and Calvet. Densities of $C_8F_{17}Br$ have been measured by picnometrical method in the small temperature range from 293 to 343 K with the accuracy $\leq 1 \cdot 10^{-4} g \cdot cm^{-3}$.

A second-order group additive scheme has been applied using full-matrix, least-squares method to predict the vaporization enthalpies of PFOC. To decrease the differences between the experimental and estimated values, we apply more extended parameterization, which considers next to nearest-neighbor interaction in the molecule. The enthalpies of vaporization are calculated from the formula

$$\Delta_{vap}H^0 = \sum_{i=1}^n H_i \cdot m_i,$$

where m_i is the linear independent numbers of atom groups in molecule, and H_i is the group value (Table 1). The values of H_i were calculated by least-squares method (LSM) on the basis of the enthalpies of vaporization obtained in this work and taken from the literature or investigated ours earlier for some perfluoroalkanes, perfluoroalkylcyclohexanes and *cis*- and *trans*-perfluorodecalines. The estimated values $\Delta_{vap}H_{est}$ for twelve PFOC are in good agreement (0.7 %) with experimental ones, $\Delta_{vap}H_{exp}^0$. The differences ($\Delta_{vap}H_{exp}^0 - \Delta_{vap}H_{est}$) for the three compounds, which were not included in scheme, are ranged from 0.02 to 0.8 $kJ \cdot mol^{-1}$ ($\leq 2 \%$).

Table 1 Listing of groups and group values of some perfluoroorganic compounds

Group*	Constants H_i	Group values ($kJ \cdot mol^{-1}$) for			
		Perfluoro-alkanes	Perfluoro-cyclocarbons	Perfluoro-dicyclocarbons	1-Br-(PFOC)
C-(C _F)(F) ₃	H_1	6.94 ± 0.11			
C-(C _F)(F) ₂	H_2	4.53 ± 0.04			
C-(C _F) ₃ (F)	H_3	1.33 ± 0.20			
C _c -(C _F) ₂ (F) ₂	H'_2		4.91 ± 0.04		
C _c -(C _F) ₃ (F)	H'_3		2.54 ± 0.18		
C _{c.d.} -(C _F) ₃ (F)	$H''_{3(trans)}$			3.08 ± 0.15	
	$H''_{3(cis)}$			3.47 ± 0.15	
Br-(C _F)(F) ₂	H_4				9.05 ± 0.15

*C_F denotes a carbon atom connected with the fluorine atom; C_c and C_{c.d.} denote a carbon atom in a monocycle and a carbon atom, which is common for two cycles, respectively.

Influence of Salts on the Phase Behavior of Ternary Liquid Systems with a Closed Delamination Field

Cherkasov D.G., Smotrov M.P., and Il'in K.K.

Saratov State University named after N.G. Chernyshevsky, Saratov 410012, Russian Federation

ilinkk@info.sgu.ru

The interest in ternary liquid systems with a closed delamination field is due to their introduction into production practice as non-traditional extraction systems. Introduction of salts with a salting-in or salting-out effect into such systems makes it possible to control the temperature-concentration range of the delamination field and, therefore, to optimize the corresponding technological process. However, polythermal studies of the phase diagrams of the appeared quaternary systems salt + three solvents have almost not been undertaken, no schemes of their topological transformation with temperature changes have been developed, and no regularities of their transformation have been revealed.

The purpose of our study was to reveal regularities of the influence of salts with salting-in and salting-out effects on the phase behavior of a ternary liquid system with a closed delamination field in a wide temperature range at constant pressure. The previously studied water + pyridine + butyric acid system was chosen as the ternary liquid system, whose phase diagram contains a closed delamination field disappearing above 52.0°C [1]. Three quaternary systems were modeled, namely:

No	System	Number of cuts	t , °C
1	Potassium chloride + water + pyridine + butyric acid	3	5–90
2	Potassium nitrate + water + pyridine + butyric acid	3	5–90
3	Potassium iodide + water + pyridine + butyric acid	6	5–145

The following phase states were found in the component mixtures of all the systems studied: monotectics, delamination, saturated and unsaturated solutions. It was found that even small concentrations of potassium chloride, which has a strong salting-out effect, in mixtures of the components of system (1) led to a significant decrease in solubility in the ternary liquid system. Potassium nitrate (system 2), which has a larger anion radius as compared to KCl, had a weaker salting-out effect on the mixture components of the ternary liquid system. In addition, it was found that small concentrations of potassium nitrate (up to ~5 wt. %) were also able to have a weak salting in effect upon water-organic mixtures within 25–40°C. When studying the component mixtures of this system, a method was proposed for locating the critical end point, the critical tie line of the monotectic state in the quaternary systems salt + three solvents.

For the first time, it was revealed that low KI concentrations (~6 wt. %) in system (3) had a strong salting-in effect on the heterogeneous mixtures of the ternary liquid system, leading to their complete homogenization even at relatively low temperatures. Increasing the concentration of KI with a simultaneous temperature increase led to the loss of the saltin-in properties and transition to salting-out. Therefore, the salt at any concentrations and temperatures cannot have a salting-in effect only.

In systems (1), (2) and (3), the invariant temperature of contact between the fields of two monotectic phase states by critical tie lines inside the composition tetrahedron was estimated, whose value was proposed to be used for comparative evaluation of the salting out effect of a salt upon ternary liquid mixtures. It has been established that the value of this temperature increases with an increase in the salt anion radius in the row $\text{Cl}^- - \text{NO}_3^- - \text{I}^-$, and the salting out effect decreases.

[1] D.G. Cherkasov, M.P. Smotrov. K.K. Ilin, *Rus. J. Appl. Chem.* 2008. 81. 218.

Conformational Equilibrium and Polymorphism of Mefenamic Acid in Supercritical Carbon Dioxide

*Oparin R.D.*¹, *Krestyaninov M.A.*¹, *Idrissi A.*², *Kiselev M.G.*¹

¹ Institute of Solution Chemistry of Russian Academy of Sciences, Ivanovo, Russia; ²Laboratoire de Spectrochimie Infrarouge et Raman, Université de Lille, France

r.d.oparin@yandex.ru

In this work, we have studied the conformational equilibrium of mefenamic acid (MA) molecules diluted in supercritical carbon dioxide (scCO₂) being in contact with MA crystalline form under isochoric heating conditions in the temperature range of 80–220°C and pressure range of 172–460 bar that are corresponding to the 1.10 value of critical density of CO₂. For this study we used designed by us the high-pressure-high-temperature optical cell. A combination of experimental (*in situ* IR and *in situ* Raman as well as micro IR and micro Raman spectroscopy) and computational (quantum chemical calculations) methods has been applied for this study.

Preliminary conformational search has been performed within quantum chemical calculations. It was based on the analysis of the potential energy surface scan. The structure of each conformer corresponded to the local minimum of potential energy, which was confirmed by frequency calculations. 16 MA conformers have been discovered, and 4 most stable conformers were further taken into account. The calculated vibration parameters of certain functional groups of these conformers have been further used for analysis of IR spectral data.

On the base of *in situ* IR spectroscopy results it has been found that the temperature increase in the range of 80–160°C results in increase of concentration of MA in scCO₂ fluid phase. However no conformational transitions of MA molecules are observed. With further heating up to 190°C the MA concentration in scCO₂ phase continues increasing. At the same time the conformational transitions of acid molecules occur. Upon staying of the binary system MA - scCO₂ at T=190°C the full transition of the first conformational state into the second one takes place. An analysis both of MA crystalline form being in contact with scCO₂ and MA form under ambient pressure by *in situ* Raman spectroscopy has shown that above 160°C the probability of its polymorphic transformation arises. However a full polymorphic transformation occurs only at 190°C.

It has been also shown that the presence of a supercritical fluid medium reduces the melting temperature of mefenamic acid to 190°C from 230–232°C (at normal pressure). This phase transition linked with melting of MA leads to the occurrence of critical phenomena in system. However when the temperature is increased further (up to 220°C) these critical phenomena disappear. Along with this in the temperature range of 200–220°C in scCO₂ phase MA exist only in the second conformational state.

An additional analysis of processed and crystallized from scCO₂ medium MA samples by micro IR and micro Raman spectroscopy has shown that these samples are pure polymorph II. It has been also found that a thermal decomposition of MA does not occur up to highest temperature studied.

Thus it has been found that there are clear correlations between the polymorphic modifications of the MA crystalline form and the conformational manifold of its molecules in the scCO₂ phase when they are in equilibrium with each other. Namely, it has been proved that in the case of interface of two phases the certain polymorph of the crystalline form provokes the formation of the corresponding conformer in the supercritical solution phase.

Acknowledgements This work was supported by the Russian Foundation for Basic Research (grants No. 18-03-00255 and 17-03-00459) and by Russian Government contract N. 01201260481

Joint Approximation of Enthalpy Increments and Heat Capacity Data for Substances in the Condensed State

Sineva M.A.¹, Aristova N.M.¹, Belov G.V.^{1,3}, Lavrinenko Ya.^{1,2}, Morozov I.V.^{1,2}

¹Joint Institute for High Temperatures of Russian Academy of Sciences, Moscow, Russia;

²Moscow Institute of Physics and Technology, Dolgoprudny, Russia;

³Department of Chemistry, Lomonosov Moscow State University, Moscow, Russia

maria.a.sineva@gmail.com

Experimental data on thermodynamic properties of substances in the condensed state require fitting with approximation functions to be used for thermodynamic modeling and other studies. Filling databases (IVTANTHERMO, NASA etc.) with new information requires fitting data with preset polynomials [1-2]. There are various codes for processing thermodynamic data. Some of them are meant for low-temperature heat capacity, others for high temperature data. There is a significant amount of methods for processing data on enthalpy increments obtained by classic calorimetry.

A new computer program based on a combination of fitting algorithms is proposed for analyzing experimentally obtained enthalpy and heat capacity of substances in the condensed state. The program is supposed to unite all processing steps to combine and analyze available data of several types simultaneously. The program comes in the forms of a standalone application and web application. The enthalpy increment data can be fitted by a polynomial of a chosen degree which can be used at the next step to process heat capacity dependence on temperature. Provided the user has high temperature heat capacity experimental data, it can be fitted by a polynomial combined of elementary functions picked manually or by preset combinations. The results can be exported in various database formats.

The application was used for processing data on thermodynamical properties of uranium dioxide [3].

The work is supported by the Basic Research Program of the Presidium RAS “Condensed matter and plasma at high energy densities” (coordinated by Fortov V.E.).

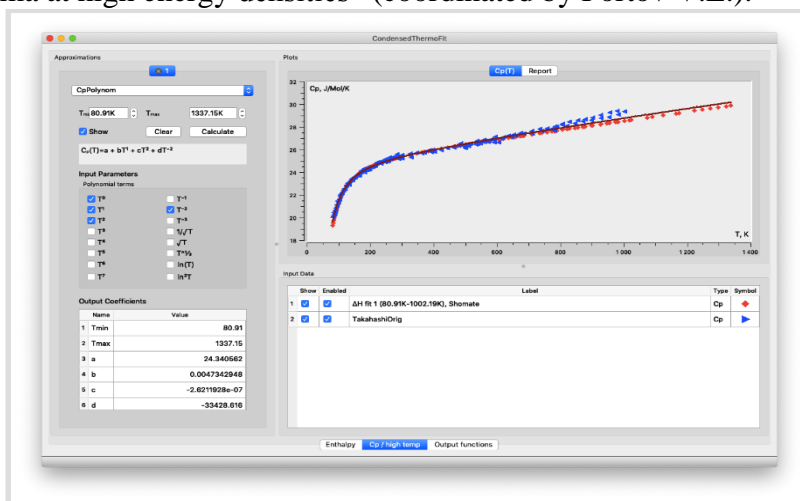


Figure 1. General view of the application's interface: fitting of the heat capacity

[1] G.V. Belov, N.M. Aristova, I.V. Morozov, M.A. Sineva. *J. Math. Chem.* 2017 55 1683.

[2] G.V. Belov, S.A. Dyachkov, P.R. Levashov et al // *J. Phys. Conf. Ser.* 2018. V. 946 P. 012120.

[3] N.M. Aristova, G.V. Belov, I.V. Morozov, M.A. Sineva // *High Temperature.* 2018. V. 56, No. 5. P. 652–661.

FRIDAY, 21.06.2019

**SECTION 1: Development of General Methods and Tools
of Chemical Thermodynamics: New Experimental
Techniques, Theory and Computer Simulation**

Driving Forces of the Clustering in Solutions

Medvedev N.N.^{1,2}

¹Novosibirsk State University, Novosibirsk, Russia;

²Institute of Chemical Kinetics and Combustion, SB RAS, Novosibirsk, Russia

nikmed@kinetics.nsc.ru

It is usually considered that the clustering in solutions is determined, mainly, by the direct interaction between molecules, at least at relatively low concentrations of solutions. In addition, it is well known that in aqueous solutions there is a so-called hydrophobic interaction, leading to the association of the dissolved molecules due to the restructuring of the hydrogen bond network around the resulting cluster. The next important factor contributing to the clustering of dissolved molecules is related to the impermeability of atoms and molecules - the effect of excluded volume. It defines the condensed phase and is essential at high concentrations of the solution, where the role of specific interactions becomes secondary in the structural organization. However, we draw attention to the fact that even at sufficiently small concentrations, the effect of the excluded volume should be taken into account. This is indicated by our recent results obtained from molecular-dynamic simulation of aqueous solutions of trimethylamineoxide. It was found that the spatial distribution of these molecules in a solution resembles the distribution of randomly thrown impermeable spheres in a fairly wide range of concentrations. In addition, we note that the "hydrophobic interaction", understood as the "water-mediated" interaction between the dissolved molecules, should have a broader meaning. It exists not only between hydrophobic molecules, or between molecules that have pronounced hydrophobic parts (such as tert-butanol), but also without such parts (for example, urea). Thus, the reorganization of the hydrogen bond network, facilitating the association, also takes place for other molecules that are usually not considered as hydrophobic.

From the study of molecular dynamic models of aqueous solutions of various non-electrolytes (osmolytes, alcohols), we conclude that even for fairly small concentrations, when interpreting the structure of the solution, all three above-mentioned driving forces should be considered simultaneously. Only in this case, it is possible to get reliable conclusions about the nature of the formed clusters and about the structure of the solution as a whole.

Acknowledgements The financial support of RFBR №18-03-00045

Thermodynamics of Melting/Freezing Transition in Molecular Layers from a Monte Carlo Simulation: a Direct Evaluation of the Chemical Potential

Ustinov E.A.

Ioffe Institute, Russian Federation

eustinov@mail.ioffe.ru

Over the past decades a great attention was paid to molecular modeling of the two-dimensional liquid-solid phase transition in molecular layers adsorbed on a substrate surface. The main obstacle in this way stems from a considerable difficulty in evaluating the chemical potential of the ordered monolayer directly by a molecular simulation. To circumvent this problem several tricks have been proposed to allow a thermodynamic integration based on an idea of the Einstein crystal, Wigner-Seitz cell, λ -integration method and so on. Although those methods are accurate, they are technically quite involved and time-consuming.

In this study an alternative approach is proposed on the basis of a kinetic Monte Carlo (kMC) algorithm and a method of external potential imposed on the elongated simulation cell [1,2]. This technique is illustrated in Fig. 1 for the system H_2 – graphite at 20 K. The hexagonally packed hydrogen molecular layer is placed in the central section of the cell. Due to the external potential (the lower panel in Fig. 1) imposed on the left and right sides of the cell, the intrinsic chemical potential is lower than that in the central section and, therefore, hydrogen presents there as the gas phase. The intrinsic and the total chemical potential can be easily determined in the gas fractions in the framework of kMC. Since at the equilibrium the total chemical potential is the same over the cell, it coincides with that of the crystalline layer. An important advantage of this method is that the lattice constant and the tangential pressure are self-adjusting parameters. The chemical potential is determined *directly* and the melting transition can be modeled by gradual changing the external potential or the number of molecules in the cell.

An interesting feature has been established [3] that the van der Waals loop in the range of the liquid-solid transition is an artefact of a small simulation cell and it disappears when the number of molecules exceeds several thousand in the cell with the uniform density distribution. This means that the chemical potential of the transition zone can be determined directly with the kMC or by the thermodynamic integration.

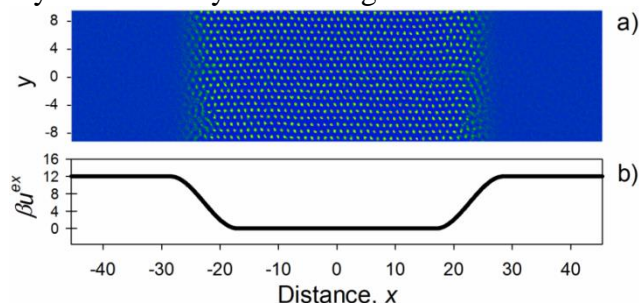


Figure 1. (a) Density distribution of hydrogen over the simulation cell at 20 K. The number of molecules is 900. (b) The external potential imposed on the cell.

[1] E. A. Ustinov, *Carbon*, 2016, 100, 52.

[2] E. A. Ustinov, *J. Chem. Phys.*, 2017, 147, 014105.

[3] E. A. Ustinov, *J. Phys. Chem. C*, 2018, 122, 23591.

Application of the Specific Ion Interaction Theory for Investigation of Indium (III) Complexation

Ukhov S.A.

Kaluga Branch of the N.E. Bauman Moscow State Technical University, Kaluga 248000, Russia

ukhov-s@mail.ru

The principal aim of this work is the development of modeling of indium (III) state in some aqueous solutions in a wide range of components concentrations for description and prediction of its electrochemical and chemical behaviour. The specific ion interaction approach is applied. According to Brønsted-Guggenheim-Scatchard's model (Specific ion Interaction Theory, SIT) [1] logarithm of molal activity coefficient of aqueous species i is equal to:

$$\lg \gamma_i = -z_i^2 \cdot \frac{0.51 \cdot \sqrt{I_m}}{1 + 1.5 \cdot \sqrt{I_m}} + \sum_j \varepsilon(i, j, I_m) \cdot m_j,$$

where z_i is the charge of i , m_j is the molality of the ion j , $\varepsilon(i, j, I_m)$ is the specific interaction coefficient (SIC) between i and j , in a solution of I_m molal ionic strength. At that, $\varepsilon(i, j) = \varepsilon(j, i)$, $i \neq j$. The thermodynamic overall complexes formation or hydrolysis constants ($\lg \beta^{m_0}$) were calculated (see table 1.). The quotients of cationic and anionic complexes parts in SIC are separated according to empiric Ciavatta's approach (with $\varepsilon(\text{In}^{3+}, \text{ClO}_4^-) = 0.50$, $\varepsilon(\text{In}^{3+}, \text{Cl}^-) = 0.3$, $\varepsilon(\text{Na}^+, \text{SO}_4^{2-}) = -0.12$): $\varepsilon(\text{In}_p \text{A}_n (\text{OH})_r^{3p-2n-r}, \text{N}^+ + \text{X}^-) = K_K \cdot \varepsilon(\text{In}^{3+}, \text{X}^-) + K_A \cdot \varepsilon(\text{A}^{z-}, \text{N}^+) + K_{\text{OH}} \cdot \varepsilon(\text{OH}^-, \text{N}^+)$

Comparison of results with Pitzer's and others data [2] shows adequacy of the SIT approach.

Table 1. Molal thermodynamic parameters of indium (III) ionic equilibria in aqueous solutions.

Species $\text{In}_p \text{A}_n (\text{OH})_r^{3p-2n-r}$	$\lg \beta^{m_0}$	K_K	K_A	K_{OH}
InCl^{2+}	3.278* ÷ 3.351**	35.0/50	0.6/3.8	
InCl_2^+	5.236	30.2/50	0.0/3.8	
InCl_3^0	5.488*	16.0/50	3.0/3.8	
InCl_4^-	4.42	11.6/50	7.4/3.8	
InCl_5^{2-}	2.735	1/6	(5/6) · $K_A(\text{InCl}_6^{3-})$	
InCl_6^{3-}	0.706	0.00	36.2/12.5 (H^+) 11.9/3.8 (Na^+) 36.1/11 (Li^+) 2.959 (K^+)	
$\text{In}_2\text{Cl}^{9+}$	1.83	10/6	2/4	
InOH^{2+}	-3.447	29.0/50		0.7/4.0
$\text{In}(\text{OH})_2^+$	-6.877*	17.2/50		2.8/4.0
$\text{In}(\text{OH})_3^0$	-12.4***	8/50		4/4.0
$\text{In}_2(\text{OH})_2^{4+}$	-5.172	8/6		4/4
$\text{In}_4(\text{OH})_6^{0+}$	-14.921	12/6		12/4
InOHCl^+	0.244	23.7/50	0.0/3.8	1.4/4.0
$\text{In}_2\text{OHCl}^{4+}$	0.116	8/6	2/4	2/4
InSO_4^+	3.890	10.9/50	2.6/12	
$\text{In}(\text{SO}_4)_2^-$	5.620	19.2/50	9.2/12	
$\text{In}(\text{SO}_4)_3^{3-}$	4.74	0.00	49.0/12 (Na^+) 9.9/3 (H^+) ***	

* – NaClO_4 , ** – HClO_4 , *** – estimated. $I_m = 0 - 6 \text{ mol/kg}$, $T = 20 (\text{SO}_4^{2-}) - 25 \text{ }^\circ\text{C}$, $\text{pH} < 5.5$.

[1] C. Bretti, C. Foti, N. Porcino, S. Sammartano, *J. Solut. Chem.*, 2006, 35(10), 1401-1415.

[2] B. Radionov, G. Maltsev, *Indium in aqueous solutions*, 2014, 352 p. LAP, Saarbrücken. in Rus.

A Promising Hybrid Methane Hydrate Inhibition on the Basis of Polyurethane for Hydrate Management Risk: Thermochemistry, Kinetics and Phase Behavior

Varfolomeev M.A., Farhadian A.

Department of Physical Chemistry, Kazan Federal University, Kremlevskaya str. 18, 420008 Kazan, Russian Federation

Mikhail.Varfolomeev@kpfu.ru

Formation of gas hydrates is a problem in the petroleum industry where the gas hydrates can cause blockage of the flow lines. This is an important topic in the chemical thermodynamics and phase equilibrium fields. Kinetic hydrate inhibitors (KHIs) and Anti-Agglomerant hydrate inhibitors (AAs) are two main types of inhibitors that are used to prevent gas hydrate blockages and they have been used in the field successfully. In this study, we present a powerful and completely soluble in water class of KHI/AAs based on polyurethane. The hydrate inhibition performances of KHIs were assessed in a high-pressure autoclave cell through two kinds of onset times of hydrate formation: the time when hydrate crystals are initially observed by naked eyes, and the time when rapid and continuous dropping of system pressure begins. The phase diagrams of binary mixture of methane and water or aqueous solutions of inhibitors were studied in details. Also, the performance of this new KHI was investigated by high-pressure micro-differential scanning calorimeter (HP- μ DSC). The thermochemistry of phase transitions (hydrate formation and decomposition) was measured. The results of both analyses demonstrated the best performance of these inhibitors in delay induction time (5-18 times) and reduce hydrate growth rate (2.7 times), also they would not increase hydrate dissociation temperature in comparison with pure water. Since it has been reported that, the highest resistance-to-flow was observed for systems with around 60% water-cut, where sharp and periodic local maxima in the torque were observed in the autoclave. To simulate the mixture of water and liquid hydrocarbon encountered in flow lines, decane was added corresponding to an initial 60% water-cut. The torque remained stable during the hydrate onset and growth, suggesting the hydrate formed in the presence of WPUUs did not aggregate or deposit inside the autoclave and show the AAs performance of WPUUs. This study introduces both kinetic hydrate inhibition and anti-agglomeration using waterborne polyurethane polymers. These results suggest that the waterborne technique can be utilized as a hybrid hydrate inhibitor because kinetic hydrate inhibition performance can be coupled with the anti-agglomeration performance of the base waterborne polyurethanes.

Acknowledgements: This work has been carried out on the basis of the Russian Government Program of Competitive Growth of Kazan Federal University and was supported by the Russian Foundation for Basic Research Project N 18-05-70121.

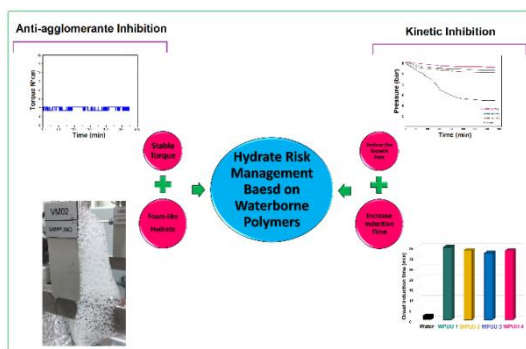


Figure 1. Waterborne polyurethane polymers as KHI/AAs.

Transformation from 2nd to 3rd Generation of Critically Assessed Thermodynamic Data for the Elements

Khvan A.V.¹, Dinsdale A.T.²

¹Thermochemistry of Materials SRC, NUST MISIS, Russia;

²Hampton Thermodynamics Ltd, UK

avkhvan@gmail.com

The second half of the 20th century has seen a rapid development of computer techniques in materials science including the methods of computational thermodynamics, a large part of which were gathered together under the umbrella of the scientific field and society entitled “Calculations of Phase Diagrams and Thermochemistry (CALPHAD)”. A significant step in the CALPHAD development took place between 1985 and 1991 when SGTE developed and published its database for the pure elements [1]. This database now forms the basis for almost all thermodynamic assessments for alloy systems and is the backbone of all commercial thermodynamic databases, which are widely used by materials scientists for the prediction of materials properties and also for the control of industrial plants and processes. However, now, there is growing awareness that these data and the way in which they are modelled will not be suitable for the needs of the materials science community for the next 25 years. A collaborative international research program is underway towards the development of a new set of data based on more physically realistic models to represent the variation of the thermodynamic properties of the crystalline and liquid phases with temperature and composition.

These models are based on the results of a series of “Ringberg” workshops [2-3] which laid down the fundamental basis which could be used to generate the new sets of data. The new models are more complicated to use and require also serious changes in modelling of data in binary and ternary systems.

In the present talk we will discuss the reasons for the transformation from the 1991 SGTE Pure elements database (2nd generation CALPHAD), describe the new models and highlight some of the implications for the critical assessment of data using some recent examples where they have been applied.

Acknowledgements The work was carried out with financial support from the Ministry of Education and Science of the Russian Federation in the framework of Increase Competitiveness Program of NUST «MISiS» (№K2-2019-003), *implemented by a governmental decree dated 16th of March 2013, N 211*

[1] A. T. Dinsdale, *Calphad*, 1991, 15, 317.

[2] M. Chase, I. Ansara, A. Dinsdale, G. Eriksson, G. Grimvall, H. Hoglund, H. Yokokawa, *Calphad*, 1995, 19, 437.

[3] J. Ågren, B. Cheynet, M.T. Clavaguera-Mora, K. Hack, J. Hertz, F. Sommer, U. Kattner. *Calphad*, 1995, 19, 449

Vaporization Thermodynamics of Tetramethylammonium Iodide Revisited: a Multitechnique Investigation

Brunetti B.¹, Ciccioli A.², Latini A.², Panetta R.², Patterson E.V.³, Vecchio Cipriotti S.⁴

¹Istitute for Nanostructured Materials, CNR, Sapienza University of Rome, Department of Chemistry, Italy;

²Sapienza University of Rome, Department of Chemistry, Italy;

³Stony Brook University, Department of Chemistry, USA

⁴Sapienza University of Rome, Department of Basic and Applied Science for Engineering, Italy

andrea.ciccioli@uniroma1.it

Alkylammonium lead halide perovskites are currently considered with great hope as possible light harvesting materials for photovoltaic devices. However, it is now well-known that their low thermal and chemical stability is a serious drawback for large-scale applications. Therefore, the investigation of the thermal decomposition pathways of these materials is important to put in place effective protection strategies and to identify possible chemical modifications [1].

To this end, the study of thermodynamic and kinetic properties of the thermal decomposition of simple alkylammonium halides, which has been the subject of a number of studies in the past [2], is becoming again of interest [3] as a first step to tackle the more complex study of the corresponding perovskites.

The vaporization/decomposition behaviour of tetrasubstituted ammonium halides (R_4NX , $X = Cl, Br, I$) is expected to take place by processes different from those displayed from mono-, di- and trisubstituted ones due to the lack of hydrogen atoms bound to the nitrogen atom. Indeed, the latter may in principle follow at least two different decomposition pathways [4], according whether the N-H or the N-C bond is broken, with formation of HX or RX, respectively, in the gas phase:



where $p = 1, 2, 3$. For tetrasubstituted halides R_4NX ($p = 4$), only process (2) can take place, with formation of R_3N and RX . However, although often overlooked in the literature, the vaporization as gaseous “intact ion pair” $R_4NX(g)$ cannot be ruled out.

In this work, we present the results of a combined experimental/computational study aimed at clarifying the vaporization behaviour of tetramethylammonium iodide, $(CH_3)_4NI$. Knudsen Effusion Mass Loss and Knudsen Effusion Mass Spectrometry measurements were carried out in the overall temperature range 440-540 K, as well as combustion calorimetry and TG-DTA experiments, in order to get new information on the thermal decomposition pathway of this compound and related thermodynamic properties. The results obtained from the different techniques are compared and discussed with the help of theoretical calculations.

[1] A. Ciccioli, A. Latini, *J. Phys. Chem. Lett.*, 2018, 9, 3756.

[2] M. Sawicka, et al., *Chem. Phys.*, 2006, 324, 425.

[3] I.L. Ivanov, et al., *Thermochim. Acta*, 2017, 658, 24.

[4] Juarez-Perez, et al. *Energy Environ. Sci.*, 2016, 9, 3406–3410.

FRIDAY, 21.06.2019

**SECTION 5: Thermodynamics of Functional Materials
and Engineered Self-Assembly**

High-Temperature Thermodynamic Properties and Thermal Expansion of Some RE Tantalates for TBC Materials

Gavrichev K.S.¹, Guskov V.N.¹, Ryumin M.A.¹, Tyrin A.V.¹, Khoroshilov A.V.¹, Ashmarin A.A.²

¹ Kurnakov Institute of General and Inorganic Chemistry, RAS, Russia;

² Baikov Institute of Metallurgy and Materials Science, RAS, Russia

gavrich@igic.ras.ru

Application of new materials allows to increase the efficiency of power plant turbine. One of the ways to improve the efficiency and lifetime of the turbine is the use of thermal barrier coatings (TBC), which allows to increase the temperature of gases acting on the turbine blades. Requirements for such materials (such as high melting point, absence of phase transformations, low thermal conductivity, low ionic conductivity, compatibility with the metallic material of the part (superalloy)) significantly limit the range of substances that can be used as TBC materials.

We believe that RE tantalates are the promising substances for TBC materials, because they meet the most of specified criteria.

RE orthotantalates $RETaO_4$ (RE = Nd, Sm, Gd, Y, Dy, Yb, Lu) were synthesized by the reverse sedimentation with the following drying and calcination at temperatures above 1200°C. Phase composition and lattice parameters were determined using X-ray diffraction (D8 Advance XRD diffractometer, Bruker). DSC/TG study and measurement of high-temperature heat capacity in the range 25-1200°C were conducted in Netzsch STA 449 F1 Jupiter. Measurements of temperature dependences of lattice parameters were carried out in the range 25-900°C in Shimadzu X-ray diffractometer with HA-1001 high-temperature chamber. Thermal expansion coefficients were calculated based on variation of lattice parameters.

It is known that RE tantalates crystallize in monoclinic M' and M structures, which undergo the reversible phase transition to tetragonal phase at very high temperatures.

Detailed X-ray study of composition of obtained specimens revealed that it is possible to synthesize the M monoclinic single-phase substance only at annealing above 1200 C, while at lower temperatures the mixture of M' and M phases.

DSC study and heat capacity measurements demonstrated the absence of phase transitions in M -phase for (Nd, Sm, Gd, Y)TaO₄ and in M' -phase for (Yb, Lu)TaO₄ in the region 25-1200°C. Obtained experimental data on heat capacity of $RETaO_4$ were fitted by the Meier-Kelley equation. Based on the obtained results we proposed that M modification is stable for RE=Nd, Sm, Gd, Y, Dy, while M' -metastable one. For ytterbium and lutetium orthotantalates M' -phase is stable in the range 25-1200°C.

Acknowledgements. The financial support of Russian Science Foundation (grant 18-13-00025) is highly appreciated.

In a Search for Enhanced Secondary Electron Emission: is there any Component Interactions in MgO-RuO₂ System?

Zherikova K.V.¹, Vikulova E.S.¹, Vasilyeva I.G.¹, Zabuslaev S.V.²

¹ Nikolaev Institute of Inorganic Chemistry SB RAS, Russia;

² JSC Katod, Russia

ksenia@niic.nsc.ru

High-emission materials are in demand in a wide field of practical application: from photomultipliers, electron multipliers, which are important elements of many high-precision devices (mass spectrometers, night vision devices, thermal imagers, cosmic radiation transmitters, etc.) to plasma displays. Currently, MgO coatings are the most common materials among the film emitters of secondary electrons for signal amplifiers, the most effective of which is turned out to be obtained by gas-phase processes. Obviously, a non-conductive material cannot maintain a high level of emission for a significant period of time due to surface charging. Thus, it is necessary for the effective functioning of MgO emitters to “run off” a positive charge. It can be achieved by heterogeneous doping of the oxide lattice and/or forming composites with a conducting layer.

So, in a search for enhanced secondary electron emission materials we used Metal Organic Chemical Vapor Deposition to obtain MgO+RuO₂ films. Among the wide variety of gas phase deposition methods, the MOCVD method has several principal advantages. First of all, it is a reasonable opportunity to choose precursors which physicochemical properties determine the type of reactions in the reactor and the state of the final product (stoichiometry, purity, dimension, crystallinity). To form multicomponent coatings, the key moment of choice is the thermal compatibility of precursors in co-deposition processes without direct chemical interaction. Thus, the complexes of magnesium and metal dopant (Ru) were selected based on information on their volatility and thermal stability from a database obtained by us and collected from literature. According to the research results, several volatile complexes of magnesium and ruthenium of various classes (beta-diketonates, their derivatives, cyclopentadienyls) were selected, which allowed us to establish how the nature of the precursor affects the emission characteristics of the films. The compounds were synthesized, purified and accurately characterized by melting points, elemental analysis, NMR and IR spectroscopy, mass spectrometry, and X-ray diffraction to confirm their chemical and phase purity. Thermal properties were investigated properly by effusion, transpiration and static methods as well as difference scanning calorimetry in order to get precision information about precursors' saturated vapor pressures in a wide temperature range.

The deposition was performed on planar silicon substrates and unique model objects: “gap structures” with a high aspect ratio, imitating components of modern 3D electron multipliers, for example, microchannel plates. Oxygen and argon were used as reactant and carrier gas respectively. The precursor concentrations were varied by evaporator temperatures. A set of traditional and original methods (X-ray diffraction, scanning electron microscopy, X-ray photoelectron spectroscopy, stoichiographic method of differential dissolution) was applied to study in detail the deposition process of the MgO and RuO₂ thin films and obtain deep sight into film microstructure, phase and chemical composition. The complex investigation was called to answer if there is any interaction between the components of the binary system. It was found that at varying ratios of precursors' vapors, reactant and carrier gases the test films differed considerably in morphology, phase state and especially in mutual spatial distribution on the surface of substrates. The different states of the films also resulted in different emission properties with coefficient of secondary electron emission varying between 7 and 3 eV. Thus, the main factors responsible for the emission properties have been found.

Acknowledgements The study was funded by RFBR according to the research project № 18-08-01105 A.

Formation of Refractory Hafnium- and Tantalum-Containing Compounds on Silicon Carbide Support by the Reactive Chemical Vapor Deposition

Lozanov V.V., Baklanova N.I.

Institute of Solid State Chemistry and Mechanochemistry SB RAS, Russia

lozanov.25@gmail.com

Silicon carbide and SiC-based composites reinforced by SiC or C fiber are widely used for high temperature applications. Their wide usage is due to the formation of glassy SiO₂ layer on the surface that it prevents the further oxidation. However, the reaction between SiC and SiO₂ with formation gaseous SiO and CO (so-called active oxidation) at temperatures above 1400°C leads to vaporization of glass and degradation of the mechanical properties of SiC-based materials [1]. A promising approach to prevent degradation of SiC-based materials is to deposit the protective coatings, e.g. carbides or silicides of early transition metals. These compounds oxidize with the formation of stable oxide scale. Reactive chemical vapor deposition (RCVD) is a convenient method to synthesize the refractory Hf- and Ta-based compounds as thin coatings at temperatures as low as 1000°C. Thus, the aim of the work is the study the formation of the Hf- and Ta-based refractory compounds on the SiC substrate under RCVD conditions.

Earlier it was shown that the fluorine-containing gas phase is one of the promising environment for synthesis of the carbide coatings on carbon substrate at 1000°C [2, 3]. To analyze the heterogeneous equilibria in the M (Hf, Ta) – C – Si – O – F systems of interest and to clarify the possibilities of the carbide and silicide formation on SiC support, the thermodynamic modelling was carried out. The calculation of the gas phase composition showed that the main components of the gas phase over SiC support are the hafnium and silicon fluorides. At the same time, hafnium carbide and silicon are formed as solid phases in the “SiC” zone. The Si : HfC ratio is not equimolar, and silicon can partially dissolve in the gas phase as SiF_x. In the tantalum-containing system, the solid phases, such as TaC and C, are formed in the “SiC” zone. The main components of the gas phase are silicon fluorides. It should be noted that the tantalum fluoride partial pressures in the SiC-rich zone are lower than those in the Ta-rich zone.

The thermodynamic modelling conclusions are in agreement with the results of the RCVD processes in the M (Hf, Ta) – C – Si – O – F systems at 1000°C and total pressure 760 torr. Indeed, the formation of the HfC and HfSi phases on the SiC support was detected in the Hf-containing system. Formation of HfSi phase can be explained by the reaction of silicon with lower fluorides HfF_n (n ≠ 4). In Ta-containing system three phases TaC, Ta₂C and Ta₅Si₃ were formed on the SiC support. Results of thermodynamic modelling are in agreement with XRD and SEM/EDS analysis data. The mechanism of reactions will be discussed.

Acknowledgements. The financial support of Russian Foundation for Basic Research (RFBR) by grant No. 18-29-17013

[1] N.S. Jacobson, D.L. Myers, *Oxid. Met.*, 2011, 75, 1.

[2] V.V. Lozanov, S.V. Sysoev, N.I. Baklanova, *Inorg. Mater.*, 2015, 51, 679.

[3] V.V. Lozanov, S.V. Sysoev, N.I. Baklanova, *Inorg. Mater.*, 2016, 52, 661.

The Identification and Stabilization of New Phases in Ga – S and In – S Systems

Zavrazhnov A.Y.¹, Nekrylov I.N.¹, Brezhnev N.Y.¹, Malygina E.V.¹, Kosyakov A.V.¹, Sidey V.I.², Volkov V.V.³

¹ Voronezh State University, Voronezh, Russia;

² Uzhgorod National University, Uzhgorod, Ukraine;

³ Institute of General and Inorganic Chemistry, Moscow, Russia

alzavr08@rambler.ru

Recently [1, 2] we argued that, in contrast to traditional views on the Ga – S and In – S systems [3, 4], the phase diagrams of these systems are sophisticated in the regions of pre-melting temperatures and concentrations between 50 and 60 mol.% of sulfur. With respect to the Ga – S system, using two independent methods of thermal analysis (DTA and ChTA [1, 2]), it was argued that in a narrow temperature range (877 – 922°C) exists a new phase (σ -phase) with a sulfur content of ~59.0 mol % [1]. Concerning the In – S system we also found a new phase, which exists in a narrow temperature range (~665 – 690°C) and can be described as a polymorphous modification of InS [2]. The concentration region near the 60 % - content of sulfur is complicated for this diagram too: three phases manifest themselves near the A_2B_3 stoichiometry (spinel-type $In_{3-x}S_4$, tetragonal In_2S_3 and high-temperature modification In_2S_3' [2]).

In this work we provide the direct evidences that the high-temperature phase in the Ga - S system (σ -phase) really exists. For that purpose we involved the high-speed quenching procedure and further structural analysis with the use of XRD and transmission electron microscopy (TEM). It was found that the σ -phase has the defect zinc-blende structure ($F\bar{4}3m$, $a = 5.210 \text{ \AA}$). Out of the range of stability this phase simultaneously easily decomposes to the heterogeneous composite of monoclinic Ga_2S_3 (Cc , $a = 11.14$, $b = 6.41$, $c = 7.04 \text{ \AA}$, $\beta = 121.2^\circ$) and layered hexagonal β -GaS ($P6_3/mmc$, $a = 3.59(1)$, $c = 15.47 \text{ \AA}$). Also we made an effort to stabilize this metastable (at room temperature) phase by some impurities. In case of the iron dopant we expanded the temperature range, where the σ -phase exists as stable solid. Due to the introducing of iron into this sulfide we can prepare the phase type as zinc-blende without quenching. The solubility of iron in the σ -phase is very high. It reaches 49 mol.% FeS along the $Ga_{41}S_{59}$ - FeS cross-section of the ternary Fe – Ga – S diagram.

In order to check our results concerning the In – S diagram the similar experiments were done in this system too. Considering the fact that σ -phase in the Ga – S system and the $In_{3-x}S_4$ -phase are similar in composition (molar sulfur content), the features and differences in these structures are considered.

Acknowledgements. This work was supported by RFBR, project 18-33-00900-mol-a.

1. A. Zavrazhnov, S. Berezin, A. Kosyakov et al, *J. Therm. Anal. Calorim.*, 2018, 118, 483
2. S. Berezin, M. Berezina, A. Zavrazhnov, *Inorg. Mater. (Russian)*, 2013, 49, 555-563.
3. V.P. Zlomanov, A.V. Novosyelova *P-T-x-phase diagrams of the metal-chalcogen systems*, 1987. Nauka, Moscow. (in Russian).
4. Greenberg J. *Thermodynamic basis of crystal growth: P-T-X phase equilibrium and non-stoichiometry*, 2002. Springer-Vcrlag Berlin Heidelberg.

The Thermodynamic Approaches for Zirconia Based Precursors and Ceramics Investigation

Kurapova O.Y., Shugurov S.M., Lopatin S.I., Vasil'eva E.A., Konakov V.G.

St. Petersburg University, Department of physical chemistry, St. Petersburg, Russia

o.y.kurapova@spbu.ru

Due to their exceptional anion conductivity at high temperatures cubic zirconia solid solutions are widely used as solid electrolyte (SE) materials in different electrochemical devices. However the search of the optimal ceramic compositions for their long-term use in the aggressive atmosphere of industrial processes remains a great challenge for science and technology. The precise knowledge of the thermochemical data on thermal prehistory, temperature and concentration dependence of the electromotive force (EMF) on ambient oxygen, temperatures makes it possible to develop high-performance zirconia based SE for in-situ measurements at extremely high temperatures in the aggressive ambience. Thus the goal of the present work was the detailed investigation of thermochemical behavior of M_xO_y - ZrO_2 systems ($M = Ca^{2+}, Y^{3+}, Ce^{4+}, La^{4+}$) via the systematic thermochemical approach that includes simultaneous thermal analysis (STA), EMF measurement and high-temperature mass spectroscopy. The synthesis of precursors powders was performed by reversed coprecipitation from aqueous solutions under the optimal conditions and by conventional solid state synthesis including milling into a planetary mill. The phase transitions, so as possible exo- and endo-effects were investigated by STA. Then the precursors was cold pressed into the pellets and hydrostatically pressed. The pellets were annealed at 1550-1600 °C for 2-3 hours. Following galvanic cell $O_2 (PO_2(1)), Pt | SE | Pt, (PO_2(2) = 0.21 \text{ atm.})$ was used for SE sensor properties investigation. The evaporation experiments were carried out using Knudsen effusion technique combined with mass spectrometric analysis of vapor composition. It was show that the value of crystallization enthalpy up on the phase transition "amorphous precursor \rightarrow crystal-line solid solution" can serve the criteria for crystallization completeness of metastable cubic solid solutions in $CaO-ZrO_2$ system. Phase stabilization of the metastable crystalline solid solution at 400 - 1000 ° C is due to kinetic factors. YSZ ceramics manufactured from powders with the mean particle size 40-140 nm shows the highest values of oxygen ion transfer number i.e. 0.97-0.98 at 600-800 °C. SE manufactured from precursors with the mean particle size 40-140 nm shows higher sensor characteristic i.e. temperature and oxygen concentration EMF dependencies, EMF ($E_{Nernst} - E_{real}$), tion, response time, then ceramics, manufactured by conventional solid state synthesis. Sensors with YSZ, 9CSZ and 15CSZ solid electrolytes showed linear EMF response to relative oxygen partial pressure in all the investigated $p(O_2)$ range. The deviation from the theoretical value is minimal in case of sensor with 9CSZ solid electrolyte. The components of $La_2O_3-ZrO_2$ system evaporate separately: there is no temperature range where lanthanum and zirconium gaseous species are present together. It was found that the activities of lantania in all concentration range of condensed phase have low negative deviation from ideal case whereas zirconia activities has strong negative deviation from ideal case. The work was supported by the President's grant for young scientists # MK-2703.2019.3.

Thermodynamics of Al₂M₃ Metalclusters (M= 3d-Element) According to Quantum-Chemical Calculation by DFT Method

Mikhailov O.V.¹, Chachkov D.V.²

¹ Kazan National Research Technological University, 420015 Kazan, Russia;

² Kazan Department of Joint Supercomputer Center of Russian Academy of Sciences – Branch of Federal Scientific Center "Scientific Research Institute for System Analysis of the RAS", 420111 Kazan, Russia

olegmkhlv@gmail.com

As known, nanoparticles of elemental metal of *p*- and *d*-elements and their compositions that are also a kind of "precursor" for nanoparticles of metal oxides and metal sulfides, acquired great importance in modern chemistry and chemical technology. Nanoparticles containing such widely distributed in natural life metals as aluminum and 3*d*-elements (M), that now occupy key positions in metallurgy and in chemical technology and also belong to different categories of chemical elements, are rather interesting objects from a purely academic and a practical point of view. Such nanoparticles composed of metal clusters with Al-Al, M-M and Al-M chemical bonds. In this connection, it becomes quite relevant task associated, firstly, with detection of the possibility of the existence of nanoparticles of a particular chemical composition, consisting of various metals, and secondly, the identification of all the possible for them structural forms and their thermodynamic characteristics using modern quantum-chemical calculations by the most popular current method of density functional theory (DFT). Diatomic and triatomic "composite" (AIM) metal clusters containing atoms of *p*- and *d*-elements, however, have limited interest, because of their structure are trivial – only linear and triangular respectively. For four-atomic and five-atomic (AIM) metal clusters, structural possibilities is much wider; for each of them, the two geometric bodies, in the tops of which are M and Al atoms, namely – a flat rectangle and a tetrahedron in the case of four-atomic clusters, trigonal bipyramid and tetragonal pyramid in the case of five-atomic ones, are possible in principle. As far as we know, quantum-chemical calculations of molecular structures (AIM) metal clusters using any variant of DFT method, were not been carried out hitherto.

The results of molecular structures and thermodynamic characteristics calculation (standard enthalpy $\Delta H_{f,298}^{\circ}$, standard entropy $S_{f,298}^{\circ}$ and standard Gibbs energy of formation $\Delta G_{f,298}^{\circ}$) of metal clusters having Al₂M₃ composition (M = Ti, V, Cr, Mn, Fe, Co, Ni, Cu, Zn), using DFT OPBE/TZVP method and Gaussian09 program, are presented and discussed in the given report. It was found that each of these metal clusters can exist in a fairly significant number of conformations, which differ substantially in its stability, and the geometric and standard thermodynamic parameters. The values of these parameters for the most sustainable from an energy point of conformations, and their corresponding molecular structures, have been presented. Besides, neither parameters of molecular structures nor the standard thermodynamic characteristics of formation of Al₂M₃ metal clusters considered does not show any correlation with the electron configuration of the M atoms and with the values of their atomic radiuses[1-3].

Acknowledgements The quantum-chemical calculations were made in the Kazan Department of Joint Supercomputer Center of Russian Academy of Sciences – Branch of Federal Scientific Center "Scientific Research Institute for System Analysis of the RAS". The present research was carried out with financial support in the framework of draft № 4.5784.2017/8.9 to the competitive part of the state task of the Russian Federation on the 2017–2019 years.

[1] O.V. Mikhailov and D.V. Chachkov, *Russ. J. Gen. Chem.*, 2016, 86, 1991.

[2] O.V. Mikhailov and D.V. Chachkov, *Struct. Chem.*, 2018, 29, 1543.

[3] O.V. Mikhailov and D.V. Chachkov, *Russ. J. Inorg. Chem.*, 2018, 63, 786.

SATURDAY, 22.06.2019
PLENARY SESSION

Estimation of Thermodynamic Properties of Substituted Benzenes Related to their Environmental Mobility

Monte M.J.S., Almeida A.R.R.P.

Centro de Investigação em Química, CIQUP, Department of Chemistry and Biochemistry, Faculty of Science, University of Porto, Portugal

mjmonte@fc.up.pt

Substituted benzenes are often used in the synthesis of other chemical compounds and employed in important industrial applications. The widespread use of some of those compounds is a source of concern that requires trustful information on their environmental fate. So, the knowledge of vapor pressures, solubility in water, and of partition and distribution coefficients, among others, is needed for guessing their distribution fate between air, water and soil. Some of these properties are difficult to determine experimentally for the existing compounds (and obviously impossible to measure for those that were never synthesized), requiring the use of calculations based on prediction methods.

This talk will address user friendly methods for accurate prediction of several properties, at the temperature 298.15 K, such as the standard Gibbs energies of sublimation or vaporization (and then of vapor pressures), solubility in water, Gibbs energies of hydration, etc. Similar approaches yielded accurate estimations for several halogenated benzenes that were reported before [1,2]. New predictive equations of those properties that may be applicable to a larger number of different non-ionizable benzene substituents will be presented.

Acknowledgements

Thanks are due to Fundação para a Ciência e Tecnologia (FCT) Lisbon, Portugal, for the financial support to Project UID/QUI/00081/2013 and for the award of the postdoctoral fellowship (SFRH/BPD/97046/2013) to A.R.R.P Almeida.

[1] M.J.S. Monte, A.R.R.P. Almeida and J.F. Liebman, *Chemosphere*, 2015, 138, 478.

[2] M.J.S. Monte and A.R.R.P. Almeida, *Chemosphere*, 2017, 189, 590.

Phase Equilibria in Reactive Biocatalytic Processes

Smirnova I.

Institute of Thermal Separation Processes, Hamburg University of Technology,
Eissendorfer Straße 38, 21073 Hamburg, Germany

irina.smirnova@tuhh.de

In the recent years process intensification of biocatalytic reactions gains more and more attention, especially in terms of the bioeconomy development. Thereby, the productivity of biocatalysts is often limited by various factors like inhibition by product formation, the position of the reaction equilibria or toxicity of the formed product. A useful tool to overcome these bottlenecks is a direct combination of unit operations with a biocatalytic reaction in one apparatus (reactive unit operations). By removing the formed products into a separate phase, toxic effects as well as inhibition effects can be minimized. Moreover, by shifting the reaction equilibrium an increased yield can be expected. This concept is well established for chemical reactions (reactive distillation, reactive absorption, reactive extraction), however still not fully explored for biocatalysis. Here often batch operations are suggested, whereas their transfer to continuous processes is still challenging. We believe that the combination of reaction and separation (in terms of reactive unit operations) has even larger potential to be generally realized as continuous process, especially using suitable contactors in counter-current flow [1]. However, the basis of the implementation of such processes is the knowledge of phase equilibria in the corresponding systems. Thereby, the type of the equilibria ranges from VLE data needed for distillation of ternary to quaternary mixtures to complex LLE behavior including self-organisation in surfactant-containing systems for liquid-liquid extraction. Moreover, the reaction kinetics should be considered simultaneously.

In this contribution different types of phase equilibria for reactive distillation, extraction and adsorption with biocatalysis are discussed. Specific challenges in treating the biocatalysis are also addressed. Several processes being implemented based on such thermodynamic data are illustrated.

[1] M.Blatkiewicz, O.Fellechner, I.Smirnova “Hybrid unit operations for *in situ* product removal for enzymatic reactions: a review” Chemie Ingenieur Technik 2019 (submitted)

Mesoscopic Non-Equilibrium Organic Periodic Self-Assembly

Koltsov S. and Skorb E.V.

ITMO University, Lomonosova str. 9, St. Petersburg 191002, Russia

skorb@corp.ifmo.ru

We propose a formation of organic periodic structures at macrolevel formed from precipitation reactions composed at microlevel of aggregates of melamine (M) and cyanuric acid (CA) in layered gel solutions (Figure 1). The structure is sensitive to a number of conditions including the concentration of M and CA, temperature, pH, and the presence of other organic compounds.

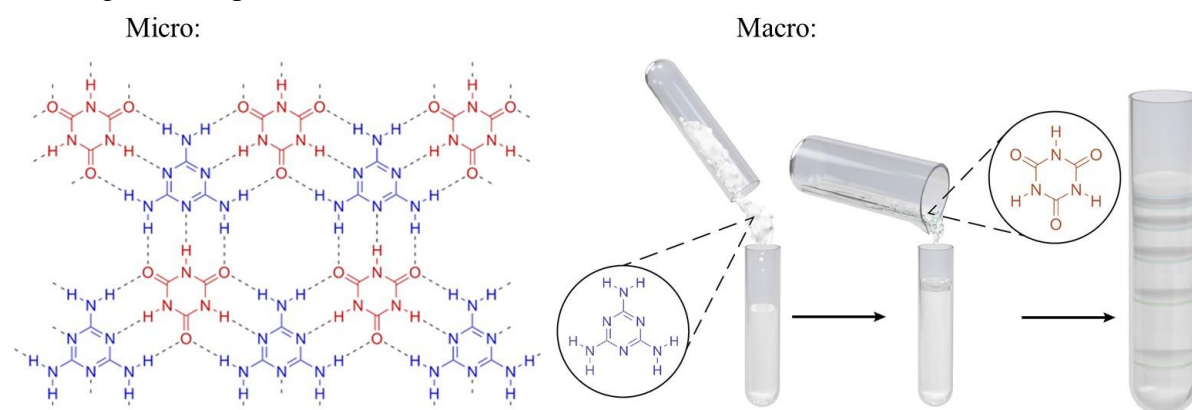


Figure 1. Representation of the experimental setup and formation of melamine-cyanuric acid assemblies (M•CA) in precipitation bands. Hot agar solution contained melamine is poured in tube and that cooled up to room temperature. Once the thermal equilibrium is reached and agar gel is formed, second solution of cyanuric acid is poured. Upon time bands of small melamine cyanurate appear.

The model formulates reaction–diffusion equations for all components intervening in the process. The reactive parts in these equations follow from the analysis of the non-equilibrium self-assembly process undergone by the mesoparticles which make up the patterns. The modelling values found for the structures diameter and the rings position are in agreement with the experiments. The results for the system temperature with peaks at the rings positions suggest that heat accumulates at these positions as a consequence of the dissipation inherent to the non-equilibrium self-assembly process. Our model enables us to rationalize how from non-homogeneous initial conditions a transient self-organization process involving formation of self-assembled structures may produce macroscopic patterns. Previously, in layered gel solutions, the structures have only been reported to form in the bottom layer. Both experiments and simulations show that by varying concentration of the two components, it is possible to control formation of the structures in both the top (the solution containing CA) and bottom (the solution containing M) layers. Finally, periodic structures are shown to form both left and right-handed helical arrangements; demonstrating a mechanism in which chiral structures can be amplified from achiral organic molecules. It can, in general, be used to analyze pattern formation due to diffusion–reaction–precipitation processes with potential applications in the design of advanced biomaterials.

Acknowledgements. The work was supported by RSF grant no. 17-79-20186 and by the Government of Russian Federation (grant 08-08).

SATURDAY, 22.06.2019

**SECTION 2:: Thermodynamics of Liquids, Fluid
Mixtures, and Phase Equilibria**

Effect of Fluctuations on Diffusivity in Liquid Solutions

Norman G.E., Orekhov M.A.

National Research University Higher School of Economics, Russian Federation

maksim.orekhov@phystech.edu

Mechanisms of diffusivity in liquid solution are investigated using molecular dynamics simulation. The decomposition of diffusivity into collective motion of particle with its nearest neighbors and motion with change of the nearest neighbors is considered. Fluctuations on these diffusivity components are considered.

It is found that ion diffusivity in liquid significantly increases at particular ion sizes [1]. These sizes correspond to the change of the ion coordination number that appears when ion size increases (figure 1). This leads to increase of the diffusivity due to fluctuations of the ion solvation shell. The result is shown to be general and appear in different liquids. It is supported by direct molecular dynamics simulations and theoretical model of the effect. This allows to estimate ion sizes that correspond to enhanced diffusivity by examination of the ion coordination number.

Liquid diffusivity is known to increase with simulation box size in molecular dynamics [2,3]. It is found that statistical uncertainty of diffusivity also increases with system size. This result is obtained under the restriction of the constant computational complexity of the simulation. This means that increase of the system size and number of particles is balanced by the decrease of the trajectory length. Increase of the uncertainty is shown for pure liquids and liquid solutions by direct estimation of diffusivity variation from molecular dynamics.

This effect is caused by the increase of the diffusivity fluctuations caused by the collective hydrodynamics that appear at large number of particles. On the other hand, systems with small number of particles do not have such collective motions and thus have smaller statistical uncertainty of diffusivity.

Acknowledgements The abstract was prepared within the framework of the HSE University Basic Research Program and funded by the Russian Academic Excellence Project '5-100'

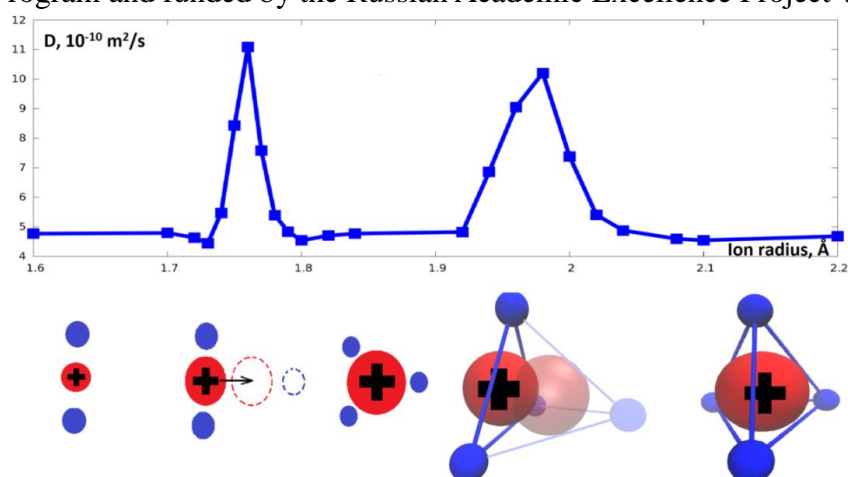


Figure 1. Dependence of ion diffusivity on ion radius in Lennard-Jones liquid with a single ion. Corresponding configurations of ion with its solvation shell are shown.

[1] M.A. Orekhov, *Phys.Chem.Chem.Phys.*, 2017, 19, 32398.

[2] In-Chul Yeh and Gerhard Hummer, *J. Phys. Chem. B* 2004, 108, 15873-15879.

[3] O.A. Moulton, et al., *J. Chem. Phys.* 2016, 145, 074109.

Anomalous Behavior of Dispersion Curves in Water-Like Systems and Water

Fomin Yu.D., Tsiok E.N., Ryzhov V.N. and Brazhkin V.V.

Institute for High Pressure Physics RAS

fomin314@mail.ru

Collective excitations are of great importance for the physics of solids [1]. Many theories of solids are really the theories of collective excitations in solids (phonons), for instance, Debye model of crystal. Recently it was shown that collective excitations are of the same importance in the description of liquids [2]. Because of this it becomes important to investigate the dispersion curves of collective excitations in different liquids.

In the present paper we consider dispersion curves of the longitudinal excitations of a model core-softened liquid (Repulsive shoulder system [3]) and SPC/E model of water [4]. We show that both systems demonstrate anomalous behavior of the excitation frequencies: the frequencies of the excitations can decrease with temperature along isochors, while in normal liquids they should increase. This observation allows to introduce one more water anomaly – the anomalous dependence of excitation frequencies on temperature [5].

This work was carried out using computing resources of the federal collective usage center "Complex for simulation and data processing for mega-science facilities" at NRC "Kurchatov Institute", <http://ckp.nrcki.ru>, and supercomputers at Joint Supercomputer Center of the Russian Academy of Sciences (JSCC RAS). The work was supported by Russian Fund of Basic Research (Grant No 18-02-00981).

- [1] N. W. Ashcroft, and N. D. Mermin, Solid State Physics, Saunders Colledge Publishing (1976).
- [2] D. Bolmatov, V. V. Brazhkin, and K. Trachenko, Sci. Rep. 2012; 2, 421-427 (2012).
- [3] Yu. D. Fomin, N. V. Gribova, V. N. Ryzhov, S. M. Stishov, and Daan Frenkel, J. Chem. Phys. 129, 064512 (2008).
- [4] H. J. C. Berendsen, J. R. Grigera, and T. P. Straatsma, J. Phys. Chem. **91**, 6269 - 6271 (1987).
- [5] Yu. D. Fomin, E. N. Tsiok, V. N. Ryzhov, V. V. Brazhkin, arXiv:1812.09695 (2018)

Precise Experimental Study of Water Thermodynamics up to the Record Pressures 12 kbar

Brazhkin V.V., Dzhavadov L.N., Fomin Yu.D., Tsiok E.N., Ryzhov V.N.

Institute for High Pressure Physics, Russian Academy of Sciences,
108840 Troitsk, Moscow, Russia

brazhkin@hppi.troitsk.ru

Water is the most ubiquitous and the most important substance on the Earth. At the same time, water is the strangest liquid, which demonstrate dozens of different anomalies. There are a lot of empirical and semi-ab-initio interparticle potentials elaborated to describe water “puzzles” including hypothetical transitions in undercooled state and second critical point.

The equation of state for water is well-studied up to 10 kbar. Meanwhile the heat expansion coefficient and heat capacity of water is known with high accuracy up to 1-2 kbar only. There were a very few attempts to study water thermodynamics up to 5 kbar (with moderate accuracy 5-10%).

We present for the first time the data of precise measurements of all thermodynamic characteristics for water – heat capacity, heat expansion coefficient, equation of state etc. up to 12 kbar and 500K.

The accuracy of measurements of all properties is about 1.5%.

These data allow us to get deep insight into water behavior at high compression and can serve as a crucial test to check the validity of different intermolecular potentials.

Acknowledgements The work was supported by the Russian Foundation for Basic Research. This work was partially carried out using computing resources of the federal collective usage center «Complex for simulation and data processing for mega-science facilities» at NRC "Kurchatov Institute", <http://ckp.nrcki.ru/> and supercomputers at Joint Supercomputer Center of the Russian Academy of Sciences (JSCC RAS).

Thermodynamic Peculiarities and Phase Diagrams of Biofuel Systems

Toikka M.A., Golikova A.D., Pulyalina A.Yu.

Saint Petersburg State University, Saint Petersburg, Russia

m.toikka@spbu.ru

Biofuel takes one of the leading places among alternative energy sources. The organization of biofuel production requires an overestimated amount of raw materials and can be optimized due to the greater inclusion of scientifically-based methods, taking into account the basic thermodynamic and kinetic aspects [1, 2]. The use of natural raw materials determines the complex processes and compositions of industrial mixtures in the production of biofuels, which requires not only the application of existing fundamental methods for analyzing complex systems, but also their development. Multicomponent heterogeneous reacting mixtures formed in the processes of synthesis, separation, purification liquid biofuels are the objects of this project. The development of experimental and theoretical methods for analyzing the phase and chemical equilibria of reacting systems with liquid phase splitting taking into account the kinetic regularities of chemical reactions in heterogeneous mixtures is the main goal of this work. Systems with hydrolysis-synthesis of esters (ethyl acetate, propyl acetate, butyl acetate, ethyl propionate, etc.) were selected as experimental objects of study. This paper presents new experimental data on phase and chemical equilibria, including critical phenomena, in systems formed by biofuel components. The obtained experimental kinetic information will make it possible to avoid the unjustified use of kinetic models in the case of complex reaction systems and at the same time propose new and sufficiently adequate models of the kinetic behavior of reaction systems with the separation of the reacting mixture. For the development of the phenomenological theory of chemical processes, methods of nonequilibrium thermodynamics were also applied, primarily, the assessment of the possibility of studying combined phase and chemical processes within the framework of a linear approximation and when deviating from linear laws.



Acknowledgements This study was supported by Russian Foundation for Basic Research: M.A. Toikka, A.D. Golikova and A.Yu. Pulyalina are grateful for the research Grant No. 18-33-20138 mol_a_ved. Alexandra Golikova acknowledges for the Scholarships of President of Russian Federation (SP-2680.2018.1).

[1] B. Bharathiraja, et al., *Renewable & Sustainable Energy Reviews*, 2017, 68, 788-807.

[2] E. Nagy, P. Mizsey, J. Hancsok, S. Boldyryev, P. Varbanov, *Chemical Engineering And Processing*, 2015, 98, 86-94.

Topological Transformation of the Phase Diagrams of Ternary Systems Salt + Water + Organic Solvent, Including a Binary Liquid System with a Closed Binodal Curve

Smotrov M.P., Cherkasov D.G., and Il'in K.K.

Saratov State University named after N.G. Chernyshevsky, Saratov
410012, Russian Federation

illinkk@info.sgu.ru

This paper is devoted to our study of topological transformation of the phase diagrams of the ternary salt + water + butoxyethanol system. The water + butoxyethanol system is a binary system with a closed delamination field (LCST = 47.9°C, UCST = 130.3°C). We previously studied the effect of adding various salts on the phase behavior of mixtures of the critical composition of this liquid system. Based on these studies, three ternary systems were modeled, namely: potassium formate (nitrate, perchlorate) + water + butoxyethanol.

Phase equilibria in mixtures of the components of the ternary systems were studied by the visual-polythermal method in a range of 10–150°C. Analysis of the isotherms of the ternary potassium formate (nitrate, perchlorate) + water + butoxyethanol systems showed that potassium formate and nitrate had a salting-out effect. It was established that increasing temperature enhanced their salting-out effect. Potassium perchlorate has a salting-in effect at relatively low temperatures, which turns into salting-out at higher ones. It was found that introduction of potassium formate and nitrate into the mixture of the critical composition of the binary water + butoxyethanol system led to a decrease in the LCST and an increase in the UCST of this system, while addition of potassium perchlorate led to an increase in the LCST and a decrease in the UCST. When the concentration of potassium perchlorate was more than 5.8 wt% and temperature was below 141.0°C, no delamination was observed in the ternary potassium perchlorate + water + butoxyethanol system. However, at 141.0°C, delamination in the ternary system appeared again.

We calculated the distribution coefficient K_d of butoxyethanol between the organic and aqueous phases of the monotectic state. K_d in the system with potassium nitrate rises significantly with increasing temperature ($K_d = 15.2$ at 25°C, $K_d = 949$ at 150°C). However, the K_d value in the system with potassium formate varies little with increasing temperature ($K_d = 941$ at 25°C, $K_d = 989$ at 150°C). This can be explained by the higher temperature solubility coefficient of potassium nitrate in water than that of potassium formate. However, the K_d of butoxyethanol in the system with potassium formate is high even at 25°C, which indicates a stronger salting-out effect of this salt. Potassium perchlorate even at 150°C has a very weak salting-out effect ($K_d = 3.0$). The salting out effect in the series HCOOK–KNO₃–KClO₄ monotonically decreases with increasing anion radius.

The obtained results confirm our previously developed generalized scheme of topological transformation of the phase diagrams of the ternary systems salt + binary solvent with salting-in and salting-out with temperature change for the cases when the constituent liquid system is characterized by a closed binodal curve [1].

[1] M. Smotrov, *Topological transformation of the phase diagrams of ternary systems salt + binary solvent with salting-in–salting-out*, Diss. PhD in chem. sci., 2012, 281 p. Saratov State Univ., Saratov, Russian Federation

Visual Studies of Methane Hydrate Formation on the Water – Oil Boundaries

Adamova T.P.^{1,2}, Stoporev A.S.^{1,3,4}, Manakov A.Yu.^{1,3}

¹Nikolaev Institute of Inorganic Chemistry SB RAS, Russian Federation;

²Novosibirsk State Pedagogical University, Russian Federation

³Novosibirsk State University, Russian Federation

⁴Gubkin University, Department of Physical and Colloid Chemistry, Russian Federation

adamova@niic.nsc.ru

Visual studies of the growth of methane hydrate at the interface of water with three kinds of methane-saturated crude oils were performed at supercooling ~ 20 °C. The results were compared with the growth of methane hydrate at the interfaces of water–methane and water–methane-saturated decane or toluene. The average rates of hydrate film growth measured for the water–oil interfaces vary within the range of $0.8\text{--}1.0$ mm s⁻¹, which is somewhat lower than the average growth rate at the water–methane and water–decane (toluene) interfaces (1.6 mm s⁻¹). It was found that in some cases hydrate nucleation proceeded not on the water–oil boundary but at the walls of the cell. Spontaneous intrusion of oil formations (drops, serpentlike formations) into the aqueous phase was observed in some experiments. These formations are likely to originate from oil catching by the bundles of needlelike hydrate crystals due to the capillary effect. Intense growth of the hydrate on the walls of the cell was observed for two kinds of crude oils. It was demonstrated that one of the factors blocking hydrate growth on the cell walls may be the presence of naphthenic acids (natural surface-active substances) in the oil phase.

Acknowledgements. This work was supported by Russian Science Foundation grant №17-17-01085.

PVT and Phase Transition Properties of Binary Mixture of *n*-Hexane+IL in the Critical and Supercritical Regions

Abdulagatov I.M.^{1,2}, Rasulov S.M.³, Isaev I.A.,³ Orakova S.M.³

¹Dagestan State University, Russia;

²Geothermal Research Institute of the Russian Academy of Sciences, Russia;

³Institute of Physics of the Dagestan Scientific Center of the Russian Academy of Sciences, Russia

ilmutdina@gmail.com

PVT and phase transition properties (saturated liquid and vapor densities) and two-phase (vapor-pressure) properties of binary mixture of *n*-hexane+IL (1 – Ethyl – 3methylimidazoliumbis [trifluoromethylsulfonyl] imide) near the critical point of pure solvent (*n*-hexane), have been measured. One (L or V) two (L+G or L+L) and three-phase (L+L+G) *PVT* measurements were made for 9 isochores between (65.4 and 663.4) kg·m⁻³ over the temperatures range from (300 to 757) K using a constant-volume piezometer technique. The measurements were made for one concentration of 0.1 wt fraction. The combined expanded uncertainty of the density, ρ , pressure, P , and temperature, T , measurements at 95 % confidence level with a coverage factor of $k = 2$ is estimated to be 0.1 %, 0.15 %, and 15 mK, respectively. The measurements were concentrated in the two- and three-phase regions in the immediate vicinity of the (L+G, L+L, and L+L+G) phase-transition temperatures to precisely determine the phase boundary properties (P_S, T_S, ρ_S) on L+G, L+L, and L+L+G equilibrium curve. The L+G, L+L, and L+L+G phase transition temperatures (T_S) for each studied liquid and vapor isochores were accurately obtained using the isochoric (P - T) break point technique (quasi-static barograms method, $P-\tau$). The values of the critical parameters (P_C, T_C, ρ_C) were estimated using the measured vapor-pressure and liquid-gas coexistence curve data. The measured results were interpreted in term of Krichevskii parameter principle. The value of the Krichevskii parameter was estimated from direct P - x measurements along the critical isotherm - isobar of pure solvent (*n*-hexane). The thermodynamic ($\bar{V}_2^\infty, \bar{H}_2^\infty, K_D^\infty, B_{12}$) and structural ($N_{exc}^\infty, C_{12}, H_{12}$) properties of dilute *n*-hexane+IL mixture near the critical point of pure solvent (*n*-hexane) were calculated using the Krichevskii parameter principle. The effect of chemical reaction on phase transition parameters (P_S, T_S, ρ_S) and measured values of *PVT* were studied.

SATURDAY, 22.06.2019

**SECTION 4: Thermodynamics of Interfacial and
Confined Phenomena**

Dynamic Surface Elasticity of Protein/Surfactant Solutions

Noskov B.A.¹, Lin S.-Y.², Milyaeva O.Y.¹, Krycki M.M.¹

¹St.Petersburg State University, Russia;

²Taiwan National University of Science and Technology, Taiwan

b.noskov@spbu.ru

Ionic surfactants at low concentrations influence mainly the charge of protein globules and thereby the adsorption kinetics. The increase of surfactant concentration results in noticeable changes of the protein tertiary structure. The main characteristic features of kinetic dependencies of the dynamic surface elasticity are determined by the protein tertiary structure and therefore the dilational surface rheology gives a possibility to estimate the conformational transitions in the course of adsorption [1]. Adsorption of globular and non-globular proteins, or the protein/surfactant complexes, leads to different kinetic dependencies of the surface elasticity [2]. In the latter case the surface elasticity has a maximum due to the formation of the distal region of the surface layer. If the distribution of positive and negative charges along the protein chain is strongly inhomogeneous, the kinetic dependencies of the dynamic surface elasticity can have two local maxima corresponding to the consecutive displacement from the proximal region of two different parts of the macromolecule. In this case cationic and anionic surfactants have different influence on the two peaks of the dynamic surface elasticity. The adsorption of the complexes of globular proteins and ionic surfactants leads to a maximum of the dynamic surface elasticity corresponding to the destruction of the protein tertiary structure, if the protein and surfactant have opposite charges. If the both solutes are similarly charged, the maximum can appear only at the high solution ionic strength. The peculiarities of the protein – surfactant interactions influence the number of peaks, the absolute values of the dynamic surface elasticity and the adsorption rate.

Acknowledgements. This work was supported by Ministry of Science of Taiwan and Russian Foundation for Basic Research (project № 19-53-52006 MHT_a).

[1] B.A. Noskov, M.M. Krycki, *Adv. Colloid Interface Sci.* 247 (2017) 81.

[2] B.A. Noskov, *Adv. Colloid Interface Sci.* 206 (2014) 222.

Deformation Induced by Fluid Adsorption: Enhanced Flexibility and Pore Size Distribution

Kolesnikov A.L.¹, Budkov Yu.A.^{2,3}, Möllmer J.¹, Adolphs J.⁴, Georgi N.⁵, Hofmann J.¹

¹ Institut für Nichtklassische Chemie e.V., Leipzig, Germany;

²Tikhonov Moscow Institute of Electronics and Mathematics, School of Applied Mathematics, National Research University Higher School of Economics, Moscow, Russia;

³G.A. Krestov Institute of Solution Chemistry of the Russian Academy of Sciences, Ivanovo, Russia;

⁴Porotec GmbH, Hofheim am Taunus, Germany;

⁵GMBU, Halle (Saale), Germany

kolesnikov@inc.uni-leipzig.de

The deformation of a porous solid can be caused by the different external stimuli, like e.g. mechanical stress, sound, temperature changes or sorption of fluid molecules. The last stimulus, one of the most unexplored, attracted great attention of researchers in the last decades [1,2]. A significant success was achieved both in theoretical description [1,3] of the sorption-induced deformation and in the development of experimental techniques [1] of sorption induced deformation measurements. The sorption of fluid molecules onto the surface of a porous sample induces stress, which in turn causes the strain. The shape of experimental strain isotherms could be concave, convex and the combination of both of them.

In this work, we investigate the deformation of mesoporous materials with cylindrical pores induced by the fluid sorption. The model [4] is based on the DBdB (Derjaguin-Broekhoff-de-Boer) theory, used for the description of the adsorption process and on the Hook's law for the description of elastic energy of the porous material. We considered only the volumetric deformation of the sample; however, the effect of coupling between deformation process and adsorption process was taken into account. The system of self-consistent equations, defining adsorbed amount and volumetric strain is the result of the model. We investigated the effects of the pore size distribution (PSD) on the strain isotherms. The account for PSD helped to reproduce the hysteresis on the strain isotherm more accurately. In addition, the effect of decreasing the bulk modulus was investigated. At low values of bulk modulus, the model qualitatively reproduces some features of the sorption isotherms on the highly deformable materials (for example aerogels). Also, the model was tested on the experimental data from the literature, namely we described the sorption and strain isotherms of water on Vycor glass [5].

Acknowledgements The authors gratefully acknowledge the financial support from Bundesministerium für Wirtschaft und Energie (BMWi) as part of the program "Zentrales Innovationsprogramm Mittelstand" (AiF-ZIM)" (ZF4129902GM5).

[1] G.Y. Gor et al. *Appl. Phys. Rev.*, 2017, 4, 011303.

[2] G.Y. Gor et al, *Langmuir*, 2013, 29, 8601-8608.

[3] O. Coussy, *Poromechanics*, 2004, John Wiley & Sons.

[4] A.L. Kolesnikov et al, *Langmuir*, 2018, 34, 7575 – 7584.

[5] C.H. Amberg et al, *Can. J. Chem.*, 1952, 30, 1012-1032.

Thermodynamic Modeling of Confined Fluid: From Incompressible to Compressible Matrices

Sermoud V. de M.^{1,*}, Barbosa G.D.², Segtovich I.S.V.², Barreto Jr. A.G.², Tavares F.W.^{1,2}

¹Universidade Federal do Rio de Janeiro, Brazil; EQ/EPQB: Programa de pós graduação em engenharia de processos químicos e bioquímicos;

²Universidade Federal do Rio de Janeiro, Brazil; COPPE/PEQ: Programa de pós graduação em engenharia química

*vsermoud@gmail.com

The thermodynamic modeling of confined fluids and adsorption is important to several systems of practical interest, as shale gas exploration and chromatography for analysis and separation of pharmaceutical compounds.

In general, an increase in pressure induces a solid matrix into shrinking, but in an adsorption system it would also favor the adsorption of more molecules. On its turn, the increase in adsorbed quantity may induce an expansion of the matrix. The result of this swelling is an apparent negative compressibility of the adsorption system. Furthermore, it has been observed that metal-organic frameworks can also undergo isostructural phase transitions [1].

Recent advancements in thermodynamic modelling of clathrate hydrates [2] have been able to model these phenomena in gas hydrate systems. The core of the model innovations is the calculation of a pressure difference between the solid solution of the adsorption system at equilibrium and the isochoric reference of the unoccupied matrix. This pressure difference can be related to calculations of the increased pressure of a fluid in a pore with fixed volume, from the modelling of confined fluids [3].

In the present work, we apply the pressure shift model for adsorption systems other than clathrate hydrates, as is the case of MOFs and zeolites, where a pore size distribution exist, in contrast with well characterized cages of clathrate compounds, and investigate qualitative and quantitative predictions.

Acknowledgements The financial support of CAPES, PETROBRAS, ANP

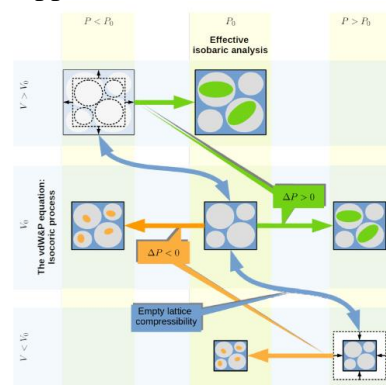


Figure 1. Schematic representation of how the pressure shift is responsible for volume differences for hydrates of different guests at a specified pressure. From reference [2]

[1] M. Zhou, K. Wang, Z. Men, et al., *Cryst. Eng. Comm.*, 2014, 20, 4084.

[2] I. S. V. Segtovich, F. de A. Medeiros, C. R. de A. Abreu, F. W. Tavares, *XI Iberoamerican conference on phase equilibria and fluid properties for process design*, 2018, 1, 71.

[3] G. D. Barbosa, L. Travalloni, M. Castier, F. W. Tavares, *Chem. Eng. Sci.*, 2016, 153, 212.

Limitations of the Single-Site Approach to Describing Adsorption in Structure-I Clathrate Hydrates

Lasich M., Tumba K.

Mangosuthu University of Technology, South Africa;

lasich.matthew@mut.ac.za

Clathrate hydrates are ice-like non-stoichiometric compounds consisting of a hydrogen-bonded water lattice enclathrating a guest gas species which stabilizes the crystal structure and influences the geometry of the clathrate hydrate crystal. Structure-I clathrate hydrates are conventionally described using two different site types, as the unit cell consists of two 5^{12} polyhedral cavities and six $5^{12}6^2$ cavities. However, the structure-I crystal is simply the Weaire-Phelan structure [1], which is a solution to the well-known Kelvin problem of determining a foam of bubbles with equal volume and minimal inter-bubble surface area. Hence, although the two cavity types in structure-I lattice are nominally different, they possess approximately equal volumes. This feature was exploited in the recent past to calculate clathrate hydrate phase equilibria indirectly from grand canonical Monte Carlo simulations [2] using van der Waals-Platteeuw theory [3]. This contribution examines the utility of this approach by examining the limits, in terms of temperature and gas fugacity, of the application of a single-site description. Grand canonical Monte Carlo simulations were used to model adsorption of methane, ethane, ethane, carbon monoxide, and hydrogen sulphide in the structure-I hydrate lattice over a range of fugacity values for the temperature range $270 \text{ K} \leq T \leq 300 \text{ K}$. The accurate TIP4P/Ice potential [4] was used to describe water, the organic species were described using the Transferable Potentials for Phase Equilibria (TraPPE) [5], and the remaining species were described using a united-atom Lennard-Jones potential calculated from the critical point [6]. The results of the molecular simulations were used to develop guidelines for the use of the single-site approach for the structure-I clathrate hydrates under consideration.

Acknowledgements All calculations were performed using the facilities of the Centre for High Performance Computing (CHPC) in Cape Town.

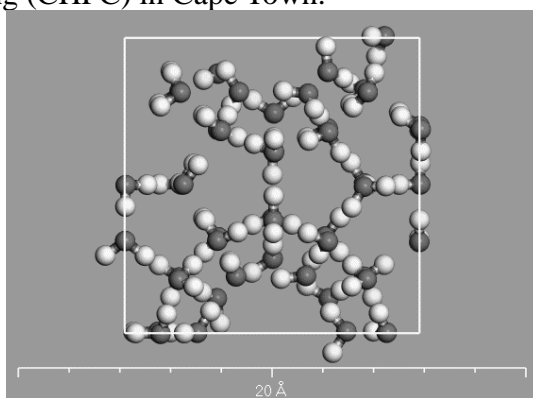


Figure 1. Structure-I crystal unit cell. White atoms are hydrogen, and shaded atoms are oxygen.

- [1] D. Weaire and R. Phelan, *Philos. Mag.*, 1994, 69, 107.
- [2] M. Lasich, A.H. et al., *Fluid Ph. Equilibria*, 2014, 369, 65.
- [3] J.H. van der Waals and J.C. Platteeuw, *Adv. Chem. Phys.*, 1959, 2, 1.
- [4] J.L.F. Abascal, E. Sanz, R.G. Fernández, C. Vega, *J. Chem. Phys.*, 2005, 122, 234511.
- [5] M.G. Martin and J.I. Siepmann, *J. Chem. Phys. B*, 1998, 102, 2569.
- [6] J.J. Potoff and A.Z. Panagiotopoulos, *J. Chem. Phys.*, 1998, 109, 10914.

Influence of Confinement on Melting of Two-Dimensional Core-Softened System

Tsiok E.N., Fomin Yu.D., Ryzhov V.N.

Institute for High Pressure Physics, Russian Academy of Sciences,
108840 Troitsk, Moscow, Russia

elena.tsiok@gmail.com

Two-dimensional and quasi-two-dimensional systems that exist under conditions of a strong spatial constraint in one direction (confinement) are widespread in nature and technology. Processes involving adsorbed ions, nano- and microparticles, as well as colloidal suspensions and emulsions are ubiquitous in physical, chemical and biological systems, technologies of novel materials. In contrast to the 3D case, where melting always occurs through a standard first order transition, several scenarios are known for the microscopic description of 2D melting. The main reason for this difference is a significant increase in fluctuations in 2D systems compared to the case of three dimensions.

We performed molecular dynamics simulations. The LAMMPS package was used. We investigated phase diagrams of a quasi-two-dimensional system (20 thousand particles) with the core-softened potentials with two length scales [1, 2], which simulates the behavior of colloids and water under confined conditions.

It has been shown that the phase diagram of purely two-dimensional system with the core-softened potentials consists of different crystalline phases. At high densities in the phase diagram, there are phases with triangular and square symmetry of the lattice, as well as a dodecagonal quasicrystals [3], and the triangular lattice at low densities with a maximum on the melting curve. Thermodynamic, dynamic and structural anomalies are presented in these systems, and the order of these anomalies is inverted compared to the order of anomalies in 3D case [4].

It was shown that, depending on the position in the phase diagram, the system can melt both in accordance with the Berezinsky-Kosterlitz-Tauless-Halperin-Nelson-Young (BKTHNY) scenario and through the first order phase transition, as well as in accordance with the third scenario with one transition of the first order and one continuous transition.

The main goal of the work is to compare the phase diagrams and the melting scenario of purely two-dimensional and quasi-two-dimensional systems in order to identify the confinement influence on the phase boundaries position. The walls are located at height z and repel the particles with Lennard-Jones 9-3 potential. The pore width H varied from 0.3 to 3.0 and from 10 to 40 (in dimensionless units). We studied water-like anomalies depending on pore width.

Acknowledgements The work was supported by the Russian Foundation for Basic Research (Grant No 17-02-00320). This work was carried out using computing resources of the federal collective usage center «Complex for simulation and data processing for mega-science facilities» at NRC "Kurchatov Institute", <http://ckp.nrcki.ru/> and supercomputers at Joint Supercomputer Center of the Russian Academy of Sciences (JSCC RAS).

[1] Yu. D. Fomin, et al., *J. Chem. Phys.*, 2008, 129, 064512.

[2] S. V. Buldyrev *et al.*, *J. Phys.: Condens. Matter*, 2009, 21, 504106.

[3] N. P. Kryuchkov, et al., *Soft Matter*, 2018, 14, 2152.

[4] D. E. Dudalov, et al, *Soft Matter*, 2014, 10, 4966.

Whether the Heat Capacity of Nanoparticles can be Negative?

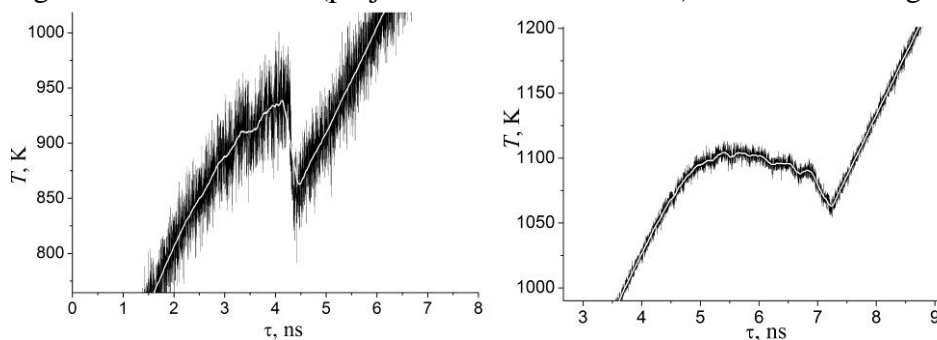
Talyzin I.V., Samsonov V.M.

Tver State University, Russia

talyzin_igor@mail.ru

According to available papers, the heat capacity C of nanoparticles (NPs) can either increase or decrease with diminishing their size and be twice and more times higher than for the corresponding bulk phase (reference see in our paper [1]). However, in [1, 2] we justified that so high values of C can not be realized in NPs and nanostructures materials. Then negative heat capacities were experimentally observed on sodium NPs [3] and theoretically justified in [4]. In molecular dynamics (MD) experiments [5] the negative heat capacity was observed in a vicinity of the melting point of Ag NPs consisting of 856 atoms. In the present work we have simulated Ag NPs in a wide enough size range from 3 to 12 nm. In the course of our simulations, by using the adiabatic MD, some small quantities of heat were put into particle (by rescaling velocities of all the atoms). Then the particle relaxed for a prescribed time τ . If the energy is put into the system by small portions, a plateau appears in the $T(\tau)$ dependence where T is the NP temperature. Afterwards the temperature T diminishes (Figure 1). Respectively, the potential term dU/dT into the molar heat capacity $C_V = (3/2)R + dU/dT$ becomes negative where R is the molar gas constant and U is the potential term into the molar internal energy. The values of the melting temperature T_m , of its jump during the adiabatic relaxation of Ag NPs as well as of C_V are evaluated. The $U(T)$ dependence in [5] corresponds to $C_V \approx -56$ J/mol·K. According to our evaluations we have also obtained negative values of C_V in the range from -30 to -70 J/mol·K but for bigger Ag NPs containing from 2093 to 50141 atoms. For NPs consisting of 1055 atoms we have also obtained a negative value of C_V approximately equal to -4 J/mol·K that is smaller by order of magnitude in comparison with [5].

Acknowledgements Financial support of RFBR (grant No 18-03-00132) and Ministry of Science and Higher Education of RF (project No 3.5506.2017/BP) is an acknowledged.



a b

Figure 1. Kinetic dependencies for Ag NPs consisting of 1055 (a) and 50141 (b) atoms in a vicinity of their melting point.

- [1] S.L. Gafner, L.V. Redel, Yu.Ya. Gafner, V.M. Samsonov, *J Nanopart Res.*, 2011, 13, 6419.
- [2] V.M. Samsonov, et al., *Eurasian Chem. Tech Journal*, 2012, 14, 305.
- [3] M. Schmidt, et al., *Phys. Rev. Lett*, 2001, 86, 1191.
- [4] M.A. Carignano, I. Gladich, *EPL (Europhysics Letters)*, 2010, 90, 63001.
- [5] J. Cui, L. Yang, Y. Wang, *Integrated Ferroelectrics*, 2013, 145, 1.

Nucleation in Superheated Solutions of Simple Liquids

Baidakov V.G., Kaverin A.M.

Institute of Thermal Physics, Ural Branch of the Russian Academy of Sciences, Russia

baidakov@itp.uran.ru

The kinetics of spontaneous boiling-up of superheated solutions with partial (methane–helium, ethane–nitrogen) and complete (oxygen–nitrogen, krypton–argon) solubility of the components has been investigated by the method of lifetime measurement. Experiments were conducted in the range of pressures from atmospheric to that close to critical at nucleation rates from 10^5 to 10^8 s⁻¹m⁻³. The data obtained have been compared with classical nucleation theory (CNT) in a macroscopic approximation, i.e. without allowance for the size dependence of the surface tension of critical bubbles. The surface tension of solutions at a plane interface σ_∞ has been measured by the differential capillarity method. It has been found that attainable superheating temperatures T_n of pure liquids are always lower than values obtained from CNT. As the solute is added into the solvent, the discrepancy between theory and experiment in T_n decreases, and close to the equimolar composition the superheating temperatures achieved in experiment exceed their theoretical values.

Properties of critical bubbles have been calculated in the framework of a gradient repretation of the van der Waals capillarity theory. All the parameters of the free energy functional of an inhomogeneous bubble – liquid system have been determined on the basis of experimental data: the density of the free energy of a homogeneous solution from data on p , ρ , T , x – properties and the matrix of influence coefficients from the results of measurement of the surface tension of pure components. Functional minimization has been used to calculate the work of its formation W_* of critical bubble. The radii of the surface of tension R and the value of the surface tension σ of a critical nucleus have been determined from the obtained values of the work with the use of conditions of mechanical and real equilibrium of vapor bubbles and the Gibbs equation for W_* .

For pure components the surface tension of critical bubbles is a monotonically decreasing function of the curvature of the surface of tension (Fig. 1). On addition of the substance being dissolved into the solvent the monotonic character of the dependence $\sigma(R)$ is disturbed. Close to the equimolar composition the function $\sigma(R)$ has a characteristic maximum. Such a behavior means that in a solution, as distinct from a pure liquid, superheatings may exceed their theoretical values obtained in a macroscopic approximation.

Acknowledgements The financial support of the Russian Foundation for Basic Research (project No. 18-08-00403A).

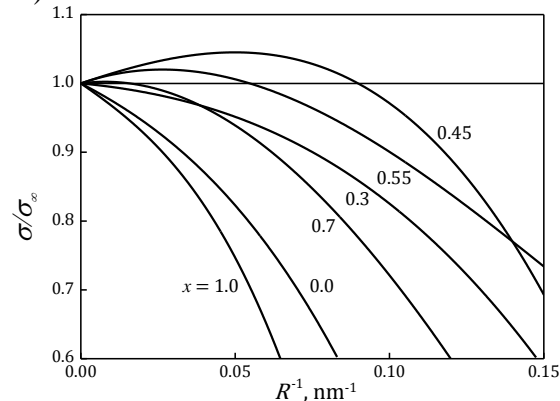


Figure 1. Dependence of the reduced surface tension of critical bubbles of oxygen–nitrogen solution on the curvature of surface tension at different concentrations x and $T = 120$ K.

SATURDAY, 22.06.2019

SECTION 3: Thermochemistry and Databases

Thermodynamic Study of α -, β -, γ -Cyclodextrin Hydrates Dehydration Processes

Zelenina L.N., Chusova T.P., Rodionova T.V.

Nikolaev Institute of Inorganic Chemistry, Novosibirsk, Russia

b. zelenina@niic.nsc.ru@spbu.ru

α -, β - and γ -cyclodextrins (CDs) are cyclic macromolecules consisting of 6, 7, or 8 glucopyranose units, respectively. These units form hollow truncated cone cavity with hydrophilic exterior and hydrophobic interior. A wide range of guest molecules can be included in the CD cavities, forming host-guest inclusion complexes. These inclusions may lead to beneficial changes of CD physicochemical characteristics such as solubility, thermal stability, volatility, resistance to oxidation, visible and UV light, etc. Due to these properties CDs are widely used in analytical chemistry, catalysis and also in pharmaceutical, food and cosmetic industries. Water plays an important role in formation of the CDs inclusion complexes because the process of complex formation is essentially a replacement reaction of water molecules located in CD cavities by hydrophobic guest molecules. Meanwhile, quantitative data on equilibria between CDs and H₂O are very scant and contradictory [1, 2], which makes it difficult to produce high-quality materials.

The purpose of this work is a comprehensive study of the α -, β - and γ -CD hydrates dehydration processes by static method with glass membrane-gauge manometers. Limiting errors for used setup were 0.5 Torr, 0.5 K and 0.01 formula units in values of pressure, temperature and solid phase composition, accordingly [3]. The measurements have been realized in the wide intervals of temperature ($313 \leq T/K \leq 506$), pressure ($1 \leq p/\text{Torr} \leq 760$) and composition ($\text{CD} \cdot x \text{H}_2\text{O}$, $2.6 \leq x \leq 15$).

As a result of this study thermal stability of investigated compounds was established, temperature dependences of pressure for dehydration processes were obtained (four types of dehydration processes were studied), enthalpies and entropies of dehydration were determined and Gibbs energy of bonding water with CDs was calculated. On the base of information obtained the conclusions about the nature of the interactions between host and guest molecules (water) were drawn.

Accumulation of quantitative information on dehydration processes of α -, β -, γ -CDs hydrates will allow one to synthesize functional materials with desired properties in future.

[1] G. Bettinetti, Cs. Novák, M. Sorrenti, *J. Thermal Analysis and Calorimetry*. 2002, 68, 517.

[2] A.Yu. Manakov, T.V. Rodionova, L.S. Aladko, G.V. Villevald, J.S. Lipkowski, L.N. Zelenina, T.P. Chusova, T.D. Karpova, *J. Chem. Therm.* 2016, 101, 251.

[3] L.N. Zelenina, T.P. Chusova, S.A. Sapchenko, E.A. Ukraintseva, D.G. Samsonenko, V.P. Fedin, *J. Chem. Therm.* 2013. 67.128

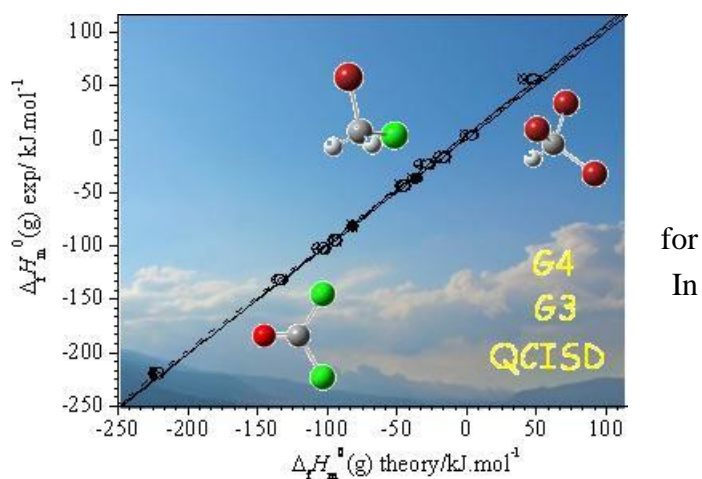
Thermochemical Properties of Halogen-Containing Organic Compounds with Influence on Atmospheric Chemistry: a Computational Study

Dávalos J.Z., Notario R., Cuevas C.A., Oliva J.M., Saiz-Lopez A.

Institute of Physical Chemistry “Rocasolano”-CSIC, Serrano 119-28006, Madrid, Spain

jdavalos@iqfr.csic.es

We have computationally studied the thermochemical properties of a wide variety of halogen-containing organic compounds (including radicals) with relevance on several atmospheric chemical processes, such as catalytic ozone destruction. A reliable estimation of the standard molar enthalpies of formation, $\Delta_f H_m^0(g)$, and the carbon-halogen bond dissociation enthalpies, *BDE*, in the gas phase at 298.15 K has been performed, by means of atomization [1] and isodesmic reactions methods [2], using *Gn* ($n = 3, 4$) [3,4], MP2 and QCISD levels of theory. *Gn* methodologies, particularly G4 have been shown to be an accurate theoretical method to provide reliable $\Delta_f H_m^0(g)$ and *BDE* values chlorinated and brominated species. In several cases these values are very close to those obtained by the most accurate, and consequently most time consuming, methods such as coupled-cluster CCSD(T) level of theory [5].



- [1] A. Nicolaidis, A. Rauk, MN Glukhovtsev, L. Radom. *J. Chem. Phys.* 1996, 100, 17460.
- [2] J.Z. Dávalos, R. Herrero, J.C.S. Costa, L.M.N.B.F. Santos, J.F. Liebman. *J. Phys. Chem. A* 2014, 118, 3705
- [3] L.A. Curtiss, K. Raghavachari, P.C. Redfern, V. Rassolov, J.A. Pople. *J. Chem. Phys.* 1998, 109, 7764.
- [4] L.A. Curtiss, P.C. Redfern, K. Raghavachari. *J. Chem. Phys.* 2007, 126, 084108.
- [5] J.Z. Dávalos, R. Notario, C.A. Cuevas, J.M. Oliva, A. Saiz-Lopez. *Comp. Theor. Chem.* 2017, 1099, 36

Calorimetric Investigation of Carbosilane and Carbosilanecyclesiloxane Dendrimers of Versatile Structure

Samosudova Ya.S., Markin A.V., Smirnova N.N., Sologubov S.S., Sarmini Yu.A.

National Research Lobachevsky State University of Nizhni Novgorod, Russia

sayanina@yandex.ru

Dendrimers and corresponding to them dendrons are represented unique monodisperse macromolecules with regular and hyperbranched three-dimensional architecture. The main features of dendrimers are their hyperbranched topology, low polydispersity, lack of links which are characterized for big macromolecules, and the large number of terminal groups. In addition, they are characterized by low deitrication temperatures, high solubility and low viscosity in solutions and melts. The combination of the structural perfection of dendrimers and the possibility of modifying their groups underlie the development of functional nanoscale materials with unique electronic, optical, magnetic and chemical properties necessary for modern nanotechnology. Liquid crystal (LC) dendrimers occupy a special position among a wide number of dendritic molecules due to their specific molecular structure combining the flexible spherical architecture of the dendrimer with the presence of rigid rod-like mesogenic groups capable to forming anisotropy of the LC-mesophase. To date, various LC dendrimers have been synthesized based on polyorganosiloxane, carbosilane, polyimine, and other dendritic structures.

Obviously, the task of precision thermodynamic values accumulation for compounds of this class and receiving of practically important dependences as «thermodynamic property – composition» is actual.

The investigated in this work dendrimers were synthesized and described in terms of composition and structure at N.S. Enikolopov Institute of Synthetic Polymer Materials, Russian Academy of Science, in the scientific group of academician A.M. Muzafarov. The composition and structure of the samples were confirmed by elemental analysis and the methods of ^1H NMR spectroscopy and IR spectroscopy.

First the temperature dependences of the heat capacity of carbosilane and carbosilanecyclesiloxane dendrimers with various architecture of surface layer have been determined in a wide temperature range by the methods of precision adiabatic calorimetry and differential scanning calorimetry. The physical transformations were detected and their standard thermodynamic characteristics were estimated and analyzed. Thus, the phase transitions, anomalies and high-temperature «nanosized transition» and their thermodynamic quantities were interpreted with structural properties.

The experimental data were used to calculate standard thermodynamic functions, namely the heat capacity $C_p^0(T)$, enthalpy $H^0(T) - H^0(0)$, entropy $S^0(T)$ and free Gibbs for different physical states and the standard entropies of formation of dendrimers at $T = 298.15$ K.

Acknowledgements: This work was performed with the financial support of the Ministry of Education and Science of the Russian Federation (Contracts Nos. 4.5706.2017/8.9 and 4.6138.2017/6.7) and the Russian Foundation for Basic Research (Project No. 18-33-00905 mol_a, 19-03-00248).

Milestone Thermodynamics of the Renewable Fuels and Hydrogen Storage

Verevkin S.P.^{1,2} Pimerzin A.A.²

¹Department of Physical Chemistry, University of Rostock, Rostock, Germany;

²Chemical Department, Samara State Technical University, Samara, Russia

sergey.verevkin@uni-rostock.de

Biofuels derived from biomass are a promising alternative energy source due to the potential for such fuels to be carbon neutral. Efficient process design requires accurate thermodynamic property information. We set an establishing benchmark thermodynamic properties and prediction of feasibility for the renewable fuel processing and alternative to conventional hydrogen storage technologies as a main goal of this project. The complex of modern thermochemical and theoretical methods was designed, developed and established in the Thermochemical lab at the Samara State Technical University. The procedure included extended experiments, critical evaluation of available data and prediction of the missing thermodynamic properties in order to provide the best possible property values as the milestones for the assessment of the feasibility of processes intended for valorisation of the natural products and the optimal hydrogen storage using favourable chemical reactions. Focus of our project has been on thermodynamic analysis of the following processes: production of dimethylfuran for liquid fuels from biomass, utilization of building block chemicals produced from sugars and lignocellulosic biomass via biological or chemical conversions, and utilization of glycerol. A challenging part of the project has been thermodynamic analysis and selection of liquid organic heteroaromatics for hydrogen storage as an auspicious alternative to conventional technologies.

Acknowledgements This research was supported by the Government of Russian Federation (decree №220 of 9 April 2010) agreement №14.Z50.31.0038.

Thermodynamic Study of Tetramethylammonium Iodide. Thermal Behavior, Molar Isobaric Heat Capacities and Thermodynamic Functions

Brunetti B.¹, Ciccioli A.², Latini A.², Vecchio Cipriotti S.³

¹Istitute for Nanostructured Materials, CNR, Sapienza University of Rome,

Department of Chemistry, P.le A. Moro 5, I-00185 Rome, Italy;

²Sapienza University of Rome, Department of Chemistry, P.le A. Moro 5, I-00185 Rome, Italy;

³Sapienza University of Rome, Department of Basic and Applied Science for Engineering,
Via del Castro Laurenziano 7, I-00161 Rome, Italy

stefano.vecchio@uniroma1.it

Tetraalkylammonium halides have received great interest in the past due to their properties, with particular reference to the low clustering tendency that makes them ideal chemical standards for ESI(+)-IMS/MS [1]. In addition, tetraalkylammonium cations, considered as the archetypal hydrophobic cations, combine in many environmental and biological processes both charge and hydrophobicity [2]. In particular, tetramethylammonium iodide ((CH₃)₄NI, denoted as TMAI) can be considered as a simpler model to study the thermal decomposition pathways of tetramethylammonium lead iodide, belonging to the class of perovskites currently considered with great expectations as possible light harvesting materials for photovoltaic devices.

In this study, we present the thermal behavior study of TMAI by means of simultaneous Thermogravimetry-Differential Thermal Analysis (TG-DTA) experiments under inert (Ar) atmosphere up to 500°C. A single step of mass loss is evidenced between 300 and 450°C, accompanied by an endothermic effect. The reaction mechanism is described in the light of the gases evolved upon heating in the suitable temperature range according to the analysis of Fourier Transform InfraRed (FTIR) spectra (being the spectrophotometer coupled to the TG apparatus). In order to complete this investigation a kinetic study of the thermal decomposition has been carried out using two different isoconversional methods [3,4], and the dependence of activation energy on the degree of conversion for each method will be presented and discussed.

Differential scanning calorimetry (DSC) experiments have been carried out (in three replicates) at low heating rate (2 K min⁻¹) under Ar atmosphere to determine the molar isobaric heat capacity $C_{p,m}$ of TMAI above the solid from ambient temperature to 533 K. A second polynomial function was used to fit the temperature dependence of the experimental $C_{p,m}$ values. Then, the thermodynamic enthalpies and entropies of the solid (related to the reference temperature of 298.15 K) were calculated from the temperature integral of the $C_{p,m}$ and $C_{p,m}/T$ data, respectively.

[1] J. Vildanoja, A. Sysoev, A. Adamov and T. Kotiaho, *Rapid Commun. Mass Spectrom.*, 2005, 19, 3051.

[2] D. Bhowmik, N. Malikova, G. Meriguet, O. Bernard, J. Teixeira and P. Turq, *Phys. Chem. Chem. Phys.*, 2014, 16, 13447.

[3] T. Akahira, T. Sunose, *Res. Report Chiba Inst. Technol. (Sci. Technol.)*, 1971, 16, 22.

[4] T. Dubaj, Z. Cibulkova, P. Simon, *J. Comput. Sci.*, 2015, 36, 392.

Development of the IVTANTHERMO-Online Thermodynamic Database for Pure Substances

Morozov I.V.^{1,2}, Belov G.V.^{1,3}, Dyachkov S.A.^{1,3}, Levashov P.R.^{1,3}, Minakov D.V.^{1,3}

¹Joint Institute for High Temperatures of Russian Academy of Sciences, Moscow, Russia;

²Moscow Institute of Physics and Technology, Dolgoprudny, Russia;

³Department of Chemistry, Lomonosov Moscow State University, Moscow, Russia.

morozov@ihed.ras.ru

Thermodynamic databases play essential role in a wide range of applications such as rocket engine engineering, nuclear power, chemical technology, metallurgy, resource usage, waste recycling, etc. The IVTANTHERMO information system [1] based on the reference book [2] has made a significant contribution to the accumulation of thermodynamic data. It has been developed since 1966 in the Institute of High Temperatures of the Academy of Sciences of the USSR. Nowadays the development is continued in the Department for Thermophysical Data of JIHT RAS.

The IVTANTHERMO system includes the database which contains more than 3400 substances, formed of 96 chemical elements, as well as supplementary software for analysis of experimental results, data fitting, calculation and estimation of thermodynamical functions and thermochemistry quantities. In this report we present a next generation of the IVTANTHERMO database and related software called “IVTANTHERMO-Online” [3] (figure 1). It has an extensible database design, user-friendly web interface with client-server architecture and a number of features for online and offline data processing. The new system enables to handle multiple versions of each block of data, to store additional information for users and experts (such as comments, bibliography, experimental data, molecular structure, etc.), to present data in multiple forms, to attach calculation services and link with other databases. The substances can be searched using their names, formula, atomic composition or CAS numbers. The supplementary software includes cross-platform or web based modules for calculation of chemical composition, data fitting and calculation of thermodynamic properties using the data from experiments and quantum chemistry computations.

The work is supported by the Basic Research Program of the Presidium RAS “Condensed matter and plasma at high energy densities” (coordinated by Fortov V.E.).

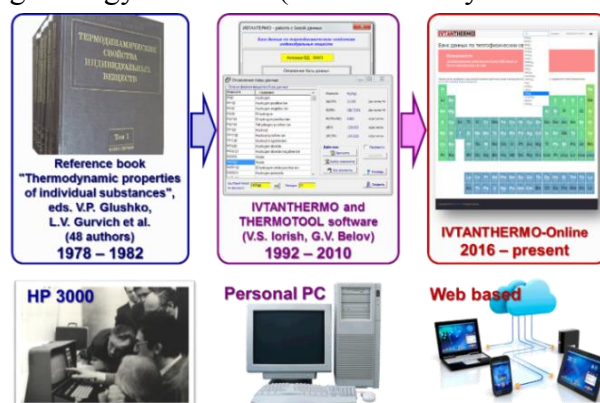


Figure 1. Development of the thermodynamic databases in JIHT RAS.

[1] G.V. Belov, V.S. Iorish, V.S. Yungman, *CALPHAD*, 1999, 23, No. 2, 173.

[2] L.V. Gurvich, G.A. Bergman, I.V. Veyts, et al, edited by V.P. Glushko, *Thermodynamic Properties of Individual Substances*, 1984, Moscow, Russia.

[3] Belov G.V., et al., *J. Phys. Conf. Ser.*, 2018, 946, 012120.

Thermochemistry of Polycyclic Hydrocarbons. Energy Characteristics of Bonds and Radical's Reorganization

Miroshnichenko E.A.¹, Kon'kova T.S.¹, Pashchenko L.L.²

¹Semenov Institute of Chemical Physics, Russian Academy of Sciences, Moscow, Russia;

²Chemical Department, Lomonosov Moscow State University, Moscow, Russia

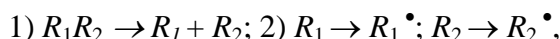
eamir02@mail.ru

In this work the calculation scheme by "double difference method" of formation enthalpies of cyclic radicals and bond dissociation energies is offered. Using fundamental equations of the chemical physics, the new calculation method is offered to determine the energies of reorganization of molecules fragments into radicals. Formation enthalpies of cyclic and frame radicals are determined. Reorganization energies of these radicals and bond chemical energies are calculated.

Energies of a dissociation of bonds, D , and enthalpies of formation of radicals, $\Delta_f H^\circ R^\bullet$; the major power characteristics of molecules and the radicals, the formations of substance connected with an enthalpy, $\Delta_f H^\circ (R_1 R_2)$, the equation

$$D(R_1 - R_2) = \Delta_f H^\circ R_1^\bullet + \Delta_f H^\circ R_2^\bullet - \Delta_f H^\circ (R_1 R_2) \quad (1)$$

The fundamental equations of chemical physics contain N. N. Semenov's representation that monomolecular radical process of decomposition of compound $R_1 R_2$ on bond $R_1 - R_2$ occurs in two stages:



where R_1 and R_2 - fragments of molecules, and R_1^\bullet and R_2^\bullet - radicals to which investigated compound breaks up. At transition from a fragment of molecule R to radical R^\bullet it is allocated energy of reorganization of a fragment of a molecule in a radical ε (named usually by "energy of reorganization of a radical").

$$E = D(R_1 - R_2) - \varepsilon_{R1} - \varepsilon_{R2}; \Delta_{at} H = \sum \Delta_f H_{(at)} - \Delta_f H^\circ = \sum E_i \quad (2)$$

where $\Delta_{at} H$ - an enthalpy of an atomization of compound (value return enthalpies of formation from atoms); E_i - average thermochemical energies of bonds; ε_{R1} and ε_{R2} - energies of reorganization of fragments of molecules in radicals. Directly from the equation (2) it is impossible to define energies of a dissociation of bonds as energies of reorganization of fragments of molecules in radical's ε_R are unknown. On the basis of enthalpy of formation of cyclic and frame compounds and their radicals in the gas phase [1], the energies of radical reorganization are determined. For calculations used the thermochemical data for monocyclic compounds from cyclopropane to cyclohexane, cyclododecane and adamantane, cuban and other substances and related radicals.

Table 1. Energies, ε_R , of the reorganization of a number of cyclic and frame radicals, $\text{kJ} \cdot \text{mol}^{-1}$

Radical	ε_R	Radical	ε_R	Radical	ε_R
$\text{C}^\bullet\text{H}_3$	23.4(23.2 ^[1])	cyclo- $\text{C}_3\text{H}_5^\bullet$	33.7	adamantan-1-yl, $\text{C}_{10}\text{H}_{15}^\bullet$	6.5
$\text{C}^\bullet\text{H}_2$	54.5	cyclo- $\text{C}_4\text{H}_9^\bullet$	-1.3	adamantan-2-yl, $\text{C}_{10}\text{H}_{15}^\bullet$	2.21
C^\bulletH	41.8	cyclo- $\text{C}_5\text{H}_9^\bullet$	-10.6	bicyclooctane-1-yl, $\text{C}_8\text{H}_7^\bullet$	78.9
$\text{C}_2\text{H}_5^\bullet$	5.1(-5.6 ^[1])	cyclo- $\text{C}_6\text{H}_{11}^\bullet$	7.1(-10.6 ^[1])	trans-decahydro-	
$n\text{-C}_3\text{H}_7^\bullet$	6.8(-6.2 ^[1])	$n\text{-C}_6\text{H}_{13}^\bullet$	2.6(-13.0 ^[1])	naphthalene-1-yl, $\text{C}_{10}\text{H}_{17}^\bullet$	6.5
$i\text{-C}_3\text{H}_7^\bullet$	0.0(-14.7 ^[1])	$(\text{C}_2\text{H}_5)_2\text{C}^\bullet\text{H}$	0.8	norbornyl-1(bicyclo-	
				[2,2,1]hept-1-yl, $\text{C}_7\text{H}_{11}^\bullet$	6.1
$n\text{-C}_4\text{H}_9^\bullet$	5.5(-13.0 ^[1])	$(n\text{-C}_3\text{H}_7)(\text{CH}_3)\text{C}^\bullet\text{H}$	4.9		
$i\text{-C}_4\text{H}_9^\bullet$	6.2(-9.8 ^[1])	$(\text{C}_2\text{H}_5)(\text{CH}_3)_2\text{C}^\bullet$	-2.6		
$s\text{-C}_4\text{H}_9^\bullet$	1.2(-14.6 ^[1])	$(\text{CH}_3)_3\text{CC}^\bullet\text{H}_2$	6.5		
$t\text{-C}_4\text{H}_9^\bullet$	-2.8(-13.5 ^[1])	$n\text{-C}_5\text{H}_{11}^\bullet$	3.4(-13.0 ^[1])		

[1] Y. Luo, *Comprehensive Handbook of Chemical Bond Energies*, CRC Press, New York, 2007, 1655

SATURDAY, 22.06.2019

**SPECIAL SESSION: “100 Years from Birthday of Acad.
Mikhail M. Schultz”**

M.M. Schultz and Thermodynamics: First Steps, but what were Significant!

Rusanov A.I.

St.Petersburg State University, Russian Federation

airusanov@mail.ru

The activity of M.M. Schultz (below MM) was multilateral. To choose the main direction, probably, this could be coming from B.P. Nikolsky the electrochemistry of glass. However, in the life of MM there was a period (from the beginning of the 50s) when it was completely absorbed by thermodynamics. At that time, same Nikolsky sent him for an internship at the department of the theory of solutions, headed by A.V. Storonkin. Under his leadership, the St. Petersburg thermodynamic school was in its heyday and reached one of the first places in the world (I can only compare it with the Van der Waals school in Holland).

The authority of A.V. Storonkin (together with Gibbs and van der Waals, whose ideas he developed) was unlimited, but MM was the first who dared to argue with him. Moreover, in this dispute, he won. It was about applying the conditions of stability, previously known only for homogeneous (single-phase) systems, to heterogeneous (multi-phase) systems. The idea belonged to MM, but, brought up on classical concepts, A.V. Storonkin first met her with doubt. However, if the argument is honest, two clever people cannot argue for a long time. Soon they united on the MM platform. In their first publication [1] in 1954, they began a remarkable series of papers on the chemical potentials of heterogeneous complexes. The main idea was that any combination of phases in a heterogeneous system can be distinguished as a heterogeneous complex and apply thermodynamic relations to it separately. The most fundamental result of this cycle is the rule of extremes of chemical potentials, which generalizes the Konowalow laws. As for the applied side, one of the most important results was the development of a scheme for calculating the properties of the two-component phase through the chemical potential of the third component (usually the solvent) in an equilibrium adjacent three-component phase. This scheme known under the name of “third component method”, has found wide application in the study of solid solutions and has been tested in numerous theses at the university.

By that time, I appeared at the department. One day, rereading Gibbs, I stumbled upon a sensation: Gibbs already has proved the reduced Le Chatelier–Brown principle, made by him even before the work of these authors. It is surprising that no one has noticed this earlier, but the explanation is very simple. The whole conclusion is given in verbal form without a single formula, which is so uncharacteristic of Gibbs. Naturally, it was not difficult to translate Gibbs' conclusion into mathematical language. The reduced Le Chatelier–Brown principle requires the inequality

$$(dY_i / dy_i)_{Y_k} < (dY_i / dy_i)_{y_k}$$

where Y_i and Y_k are generalized forces (say, chemical potentials), whereas y_i and y_k are conjugate generalized coordinates. Replacing fixing an extensive parameter by fixing an intensive one always leads to a decrease in the derivative. It vanishes when all the intensive parameters are fixed. Thus, the entire reduced Le Chatelier–Brown principle is a chain of inequalities ending in zero. Like the authors who gave the name to the principle, Gibbs also referred to homogeneous systems. Considering the above, it was suggested that this principle be generalized to heterogeneous systems. It turned out that just at this time the reduced principle of Le Chatelier–Brown was studied by MM, and now I have found a common platform with him [2].

[1] М. Шульц, А. Сторонкин, Вестник ЛГУ, сер. 4, 1954, вып. 11, 153.

[2] А. Русанов, М. Шульц, Вестник ЛГУ, сер. 4, 1960, вып. 1, 60

Mikhail Mikhailovich Shultz and his Thermodynamic Investigations

Toikka A.M.

St.Petersburg State University, Russia

a.toikka@spbu.ru

This presentation is devoted to 100-year jubilee of outstanding Russian scientist academician Mikhail Mikhailovich Shultz. The lecture is the review of his scientific activity in the area of chemical thermodynamics and related fields. These researches of academician M. Shultz cover a wide range of thermodynamic tasks both of basic and applied importance including the problems of material science. Most of the results are of particular importance for the solution of modern fundamental thermodynamic problems. Some of them will be briefly discussed in the lecture, e.g. the problem of isothermal-isobaric changes of chemical potentials in ternary systems (published with A.V. Storonkin [1]) and reduced Le Chatelier – Braun principle (the study with A.I.Rusanov [2]). Other results, activities and role of academician M. Shultz in the development of chemical thermodynamics in Russia will be also presented. Author also include in the lecture his own impressions connected with the meetings with Mikhail Mikhailovich Shultz [3] and some main stages of the biography related to the work in Saint Petersburg (Leningrad) State University.



Academician Mikhail Mikhailovich Shultz (1919-2006)

- [1] A.V. Storonkin, M.M. Shultz, *Zh. Fiz. Khim. (J. Phys. Chem. USSR)*, 1960, 34, 2167 (in Russian).
- [2] A.I. Rusanov, M.M. Shultz, *Vestnik Leningrad Univ., Ser. 4, Phys. Chem.* 1960, 4, 60 (in Russian).
- [3] A.M. Toikka, *Saint Petersburg University*, 2006, 206 53 (in Russian).

Developing of Thermodynamic Approach to Study of Oxide Systems and Materials by Academician M.M. Shultz

Stolyarova V.L.

St.Petersburg State University, Russia

v.stolyarova@spbu.ru

Among the outstanding studies by M.M. Shultz on materials science that are carefully analyzed and discussed in [1] thermodynamic approach is one of the most valuable input for understanding and prediction of high temperature behavior of oxide materials. These investigations are the continuation of the best traditions of physicochemical school available in Saint Petersburg University that were done together with A.V. Storonkin [2, 3], B.P. Nikol'skii [4] and A.I. Rusanov [5]. Validity of this approach [6] was successfully illustrated in the variety of oxide systems and materials such as glasses, ceramics and coatings [7-10]. Carrying out the systematic thermodynamic studies of various types of oxide systems simultaneously as the combination of high temperature mass spectrometric [11], calorimetric [12] and EMF [13] methods allowed to obtain further a lot of unique information included nowadays in the modern international thermodynamic data bases as well as to develop statistical thermodynamic approaches for analyzing and modeling of phase diagrams [14, 15]. In more details the importance of this approach is considered using results obtained by high temperature mass spectrometric method summarized in the reviews for series of borate, silicate, germanate, phosphate, zirconate and hafnate systems and materials [16-20].

- [1] N.B. Borisova and M.P. Semov, *Mikhail Mikhailovich Shultz*, 2004, Chapter, 14-35. Nauka, Moscow, Russian Federation.
- [2] A.V. Storonkin and M.M. Shultz, *Vestnik of the St. Petersburg University: Mathematics*, 1954, 11, 127.
- [3] M.M. Shultz and A.V. Storonkin, *Vestnik of the St. Petersburg University: Mathematics*, 1956, 22, 111.
- [4] B.P. Nikol'skii and M.M. Shultz, *Zhurnal Fizicheskoi Khimii*, 1962, 34, 1327.
- [5] A.I. Rusanov and M.M. Shultz, *Vestnik of the St. Petersburg University: Mathematics*, 1960, 4, 60.
- [6] M.M. Shultz, *Vestnik of the St. Petersburg University: Mathematics*, 1963, 4, 174.
- [7] M.M. Shultz, *J. Non-Crystalline Solids*, 1985, 73, 91.
- [8] M.M. Shultz, *Transactions Indian Ceramic Soc.*, 1987, 46, 95.
- [9] M.M. Shultz, *Sorosovskii obrazovatelynyi zhurnal*, 1996, 3, 49.
- [10] M.M. Shultz, *Glass Physics and Chemistry*, 1998, 24, 224.
- [11] M.M. Shultz, V.L. Stolyarova and G.A. Semenov, *J. Non-Crystalline Solids*, 1980, 38&39, 581.
- [12] M.M. Shultz, V.M. Ushakov and N.V. Borisova, *Doklady Akademii Nauk SSSR.*, 1985, 283, 179.
- [13] E.L. Kozhina and M.M. Shultz, *Glass Phys. Chem.*, 1996, 22, 338.
- [14] M.M. Shultz, N.V. Borisova and E.L. Kozhina, *Khimiya Silikatov i Oksidov*, 1982, Chapter, 3-19. Nauka, Leningrad, Russian Federation.
- [15] M.M. Shultz, N.M. Vedishcheva and B.A. Shakhmatkin, *Thermochim. Acta*, 1987, 110, 443.
- [16] V.L. Stolyarova, *High Temperature Science*, 1990, 26,405.
- [17] V.L. Stolyarova, *Rapid Commun. Mass Spectrom.*, 1993, 7, 1022.
- [18] V.L. Stolyarova, *Russ. Chem. Revs.*, 2016, 85, 60.
- [19] V.L. Stolyarova, *Applied Solid State Chem.*, 2017, 1, 26.
- [20] V.L. Stolyarova, *Calphad*, 2019, 64, 258.

SUNDAY, 23.06.2019

PLENARY SESSION

Thermochemistry of Water Vapor/Refractory Oxide Reactions at Elevated Temperatures

Jacobson N.S.¹, Myers D.L.², Bauschlicher Jr.C.W.³, Opila E.J.⁴

¹NASA Glenn Research Center, Cleveland, OH, USA;

²East Central University, Ada, OK, USA

³NASA Ames Research Center, Moffett Field, CA, USA

⁴University of Virginia, Charlottesville, VA, USA

nathan.s.jacobson@nasa.gov

The interactions of water vapor and refractory oxides is important in combustion applications. The water vapor combustion product reacts with an oxide on a structural component to form a volatile metal hydroxide or oxyhydroxide. To understand and model these reactions, accurate thermochemical data are required for both the gas phase product and solid oxide reactant [1, 2]. At NASA we have studied the Si-OH, Cr-OH, Ti-OH, and Ta-OH systems using both experimental and quantum chemistry methods. The first step is to identify the primary vapor species, which is conducted with direct mass spectrometric identification and/or methodically determining the pressure dependence on H₂O and O₂. Enthalpies and entropies of reaction are determined with the transpiration method. In this classic technique, the oxide and water vapor are carefully equilibrated and the products are collected downstream for analysis. Quantum chemistry calculations provide accurate structural and spectroscopic data for heat capacities and thermal functions. Theory provides relative stabilities when several vapor species are generated and provides an independent check on the experimental enthalpy of formation. Our current state of knowledge of gaseous hydroxides is summarized.

[1] J. Hastie, *High temperature vapors: science and technology*. Academic Press, 1975.

[2] P. J. Meschter, E. J. Opila and N. S. Jacobson, *Annual Review of Materials Research*, 2013, 43, 559.

Microphase Separation in Polyelectrolytes

Kramarenko E.Yu.¹, Rumyantsev A.M.², Gavrilov A.A.¹

¹Faculty of Physics, Lomonosov Moscow State University, Russia;

²Institute for Molecular Engineering, University of Chicago

kram@polly.phys.msu.ru

The possibility of microphase separation in a solution of a weakly charged polyelectrolyte under poor solvent conditions, i.e. polymer density modulations with formation of alternate polymer-rich and polymer-poor nanodomains, was first theoretically predicted in [1,2], since then this phenomenon has been studied in various polyelectrolyte systems. In this talk, we discuss the main physical mechanism stabilizing mesophases in polyelectrolytes in comparison with that in block-copolymers. Furthermore, we consider some new aspects of microphase separation in polyelectrolytes. First, we study the effects of ionic association, i.e. ion pair and multiplet formation between counterions and ions in polymer chains, as well as dielectric mismatch between polymer and solvent on the stability of microphase separated structures in polyelectrolyte solutions. We demonstrate a possibility of a qualitatively new type of microphase separation realized at high polymer concentrations where ion association processes are the most pronounced. The driving force for the microphase formation of a new type is more favorable ion association in polymer-rich domains where ionomer-type behavior takes place. Second, we predict a microphase separation in a blend of oppositely and weakly charged polyelectrolytes being immiscible when uncharged by a complex theoretical approach including a strong segregation theory and DPD simulations. In case of a symmetrical mixture, the theoretical dependence of the lamella period on the Flory-Huggins incompatibility parameter, $D \sim \chi^{1/6}$, is quantitatively confirmed in simulations. Some other morphologies, in particular, hexagonal one and bcc are predicted for asymmetrical compositions.

Acknowledgements The financial support of Russian Foundation for Basic Research (project 18-53-45020) is gratefully acknowledged.

[1] V. Yu. Borue, I. Ya. Erukhimovich, *Macromolecules*, 1988, 21, 3240.

[2] J. F. Joanny, L. Leibler, *J. Phys. France*, 1990, 51, 545.

[3] A.M. Rumyantsev, E.Yu. Kramarenko, *Soft Matter*, 2017, 13, 6831.

Compressibility of Confined Simple Fluid from an Equation of State and Molecular Simulation

Dobrzanski C.D., Corrente N., Gor G.Y.

New Jersey Institute of Technology, USA

gor@njit.edu

Compressibility of a fluid in a porous medium determines the response of the medium to mechanical loads, and elastic waves propagation in particular [1]. If the pores of the medium are in the nanometer range, many thermodynamic properties of the fluid confined in such pores are altered. Our theoretical results show that the fluid compressibility is not an exception [2,3].

Here, we use two methods for calculating the compressibility of a fluid in nanoconfinement. The first method employs the grand canonical Monte Carlo simulation, in which the compressibility can be calculated from the fluctuations of number of molecules in the system [3]. The second method uses van der Waals equation of state extended for confined fluids [4]. We illustrated both methods with an example of Lennard-Jones argon confined in cylindrical silica pores. We showed that the two methods give consistent predictions, and agree with experimental measurements [5].

Our main result is the relation between the fluid compressibility and the pore size. We predicted a simple trend: the isothermal modulus (1/compressibility) is enhanced linearly with reciprocal pore size (see Figure 1). This dependence provides an unambiguous relation between the pore size and the compressibility, which can be probed experimentally using ultrasound. Therefore, our results set up the grounds for characterization of fluid-saturated porous samples based on the data on ultrasound propagation [6].

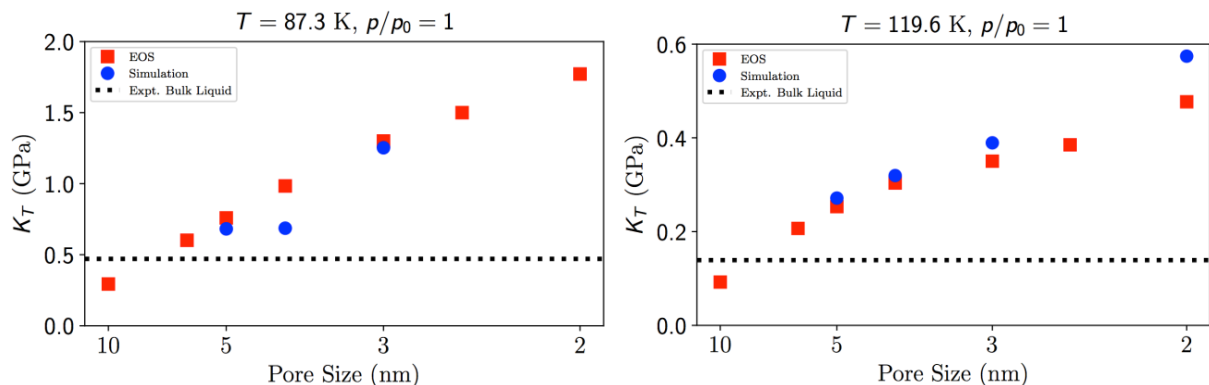


Figure 1. Theoretical predictions of isothermal modulus of liquid argon confined in pores of various sizes at temperatures 87.3 K and 119.6 K.

[1] M. A. Biot, *J. Acoust. Soc. Am.*, 1956, 28, 168.

[2] G. Y. Gor, *Langmuir*, 2014, 30, 13564.

[3] C. D. Dobrzanski, M. A. Maximov, G. Y. Gor, *J. Chem. Phys.*, 2018, 148, 054503.

[4] L. Travalloni, M. et al., *Chem. Eng. Sci.*, 2010, 65, 3088.

[5] K. Schappert, R. Pelster, *J. Phys.: Condens. Matter*, 2013, 25, 415302.

[6] M. A. Maximov, G. Y. Gor, *Langmuir*, 2018, 34, 15650

Critical Condition of Macromolecule Adsorption: Application for Size-Independent Separations

Vishnyakov A.V.^{1,2}, Santo K.P.², Rasmussen R.^{2,3}, Neimark A.V.², Brun E.³

¹Skolkovo Institute of Science and Technology, Moscow, Russia;

²Rutgers the State university of NJ, Piscataway NJ, USA

³DuPont Central Research & Development, Wilmington, DE, USA

a.vishnyakov@skoltech.ru

Adsorption of macromolecules is widely used in their detection, separation and immobilization. A macromolecule can be broadly defined as a chemically and structurally stable object much larger than atomic diameter but substantially smaller than 1 micrometer (e.g. a polymer, nanoparticle, colloidal aggregate etc). Adsorption of macromolecules is generally controlled by two factors: entropic penalty due to configurational restrictions and enthalpic attraction. Both factors depend on size and the chemical composition of the adsorbate. Correspondingly, adsorption can be applied to separate macromolecules by size or by chemistry. The latter, size-independent separations are very important from the practical point of view but also difficult to achieve.

A set of conditions, where the entropic repulsion and enthalpic attraction effectively cancel each other making adsorption equilibrium size-independent is identified as the critical point of adsorption. The talk explains the critical condition on several important examples: linear homopolymers on flat and porous surfaces and functionalized nanoparticles in channels grafted by polymer brushes. The concept of critical condition is applied to gradient elution chromatographic separations, where the analyte mobility is controlled by solvent composition that gradually changes with time. We consider two types of analytes: homo- and heteropolymers and functionalized nanoparticles of different sizes. These systems exhibit a transition between the adsorption regime (small analytes elute first) to the hydrodynamic regime (large analytes elute first). Using Monte Carlo and dissipative particle dynamics simulations, we predict analyte adsorption and mobility and explore different systems for existence of critical conditions leading to size-independent separations. The theoretical study facilitates developing experimental methods in polymer and nanoparticle chromatography.

Acknowledgements The studies were supported by NSF grant **1510993**.

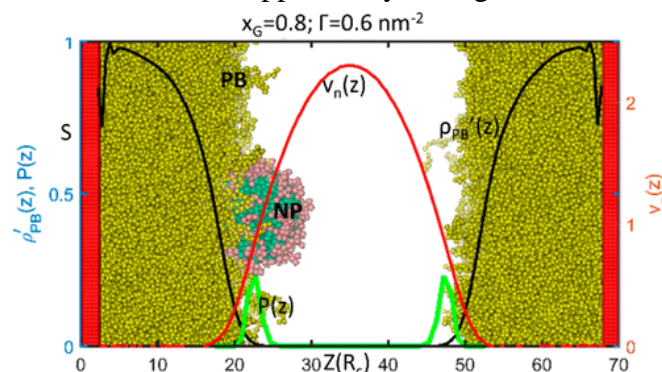


Figure 1. Snapshot of a functionalized nanoparticle adsorbed on a polymer brush with polymer density and solvent velocity profiles

[1] KP Santo, A Vishnyakov, Y Brun, AV Neimark *Langmuir* 34 (4), 1481-1496 (2018)

[2] CJ Rasmussen, A Vishnyakov, AV Neimark; *J Chem Phys* 135 (21), 21410 (2013)

[3] CJ Rasmussen, A Vishnyakov, AV Neimark; *Adsorption* 17 (1), 265-271 (2011)

On Size Dependence of Surface Tension and Surface Energy

Samsonov V.M., Sdobnyakov N.Yu., Talyzin I.V., Bazulev A.N., Vasilyev S.A.

Tver State University, Russia

samsonoff@inbox.ru

Dedicated to 100th anniversary of the birth of Prof. L.M. Shcherbakov

The problem of the size dependence of the surface tension γ and the surface energy ε is on the top problems of physics and chemistry of surface phenomena. Using the Gibbs adsorption equation, Tolman obtained his well-known formula predicting that γ diminishes under diminishing the droplet radius R . In 60s an analogous equation for the specific surface free energy σ was obtained by L.M. Shcherbakov [1]. Moreover, in [1] a concept of the Type II capillary effect was put forward and partially justified. According to [1], effects caused by the surface energy itself were referred to as Type I capillary effects. Respectively, Type II capillary effects are due to dependences of surface properties on the size and shape of a small object. No wonder that L.M. Shcherbakov could not develop the concept under discussion in its entirety. In 60s as well for very small R Rusanov predicted the linear correlation [2]

$$\gamma = KR \quad (1)$$

between γ and R (where K is a proportionality coefficient). For a long time this formula was beyond the scope of scientists. In 1992 only E. Vitol [3] calculated values of the K parameter for some solid and liquid metals. For this purpose experimental data on the particle evaporation rate were used. Recently [4] we recalculated values of K and estimated intervals of the reliability of determination of this parameter. The size dependence of the specific surface energy ε has been even less studied than the size dependence of γ . However, from the Gibbs-Helmholtz equation $\sigma = \varepsilon + T(d\sigma/dT)$ it follows that if Eq.(1) is fulfilled, an analogous linear correlation

$$\varepsilon = K_\varepsilon R \quad (2)$$

should be also fulfilled where $K_\varepsilon = K - T(dK/dT)$. In our papers [4, 5] the size dependence of ε was investigated for modeling icosahedral metal nanoparticles using the tight-binding potential. It was found that the $\varepsilon(R)$ dependence should be more complex than the simple linear dependence (2). The $\varepsilon(R)$ dependence for solid metal nanoparticles obtained in our MD experiments demonstrates a much more complex oscillating behavior. Such a behavior can be explained in terms of the subsequent filling of the atomic shells in the course of growing the particle size. The result concerning the oscillating behavior of the $\varepsilon(R)$ dependence agrees with an analogous conclusion made in [6]. Some other results on the $\gamma(R)$ dependence, including its nonmonotonic behavior [7] are also planned to be discussed.

The work was supported by the Ministry of Education and Science of the Russian Federation in the framework of the State Program in the Field of the Research Activity (No. 3.5506.2017/BP) and by Russian Foundation for Basic Research (project No. 18-03-00132).

[1] L.M. Shcherbakov, in “*Research in surface forces*”, Ed. by B.V. Deryagin, 1966, V. 2, p. 26. Consultants bureau, N.Y., USA,

[2] A.I. Rusanov, *Phasengleichgewichte und Grenzflächenerscheinungen*, 1978. Akademie-Verlag, Berlin, Germany.

[3] E.N. Vitol, *Kolloidnii Zhurnal*, 1992, 54, 21 (in Russian).

[4] N.Yu. Sdobnyakov, V.M. Samsonov and A.N. Bazulev, *Journal of Surface Investigation: X-ray, Synchrotron and Neutron Techniques*, 2015, 9, 968.

[5] V.M. Samsonov and A.A. Chernyshova, *Colloid Journal*, 2016, 78, 378.

[6] R.S. Berry and B.M. Smirnov, *Physics-Uspokhi*, 2005, 48, 345.

[7] T.V. Bykov and A.K. Shchekin, *Colloid Journal*, 1999, 61, 144.

POSTER SESSION I
THURSDAY, 20.06.2019

PI-1. New Study of Viscosity for the Binary System n-Alkane + 1-Alkanol

Castelo S., Gayol A., Mato M.M., Legido J.L.

Department of Applied Physics, University of Vigo, Campus As Lagoas Marcosende s/n,
36310 Vigo, Spain

fammmc@uvigo.es

In this work a study of the behavior of the viscosity of n-alkane mixtures with 1-alcohols provided with the new data obtained in recent years. For years, data and viscosity studies of n-alkane mixtures with 1 alcohol have been provided¹⁻⁴, but more recently, new viscosity data have been added⁵⁻⁸.

We provide more experimental data of the dynamic viscosity at temperatures between 288.15K and 308.15K and atmospheric pressure.

The viscosity measurements were performed with an Anton Paar AMV 200 viscometer connected to a PolyScience fluid circulation bath, which controls the temperature with an uncertainty of 10^{-2} K. This device determines the viscosity of the fluid through time measurement by dropping a steel ball rolling inside a glass capillary filled with sample⁸.

The viscosities were used to test the semiempirical relations of Grunberg-Nissan⁹, McAllister¹⁰, Auslander¹¹ and Teja¹².

Acknowledgements We thank María Perfecta Salgado González for her collaboration with the technical measurements. We are also thankful for the financial support provided by the project ED431C 2016-034 by “Xunta de Galicia” of Spain. This project is co-financed with FEDER funds.

- [1] R. Bravo, M. Pintos, A. Amigo, M.García, *Phys. Chem. Liquid*, 1991, 22, 245–253.
- [2] N. V.Sastry, M. K.Valand, *J. Chem. Eng. Data*, 1996, 41, 1426-1428.
- [3] J. Nath, J.G. Pandey, *J. Chem. Eng. Data*, 1997, 42, 1137-1139.
- [4] E. Jiménez, C. Franjo, L. Segade, J.L. Legido, M.I. Paz Andrade, *J. Sol. Chem.*, 1998, 27, 569–579.
- [5] A. Randová, L. Bartovská, *Journal of Molecular Liquids*, 2017, 242, 767–778.
- [6] A. Guzmán-López, G.A. Iglesias-Silva, F. Reyes-García, A. Estrada-Baltazar, *J. Chem. Eng. Data*, 2017, 62, 780–795.
- [7] G. A. Iglesias-Silva, A. Guzmán-López, G. Pérez-Durán, M. Ramos-Estrada, *J. Chem. Eng. Data*, 2016, 61, 2682–2699.
- [8] M. J. Pastoriza-Gallego, C. Casanova, R. Paramo, B. Barbes, J. L. Legido, M. M. Piñeiro, *J. Applied Physics*, 2009, 106, 64301.
- [9] L. Grunberg, A. Nissan, *Nature*, 1949, 164, 799-800.
- [10] R. A. McAllister, *AIChE J.*, 1960, 6, 427-431.
- [11] G. Auslander, *Br. Chem. Eng.* 1964, 9, 610.
- [12] A. S.Teja, P. Rice, *Chem. Eng. Sci.* 1981, 36, 7-10.

PI-2. Surface Tension of the Ternary System Diethyl Carbonate + *p*-Xylene + *n*-Decane

Gayol A.¹, Casás L.², Mato M.M.¹, Legido J.L.¹

¹Department of Applied Physics, University of Vigo,
Campus As Lagoas Marcosende s/n,36310 Vigo, Spain

²Univ. Pau & Pays Adour, Laboratoire de Thermique,
Énergétique et Procédés-IPRA,EA1932, 64000 Pau, France

fammmc@uvigo.es

The present paper describes an experimental study of surface tension in the temperature range from 288.15 K to 308.15 K and at atmospheric pressure for the ternary system¹⁻³ diethyl carbonate + *p*-xylene + *n*-decane. The surface tension values were adjusted by a third degree polynomial equation:

$$\sigma = A_{00} + A_{11} \cdot x_1 + A_{21} \cdot x_2 + A_{31} \cdot x_3 + A_{12} \cdot x_1^2 + A_{22} \cdot x_2^2 + A_{32} \cdot x_3^2 + A_{13} \cdot x_1^3 + A_{23} \cdot x_2^3 + A_{33} \cdot x_3^3$$

Diethyl carbonates have many industrial applications, principally due to the fact that they have been developed as gasoline additives, lubricants and as alternatives for chlorofluorocarbons (CFCs) with new HFC (hydrofluorocarbons)⁴⁻⁷ refrigerants. As a result of this, there has been an important increase in theoretical and experimental research of dialkyl carbonates and their mixtures with other compounds^{8,9}.

Acknowledgements We thank María Perfecta Salgado González for her collaboration with the technical measurements. We are also thankful for the financial support provided by the project ED431C 2016-034 by “Xunta de Galicia” of Spain. This project is co-financed with FEDER funds.

- [1] A. Gayol, L.M. Casás, A.E. Andreatta, R.E. Martini, J.L. Legido. *Journal of Chemical Engineering Data*, 2013, 58, 758-763.
- [2] L. Mosteiro, L.M. Casás, M.R. Currás, A.B. Mariano, J.L. Legido. *Journal Chemical Thermodynamics*. 2011, 43, 1984-1990.
- [3] L. Mosteiro, L.M. Casás, J.L. Legido. *Journal Chemical Thermodynamics*. 2009, 41, 695-704.
- [4] T. Takeno, K. Mizui, K. Takahatai, K. Proceedings of the International Compressor Engineering Conference at Purdue. Purdue University, W. Lafayette, IN, USA, 1992.
- [5] K. Takahata, M. Tanaka, T. Hayashi, N. Sakamoto. Proceedings of International Refrigeration Conference at Purdue. Purdue University, W. Lafayette, IN, USA, 1994.
- [6] T. Hayashi, T., M.Tanaka, K. Takeuchi, K. Takahata, N. Sakamoto. Proceedings of the International Refrigeration Conference at Purdue. Purdue University, W. Lafayette, IN, USA, 1996.
- [7] H.O. Spauschus, Bull. Int. Inst. Refrig. 1997, 1, 2-12.
- [8] E.R. López, E.R. A.M. Mainar, J.S. Urieta, J. Fernández. *Journal Chemical. Engineering Data*, 2009, 54, 2609–2615.
- [9] J. M. Pardo, C.A. Tovar, J. Troncoso, E. Carballo, L. Romani, *Thermochimica Acta*, 2005, 433, 128–133.

PI-3. Thermal Properties of Mixtures of Montmorillonite with Water

Rosino J., Tobar J.L., Gómez C.P., Mato M.M., Mourelle M.L., Legido J.L.

Department of Applied Physics, University of Vigo, Campus As Lagoas Marcosende s/n,
36310 Vigo, Spain

jlftobar@gmail.com

In this work density, thermal conductivity, specific heat and thermal diffusivity of mixtures of montmorillonite + water at different concentrations are presented. The experimental results were compared with those obtained from mixtures with other clays.

The mixtures were prepared by weight using an analytical Acculab ALC-210.4 balance [1]. Density of the mixtures was measured by the pycnometer method [2]. The equipment used to measure thermal conductivity was a KD2 Pro Thermal Properties Analyzer [3] and specific heat capacity was measured with a CALVET calorimeter [4]. Thermal diffusivity was determinate from the experimental data of density, thermal conductivity and specific heat [5]. All measurements taken had been calculated at 298.15 K and 308.15 K and atmospheric pressure.

Acknowledgements We thank to María Perfecta Salgado González for her collaboration with the technical measures. We are also thankful for the financial support provided by the project ED431C 2016-034 by “Xunta de Galicia” of Spain. This project is co-financed with FEDER funds.

References

- [1] M.M. Mato, L.M. Casás, J.L. Legido, C.P. Gómez, L.M. Mourelle, D. Bessières, F. Plantier. *Journal of Thermal Analysis and Calorimetry*, 2017, 130, 1, 479.
- [2] V. Caridad, J.M. Ortiz de Zárate, M. Khayet, J.L. Legido. *Applied Clay Science*, 2014, 93–94, 23.
- [3] M.J. Pastoriza-Gallego, L. Lugo, J.L. Legido, M.M. Piñeiro. *Nanoscale Research Letters*, 2011, 6, 560.
- [4] N. Glavaš, M.L. Mourelle, C.P. Gómez, J.L. Legido, N.R. Šmuc, M. Dolenc, N. Kovač. *Applied Clay Science*, 2017, 135, 119.
- [5] L. M. Casás, M. Pozo, C. P. Gómez, E. Pozo, L. D. Bessières, F. Plantier, J. L. Legido. *Applied Clay Science*, 2013, 72, 18.

PI-4. Measurement of Binary Vapour-Liquid Equilibrium for High Relative Volatility Systems

Narasigadu C.^{1,2}, Moodley K.¹, Raal J.D.¹

¹Thermodynamics Research Unit, School of Engineering, University of KwaZulu-Natal, Howard College Campus, King George V Avenue, Durban, 4041, South Africa;

²Department of Chemical Engineering, Mangosuthu University of Technology, 511 Mangosuthu Highway, Umlazi, 4031, South Africa

narasigadu.caleb@mut.ac.za

A specialised still with a novel annular Cottrell pump was used for the measurement of vapour-liquid equilibrium (VLE) data by the dynamic-analytic approach at low pressures. This still, similar to a previously employed still^[1], improves VLE measurement of high relative volatility systems. Test systems of ethanol + *n*-nonane at 343.21 K and ethanol + *n*-decane at 101.3 kPa were measured to confirm the reliability of the apparatus. Thereafter novel data were measured for the ethanol + *n*-nonane system at 323.21 and 333.21 K and the ethanol + *n*-decane system at 328.17, 338.17 and 348.16 K.

The combined method for data regression incorporating the NRTL^[2] activity coefficient model and the virial equation of state with the Hayden and O'Connell^[3] correlation was used. The minimisation of pressure residuals was used to fit the experimental data. UNIFAC predictions were also conducted which revealed significant discrepancy between experimental and predicted data thus highlighting the importance of precise experimental data in these types of systems. All the experimental data were subjected to thermodynamic consistency testing^[4-6] which concluded that all the data were consistent.

[1] J.D. Raal, R.K. Code, D.A. Best, *J. Chem. Eng. Data*, 1972, 17, 211-216.

[2] H. Renon, J. Prausnitz, *AIChE J.*, 1968, 14, 135-144.

[3] J.G. Hayden, J.P. O'Connell, *Ind. Eng. Chem. Process Des. Dev.*, 1975, 14, 209-216.

[4] O. Redlich, A.T. Kister, *Ind. Eng. Chem.*, 1948, 40, 345-348.

[5] H.C. Van Ness, S.M. Byer, R.E. Gibbs, *AIChE J.*, 1973, 19, 238-244.

[6] L.J. Christiansen, A. Fredenslund, *AIChE J.*, 1975, 21, 49-57.

PI-5. Internal Pressure in Water + 1,3-Dimethylurea Mixtures

Egorov G.I., Makarov D.M.

G.A. Krestov Institute of Solution Chemistry of the Russian Academy of Sciences, Ivanovo, Russia

gie@isc-ras.ru

The internal pressure P_{int} determines the change in the internal energy of the system with a slight isothermal expansion, is well determined from experimental data and is described by the equation:

$$P_{\text{int}} = -(\partial U / \partial V)_{T,x} = P - T(\partial P / \partial T)_{V,x} = P - T(E_{P,m} / K_{T,m})_{T,P,x}$$

The magnitude of the internal pressure of the system P_{int} is related to the cohesion energy density, and its dependence on temperature, external pressure and molar volume can be used to observe structural changes in the liquid mixture. It was previously shown that the strongest changes in the values of the internal pressure depending on temperature are observed in those liquid-phase systems where association processes take place, or in solvents with a developed network of hydrogen bonds. The values of the internal pressure of liquids in the temperature range from 278 to 323 K and pressures from 0.101 MPa (atmospheric) to 100 MPa, as a rule, change monotonically both with increasing temperature and with increasing pressure. With increasing pressure at low temperatures, the values P_{int} decrease, and at high temperatures they increase.

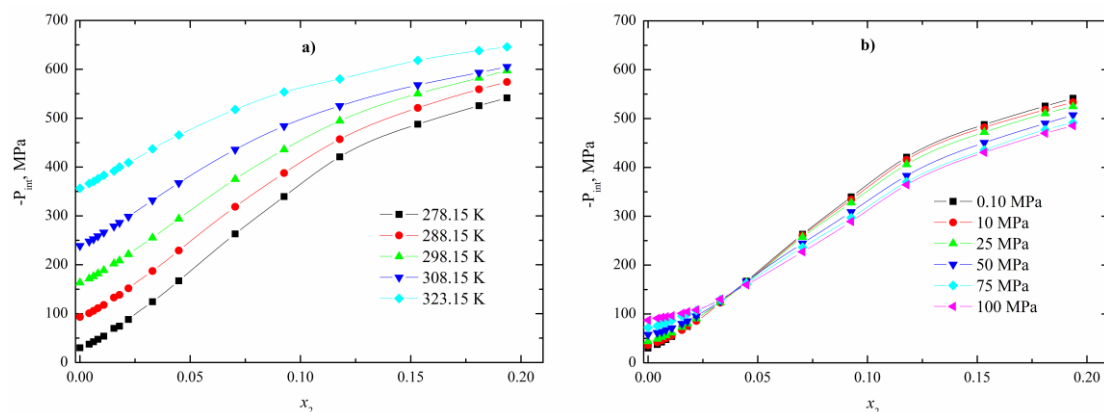


Figure 1. The dependence of the internal pressure on the molar fraction of 1,3-dimethylurea: (a) at 0.101 MPa and different temperatures, (b) at 278.15 K and various pressures.

The obtained temperature, pressure dependences of the internal pressure of the water + 1,3-dimethylurea mixture in the report are compared with similar dependencies of the internal pressure of the water + urea [1] and water + methylurea [2] mixtures.

References:

1. D.M. Makarov, G.I. Egorov // J. Chem. Thermodyn. 2018, 120, 164–173.
2. G.I. Egorov, D.M. Makarov // J. Chem. Eng. Data, 2017, 62, 4383–4394.

Acknowledgements: This work was supported by the Russian Foundation for Basic Research (project 18-43-370010 r_center_a).

PI-6. Effect pressure on the Intermolecular Interactions of N-Methylacetamide with Water

Makarov D.M., Egorov G.I., and Kolker A.M.

G.A. Krestov Institute of Solution Chemistry of the Russian Academy of Sciences, Ivanovo, Russia

gie@isc-ras.ru

N-methylacetamide are of great interest due to the presence of amide group in its structure, which can be considered as a model for investigation of peptide bond. The intermolecular interactions of this functional group with water play an important role in the structure formation and, thus, determine the properties of many biological systems.

The compressibility coefficients, $k = (V_0 - V)/V_0$, of binary aqueous solutions of N-methylacetamide have been measured within $x_2 = 0 \div 0.5$ (N-methylacetamide mole fraction) at 298.15 K and at pressures from atmospheric one to 100 MPa. The molar isothermal compressibilities of solutions, $K_{T,m}$, the partial molar volumes of water, \bar{V}_1 , and N-methylacetamide, \bar{V}_2 , the limiting partial molar volumes of N-methylacetamide in water, \bar{V}_2^∞ , and the limiting partial molar isothermal compressibilities of N-methylacetamide, $\bar{K}_{T,2}^\infty$, have been calculated.

It was established that the molar isothermal compressibility went down with the first portions of N-methylacetamide in water and reached its minimum at $x_2 \approx 0.18$. The concentration dependence of the partial molar volume of N-methylacetamide passed through its minimum at $x_2 \approx 0.07$; the extreme depth increased with the pressure growth. The limiting partial molar volumes of N-methylacetamide in water decreased with the pressure increase and the limiting partial molar isothermal compressibilities of N-methylacetamide were positive at all state parameters studied. These results agree with the idea about the looser structure of water within the hydration sphere of N-methylacetamide as compared with the structure of bulk water.

Acknowledgements: This work was supported by the Russian Foundation for Basic Research (projects 17-03-00309a and 18-43-370010 r_center_a).

PI-7. Experimental Determination of (p, ρ, T) Data of Liquid Toluene and n-Tetradecane in a Wide Range of State Parameters

Shchamialiou A.P.¹, Samuilov V.S.¹, Holubeva N.V.¹, Paddubski A.G.¹, Drăgoescu D.², Sirbu F.²

¹Mogilev State University of Food Technologies, Belarus;
²„Ilie Murgulescu” Institute of Physical Chemistry, Romania

shche70@mail.ru

The present paper deals with experimental determination of density for liquid toluene and n-tetradecane. A review of the open literature has shown that the experimental data on thermodynamic properties for liquid n-tetradecane are scarce. In this work, the density of a much more commonly studied liquid – toluene – was also measured, which allowed to confirm the reliability and accuracy of the apparatus, along with obtaining of additional data for this liquid in a wide range of temperatures and pressures.

For a further investigation of the thermodynamic properties of the above mentioned substances, the measurements of density, over the temperature range 273.65-473.15 K and at pressures up to 140.1 MPa, for the liquid toluene and over the temperature range 298.15-433.15 K and at pressures up to 100.1 MPa, for the liquid n-tetradecane have been done. The samples of toluene and n-tetradecane were obtained from ECOS1 and Aldrich, with a stated minimum purity of 99.5 and 99%, respectively. Further purification of the samples was not performed.

The density measurements have been effected by means of a apparatus Anton Paar DMA HPM vibration-tube densimeter. The temperature has been measured with a platinum resistance thermometer Hart Scientific (model: 5608), with an uncertainty of 0.02 K. The pressure has been measured with an MP-2500 dead-weight pressure gage, with an uncertainty of 0.05%. Densitometer has been calibrated using the model proposed by Bouchot and Richon [1]. Some changes have been made to the original calibration procedure, described in detail [2]. The overall uncertainty in density measurements is estimated to be 0.03%.

A comparison of measured densities values for pure toluene and n-tetradecane with the available in the literature data has been performed. The most reliable data on the density of toluene and n-tetradecane agree with the results of measurements within 0.2 and 0.1%, respectively. The Tate equation of state was used as an approximation equation.

Acknowledgements. This research has been carried out in the framework of the joint project T18RA-007, with the financial support of the Belarusian Republican Foundation for Fundamental Research and the Romanian Academy.

The Romanian authors want to express their acknowledgement to the Romanian Academy, for the financing the research programme “Chemical thermodynamics and kinetics. Quantum chemistry” of the “Ilie Murgulescu” Institute of Physical Chemistry. The financial support of the EU (ERDF) and Romanian Government, which allowed for the acquisition of the research infrastructure under POS-CCE O 2.2.1 Project INFRANANOCHEM - Nr. 19/01.03.2009, is also acknowledged.

[1] C. Bouchot, D. Richon, *Fluid Phase Equilib.*, 2001, 191, 189.

[2] T.S. Khasanshin, V.S. Samuilov, A.P. Shchamialiou, F.M. Mosbakh, D. Dragoescu, F. Sirbu, *Fluid Phase Equilib.*, 2018, 463, 121.

PI-8. Determination of Thermodynamic Properties of Liquid Toluene and n-Tetradecane in a Wide Range of Temperatures and Pressures Based on Dissimilar Initial Data

Shchamialiou A.P.¹, Samuilov V.S.¹, Holubeva N.V.¹, Drăgoescu D.², Sîrbu F.²

¹Mogilev State University of Food Technologies, Belarus;

²„Ilie Murgulescu” Institute of Physical Chemistry, Romania

shche70@mail.ru

The speed of sound data for the obtaining of thermodynamic properties have been used for many years. Such calculations representing a useful tool for the indirect determination of thermodynamic properties, which are particularly difficult to obtain, especially at high pressures. Earlier, the methods for determination of these properties for a compressed liquid were developed with simultaneous use of initial data on the density and speed of sound at elevated pressures. All literature available data of thermodynamic properties can be used in the development of the fundamental equations of state. In this work, based on the all available measurements of thermodynamic properties, these properties of liquid toluene and n-tetradecane have been calculated. We used the data on density, sound velocity, isobaric and isochoric heat capacity, isothermal compressibility, as initial data for calculating the thermodynamic properties, for both toluene and n-tetradecane.

The calculation method uses a simple dependence of specific volume on pressure:

$$v = \frac{1 + A(p + B)^{1/3}}{C + D(p + B)^{1/3}},$$

where p is pressure; A , B , C , D are temperature dependent parameters.

The isobaric specific heat capacity at atmospheric pressure was fitted with a simple equation:

$$c_{p0} = e_0 + e_1T + e_2T^k,$$

where e_0 , e_1 , e_2 , k are constants.

As a result of processing the initial data, the values of the parameters of equation were determined. The system of internally consistent values of the thermodynamic properties of liquid toluene and n-tetradecane was obtained using the values of this parameters and known differential thermodynamic relations.

The values of density, speed of sound, isobaric and isochoric heat capacity, isobaric expansion coefficient, isothermal and isentropic compressibility for toluene, over a temperature range from 273.15 K to 433.15 K and pressures up to 140 MPa, as well as for and n-tetradecane, at temperatures from 298.15 K to 433.15 K and pressures up to 100 MPa have been obtained.

The validity of the calculation method is confirmed by a good agreement between the obtained results and a large number of measurements of the various thermodynamic properties for liquid toluene, as well as n-tetradecane.

Acknowledgements. This research has been carried out in the framework of the joint project T18RA-007, with the financial support of the Belarusian Republican Foundation for Fundamental Research and the Romanian Academy.

The Romanian authors want to express their acknowledgement to the Romanian Academy, for the financing the research programme “Chemical thermodynamics and kinetics. Quantum chemistry” of the “Ilie Murgulescu” Institute of Physical Chemistry. The financial support of the EU (ERDF) and Romanian Government, which allowed for the acquisition of the research infrastructure under POS-CCE O 2.2.1 Project INFRANANOCHEM - Nr. 19/01.03.2009, is also acknowledged.

PI-9. Volumetric and Caloric Properties of Liquid Cesium–Bismuth Alloys

Stankus S.V., Khairulin R.A., Abdullaev R.N., Savchenko I.V., Yatsuk O.S.

Kutateladze Institute of Thermophysics, Novosibirsk, Russia

stankus@itp.nsc.ru

According to a number of studies, the chemical bonds between different atoms in the alloys of alkali metals with bismuth have a mixed ionic and metallic character. This is due to the fact that bismuth, although considered a metal element, is much more electronegative than alkali metals. Measurements of the electrical resistivity and thermodynamic activity of alkali–bismuth melts indicate the existence of associated ionic complexes in the liquid phase. The concentration of these complexes reaches a maximum at certain stoichiometric compositions. The change in the structure of the alkali–bismuth melts under changes of their composition should lead to features in the concentration dependences of the structure-sensitive properties of these systems. However, most of the properties of liquid alloys of alkali metals with bismuth have not been experimentally investigated to date. In this work, we present the new experimental data on the density, enthalpy and heat capacity of a number of cesium–bismuth melts. The density was measured by the gamma-ray attenuation technique. The caloric properties were investigated using the drop calorimeter of isoperibol type. Using the obtained results, the temperature and concentration dependencies of the investigated properties of the liquid Cs–Bi system were constructed. An analysis showed that the behavior of the molar volume, thermal expansion coefficient, enthalpy, and heat capacity substantially deviates from the laws of an ideal solution. A correlation between the volumetric and electrical properties of the cesium–bismuth melts was revealed. The presence of maxima on the concentration dependences of thermophysical properties confirms the possibility of formation of associated complexes in melts with partially ionic character of interatomic interaction. Based on the measurement results, the position of the liquidus curve in the Cs–Bi phase diagram was clarified.

Acknowledgements This study was supported by the Russian Science Foundation (Grant No. 16-19-10023).

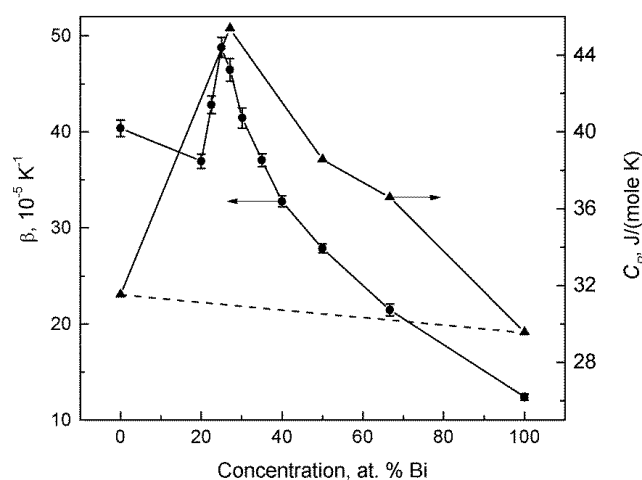


Figure 1. Concentration dependences of the volume coefficient of thermal expansion (950 K) and isobaric heat capacity (1000 K) of the melts of the cesium-bismuth system.

PI-10. Chemical Interaction in the Na,Rb||F,I,CrO₄ Quaternary Reciprocal System

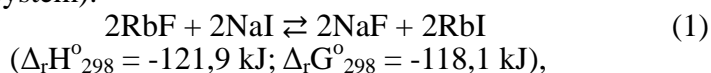
Babenko A.V., Egorova E.M., Garkushin I.K.

Samara State Technical University, Russia;

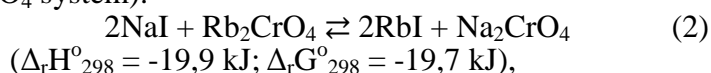
anastasya.babenko2010@yandex.ru

The Na,Rb||F,I,CrO₄ quaternary reciprocal system was studied, composition prism presented in figure 1. Using theory of graphs [1], the Na,Rb||F,I,CrO₄ system was divided into simplexes. The lower dimensionality (two-component and three-component systems) data were used for connecting points determination, as well as a preliminary calculation of the standard enthalpies $\Delta_r H^\circ_{298}$ and Gibbs energies $\Delta_r G^\circ_{298}$ of reactions occurring at conversion points of triple reciprocal systems, that bound the Na,Rb||F,I,CrO₄ quaternary reciprocal system:

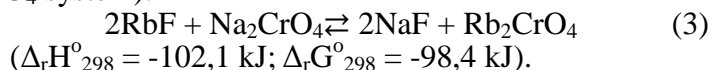
point K₁ (Na,Rb||F,I system):



point K₂ (Na,Rb||I,CrO₄ system):



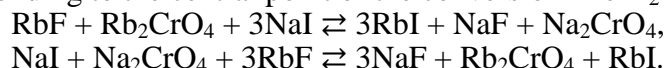
point K₃ (Na,Rb||F,CrO₄ system):



The thermodynamic characteristics of the individual salts are taken from [2].

As shown the system partition, the stable secant complex of the quaternary reciprocal system Na,Rb||F,I,CrO₄ is formed by two stable triangles. Each stable triangle intersects the metastable triangle forming the conversion line (fig.1).

Summing up the reactions (2) and (1) ((1) and (3)) for the compositions of the full conversion points K₂ and K₁ (K₁ and K₃), the exchange reaction was obtained, occurring in the composition corresponding to the central point of the conversion line K₂–K₁ (K₁–K₃):



The triangular plane formed by the K₂–K₁ and K₁–K₃ conversion lines reflects the interaction of three pairs of salts in the Na,Rb||F,I,CrO₄ system.

The reaction products are crystallizing phases in the corresponding stable simplexes of the system, which is confirmed by the results of the experimental study using differential thermal analysis.

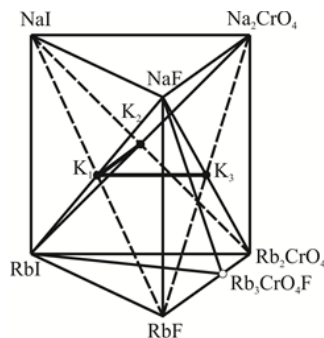


Figure 1. . Composition prism of the Na,Rb||F,I,CrO₄ system

[1] O. Ore, *Theory of graphs*, 1980, 336 p. Nauka, Moscow, Russia.

[2] V. P. Glushko, *Thermal Constants of Materials. Handbook*, 1981, Vol. 10, Pts. 1 and 2. VINITI, Moscow, Russia.

PI-11. Thermodynamical Properties of L-Carnosine on Solid and Liquid Phase

Kuritsyna A.A.¹, Tyunina V.V.¹, Mezhevoi I.N.², Tyunina E.Yu.², Badelin V.G.²

¹Ivanovo State University of Chemistry and Technology, Russia;

²G.A. Krestov Institute of Solution Chemistry, Russian academy of Sciences

kaa_isc@mail.ru

Thermodynamic studies of crystalline peptides cause a lot of attention, since these systems can be used as molecular materials, drugs and biomimetics. They are zwitterions linked with each other by dipole-dipole interactions, hydrogen bonds and Van der Waals interactions. L-Carnosine (Car) is a dipeptide, made up of β -alanine and L-histidine, bound together by means of a peptide linkage, found in different body organs. Carnosine is found naturally mainly in the skeletal muscles, central nervous system, olfactory neurons and in the lens of the eye in some vertebrates, including humans. Due to its antioxidant, protective, chelating, anti-glycation activity, this dipeptide can be used to prevent and treat diseases such as diabetes, neurodegenerative diseases, diseases of the sense organs and cancers. The crystal structure of Car has been reported. However, the thermal and solvation properties of Car still need to be investigated. Here, we provide the first study of this dipeptide both in solid and liquid phase via thermochemical techniques. Enthalpies of solution of the Car in water have been determined with the isoperibol solution calorimeter at 298 K and heat capacities of solid Car have been obtained with the DSC calorimeter.

The behavior of the sample as a function of temperature was studied by DSC 204 F1 Phoenix differential scanning heat flux calorimeter (NETZSCH, Germany) with a high sensitivity μ -sensor. The sample was heated at the rate of 10 K min^{-1} in an argon atmosphere and cooled with gaseous nitrogen. The analysis of the results showed that measurements error of the specific heat capacity of the crystalline substance was within $\pm 0.003 \text{ J}\cdot\text{g}^{-1}\text{K}^{-1}$. The molar heat capacities ($C_{p,m}^0(\text{cr})$) of Car increase with rising temperature and does not show any peculiarities in the range (205–475) K. Thermal properties (temperatures, mass losses) associated with decomposition processes of the Car were measured in the temperature ranging from 293 to 623 K. The temperature range in which the decomposition processes (decomposition prevails due to the high temperature) of Car take place was to be (531–563) K.

The sublimation of Car was investigated by Knudsen's effusion method with mass spectrometric vapor composition control. Fragmentation of molecule under electron ionization was discussed. It was showed that this dipeptide have a fairly low vapor pressure. The zwitterionic character of their molecules decreases their volatility. Its mass spectrum contains mostly light ions. Using the correlation equation of "structure-property" for peptides series [1], the molar standard enthalpy of sublimation at $T = 298.15 \text{ K}$, was derived as $\Delta_{\text{sub}}H_m^0 = 179 \text{ kJ}\cdot\text{mol}^{-1}$ for Car.

Experimental measurements of enthalpies of solution were performed in the range of molalities of the Car from (0.002 to 0.008) $\text{mol}\cdot\text{kg}^{-1}$. Standard uncertainties for temperature, pressure and molality are $\pm 0.01 \text{ K}$, $\pm 0.5 \text{ kPa}$ and $\pm 1\cdot 10^{-6} \text{ mol}\cdot\text{kg}^{-1}$, respectively. The standard enthalpies of solution of Car in water are positive. The molar enthalpy of solvation at infinite dilution (i.d.) ($\Delta_{\text{solv}}H_m^\infty$) of the Car in aqueous solution was determined, calculated from the differences between the obtained molar enthalpy of solution at i.d. of the Car ($\Delta_{\text{sol}}H_m^\infty = 8.01 \text{ kJ}\cdot\text{mol}^{-1}$) and the molar standard enthalpy of sublimation. The results were discussed in terms of solute-solvent and solute-solute interactions in liquid phase.

Acknowledgements The reported research was funded by Russian Foundation for Basic Research and the government of the Ivanovo region of the Russian Federation, grant № 18-43-370018.

[1] V. Badelin, et al., *Russ.J. Phys. Chem.*, 2012, 86A, 457.

PI-12. Phase Equilibrium and Structure of Acrylic Blocks and Gradient Copolymers

Nikulova U.V., Chalykh A.E., Khasbiullin R.R., Gerasimov V.K.

A.N. Frumkin Institute of Physical Chemistry and Electrochemistry
Russian Academy of Sciences, Russia

ulianan@rambler.ru

Thermal properties of the block, gradient and statistical copolymers of styrene and *n*-butyl acrylate with styrene content from 7 to 60 % and M_w from 21000 to 67000, obtained by the methods of PAFT-copolymerization [1], have been studied by DSC. Experimental data on the temperature values for the coexisting phases compositions are obtained by optical interferometry by mixing copolymers with homopolymers of different M_w . Within the framework of the Flory-Huggins-Scott theory, paired interaction parameters are calculated. Constructed generalized phase and physical state diagrams.

It is established that statistical, gradient and block copolymers with a low styrene content have one glass transition temperature, close to additivity. Block copolymers with a high styrene content (above 46 %) have two glass transition temperatures (Fig. 1). This fact is associated with the presence in the gradient copolymer of extensive statistical regions between the block ones. Block copolymer behaves like a two-phase system, starting with a certain length of styrene block.

Statistical, gradient, and block copolymers with a low styrene content show the classic diagram with UCST (Fig. 2). For block copolymer with a high styrene content, due to the formation of phase grids, there is a stage of prolonged swelling of the copolymer in PS followed by complex and irreversible phase decomposition. The data are in agreement with the results of structural and morphological studies using transmission electron microscopy.

Acknowledgements The financial support of Russian Foundation for Basic Research (RFBR) – project №17-03-00197.

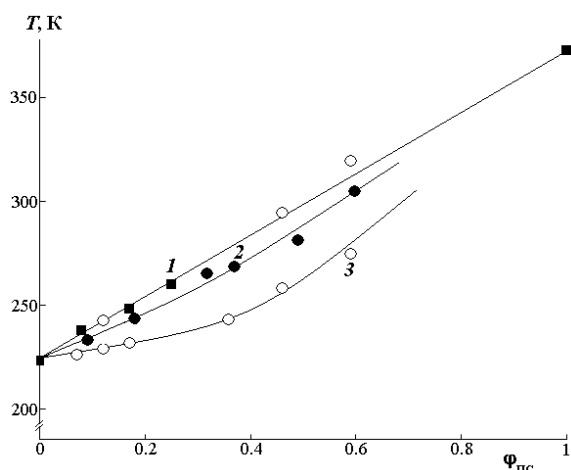


Figure 1. The dependence of the glass transition temperature of statistical (1), gradient (2) and block copolymers (3) on the styrene content.

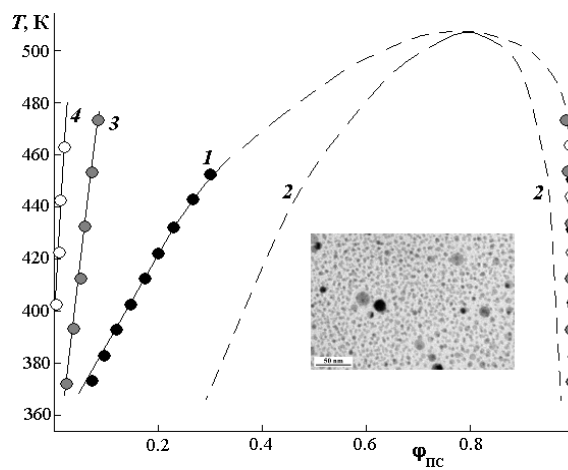


Figure 2. Phase diagram of the block-SBAS-7 with PS-4100 (1), PS-9000 (3) and PS-30000 (4). Also, the calculated data for the spinodal curve of block SBAS-7 with PS-4100 (2) and micrograph of block copolymer are given.

[1] E.V. Chernikova, et al., *Polymer Science B*. 2013. V. 55. № 3–4. P. 176.

PI-13. The Influence of Solute-Solute and Solute-Solvent Correlations on Urea-Urea and Tetramethylurea-Tetramethylurea Pair Interactions in Water

*Kustov A.V.^{1,2}, Antonova O.A.^{1,2}, Smirnova N.L.^{1,2}, Kruchin S.O.,¹
Ivanov E.V.¹, Makarov V.V.²*

¹Krestov Institute of Solution Chemistry of Russian Academy of Sciences, Russian Federation;
²Ivanovo State University of Chemistry and Technology, Russian Federation

kustov@isuct.ru

Water reveals a unique ability to hydrate biological species leading to the appearance of a driving force for them to adopt special structures in ways where hydrophilic units are exposed to water and the hydrophobic ones are mainly sequestered from solvent molecules. Similar but much weaker solvent-induced forces are believed to appear in non-aqueous solvents with the three dimensional H-bond network such as glycols, amino alcohols etc [1]. We are currently involved in the intensive and continuing study on the behavior of hydrophobic and hydrophilic species in water, ethylene glycol (Eg) and formamide (see [2, 3] and references therein). Here, we present the results of our thermochemical and volumetric investigations on pair and triplet interactions occurring between urea (U) or tetramethylurea (TMU) molecules in water at different temperatures. The corresponding pair and triplet interaction parameters obtained *via* the virial expansion technique are given below. In the report these and other (g_{AA} , $-T\delta_{AA}$, c_{pAA}) thermodynamic quantities will be compared for hydrophilic (U) and hydrophobic (TMU) species. Special attention will be paid to the extraction of the contribution from the direct solute-solvent interactions into the y_{AA} values. The similar trends and principal differences in the behavior hydrophilic and hydrophobic species at different temperatures will be highlighted and discussed.

Acknowledgements The financial support of this research by RFBR Grant 18-03-00016 –a is gratefully acknowledged.

Table. Enthalpic and volume pair (h_{AA} , v_{AA}) and triplet (h_{AAA} , v_{AAA}) interaction parameters for U and TMU in water obtained in the Lewis-Randall standard state

T/K	$h_{AA}/J \text{ kg/mol}^2$;	$v_{AA}/\text{m}^3 \text{ kg/mol}^2$	$h_{AAA} / J \text{ kg}^2/\text{mol}^3$	$v_{AAA}/ \text{m}^3 \text{ kg}^2/\text{mol}^3$
U				
298.15	-335(24)	0.01(0.02)	27(13)	-
308.15	-145(16)	-0.01(0.02)	-53(8)	-
318.15	-77(35)	-0.03(0.03)	-65(17)	-
TMU				
298.15	2346 (163)	-1.51(0.03)	-240(84)	-
308.15	2002 (276)	-1.21(0.03)	-180 (145)	-
318.15	1730 (175)	-0.88(0.05)	-178 (94)	-

[1] N.A. Chumaevskii, M.N. Rodnikova, J. Barthel, *J. Mol. Liq.*, 2004, 115, 63.

[2] A.V. Kustov, O.A. Antonova, N.L. Smirnova, *J. Chem. Thermodyn.*, 2019, 130, 114.

[3] A.V. Kustov, O.A. Antonova, N.L. Smirnova, A.A. Kladiev, A.A. Kladiev, T.V. Kudayarova, M.S. Gruzdev, D.B. Berezin, *J. Mol. Liq.*, 2018, 263, 49.

PI-14. Thermodynamics of Solution of 3,5-Diamino-1,2,4-Triazole and 3,5-Diamino-1-Phenyl-1,2,4-Triazole in Water

Kustov A.V.^{1,2}, Kudayrova T.V.², Antonova O.A.^{1,2}, Smirnova N.L.^{1,2}

¹Krestov Institute of Solution Chemistry of Russian Academy of Sciences, Russian Federation;

²Ivanovo State University of Chemistry and Technology, Russian Federation

kustov@isuct.ru

In this work we focus on the first thermodynamic study of aqueous solutions of two heterocycles *i.e.* 3,5-diamino-1,2,4-triazole and 3,5-diamino-1-phenyl-1,2,4-triazole which is known to be an extremely versatile synthetic base for a variety of medical applications [1]. We describe here synthesis, identification as well as calorimetric, solubility and partition experiments in water and 1-octanol/water biphasic system. The investigation of triazoles behavior in a solid state to study possible hydrate formation or phase transitions is also provided. The results are compared with those for some hydrophobic (see Figure below) or hydrophilic species and discussed in terms of solute-solvent interactions and water-induced forcers occurring in a liquid phase.

Acknowledgements This work was supported by the Russian Science Foundation (Grant 18-73-00217).

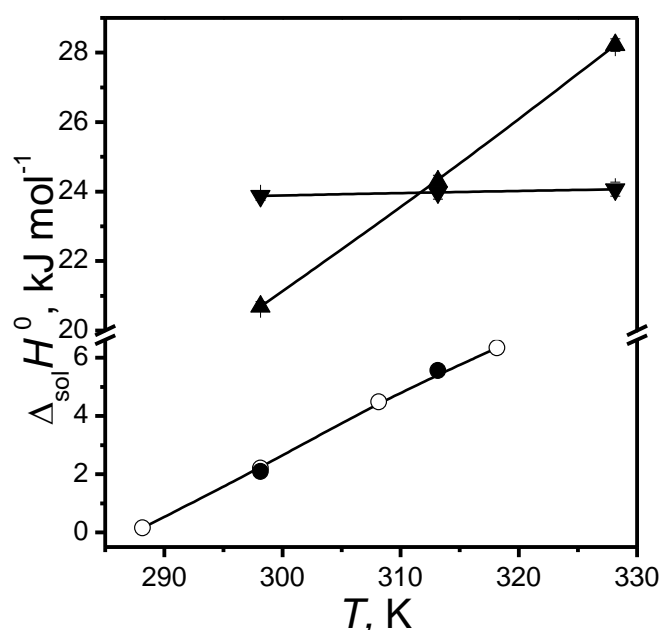


Figure. Temperature dependence of standard enthalpies of solution of 3,5-diamino-1,2,4-triazole (▼), 3,5-diamino-1-phenyl-1,2,4-triazole (▲) and benzene (○, ●) in water. Points are experimental values, lines represent linear functions, error bars give the twice standard deviation; (○) – values from ref. [2].

[1] J.K. Shneine, Y.H. Alaraji, *International J. Science and Research*, 2016, 5, 1411.

[2] D. Hallén, S.O. Nilsson, I. Wadsö, *J. Chem. Thermodyn.*, 1989, 21, 529.

PI-15. Enthalpic Parameters of Pair Interactions between Urea and Tetramethylurea Molecules in Ethanediol at 298 - 318 K

Batov D.V., Smirnova N.L., Kustov A.V., Antonova O.A.

Krestov Institute of Solution Chemistry of Russian Academy of Sciences, Russian Federation

bat21dv@yandex.ru

It is believed that in non-aqueous media, especially, in solvents with hydrogen bonding systems, the phenomena associated with the solvent ordering around non-polar objects and the corresponding tendency to an aggregation of apolar species may occur. One way to solve this problem is to provide a comparative study of solutions of hydrophobic tetramethyl urea (TMU) and hydrophilic urea (U) species in water and an appropriate non-aqueous solvent such as ethanediol (Eg). Some experimental evidence for solvophobic interactions between tert-butanol and TMU molecules in Eg have been found elsewhere [1, 2]. Here, we study urea and tetramethylurea behavior in Eg to characterize the solvophobic interaction. The enthalpic parameters of the U-U and TMU-TMU pair interactions at 298.15, 308.15 and 318 K have been obtained from the enthalpies of dilution data ($\Delta_{dil}H$). These quantities for solutions containing 1, 1.3 and 1.6 moles U or TMU in 1 kg Eg were determined by the calorimetric method. The data obtained were approximated *via* the equation based on the McMillan-Mayer formalism [3].

$$\frac{\Delta_{dil}H}{m_f(m_f - m_i)} = h_{AA} + h_{AAA}(m_f + m_i)$$

In this equation, m_i and m_f are the initial and final concentrations of the solution; h_{AA} and h_{AAA} are the enthalpic parameters of the pair and triple interaction between solute molecules. The temperature dependence of the enthalpic parameters for urea solutions is shown in the figure 1. Possible reasons leading to the increase of h_{AA} parameters with increasing temperature will be discussed.

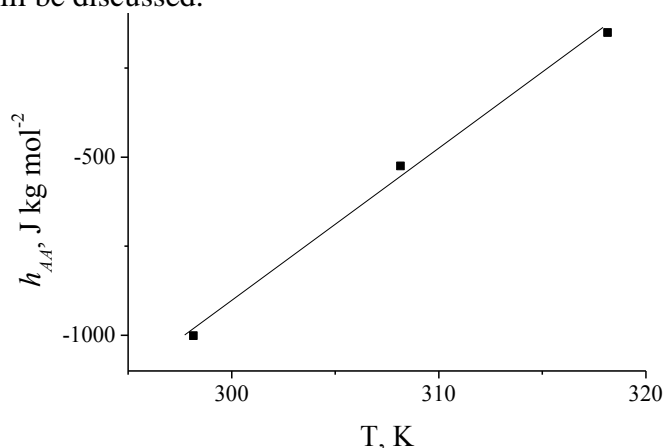


Figure 1. The temperature dependence of the enthalpic parameters of pair interactions for urea solutions.

Acknowledgements. This work was supported by the Russian Foundation for Basic Research (project 18-03-00016).

[1] I. A. Chaban, et al., *J. Mol. Liq.*, 1999, 80, 27.

[2] M. N. Rodnikova, *J. Mol. Liq.*, 2007, 136, 211.

[3] G. Barone, et al., *J. Chem. Soc., Faraday Trans. I*, 1981, 77, 1569.

PI-16. Heat Capacity and Structural Changes Associated with Solvation of Polar and Apolar Groups in Water and Ethylene Glycol

Krest'yaninov M.A.¹, Kustov A.V.^{1,2}, Batov D.V.¹, Ivanov E.V.¹, Makarov V.V.²

¹Krestov Institute of Solution Chemistry of Russian Academy of Sciences, Russian Federation;

²Ivanovo State University of Chemistry and Technology, Russian Federation

kustov@isuct.ru

Experiments and computer simulations show that the “open” structure of water results from the high degree of angular ordering in a liquid phase [1]. It has been found that the probability distribution of H-bond angles made by each water to its neighbours is bimodal both in a pure liquid and aqueous solutions, it being crucially dependent of the hydrophobicity/hydrophilicity of solute molecules [1]. The effect of hydrophobic species is essentially geometric: they tend to displace the more weakly H-bonded facial water in the coordination shell, thus reducing the population of more bent H-bonds. In contrast, polar solutes usually shift the distribution of water–water H-bond angles towards the more bent form. These structural changes lead to totally different heat capacities of hydration. For apolar solutes they are large and positive, whereas for polar ones they are negative. We have performed molecular dynamics simulations (DL_POLY Classic 1.9) of water, ethylene glycol (Eg) and solutions of urea and tetramethylurea in both solvents using various potential functions at 288-308 K. The computed distribution of solvent-solvent H-bond angles both in water and Eg are found to be bimodal independently of the potential function used. The similar phenomenon is observed in aqueous solutions of U and TMU (see Figure 1). The apolar groups of TMU and amino groups of U induce the slight increase of the linear H-bonds in the first hydration shell, whereas carbonyl oxygen gives the opposite effect. The contributions of different solute fragments into heat capacities of hydration are computed *via* the H-bond random network model [1], compared with the experimental quantities and briefly discussed in terms of the solvophobic solvation phenomenon.

Acknowledgements The financial support of this research by RFBR Grant 18-03-00016–a is gratefully acknowledged.

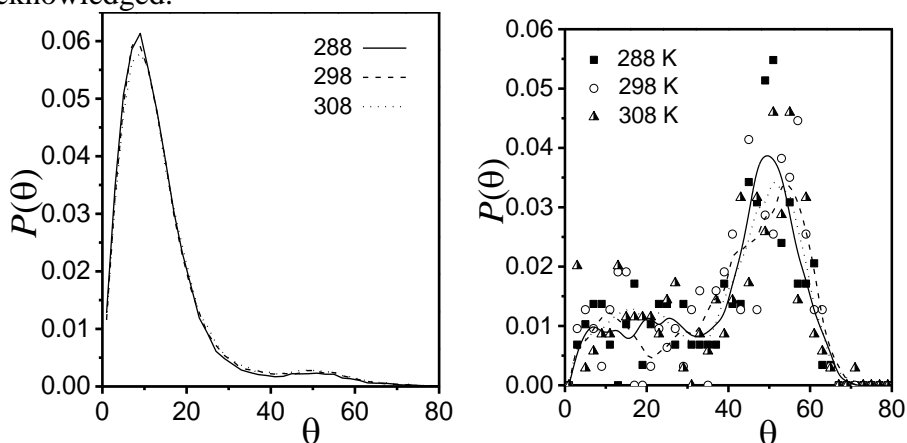


Figure 1. The probability of H-angles distribution (Θ is the smallest HOO angle for two neighbor waters) in an aqueous solution around methyl group of TMU (left-hand side) and carbonyl oxygen (right-hand side).

[1] K.R. Gallagher, K.A. Sharp, *J. Amer. Chem. Soc.*, 2003, 125, 9853.

PI-17. Extractive Crystallization of Sodium Chloride in the Ternary System Sodium Chloride–Water–Diisopropylamine

Danilina V.V. and Cherkasov D.G.,

Saratov State University named after N.G. Chernyshevsky, Saratov 410012, Russian Federation

ilinkk@info.sgu.ru

Traditional methods of obtaining salts by evaporation of their aqueous solutions are often very energy-expensive and do not always lead to obtaining the desired high-quality product. The process of extractive crystallization under the action of organic solvents, which are often called “antisolvents” in the literature, is one of the promising modern methods to obtain various salts. An organic solvent is added to aqueous salt solutions, which, on the one hand, leads to a decrease in the salt solubility with some fraction of it to precipitate, and on the other hand, delamination of the water-organic mixture into two liquid phases is observed. The organic phase is then separated and recycled.

The paper is devoted to the study of phase equilibria and critical phenomena in component mixtures of the ternary system sodium chloride + water + diisopropylamine in order to clarify the possibility of its usage for extractive crystallization of sodium chloride and isolation of the amine from its aqueous solutions under the action of this salt. The study was carried out by the visual-polythermal method in component mixtures of ten sections of the composition triangle of the ternary system in a range of 10.0-90.0°C.

The following phase states were observed in the components mixtures: saturated and homogeneous solutions, monotectics, and delamination. The solid phase was identified as NaCl at all temperatures. The temperature dependences of the composition of the critical solution of the separation area were found. Analysis of the plotted phase diagrams of the system at 10.0, 25.0, 27.3, 40.0 and 90°C made it possible to evaluate the efficiency of using the amine in the process of extractive crystallization of the salt, as well as the effect of salting out of diisopropylamine from its aqueous solutions under the action of the salt at several temperatures.

To assess the efficiency of salting out of diisopropylamine from its aqueous solutions under the action of sodium chloride, we found the temperature dependence of the distribution coefficient of the amine between the equilibrium liquid phases of the monotectic state. At all temperatures, the organic phase was significantly enriched in the amine, while its content in the aqueous phase was negligible. The high values of the distribution coefficient of diisopropylamine (more than 300 in the range of 40-90°C) indicate that sodium chloride is a very effective salting-out agent of this amine. The amine content in the organic phase reached 93-96 wt. %, which is a favorable factor for the process of extractive crystallization and subsequent amine recycling.

To assess the efficiency of the use of diisopropylamine in extractive crystallization of sodium chloride, we calculated the mass of the salt in the precipitate using the triangle center of gravity rule using a designed computer program, which allowed us to find the optimal conditions for extractive crystallization of NaCl. To calculate the salt mass precipitated under the action of the amine, an unsaturated water-salt solution containing 25 wt. % of sodium chloride was chosen. It was established that the salt yield increased with increasing amine content in the temperature range 10.0-40.0°C. It was concluded that temperature almost did not affect the salt yield; it increased with an increase in the diisopropylamine content in the mixture, reaching a maximum value (~45%) with the highest amine content (up to 90 wt.%).

PI-18. Vapor Pressure of Dipropylene Glycol Methyl Ether and Vapor-Liquid Equilibria of its Aqueous Mixture: Experimental Measurements by The Static Method and Modeling Development

Dimitrov O.¹, Neau E.¹, Raspo I.¹, Guichardon P.¹, Dergal F.², Mokbel I.^{2,3}, Jose J.², Testa A.⁴

¹*Aix Marseille Université, CNRS, Centrale Marseille, M2P2 UMR 7340, Marseille, France;*

²*Univ Lyon, Université Claude Bernard Lyon 1, Laboratoire Multimatériaux et Interfaces, UMR 5615, F-69622 Lyon, France;*

³*Univ Lyon, Université Jean Monnet, F-42023 Saint-Etienne, France;*

⁴*ATDveloppements, 73, rue du Douard, F-13685 Aubagne, France;*

oleksandr.dimitrov@centrale-marseille.fr

Nowadays, the organic solvents are very widely spread in chemical and process engineering. In every industry the solvent choice is essential: many criteria should be considered in order to respect all the international rules and regulations. Therefore, not only the solvent power and volatility criteria, but the effect on the human body, the carcinogenicity as well as the environment and atmosphere impact, make a significant influence on solvent choice.

The dipropylene glycol methyl ether (DPM) is used in paint and ink industries, wood stains, textile processes, dry cleaning soaps and cleaning compounds. This solvent, having a great degreasing and dissolving power, respects the modern international regulations in terms of toxicity, biodegradability, ozone layer protection etc.

The problem, however, is a huge lack of the experimental thermo-physical and thermodynamic data for this compound. For example, some properties such as the normal boiling temperature, molar mass and density could be found in respective technical sheets provided by the solvent suppliers, but data concerning its vapor-liquid equilibria (VLE) have not yet been published, although these data are necessary for the solvent treatment process design (such as distillation).

This work represents a first path towards the construction of the database of DPM vapor pressure and VLE of its aqueous mixtures. We have studied the pure compound vapor pressures as well as the isothermal VLE for water and DPM binary mixture for temperatures ranging from 283.15 to 363.15 K.

The measurements were carried out using the static method. Its principle is to use a static cell that is filled with the testing liquid (pure compound or gravimetrically prepared binary mixture) previously degassed. The cell is placed into a thermal bath keeping the temperature constant. The saturated vapor is formed above the liquid in the static cell. Its pressure is then measured and one experimental P, T, x point is obtained. The measurements continue for all needed compositions and temperatures, so the bubble pressure curves can be constructed. Then, using the obtained experimental points, they were correlated with different equations (Antoine, Clapeyron, Wagner, Lee-Kesler etc) and all the corresponding coefficients were obtained in order to estimate vapor pressures at undetermined temperatures (and in the explored range).

The dew pressure curves were then calculated using well-known VLE semi-empirical models such as Wilson, Van Laar, NRTL Original, UNIQUAC. In the frame of this study, we have also investigated the ability to predict this VLE by the EoS-g^E approach using the NRTL-PR model.

PI-19. Synthesis of the Compounds with High Partial Pressure of Arsenic

Kostyanko A.A.¹, Sineva S.I.^{2,3}, Starykh R.V.³

¹Peter the Great St. Petersburg Polytechnic University, Russia;

²University of Queensland, Australia,

³LLC Gipronickel Institute

alena.alena.1512@mail.ru

The technique of arsenic-contained compounds synthesis has been developed for the study of the phase equilibria in the Fe-As-Cu-S quaternary system.

It is well-known, that arsenic, sulphur and their compounds are characterised by extremely high partial pressures at high temperatures. In particular, at melting temperature (817 °C) arsenic has partial pressure 38.2 atm. [1]. Also high partial pressure is observed for arsenic sulphides, heated up to 300 - 400 °C [1, 2, 3]. Moreover, the Fe-As-S и Cu-As-S ternary systems have wide range area of miscibility gap [4, 5], that makes it difficult to obtaining the homogeneous sample of the given composition. Available techniques of synthesis of arsenic-contained compounds are extensively described in [4, 5, 6], however, these methods are time-consuming and can lead to discrepancies between desired and obtained compositions, as they include the process of selective dissolution of phases inside the water substances. Therefore, the authors, relying on their experience of operating with volatile and aggressive compounds [7, 8] have developed the unique technique of arsenic-contained compounds synthesis with the applying of high pressure furnace.

The high pressure furnace can operate up to 70 atm pressure and 950 °C.

The arsenic-contained experimental samples, sealed in vacuumed silica ampoules, were synthesised during two stages. At the first stage they were heated up to 950 °C with the heating rate of 25 °C/min. High purity argon was used to create the external overpressure. The ampoules were held at the final temperature during the half on hour, then cooled inside the furnace. The second stage is the heating of the same ampoule at atmosphere pressure up to 1200 °C to reach the liquid state of samples. After high temperature holding ampoules were quenched into the water.

Described technique was successfully used for synthesis of arsenic sulphides and arsenides of stoichiometric compositions as well as for samples of the Fe-As-S and Cu-As-Fe ternary systems.

The details of construction of high pressure furnace and developed technique will be discussed during the conference.

The project was supported by RFBR grant No. 18-29-24166.

[1] Н.И. Копылов, Ю.Д. Каминский, *Мышьяк*, 2004, 44. Под ред. Г.А. Толстикова, Новосибирск, Россия.

[2] N. Chakraborti; D.C. Lynch, *Metall. Trans. B*, 1983, 14B (2), 239-251.

[3] М.М. Spivak, N.T. Skosyrev, I.O. Fedulov, *Kompleks. Ispol'z. Mineral'n. Syr'ya*, 1989, (3), 86-87.

[4] L.A. Clark, *Econ. Geol.*, 1960, 55, 1345-1381; 1631-1652.

[5] P.B. Barton, *Geochim. Cosmochim. Acta*, 1969, 33, 841-857.

[6] Э.Г. Мильке; С.М. Исабаев; Л.Ф. Сивак; Х.М. Кузгибекова, Патент Российской Федерации номер 2060947.

[7] E. Yu Kononova, S. I. Sineva, G. V. Semenova, T. P. Sushkova. Phase equilibria in the Sn-As-Ge and Sn-As-P systems. *Journal of Thermal Analysis and Calorimetry*, September 2014, Volume 117, issue 3, pp 1171-1177

[8] Илатовская М.О., Sineva S.I., Starykh R.V. Phase equilibria in the ternary Fe-Co-S system // CALPHAD: Computer Coupling of Phase Diagrams and Thermochemistry 59 (2017) 31–39

PI-20. Repeatings of DMPC Multilamellar Membranes Meltings Dramatically Change the Thermodynamic Parameters Registered by Differential Adiabatic Scanning Microcalorimetry Method

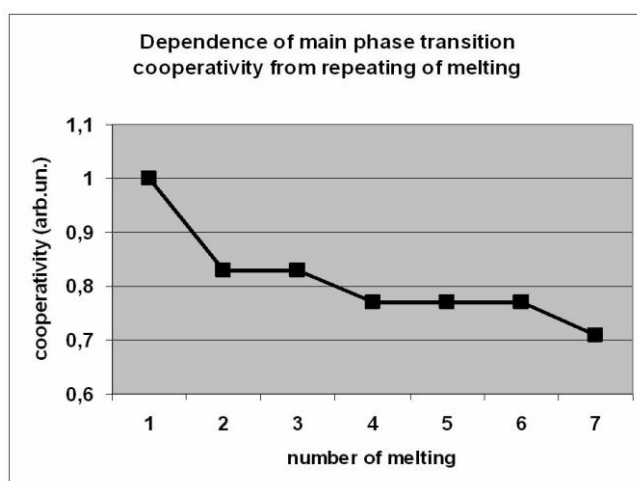
Alekseeva O.M.¹, Kremntsova A.V.¹, Kim Yu.A.²

¹ Emanuel Institute of Biochemical Physics RAS, Moscow, Russia;

² Institute of Cell Biophysics, RAS., Moscow region, Pushchino, Russia

olgavek@yandex.ru

The properties of biological objects are very variable. Thus animal's biomembranes change its parameters very often and fast, in order to be in harmony with demands of entire of animal organism. One of the interesting events were occurred when the body sleeps or when the organism fills and wakes up when usual sleeps or when hibernation sleeps. The temperatures of body change dramatically even sometimes on several degrees [1]. By this the properties of membranes change dramatically too. The microviscosity changes, fluidity and solidity changes too. Functional activities of membrane bounded integral or associated proteins correlate with these membrane's modifications. They are determined by the interaction of all components of membrane, including lipids. By these facts we tested the phase transitions of lipid components of biomembranes under the temperatures changes. The experimental object - multilammellar liposomes were formed from phospholipid dimyristoyl phosphatidylcholine (DMPC). The phase state of DMPC at multilammellar liposomes has been examined by means of differential adiabatic scanning microcalorimetry (DSC) when melting were repeated. The heating and cooling were repeated 7 times. The kind of thermograms curves were changing. The peak of main endothermic phase transition was becoming smaller than at first melting. Stapes by stapes the cooperativity of melting of DMPC microdomains decreased that was presented at figure. The temperature at maximum of peak of main phase transition was lowered too. This phenomenon suggested to the disrupting of microdomain organization at DMPC multilammellar liposomes under the repeating of temperature changing. These data supported that the events at bio membranes that occurred under the slipping processes, may influence to the bioactivity.



1 D.P. Kharakoz "About the possible physiological role of phase transition "liquid-solid" at biological membranes", *Successes of Biol. Sciences*, 2001, 41, 264

PI-21. Features of the Association of Biocompatible Ionic Liquids: the Case of Holin-Based Amino Acid Ionic Liquids

Fedotova M.V.¹, Kruchinin S.E.¹ Chuev G.N.²

¹ G.A. Krestov Institute of Solution Chemistry of the Russian Academy of Sciences, Akademicheskaya St., 1, Ivanovo, 153045, Russia;

² Institute of Theoretical and Experimental Biophysics of the Russian Academy of Science, Pushchino, Moscow Region, 142290, Russia

genchuev@rambler.ru

Biocompatible ionic liquids (bioILs) with biologically active cation and anion are one of the most promising classes of the compounds are biocompatible ionic liquids (BIH). Their low toxicity and biodegradability allow using bioILs in pharmaceuticals and medicine [1]. BioILs are able to exhibit antimicrobial activity, to prevent deactivation and maintain the structural stability of enzymes, to stabilize the native structure of proteins [2, 3]. However, the ion interactions in BioILs (association) can significantly affect their biological activity. Therefore the study of the features of ion association is necessary for control and regulation the ability of bioILs to perform a specified function. New choline(Ch)-based amino acid bioILs ([Ch][AA]) recently synthesized are among such compounds [4, 5]. Paper size: A4. Margins: 2.5 cm on the top and bottom, 2.0 cm on the right and left sides.

Here we present the results for bioILs [Ch][AA] ([AA] = [Gly], [Ala], [Pro]) obtained by the integral equation method in the framework of the 1D-RISM (Reference Interaction Site Model) approach. The features of ion association in these bioILs were analyzed on the base of radial distribution functions (RDFs) and potentials of mean force (PMFs). It was found that the cation-anion interaction can be realized both by hydrogen bonding and by Coulomb attraction. The number of counterions near the interacting functional groups and the number of H-bonds are determined. As it was established, there is a possibility for association of [AA] anions. The results obtained are in satisfactory agreement with the available literature data.

Acknowledgements This work was supported by the Russian Foundation for Basic Research with Grant 18-43-370003-r_a.

[1] K. Egorova, E. Gordeev and V. Ananikov, *Chem. Rev.*, 2017, 117, 7132.

[2] X.-D. Hou, Q.-P. Liu, T. Smith, N. Li and M.-H. Zong, *PLoS ONE*, 2013, 8, 59145.

[3] A. Yazdani, M. Sivapragasam, J.-M. L  v  que and M. Moniruzzamanet, *J. Microb. Biochem. Technol.*, 2016, 8, 415.

[4] Q.-P. Liu, X.-D. Hou, N. Li and M.-H. Zong, *Green Chem.*, 2012, 14, 304.

[5] S. De Santis, G. Masci, F. Casciotta, R. Caminiti, E. Scarpellini, M. Campetella and L. Gontrani, *Phys. Chem. Chem. Phys.*, 2015, 17, 20687

PI-22. Phase Solubility Diagrams of the 4-Aminobenzoic Acid Cocrystal

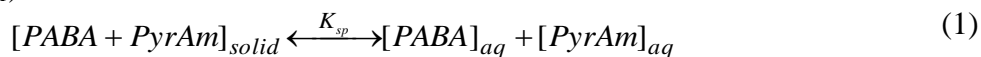
Drozd K.V., Manin A.N.

G.A. Krestov Institute of Solution Chemistry of the Russian Academy of Sciences, Russia

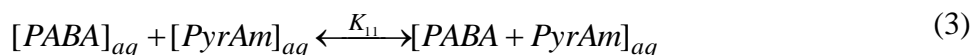
ksdrozd@yandex.ru

Pharmaceutical cocrystal is stoichiometric molecular complex which contains an active pharmaceutical ingredient and an acceptable cocrystal former in crystal lattice via non-covalent interactions (hydrogen bond, van der Waals force, π - π interaction) [1, 2]. Understanding cocrystal solubility behavior is vital for cocrystal screening and preparation for solution cocrystallization.

4-Aminobenzoic acid (PABA) is known as vitamin B10 and is involved in the production of folic acid in bacteria [3]. PABA has been the subject of many scientific investigations, due to not only its pharmaceutical and biological properties, but also its ability to form various multi-component solid forms: salts, cocrystals, solvates, complexes with cyclodextrins and etc. PABA has been reported to form a pharmaceutical cocrystal with pyrazinamide (PyrAm) [4]. PyrAm is an antimicrobial agent that is most commonly used for treatment of active tuberculosis. In the present work, phase solubility diagrams of [PABA+PyrAm] cocrystal in buffer pH 7.4 were constructed at 293.15, 298.15, 303.15, 308.15 and 313.15 K under atmospheric pressure. The solubility behavior of [PABA+PyrAm] cocrystal was investigated on the basis of a mathematical model considering solubility product (K_{sp}) and solution complexation (K_{11}):



$$K_{sp} = [PABA]_{aq} \cdot [PyrAm]_{aq} \quad (2)$$



$$K_{11} = \frac{[PABA + PyrAm]_{aq}}{[PABA]_{aq} \cdot [PyrAm]_{aq}} \quad (4)$$

The region where the [PABA+PyrAm] cocrystal is the only thermodynamic stable solid phase, the solubility of cocrystal depends mainly on the cofomer (PyrAm) concentration. The solubility of the [PABA+PyrAm] cocrystal increases with the increase of temperature, and decreases with the increase of PyrAm concentration. According to obtained data, K_{sp} and K_{11} are affected by temperature. K_{sp} is proportional to the solubility of cocrystal and increases with increasing temperature. K_{11} decreases with increasing temperature, which is opposite to K_{sp} . At each temperature, ΔG_f° is negative which indicates the formation of cocrystal is spontaneous even at high temperature of 40°C.

Acknowledgements This work was supported by the Russian Science Foundation (№ 17-73-10351).

[1] N.J. Babu, A. Nangia, *Cryst. Growth Des.*, 2011, 11, 2662.

[2] S. Aitipamula, R. Banerjee, A.K. Bansal, K. Biradha, M.L. Cheney, A.R. Choudhury, G.R. Desiraju, A.G. Dikundwar, R. Dubey, N. Duggirala, *Cryst. Growth Des.*, 2012, 12, 2147.

[3] T.-Y. Chang, M.-L. Hu, *J. Nutr. Biochem.*, 1996, 7, 408.

[4] S.H. Thorat, S.K. Sahu, R.G. Gonnade, *Acta Cryst. C*, 2015, 71, 1010.

PI-23. Ion-Dipole Interactions During the Complex Formation of d-Metal Ions with Some Organic Derivatives of Hydrazine

Amerkhanova Sh.K., Shlyapov R., Uali A.S.

L.N. Gumilyov Eurasian National University, Kazakhstan

amerkhanovashk@gmail.com

The coordination compounds of hydrazides and their derivatives are considered as promising compounds for medicine and pharmacology. The resistance to the action of the solvent is the most important characteristics of resistance from a practical point of view. Investigations of complex compounds of biogenic metals with N, S, O-donor ligands in solutions are of great interest due to the need to solve a number of practical problems, and the need for a detailed understanding of the processes in such systems, which can be used for simulating biological objects.

The dissociation constants of N-morpholinyl acetic acid hydrazide in an aqueous ethanol solvent had been determined by potentiometric method [1]. The influence of the mole fraction of ethanol on the thermodynamic components of the complexation process of an organic ligand with cobalt(II) and zinc(II) ions in solution had been established. It is shown that the relative associativity (the proportion of hydrogen bonds) in a mixed solvent increases with increasing volume content of ethanol. This indicates the preferential solvation of water molecules with ethanol in the range of 50-90 vol.%, Therefore, the autoprotolysis constant of the mixed solvent (pK_s) will decrease [2].

Table 1 Physical-chemical properties of the solvent and hydrazide N-morpholinyl acetic acid (L)

Parameter	C _{EtOH} , % (v/v)				
	10	30	50	70	90
pK _s (EtOH-H ₂ O)	14.02	14.35	14.65	15.23	16.62
pK _a (L)	8.37	8.02	8.30	8.91	8.12
pK _b (L)	5.65	6.33	6.35	6.32	8.50

A tendency has been revealed to change the acid-base properties of the organic ligand in an aqueous ethanol environment. The acidity and basicity constants of the ligand had been determined, on the basis of which the stability constants of the d-metal complexes had been calculated. The enthalpy, entropy, Gibbs energy of formation of complexes of nitrogen-containing ligand with Zn (II), Co (II) ions, transfer of ligand, metal complexes from ethanol to aqueous-organic solvent had been calculated.

[1] M. Kurtoglu, N. Birbicer, U. Kimyonsen and S. Serin, *Dyes and Pigments*, 41, 1999, 143.

[2] M. Faraji, A. Farajtabar and F. Gharib, *J. Appl. Chem. Res.*, 2009, 9, 7.

PI-24. TPT-Modeling of the Liquidus Surface in Molten Alkali Metal Halides with the Inclusion of the Ion Polarization Effect

Davydov A.G., Tkachev N.K.

Institute of High Temperature Electrochemistry UB RAS, Russia

A.Davydov@ihete.uran.ru

The study of thermodynamic properties and phase equilibria in salt melts is an important direction in the field of materials science. The theoretical description of the properties of molten salts is carried out today mainly using molecular dynamic (MD) simulations or based on *ab initio* methods with subsequent MD calculations. The authors of this report are developing an approach to describing phase equilibria in molten salts based on thermodynamic perturbation theory (TPT). In our report, we will present the results of TPT-modeling of the liquidus surface in molten alkali metal halides.

The calculation of the liquidus surface was carried out based on the equality of the chemical potentials of the liquid and solid phases. Most attention was paid to the calculation of the free energy of the liquid melt. Since the salt is a mixture of single cations and anions above the melting point, the system of charged hard spheres (CHS) in the mean spherical approximation was chosen as the reference system. In this case, less strong polarization interactions of ions can be taken into account as a perturbation of the system. In our work, polarization interactions of ions were taken into account in the framework of the variational TPT-approach:

$$F \leq F_{Ref} + 2\pi N\rho \sum_{i,j} x_i x_j \int_0^{\infty} \varphi_{ij}^1(R) \cdot g_{ij}^0(R) R^2 dR. (1)$$

At the same time, from the point of view of computational costs, the most convenient was to go to the Fourier representations of the interaction potential and the radial distribution function:

$$F \leq F_{ref} + \frac{N}{4\pi^2} \sum_{i,j} \sqrt{x_i x_j} \int_{d_{ij}}^{\infty} \varphi_{ij}^1(k) \cdot [S_{ij}^0(k) - \delta_{ij}] k^2 dk + \frac{N}{2} \cdot \lim_{k \rightarrow 0} \varphi_{ij}^1(k), (2)$$

where indices 0 and 1 refer to the reference system and the energy additive, respectively.

Radial distribution functions, as can be seen from (1) and (2), are related to structural factors through the inverse Fourier transform. The latter, in its turn, can be calculated from the Fourier representations of direct correlation functions, which are derived in this the work, but have a quite bulky form and they are omitted in the text.

The interaction potential in inverse space is as follows:

$$\varphi_{ij}^1(k) = -\pi k E_{ij} \left[\frac{\sin(kd_{ij})}{(kd_{ij})^2} + \frac{\cos(kd_{ij})}{kd_{ij}} + \text{Si}(kd_{ij}) \right], (3)$$

where $\text{Si}(kd_{ij})$ is the integral sinus, and E_{ij} is used in the work in two forms:

$$E_{ij}^{(I)} = (Z_i e)^2 \alpha_j + (Z_j e)^2 \alpha_i, (4)$$

$$E_{ij}^{(II)} = \frac{(\varepsilon - 1)b_i^3 - (\varepsilon + 2)\alpha_i}{(2\varepsilon + 1)b_i^3 - 2(\varepsilon - 1)\alpha_i} \cdot \frac{(Z_j e)^2 b_i^3}{\varepsilon} + \frac{(\varepsilon - 1)b_j^3 - (\varepsilon + 2)\alpha_j}{(2\varepsilon + 1)b_j^3 - 2(\varepsilon - 1)\alpha_j} \cdot \frac{(Z_i e)^2 b_j^3}{\varepsilon}. (5)$$

Acknowledgements The reported study was funded by RFBR according to the research project № 18-33-01234

PI-25. Liquid Organic Hydrogen Carriers. Chemical Equilibrium of Hydrogenation Reactions of Condensed Aromatic Hydrocarbons

*Vostrikov S.V.¹, Konnova M.E.¹, Pimerzin A.A.¹, Martynenko E.A.¹,
Verevkin S.P.^{1,2}, Pimerzin A.A.¹*

¹Samara State Technical University, Samara, Russia;
²Institute of Chemistry, University of Rostock, Germany

vostrikov.sv@samgtu.ru

With the depletion of fossil fuels there is high demand to seek renewable energy sources that can substitute fossil fuels to enable the sustainable development of our economy. However, without solving the problem of saving large amounts of energy for an unlimited time, the total transition to renewable energy sources is very problematic. The use of hydrogen as an alternative energy source is quite obvious, since more than energy-saturated molecule simply does not exist. Practical implementation of methods for the storage and release of hydrogen faces certain difficulties.

Many studies have been focused on solving this problem, and the use of unsaturated organic compounds as hydrogen storage is considered as one of the most promising areas today. This is due to the relatively high hydrogen capacity of organic compounds, the possibility of its multiple use, safety of use, proximity to traditional motor fuels.

The purpose of this paper is to examine the thermodynamic properties of promising liquid organic hydrogen carriers. Diphenyl, anthracene, phenanthrene and acenaphthen have been chosen as objects of study, which reliable data on chemical equilibrium are absent in the literature. The catalytic hydrogenation-dehydrogenation was carried out in a heated autoclave over a Pt and Pd catalysts with varying reaction conditions: temperature (548-623 K), pressure (20-90 atm), hydrogen/LOHC ratio (0-28 mol/mol). The substances was dissolved in n-heptane in the amount of 2% wt. The fully hydrogenated product was then used as reactant in the dehydrogenation reaction. For each system, the achievement of an equilibrium state was proved by the invariance of the composition of the equilibrium mass over time by varying the type and amount of the catalyst, as well as by achieving an equilibrium state on the part of the reagent and the product. Analysis of the reaction mixture was done with GC, identification of the components was performed by GCMS method.

The conference materials will present the results of experimental determination of equilibrium compositions, equilibrium constants, thermodynamic characteristics of the studied reactions, conditions of exhaustive selective hydrogenation-dehydrogenation of substrates on Pt and Pd catalysts, and conclusions will be made about the relationship "structure-property" in hydrogenation-dehydrogenation reactions with involving polycyclic aromatic hydrocarbons.

Acknowledgments

This research was supported by the Government of Russian Federation (decree №220 of 9 April 2010) agreement №14.Z50.31.0038.

PI-26. How Liquid Organic Hydrogen Carriers. Chemical Equilibrium of Hydrogenation Reactions of Some N-Heterocycles

Konnova M.E.¹, Vostrikov S.V.¹, Chernova M.M.¹, Verevkin S.P.^{1,2}, Pimerzin A.A.¹

¹Samara State Technical University, Samara, Russia;

²Institute of Chemistry, University of Rostock, Germany

mariaknv@gmail.com

Under the renewable energy refers to alternative sources such as solar radiation energy, the potential energy of wind and water, geothermal energy, biomass energy, etc., which are beginning to replace fossil hydrocarbons. There are ambitious goals in many parts of the world to raise the share of renewable energy in the total volume of its production. A key hurdle for the massive integration of some of the most important sources of renewable energy into our energy system is their intermittent character [1]. One solution to this problem is the transition from electricity to a new energy source - hydrogen. In this case, the problem of accumulating huge reserves of renewable energy confined to the problem of "preserving" large volumes of hydrogen, the so-called problem of hydrogen batteries. The use of liquid organic hydrogen carriers as a medium for the storage and transportation of hydrogen is one of the solutions to the current problem.

It is necessary to have information on the thermodynamics of the catalytic hydrogenation-dehydrogenation reaction of organic molecules for the successful selection of effective samples of liquid organic hydrogen carriers.

In this work, the objects of study have been selected indoline, N-methylindole, 2-methylquinoline and 4,4'-bipyridine. The experiment to study the chemical equilibrium of hydrogenation-dehydrogenation reactions was carried out in an autoclave with a magnetic stirrer on Pt and Pd catalysts with varying temperature, pressure, and hydrogen:feed ratio. The compositions of the reaction mixtures were determined by GC and GHMS. The achievement of equilibrium by the system was confirmed by the constant ratio of the components concentrations characterizing the equilibrium constant of the corresponding reaction, while varying the reaction time, the ratio of reactants and the concentration of the catalyst. Chemical equilibrium constants were obtained for the liquid and gas phases.

The experimental chemical equilibrium constants of the hydrogenation-dehydrogenation reactions have served as the basis for calculating the enthalpy and changes in the entropy of reactions. Also the work presents the dependences of the equilibrium compositions on temperature, the ratio of hydrogen: substrate and contact time. The model was proposed for describing the conditions of exhaustive hydrogenation and dehydrogenation of the studied substances. The dependence of the selectivity and degree of conversion of substrates on the process conditions was evaluated. The results of the experiment were compared with the data of quantum chemical calculations of chemical equilibrium for the studied systems. Conclusions have been drawn about the relationship "structure-property" in the hydrogenation-dehydrogenation reactions involving aromatic N-heterocycles.

Acknowledgments. This research was supported by the Government of Russian Federation (decree №220 of 9 April 2010) agreement №14.Z50.31.0038.

References

[1] D. Teichmann, W. Arlt, P. Wasserscheid, R. Freymann A future energy supply based on Liquid Organic Hydrogen Carriers (LOHC), *Energy Environ. Sci.*, 2011, 4, 2767

PI-27. Modeling of Thermodynamic Characteristics for Polysubstituted Crystals with a M-Type Hexaferrites Structure

Zaitseva O.V., Zhivulin D.E., Chernukha A.S., Galkina D.P., Vakhitova E.R.

South Ural State University, 76, Lenin Ave., Chelyabinsk 454080, Russia

nikonovaolga90@gmail.com

M-type hexaferrites with magnetoplumbite structure are known for more than half a century. Thanks to their properties, they are widely used in various fields of science and technology, especially in the storage and recording of information, as well as in the fabrication of permanent magnets. In recent decades, researchers found the ability to control the properties of hexaferrites by replacing a part of iron atoms with atoms of other elements. As a rule, there is one substitute. The aim of this research was to study the possibility of creating high-entropy phases with a structure of M-type hexaferrites, i.e. polysubstituted solid solutions, where the stabilization of the structure is facilitated by high configuration entropy of components mixture.

The creation of high entropy phases with the structure of M-type hexaferrites and the improvement of their compositions, as well as the technology development for fabrication of such materials require their thermodynamic description. This was the aim of the present study. Such work is necessary due to the fact that these results should allow to calculate the phase diagrams of multicomponent systems, where polysubstituted crystals with the structure of M-type hexaferrites are formed, as well as to simulate the formation processes of solid solutions with the structure of hexaferrite during cooling of multicomponent oxide melts.

Within this study, a model that allows us to describe and explain the experimentally obtained results was developed, relating to the equilibrium between the low entropy phases and high entropy solid solutions with the M-type hexaferrites structure, that are formed in the BaO–PbO–ZnO–SrO–CaO–Fe₂O₃–Mn₂O₃–Al₂O₃ system at different temperatures.

In this study, the selection of a suitable thermodynamic model for the variable composition phase (high-entropy oxide solid solution with the M-type hexaferrites structure) was done. In addition, the parameters identification for this selected model was carried out. The thermodynamic models of interested us solutions include the different variants of the sublattice model, combined with different approaches to describe the deviation from the ideality within a single sublattice, as well as different variants of a quasi-chemical model.

In results, it was demonstrated that currently available experimental data with reasonable accuracy can be described by a two-sublattice model, where a solid solution (MR₁₂O₁₉) is represented as a set of sublattices formed by divalent cations (M²⁺) and dual-charge anions (R₁₂O₁₉²⁻). Within each of the sublattices, the deviation from the ideality is described by means of Redlich-Kister polynomials. In addition, the projects were developed in MathCad that can be used to enrich the parametric software for modeling of solid solutions for studied systems. Part of this work was carried out using the FactSage software (version 7.2), where a user database was created with the data found in the course of this study.

The results of this work gave the possibility to plot (by CALPHAD algorithms) sections of phase diagrams that characterize the phase equilibria in the studied systems during and after the crystallization of a multicomponent oxide melt.

Acknowledgements The reported study was funded by RFBR according to the research project № 18-38-00736.

PI-28. Calorimetric Study of Binding of Substituted Benzoic Acids to Bovine Serum Albumin

Khaibrakhmanova D.R., Nikiforova A.A., Sedov I.A.

Kazan Federal University, Russia

diliara.khaibrakhmanova@gmail.com

Serum albumin is a major plasma protein acting as a carrier of many substances in the blood, particularly drugs. Thermodynamics of binding with albumin determine the values of the fraction of free active form of drugs in blood and influence overall pharmacodynamic and pharmacokinetic properties. Development of structure–property relationships allowing to predict the affinity of drug candidates to albumin is a very important task. Experimental data on the binding constants of compounds with different structure are essential to deduce such relationships.

Despite quite a large number of binding constants available from different studies, there is a strong disagreement between values reported by different authors. Reported values of equilibrium constants of binding with albumin are strongly dependent on its concentration, the ligand/protein ratio, method of measurement and data evaluation.

In the present work, binding of different substituted benzoic acids to bovine serum albumin was studied using capillary differential scanning calorimetry. In general, binding with ligands increases the denaturation temperature of albumin, and tighter binding leads to a more pronounced increase. The results of such experiments are well reproducible. The influence of ligand/protein molar ratio on the denaturation temperature shift for different ligands was studied. A model allowing to calculate the affinity parameters from the magnitude of the shift at different ligand concentration is proposed. The results are compared with the binding constants determined using traditional spectrofluorimetric titration method. Correlations of the obtained affinity parameters with the structural descriptors and thermodynamic properties of ligands are developed. A pronounced influence of the hydrophobicity and acidity of ligands on the binding affinity is shown.

PI-29. Asymptotically Exact Equation for Describing Phonon Heat Capacity of Solids in a Wide Temperature Range

Bespyatov M.A., Naumov V.N.

Nikolaev Institute of Inorganic Chemistry,
Siberian Branch of the Russian Academy of Sciences, Russia

bespyatov@niic.nsc.ru

It is well known that heat capacity $C(T)$ of solids on asymptotics (at low and high temperatures) can be described within the framework of universal behavior, which is determined by the validity of the limit laws in its description. At low temperatures, the Debye limit law [1] is widely used, within which for all solids a phonon component of heat capacity is proportional to T^3 and is determined by only one parameter — the Debye temperature. At high temperatures, all vibrational modes of a crystal are excited, and the heat capacity inevitably approaches the limiting Dulong-Petit law [2]. Description at medium temperatures is currently an unsolved problem.

We propose a new equation for describing phonon heat capacity of solids in a wide temperature range:

$$C(T) = \left[\left(\frac{T}{\Theta} \right)^{-\alpha\beta} + 1 \right]^{-\frac{1}{\alpha}}, \quad (1)$$

where α and β are dimensionless parameters that can be determined from experiment; Θ is a parameter that has the dimension of temperature; $C(T) = C_V/(3Rn)$; R is the universal gas constant; n is the number of atoms in the mole. The equation has three parameters. The correct asymptotic behavior at high and low temperatures will be preserved when these parameters change.

Equation (1) will easily be converted to the linear equation view:

$$Y = A - BX$$

$$Y = \frac{1}{\alpha} \ln \left(\frac{1 - C(T)^\alpha}{C(T)^\alpha} \right); X = \ln T; A = \beta \ln \Theta; B = \beta. \quad (2)$$

Equation (2) is convenient for finding the unknown parameters α , β , Θ . Note that Y depends on the unknown parameter α , which must be chosen in such a way that the experimental data $C(T)$ are best described by the linear equation (2).

The description of phonon heat capacity by the proposed equation was performed for a wide range of objects, including model objects with different degrees of anisotropy, elements, simple and complex compounds, including molecular crystals. This consideration shows that the accuracy of the description can be obtained at a level of from 0.1% to 1%.

Equation (1) can be used to extrapolate heat capacity to 0 K, to separate experimental heat capacity into components, as well as to isolate various anomalies associated with phase transformations.

Acknowledgements The reported study was funded by RFBR according to the research project № 19-03-00385.

[1] P. Debye, *Ann. Phys.*, 1912, 39, 789.

[2] A.-T. Petit, P.-L. Dulong, *Ann. Philos.*, 1819, 14, 189

PI-30. The Two-Parameter Equilibrium Constant for Gas Reactions

Vitvitskiy A.I.

Saint Petersburg, Russia

avitvitskiy@mail.ru

In the single act of reversible transformation of gaseous substances by chemical equations with integer stoichiometric coefficients in the general case (table, reactions 1-3), there are groups of molecules (Σb_i and Σd_i) of equal mass with a potential number of transformation acts equal to one mole ($N_A = 6.02214 \times 10^{23}$). At temperature T (K) and pressure P (Pa), initially nonequilibrium initial substances come to the equilibrium state $N_{Ab} \rightarrow (N_{pb} + N_{pd}) \leftarrow N_{Ad}$, where $N_{Ab} = N_{Ad} = N_A = N_{pb} + N_{pd}$. The equilibrium fraction the N_{pd} groups Σd_i (α_p) and the equilibrium fraction the N_{pb} groups Σb_i (β_p) from the initial number of the N_A are $\alpha_p = N_{pd}/N_A = (1 + \beta_p/\alpha_p)^{-1}$ and $\beta_p = N_{pb}/N_A = (1 + \alpha_p/\beta_p)^{-1}$ with the observance of the equality $\alpha_p + \beta_p = 1$. For $\beta_p > 0.5$, $\beta_p/\alpha_p = N_{pb}/N_{pd}$ is the number of Σb_i equilibrium groups per one Σd_i group; for $\alpha_p > 0.5$, $\alpha_p/\beta_p = N_{pd}/N_{pb}$ is the number of Σd_i equilibrium groups per one Σb_i group; for $\alpha_p = \beta_p = 0.5$ ($N_{pd}/N_{pb} = 1$), for each Σd_i group there is one Σb_i group.

When $\Sigma b_i \neq \Sigma d_i$, the graphical dependence of the logarithm of the quantities α_p/β_p (or β_p/α_p) on $1/T$ represents two straight sections with different inclination. Rectilinear segments can be combined [1] into one logarithmic straight line with the help of the same type compound equilibrium constant (K_p) with two individual coefficients-parameters T_m and P_m

$$K_p = (P_m/P) \times \exp(1 - T_m/T) = \exp(T_m/T_x - T_m/T),$$

where at $\alpha_p = \beta_p = 0.5$ and $K_p = 1$ $P_m/P = \exp(T_m/T_x - 1)$ or $P_m = P \times \exp(T_m/T_x - 1)$.

The relationship K_p , α_p (> 0.5), and β_p (> 0.5) shown in reactions 1–3 (table) allows us to determine the coefficients T_m and P_m from two values α_p or β_p . The two-parameter constant K_p is applicable for calculating the values of α_p and β_p under broad conditions (at $T \leq T_m$ and $P > 0$) for macro and micro systems. The error in calculating α_p and β_p is comparable with the error in the data used in determining the values of T_m and P_m .

At temperature T , the absolute value of heat (enthalpy) for the N_A conversion of Σb_i or Σd_i groups of reactions 1-3 (Q_T , J/mol), including at 298.15 K, does not depend on pressure and is determined by the equation $|Q_T| = R(T_m - T)$, where $R = 8.31447$ J/mol.

Table Characteristics of the equilibrium state of reactions 1-3

$\Sigma(b_i B_i) = \Sigma(d_i D_i)$	T_m/P_m	T_x^* , K	Conditions	$(\alpha_p, \beta_p) - f_{Kp}$
$o\text{-H}_2 = p\text{-H}_2$ [2]	$\frac{170.23 \text{ K}}{3.3336 \times 10^5 \text{ Pa}}$	77.699	$T \leq T_x$ $T \geq T_x$	$\alpha_p = (1 + K_p)^{-1} \geq 0.5$ $\beta_p = (1 + K_p^{-1})^{-1} \geq 0.5$
$2\text{NO}_2 = \text{N}_2\text{O}_4$ [2]	$\frac{7283.6 \text{ K}}{7.764 \times 10^{13} \text{ Pa}}$	339.45	$T \leq T_x$ $T \geq T_x$	$\alpha_p = (1 + K_p^{1/2})^{-1} \geq 0.5$ $\beta_p = (1 + K_p^{-1})^{-1} \geq 0.5$
$2\text{H}_2 + \text{O}_2 = 2\text{H}_2\text{O}$ [3]	$\frac{58512 \text{ K}}{3.206 \times 10^{10} \text{ Pa}}$	4282.0**	$T \leq T_x$ $T \geq T_x$	$\alpha_p = (1 + K_p^{1/3})^{-1} \geq 0.5$ $\beta_p = (1 + K_p^{-1/2})^{-1} \geq 0.5$

* At $P = P_n = 101325$ Pa. ** At $P = 100 \times P_n$ $T_x = 6458.6$ K.

[1] Anatoly Vitvitskiy, *Chemicals, Conditions of equilibrium states and conversion* (in Russian). <https://www.lap-publishing.com>. ISBN-13: 978-3-330-08416-2, 64 p. Published 2017.05.12.

[2] H. Zeise, *Thermodynamik*, 1954, Band 3, Halfte 1 (Tabellen), 135, 145. Leipzig, Germany.

[3] N. Bjerrum, *Zeitschr. Physik. Chemie*, 1912, 79, 5, 513-536.

PI-31. Approaches to the Equilibrium Composition Calculations for the Conversion of Diesel Fuel

Uskov S.I.^{1,2}, Potemkin D.I.^{1,2}, Snytnikov P.V.^{1,2}, Belyaev V.D.^{1,2}, Sobyenin V.A.^{1,2}

¹Novosibirsk State University, Russia;

²Borescov Institute of Catalysis SB RAS, Russia

uskov@catalysis.ru

Recently there has been a growing interest in solid oxide fuel cells (SOFC). A lot of studies are dedicated to new approaches to use traditional fuels to power SOFC. Diesel fuel is a promising material to power SOFC due to its high energy density. However, it cannot be used without prior conversion to synthesis gas. Steam reforming (SR), partial oxidation (PO) and autothermal reforming (ATR) are suggested to obtain synthesis gas from diesel. Certain difficulties may occur during this processing, the most complicated one being carbonization. This work is aimed at determining reaction conditions which would provide carbon-free operation of SR, PO and ATR.

Calculations were carried out using the HSC Chemistry 7.1 software. An approach was used which consisted of substitution of C_nH_{2n+2} by C and H_2 in order to simulate diesel fuel with a certain average atomic ratio of H/C in the fuel. The substitution was proved to allow obtaining the same results for SR and PO as if an actual hydrocarbon mixture was chosen as an initial reaction substance. Figure 1 shows an example of the calculations of equilibrium composition for the SR of a fuel with H/C ratio of 1.8. It is seen that the temperature corresponding to the absence of carbon deposition significantly depends on the initial water content. The less initial water content the higher temperature is required to perform the process in the carbon-free mode.

It was shown that the range of carbon-free reaction conditions is restricted in case of PO and high temperature is required. Carrying out the PO process at reasonable temperature is possible only at high O_2/C ratio (> 0.6) which is unacceptable because diesel combustion prevails at these conditions. Calculations of ATR were performed using a model mixture of 40 mol. % hexadecane, 35% decahydronaphthalene, 20% hexylbenzene and 5% 1,2-dimethylnaphthalene. The reactions were equalized by heat under the following conditions: 700-800 °C, $H_2O/C = 2.5-3.0$ and $O_2/C = 0.2-0.3$. At these conditions there was no carbon deposition, methane content was below 0.1 vol. % and the total yield of synthesis gas decreased insignificantly with temperature. The calculated data were confirmed experimentally by the stable operation of $Rh/Ce_{0.75}Zr_{0.25}O_{2-\delta}$ catalyst in SR and ATR of n-hexadecane [1] and diesel fuel.

Acknowledgements This work was supported by RFBR project 18-29-24015 mk.

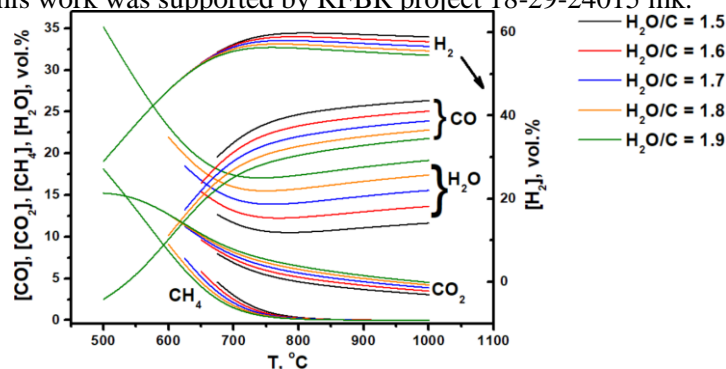


Figure 1. An example of the calculation of the equilibrium composition for the SR of a diesel fuel with average atomic H/C ratio of 1.8. Each curve originates under conditions corresponding to the absence of carbon formation.

[1] T.B. Shoykhorova et.al, Applied Catalysis B: Environmental, 2018, 237, 237–244.

PI-32. Investigation of Evaporation of HfC_x and ZrC_x Near and Above Melting Point

Frolov A.M., Sheindlin M.A., Falyakhov T.M., Petukhov S.V.

University Joint Institute for High Temperatures, Russia

matotz@gmail.com

Hafnium and zirconium carbides are ultra-high temperature ceramics (UHTCs) – a group of refractory material possessing unique thermophysical characteristics. Their most notable property – high melting temperature – stimulates big interest for their application in extreme conditions. However high-temperature behavior of the substances is studied poorly. For instance, the latest data on evaporation of HfC_x and ZrC_x was obtained at temperatures below 3200 K, i.e. only for solid state [1,2]. In the [3] a combination of laser heating with millisecond pulses with time-of-flight mass-spectrometry was successfully proposed for investigating evaporation of liquid substance with rapidly changing stoichiometry – uranium dioxide.

In the present work the evaporation of HfC_x and ZrC_x was investigated using the method akin to one utilized in [3] with several improvements of the experimental setup. Samples of ZrC_x and HfC_x were prepared by sintering of mixtures of Hf or Zr with carbon and had compositions lying within homogeneity domain ($0.4 < x < 1$). The sintered samples were partially melted using long (~100 ms) laser pulses in order to increase the density. The spectral emissivities of solid and liquid surfaces were measured using polychromatic pyrometer. The analysis of evaporation was performed using millisecond laser pulses with the optimized shape to obtain linear time dependence of the temperature. The temperature was measured utilizing fast ad hoc brightness micropyrometer at 905 nm. The temperature dependences of relative partial pressures were measured in each experiment. The heats of evaporation of different vapor species were calculated. For the first time the temperature dependence of the ratio C/Me over liquid HfC_x and ZrC_x were measured. It was found that the ratio C/Zr in vapor over ZrC_x with various initial compositions tends to the value of 0.2 at the temperature above 4000 K.

Acknowledgements The reported study was funded by RFBR according to the research project № 18-38-00837.

[1] C. Stearns, F. Kohl, *NASA TN D-7613*, 1974

[2] H. Jackson, W. Lee. *Comprehensive Nuclear Materials*, 2012, 2, 339-372. Elsevier, London, UK.

[3] R. Pflieger, J-Y. Colle, I. Iosilevskiy, M. Sheindlin., *J. Appl. Phys*, 2011, 109, 033501

PI-33. Solubility of Drug Compounds in Supercritical Carbon Dioxide. Molecular Dynamics Simulation

Ivlev D.V., Kalikin N.N., Kiselev M.G.

G.A. Krestov Institute of Solution Chemistry of the Russian Academy of Sciences

dvi@isc-ras.ru

In recent years there has been an increasing level of interest in utilizing supercritical fluid technology for processing pharmaceutical materials. The use of supercritical carbon dioxide as a solvent is of particular interest because of its low critical parameters ($T_c=31,2^\circ\text{C}$, $P_c=72,9\text{bar}$), low toxicity, and relative low cost. Currently, there are many experimental methods for determining the solubility of drug compounds in supercritical CO_2 , however, they are quite expensive.

Earlier in our article [1], a method for calculating of solubility using molecular dynamic (MD)simulation was tested. Satisfactory agreement of the calculated results with experimental data was obtained. In this report, MD simulation of drug compounds (ibuprofen, naproxen, and ketoprofen) in supercritical carbon dioxide was carried out in a wide range of parameters. Features of solubility behavior depending on the parameters of the state are discussed in the report.

Acknowledgements The financial support of this work was supported by grants from Russian Foundation of Basic Researches (grants nos. A 18-29-06008 and 18-03-00255).

[1] Y.A. Budkov, A.L. Kolesnikov, D.V. Ivlev et al. *Journal of Molecular Liquids*, 2019, 276, 801.

PI-34. Classical DFT Based Method of the Solubility Estimation of Sparingly Soluble Compounds in SC CO₂

Budkov Y.A.^{1,2}, Kalikin N.N.¹, Kolesnikov A.L.³, Ivlev D.V.¹, Kiselev M.G.¹

¹G.A. Krestov Institute of Solution Chemistry of the Russian Academy of Sciences, Russia

²Tikhonov Moscow Institute of Electronics and Mathematics, National Research University Higher School of Economics, Russia

³Institut für Nichtklassische Chemie e.V., Germany

nikolaiKalikin@gmail.com

Development of the efficient non-empirical method for solubility assessment of the poorly soluble compounds in the supercritical fluids is a serious problem for the chemical thermodynamics. As is well known, solubility of the solid sparingly dissolved compounds in the supercritical fluid under the imposed conditions can be defined by the two thermodynamic processes: compound molecules sublimation from solid to gas phase and their solvation in the supercritical fluid. Thus, to quantitatively estimate solubility value, one has to know the sublimation and solvation free energies. The first contribution can be obtained from the experimental data, available in literature. In the presented method [1] the solvation free energy is estimated within the classical DFT. Solvent and solute molecules are modelled as spherically symmetric particles with Lennard-Jones interactions between them. Contribution to the excess Helmholtz free energy of the hard spheres is obtained within the Rosenfeld's Fundamental Measure Theory (FMT) [2]. Effective potential of interaction between the molecules in the attractive contribution to the excess Helmholtz free energy is obtained via the Weeks-Chandler-Anderson (WCA) procedure [3]. The parameters of the solute-solute and solvent-solvent interaction potentials are obtained from the fit of the critical pressure and temperature values, which are taken from the literature [4]. The solvation Gibbs free energy is calculated as the excess grand potential. To test our methodology, we estimated solubility of ibuprofen in supercritical CO₂. The obtained values of solubility are underestimated, as compared to the experimental data or the results of the molecular dynamic simulations. It can be explained by the fact that the classical DFT does not take into account Coulomb interactions. Nevertheless, the obtained values of pressure crossovers are very close to those obtained experimentally.

Acknowledgements: This work was supported by grants from Russian Foundation of Basic Researches (grants nos. A 18-29-06008 and MK 18-03-00255). The authors acknowledge Russian Federal Program (grantno. RFMEFI61618×0097) for support. K.A.L. gratefully acknowledge the financial support from Bundesministerium für Wirtschaft und Energie (BMWi) as part of the program "Zentrales Innovationsprogramm Mittelstand (AiF-ZIM)" (ZF4129902GM5).

[1] Y.A. Budkov, A.L. Kolesnikov, D.V. Ivlev, N.N. Kalikin and M.G. Kiselev, *Journal of Molecular Liquids*, 2018, 276, 801.

[2] Y. Rosenfeld, *Phys. Rev. Lett.*, 1989, 63, 980.

[3] J. Weeks, D. Chandler and H. Andersen, *J. Chem. Phys.*, 1971, 54, 5237.

[4] C. Garlapati and G. Madras, *Thermochim. Acta*, 2009, 496, 54–58.

PI-35. Thermovap – Calculation Program of Vaporization Enthalpy and Heat Capacity Organic Compounds

Krasnykh E.L., Kazakov A.K., Portnova S.V.

Samara State Technical University, Russia

kinterm@samgtu.ru

The Thermovap program is designed to calculate the enthalpies of vaporization and change heat capacities of the “liquid – vapor” for a number of classes of organic compounds except cyclic and aromatic substances.

A program is based on graph theory and available literature data on $\Delta_{\text{vap}}H_m^o(298.2)$ and $\Delta_l^sCp^o(298.2)$ [1-3].

The calculation procedure is based on the linear dependence $\Delta_{\text{vap}}H_m^o(298.2)$ and $\Delta_l^sCp^o(298.2)$

of total index $^{0-3}\chi$ determined by equation: $^{0-3}\chi = ^{0-3}\chi_f + \chi_{MM}$

The index $^{0-3}\chi_f$ is the contribution from the molecular structure estimated by connectivity indices from zero to the third order $^{0-3}\chi_f = ^0\chi + \frac{1}{2}^1\chi + \frac{2}{3}^2\chi + \frac{3}{4}^3\chi$, $^0\chi = \sum_1^n 1/Ln(\delta_i)$ - is the zero order connectivity index and determines the contribution of atoms or a group of atoms; $^1\chi = \sum_1^m 1/Ln(\delta_i\delta_j)$ - is the first order connectivity index and determines the contribution of two valently bonded atoms; $^2\chi = \sum_1^p 1/Ln(\delta_i\delta_j\delta_k)$ - is the second order connectivity index and determines the contribution to the three successively located atoms; $^3\chi = \sum_1^r 1/Ln(\delta_i\delta_j\delta_k\delta_l)$ - is the third order connectivity index and determines the contribution to the four successively located atoms. Values of descriptors present in table 1.

The index χ_{MM} is the contribution from intermolecular interactions determined by equation:

$\chi_{MM} = (-3,249 \cdot Ln(m \cdot ^{0-3}\chi_{alk}) + 14,806) \cdot (n-1)$ for esters and $\chi_{MM} = 11,3$ for alcohols. For other classes χ_{MM} is zero.

Table 1. The values of descriptors.

Descriptor	Value	Descriptor	Value	Descriptor	Value
—CH ₃	1,4773	—C— 	7,5949	—O—	1,6062
—CH ₂ —	1,6201	—C=O H	1,1319	—C=O O—	1,1467
—CH— 	2,3685	—OH	1,2115	—C— O	1,1664

A vaporization enthalpy $\Delta_{\text{vap}}H_m^o(298.2)$ and difference of the molar heat capacities of the gaseous and the liquid phase $\Delta_l^sCp^o(298.2)$ were estimated by equations:

$$\Delta_{\text{vap}}H_m^o(298.2) = 1,6883 \cdot ^{0-3}\chi + 2,0781 \quad \Delta_l^sCp^o(298.2) = -2,416 \cdot ^{0-3}\chi - 11,0$$

The program is available to download on a link <http://tonhs.samgtu.ru/node/13>.

Acknowledgements The financial support of RFBR № 18-08-00574 A.

[1] E. L. Krasnykh *Journal of Structural Chemistry*. 2008, 48, 4, 1026.

[2] Krasnykh and S. V. Portnova. *Journal of Structural Chemistry*. 2017, 58, 6, 706.

[3] Krasnykh and S. V. Portnova. *Journal of Structural Chemistry*. 2016, 57, 3, 437.

PI-36. The Use of Density Functional Theory in the Calculation of Structural, Energetic and Thermodynamic Characteristics of Triethylammonium - Based Protic Ionic Liquids

Fedorova I.V., Krestyaninov M.A., Safonova L.P.

G.A. Krestov Institute of Solution Chemistry of the Russian Academy of Sciences, Russia

fiv@isc-ras.ru

The results of structural, energetic and thermodynamic analysis of ten ion pairs and their relevance for the physicochemical properties of triethylammonium (TEA) - based protic ionic liquids are reported. Dihydrogen phosphite (H_2PO_3), dihydrogen phosphate (H_2PO_4), hydrogen sulfate (HSO_4), mesylate (MsO), triflate (TfO), besylate (Bsu), metanilate (MTN), sulfamate (SAM), tosylate (PTSA) and 3-nitrobenzenesulfonate (NBSu) anions were taken for the present computations. The calculations were mainly performed by dispersion corrected density functional theory method (B3LYP-GD3). The dispersion correction was found to contribute significantly to the interaction energy, but it has a small effect on the optimized geometries of the studied ion pairs. The interaction triethylamine with each of the investigated acids leads to proton transfer from acid to amine and formation of ions held together in the ion pair by the electrostatic interaction, dispersion forces and hydrogen bond. Negative Gibbs free energy values show that the ion pair formations from amine and acid molecules are thermodynamically favorable and that the process proceeds spontaneous. The anions that possess a smaller gas phase proton affinity (PA) have the tendency form more thermodynamically stable ion pairs with triethylammonium cation. There is a linear relationship between the decomposition temperatures of TEA-based PILs [1, 2] and the calculated free energies of the ion pair formation. Here, the greater the energy value, the higher is the decomposition temperature. The calculated characteristics of the hydrogen bonding in all the studied ion pairs of TEA completely satisfy the geometrical (interatomic distances in the N-H...O fragment and H-bond angle), energetic (hydrogen bond energy) and electron-topological (electron density and its Laplacian at (3; -1) bond critical point) criteria of H-bonds indicating that they can be identified as strong H-bonds. Among the analyzed systems the ion pair of TEA with anions of phosphorus acid has the strongest hydrogen bonds while there is the weakest H-bonding interaction in triethylammonium triflate. The interaction energy between ions in the ion pairs of TEA increases with the PA parameter growth in the following order: TfO < NBSu < HSO_4 < Bsu < SAM < PTSA < MTN < MsO < H_2PO_4 < H_2PO_3 . For evaluating the possibility of molecular complex formation in these TEA-based PILs, the simulation of proton transfer from cation to anion along the hydrogen bond in the ion pair was performed by the scan technique of proton transfer coordinate along the potential energy surface. Based on the obtained results, the spontaneous proton transfer in the ion pairs of TEA is very unlikely. The changing the acid anion within the ion pairs of TEA has a minor effect in the energy profile for proton transfer.

Acknowledgements This work was partially financed by the Russian Foundation for Basic Research and the government of the region of the Russian Federation, grant № 18-43-370009.

[1] L.E. Shmukler, M.S. Gruzdev, N.O. Kudryakova, Yu.A. Fadeeva, A.M. Kolker, L.P. Safonova, *RSC Advances*, 2016, 6, 109664.

[2] L.E. Shmukler, M.S. Gruzdev, N.O. Kudryakova, Yu.A. Fadeeva, A.M. Kolker, L.P. Safonova, *J. Mol. Liq.*, 2018, 266, 139.

PI-37. Solubility of Caffeine in the Binary Solvent Carbon Tetrachloride – Methanol

Golubev V.A., Kiselev M.G

G.A. Krestov Institute of Solution Chemistry of the Russian Academy of Sciences, Russia

vag@isc-ras.ru

In this work the results of the experimental and theoretical study of caffeine solubility in the binary solvent carbon tetrachloride – methanol are presented. These binary mixtures are characterized by nonideal deviations caused by the methanol self-association. The effect of molecular association on thermodynamic properties of the binary mixtures methanol – carbon tetrachloride was described in [1].

The solubility of caffeine in binary solvent was investigated by gravimetric method at temperature of 298 K. According to the data obtained, the concentration dependence of the caffeine solubility has the maximum in the region of 0.5 mole fraction of methanol. The extreme behavior of concentration dependence of solubility was analyzed in the framework of ASL model (Associated Solution + Lattice) based on the associative equilibrium theory and the simple lattice model [2,3]. The logarithm of the activity coefficient of the solute (S) in this model is the sum of the chemical $(\ln \gamma_S)_{chem}$, combinatorial $(\ln \gamma_S)_{comb}$ and residual contributions:

$$(\ln \gamma_S) = (\ln \gamma_S)_{chem} + (\ln \gamma_S)_{comb} + (\ln \gamma_S)_{res}.$$

The parameters of the model are the equilibrium constants of the association reactions, the geometric characteristics of the molecules of the mixture components and the binary interaction parameters. According to the data obtained, the solubility dependence mainly determined by caffeine – methanol heteroassociation.

Acknowledgements This work was supported by the Russian Foundation for Basic Research [grant No. 18-03-00255-A].

[1] V.A. Durov and I.Yu. Shilov, *J. Mol. Liq.*, 2001, 92, 165.

[2] V.A. Golubev, M.Yu. Nikiforov and G.A. Alper, *Rus. J. Phys. Chem. B.*, 2015, 9, 1054.

[3] V.A. Golubev, M.Yu. Nikiforov, G.A. Alper and R.D. Oparin, *Rus. J. Phys. Chem. B.*, 2016, 10, 1166.

PI-38. On the Possibility of Realization of Labile States

Fedorov P.P.

Prokhorov General Physics Institute of the Russian Academy of Sciences, Russia

ppfedorov@yandex.ru

Thermodynamic equilibria are divided into three types: stable, metastable, and labile (Fig.1). It is generally accepted that labile states are unrealizable, because there is no force that returns the system to its original state, and after the fluctuation out of equilibrium, the system moves away from it with acceleration [1]. However, there are experimental data that refute this postulate.

$Ba_{1-x}Ca_xF_2$ samples with fluorite-type structure were prepared by high-energy ball milling. Solid solution samples show no signs of decay when stored at room temperature for several years. However DSC measurements revealed exothermic decomposition at temperatures of about 450 °C. Decomposition was also observed by high temperature X-ray experiments. As a product two phases with compositions close to pure BaF_2 and CaF_2 were obtained. [2].

Fig. 1 shows the general scheme of stable, metastable and labile state, and the proposed state diagram for the system CaF_2 - BaF_2 . Apparently, the crystalline solid solution $Ba_{1-x}Ca_xF_2$ is in labile state, i.e. its transition to the equilibrium state is not associated with overcoming the potential barrier. Indication of this is the lack of abrupt beginning of the exothermic effect (smooth onset, see Fig. 2). Apparently, the relative stability of the crystalline samples of the solid solution $Ba_{1-x}Ca_xF_2$ is due to the extremely low values of the diffusion coefficients of the cations. The system is “falling”, but very slowly.

Solid solutions crystals must undergo spinodal decomposition during the cooling process. However, in this case there are no signs of it. Systems in labile state can be the basis of new functional materials.

Acknowledgements The author is grateful to Andre Düvel, Paul Heitjans, Valery Voronov, and Aleksandr Pynenkov for participating in the experiment and discussing the results

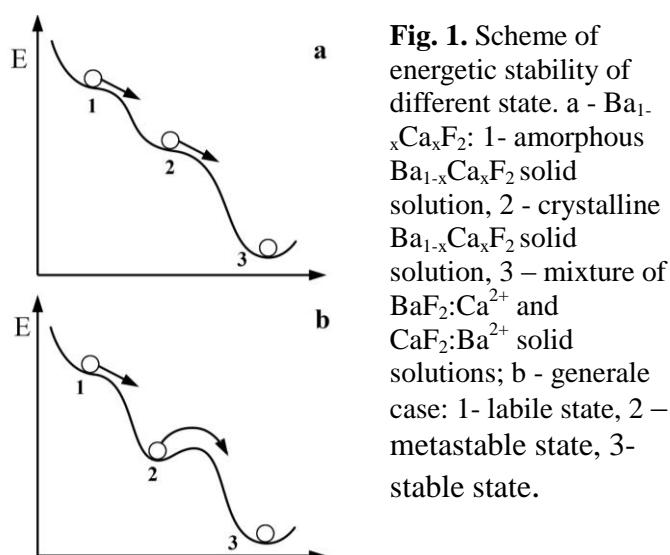


Fig. 1. Scheme of energetic stability of different state. a - $Ba_{1-x}Ca_xF_2$: 1- amorphous $Ba_{1-x}Ca_xF_2$ solid solution, 2 - crystalline $Ba_{1-x}Ca_xF_2$ solid solution, 3 – mixture of $BaF_2:Ca^{2+}$ and $CaF_2:Ba^{2+}$ solid solutions; b - generale case: 1- labile state, 2 – metastable state, 3- stable state.

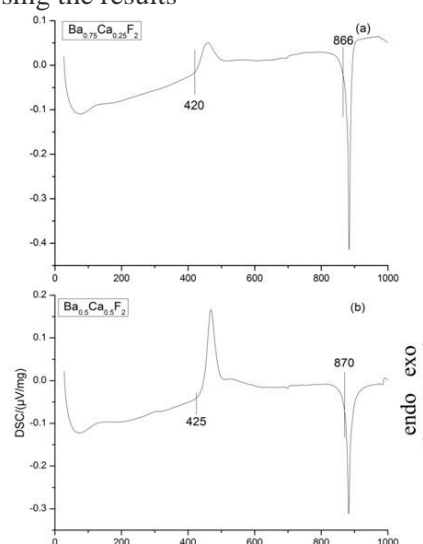


Fig.2. DSC curves

[1] A.V. Storonkin, *Thermodynamic of heterogeneous systems*, 1967, 448 pp, Leningrad State University, Leningrad, USSR (in Russian) c.

[2] A. Düvel, P. Heitjans, P.P. Fedorov, V.V. Voronov, A.A. Pynenkov and K.N. Nishchev. *Solid State Science*, 2018, 83,188. DOI: 10.1016/j.solidstatesciences.2018.05.011

PI-39. A New Equation of State for Solids Based on Linear Combination of Planck-Einstein Functions

Perevoshchikov A.V., Kovalenko N.A., Uspenskaya I.A.

Lomonosov Moscow State University, Russian Federation

andreyperev94@gmail.com

Recently a new method for approximating the standard thermodynamic functions was proposed [1]. This method is primarily based on analytical description of temperature dependence of isobaric heat capacity of solids. It was pointed out that for substances not undergoing phase transformations within the temperature interval from 0 to $T(K)$ standard thermodynamic functions $C_p^\circ(T)$, $S^\circ(T)$ and $H^\circ(T)-H^\circ(T_{ref})$ could be easily calculated into each other with the help of linear combination of Planck-Einstein functions.

The purpose of current work was to expand this approach by introducing of two additional variables – volume and composition. So, probability of solid solution description as well as P - V - T data for solids by means of linear combination of Planck-Einstein functions was investigated. Moreover, additional task was to consider the potential of these functions as general equation of state included both thermal and caloric equations of state.

To demonstrate the possibility of using Planck-Einstein functions for description P - V - T data magnesium oxide was chosen as a test system. The use as a base function the dependence of heat capacity (and Gibbs energy, consequently) from temperature and pressure together with well-known thermodynamic relations allows to calculate the change in volume of magnesium oxide depending on changes of temperature and pressure. As a result, an analytical dependence of the function $C_p(T,P)$ based on linear combination of Planck-Einstein functions was found, which is consistent with P - V - T data for magnesium oxide in a wide range of temperatures (up to 1350 K) and pressures (up to 25 GPa) with an error comparable with the measurement accuracy.

Experimental data for thermodynamic functions of solid solutions are not widely presented in literature. However there are few systems with enough composition dependent data that allowed us to try to model it properly. Parameters of special model based on linear combination of Planck-Einstein functions were determined during the processing of the experimental data on the ThO_2 - PuO_2 , InAs - InP , InP - GaAs systems. The estimation of parameters was performed by minimization sum of squares of residuals. 95 % confidence intervals for parameters were calculated, only statistically significant parameters were used. As a result heat capacities of solid solutions were described. The model allows to estimate the entropy of mixing and enthalpy increments for systems under investigation.

Acknowledgements This work was performed as part of the project "Chemical Thermodynamics" (AAAA-A16-116061750195-2).

[1] G.F. Voronin and I.B. Ku

PI-40. Derivation of Effective Intermolecular Potential for Water via Molecular Modeling

Volkov N.A., Shchekin A.K.

Saint Petersburg State University, Russia

nikolay.volkov@spbu.ru

The effective intermolecular potential of interaction of water molecules was obtained for the coarse-grained water model, which we constructed on the basis of the TIPS3P all-atom three-center water model. To obtain the intermolecular potential we used the alignment of the structural properties (radial distribution functions) of water in the all-atom and coarse-grained representations using the molecular dynamics and Monte Carlo methods. The effective intermolecular potential was obtained by us both in the tabulated and in the analytical form.

The procedures for building the effective potentials of interactions using the structural properties are described in details, e.g., in [1]. In order to get the effective potential we carried out an all-atom molecular dynamics (MD) simulation using the MDynaMix program [2] and several coarse-grained (CG) Monte Carlo (MC) simulations together with the Iterative Boltzmann Inversion procedure [3-5] using the in-house programs. First, we performed an all-atom MD simulation of the system of 3200 TIPS3P molecules in the NPT statistical ensemble at $T = 298$ K and $P = 1$ atm. The average volume of the system appeared to be $\langle V \rangle = 44.91 \times 44.91 \times 44.91 \text{ \AA}^3 = 90579 \text{ \AA}^3$. Then the $g(r)$ for the TIPS3P water molecules (their centers of mass) was obtained. The second step was to simulate a system of 3200 CG water molecules by the MC method in the NVT ensemble ($N = 3200$, $V = 44.91 \times 44.91 \times 44.91 \text{ \AA}^3 = 90579 \text{ \AA}^3$, $T = 298$ K). A CG water molecule was represented by a hard sphere with an additional potential acting beyond the hard sphere radius. This additional potential was gradually tuned using the Iterative Boltzmann Inversion procedure in order to fit the $g(r)$ of the CG water molecules to the $g(r)$ of the TIPS3P water molecules obtained earlier during the all-atom MD simulation. After getting the effective potential for the CG water molecules we tried to represent it by a polynomial (see Fig.1). It seems that a polynomial of the power 20 gives the best fit. The obtained effective intermolecular potential for water can be used, e.g., for studying the nucleation using the density functional theory and the methods of molecular modeling.

Acknowledgements This work was supported by the Russian Foundation for Basic Research (grant 18-53-50015 ЯФ_a).

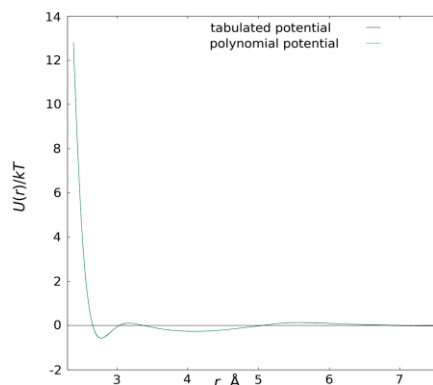


Figure 1. The effective intermolecular potential for water in tabulated and analytical forms.

- [1] A.P. Lyubartsev, A. Laaksonen, *Lecture Notes in Physics*, 2004, 640, 219.
- [2] A.P. Lyubartsev, A. Laaksonen, *Comput. Phys. Commun.*, 2000, 128, 565.
- [3] W. Schommers, *Phys. Rev. A*, 1983, 28, 3599.
- [4] A.K. Soper, *Chem. Phys.*, 1996, 202, 295.
- [5] D. Reith, M. Putz, F. Muller-Plathe, *J. Comp. Chem.*, 2003, 24, 1624.

PI-41. Colloidal Aggregation of Asphaltenes Studied with Brownian Dynamics and Monte Carlo Simulations

Taherkhani F.^{1*}, Vishnyakov A.^{1,2}, Kolattukudy P. Santo²

¹Skolkovo Institute of Science and Technology, Moscow, Russia;

²Rutgers the State university of NJ, Piscataway NJ, USA

F.Taherkhani@skoltech.ru

Asphaltenes and resins constitute the heaviest fraction of crude oil. Their aggregation caused by change in external conditions is a phenomenon of a significant practical importance that is still insufficiently understood. The talk reports Brownian dynamics and hybrid Monte Carlo/Brownian dynamics simulations of asphaltene aggregation, by assuming a *colloidal model* in which the asphaltenes are dispersed in form of primary nanoclusters (PN) modelled as individual particles. PN experience short range attraction (which effectively takes into account van der Waals interactions and hydrogen bonding between the polyaromatic cores at short distances) a longer range repulsion (which accounts for the steric interactions between the aliphatic chains of asphaltenes and resins adsorbed at nanocluster surface). Finally, we propose a new modelling approach that accounts for redistribution of aliphatic chains on primary cluster association.

With this model, we explore the mechanisms of asphaltene aggregation upon oil dilution with aliphatic solvents at different resin concentration, paying attention to both thermodynamic and kinetic factors. The agglomeration process involves initial diffusion-limited aggregation, internal rearrangement within the aggregates that gradually converts loose initial aggregates into compact 3D structures and aggregate coalescence. We discuss how the roles of each factor depends on the chemical structure of asphaltene molecules and resin concentration. We distinguish different aggregation regimes leading to bulk precipitation, long-living fractal structures and gels.

Acknowledgements The studies were supported by PRF grant 54610-ND6

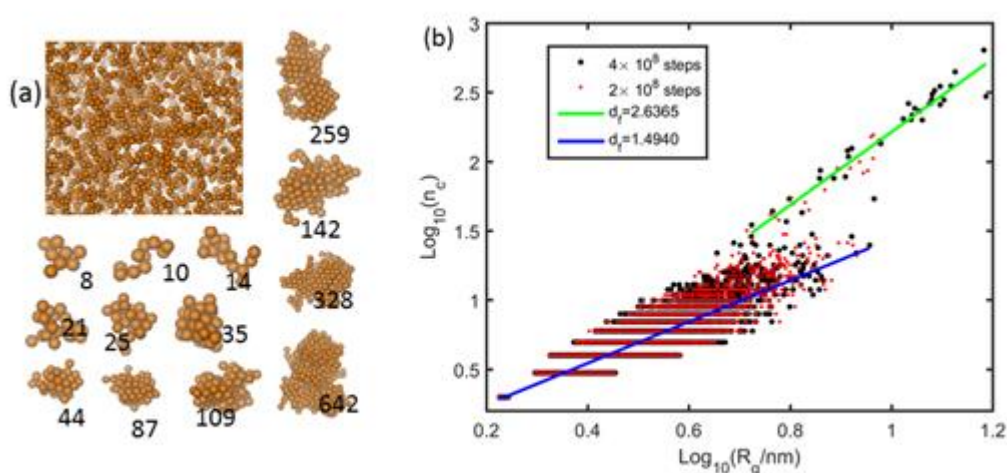


Fig.1. (a) Agglomerates of difference sizes formed with a moderate attraction and repulsion between the particles. (b) The radius of gyration vs the aggregation number of the clusters.

PI-42. Approximation of Thermodynamic Properties by Expanded Einstein Model: Possibilities and Problems

Babkina T.S., Ivanov A., Konstantinova N.M., Uspenskaya I.A.

Lomonosov Moscow State University, Russian Federation

ivanovas.chem@mail.ru

Multiple Einstein functions (MEF) as described in the work of Voronin and Kutsenok [1] allow standard thermodynamic functions to be approximated with an accuracy corresponding to experimental measurements from 0 K up to the melting point.

Using this approach the experimental $C_p(T)$ data can be approximated by the following equation

$$C_p(T) = 3R \sum_i \alpha_i \frac{(\Theta_i/T)^2 e^{\Theta_i/T}}{(e^{\Theta_i/T} - 1)^2} \quad (1)$$

Then an integration of the Eq. (1) with addition of $3/2R\theta_E$ (which corresponds to zero-point lattice vibration) leads to the following expressions for thermodynamic functions:

$$S^\circ(T) = 3R \sum_i \alpha_i \left(\frac{\Theta_i/T}{e^{\Theta_i/T} - 1} - \ln(1 - e^{-\Theta_i/T}) \right) \quad (2)$$

$$H_T^\circ(T) - H_0^\circ = \frac{3}{2} \theta_E + 3R \sum_i \alpha_i \Theta_i (e^{\Theta_i/T} - 1)^{-1} \quad (3)$$

where α_i , Θ_i ($i = 1, 2, \dots$) are parameters determined by fitting the experimental heat capacity data to equation (1), θ_E is a true Einstein temperature of substance under investigation.

Critical review of available data for solid and liquid phases of Sn, Si and Ge were performed. Adiabatic calorimetry and enthalpy increment measurements for solids were fitting simultaneously with CpFit program (available at <http://td.chem.msu.ru/develop/cpfit/>). As a result, a set of self consistent thermodynamic properties of pure solid elements were obtained. One of interesting and useful result of MEF applying is a possibility to estimate the entropy and enthalpy of transition at temperature of reversible phase transformation α -Sn \leftrightarrow β -Sn (the transformation from the white tin to grey tin is very difficult). Result of reassessment for α -tin (grey) and β -tin (white) were compared with *ab initio* calculations of C_p performed within the framework of density functional theory using the Vienna *ab-initio* simulation package VASP code [2-4]. The good agreement of *ab-initio* calculations and estimation carried out based on the Voronin and Kutsenok method is obtained.

The possibility to describe $C_p(T)$ in premelting area and after melting point with multiple Einstein functions and additional term [5] was investigated. It was shown that in some cases it's possible to describe available data within the experimental error and to predict a correct limited behavior of thermodynamic functions.

Acknowledgements This work was performed as part of the project "Chemical Thermodynamics" (AAAA-A16-116061750195-2).

1. Voronin G.F., Kutsenok I.B. J. Chem. Eng. Data 2013; 58:2083-2094
2. Kresse G., J. Hafner J. Phys. Rev. B 1993; 47 (1): 558-561.
3. Kresse G., J. Hafner J. Phys. Rev. B 1994; 49: 14251-14269.
4. Kresse G., Furthmuller J. Comput. Mater. Sci. 1996; 6: 15-50.
5. Voskov A.L., Kutsenok I.B., Voronin G.F. Calphad, 2018; 61: 50-61

PI-43. A New Method to Calculate the Change in Ion Solvation Energy at Ion Transfer Between Two Nonlocal Dielectric Media Possessing Different Correlation Lengths

Rubashkin A.A.¹, Iserovich P.², Vorotyntsev M.A.³

¹Institute of Cytology, Russian Academy of Sciences, Saint-Petersburg, Russia;

²State University of New York, Downstate Medical Center, New York, 11203 USA;

³D. I. Mendeleev University of Chemical Technology of Russia, Moscow, Russia

andrey.rubashkin@gmail.com

Novel approximate procedure for calculation of potential distribution and ion solvation energy in nonlocal dielectric media [1] is used here for calculation of the ion resolution energy, $\Delta W_{m1 \rightarrow m2} = (W_2 - W_1)$, i.e. the difference between the ion solvation energies at it transfer between two medias with different correlation lengths. As in [2,3] a procedure [1] takes into account cut-out ion cavity effect. Total charge of the ion, e , is composed of two contributions: $e = q_{cav} + q_{ext}$, were q_{cav} is a charge inside cavity, and q_{ext} is related to the ionic charge density outside the cavity $\rho_{ext}(r)$, which is a function of distance from a center of an ion [4] and r_i is a radius of Born sphere of an ion:

$\rho_{ext}(r) = \rho_0 (4 \pi \eta)^{-1} \exp[-(r - r_i) / \eta]$, $\rho_0 = q_{ext} (r_i^2 + 2 r_i \eta + 2 \eta^2)^{-1}$ for $r > r_i$, (1) We derived Eq. (2) for resolution energy were k is a wave vector:

$$\Delta W_{m1 \rightarrow m2} = (1/\pi) \int_0^\infty [1/\varepsilon_1(k) - 1/\varepsilon_2(k)] \left[q_{cav} \sin kr_i / kr_i + (4\pi/k) \int_{r_i}^\infty r \rho_{ext}(r) \sin kr dr \right]^2 dk, \quad (2)$$

The dependence of

$\Delta W_{m1 \rightarrow m2}$ from Λ_2/Λ_1 (Fig. 1) originates from the difference of the inverse dielectric functions in two liquid phases (Eqs. (3)–(4)). For water $\varepsilon_2 = 4.9$, $\varepsilon_3 = 78$, $C_3 = (1/\varepsilon_2 - 1/\varepsilon_3)$. A correlation length in water $\Lambda_1 = 3 \text{ \AA}$. OS is overscreening effect in $\varepsilon^{OS}(k)$ (Eq. (4)), were $\lambda = 0.15 \text{ \AA}$ [4]. The second media is a mixture of water with proteins, so for it should be $\Lambda_2 > \Lambda_1$. $1/\varepsilon_1^{3mod}(k) - 1/\varepsilon_2^{3mod}(k) = -C_3 \{1/[1+(k\Lambda_1)^2] - 1/[1+(k\Lambda_2)^2]\}$, for $\varepsilon(k)$ without OS, (3) $1/\varepsilon_1^{OS}(k) - 1/\varepsilon_2^{OS}(k) = k^2 C_3 \{ \Lambda_1^2/[1+(k\Lambda_1)^2] - \Lambda_2^2/[1+(k\Lambda_2)^2] \} / [1+(k\lambda)^2]$, for $\varepsilon(k)$ with OS. (4) On Fig. 1 solid curves (1,2) for 3mod $\varepsilon(k)$ with OS effect. Points (1',2') for 3mod $\varepsilon(k)$ without OS. Curve 1 and points 1' for ion charge only inside cavity ($q_{cav} = e$, $q_{ext} = 0$). Curve 2 and points 2' for ion charge as inside and outside cavity ($q_{cav} = 0.51e$, $q_{ext} = 0.49e$, $\eta = 0.35 \text{ \AA}$).

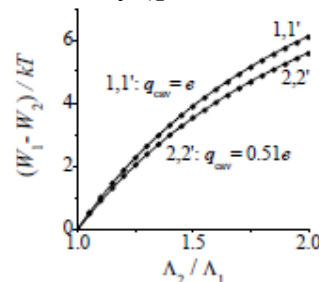


Figure 1. Na⁺ resolution energy, $-\Delta W_{m1 \rightarrow m2}$, as a function of the ratio of a long-range correlation lengths inside 2-media and in 1-media, Eqs. (1)–(4).

[1] M.A. Vorotyntsev, A.A. Rubashkin and A.E. Antipov, *Russ. J. Electrochem.*, 2018, 54, 879.

[2] M.A. Vorotyntsev, *J. Phys. C: Solid State Phys.*, 1978, 11, 3323.

[3] M.A. Vorotyntsev and A.A. Rubashkin, *Phys. Chem. Liquids*, 2017, 55, 141.

[4] A.A. Kornyshev and G. Sutmann, *J. Chem. Phys.*, 1996, 104, 1524.

PI-44. Thermodynamic Properties of Thulium Orthovanadate: a Low-Temperature Heat Capacity Study

Kondrat'eva O.N., Ryumin M.A., Morozova E.A., Gavrichev K.S.

Kurnakov Institute of General and Inorganic Chemistry of RAS, Russia

ol.kondratieva@gmail.com

Thulium orthovanadate, TmVO_4 , belongs to REEVO_4 (REE = rare earth element) and crystallizes in a tetragonal zircon-type structure (space group: $I4_1/amd$) at room temperature. Like some other members of REEVO_4 family (e.g., DyVO_4 and TbVO_4), TmVO_4 undergoes a Jahn-Teller phase transition with a lowering of the crystal symmetry from tetragonal to orthorhombic at $T_C \approx 2.1$ K, as determined from the results of optical spectroscopy, magnetic susceptibility and heat capacity measurements. Cooke et al. [1] measured heat capacity of TmVO_4 from 0.5 to 4.2 K. At the same time, the heat capacity of TmVO_4 from liquid-helium to room temperatures still remains uncharacterized.

A polycrystalline specimen of TmVO_4 was prepared by a solid state reaction method. The phase purity and chemical composition of the specimen prepared were confirmed by powder X-ray diffraction (D8 Advance XRD diffractometer, Bruker) and X-ray fluorescence spectroscopy (M4 TORNADO X-ray fluorescence spectrometer, Bruker). An adiabatic vacuum calorimeter (BKT-3, Termis, Russia) was used to measure the heat capacity of TmVO_4 in the temperature range from 10.40 to 343.24 K. An accuracy of heat capacity measurements was 2% at $T < 20$ K, 0.8% in the temperature range from 20 to 50 K, and 0.2% at $T > 50$ K.

This report discusses the results of heat capacity measurements obtained by adiabatic calorimetry (Fig. 1) and compares with the high-temperature $C_{p,m}^0(T)$ data available in the literature [2, 3]. Special attention was paid to calculation of the standard thermodynamic properties (heat capacity, entropy, enthalpy change and derived Gibbs energy). An assessment and subsequent comparison of an anomalous contribution to the total heat capacity (Schottky anomaly) of TmVO_4 with the data known for TmPO_4 were also carried out.

Acknowledgements This study used the equipment of the JRCMPR IGIC RAS and was supported by the Russian Foundation for Basic Research (RFBR), grant No 18-33-00252.

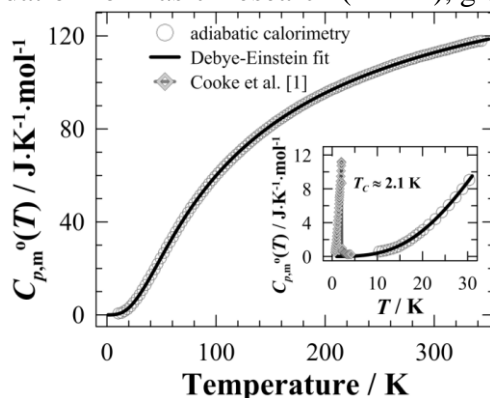


Figure 1. Low-temperature heat capacity of TmVO_4 .

- [1] A.H. Cooke, S.J. Swithenby, and M.R. Wells, *Solid States Communications*, 1972, 10, 265.
[2] L.T. Denisova, L.G. et al., *Doklady Physical Chemistry*, 2015, 463, 173.
[3] H. Yokokawa, N. Sakai, T. Kawada, and M. Dokiya, *Journal of American Ceramic Society*, 1990, 73, 649.

PI-45. Novel Bodipy Sensors for the Hydrocortisone Spectral Detection in Organic Media

Antina E.V.^{1,2}, *Ksenofontov A.A.*^{1,2}, *Antina L.A.*¹, *Berezin M.B.*¹, *Guseva G.B.*¹

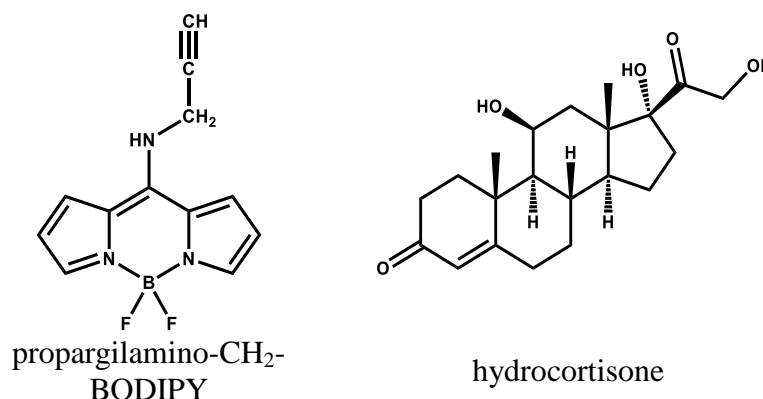
¹G.A. Krestov Institute of Solution Chemistry of the Russian Academy of Sciences, Russia

²Ivanovo State University of Chemistry and Technology, Russia

lyubov.antina@mail.ru

Modern studies of physiological and pathological processes are often based on the use of fluorescent sensors. These sensors are able to selectively bind specific metabolites into supramolecular structures and produce effective spectral signals.

At present, a number of structurally modified BF₂-dipyrromethene luminophores (BODIPY) are used for medical and bio-diagnostic purposes. They are non-toxic, have a high quantum yield of fluorescence and sensitivity of spectral characteristics to intermolecular interactions. This allows determining ultralow biomolecules concentrations (10⁻⁹ - 10⁻¹² mol / l) by spectral methods with high speed and ease of results interpretation. The self-assembly, structure and properties of the supramolecular complexes of steroid hormone hydrocortisone and BODIPY, modified by the mesopropargylamine group (propargylamino-CH-BODIPY), are presented in the report.



Hydrocortisone molecules contain aromatic cycles and several hydroxyl and keto groups. This allows the steroid to enter into intermolecular interactions of various types (donor-acceptor, acid-base, π - π -stacking) and form supramolecular complexes with complementary in structure compounds.

Spectrophotometric and fluorescent titration showed that propargylamino-CH-BODIPY is involved in the reaction of supramolecular complexation with hydrocortisone. This reaction is accompanied by a complex spectral response: an increase in the intensity of the characteristic band in the absorption spectra up to 25% and the quenching of the dye fluorescence up to 20%. The stoichiometric composition of supramolecular complexes was determined. Crystall samples of the supramolecular compound BODIPY with hydrocortisone were obtained and investigated using UV / vis, fluorescence, FTIR, PXRD, and DFT calculation. The mechanism for fluorescence quenching, the increase in the chromophore activity of the BODIPY-luminophore in the composition of the supramolecule and the prospects for its use as a steroid hormones spectral sensors are substantiated.

Acknowledgements The financial support of Russian Foundation for Basic Research (RFBR), project no. 18-33-20218 mol_a_ved

PI-46. Computer Simulation of Polyvinylpyrrolidone (PVP) Adsorption on Cellulose Nanocrystals (CNC) and The PVP-Assisted CNC Self-Assembly

Surov O.V., Voronova M.I., Gurina D.L., Zakharov A.G.

G.A. Krestov Institute of Solution Chemistry of the RAS, Russian Federation

ovs@isc-ras.ru

Cellulose nanocrystals (CNC) refer to a type of rod-like cellulose nanomaterial with a typical length of 100-300 nm, a diameter of 10-20 nm, a moderate density, a high degree of crystallinity and a very high tensile strength and modulus. The properties of CNC, viz. anisotropic particle shape, high surface charge, high mechanical strength, the possibility of chemical modification of the surface hydroxyl groups and the formation of a chiral nematic liquid-crystalline phase in aqueous dispersions and films, attract considerable attention for the design of new functional materials.

Polyvinylpyrrolidone (PVP), a water-soluble, non-toxic, non-ionic amorphous polymer with high solubility in polar solvents, has been widely used in nanoparticles synthesis. Due to the amphiphilic nature, PVP can affect morphology and nanoparticle growth by ensuring solubility in various solvents, discriminatory surface stabilization, controlled crystal growth, playing the role of a shape-control agent and facilitating the growth of specific crystal faces while preventing others.

Recently, we have revealed PVP assisted CNC self-assembly which produces highly crystalline and reasonably uniform CNC aggregates with high aspect ratio (length/width) [1].

The aim of the present research is a computer simulation for a consideration and proof of an appropriate mechanism of PVP adsorption onto different facets of CNC particles as well as a possible model of the PVP-assisted CNC self-assembly.

Acknowledgements The financial support of the Russian Science Foundation, grant number 17-13-01240.

[1] M. Voronova, N. Rubleva, N. Kochkina, A. Afineevskii, A. Zakharov and O. Surov, *Nanomaterials*, 2018, 8, 1011.

PI-47. Pharmaceutical Cocrystals of Flurbiprofen: Thermodynamic and Structural Aspects

Surov A.O., Voronin A.P.

G.A. Krestov Institute of Solution Chemistry of the RAS, Russian Federation

aos@isc-ras.ru

Cocrystals, solid forms having two or more different molecules in the crystal structure, continue to gain significant interest for their application to the design of new materials with desired functional properties. Pharmaceutical cocrystals, multi-component crystals in which at least one component is a neutral active pharmaceutical ingredient (API) and the cocrystal former is a pharmaceutically acceptable ion or molecule, have been added to the landscape of crystal forms of APIs. The differences in the molecular arrangement of an API and its cocrystals inevitably lead to altered therapeutic effects and physicochemical properties including water solubility, bioavailability and stability.

In this work we report the application of the cocrystallization approach to a low water soluble but potent non-steroidal anti-inflammatory drug flurbiprofen. Flurbiprofen belongs to BCS class II of the biopharmaceutical classification system and finds application in medical practice in oral formulations for the acute or long-term treatment of rheumatoid arthritis, osteoarthritis, or mild to moderate pain. To date, however, cocrystal formation for flurbiprofen does not seem to have been systematically explored. Thus, development of novel crystalline forms of the drug with potentially enhanced key physicochemical properties are still of considerable interest.

Cocrystal screening of the flurbiprofen resulted in three new multicomponent solids with benzamide, salicylamide and picolinamide in a 1:1 molar ratio. Cocrystal formation between the components was confirmed by differential scanning calorimetry, X-ray powder diffraction analysis and infrared spectroscopy. Crystal structures of the cocrystals were determined from powder diffraction data using synchrotron radiation source. Special emphasis was put on the influence of structural changes in the co-former molecules on pattern of hydrogen bonding and packing arrangements of the cocrystals with flurbiprofen. The binary solid-liquid phase diagrams were built and allowed identifying unequivocally the formation of cocrystals of flurbiprofen with each of the three co-formers and also their stoichiometry. In addition, binary eutectic mixtures, potentially relevant for pharmaceutical application, are also identified. In order to assess the possible applicability of the obtained crystalline forms in drug delivery, the cocrystals solubility advantage values determined from eutectic concentrations at pH 2.0 and 25.0 °C were measured. All the cocrystals were found to be more soluble compared to the pure flurbiprofen. The observed values of the eutectic constant significantly exceed unity, indicating low thermodynamic stability of the obtained cocrystals in comparison with the parent drug in pH 2.0 buffer solution. The thermodynamic stability relationships between different cocrystals of flurbiprofen were rationalized in terms of Gibbs energies of the cocrystallization reactions and further verified by performing a set of competitive and exchange mechanochemical reactions. The influence of structural changes in the co-former molecules and structural features of the cocrystals on the driving force of the cocrystallization process were discussed.

Acknowledgements *This work was supported by the Russian Foundation for Basic Research (Grant 18-33-00485)*

PI-48. Congruent Sublimation of an Organic Cocrystal: Experimental Data on Sublimation Thermodynamics and Calculated Lattice Energies

Voronin A.P.¹, Boycov D.E.^{1,2}, Vasilyev N.A.^{1,2}, Surov A.O.¹, Manin A.N.¹

¹G.A. Krestov Institute of Solution Chemistry of Russian Academy of Sciences, Ivanovo, Russia;

²Ivanovo State University for Chemistry and Technology, Ivanovo, Russia

apv@isc-ras.ru

Cocrystals are multicomponent crystals consisting of two or more neutral molecules, which are solids in their pure form under ambient conditions. Their potential use in drug delivery, energetic materials, materials for optics and electronics draws attention to the problems of rational design of cocrystals with desired properties. One of widely used descriptors for relative stability and solubility, which are essential for pharmaceutical cocrystal development, is the lattice energy of a cocrystal and its constituents in their pure form. The lattice energy of a cocrystal in these methods is obtained either from quantum chemical computations or semi-empirical schemes. The lattice energy of molecular solids corresponds to the heat required to transfer a molecule from the bulk crystal into gas phase and is numerically equal to the sublimation enthalpy at conventional 0 K. Unfortunately, the accuracy of such predictions is insufficient, since there are no experimental data on the cocrystal lattice energy in the literature. The only known results obtained by our group [1] correspond to the quasi-equilibrium sublimation process of hydroxybenzamide cocrystals which decompose during sublimation due to large differences in their saturated vapor pressures of their components. For the cocrystal to be stable, the components need to have close saturated vapor pressures (within one order of magnitude) in a wide temperature range.

The aim of present research was to find the cocrystals that are stable during sublimation in order to obtain the thermodynamic functions of the equilibrium sublimation process which may further serve as references for different theoretical schemes. At the first stage, the search of pairs of compounds with close $\Delta_{\text{subl}}G^{298}$ and $\Delta_{\text{subl}}H^{298}$ values and capable to form a robust heterosynthon was performed in the database for experimental sublimation properties of organic compounds sublimation by Perlovich [2]. Experimental screening confirmed the cocrystal formation in two out of six selected pairs. Phase stability of the [caffeine + 3-hydroxybenzoic acid] (1:1) cocrystal during sublimation up to 130°C was confirmed by high performance liquid chromatography, powder X-Ray diffraction, differential scanning calorimetry and FT-IR spectroscopy. The saturated vapor pressures of both components were determined at wide range of temperatures using the inert gas flow method, and corresponding $\Delta_{\text{subl}}G$ and $\Delta_{\text{subl}}H$ values were derived. The $\Delta_{\text{subl}}H^{298}$ value of the cocrystal was found to be comparable with that of the pure compounds. Experimental lattice energy was compared against the set of the widely used theoretical methods, including DFT calculations with periodic boundary conditions and several additive schemes including CLP/PIXEL [3], CE-B3LYP [4] and descriptors for the non-covalent interaction energy based on the QTAIMC properties in the bond critical point [5].

Acknowledgements

The present work is supported by Russian Foundation for Basic Research (project 18-33-00485)

[1] A.N. Manin, et al., *J. Phys. Chem. B*, 2014, 118(24), 6803–6814.

[2] G. L. Perlovich and O. A. Raevsky. *Cryst. Growth Des.*, 2010, 10(6), 2707–2712.

[3] A. Gavezzotti, *J. Phys. Chem. B*, 2003, 107, 2344–2353.

[4] S.P. Thomas, P.R. Spackman, D. Jayatilaka and M.A. Spackman, *J. Chem. Theory Comput.*, 2018, 14, 1614–1623.

[5] I. Mata, I. Alkorta, E. Espinosa and E. Molins, *Chem. Phys. Lett.*, 2011, 507, 185–189.

PI-49. Thermodynamic Aspects of the Formation of Composites Based on Protein with the Ability to Inhalation Administration

Boldyrev A.E., Gerasimov A.V.

Kazan Federal University, Russia

boldyrev25@gmail.com

Inhalation delivery is a promising route of drug administration. The particles of drug aerosol must have a radius between 0,5 and 1,5 μm . The use of microspherical particles based on protein matrix allows to enhance bioavailability of poorly water-soluble drugs. In the present work, spray drying method was used for the preparation of the microspherical particles of bovine serum albumin with sulfanilamide as a model drug compound. The average aerodynamic radius of the prepared particle is 1 μm . We show that the spray drying regime produces microparticles with low residual solvent content. It was found that the release time of sulfanilamide from the microspherical particles is much lower than of the pure drug. The results allow developing a strategy of the production of the protein matrix-based systems for inhalation delivery of poorly water-soluble drugs.

Protein molecules are promising carriers of drugs. In connection with this, the study of the possibility of creating inhalation preparations based on the protein matrix is an actual area of modern chemical science and pharmaceuticals.

In the present study, obtaining of albumin composites with a model hydrophobic drug – sulfanilamide, was optimized by a complex of physicochemical methods. Optimal concentrations of the components in the solution were determined to produce microspherical particles with an average diameter of 1-3 μm , which can be used in inhalation administration of drugs. The obtained particles were characterized by differential scanning calorimetry, thermogravimetry, X-ray powder diffractometry and scanning electron microscopy. Dissolution kinetics of the drug from the protein carrier was examined. It was found that dissolution rate of drug can be increased by using protein matrix.

Acknowledgements. The reported study was funded by RFBR according to the research project № 18-015-00267.

PI-50. Sorption of Water by Carbon Fibers

Petrova T.F.¹, Chalykh A.E.¹, Aliev A.D.¹, Antipov Y.V.²

¹Frumkin Institute of Physical Chemistry and Electrochemistry Russian Academy of Sciences, Russia;

²Central research Institute of special mechanical engineering, Russia

petrttt@mail.ru

Information on the sorption capacity of water vapor by carbon fibers is crucial for predicting their behavior in the operation of composite materials in wet environments. Methods of vacuum weights Mac-Ben and sorption-desorption desiccator method determined sorption isotherms of water vapor of the carbon fiber UKN-M-6K, Kulon-VM, UMT-430-12K-EP, Umatex: UMT40-3K-ER, UMT42 -12K – EP, HTS-F13-12K -800 tex, Aksaca -03-A38, M-46-JB, graphitized carbon black X-72. Measurements were carried out at $T 20 \pm 1$ °C and different values of the relative vapor pressure P/P_0 (from 0.2 to 1.0). Structural and morphological characteristics of the fibers were determined by electron microscopy, x-ray microanalysis, atomic force microscopy, and Raman IR-scattering. The porous structure was characterized by low-temperature nitrogen sorption.

It is established that the sorption capacity of carbon fibers is determined by the oxygen concentration and can be calculated with the involvement of the information on the hydration numbers of oxygen-containing groups; the mechanism of sorption of water is identical with the mechanism of sorption of nitrogen, as evidenced by the linear dependence in the coordinates of equation De Boer, the fibers are characterized by unexpressed sorption-desorption hysteresis, which indicates a low level of defects sorbents. The possibility of calculating the specific surface area of the fibers by water vapor sorption isotherms with the use of reference samples of graphite carbon black X-72 is shown.

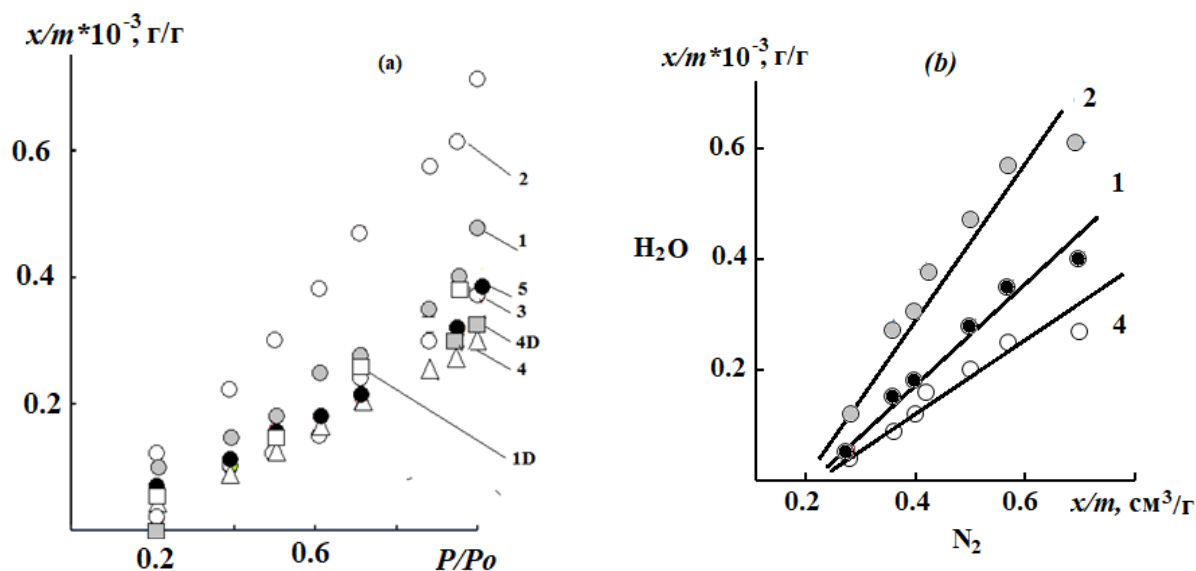


Figure 1. Isotherms of sorption (1-5) and desorption (1D, 4D) of water vapor by fibers (a)-1, 1D- UKN-M-6K; 2-HTS40 F13 12K 800 tex; 3-Umatex UMT42-12K-EP(K010); 4, 4D-Umatex UMT40-3K-EP; 5-Aksaca 03K-A38-0.3; (b) - water and nitrogen vapor sorption isotherms at De Boer coordinates.

PI-51. Heat Capacity and Thermodynamic Functions of Praseodyme Orthoniobate

Tyurin A.V., Nikiforova G.E., Ryumin M.A., Khoroshilov A.V., Gavrichev K.S

Kurnakov Institute of General and Inorganic Chemistry of RAS, Russia

tyurin@igic.ras.ru

Orthoniobates of rare earth elements are interesting objects of research, both from a scientific and applied point of view. They are promising functional materials for the potential application as phosphors, fuel cells electrolytes, humidity sensors, materials for electronic devices and microwave dielectric ceramics. They can also be a convenient model substance for studying the typical second-order phase transition.

$PrNbO_4$ is crystallized with high temperature tetragonal crystal structure (T-type, scheelite structure, space group of $I4/a$). Lowering the temperature causes structural ordering, and a reversible phase transition from the tetragonal phase to the monoclinic one (M-type, fergusonite structure, space group of $I2/a$) occurs.

The present study is aimed at experimental measurement of heat capacity and enthalpy change in the wide temperature range, with special attention to the region of phase transition, and the calculation of the standard thermodynamic functions of $PrNbO_4$.

The low-temperature heat capacity of praseodymium orthoniobate was measured by relaxation calorimetry using a Quantum Design Physical Properties Measurement System (PPMS) in the interval 2.08-100.61 K and adiabatic calorimetry using an adiabatic vacuum calorimeter BKT-3 ("Termis", Russia) in the range 89.90-340.58 K. The experimental data obtained by both methods were joint fitted using an equation that is a linear combination of the Debye and Einstein functions.

The measurements of $PrNbO_4$ heat capacity at high temperatures were carried out in the range 331 – 1371 K using a differential scanning calorimeter NETZSCH 449 F1 Jupiter®. Around the temperature of the phase transition, a small step change in heat capacity is observed on experimental DSC curves, while heating and cooling. The jump in heat capacity indicates to the second-order of the phase transition. According to dielectric measurements, the transition of praseodymium orthoniobate from the antiferroelectric state to the dielectric one occurs at 953 K [1]. The phase transition temperature T_{tr} determined by DSC was equal to 960 K.

The experimental values of the heat capacity were divided into two temperature ranges (before and after T_{tr}), and in each interval, the heat capacity was fitted by the Maier-Kelly equation. The calculation of enthalpy changes at high temperatures was made by integration of the Maier-Kelly equations and the reduction of these values to the $H^{\circ}(T)-H^{\circ}(0)$ form.

As a comparative method, the drop calorimetry measurements of high temperature enthalpy increments of $PrNbO_4$ were carried out using a SETARAM high-temperature calorimeter HTC1800K/DSC2000K. The high-temperature enthalpy change determined by two independent calorimetric methods agreed within the uncertainty of measurements.

The temperature dependencies of the standard thermodynamic functions (heat capacity $C_p^{\circ}(T)$, entropy $S^{\circ}(T)$, enthalpy change $H^{\circ}(T)-H^{\circ}(0)$ and derived Gibbs energy $\Phi^{\circ}(T)-\Phi^{\circ}(0)$) for $PrNbO_4$ were calculated over the temperature range from 2 to 1600 K.

Acknowledgements This study used the equipment of the JRCPMR IGIC RAS and was supported by the Russian Foundation for Basic Research (RFBR grant No 18-03-00343).

[1] L.L. Kukueva, L.A. Ivanova, Y.N. Venevtsev, *Ferroelectrics*, 1984, 55, 129.

PI-52. Effects of Spatial Bonds Grids of Acrylic Copolymers on their Adhesion Properties

Shapagin A.V., Shokurova N.A., Chalykh A.E.

A.N. Frumkin Institute of Physical Chemistry and Electrochemistry RAS, Russia

shapagin@mail.ru

In order to develop methods of controlling copolymer adhesion properties the effect of chemical bonds grid on the physicomechanical and energy characteristics of acrylic copolymers was investigated.

The object of the study was a statistical copolymer of butyl acrylate (70%), vinyl acetate (25%) and acrylic acid (5%). The adhesive macromolecules were cross-linked by carboxyl groups of acrylic acid at room temperature. A polyisocyanate (Desmodur 3300) was used as a crosslinking agent. The concentration of polyisocyanate varied from 0.26 to 5 parts by mass. The density of spatial bonds grid was studied using ATR IR spectroscopy (Nicolet iN10) and DSC (Netzsch DSC 204 F1 Phoenix). The chemical grid density was monitored by the intensity of characteristic bands of 2274 (N=C=O) and 1689 cm^{-1} (C=O) of isocyanate IR spectra corresponding to asymmetric vibrations of named bonds (Fig. 1). The energy characteristics of adhesive surface were determined by the static sessile drop method (EasyDrop). An elastic modulus and adhesion characteristics were investigated on a Zwick/Roell Z010 tensile testing machine. Adhesive properties were determined by peeling at an angle of 180° of adhesive applied to test surfaces made of polished steel and PET.

It is shown that with increasing of isocyanate concentration, an increase in the density of the chemical bonds grid occurs, as evidenced by an increase in the tensile modulus and a character change of the stress-strain curve. It is established that the increase in the density of the grid leads to a decrease in the copolymer adhesive characteristics. The isocyanate concentration ranges that provide cohesive and adhesive peeling mechanisms were determined. Based on the glass transition temperatures of systems with various crosslinker contents, the macromolecular mass between the nodes of the spatial grid of chemical bonds was estimated and the concentration of polyisocyanate (0.19 parts by mass) was determined at which a chemical grid with a high conversion degree was formed.

Acknowledgements The financial support of Russian Foundation for Basic Research (RFBR) – project №17-03-00197.

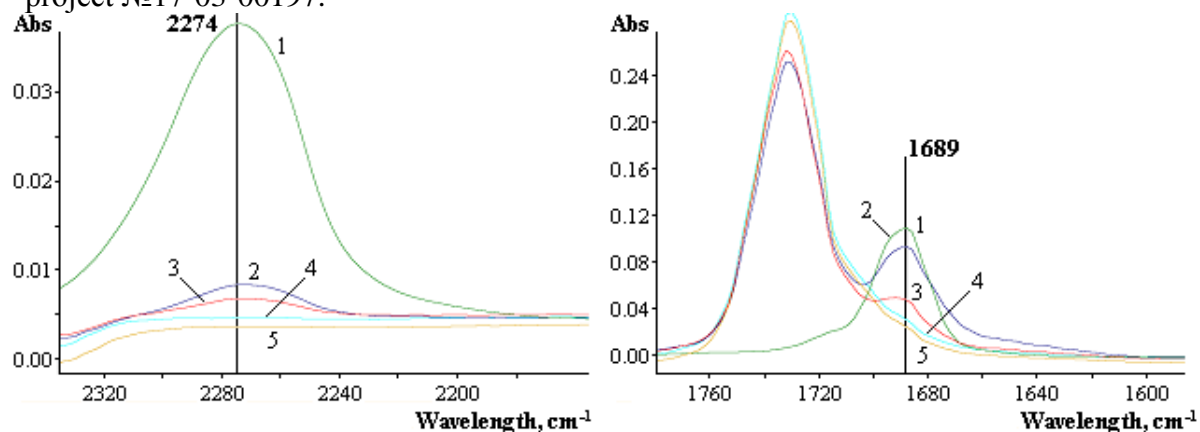


Figure 1 Fragments of the IR spectra of polyisocyanate (1) and terpolymers with various polyisocyanate concentration: 2 – 5 p.b.m.; 3 – 3 p.b.m.; 4 – 0,4 p.b.m. ; 5 – 0,26 p.b.m.

PI-53. Thermodynamic Modeling of the Behavior of A^2B^6 Compounds in a Wide Range of Temperatures and Pressures

Ilinykh N.I.^{1,2}, Kovalev L.E.³

¹Ural Technical Institute of Telecommunications and Informatics, 15, Repin Str, Ekaterinburg, Russia, 620109;

²Institute of Metallurgy, Ural Branch of Russian Academy of Sciences, 101, Amundsen STR, Ekaterinburg, Russia, 620016;

³Uman National University of Horticulture, 1 Institutskja st., Uman, Cherkasskaja obl., Ukraine, 20305

ninail@bk.ru

Semiconductor compounds of the A^2B^6 group are promising materials to creation of unique instruments of optics, optoelectronics, acoustoelectronics, nanoelectronics, laser technology, detecting ionizing radiations. For example, zinc selenide crystals are increasingly applied in the infrared, LED, and fiber optic technology as the detectors of X-rays and elementary particles. Crystals of zinc chalcogenides (ZnSe and ZnS) doped with ions of transition metals (Fe^{2+} , Co^{2+} , Cr^{2+}) are promising materials for creating active media of tunable solid-state lasers.

For growing crystals it is necessary to know the properties of these materials in liquid and solid states. It should be noted that physical and chemical properties of A^2B^6 compounds and alloys are investigated good enough in solid state. However, for liquid phase the information is lack. This is due to the great difficulties in working with these substances: high melting points, high pressures of own vapors, chemical aggressiveness of the gas phase and melts, toxicity. The lack of data constrains the development of all technologies for obtaining these materials, which, in turn, limits the possibilities of their practical application.

In the present work using the TERRA software [1] and thermodynamic modeling method [2] the thermodynamic characteristics and equilibrium composition of the condensed and gas phases formed during the equilibrium heating of ZnSe, ZnS, CdSe, CdS, in wide range of temperatures (300-3000 K) at different common pressures (1, 10, 10^2 , 10^3 , 10^4 , 10^5 , 10^6 , 10^7 , 10^8 , 10^9 Pa) in an argon atmosphere were studied. Temperature dependences of the content of condensed and gas phases and thermodynamic state parameters for each of the systems studied over a wide temperature and pressure ranges have been constructed.

[1] B.G. Trusov, *Vestnik of Bauman Moscow State Technological University*, 2012, Vol. 2 (special Issue), 240.

[2] N.A. Vatolin, G.K. Moiseev, B.G. Trusov, *Thermodynamic modeling in high temperature inorganic systems*, 1994, Metallurgia, Moscow (in Russian).

PI-54. Thermodynamic Modeling of the Equilibrium Composition and Thermodynamic Characteristics of SiC

Ilinykh N.I., Verhovtsev A.Ju.

Ural Technical Institute of Telecommunications and Informatics, 15
Repin Str, Ekaterinburg, Russia, 620109

ninail@bk.ru

In the present work thermodynamic modeling of the equilibrium composition and thermodynamic characteristics of SiC was carried out in an atmosphere of argon, oxygen and air in the temperature range 300–4000 K with total pressures (MPa): 10^{-6} , 10^{-5} , 10^{-4} , 10^{-3} , 10^{-2} , 0.1, 1, 10, 10^2 , 10^3 , 10^4 .

For modeling of the phase and chemical equilibria the software "TERRA" was used [1]. The initial compositions of the modeling systems (mass. %) were following: 1) 99% SiC + 1% Ar; 2) 99% SiC + 1% O₂; 3) 99% SiC + 0.79% N₂ + 0.21% O₂.

The temperature dependences of the thermodynamic characteristics and equilibrium composition of the condensed and gas phases formed during the equilibrium heating of SiC in an argon, oxygen, and air atmosphere at different pressures are investigated.

It is shown that the main component of the condensed phase formed upon heating of SiC in a wide range of temperatures and pressures in an argon atmosphere is SiC, and a small amount of Si and C is also observed; in oxygen atmosphere - SiC and SiO₂; in the atmosphere of air - SiC, SiO₂ and Si₃N₄. The main components of the gas phase that are formed when SiC is heated in an argon atmosphere are Si, Ar, C, C₂, C₃, SiC; in an oxygen atmosphere - Si, O, O₂, C, C₂, C₃, SiO; in the atmosphere of air - Si, Ar, C, C₂, C₃, SiC, N, N₂, CO, O₂. It is shown that the evaporation temperature of SiC depends significantly on pressure. In the pressure range of 1-10⁶ Pa, the dependence $T_{isp}(P)$ is linear and can be described by the equation: $T_{isp} = A + B \ln P$, where A and B are constants, P is pressure, Pa.

A comparative analysis of the temperature dependences of the contents of the components of the condensed and gas phases with the temperature dependences of the state parameters of the SiC + gas system (gas - argon, oxygen or air) shows that there is a correlation between them: kinks in the dependences are observed at the same temperatures. Similar patterns are observed at all studied pressures.

Thus, it was found that silicon carbide has a high thermal stability under extreme conditions (elevated pressures and temperatures) in argon, oxygen and air atmospheres.

The high working temperature and radiation resistance of silicon carbide make it an almost indispensable semiconductor material for the development of devices operating in harsh environments, in particular for space application.

[1] B.G. Trusov, *Vestnik of Bauman Moscow State Technological University*, 2012, Vol. 2 (special Issue), 240.

PI-55. Thermodynamic Aspects of Structure Formation in Oil Dispersed Systems During Transportation

Boytsova A., Kondrasheva N.

Saint Petersburg Mining University, Russia

cadaga@mail.ru

The modern oil transportation system is characterized by mixing of different type of crudes such as heavy resin-asphaltenic and light paraffinic crude. The obtained blend is typically described as incompatible and leads to structure formation, blocking pipelines and equipment. The goal is a comparative assessment of structural properties and thermodynamic activation parameters for viscous flow in crudes of various composition in a broad range of temperatures and shear rates and determination of incompatibilities of crudes of different nature.

Crudes from Timan-Pechora region were used. Crudes of Yarega and Usinsk fields are heavy naphthene-aromatic resin-asphaltenic and Kharyaga crude is light paraffinic. West-Tebuk and Ukhta (oil mixture transported in the main pipeline "Usinsk-Ukhta") crudes are naphthene by K factor and paraffinic by paraffin wax content; crudes are of medium gravity. Standard instruments and methods corresponding to requirements of GOST's were used to study physical and chemical properties of Timan-Pechora crudes. Rheology was determined using rotary rheometer Rheotest RN 4.1 with "cylinder-cylinder" measuring system in thermostated cell in shear rate range from 0 s^{-1} to 300 s^{-1} and temperature range from 10 to 70°C .

It was found that type of liquid depends on temperature and shear rate and goes from pseudoliquid with yield point to Newtonian at temperature above temperature of phase transition and shear rate higher than 10 s^{-1} . Thixotrophy energy depends both on content of resins and asphaltenes and amount of light fractions. Thixotrophy energy is non-additive parameter and sharply decreases for compound of heavy and light crudes. Mixture of heavy yarega crude and light west tebuk crude has a potential range for structure formation. Temperatures of phase transition for each oil sample and thermodynamic activation parameters for viscous flow in a broad range of temperatures and shear rates are investigated in accordance with Arrhenius equation of viscosity and theory of activated complex (table 1). In general, structure of activated condition is less organized that of the initial condition at the increasing of T and shear rate. Process is related to destruction of supramolecular structures and sharp decreasing of the number of activated complexes. Paraffin crudes have the largest number of activated complexes at temperatures below phase transition. Structural changes are conditioned by enthalpic factor - strength performance.

Results can be used for predicting and preventing structure formation during production, transport and storage of crudes with various content of solid paraffins, resins and asphaltenes. High temperature or fluid flow velocity can be used to decrease structure formation in paraffin crudes for the purpose of optimizing their production and transportation; while use of blending with light crude is optimal for heavy naphthene-aromatic crudes, but in this case incompatibility of mixture should be tested.

Table 1. Activation energy of viscous flow at different shear rate, kJ/mole

Crude	Phase transition $T_L, ^\circ\text{C}$	0,15 1/s		100 1/s		200 1/s		300 1/s	
		Below T_L	Above T_L	Below T_L	Above T_L	Below T_L	Above T_L	Below T_L	Above T_L
Yarega	-	57,9		57,9		55,4		52,1	
W.Tebuk	30	215,6	30,5	96,2	20,2	83,8	19,4	76,4	19,0
Kharyaga	40	247,2	33,7	104,9	25,3	94,6	22,9	85,4	22,3
Usinsk	-	37,8		36,9		36,6		36,5	
Ukhta	23	352,9	24,3	129,7	23,4	106,4	23,4	96,3	23,1

PI-56. Thermal Expansion of Complex Phosphates, Containing Copper, Iron and Zirconium

Glukhova I.O., Asabina E.A., Pet'kov V.I.

Lobachevsky University, Nizhny Novgorod, Russia

IO-Glukhova@yandex.ru

The phosphates $\text{Cu}_{0.5(1+x)}\text{Fe}_x\text{Zr}_{2-x}(\text{PO}_4)_3$ are of research interest as prospective catalysts for dimethyl ether synthesis. The compounds are characterized by the framework structure and crystallize in $\text{Sc}_2(\text{WO}_4)_3$ (SW) type with monoclinic symmetry of the unit cell (space group $P2_1/n$). For industrial application of the phosphate catalysts it is necessary to know their thermal behavior (in particular, thermal expansion).

In the present investigation, the samples of the compositions $\text{Cu}_{0.5(1+x)}\text{Fe}_x\text{Zr}_{2-x}(\text{PO}_4)_3$ with ($0 \leq x \leq 0.7$) were synthesized by Pechini route. Final annealing temperature was 943 K for all samples. X-ray diffraction (XRD) patterns obtained on Shimadzu XRD 6000 diffractometer (CuK_α radiation, $\lambda=1.54178 \text{ \AA}$) demonstrated SW solid solutions formation and indicated phase purity of the final products. Scanning electron microscopy results combined with electron microprobe data (microscope JEOL JSM-7600F) confirmed their chemical compositions and absence of impurities of other elements.

Thermal expansion of the obtained compounds was investigated by XRD method within the range $298 \leq T/\text{K} \leq 473$. Linear and volume thermal expansion coefficients (TEC) of the samples were calculated from the temperature dependencies of their lattice parameters.

The results indicated anisotropic character of the thermal expansion of the studied phosphates in the a , b and c crystallographic directions. Their volume expansion coefficients α_V were in the range $(2.44\text{--}7.82) \cdot 10^{-5} \text{ K}^{-1}$. Inclusion of iron into the $\text{Cu}_{0.5(1+x)}\text{Fe}_x\text{Zr}_{2-x}(\text{PO}_4)_3$ lattice led to decrease of TEC (Fig. 1). This effect is caused by the overall decrease of lattice volume with substitution of Zr^{4+} (ionic radius 0.72 \AA) with Fe^{3+} (0.65 \AA) and as x grows.

The obtained results will be useful for choosing the operation conditions for the industrial processes with using the phosphate catalysts.

Acknowledgements This work was supported by Russian Foundation for Basic Research, projects Nos 18-33-00248, 18-29-12063.

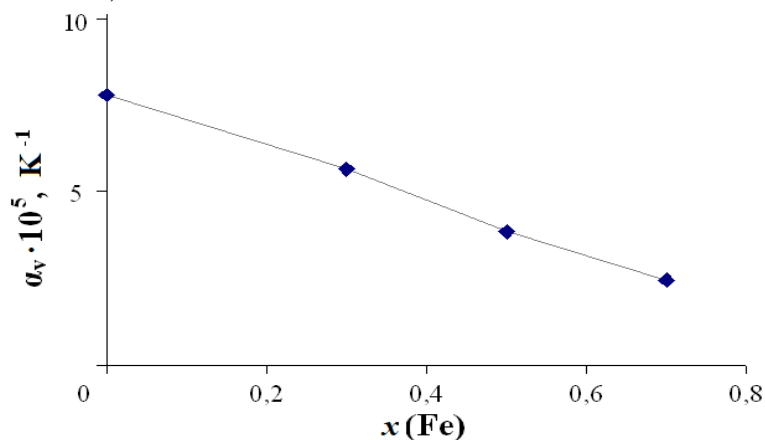


Figure. Thermal expansion coefficient (TEC) of the $\text{Cu}_{0.5(1+x)}\text{Fe}_x\text{Zr}_{2-x}(\text{PO}_4)_3$ against Fe amount.

PI-57. Thermodynamic Properties of the NZP Compounds M²⁺Ti₄P₆O₂₄ (M – Ni, Zn)

Glukhova I.O., Asabina E.A., Pet'kov V.I., Smirnova N.N., Markin A.V.

Lobachevsky University, Nizhny Novgorod, Russia

IO-Glukhova@yandex.ru

Double phosphates of titanium and d-transitions metals in oxidation state +2 are considered as prospective formaldehyde synthesis catalysts [1]. Most of them belong to NZP (NASICON) structural type and are characterized by stability under high temperature, pressure and aggressive media.

Sol-gel method and Pechini technique with further calcination till 1023 K (Ni) and 1223 K (Zn) were applied to obtain phosphates M²⁺Ti₄P₆O₂₄ (M – Ni, Zn). Powder X-ray diffraction (Shimadzu XRD-6000 diffractometer; CuK α radiation, $\lambda=1.54178$ Å), IR-spectrometry (Shimadzu FTIR 8400S spectrometer; 400-4000 cm⁻¹), electron microscopy (microscope JEOL JSM-7600F) were employed to identify phase purity, homogeneity and composition of the samples. From the results, both phosphates crystallize in NZP structural type and do not have any phase transitions from room temperature to 1073 K (Ni), 1273 K (Zn). Structure refinement of the samples was provided with Rietveld method. The calculated lattice parameters are collected in Table 1.

Table 1. Lattice parameters of M²⁺Ti₄P₆O₂₄ (M – Ni, Zn).

Sample	Space group	Parameters			
		a, Å	b, Å	c, Å	R _{wp} / R _p / S
NiTi ₄ P ₆ O ₂₄	R $\bar{3}$	8.4612(19)	20.977(4)	1300.6(5)	5.69 / 4.23 / 2.96
ZnTi ₄ P ₆ O ₂₄	R $\bar{3}c$	8.4578(8)	21.1632(17)	1311.07(21)	5.93 / 4.29 / 3.03

Experimental data of heat capacity were received using firstly adiabatic vacuum calorimetry on calorimeter BCT-3 ‘Termis’ in the range 5.5-350 K and then differential scanning calorimetry on calorimeter DSC 204 F1 Phoenix with μ -sensor within temperature range 340-650 K. For both samples the heat capacity smoothly increases as the temperature grows. As the temperature approaches 6.5 K, both curves have a bend, which presumably indicates the presence of a phase transition at temperatures below 6.5 K. Their temperature dependences are devoid of any anomalies in the rest of the temperature range. The fractal dimension D of phosphates was calculated from experimental data on the low-temperature (35≤T/K≤50) heat capacity and equal 3, thus the topology of the phosphate’s structures was estimated as framework.

The calculation of $H^{\circ}(T) - H^{\circ}(6.5)$ and $S^{\circ}(T) - S^{\circ}(6.5)$ were made by the numerical integration of the $C_p^{\circ} = f(\ln T)$ and $C_p^{\circ} = f(T)$ dependencies, respectively. The $\Phi^{\circ}(T) - \Phi^{\circ}(6.5)$ functions were computed from the enthalpies and entropies at the corresponding temperatures.

Acknowledgements This work was supported by Russian Foundation for Basic Research, projects Nos.18-33-00248, 18-29-12063.

[1] E. Asabina, V. Pet'kov and I. Glukhova, *Inorganic materials*, 2015, 51, 793.

PI-58. Vaporization and Thermodynamics of the Ceramics Based on the Y_2O_3 - ZrO_2 - HfO_2 system

Vorozhtcov V.A.¹, Stolyarova V.L.¹, Lopatin S.I.¹, Karachevtsev F.N.²

¹ Saint Petersburg State University, Russia;

² All-Russian Research Institute of Aviation Materials, Russia

st011089@student.spbu.ru

Zirconia stabilized by the rare earth oxides is known to be promising for development of refractory materials for a variety of high temperature applications. The main limitation of zirconia stabilized by the rare earth oxides is narrow working temperature range less than 1273 K. Addition of hafnia is assumed to improve the working temperature and phase stability of the zirconia based ceramics. Therefore, the Y_2O_3 - ZrO_2 - HfO_2 system is considered as a prospective base for highly refractory ceramics, such as thermal barrier coatings, casting molds for gas turbine engine blades and the advanced materials for nuclear industry. However, increased temperatures of synthesis and application may lead to selective vaporization of the components of the system considered. This is the reason for the present investigation of vaporization processes and thermodynamic properties of the Y_2O_3 - ZrO_2 - HfO_2 system.

Nine ceramic samples in the Y_2O_3 - ZrO_2 - HfO_2 system were synthesized in the present study by the solid-state method. The chemical compositions of the samples after synthesis were confirmed by X-ray fluorescence analysis. The vaporization processes and thermodynamic properties of ceramics based on the Y_2O_3 - ZrO_2 - HfO_2 system were studied by the high temperature mass spectrometric method using a tungsten twin effusion cell.

The gaseous phase over the samples under consideration at the temperature 2660 K was found to consist of the YO, ZrO, ZrO_2 , HfO and O vapor species. The tendencies of the composition changes in the condensed phase of these samples due to the selective vaporization of the components were studied by the complete vaporization method, Fig. 1. The YO, ZrO, ZrO_2 , HfO and O partial pressures, the vaporization rates of the samples and the Y_2O_3 , ZrO_2 and HfO_2 activities were determined at the temperature 2660 K not only for the initial compositions of the samples, but also for the sample compositions obtained because of the Y_2O_3 and ZrO_2 selective vaporization and shown in Fig. 1. Using the values of the Y_2O_3 , ZrO_2 and HfO_2 activities the Gibbs energies of formation and the excess Gibbs energies were found in the Y_2O_3 - ZrO_2 - HfO_2 system indicating negative deviations from ideality at the temperature 2660 K. The excess Gibbs energies in the Y_2O_3 - ZrO_2 - HfO_2 system were approximated using the Redlich-Kister algebraic representation.

Acknowledgements The financial support of the Russian Foundation for Basic Research through the Project No. 16-03-00940.

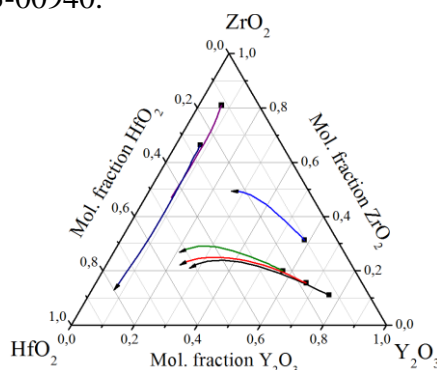


Figure 1. Directions of the composition changes of the samples in the Y_2O_3 - ZrO_2 - HfO_2 system caused by the Y_2O_3 and ZrO_2 selective vaporization at the temperature 2660 K.

PI-59. Thermodynamic Properties of Diatomic Argon Compounds

Maltsev M.A.^{1,2}, *Morozov I.V.*¹, *Osina E.L.*¹

¹ Joint Institute for High Temperatures of Russian Academy of Sciences, Russia;

² Moscow Institute of Physics and Technology, Dolgoprudny, Russia

maksim.malcev@phystech.edu

The diatomic argon compounds are of importance for different plasma sources that contain argon as a basic gas. One of these applications is the mass spectrometry with inductively coupled plasma (ICP-MS). In such experiments the signals from the argon compounds can disturb measured spectra significantly [1]. Therefore, for accurate processing of the ICP-MS results it is necessary to obtain the thermodynamic functions of the compounds of argon with other gases (H, O, etc.) and metal ions. It allows to estimate concentrations of these compounds in the ICP-MS plasma. However, there is a lack of information about such properties in the literature. In this work we report on calculations of the partition function and thermodynamic properties of such diatomic argon compounds as ArCo^+ , ArV^+ , Ar_2 , Ar_2^+ , ArH , ArH^+ , ArO and ArO^+ .

We used the method based on resolving the one-dimensional Schrödinger equation with a given interatomic potential and finding the energy spectra of the diatomic molecule [2,3]. First the LEVEL code (version 8.2) [4] is used to compute discrete eigenvalues of the rotationless energies and vibronic constants. Then the rovibronic energy spectrum is calculated that takes into account rotation of the diatomic molecule. Using the energy spectrum, it is possible to calculate internal partition function and thermodynamic functions of the molecule.

The given algorithm is implemented as a “Partition Function” program. This program uses the information of rotationless potential functions for various electronic states of the molecule and computes the main thermodynamic functions. Additionally, it approximates acquired functions with polynomials that are traditionally used in [3]. It allows to compute the contribution of different electronic states into the internal partition function and thermodynamic functions (see Fig.1).

The work is supported by the Basic Research Program of the Presidium RAS “Condensed matter and plasma at high energy densities” (coordinated by Fortov V.E.).

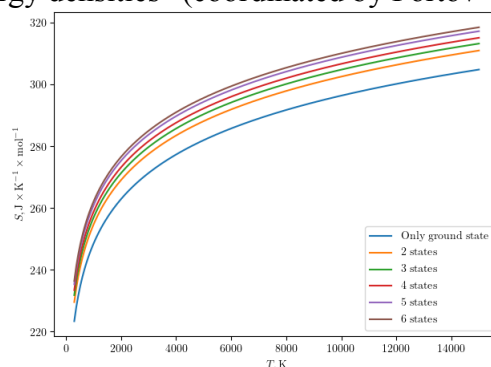


Figure 1. Calculated temperature dependence of the entropy of ArO using different number of electronic states

[1] T.M. Witte and R.S. Houk, *Spectrochimica Acta Part B*, 2004, 69, 25-31.

[2] M.A. Maltsev, A.N. Kulikov and I.V. Morozov, *J. Phys. Conf. Ser.*, 2016, 774, 12023.

[3] L.V. Gurvich, G.A. Bergman and I.V. Veyts *Thermodynamic Properties of Individual Substances*. Vol.1 parts 1 and 2, Moscow, Russia.

[4] R.J. Le Roy *J. Quant. Spectrosc. Radiat. Transfer*, 2016, 186, 167.

PI-60. Phase Transitions in *n*-Butanol-Propionic Acid-*n*-Butyl Propionate-Water System at 333.15 K

Skvortsova I., Toikka M.

Saint Petersburg State University, Russia;
Department of chemical thermodynamics and kinetics

st059141@student.spbu.ru

Scientific developments devoted to the modification of diverse technological processes have always been and will be directed toward reducing energy costs and increasing the product yield. In order to improve the production of any substance, it is necessary to take into account the individual physical and chemical characteristics of it. This is why phase transition in a reactive mixture should be investigated before starting the synthesis of *n*-butyl propionate that has great significance in the chemical industry as a solvent and in the food industry as a flavoring agent.

Liquid-liquid equilibrium in *n*-butanol - propionic acid - *n*-butyl propionate-water system at 333.15 K has been analyzed using two independent methods: gas chromatography and “cloud-point” technique. The first one allowed determining the compositions of the coexisting phases. Data on peak heights have been obtained from chromatograms and then converted into equilibrium compositions by internal normalization and relative calibration methods. The second approach has made it possible to construct the whole binodal curve and verify the received results.

Based on the experimental data, a solubility surface has been constructed for easier perception (Fig. 1). It depicts the regions of concentrations where the synthesis of *n*-butyl propionate will not be effective as the final obtained product will be a part of the heterogeneous system. To fix a proper temperature dependence, literature data have been used and it proved that with a temperature increase, the mutual solubility of substances rises. [1]

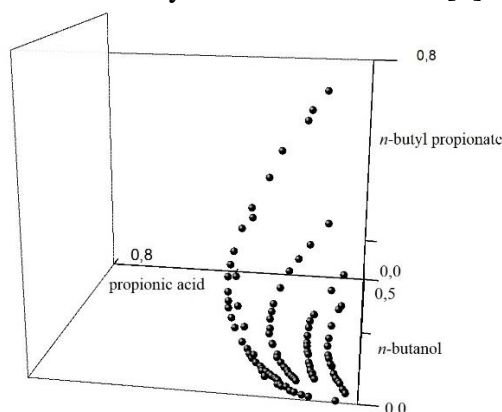


Figure 1. Solubility curves for quaternary system with *n*-butyl propionate synthesis reaction.

Acknowledgements: *Toikka M. is grateful to the Russian Science Foundation (grant 17-73-10290) for the support of this study.*

[1] Maria Toikka, Dariya Trofimova, Artemiy Samarov

PI-61. Thermodynamic Solubility of Two Different Dihydropyridine Compounds in Various Alcohols at 298.15-328.15 K

Lava D., Parmar D. and Baluja S.

Some new dihydropyrimidine compounds have been synthesized and the solubility of these dihydropyridine compounds were studied in some alcohols using gravimetric method at different temperatures ranging from 298.15 K to 328.15 K. The solubility data of compounds in different solvents were regressed by modified Apelblat and Buchowski-Ksiazczak λh models. Some thermodynamic parameters such as enthalpy, Gibb's energy and entropy of dissolution have also been calculated. It is observed from these parameters that dissolution process is endothermic and spontaneous in all the studied solvents. Further, dissolution of compounds in studied solvents cause more ordered structure in these solutions.

PI-62. The Influence of Rare-Earth Elements on Glass-Forming Ability of Al-Ni-Co-Rem Amorphous Alloys

Rusanov B.A.¹, Sidorov V.E.^{1,2}, Svec Sr. P.³, Svec P.³, Janickovic D.³, Moroz A.I.¹

¹Ural State Pedagogical University, Russia;

²Ural Federal University, Russia;

³Institute of Physics, Slovak Academy of Sciences, Slovakia

rusfive@mail.ru

Al-TM-REM amorphous alloys exhibit good mechanical characteristics combining high strength and plasticity (tensile strength reaches 1000 MPa) with the excellent corrosion resistance and heat resistance, which enable one to consider them for use as protective coating materials in aviation and space industry. However, their glass-forming ability (GFA) is rather low and should be improved.

In this work we investigated the influence of REM (Nd, Sm, Gd, Tb, Yb) additions and variation of 3d-metals (Ni, Co) content on GFA of Al-Ni-Co-REM metallic glasses.

Amorphous ribbons (width - 2 mm, thickness - 39-45 μm) of $\text{Al}_{86}\text{Ni}_4\text{Co}_4\text{REM}_6$ and $\text{Al}_{86}\text{Ni}_6\text{Co}_2\text{REM}_6$ (REM = Nd, Sm, Gd, Tb, Yb) compositions were produced by a standard planar flow casting method in the controlled atmosphere of argon. The structure of the ribbons was studied by X-ray diffraction on a Bruker D8 diffractometer (Cu $K\alpha$) in parallel beam configuration. These investigations show that all the ribbons were fully amorphous. Their kinetics of crystallization was studied by DSC on a Perkin Elmer apparatus and electric resistivity determined by a standard four-probe method.

It was found that Al-(Ni+Co)-REM metallic glasses are characterized by a higher (~100 K) temperature stability of amorphous state in comparison with Al-Ni-REM and Al-Co-REM alloys. The light lanthanides (Nd, Sm, Gd) shift the crystallization onset up to 570 K, whereas the heavy REM (Tb, Yb) provide the beginning of crystallization at 508 K. The peculiarities in crystallization behavior are connected with the electronic structure of REM.

PI-63. Partitioning Behavior of L-Tryptophan in Aqueous-Salt Biphase Systems Formed by Aminoacid Alkylimidazolium Ionic Liquids

Korchak P.A., Safonova E.A.

Saint-Petersburg State University, Institute of Chemistry Russia

st034758@student.spbu.ru

The problems of purification, preconcentration or extraction of biomolecules are the actual challenges in biotechnology [1]. Owing to their inflammability and low toxicity, ionic liquids (ILs) can be a good alternative to the most of organic extracting agents. Thus, the aqueous mixtures of ILs with inorganic salts forming aqueous biphasic systems (ABSs) are of particular interest. Due to the ability to split into two liquid phases with a distribution of solute between phases, these ABSs are considered as high-potential particularly for an enhanced extraction of biomolecules. One of the important advantages of ILs is a possible modification of their chemical structure resulting in the required changes of their physicochemical properties. Among the modified ILs, amino acidic ILs (AAILs) attracts much attention [2] also because of their biodegradability and even less toxicity in comparison with their halide analogues. However, the extraction ability of ABSs containing these ILs is poorly studied.

The main aim of this work was to investigate the effect of chemical structure of 1-alkyl-3-methylimidazolium ILs on the distribution of solute (L-tryptophan) in the ABS. AAILs under study are 1-alkyl-3-methylimidazolium ILs with aminoacidic anions $[C_n\text{mim}]X$, where n is a number of carbon atoms in the alkyl chain of AAIL = 4, 8; $X = [\text{Leu}]$ (L-Leucinate), $[\text{Val}]$ (L-Valinate), $[\text{Lys}]$ (L-Lysinate). K_3PO_4 was inorganic salt used as a salting-out agent. To study the distribution of L-tryptophan, the systems also contained small quantities of the solute.

As a result, a series of chemically modified ILs was synthesized. The new data on the partition coefficients of L-tryptophan in ABSs with the AAILs were obtained. The main features associated with the presence of aminoacidic anions in the composition of ILs were considered in comparison with the halide ILs. It was found that the higher partition coefficients are observed in the AAIL-based systems than in the systems with halide analogues [3].

The results are helpful to find the ABS with the desired properties, e.g. its extraction capacity, what is one of the major aspects of their practical application. Moreover, these data could be useful for a development of “green” extraction methods. The next step of this work is molecular-thermodynamic modeling of phase behavior and extracting ability of the ABSs under consideration by means of ePC-SAFT equation of state.

Acknowledgements

Spectroscopic and NMR measurements were performed at the Research park of St. Petersburg State University (Center for Magnetic Resonance and Center for Chemical Analysis and Materials Research).

[1] Freire M.G. et al. *Chem. Soc. Rev.*, 2012, 41, 4966–4995.

[2] Alopina E. et al. *Colloid Surf. A Physicochem. Eng. Asp.*, 2018, 544, 137-143.

[3] Korchak P. Abstract from International Student Conference “*Science and Progress-2018*”, 2018, 51

PI-64. How Strong are Intramolecular Interactions in Nitrobenzaldehydes?

Siewert R.,¹ Verevkin S.P.^{1,2}

¹Department of Physical Chemistry University of Rostock, Germany;

²Competence Centre CALOR, Faculty of Interdisciplinary Research,
University of Rostock, Rostock, Germany

riko.siewert@uni-rostock.de

The investigation of energetic effects between substituents on benzene has long been an important field of scientific and industrial research. For the synthesis of benzene derivatives, the electrophilic aromatic substitution is one of the most prominent pathways. The regioselectivity and the reactivity of this reaction is crucially dependent on the interactions between the ring substituents. Although di-substituted benzenes are the basis for the understanding of this interaction, there is still not enough reliable thermodynamic data for the quantification of substitution effects. We have continued studies on the thermochemical properties of *ortho*-, *meta*-, and *para*-di-substituted benzenes in order to quantify the pairwise-interactions in the benzene ring.

In this work, we have investigated the intramolecular interactions in *ortho*-, *meta*-, and *para*-nitrobenzaldehydes. Thermal behavior of these compounds was studied by DSC. Molar enthalpies of formation in the crystalline state have been obtained from the combustion calorimetry experiments. Standard molar enthalpies of sublimation were derived from the vapor pressure - temperature dependences measured by the transpiration method. From these experimental values, molar enthalpies of formation in the gaseous state have been obtained.

High-level quantum-chemical calculations on the G4-level of theory have been performed for validation of experimental gas phase enthalpies of formation. The quantum-chemically calculated enthalpies of formation in the gas phase have been determined with help of the atomization procedure, as well as with well-balanced distribution reactions.

Gas phase molar enthalpies of formation of nitrobenzaldehydes calculated by the G4 method were in good agreement with the experimental values. Experimental data on vaporization enthalpies, as well as on enthalpies of formation in the gaseous and in the liquid state have been used for quantification of intramolecular interactions of nitro- and carbonyl substituents in the benzene ring. This set of nearest and non-nearest neighbor interactions between substituents have been suggested for a quick appraisal of the vaporization and formation enthalpies of substituted benzenes.

POSTER SESSION 2

FRIDAY, 21.06.2019

P11-1. The Modified SIT Conception for Evaluation of Ionic Equilibria in Concentrated Mixed Electrolytes Solutions

Ukhov S.A.

Kaluga Branch of the N.E. Bauman Moscow State Technical University, Kaluga 248000, Russia

ukhov-s@mail.ru

According to Brønsted-Guggenheim-Scatchard's model (Specific ion Interaction Theory, SIT) [1, 2] logarithm of molal activity coefficient of aqueous species i is equal to:

$$\lg \gamma_i = -z_i^2 \cdot \frac{0.51 \cdot \sqrt{I_m}}{1 + 1.5 \cdot \sqrt{I_m}} + \sum_j \varepsilon(i, j, I_m) \cdot m_j,$$

where z_i is the charge of i , m_j is the molality of the ion j , $\varepsilon(i, j, I_m)$ is the specific interaction coefficient (SIC) between i and j , in a solution of I_m molal ionic strength. At that, $\varepsilon(i, j) = \varepsilon(j, i)$, $i \neq j$. In original SIT same charge ion and uncharged species interactions are negligible, i.e. $\varepsilon(i, j) = 0$. But this postulate is inadequate in mixed electrolytes and for approximation by modeling of ionic equilibria of trace elements [3]. Independent evaluations shows as dependence of SIC from ionic media as well as need of their adjustment. The classical SIT model is modified by the introduction of some mixing parameters for anion–anion and cation–cation interactions (see table 1.).

Standard square deviation of SIC in the fit of activity factors is ≤ 0.005 .

The estimation of water ionic product is correct up to $I_m \sim 10$ m (NaClO_4) according to equation:

$$pK_w^m = 13.997 - \frac{1.02 \cdot \sqrt{m_{NX}}}{1 + 1.5 \cdot \sqrt{m_{NX}}} + [\varepsilon(H^+, X^-) + \varepsilon(OH^-, N^+) + \varepsilon(OH^-, X^-) + \varepsilon(H^+, N^+)] \cdot m_{NX} - \lg a_w,$$

where m_{NX} is the molality of background electrolyte N^+X^- (for instance $\text{Na}^+\text{ClO}_4^-$), a_w is the actual water activity, with maximal real error 0.02. Ternary interactions (with counterions) introduced in the complicated Pitzer's model, are not contemplated in this simplified SIT model. Parameters are also used to calculate the pH of some solutions and the solubility products of some hydroxides.

Table 1. Fixed and evaluated values of specific interaction coefficients. T = 25 °C.

Specific ion interaction coefficient	Ionic strength ranges (mol/kg)			References
	0 – 1 m	0 – 3.5 m	0 – 6 m	
$\varepsilon(H^+, OH^-)$			0.00	[4]
$\varepsilon(H^+, ClO_4^-)$	0.120	0.14	0.146	[5]
$\varepsilon(H^+, Cl^-)$	0.110	0.12	0.125	[5]
$\varepsilon(Na^+, OH^-)$	0.032	0.040	0.055	[5]
$\varepsilon(Li^+, OH^-)$	-0.060		-0.0248 (0 – 4 m)	[5]
$\varepsilon(K^+, OH^-)$	0.0814	0.090	0.0974	[5]
$\varepsilon(OH^-, ClO_4^-)$		-0.026	-0.041	[4], this work
$\varepsilon(OH^-, Cl^-)$		-0.026	-0.041	[4], this work
$\varepsilon(Na^+, H^+)$		0.00	-0.005	This work
$\varepsilon(Li^+, H^+)$			-0.034	This work
$\varepsilon(K^+, H^+)$	0.00 (0 – 1.05 m)		-0.015 (0 – 4.8 m)	This work
$\varepsilon(Cl^-, ClO_4^-)$			0.00	[4], this work

[1] P.L. Brown, C. Ekberg, *Hydrolysis of Metal Ions*, 2016, 917 p. Wiley, Weinheim, Germany.

[2] P. Sipos, *J. Mol. Liq.*, 2008, 143(1), 13-16.

[3] I.V. Mironov, *Medium effect and complexation in electrolyte solutions*, 2003, 239 p. (Ed. V.I. Belevantsev). INKh SO RAN, Novosibirsk, Russia. (in Russian).

[4] S. Pivovarov, *J. Colloid Interface Sci.*, 2005, 291(2), 421-432.

[5] C. Bretti, C. Foti, N. Porcino, S. Sammartano, *J. Solut. Chem.*, 2006, 35(10), 1401-1415.

PII-2. A New Quartz Crystal Microbalance (QCM) to Determine Sublimation and Vaporization Enthalpies

Brunetti B.¹, Ciccioli A.², Magi M.³, Vecchio Cipriotti S.³

¹Istituto for Nanostructured Materials, CNR, Sapienza University of Rome, Department of Chemistry, P.le A. Moro 5, I-00185 Rome, Italy;

²Sapienza University of Rome, Department of Chemistry, P.le A. Moro 5, I-00185 Rome, Italy;

³Sapienza University of Rome, Department of Basic and Applied Science for Engineering, Via del Castro Laurenziano 7, I-00161 Rome, Italy

stefano.vecchio@uniroma1.it

A new quartz crystal microbalance (QCM) has been constructed for the determination of vapor pressures and sublimation or evaporation enthalpies of low volatile molecular or ionic compounds.

The extremely high sensitivity of the QCM has been demonstrated [1] to allow measuring very low mass loss rates in comparison with those considered in other conventional techniques. In fact, when small masses have been deposited on a quartz crystal surface the increase of its thickness leads to a shift of its resonance frequency (6 MHz in our study) that can be precisely measured and directly related to the mass deposited. Combination of vacuum conditions and high sensitivity in measuring the shift of the crystal frequency allow exploring lower temperature and vapor pressure ranges.

In our newly constructed apparatus, a rotary and a turbo molecular pump provide vacuum conditions. The sample crucible is located in a resistance-heated copper block. A Pt100 thermoresistance placed in a hole drilled in the copper block measures the sample temperature. The quartz crystal is placed 25 mm above the sample surface, exactly like in the apparatus used in [1]. Its temperature is kept constant by circulating water at 20 °C.

In order to test the internal consistency of the equipment, suitable tests on very pure recommended reference compounds such as benzoic acid, cadmium, zinc were performed. The method developed in this work paves also the way to obtain reliable values of vaporization enthalpies of thermally unstable ionic liquids. Test measurements were carried out on prototypical aprotic ionic liquids of the imidazolium class, whose vapor pressures and evaporation enthalpies are well known from literature [2].

[1] S. P. Verevkin, D. Zaitsau, V.N. Emelyanenko and A. Heintz, *J. Phys. Chem. B*, 2011, 115, 12889.

[2] B. Brunetti, A. Ciccioli, G. Gigli, A. Lapi, N. Misceo, L. Tanzi, S. Vecchio Cipriotti, *Phys. Chem. Chem. Phys.*, 2014, 16, 15653.

PII-3. Stability of Nanoclusters of Methane and Carbon Dioxide Hydrates: Effects of Particle Size

Sizova A.A., Sizov V.V., Brodskaya E.N.

St. Petersburg State University, Russia

shapovalovaaa@mail.ru

Gas hydrates are crystalline solids comprised of gas molecules enclosed in cavities of water lattice. Methane hydrate is the most abundant gas hydrate occurring in nature and it is considered as alternative source of fossil fuel. The possible way to enhance the methane production from hydrates deposits is the injection of carbon dioxide followed by the CO₂ hydrate formation. Thus, the hydrate stability data are necessary for the technology development. Hydrates can exist in nature in dispersed state (in particular, in the form of nanoclusters) and their melting points can differ from that of the bulk phase.

In the present study the molecular dynamics simulation of CO₂ and CH₄ hydrates nanoclusters stability was provided. Spherical hydrates particles were considered over a wide range of temperatures (180-280 K) and constant pressure. The melting points were determined on the basis of local structure, potential energy and diffusion coefficients variations accompanying the increase of temperature. The melting temperatures of CO₂ and CH₄ hydrates nanoclusters of various size were obtained and compared with melting temperatures of the bulk hydrate phase.

Acknowledgements. This work was supported by the Russian Foundation for Basic Research (grant no. 18-03-00654 A).

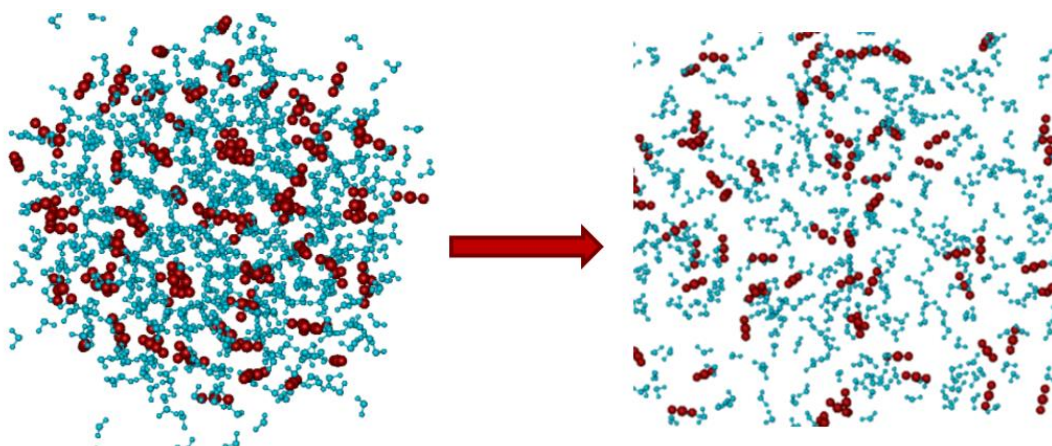


Figure 1. Melting of the CO₂ hydrate nanocluster: system configurations at 180 K (left) and 280 K (right).

PII-4. New Units of Solutions Concentration

Kadtsyn E.D.^{1,2}, Anikeenko A.V.^{1,2}, Medvedev N.N.^{1,2}

¹Novosibirsk State University, Russia;

²Voevodsky Institute of Chemical Kinetics and Combustion, Russia

kadtsyn@kinetics.nsc.ru

Using molecular dynamics models of solutions one can calculate the *volume fraction* of a component in the solution in the other manner than it is usually done in experimental chemistry. The volume fraction of a component is usually defined as a ratio of the volume of the pure component to the total volume of the solution. On the other hand, it is known that the volume per solute molecule can highly differ in solution and in the pure substance. However, having a molecular dynamics model of the solution one can calculate the volume fraction directly, as the ratio of the volume occupied by the solute molecules to the total volume of the model, $\eta = V_{\text{solut}} / V_{\text{solution}}$. Following the physicists, this parameter can be also called as the *packing fraction*. Such a definition of the solution concentration was used in [1, 2], where spatial distributions of trimethylamine-N-oxide (TMAO) and tert-butyl alcohol (TBA) molecules in aqueous solutions at different concentrations were compared with the ones for the random spheres system at the same packing fractions. The volume of the solute was calculated as the sum of volumes of the solute molecules defined as spheres with an effective radius estimated from the left front of $g(r)$ for the appropriate molecules. In current work, we propose to use Voronoi volumes of the solute molecules to define the volume of a solute component. Differences of these two approaches is discussed. We have obtained all-atom molecular dynamics models of aqueous solutions of urea, TBA and TMAO in a broad concentration range, up to $x=10$ mol %. Concentration dependences of the appearing clusters (mean size and topology) is investigated. It was shown that clusters properties of TMAO coincide greatly with the ones for random spheres, while there are some differences for clusters properties of TBA and urea. These cluster properties are sufficiently influenced by the excluded volume, connected to the molecules impermeability. Using the proposed packing fraction η for concentration of solution, one can to compare solutions of solute molecules of different size when structure of solution is studied.

Acknowledgements: The financial support of RFBR 18-03-00045 and Russian Ministry of Science and Education under 5-100 Excellence Programme.

[1] Statistical geometry characterization of global structure of TMAO and TBA aqueous solutions. A.V. Anikeenko, E. D. Kadtsyn, and N. N. Medvedev, *Journal of Molecular Liquids*, 2017, 245, 35-41.

[2] Statistical geometry characterization of local structure of TMAO, TBA and urea aqueous solutions. E. D. Kadtsyn, A.V. Anikeenko, and N. N. Medvedev, *Journal of Molecular Liquids* (submitted).

PII-5. Thermodynamic Properties of Pure Vanadium

Lineva V.I.^{1,2}, *Sineva M.A.*¹, *Morozov I.V.*^{1,2}, *Belov G.V.*^{1,3}

¹Joint Institute for High Temperatures of Russian Academy of Sciences, Moscow, Russia;

²Moscow Institute of Physics and Technology, Dolgoprudny, Russia

³Department of Chemistry, Lomonosov Moscow State University, Moscow, Russia

lineva.vi@phystech.edu

Experimental data analysis of thermodynamic properties of substances in condensed state is an essential step of creating thermodynamic databases. Theoretical calculations in this field are complex, so experiments remain the main source of data. Depending on an experimental technique, the data can be obtained in the form of either enthalpy increments, or heat capacity as a function of temperature. The easiest way to process different types of data jointly is to convert the enthalpy data to the heat capacity as a derivative by temperature. Nevertheless, this method leads to large errors, so it cannot be recommended. As an alternative to this method we suggest first implementing the Shomate approximation [1] for the enthalpy increments data. After that, the obtained functions can be differentiated analytically and converted again into a discrete set of the heat capacity data for the further joint treatment with other experimental data. The second step includes an additional robustness assessment and approximation of the heat capacity-temperature dependence with an adjusted set of approximation functions. This method leads to reduction of errors and obtaining smoother and more physically justified curves. In the present work the calculations of such kind were carried using our “CondensedThermoFit” code which allows also to export the approximated functions into the “IVTANTHERMO-Online” database.

To evaluate this approach we considered thermodynamical properties of the pure vanadium in the condensed state. Measurements of its heat capacity and enthalpy increments have been carried out by many experimenters. In the temperature range from 298.15 K to the melting point (2202 K) the accepted data contains the results of [2-5] (figure 1). At the temperatures above the melting point the measurement results of [6-7] were considered.

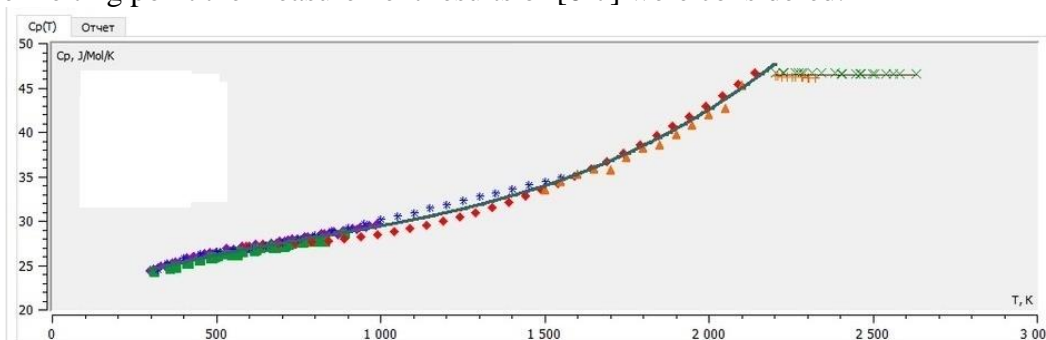


Figure 1. Heat capacity of the pure vanadium depending on the temperature: experimental data vs approximations (screenshot from the CondensedThermoFit application)

- [1] C.H. Shomate, *J. Phys. Chem.*, 1954, 58, v.4, p.368-372
- [2] B.Y. Berezin and V.Y. Chekhovskoi, *Teplofiz. Vys. Temp.*, 1977, 15, p.772-778.
- [3] Y. Takahashi et al, *J. Chem. Thermodyn.*, 1982, 14, v.10, p.977-982.
- [4] A. Cezairliyan et al, *J. Res. Natl. Bur. Stand.*, 1974, v.78A, p.143-147.
- [5] V.Y. Chekhovskoi and R.G. Kalinkina, *Teplofiz. Vys. Temp.*, 1973, 11, p.885-886.
- [6] M.G. Froberg et al, *JMSE*, 1995, 197, v.1, p.83-90
- [7] V.Y. Chekhovskoi et al, *High Temp.*, 1972, 4, v.6, p.478-486

PII-6. Molecular Dynamics Study of Melting of Alkali Halides Mixtures

Kobelev M.A., Zakiryanov D.O., Tkachev N.K.

Institute of High-Temperature Electrochemistry Ural Branch of the Russian Academy of Science,
Ekaterinburg, Russia

coulomb76@mail.ru

Binary mixtures of alkali halides (AH) are relevant objects for computer simulation, due to the fact that the configuration of the phase diagram is controlled mainly by repulsive forces and Coulomb interaction. The overwhelming majority of phase diagrams of mixtures of AH are of three types: eutectic, azeotropic mixture and with the liquid-phase miscibility gap. In the case of the mixtures with a common ion, phase diagrams of only the first two types are experimentally observed. It is of interest to determine molecular dynamics models that would allow describing the evolution of the phase diagram of a binary mixture of AH with variations in the parameters of the pair potential. The question of quantitative description of the experimentally observed liquidus curves is intriguing as well.

The molecular dynamics (MD) simulation can be carried out with sufficient accuracy to calculate the melting characteristics of alkali halides [1, 2]. This work is concerned to generalization of this method to the AH binaries. Parameters of pair interaction in our case were calculated by ab initio methods.

In this report, we present the results of calculating the liquidus and solidus temperatures for the binary mixture of LiCl-KCl at various concentrations, obtained within of the molecular dynamics. The initial MD cell consists of two crystals of LiCl and KCl, in accordance with the specified ratio of components. Figure 1 shows the curve of change in the volume of the MD cell during the simulation, under conditions of slow heating with a constant external pressure of 1 bar.

Acknowledgements The financial support of the Russian Foundation for Basic Research (Grant № 18-03-00606)

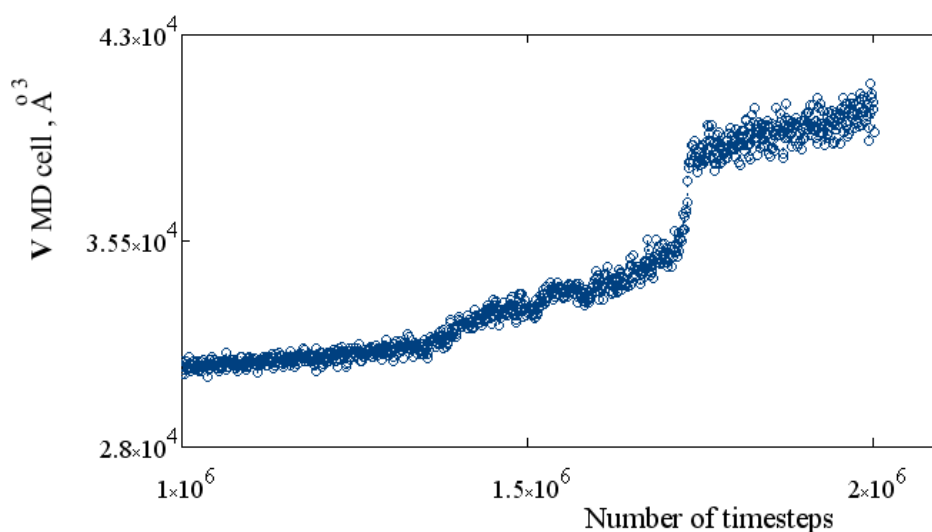


Figure 1. The volume dependence of 0.25LiCl-0.75KCl mixture at 1 bar.

[1] J.L. Aragones, E. Sanz, C. Valeriani and C. Vega, *J. Chem. Phys.*, 2012, 137, 104507.

[2] D.O. Zakiryanov, M.A. Kobelev and N.K. Tkachev, *J. Phys.: Conf. Series* (in press)

PII-7. A Quantum Chemical Simulation of the Interaction Between (α -ALA)₂ Dipeptide Zwitterion and the Dimer of Sodium Dodecyl Sulphate as Model of Micelle Fragment

*Kurbatova M.S.*¹, *Barannikov V.P.*¹, *Giricheva N.I.*²

¹Institute of Solution Chemistry, RAS, Ivanovo, Russia;

²Ivanovo State University, Ivanovo, Russia

msk@isc-ras.ru

The mechanism of interactions of organic substances with the micellar assemblies is of interest due to its numerous applications. We performed a quantum chemical simulation for the SDS... α -L-Ala- α -L-Ala...SDS complexes in dependence on the penetration depth of dipeptide zwitterion into dimer hydrophobic canal. Different positions of the dipeptide relative to an (SDS)₂ dimer have been considered: specifically, above two charged SO₄⁻ groups (complex I) or inside the hydrophobic canal of the dimer (complex II and complex III). All calculations were performed within the density functional theory (DFT) using a hybrid exchange-correlation functional with Grimme's dispersion correction B97D and 6-311++G(2d,2p) basis set. The polarizable continuum model has been used to take into account the water solvent effect. The structures of the optimized complexes are presented in Fig.1. As one can see, the formation of an intermolecular hydrogen bond between the oxygen atom of SO₄⁻ fragment in (SDS)₂ dimer and hydrogen atom belonging to ionized amino NH₃⁺ group of dipeptide is to be observed in all three complexes. There are strong ionic interactions such as SO₄⁻...Na⁺...CO₂⁻ in complexes I and III. As a result of dipeptide - (SDS)₂ dimer interaction, α -L-Ala- α -L-Ala structure undergoes deformation. It is the dihedral angle of HNCO that suffers the greatest changes in the peptide fragment, whose value for the starting structure of the isolated peptide is 177.5°. The greatest change of the HNCO angle is inherent in complex II. The energy of complex formation E_{comp} takes a more negative value in case of complexes I and III (-47.8 and -46.8 kcal mol⁻¹, respectively). Less preferable configuration is observed for complex II (-44.8 kcal mol⁻¹).

The study was financially supported by the Russian Foundation for Basic Research (grant No. 18-03-01032-a).

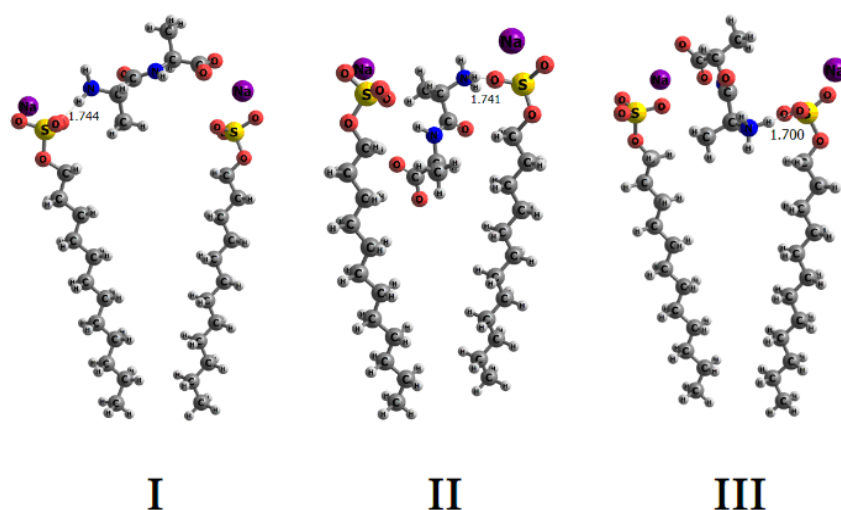


Figure 1. The structures of the optimized SDS... α -L-Ala- α -L-Ala...SDS complexes.

PII-8. KEV: a Free Software for Solving the Direct and Inverse Problems of Chemical Equilibria

Gamov G.A.¹, Meshkov A.N.²

¹Ivanovo State University of Chemistry and Technology, Russia; ²Dentsu Aegis Network Russia

georgegamov38@gmail.com

In research practice, it is regularly necessary to solve either direct or inverse problem of chemical equilibria. The first one is calculating the equilibrium concentrations of the reagents and the reaction products, if the total concentrations and equilibrium constants are known. The inverse one is determining the equilibrium constants values using the experimental data, if the total concentrations of the reagents are known. The aim of the present work is describing the algorithm and developing the software for solving those problems.

S.R. Brinkley [1] method for describing the chemical equilibria was applied. The iterative Newton method was used for calculating the equilibrium concentrations of reagents and products. The determination of equilibrium constants from experimental UV-Vis and potentiometric data was realized using minimizing function and maximal likelihood approach. A modified Hooke-Jeeves algorithm [2] was implemented for the direct search of the global minimum of minimizing function. It prevents from “ravine”-type problems that are possible in case of gradient methods using. The modifications refers to the varying search precision and learning rate, which provides the fine tuning of constants determination process and the accurate and quick search for global minimum.

A number of checks is implemented in order to help user to figure out, is whether something wrong with the calculations. The results of constants determinations displayed are accompanied with brief commentary indicating the possible problems and helping the researcher to understand, should he change the experimental design.

A separate module allows calculating the molar extinction coefficients from the full spectra of compounds at different total concentrations (calibration plot method). Using those values, KEV calculates in the end the spectra of compounds with unknown extinction coefficients, thus, providing another possibility to check the correctness of results.

KEV is an open-source software and could be used free of charge [3] in accordance with the license GPL v.3.0. Source code (*R* language [4]) is also available for free using in accordance with the license GPL v.3.0.

Acknowledgements

The study was carried out with financial support of Russian Foundation for Basic Research (projects 16-33-60017), Ministry of Science and Higher Education of the Russian Federation (project 4.7305.2017/8.9), and under grant of Council on grants of the President of the Russian Federation (project 14.Z56.18.877-MK).

[1] S.R. Brinkley, *J. Chem. Phys.*, 1947, 15, 107.

[2] R. Hooke, T.A. Jeeves, *J. ACM*, 1961, 8, 212.

[3] <https://k-ev.org/>

[4] <https://gitlab.com/a.meshkov/KEV>

PII-9. Molecular Simulations of Liquid Hydrocarbon Mixtures Viscosity

Pisarev V.V., Kondratyuk N.D.

Joint Institute for High Temperatures of RAS, Moscow, Russia

pisarevvv@gmail.com

The report presents the results of calculations of shear viscosity coefficients for one-component hydrocarbon liquids, binary and ternary mixtures using classical molecular dynamics (MD) method. The MD simulations are performed for the methane–n-butane–n-pentane system with the TraPPE-EH forcefield [1] at the temperatures from 300 K to 360 K. The shear viscosity is calculated as a function of density using the reverse non-equilibrium molecular dynamics method [2]. The viscosities of pure liquids are in good agreement with the experimental data available in literature.

The simulations show that the viscosity of the studied liquids and fluids depend strongly on density and, within the accuracy of the used simulation method, do not depend on temperature in the studied range. The use of viscosity-density correlations in hydrodynamic modeling is thus advantageous, because a unified dependence can be used for stable and metastable liquid phase.

A simple viscosity-density correlation in the Batchinski form has been tested, and it is shown that it describes well both pure hydrocarbon liquids and mixtures. The parameters for the mixtures can be obtained by simple linear mixing of the parameters for pure substances [3]. The parameters obtained from molecular simulations can be used to calculate the viscosities of hydrocarbon liquids at pressures up to 1 kbar.

Acknowledgements The work is supported by the Russian Science Foundation (project No. 17-79-20391).

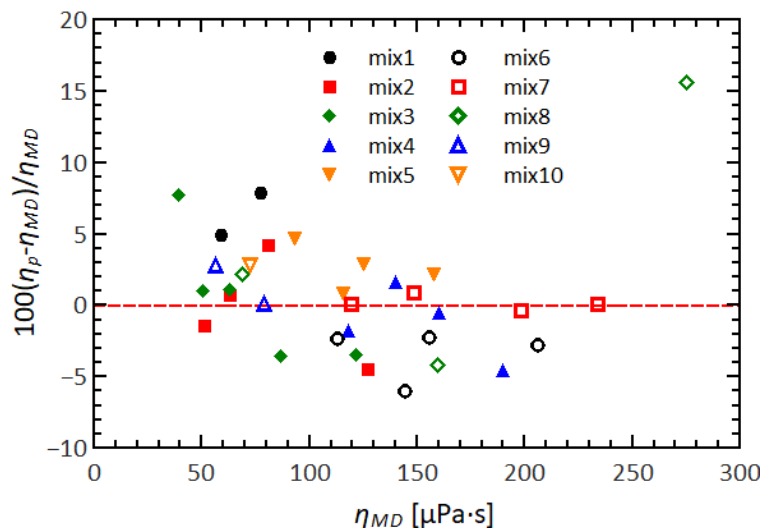


Figure 1. Quality of the Batchinski fit for various methane-n-butane-n-pentane mixtures. η_{MD} is the viscosity of a mixture obtained from a direct MD simulation, η_P is the viscosity predicted by mixing rule for the same composition and density.

[1] B. Chen, and I. Siepmann, *J. Phys. Chem. B*, 1999, 103, 5370.

[2] F. Müller-Plathe, *Phys. Rev. E*, 1999, 59, 4894.

[3] V. Pisarev, S. Mistry, *Fluid Phase Equilib.*, 2019, 484, 98.

PII-10. Thermal Behaviour of the Polystyrene Films Filled with Bentonite

Alekseeva O.V., Noskov A.V., Guseynov S.S.

G.A. Krestov Institute of Solution Chemistry, Russian Academy of Sciences;
Akademicheskaya str., 1; Ivanovo, 153045, Russia

avn@isc-ras.ru

In recent years, clay-containing composites are becoming more interesting for several research areas, such as polymer science, as well due to the perspective using of these materials in electronics, medicine, and pharmaceuticals. Insertion of these fillers results to modify the original polymer matrix, which can lead to the creation of materials with improved physicochemical properties [1]. Polystyrene (PS) is well-known film-forming polymer often used for different modifications with low molecular compounds of special properties, including aluminosilicates. Bentonite (Bent) is one of best-known and the most important clay minerals that can be used for intercalation of polymers. In the current study, the samples of the PS/bentonite composite films were produced. Also an effect of the filler content on the glass transition temperature was researched.

To fabrication of the film composites, PS and PS/Bent solutions in o-xylene were prepared at various mass ratios and stirred using a magnetic stirrer. The films were prepared by casting pure and modified polymer solutions onto a Teflon substrate followed by drying at room temperature until the solvent was completely removed.

Thermal behavior of the film materials prepared was studied using DSC. Figure shows the DSC curves for unmodified polymer and PS/Bent composites. It can be seen for all film, when the temperature rises, a break in the thermogram is observed. This break corresponds to the relaxation transition from the glassy state to the highly elastic one. Such dependences are associated with changes in the heat capacity of the material during the relaxation transition. It was found that the concentration of clay in the film affects the glass transition temperature. For unmodified polystyrene, the glass transition temperature is 70.9 °C, whereas the composites have higher T_g values: the introduction of bentonite (5 wt. %) into polystyrene leads to an increase in the glass transition temperature by almost 15 °C. The revealed effect is associated with a decrease in the mobility of polymer chain segments as a result of their interaction with clay.

Acknowledgements The study was supported by the Russian Foundation for Basic Research (project no. 18-43-370015-a).

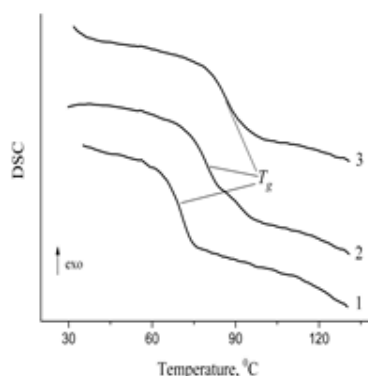


Fig. DSC curves of the PS/Bent composites films with various filler content, wt.%: 0 (1); 1 (2); 5(3).
[1] O. Alekseeva, A. et al., Cellulose, 2017, 24, 1825

PII-11. Quantum Chemical Calculation of Thermodynamic Properties of Diethyl Sulfone

Gabrielyan L.S.¹, Papanyan Z.K., Mkhitarian A.S.

Department of Chemistry, Yerevan State University, 0025 Yerevan, Armenia

lgabriel@ysu.am

Among sulfur-containing compounds sulfones are important and widely used solvents due to their unique physicochemical properties. In the recent years, extensive experimental and theoretical investigations were done to study the use of sulfones as components of electrolyte systems in lithium batteries. Theoretical studies of sulfones reported so far are limited to the first representative of sulfones, dimethyl sulfone (DMSO₂) only. The main goal of this study was to calculate different thermodynamic properties of the diethyl sulfone (DESO₂), to characterize all stable and transition state structures on the potential energy surface as well as to calculate heat of hydration of DESO₂ [1,2].

Calculations of thermodynamic and spectral properties of DESO₂ have been carried out by Gaussian 09 program package using restricted Hartree-Fock (RHF) and density functional theory (DFT/B3PW91) methods with 6-311++G(d,p) basis set. The analysis of the potential energy surface of DESO₂ revealed the existence of 4 stable conformers and 5 transition state structures with different degrees of degeneracy. The thermodynamic parameters, in particular enthalpies, as well as the vibrational spectra for the conformers of DESO₂ were determined both in the gas phase and in the aqueous solution. It was shown that heat of dissolution of DESO₂ calculated by the density functional theory (26.2 kJ/mol) is consistent with the experimental data (22 kJ/mol). From the comparison of the vibrational spectra of the stable conformers it was found that the antisymmetric stretching vibrations of the SO₂ group are very sensitive to the conformation of DESO₂, leading to the broadening of that peak in the mass-averaged spectrum.

Acknowledgements This work was supported by the RA MES State Committee of Science, in the frame of the research project N 18T-1D086.

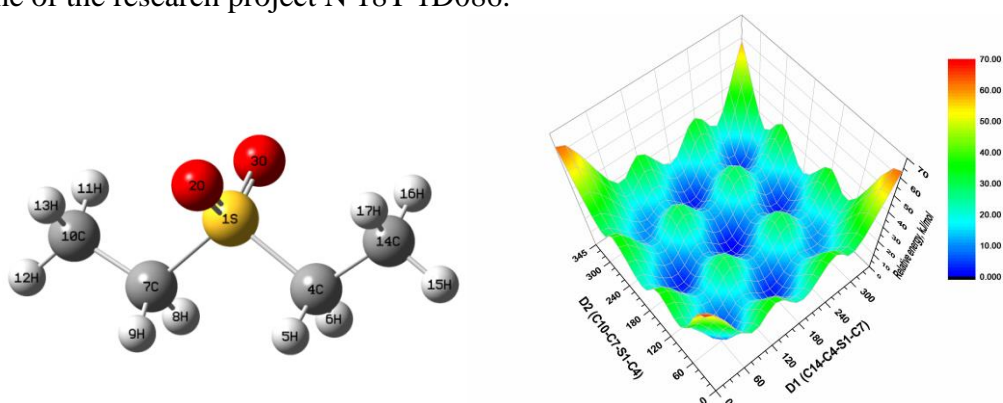


Figure 1. Optimized structure of DESO₂ and the dependence of potential energy of DESO₂ on D1(C10-C7-S1-C4) and D2(C14-C4-S1-C7) dihedral angles according to the RHF/6-311++G(d,p) calculations.

[1] Z.K. Papanyan, A.S. Mkhitarian, L.S. Gabrielyan, *Proceedings of the YSU, Chemistry and Biology Sciences*, 2018, 52, 147.

[2] A.S. Mkhitarian, et al., *Izv. Vyssh. Uchebn. Zaved. Khim. Khim. Tekhnol.*, 2018, 61, 17.

PII-12. Thermodynamic Properties of the Tl_9TmTe_6 and $TlTmTe_2$ Compounds

Mekhdiyeva I.F.¹, Imamaliyeva S.Z.¹, Sultanova S.Q.², Babanly M.B.¹

¹Institute of Catalysis and Inorganic Chemistry, ANAS, Baku, Azerbaijan;

²Baku State University, Baku, Azerbaijan

babanlymb@gmail.com

Chalcogenides of the heavy metals are important functional materials possessing thermoelectric, photoelectric, optical, and other properties. The introduction of rare-earth atoms in these compounds can improve their properties and impart them additional functionality, in particular, magnetic properties [1,2].

The design and optimization of processes for the preparation of novel complex phases are based on the data on phase equilibria and thermodynamic characteristics of the corresponding systems [3].

The aim of the present paper is the investigation of the solid-phase equilibria in the Tl-Tm-Te system in the Tl_2Te – Tl_2Te_3 – $TlTmTe_2$ compositions area and thermodynamic properties of the Tl_9TmTe_6 and $TlTmTe_2$ compounds. These compounds and phases based on them are of interest as materials with thermoelectric and magnetic properties [4, 5].

Compounds and the alloys were synthesized by direct interaction of the elemental components of high purity in evacuated (10^{-2} Pa) quartz ampules at 1000 K followed by stepwise annealing at 550 K (1000h.) and 450 K (300 h.). Studies carried out by DTA and XRD methods as well as EMF measurements of the concentration cells of the type



at 300–450 K temperature interval.

In cells (1), as an electrolyte, a glycerol solution of KCl with a $TmCl_3$ addition was used. The left electrode (cathode) was TmTe with an insignificant (0.5–1 at %) excess of tellurium; the right electrodes (anode) were equilibrium alloys from various phase regions of the Tl_2Te – Tl_2Te_3 – $TlTmTe_2$ subsystem. The methods for the preparation of the electrodes and electrolyte as well as for assembly of the electrochemical cell were described in detail in [6].

The results of the EMF measurements of the chains (1) were consistent with the solid phase diagram of the system. The analysis showed the linearity of the EMF dependences upon temperature for all alloys. Therefore, they were treated by the least squares methods and the linear equations of the type $E=a+bT$ were obtained, based on which the partial thermodynamic functions of TmTe in alloys were calculated.

Based on the solid phase equilibria diagram, the potential-forming reactions for thallium-thulium tellurides were established, and their standard thermodynamic functions of formation and standard entropies were calculated.

In the calculations, the literature data on the corresponding thermodynamic characteristics of Tl_5Te_3 , TlTe, Tl_2Te_3 were used.

References

1. *Applications of Chalcogenides: S, Se, and Te*, ed. by Gurinder Kaur Ahluwalia. Springer, 2016
2. A.R.Jha, *Rare Earth Materials: Properties and Applications*, 2014, CRC, USA.
3. S.Z.Imamaliyeva, D.M.Babanly, D.B.Tagiev, M.B.Babanly, *Russ.J.Inorg.Chem.*, 2018, 63, 1703
4. S.Bangarigadu-Sanasy, et al., *J.Alloys. Compd.*, 2014, 589, 389
5. S.Z. Imamaliyeva, et al., *J. Phase Equilib. Diffus.*, 2017, 38, 764
6. S.Z.Imamaliyeva, et al., *Russ.J.Phys. Chem. A*, 2018, 92, 2111

PII-13. Thermodynamic Investigation of the PbX-AgSbX₂ (X-Se, Te) Systems Using Two Modifications of the EMF Method

Mashadiyeva L.F.¹, Mansimova Sh.H.², Babanly D.M.¹, Shukurova G.M.², Babanly M.B.¹

¹Institute of Catalysis and Inorganic Chemistry, ANAS, Baku, Azerbaijan;

²Baku State University, Baku, Azerbaijan

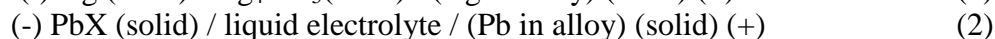
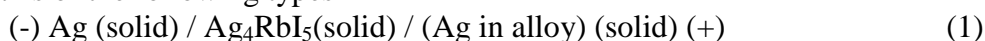
babanlymb@gmail.com

The electromotive forces method (EMF) is widely used for thermodynamic studies of complex inorganic systems [1,2]. We have previously shown that the use of concentration cells with an Ag⁺ conducting solid electrolyte makes it possible to measure the activity of the mobile component (Ag) in a complex alloy, even if it is not the least noble metal of the system [2, 3]. Ag-Pb-Sb-Se (Te) quaternary systems, whose alloys are of great practical interest as promising thermoelectric materials [4], are a typical example of such systems. Therefore, it can be expected that the combination of this modification of the EMF method with its classical variant will allow us to obtain two independent complexes of integral thermodynamic data that can significantly improve their reliability.

This work presents the results of a study of the thermodynamic properties of solid solutions in the PbX-AgSbX₂ (X-Se, Te) systems by two modifications of the EMF method. These systems are characterized by the formation of wide areas of solid solutions [5,6].

Synthesis of the starting compounds and alloys were carried out by melting of high purity elemental components in quartz ampoules under vacuum (~10⁻² Pa), followed by stepwise homogenizing annealing at 800 K (1000 h.) and 400 K (500 h.).

Concentration chains of the following types



were assembled and their EMF was measured in the temperature range of 300-450 K. The assembly of an electrochemical cell of types (1) and (2) and measurements are described in detail [1,2].

The homogeneity areas of solid solutions were identified and the partial thermodynamic functions ($\Delta\bar{G}, \Delta\bar{H}, \Delta\bar{S}$) of Ag, PbX and Pb in solid solutions were calculated based on EMF measurements data.

The standard thermodynamic functions of formation and standard entropy for solid solutions were calculated using the obtained data of partial molar functions and the corresponding thermodynamic data for Ag₂Se, Ag₂Te, Sb₂Se₃, Sb₂Te₃, PbSe, and PbTe compounds. The data obtained by two independent methods are in good agreement with each other.

References

1. A.G. Morachevskii, G.F. Voronin, V.A. Geiderikh, I.B. Kutsenok, *Electrochemical Characterization Techniques in the Thermodynamics of Metallic Systems*, 2003, Akademkniga, Moscow, Russia (in Russian).
2. M.B. Babanly, Yu.A. Yusibov, N.B. Babanly, *Electromotive force and measurement in several systems*, Ed.S.Kara. 2011, 57-78, Intech, Rijeka, Croatia
3. N.B. Babanly, et al., *J. Sol.State Electrochem.*, 2018, 22, 1143
4. A.V. Shevelkov, *Russ. Chem. Rev.*, 2008, 77, 1
5. S.H. Mansimova, K.N. Babanly, L.F. Mashadiyeva, *Chem.Probl.*, 2018, 4, 530
- L. F. Mashadiyeva, et al., *Russ. J. Electrochem.*, 2018, 54, 106

PII-14. Study of Hydrogen Reaction with $\text{Ti}_{0.9}\text{Zr}_{0.1}\text{Mn}_{1.3}\text{V}_{0.6}$ by Calorimetric Method

Anikina E.¹, Verbetsky V.¹

Lomonosov Moscow State University, Chemical Department Moscow, Russia

helena-anikina@yandex.ru

The intermetallic compounds (IMCs) overall formula AB_2 with Laves phase structure C14 reversibly absorb appreciable quantity of hydrogen and therefore they can be used as effective storage materials. The IMCs on the base of TiMn were investigated of both its technological applications and fundamental properties. Changing of optimal proportions of alloys components as well as adding the different transition metals we can create IMC having essential properties to solve the different practical tasks. In the present work we studied of hydrogen interaction with $\text{Ti}_{0.9}\text{Zr}_{0.1}\text{Mn}_{1.3}\text{V}_{0.6}$.

For calorimetric study the twin-cell differential calorimeter of a Tean-Calvet type connected with a Sieverts-type apparatus was used. The apparatus scheme and the method of measurements are described elsewhere [1]. This technique in operation permits to obtain calorimetric data simultaneously with pressure-composition isotherms.

XRD data showed that the initial sample was single-phase compound with the hexagonal Laves phase structure C14 (space group: $\text{P6}_3/\text{mmc}$) with refined lattice parameters $a=4.924(3)\text{\AA}$, $c=8.050(3)\text{\AA}$, $V=169\text{\AA}^3$, $c/a=1.63$. It was determined that $\text{Ti}_{0.9}\text{Zr}_{0.1}\text{Mn}_{1.3}\text{V}_{0.6}$ compound absorbs considerable quantity of hydrogen ($\text{H}/\text{IMC}=3.1$ at 25°C and 50 atm).

The calorimetric study was carried out from 60 to 130°C and a hydrogen pressure up to 50 atm. Absorption (desorption) partial molar enthalpy $\Delta H_{\text{abs.}}(\text{des.})$ was determined from the heat effect of the reaction: $\text{Ti}_{0.9}\text{Zr}_{0.1}\text{Mn}_{1.3}\text{V}_{0.6} \text{H}_x + y/2 \text{H}_2 \leftrightarrow \text{Ti}_{0.9}\text{Zr}_{0.1}\text{Mn}_{1.3}\text{V}_{0.6} \text{H}_{x+y}$

The P-C (P - equilibrium hydrogen pressure, $C=\text{H}/\text{IMC}$), $\Delta H=f(C)$ and $\Delta S=f(C)$ dependence (ΔH and ΔS - the partial molar enthalpy and entropy, respectively, of hydrogen reaction with IMC) were obtained.

For the $\text{Ti}_{0.9}\text{Zr}_{0.1}\text{Mn}_{1.3}\text{V}_{0.6}\text{-H}_2$ system the values of $\Delta H_{\text{abs.}}(\text{des.})$ and $\Delta S_{\text{abs.}}(\text{des.})$ changed with the experimental temperature and the hydrogen concentration in the IMC and the enthalpy values increase in the absolute magnitude with increasing of the H concentration in this system. There are two regions of constant enthalpy values in the $\Delta H - C$ dependences.

Present study showed that in the $\text{Ti}_{0.9}\text{Zr}_{0.1}\text{Mn}_{1.3}\text{V}_{0.6}\text{-H}_2$ system the $\Delta H=f(C)$ and $\Delta S=f(C)$ dependences change with temperature. The $\text{Ti}_{0.9}\text{Zr}_{0.1}\text{Mn}_{1.3}\text{V}_{0.6}\text{-H}$ system there is a large region of ordered solid solution of hydrogen in IMC and as well the formation of two hydride phases is possible at 60, 80 and 100°C . The values of $|\Delta H_{\text{plat.}}|$ increase both for absorption and desorption with the rise of C. Hydrogenation of IMC at definite temperature and pressure may cause rearrangement of crystal structure of initial IMC and formation of some new different interstitial sites which are more energetic efficient for hydrogen.

$\text{Ti}_{0.9}\text{Zr}_{0.1}\text{Mn}_{1.3}\text{V}_{0.6}$ has very good hydrogen capacity ($C\sim 3.1$) and very small hysteresis of pressure. These properties are important for use in hydrogen power engineering.

[1] Anikina E.Yu., Verbetsky V.N. *J. Alloys and Compds.*, 2002, 45-47, 330-332

PII-15. Simultaneous Measurements of The Temperature and Specific Volume Derivatives of Internal Energy of Benzene in the Critical and Supercritical Regions

Abdulagatov I.M.^{1,2}, Polikhronidi N.G.³, Batyrova R.G.³

¹Dagestan State University, Russia;

²Geothermal Research Institute of the Russian Academy of Sciences, Russia;

³Institute of Physics of the Dagestan Scientific Center of the Russian Academy of Sciences, Russia

ilmutdina@gmail.com

A new method of direct internal pressure determination in the calorimetric experiment by simultaneously measurements of the thermal pressure coefficient, $\gamma_v = (\partial P / \partial T)_v$, *i.e.* internal pressure $P_{\text{int}} = (\partial U / \partial V)_T$, and heat capacity $C_v = (\partial U / \partial T)_v$, has been developed. The method has been employed for measurements of the pressure, P , and the thermal pressure coefficient, γ_v , of benzene in the near- and supercritical regions. The method is based on a high-temperature, high-pressure, nearly constant-volume adiabatic piezo-calorimeter. Measurements were made along 10 liquid and vapor isochores in the range from (265 to 643) kg·m⁻³ and at temperatures from (346 to 616) K at pressures up to 9.17 MPa. The liquid-gas phase transition temperatures, $T_s(\rho)$, for each measured density (isochore) were measured using the quasi-static thermograms technique. The direct measured pressures, P , and temperature derivatives, $(\partial P / \partial T)_v$, have been used to calculate the internal pressure (or energy-volume coefficient) as $(\partial U / \partial V)_T = T(\partial P / \partial T)_v - P$. Internal energy-volume coefficient, $(\partial U / \partial V)_T$, is very sensitive to changes in the structure of the liquids and nature of the intermolecular interactions. Therefore, internal pressure is very important to understand of the nature of molecular interactions and in the theory of liquid and liquid mixtures. The internal pressure is very valuable thermodynamic quantity (instrument) to direct study intermolecular interactions through the macroscopic properties

$$P_{\text{int}} = -\frac{2\pi}{3} \rho^2 kT \int_0^\infty r^3 \frac{\partial \phi}{\partial r} \frac{\partial g}{\partial r} dr, \quad (1)$$

where $\phi(r)$ is the potential energy between a pair molecules separated by a distance r and $g(r)$ is the radial distribution function (probability of finding a molecule at a distance r from the reference molecule). The effect of pressure and temperature on the internal pressure of benzene was studied. The statistical structure factor $S(Q)$ of benzene can be presented through the internal pressure as

$$S(Q) = \left[1 - 6 \left\{ 1 - \frac{P_{\text{int}}}{\rho kT} \right\} \left(\frac{X \sin x - x \cos x}{x^3} \right) \right]^{-1}, \quad (2)$$

We also measured the temperature derivatives of the internal energy $(\partial U / \partial T)_v = C_v$ (isochoric heat capacity) using the same method. Thus, the present method allows simultaneously measure both temperature and volume derivatives of the internal energy, *i.e.*, $(\partial U / \partial T)_v$ (energy-temperature coefficient or isochoric heat capacity) and $(\partial U / \partial V)_T$ (energy-volume coefficient or internal pressure).

Acknowledgements: This work was supported by Russian Foundation of Basic Research (RFBR) grants № 19-08-00056 and № 18-08-00500.

PII-16. High-Temperature Heat Capacity of $\text{Pb}_{10-x}\text{Nd}_x(\text{GeO}_4)_{2+x}(\text{VO}_4)_{4-x}$ ($x = 0, 1, 2, 3$) Apatites in the Range 320–1000 K

Denisova L.T., Galiakhmetova N.A.

Institute of Nonferrous Metals and Materials Science, Siberian Federal University, Russia

antluba@mail.ru

Constant research interest in compounds with the apatite structure is aroused by the fact that they possess various properties. They are used as fluorescent and laser materials and in medicine, power generation technologies, oil refining, and environmental protection. The thermophysical properties of the $\text{Pb}_{10-x}\text{Ln}_x(\text{GeO}_4)_{2+x}(\text{VO}_4)_{4-x}$ are essentially unexplored (except for data for $\text{Pb}_8\text{La}_2(\text{GeO}_4)_4(\text{VO}_4)_2$ and $\text{Pb}_8\text{Nd}_2(\text{GeO}_4)_4(\text{VO}_4)_2$). The objectives of this work were to investigate the high-temperature heat capacity of the $\text{Pb}_{10-x}\text{Nd}_x(\text{GeO}_4)_{2+x}(\text{VO}_4)_{4-x}$ ($x = 0, 1, 3$) apatites and determine their thermodynamic properties.

$\text{Pb}_{10-x}\text{Nd}_x(\text{GeO}_4)_{2+x}(\text{VO}_4)_{4-x}$ ($x = 0, 1, 2, 3$) compounds with the apatite structure have been prepared by solid-state reactions via multistep firing of appropriate oxide mixtures in air in the temperature range 773–1073 K.

The phase composition of the samples thus prepared was determined by X-ray diffraction on a PANalytical X'Pert Pro MPD diffractometer (Netherlands) with CuK_α radiation. Table 1 compares the lattice parameters of the synthesized apatites with previously reported data. It is seen that there is satisfactory agreement.

The heat capacity C_p of the $\text{Pb}_{10-x}\text{Nd}_x(\text{GeO}_4)_{2+x}(\text{VO}_4)_{4-x}$ apatite oxides was determined by differential scanning calorimetry using an STA 449 C Jupiter thermoanalytical system (Netzsch, Germany). The C_p of all compounds is seen to increase systematically with increasing temperature, with no extrema in the $C_p(T)$ curves. It is reasonable to assume that the compounds undergo no polymorphic transformations in the temperature range studied here. The data obtained are well represented by the following equations:

$$x = 0$$

$$C_p = (861.86 \pm 1.62) + (136.4 \pm 1.7) \times 10^{-3} T - (24.29 \pm 1.74) \times 10^5 T^{-2},$$

$$x = 1$$

$$C_p = (1052.8 \pm 31.0) - (314.2 \pm 6.5) \times 10^{-3} T - (120.3 \pm 17.84) \times 10^5 T^{-2} + (34.56 \pm 3.6) \times 10^{-5} T^2,$$

$$x = 2$$

$$C_p = (964.1 \pm 16.2) - (61.86 \pm 3.5) \times 10^{-3} T - (71.86 \pm 8.63) \times 10^5 T^{-2} + (23.51 \pm 2.12) \times 10^{-5} T^2,$$

$$x = 3$$

$$C_p = (834.44 \pm 8.35) + (245.5 \pm 8.8) \times 10^{-3} T - (58.83 \pm 8.87) \times 10^5 T^{-2}$$

Table 1. Unit-cell parameters of $\text{Pb}_{10-x}\text{Nd}_x(\text{GeO}_4)_{2+x}(\text{VO}_4)_{4-x}$

a , Å	c , Å	V , Å ³	Source
$\text{Pb}_{10}(\text{GeO}_4)_2(\text{VO}_4)_4$			
10.089	7.393		[1]
10.0876(2)	7.3927(1)	651.49(2)	This work
$\text{Pb}_9\text{Nd}(\text{GeO}_4)_3(\text{VO}_4)_3$			
10.0918(2)	7.3535(2)	648.51(3)	This work
$\text{Pb}_8\text{Nd}_2(\text{GeO}_4)_4(\text{VO}_4)_2$			
10.0982(3)	7.3021(2)	642.82(4)	[2]
$\text{Pb}_7\text{Nd}_3(\text{GeO}_4)_5(\text{VO}_4)$			
10.0927(2)	7.2350(2)	638.03(3)	This work

[1]. T. Yano, Y. Nabeta and A. Watanabe, *Appl. Phys. Lett.*, 1971, 12, 570.

[2] L. T. Denisova, et al., *Inorganic Materials*, 2018, 2, 163.

PII-17. Anomalies in Thermodynamic Parameters of the $\text{Li}_2\text{CO}_3\text{-Na}_2\text{CO}_3\text{-K}_2\text{CO}_3$ - Nanopowder MgO Heterogeneous System

Zakiryanova I.D.^{1,2}, Korzun I.V.¹

¹Institute of High Temperature Electrochemistry, Russia;
²Ural Federal University, Russia

optic96@mail.ru

The thermodynamic parameters of heterogeneous systems $\text{Li}_2\text{CO}_3\text{-Na}_2\text{CO}_3\text{-K}_2\text{CO}_3$ – MgO (nanopowder) containing up to 70 vol. % magnesium oxide was obtained using the DSC method. It was established that with an increase in the specific surface area of the MgO nanopowder particles, the deviations of the reduced melting enthalpy of the salt composition from additive values increase.

An anomalous decrease in the temperature and reduced enthalpy of melting of the salt phase when increasing magnesium oxide content in the composite (Fig. 1, 2) was found.

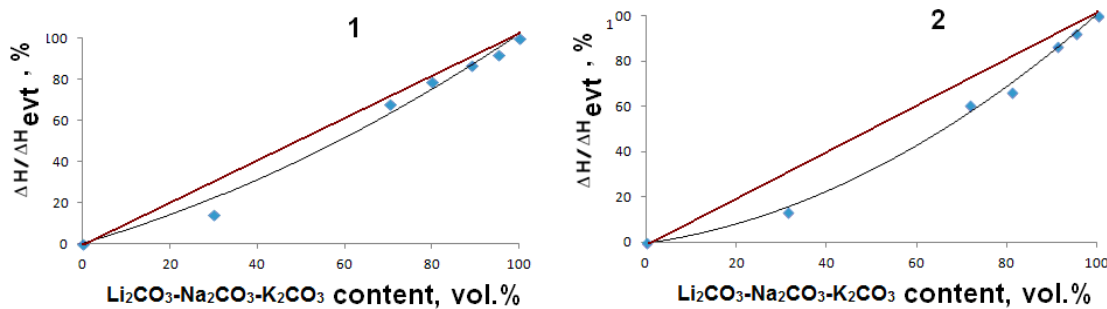


Figure 1. Deviations of the reduced enthalpy of melting of the salt phase from additive values in heterogeneous systems ($\text{Li}_2\text{CO}_3\text{-Na}_2\text{CO}_3\text{-K}_2\text{CO}_3$) – MgO: $S = 9.35 \text{ m}^2/\Gamma - 1$; $S = 15.02 \text{ m}^2/\Gamma - 2$.

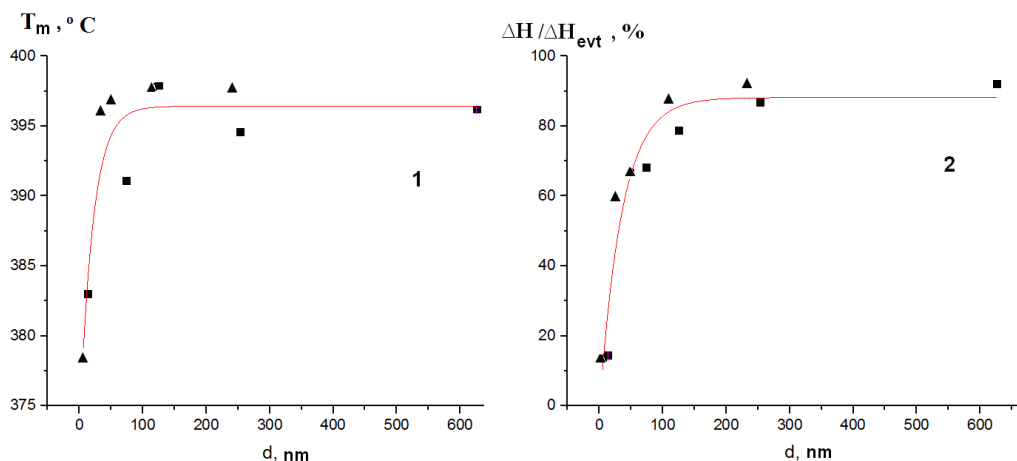


Figure 2. Dependencies of T_m and reduced enthalpy of melting of heterogeneous systems ($\text{Li}_2\text{CO}_3\text{-Na}_2\text{CO}_3\text{-K}_2\text{CO}_3$) - MgO nanopowder from the effective thickness of the salt phase interlayer between magnesium oxide particles (d) ($S = 9 \text{ m}^2/\text{g}$ - squares, $S = 15 \text{ m}^2/\text{g}$ - triangles)

PII-18. Structure and Phase Behavior of Iron(III) Schiff Base Complex with 3,6-Di-*Tert*-Butyl-Carbazole Moieties

*Kolker A.M.*¹, *Chervonova U.V.*¹, *Alexandrov A.I.*², *Gruzdev M.S.*¹,
*Ksenofontov A.A.*¹, *Pashkova T.V.*²

¹G.A. Krestov Institute of Solution Chemistry of Russian Academy of Sciences, Ivanovo, Russia;
²Ivanovo State University, Ivanovo, Russia

amk@isc-ras.ru

The novel azomethine iron (III) complex containing 3,6-di-*tert*-butyl-carbazole-fragments on periphery and PF₆⁻ counter-ion was synthesized by reaction of metal salts with the Schiff base leading to production of biligand system. X-Ray powder diffraction of polycrystalline sample of complex was done by X-ray powder diffractometer Bruker D8. The indexing shows that crystal lattice of complex is triclinic (close to monoclinic) with parameters $a=41,60 \text{ \AA}$, $b=14,41 \text{ \AA}$, $c=12,47 \text{ \AA}$, $\alpha=104,14^\circ$, $\beta=89,24^\circ$, $\gamma=93,11^\circ$; space group is P1. Unit cell contains of four molecules. Conformation of complex molecules is elongated and asymmetric, fig. 1; counter-ions are built in crystal lattice in a regular way, formation of dimer is possible at the expense of hydrogen bond N-H-F-P-F-N. Calculated density is $\rho=1,105 \text{ g/cm}^3$.

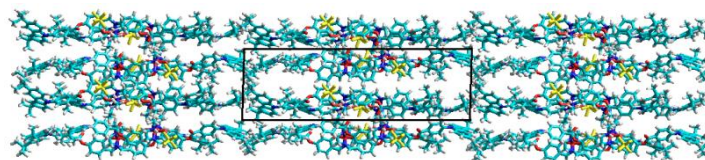


Fig. 1. Molecular packing of Fe complex in elementary cell of monoclinic crystalline lattice according to space group P1

The thermal stability and phase behavior of the complex were studied by thermogravimetric analysis (TGA) and differential scanning calorimetry (DSC). Consequently it was established that the decomposition takes place in the temperature range from 309 to 350 °C. The values of temperatures and enthalpies of the phase transitions are listed on fig. 2. Thus in the first heating cycle only melting temperature was detected ($T_m = 184.9 \text{ }^\circ\text{C}$). It should be noted that while sample was cooling, crystallization was not observing. At the repeated heating from the glass-like state ($T_g = 54.8 \text{ }^\circ\text{C}$) the substance crystallizes at $T_{cr} = 153.9 \text{ }^\circ\text{C}$ and melts subsequently at $T_m = 182.4 \text{ }^\circ\text{C}$.

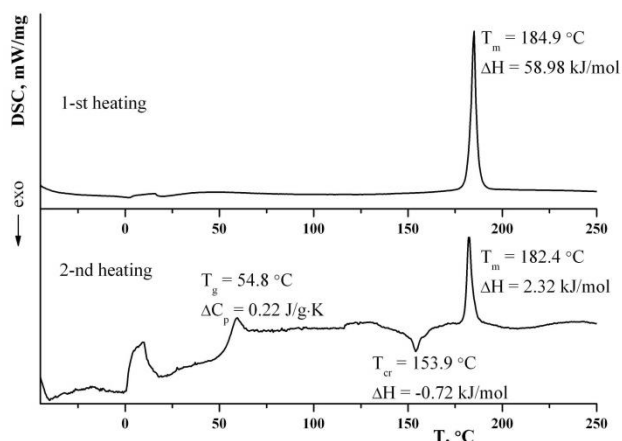


Fig. 2. The DSC curves of complex at heating cycles.

were observed for this compound.

Acknowledgements The financial support of Russian Foundation for Basic Research according to the research project № 18-29-04016_mk.

The photophysical properties of complex were studied via UV/vis and fluorescence spectroscopy in dichloromethane. The spectroscopic characteristics and the molecular parameters were explained using DFT and TDDFT theoretical calculations. It was found that π - π^* - type transition makes the major contribution to the spectral-luminescent properties of the iron(III) bis-[4-(3,6-di-*tert*-butyl-9H-carbazole-9-yl)-benzoyloxy-2-hydroxy-N'-ethyl-N-ethylenediamine] hexafluoro-phosphate. This causes a strong emission of complex. A significant Stokes shift (105 nm) and large fluorescence quantum yield (54 %) were observed for this compound.

PII-19. Thermodynamic Assessment of High-Entropy Crystalline Phase with the Magnetoplumbite Structure

Vinnik D.A.¹, Trofimov E.A.¹, Zhivulin V.E.^{1,2}, Zaitseva O.V.¹, Gudkova S.A.^{1,3}, Starikov A.Yu.¹, Kirsanova A.A.¹, Zherebtsov D.A.¹

¹South Ural State University, 76, Lenin Ave., Chelyabinsk 454080, Russia; ²South Ural State Humanitarian Pedagogical University, 69, Lenin Ave., Chelyabinsk 454080, Russia; ³Moscow Institute of Physics and Technology (State University), 9, Institutskiy per., Dolgoprudny 141700, Russia

tea7510@gmail.com

The scientific direction associated with the high-entropic oxide phases creation and study, almost recently arose and is currently in a period of rapid growth. In this case, results have already been obtained are interesting not only from the fundamental science point of view, but also promising from the point of view of practical application as constructional and functional materials.

In the course of our research, the obtaining possibilities, the formation mechanisms and properties of oxide high-entropic crystalline solid solutions with the structure of the magnetoplumbite are studied. Hexaferrites with the magnetoplumbite structure have been known for more than half a century and due to their properties - chemical inertness, mechanical hardness, high Curie temperature, coercivity and anisotropy field - are widely used in various branches of science and technology (in magneto-optics, acoustoelectronics, for microwave devices, high density information storage and rewriting devices). At the same time, modern electronics follows the path of miniaturization and, as a result, the requirements for optimizing pure materials (crystalline matrices) for specific parameters are becoming tougher. Crystalline high-entropic hexaferrite phases can become a material that will provide such opportunities for properties smooth adjustment over a wide range due to quantitative changes in their composition.

As part of the research, much attention is paid to the experimental work on hexaferrite phases obtaining by various methods. However, one of the most important research areas is the thermodynamic modeling complex of multicomponent oxide systems in which high-entropy phases with the magnetoplumbite structure can be formed. In particular, of great interest is the thermodynamic description of the high-entropy phases with the magnetoplumbite structure.

In the course of the carried out work, an analysis of the literature and our own data on stable oxide high-entropy systems was performed for the purpose of improving the solid solutions stability criteria in such systems. On the base on the analysis of literature and own experimental data (primarily on temperature and concentration limits of the stability of solid solutions in the systems under study). the thermodynamic description of high-entropy crystalline phases with the magnetoplumbite structure is made. The investigated system can be described by the formula: $(\text{Ba, Sr, Pb, Ca, La})\text{Fe}_x(\text{Al, Mn, Ti, Co, In, Ga, Cr})_{12-x}\text{O}_{19}$, with $x = 1.5-6$.

Expressions that relate the Gibbs energy of such phases with their composition and temperature are obtained. These results allow to perform a full-fledged thermodynamic simulation of phase formation processes in the system under study. The result of such simulations is sections (poly- and isothermal) of the phase diagram of the multicomponent system, as well as the ability to model the crystals growth process through non-equilibrium crystallization models.

In the research process, the software package FactSage with the supplied databases were used for the thermodynamic modeling, for the own database formation and the parameters optimization. According to the research results, an own new database has been formed, which is optimized for the description of the studied system.

Acknowledgements The financial support of Russian Science Foundation (project No. 18-73-10049).

PII-20. Thermal Properties of Iridium (I) Volatile Complexes with Cyclooctadiene-1,5 and (O,N)-Coordinated Ligands

Karakovskaya K.I.^{1,2}, *Vikulova E.S.*¹, *Zelenina L.N.*^{1,2}, *Sysoev S.V.*¹, *Morozova N.B.*¹

¹Nikolaev Institute of Inorganic Chemistry, Russia; ²Novosibirsk State University, Russia

red_garden@mail.ru

Volatile hetero-ligand complexes of iridium(I) are supposed to be promising precursors for obtaining thin coatings by chemical vapor deposition method (MOCVD) for various applications, including the medical industry. Currently, in the field of MOCVD precursors, the modern tendency can be characterized as transition from traditional (O,O)-coordinated ligands to N-substituted analogs. The reasons include optimization of the reactivity and increasing of thermal stability of compounds. However, in the case of iridium complexes, systematic studies are fragmentary. Thus, the purpose of this work is to identify the influence of substituents in (O,N)-coordinated ligands on the thermal properties of iridium complexes as well as comparison with (O,O)-donor analogs. Compounds of Ir(I) with general formula [Ir(cod)(L)], where cod = cyclooctadiene-1,5 and L = β -ketoiminate (L = R¹C(O)CHC(NR²)CH₃, R¹ = CH₃, R² = H (i-acac) **1**; R¹ = R² = CH₃ (Mei-acac) **2**; R¹ = CF₃, R² = CH₃ (Mei-tfac) **3**) or β -ketohydrzonate (R¹C(O)CHC(NN(CH₃)₂)CH₃, R¹ = CH₃ (dmha) **4**; R¹ = CF₃ (dmht) **5**) were selected for investigation and compounds with L = β -diketonate (R¹C(O)CHC(O)CH₃, R¹ = CH₃ (acac); R¹ = CF₃ (tfac)) for comparison.

The complexes were synthesized in inert atmosphere with approximately 80% yields. Compounds **1-5** were first obtained and characterized by elemental analysis, IR- and ¹H and ¹³C NMR spectroscopy, and powder X-ray diffraction. Crystal structures of complexes were determined by single-crystal XRD. Thermal properties of compounds in condensed phase were performed by thermogravimetry (TG/DTA) and differential scanning calorimetry (DSC). TG/DTA investigation was carried out using thermobalances Netzsch TG 209 F1 Iris (He, 20 mL·min⁻¹, 10 K·min⁻¹, sample mass 9-11 mg). For β -ketoiminate compounds, mass loss occurs in single step, whereas for β -ketohydrzonate ones several steps are observed. The following volatility row could be established on the base of 50% mass loss temperature for [Ir(cod)(L)]: L = tfac (479 K) > acac (496 K) > Mei-tfac **3** (507 K) > dmht **5** (513 K) > dmha **4** (521 K) > i-acac **1** (528 K) > Mei-acac **2** (538 K). Thus, decrease of volatility is observed, when donor oxygen atom in chelate ligand is replaced by N-substituted one. In addition, there is a trend of increasing thermal stability with the introduction of fluorinated substituent. In β -ketoiminate complexes, existence of methyl group at the donor nitrogen atom provides growth of volatility. Moreover, the transition from β -ketoiminate to β -ketohydrzonate ones leads to decline of thermal stability.

DSC investigation for complexes **1** and **2** was investigated using a Setaram DSC 111 calorimeter with heating rate 0.5–1.0 K·min⁻¹ and sample mass 14–17 mg. The results are presented in the **Table 1**. For these compounds there are no any phase transitions up to melting. Temperature dependencies of saturated vapor pressure for complexes **1** and **2** were measured by flow (transpiration) method. The experiments were carried out using helium as an inert gas-carrier with flow rate (0.9–2.0). The quantitative volatility row, which was constructed on the base of p(T) dependencies, is in a good agreement with the TG data.

On the base of obtained data, the optimal deposition conditions for obtaining metal coating were selected and several MOCVD experiments were carried out using **1** as a precursor.

Table 1. Thermodynamic parameters of melting and sublimation of Ir(cod)(L)

L	T _{melt.} , K	$\Delta_{\text{melt.}}H_{T_{\text{melt.}}}$, kJ·mol ⁻¹	$\Delta_{\text{melt.}}S_{T_{\text{melt.}}}$, J·(mol·K) ⁻¹	T _{sub.av.} , K	$\Delta_{\text{sub.}}H_{T_{\text{av.}}}$, kJ·mol ⁻¹	$\Delta_{\text{sub.}}S_{T_{\text{av.}}}$, J·(mol·K) ⁻¹
i-acac	428.8 ± 0.5	21.3 ± 0.5	49.6 ± 0.6	410.6 ± 0.5	119 ± 2	210 ± 5
Mei-acac	440.0 ± 0.5	22.8 ± 0.3	51.8 ± 0.6	406.4 ± 0.5	111 ± 3	188 ± 7
acac	422.5 ± 0.5	25.9 ± 0.5	61.2 ± 0.7	401.6 ± 0.5	106.6 ± 0.7	191 ± 2

PII-21. First Example of Large Anisotropic Plasticity of Organic Crystal Preserved at Cryogenic Temperatures. Structure-Property Relation

Nguyen T.T.², Arkhipov S.G.^{1,2}, Losev E.A.^{1,2}, Rychkov D.A.^{1,2}

¹Institute of Solid State Chemistry and Mechanochemistry SB RAS, Russia;

²Novosibirsk State University, Russia

rychkov.dennis@gmail.com

Mechanical properties of molecular crystals have been undeservedly disregarded up to recent time, despite its high value and vast application in industry. Among others, one can specify importance of mechanical properties of organic crystals for optoelectronics, pharmaceuticals, explosives and more futuristic artificial muscles bendable armor and weapons, mechanical actuators etc. Surprisingly, first systematic research of structure-property relation in molecular crystals has been provided only in 2005 by Reddy et al¹. In that work the mechanical basis for bendable organic crystals was suggested based on 15 examples. Further, structure-property correlation was unveiled for higher number of solids, including not only organic, but metal-organic crystals too.

To study mechanical properties of particular crystals different techniques were used: optical microscopy, SEM, AFM, both single crystal and powder XRD, Raman spectroscopy, thermal analysis, micro- and nanoindentation, different computational methods, luminescence, etc. Nevertheless, very limited studies were devoted to pressure or temperature changes in crystalline structures of bendable crystals. What is more interesting, we did not find any studies devoted to qualitative or quantitative study of mechanical properties at high pressure (which is technically a difficult task) or low temperatures. In this work we based on our previous results published by Arkhipov et al, where structure of L-leucinium hydrogen maleate (LLHM) was solved and described, and noted that it “shows interesting mechanical behavior: mechanical action on crystals of LLHM results in elastic, and then plastic, bending”².

In this work we show that crystal of LLHM preserve its property to bend as a response to external force even at cryogenic temperatures. Intensive analysis of crystal structure and corresponding thermodynamic properties was performed to unveil the bending mechanism. Significant amount of experimental³ and computational⁴ results is analyzed and summarized to fully explain the phenomenon of plasticity at cryogenic temperatures. Finally, we confirm that up to our best knowledge this is the first example of bending molecular crystal at cryogenic temperatures, and suggest that this should not be an exception for some other known crystals.

Acknowledgements This work is performed with financial support of RFBR 18-43-543004 r_mol_a grant.

[1] Reddy, C. M., et al., *Chemical Communications*, 2005, 1, 3945 - 3947.

[2] S. G. Arkhipov, et al., *Journal Acta Crystallographica Section C: Structural Chemistry*, 2015, 71 (7), 584-592.

[3] S. G. Arkhipov, et al., *Acta Crystallographica Section B: Structural Science, Crystal Engineering and Materials*, 2019 – in press.

[4] Y. V. Matveychuk, E. V. Bartashevich, V. G. Tsirelson, *Crystal Growth & Design*, 2018, 18 (6), 3366-3375.

PII-22. Thermodynamic Issues of L-Valinium Hydrogen Maleate: Crystallographic and Computational Insight

Arkhipov S.G.^{1,2}, Rychkov D.A.^{1,2}

¹Institute of Solid State Chemistry and Mechanochemistry SB RAS, Russia;

²Novosibirsk State University, Russia

rychkov.dennis@gmail.com

Pharmaceutical industry widely uses different methods of modification of crucial properties of organic materials: bioavailability, solubility rates, mechanical properties, etc. Co-crystallization is widely examined and used technique to serve the idea of changing original issues of active pharmaceutical ingredients (API), in other words target active molecule. Nevertheless, even nowadays theory of formation of new salts and cocrystals is poorly understood. Different molecules can serve as model systems for discovering principles of targeted modification of crystal structures. Series of amino acid maleates was used for such investigation.

Deep and laborious analysis shows that there is a common crystallographic peculiarity for all structures of amino acid maleates – $C^2_2(12)$ crystallographic motif. It is present for 24 (out of 26 known) maleates of amino acids – all cases, where this motif could be formed theoretically¹. Such a remark became the basis for further investigation, which can lead to a deeper understanding of co-crystals formation, at least for this structure's family. As we previously mentioned an interesting experimental phenomenon gives an assumption that $C^2_2(12)$ motif plays crucial role in co-crystal formation – difference in solubility of original compounds reaches up to 50 times, what is quite rare for such multi-component systems.

In this work we performed laborious analysis of crystal structures and vast but simple computations to correlate traditional views of 'common' crystallographic motives and real energies of intermolecular interactions² (Fig.1). For several compounds not only intermolecular energies, but also packing energies were calculated.

Acknowledgements This work is performed with financial support of RSCF 18-73-00154 grant.

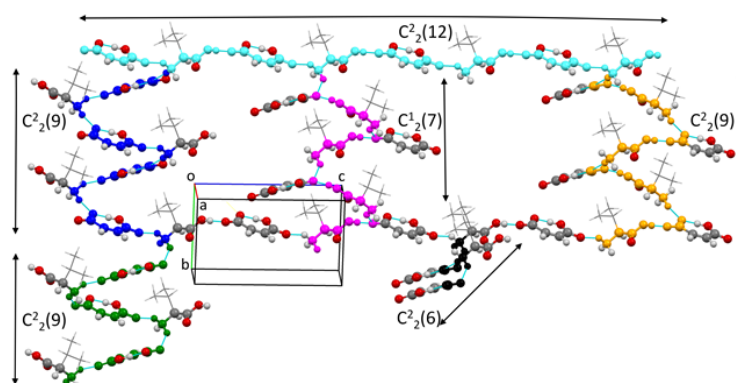


Figure 1. A fragment of the crystal structure of L-valinium hydrogen maleate showing the main structural motifs.

[1] S. G. Arkhipov, D. A. Rychkov, A. M. Pugachev and E. V Boldyreva, *Acta Crystallogr. Sect. C Struct. Chem.*, 2015, 71 (7), 584-592.

[2] D. Rychkov, S. Arkhipov and E. Boldyreva, *Acta Crystallogr. Sect. B Struct. Sci. Cryst. Eng. Mater.*, 2016, 72 (1), 160-163.

PII-23. Resonant Active Sites in Catalytic Ammonia Synthesis over Metal Alloys and Clusters

Cholach A.R., Bryliakova A.A.

Boreskov Institute of Catalysis, Russian Federation

cholach@catalysis.ru

Heterogeneous catalytic phenomena are mainly enabled by the particular sets of near-surface atoms known as active sites. The exact nature and mechanism of the catalytic promotion of these sites is still under discussion [1]. Generally, the superior activity of a catalytic site is enabled by its optimal thermodynamics, which is affected deeply by the first coordination shell. By an example of the catalytic ammonia synthesis, the report highlights the strategy for creating the tailor-made catalytic centers by optimizing the content and coordination numbers of their atoms. First, the catalytic sites M_n ($M = \text{Pt, Rh, Ir, Fe, Ru, Re}; n = 2, 3, 4$) on the metal planes have been classified by their total undercoordination Σ , as compared to bulk atoms, and the enthalpies of formation and hydrogenation of the atomic nitrogen over sites M_n were calculated semi-empirically; then, turnover frequencies (TOF) of the NH_3 synthesis were estimated using the Brønsted-Evans-Polanyi relationship. It was found that the highest TOF of a site M_n can be achieved at the specific “resonant” Σ value, whose major part is inaccessible at perfect planes because of steric reasons [2]. The creation of more active catalytic site has been resolved into the convergence of real and resonant Σ . Increase in real Σ was carried out by reducing the size of the cluster, while the change in the resonant Σ was performed through the modeling of binary alloys [3]. The synergetic catalytic effect in Fig. 1 indicates that the activity of a strong catalyst of the ammonia synthesis (Ru) can be increased by alloying with a weak catalyst (Pt, Ir, Rh) due to the optimal combination of the composition and atomic coordination of catalytic centers of the alloy. The TOF of similar sites increases with an increase in the cluster (supported particle) size of Re and Ru, and in contrast, it decreases with an increase in the cluster size of Pt, Rh, and Ir. The model of resonant catalytic sites has shown a good agreement with the reference experimental data on the TOF of metals, individual single crystals and special centers Fe- C_7 and Ru- B_5 ; it is in line with the basic concepts of heterogeneous catalysis and can be applied to other structure-sensitive catalytic reactions. One just has to fix the intermediate of rate-determining step and define its resonant Σ values, which will show the optimal structure and/or the appropriate promoter of a catalyst providing the closeness of real and resonant Σ for its active sites.

Acknowledgements The study was conducted within RFBR and Novosibirsk region project № 19-43-540012 and budget project № AAAA-A17-117041710078-1 for Boreskov Institute of Catalysis.

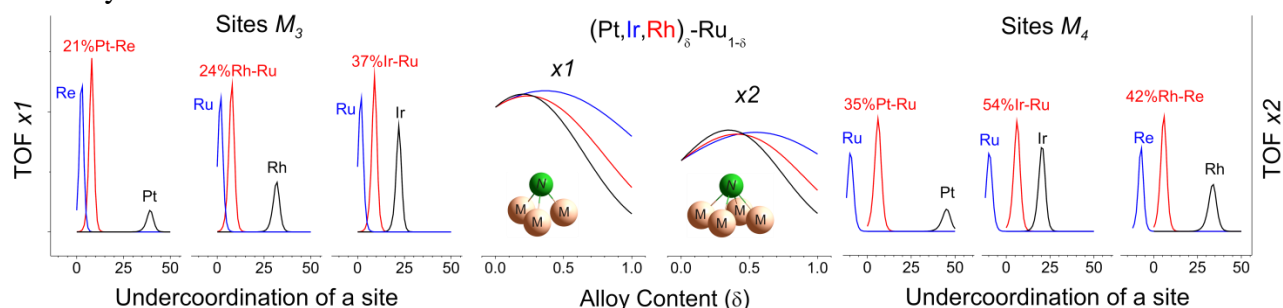


Figure 1. Synergetic behaviour of binary alloys in the catalytic ammonia synthesis.

[1] Y. Pan, X. Shen, L. A. Bentalib, Z. Peng, *Catalysis*, 2018, 8, 478.

[2] A. Cholach, A. Bryliakova, A. Matveev, N. Bulgakov, *Surface Science*, 2016, 645, 41.

[3] A. Cholach, *Applied Catalysis A: General*, 2018, 562, 223.

PII-24. Molecular Brushes Based on Polyimide and Polymethyl Methacrylate as Compatibilizers of Epoxy-Thermoplastic Mixtures

Chalykh A.E.¹, Stepanenko V.Y.¹, Budylin N.Y.¹, Shcherbina A.A.¹, Meleshko T.K.², Yakimanskij A.V.²

¹AN Frumkin Institute of Physical Chemistry and Electrochemistry, Russia;

²Institute of Macromolecular Compounds, Russia

budylin_nikita@mail.ru

It is known that the introduction into the mixture of polymers of a certain type of modifiers, usually grafted or block copolymers, makes it possible to some extent to solve the problem of controlling the phase structure of a composite material. In order to use molecular brushes based on polyimide (PI) and polymethyl methacrylate (PMMA) as a compatibilizer for mixtures of thermoplastics, the effects of brush additions on the phase structure of polymer heterogeneous systems were traced using an electronic transmission microscope (fig.1): a mixture of PMMA and PI, PMMA and PI-graft-PMMA, PMMA with PI and block copolymer PI and PMMA. It is shown that the dispersion characteristics of PI in PMMA do not change with the introduction of a molecular brush into the mixture, which forms an independent nanoscale phase. It has been established that the main polyimide chain of the molecular brush is shielded by the side chains of PMMA, while the “core-shell” conformation is maintained during the transition from solutions to films of “dry” copolymers.

The conformation of molecular brushes is characterized by high stability, while the observed surface activity of molecular brushes that is due to adhesive anchor interactions with the substrate functional groups is caused by small-scale conformational changes of side chains, orientation of ester groups of side chains with respect to the substrate, migration of these groups to the substrate surface, and their adsorption at the interface. In this case, the globular core of molecular brushes formed by the polyimide backbone remains spherical and probably does not change in volume, in agreement with the morphological data.

Acknowledgements The financial support of Russian Foundation for Basic Research, (project 14-03-00390) and the Russian Science Foundation (project № 14-13-00200).

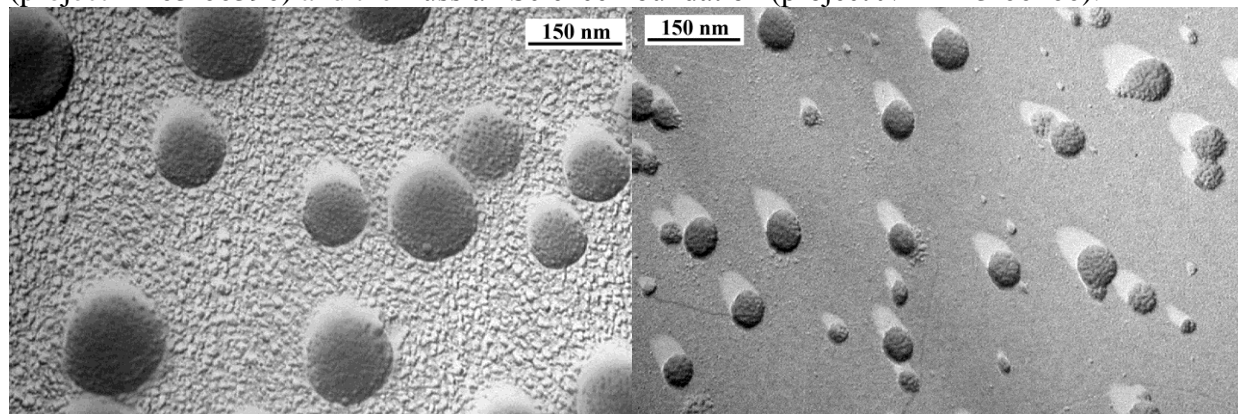


Figure 1. Structural–morphological characteristics of films of mixtures: brush – 1, PMMA – 72, PI – 18 wt. % (left) and brush – 2, PMMA – 64, PI – 16 wt. % (right).

PII-25. The Effect of the Latrepirdine on the Structure of Microsomal and Synaptosomal Membranes

Gerasimov N.Yu., Nevrova O.V., Kasparov V.V., Kovarskii A.L., Goloshchapov A.N.,
Burlakova E.B.

Emanuel Institute of Biochemical Physics RAS, 119334, Kosygina str., 4, Moscow, Russia

n.yu.gerasimov@gmail.com

The effect of neuroprotector latrepirdine on the microviscosity of the membranes of synaptosomes and microsomes isolated from the brain of mice was studied. Today, latrepirdine is considered as a perspective neuroprotector and is proposed for the treatment of many neurodegenerative diseases. The membrane structure is capable of thermo-induced generalized structural rearrangements when external influences on the cell. As a result of such transitions, many structural characteristics of the lipid bilayer are changed. Microviscosity is one of the important structural characteristics of the membrane, therefore, in this work, the effect of latrepirdine on the microviscosity of the lipid bilayer of synaptosomes and microsomes, and thermally induced phase transitions were investigated by the method of paramagnetic resonance (EPR) spin probes. 2,2,6,6-tetramethyl-4-capryloyloxypiperidine-1-oxyl (Probe I) and 5,6-benzo-2,2,6,6-tetramethyl-1,2,3,4-tetrahydro- γ -carbolin-3-oxyl (Probe II) were used as probes. It is shown that the probe I is mainly localized in the surface layer of the lipid components of the membrane, and the probe II is localized in the near protein areas. The time of rotational mobility correlation (τ_c) characterized the microviscosity of membrane components and was calculated from the obtained EPR spectra,

$$\tau_c = 6,65 \cdot 10^{-10} \times \Delta H_{+} \times ((I_{+}/L)_{0,5} - 1).$$

The dependences of the correlation times of the rotational diffusion of the probes on temperature *in vivo* for the studied membranes with chronic administration of latrepirdine were obtained. Typical structural transitions at temperatures of 16–20°C (289–293 K) and 32–38°C (305–311 K) in both the synaptosome and microsome membranes were observed for the control groups of animals. Chronic administration of latrepirdine for 15 days led to the appearance of an additional structural transition at temperatures of 24–28°C in synaptosomal membranes. This fact indicates that membrane structure of synaptosomes after neuroprotector injection changes in relation to the control. In the microsome membranes, the similar transition is not observed. Also, the microviscosity of microsome membranes is practically unchanged relative to control values. Consequently, latrepirdine reaches the synaptosomes of the brain in sufficient concentration, whereas the delivery of the neuroprotector to microsomes is impeded. This may be the reason for the lack of effectiveness of latrepirdine in the treatment of dementia. Thus, it can be concluded that it is necessary to develop the special method for the targeted delivery of latrepirdine into the cell.

PII-26. Research of the Experimental Alzheimer`S Disease to Search for the Treatment

Gerasimov N.Yu., Nevrova O.V., Krivandin A.V., Goloshchapov A.N., Burlakova E.B.

Emanuel Institute of Biochemical Physics RAS, 119334, Kosygina str., 4, Moscow, Russia

n.yu.gerasimov@gmail.com

Among the most noteworthy dementia, in connection with increasing prevalence recent decades, is Alzheimer's disease (AD). In our opinion, during the development of AD, pathological changes in the molecular and other systems are caused by disturbance of the structure of the membrane. Earlier, we showed that there are the membrane structure failures under Alzheimer's type dementia development, and the microviscosity of the membrane dramatically decreases [1]. Therefore, change of the microviscosity of membranes isolated from the forebrain of mice with experimental pathology simulating AD (samples courtesy of N.V. Bobkova, Institute of Biophysics of cell RAS) and based on the removal of olfactory bulbs was examined.

The membrane microviscosity was measured by the method of electron paramagnetic resonance of spin probes 2,2,6,6-tetramethyl-4-capryloxyloxypiperidine-1-oxyl and 5,6-benzo-2,2,6,6-tetramethyl-1,2,3 probe, 4-tetrahydro- γ -carbolin-3-oxyl. Phasic changes in the fluidity during the development of the experimental pathology of Alzheimer's disease have been revealed. The results obtained correlate with the data on changes in cognitive functions, the amount of β -amyloid. Major disorders associated with changes in the structure of the protein regions of the lipid bilayer.

The changes in the structure of the lipid bilayer of synaptosome membranes under the influence neuroprotector NT-1505 have also been studied by Electron paramagnetic resonance (EPR) of spin probes and X-ray structural analysis. The temperature dependence of the correlation time of rotational diffusion was measured by the EPR method of spin probes. It was shown that there are two thermo-induced structural transitions at temperatures of 16-20°C and at 32–38°C in the control group and with the introduction of NT-1505. By changing of the correlation time of the rotational diffusion of the probes at the temperature of 24°C, it has been established that the microviscosity of the lipid regions practically does not change with time, and dynamic changes occur in the near protein regions. This suggests that the main changes are associated with changes in the structure of proteins. The dynamics of changes under the introduction of NT-1505 had opposite character with respect to changes in the membranes of the control group.

Further, the change in the structure of the lipid bilayer of synaptosomes with the introduction of NT-1505 in concentrations of 10^{-14} and 10^{-4} mol/kg after 7 days of drug chronic administration was investigated by the X-ray structural analysis method. Diffractograms of the lipid bilayer of synaptosomes of the control group at different humidities were obtained. The introduction of NT-1505 definitely led to change in the structure of the synaptosomes lipid bilayer.

[1] N. Yu. Garasimov, A. N. Goloshchapov, and E. B. Burlakova, *Khim. Fizika* 28 (7), 82 (2009)/in russian

PII-27. Disjoining Pressure in a Thin Spherical Liquid Film within Molecular and Mechanical Approaches

Lebedeva T.S.¹, Shchekin A.K.¹, Suh D.²

¹St. Petersburg State University, Russia;

²The University of Tokyo, Japan

tpodguzova@mail.ru

Bulk pressure and normal/tangential components of the local pressure tensor in a small droplet with a solid core and a flat liquid thin film on a substrate and their relation to the disjoining pressure have been considered for the argon-like condensate. The Lennard-Jones fluid with the Carnahan-Starling model for the hard-sphere contribution to intermolecular interactions in liquid and vapor bulk phases and interfaces has been used to describe the condensate. The forces between the solid core (and the flat substrate) and condensate molecules have been taken into account as a sum of the Lennard-Jones molecular potentials with the energy parameter higher than that for the condensate-condensate interaction. The nonuniformity in the central part of the liquid film (flat and spherical) has been treated as overlapping of surface layers of solid-liquid and liquid-vapor interfaces.

The thermodynamic effects of internal inhomogeneity in small droplets at homogeneous and heterogeneous nucleation must necessarily be taken into account when comparing theory with experiment. In the case of homogeneous nucleation, these effects are manifested through the dependence of the surface tension of the critical droplet on its radius. In the case of heterogeneous nucleation on wettable solid particles, these effects can be taken into account through the dependence of the disjoining pressure on the thickness of the liquid condensate film [1-3]. For a thin flat liquid film between a solid substrate and an undersaturated vapor, a modified definition of the disjoining pressure was suggested by Rusanov and Kuni [4] as the difference in the normal component of the pressure tensor in the film and the bulk pressure in the liquid phase for a given chemical potential. However, because the normal component of the pressure tensor in the liquid film with curved interfaces depends on location inside the film even for a spherical droplet around a solid spherical core, there are some difficulties in the definition of the disjoining pressure for such films.

The disjoining pressure for a flat liquid thin film on a solid substrate in the undersaturated vapor has been computed for different film thicknesses to represent the difference between bulk values of the pressures for vapor and liquid phases. This disjoining pressure has been shown to be consistent with that in small droplets condensed on solid cores found through the thermodynamic and mechanical routes for a range of values of the droplet and core sizes [5].

Acknowledgements This work was supported by the Russian Foundation for Basic Research (grant 18-53-50015 ЯФ_a).

- [1] F.M. Kuni, A.K. Shchekin, A.I. Rusanov, B.Widom, Adv. Coll. Interface Sci.,1996, 65, 71.
- [2] A.K. Shchekin, T.S. Podguzova, Atmospheric Research, 2011, 101, 493.
- [3] A.K. Shchekin, T.S. Lebedeva, J. Chem. Phys., 2017, 146, 094702.
- [4] A.I. Rusanov, F.M. Kuni, Research in Surface Forces, 1971, 3, pp. 111–122. B.V. Derjaguin (Ed.), Consultants Bureau, New York.
- [5] A.K. Shchekin, T.S. Lebedeva, D.Suh, The overlapping surface layers and the disjoining pressure in a small droplet, Colloids and Surfaces A, submitted, 2019.

P11-28. Dynamic Surface Properties of Heptadecafluoro-1-Nonanol Solutions

Akentieva A.V.¹, Noskov B.A.¹, Lin S.-Y.²

¹St. Petersburg State University, 26 Universitetskiy pr., Petergof, St. Petersburg, 198504, Russia;

²National Taiwan University of Science and Technology, Chemical Engineering Department, 43 Keelung Road, Section 4, 106 Taipei, Taiwan

a.akentiev@spbu.ru

The interest in properties of fluorinated surfactants is mainly caused by their high thermal and chemical stability, and especially high surface activity as compared with conventional hydrocarbon surfactants. At the same time, many fluorinated compounds are toxic, poorly decompose due to their high stability and are able to accumulate in the environment. One of the main constraints on the development of new purification technologies is the limited information on the physicochemical properties of these compounds. This conclusion relates also to the surface properties of the solutions of fluorinated surfactants. The most of results on the behavior of fluorinated surfactants at the liquid surface have been obtained by the interfacial tensiometry. In particular, Lin et al. measured the kinetic surface tension dependencies of heptadecafluoro-1-nonanol solutions at water/air interface and found that the adsorption kinetics is controlled by diffusion only at relatively long adsorption times [1]. Meanwhile at the beginning of adsorption it was found the mixed adsorption mechanism. These authors have shown that the change of the adsorption mechanism is caused by a transition between liquid expanded and condensed surface phases. The methods of dilatational surface rheology are usually more informative in case of heterogeneous adsorption layers. In this study the dilatational dynamic elasticity of heptadecafluoro-1-nonanol adsorption films at the water/air interface was determined in a broad range of concentrations and surface life times. Measurements of the surface rheological properties confirmed a transition between liquid expanded and liquid condensed surface phases in the course of adsorption of heptadecafluoro-1-nonanol. The surface elasticity increased in the region of the liquid expanded surface phase, went through a shallow local minimum in the transitional region and increased strongly in the region of the liquid condensed surface phase. A mathematical model was developed to describe the dynamic surface elasticity of an adsorption layer with a coexisting region of two surface phases and taking into account the adsorption barrier. The application of the developed model to the experimental data on the dilatational surface elasticity proved that the adsorption kinetics is controlled by diffusion in the region of the liquid condensed surface phase ($\gamma < 57$ mN/m) and allowed estimation of the kinetic coefficient of the surfactant exchange between the coexisting surface phases. The obtained value proved to be less than that for the adsorption layer of hydrocarbon surfactants.

The work was financially supported by the RFBR and Ministry of Science and Technology of Taiwan (joint project № 19-53-52006 MHT_a)

[1] A. Casandra, B.A. Noskov, M. Hu, S. Lin, Adsorption kinetics of heptadecafluoro-1-nonanol : Phase transition and mixed control, *J Colloid Interface Sci.*, 2018, 527, 49.

P11-29. Dynamic Surface Properties of Fullerenol Solutions

*Timoshen K.A.*¹, *Noskov B.A.*¹, *Akentieva A.V.*¹, *Chirkov N.S.*¹, *Lin S.-Y.*², *Sedov V.P.*³,
*Borisenkova A.A.*³, *Dubovsky I.M.*³, *Lebedev V.T.*³

¹St. Petersburg State University, 198504, Russia;

²National Taiwan University of Science and Technology, 106 Taipei, Taiwan

³B.P.Konstantinov Petersburg Nuclear Physics Institute, NRC Kurchatov Institute, 188300, Russia

gaminikyl@mail.ru

Due to their unique properties fullerenes have a large area of potential applications in various branches of industry and medicine [1-3]. At the same time, their real applications are limited significantly because of their low solubility in water. To overcome this problem one can use the chemical modification of fullerenes. Promising fullerene derivatives are fullerenols in which a fullerene core, is modified by hydroxyl groups. They have a similar structure and are characterized by high solubility in water. The surface properties of solutions of a fullerenol with a large number of hydroxyl groups $C_{60}(OH)_X$ ($X = 30 \pm 2$) were investigated by the methods of dilational surface rheology, surface tensiometry, ellipsometry, Brewster angle microscopy, transmission electron and atomic force microscopies. The surface properties proved to be similar to the properties of dispersions of solid nanoparticles and differ from those of the solutions of conventional surfactants and amphiphilic macromolecules. Although the surface activity of fullerenols with a great number of hydroxyl groups is not high and these substances do not decrease significantly the surface tension at low concentrations, the fullerenol molecules form a macroscopically homogeneous adsorption layer at the solution – air interface with a high dynamic surface elasticity up to about 170 mN/m. Atomic force microscopy shows that the adsorption layer is not homogeneous at the microscale and consists of interconnected surface micro-aggregates consisting of two – three layers of fullerenol molecules. The bonds between different aggregates are weak and can be broken even by slight mechanical perturbations. The surface aggregates are not adsorbed from the bulk phase but formed in the surface layer as a result of structural rearrangements of the adsorbed molecules. The slow fullerenol adsorption is not controlled by diffusion but by an electrostatic adsorption barrier.

Acknowledgements The groups from SPbGU and from B.P.Konstantinov Petersburg Nuclear Physics Institute were financially supported by RFBR, project № 18-29-19100 (SPbGU) and project № 18-29-19008 (Konstantinov Institute).

[1] Kang, H., Lee, W., Oh, J., Kim, T., Lee, C., Kim, B. J. *Acc Chem Res.* 2016, 49 (11), 2424.

[2] Dini, D., Calvete, M. J. F., Hanack, M. *Chem Rev.* 2016, 116 (22), 13043.

[3] Zieleniewska, A., Lodermeier, F., Roth, A., Guldi, D. M. *Chem Soc Rev.* 2018, 47 (3), 702.

PII-30. Dynamic Surface Properties of DNA/Polyelectrolyte Aqueous Solutions

Chirkov N.S.¹, Noskov B.A.¹, Lin S.-Y.²

¹Institute of Chemistry, St. Petersburg State University, Russia;

²National Taiwan University of Science and Technology, Chemical Engineering Department, Taiwan

jinnhut@gmail.com

Polycations form soluble complexes with DNA in aqueous solution due to strong electrostatic attraction between the components and allow transfer of genetic material into cells [1]. Cationic polymers represent a class of nonviral carriers which can be designed to facilitate gene delivery into target cells. The corresponding biomedical interest resulted in extensive investigations of DNA-polyelectrolyte interactions in the bulk phase of aqueous solutions [2]. At the same time, the information on surface properties of these systems is scarce.

In the given work the dynamic surface properties of DNA/poly(methylalkyldiallylammonium chloride) (PMADAAC) aqueous solutions at the solution/air interface were studied by the surface tensiometry, dilational surface rheology, ellipsometry and atomic force microscopy. The deviations of the surface properties (surface elasticity, surface tension, ellipsometric angles) of DNA/poly(dimethyldiallylammonium chloride) from the values of water were close to the error limits. Measurements of the kinetic dependencies of the surface properties of DNA/poly(methylbutyldiallylammonium chloride) and DNA/poly(methylhexyldiallylammonium chloride) solutions discovered noticeable deviations from the results for solutions of individual components indicating thereby the adsorption of DNA/polyelectrolyte complexes. These deviations increased strongly at the approach to the isoelectric point. The atomic force microscopy allowed estimation of the morphology of the adsorption layer as a function of the molar ratio and total concentration of the two components.

Acknowledgements This work was financially supported by the Russian Foundation of Basic Research and the Ministry of Science and Technology of Taiwan (joint project RFFI-MSTT no. 19-53-52006 MHT_a).

[1] V. Incani, A. Lavasanifar, H. Uludağ, *Soft Matter*, 2010, 6(10), 2124-2138.

[2] S.K. Filippov, C. Koňák, P. Kopecková, L. Starovoytova, M. Špírková, P. Štěpánek, *Langmuir*, 2010, 26(7), 4999-5006.

PII-31. Theory for Charge Distribution in Ionic Liquids Near a Charged Wall

Ciach A.

Institute of Physical Chemistry, Polish Academy of Sciences, 01-224 Warszawa, Poland

aciach@ichf.edu.pl

The mesoscopic field theory for ionic systems [A. Ciach and G. Stell, *J. Mol. Liq.* **87**, 255 (2000)] is extended to the system with charged boundaries. A very simple expression for the excess grand potential functional of the charge density is developed. The size of hard-cores of ions is taken into account in the expression for the internal energy. The functional is suitable for a description of a distribution of ions in ionic liquids and ionic liquid mixtures with neutral components near a weakly charged wall. The Euler-Lagrange equation is obtained, and solved for a flat confining surface. An exponentially damped oscillatory charge density profile is obtained. The electrostatic potential for the restricted primitive model agrees with the simulation results on a semiquantitative level.

PII-32. Surfactant Adsorption in Porous Media: Adsorption Equilibria and Self-Assembly

Faria B.F., Vishnyakov A.

Skolkovo Institute of Science and Technology, Moscow, Russia

Bruna.Faria@skoltech.ru

Prediction of surfactant adsorption at solid surfaces are of a great practical interest not only for developing new detergent formulations, but is also critical for polymer and surfactant performance in enhanced oil recovery. Atomistic simulations of surfactant adsorption at mineral surfaces are difficult both because of computational expenses (due large simulations boxes required and difficulties of free energy calculations), and lack of reliable parameter sets. This presentation describes coarse-grained simulations of adsorption of different surfactants at flat surfaces using soft-core coarse-grained models. The solid-fluid interactions are parameterized from easily measurable Henry constants of reference compounds, which are small molecules consisting of the same fragments as the surfactants. The simulated structure and adsorption isotherms are systematically compared to experiments on surfaces of different hydrophobicity. Free energy perturbation and expanded ensemble techniques are applied to calculate the equilibrium between adsorbed surfactant molecules and uniform bulk surfactant solution.

PII-33. Impact of L(+)-Arabinose on Micellar Structure of Aqueous Solutions of Nonionic Surfactant Triton X-114 in a Mean Concentration Range

Levashova E.Y., Koneva A.S., Safonova E.A.

Saint-Petersburg State University, Institute of Chemistry, Russia

st055679@student.spbu.ru

Recently, the unique property of some nonionic surfactants in aqueous solutions to split into two coexisting liquid phases at the so-called cloud point temperature (CPT) has found its application in the bioextraction processes [1]. To design such processes the sugars can be used as effective additives improving the phase behavior under certain conditions [1]. These additives affect not only on the separation process, increasing the density difference between two liquid phases and decreasing CPT, but also affect the microstructure of surfactant solutions. One of the commonly used methods sensitive to any structural changes that occur in a micellar solution is viscosimetry [2]. The main goal of this work is to investigate the impact of L(+)-arabinose on viscosities of aqueous solutions of nonionic surfactant (Triton X-114) by means of dynamic viscosity measurements and NMR diffusometry at 298 K.

The data on viscosity, density and self-diffusion coefficients were obtained for aqueous solution of Triton X-114/L-arabinose, L-arabinose, and Triton X-114. Firstly, the binary systems L-arabinose/H₂O and Triton X-114/H₂O were investigated in the wide concentration range. The ternary system Triton X-114/L-arabinose/H₂O was studied at the fixed content of surfactant or sugar.

For all the systems under investigation, the nonlinear changes of dynamic viscosity vs. component' concentration were observed. The NMR diffusometry data for the Triton X-114/L-arabinose/H₂O system indicated the presence of freely diffusing species of water and L-arabinose. Moreover, it was found that L-arabinose does not incorporate into Triton X-114 aggregates.

Acknowledgements: The reported study was funded by RFBR and DFG according to the research project № 16-53-12029.

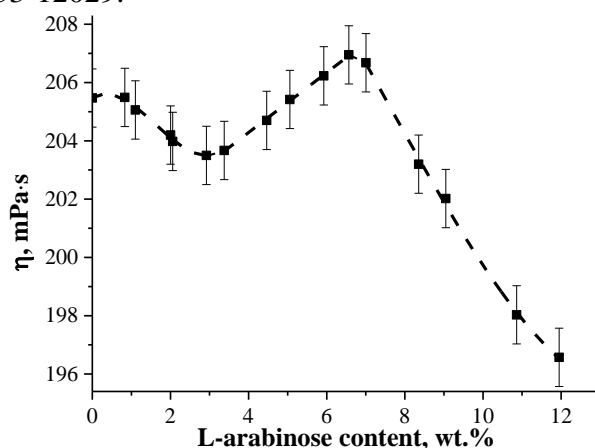


Figure 1. Data on dynamic viscosities of aqueous solutions of Triton X-114 (20 wt.%) in the presence of L-arabinose as a function of L-arabinose concentration

[1] E. Ritter, *Chemical Engineering Research and Design*, 2017, 121, 149-462.

[2] V. Lutz-Bueno, *Langmuir*, 2017, 33, 2617-2627.

PII-34. Seawater Nanodroplets Under Atmospheric Conditions. A Molecular Dynamics Simulation Study

Egorov A.V.¹, Brodskaya E.N.¹, Laaksonen A.²

¹St. Petersburg State University, Russia;

²Stockholm University, Sweden

a.v.egorov@spbu.ru

Water droplets play a key role in atmospheric chemistry [1]. Determination of their structural transformations occurring under a low pressure in a temperature range of 100-250 K is essential for understanding the physical mechanisms of atmospheric processes. However, it is challenging to characterize such transformations by experimental techniques. In this case the atomistic molecular dynamics (MD) simulations is a very promising tool to address the problem.

In the present study a 8000-molecule water nanodroplet containing 100 pairs of Na⁺ and Cl⁻ ions (the salt concentration is close to its value in the seawater at salinity 40) in vacuo was considered. The MD simulations were carried out in a canonical NVT ensemble. Temperature was kept constant by means of the Nose-Hoover thermostat. The equations of motion were solved using the Verlet leap-frog algorithm with a time step of 1.0 fs. Both the ions and water molecules are represented by non-polarizable models. To describe water the SPC/E model [2] was used. Ions interactions are described as a sum of Coulomb and Lennard-Jones (LJ) potentials. Two sets of LJ parameters taken from Refs. [3-4] were considered. No any cut-off procedure was employed in the treatment of the Coulombic forces. Structural and energetic characteristics of the droplet were calculated over a temperature range from 300 to 160 K. The system temperature was decreased in the following steps: 300, 250, 230, 210, 200, 190, 180, 170, and 160 K. Each step followed 2 ns equilibration time. The subsequent production runs were extended to 5 ns.

At the same time, a bulk sodium chloride aqueous solution of the same concentration (10 Na⁺:10 Cl⁻:800 H₂O in a cubic periodic cell) was simulated as a reference system. The simulations were carried out in the canonical NVT ensemble using the MDynaMix package [5]. Temperature was kept constant by using the Nose-Hoover method. The equations of motion were solved using the Verlet algorithm with a time step of 1.0 fs. The long-range Coulombic forces were calculated using the Ewald summation method. Model parameters, equilibration and production runs as well as the cooling protocol were the same as in the case of droplet simulations.

To examine the distributions of the ions inside the droplet the radial profiles of the local density were calculated. In addition, the profiles of the local electrostatic potential including the separate water and ions contributions as well as the translational self-diffusion coefficients were evaluated from the simulation data. The effect of the surface on the droplet structural transformations under the cooling was given a special attention.

Acknowledgements A. Laaksonen is grateful to the Swedish Science Council (VR) for scientific support. E.N. Brodskaya is grateful to the Russian Foundation for Basic Research for partial financial support, project no. 18-03-00654a.

[1] V. Vaida, *J. Chem. Phys.*, 2011, 135, 020901.

[2] H.J.C. Berendsen, J.R. Grigera and T.P. Straatsmaa, *J. Chem. Phys.*, 1987, 91, 6269.

[3] L.X. Dang, *J. Am. Chem. Soc.*, 1995, 117, 6954.

[4] I.S. Joung and T.E. Cheatham, *J. Phys. Chem. B*, 2008, 112, 9020.

[5] A.P. Lyubartsev and A. Laaksonen, *Comput. Phys. Commun.*, 2000, 128, 565.

PII-35. Thermodynamic Modeling of Fluid Systems Based on Baku Oil

Ramazanova E.E.¹, Asadov M.M.^{1,2}, Aliyev E.N.¹

¹"Geotechnological Problems of Oil, Gas and Chemistry" SRI. Azerbaijan;

²Institute of Catalysis and Inorganic Chemistry, ANAS. Azerbaijan

mirasadov@gmail.com

This report discusses the results of thermodynamic and experimental study of fluid systems based on Baku oil. A clear understanding of the effects of phase behavior is necessary when modeling multicomponent systems. This becomes important for characterizing fluids with a variable composition, in particular, oil systems.

To model the oil system, a volume balance model was chosen, where partial molar volume (\bar{v}_t) and compressibility of the fluid (c_v) are the thermodynamic parameters.

Let us assume that oil and gas phases coexist. Then the hydrocarbon system can be considered in thermodynamic equilibrium. Let us assume that the aqueous phase is independent and does not mix with the hydrocarbon phase.

Equilibrium constraints can be expressed in terms of equality of fugacity (f_c^L, f_c^V). Then the fugacity for each component in the hydrocarbon liquid phase will be equal to the fugacity in the gas phase: $f_c^L = f_c^V$.

The ratio of the mole fraction of the component (c) in the vapor phase (y_c) to the mass in the liquid phase (x_c) is expressed in terms of equilibrium coefficient (k_c).

Using critical pressure ($p_{c,c}$), critical temperature ($T_{c,c}$) and acentric factor (ω_c) of component c , the equilibrium coefficient was estimated by the expression Wilson

$$k_c = \frac{p_{c,c}}{p} \exp \left[5.371(1 + \omega_c) \left(1 - \frac{T_{c,c}}{T} \right) \right]$$

At a given pressure, temperature, and total molar composition, by thermodynamic calculation of two-phase equilibrium, the separation of the hydrocarbon system was determined. The molar fractions of the liquid phase and gas phase were determined. The number of moles of the liquid phase and the number of moles of the gas phase in the hydrocarbon liquid at a given pressure and temperature were also determined. We built the calculation algorithm and carried out calculations of two-phase equilibrium.

Volumetric changes and phase behavior of the hydrocarbon system were analyzed by the equation of state Peng and Robinson. To test thermodynamic procedures using the balance model of the compositions' volumes, a three-component fluid system was used. The properties of the three-component fluid system were changed by changing the composition (C1, C4, C10). The results of thermodynamic calculations were compared with the data obtained by PVT WinProp software. Satisfactory calculations are obtained for density, volatility and viscosity.

Acknowledgement. This work was partially financial supported by SOCAR (project No 12LR – ANAS. 2018).

PII-36. Thermodynamics and Dielectric Properties of As₂S₃–As₂Se₃–InSe

Asadov M.M.¹, Mustafaeva S.N.², Lukichev V.F.³

¹Institute of Catalysis and Inorganic Chemistry, ANAS. Azerbaijan;

²Institute of Physics, ANAS. Azerbaijan;

³Institute of Physics and Technology RAS. Russia

mirasadov@gmail.com

As₂S₃–As₂Se₃ liquidus and solidus lines with continuous rows of liquid and solid solutions are thermodynamically described in terms of ideal and regular solution models. Standard thermodynamic functions of InAs₂Se₄, In₃As₂Se₆, InAs₂S₃Se, In₃As₂S₃Se₃ phase formation, which are formed on the boundary systems, and detected InAs₂SSe₃, In₆As₄S₃Se₉, InAs₂S₂Se₂ phases in As₂S₃–As₂Se₃–InSe system, are calculated. Taking into account the data on boundary systems and InAs₂SSe₃, In₆As₄S₃Se₉, InAs₂S₂Se₂ compounds, the As₂S₃–As₂Se₃–InSe system was triangulated and an isothermal section was constructed at 300 K (Figure).

The kinetic, thermodynamic, and dielectric properties of samples of the As₂S₃–As₂Se₃–InSe system are studied. Using the model of linear isoconversion for glassy samples, the activation energy $E_a = 145\text{--}155$ kJ / mol for crystallization at glass-crystal transition was estimated.

The phase diagram for As₂S₃–As₂Se₃ is approximated. The concentration-temperature dependences of the Gibbs free energy of $1-x(\text{As}_2\text{S}_3) \cdot x(\text{As}_2\text{Se}_3)$ and heat capacity and band gap are constructed.

The dielectric properties of the $0.2(\text{As}_2\text{S}_3) \cdot 0.8(\text{As}_2\text{Se}_3)$ solid solution in alternating electric fields with a frequency of $f = 20\text{--}10^6$ Hz are studied. The laws of variation of the dielectric coefficients and the conductivity of the $0.2(\text{As}_2\text{S}_3) \cdot 0.8(\text{As}_2\text{Se}_3)$ sample are established depending on the frequency of the alternating electric field. The density of localized states near the Fermi level $N_F = 8.8 \cdot 10^{18} \text{ eV}^{-1} \cdot \text{cm}^{-3}$ is estimated, the energy spread of these states is $\Delta E = 0.04$ eV, the average distance is $R = 112 \text{ \AA}$, and hopping time of charge carriers in the forbidden zone is $\tau = 10^{-4}$ s.

Acknowledgements. This work was partially financial supported by Science Development Foundation under the President of the Republic of Azerbaijan (grant No EIF-BGM-3-BRFTF-2 + / 2017-15 / 05/1-M-13; grant No EIF-BGM-4-RFTF-1 / 2017-21 / 05/1-M-07) and RFFR (Az_a2018, project No 18-57-06001).

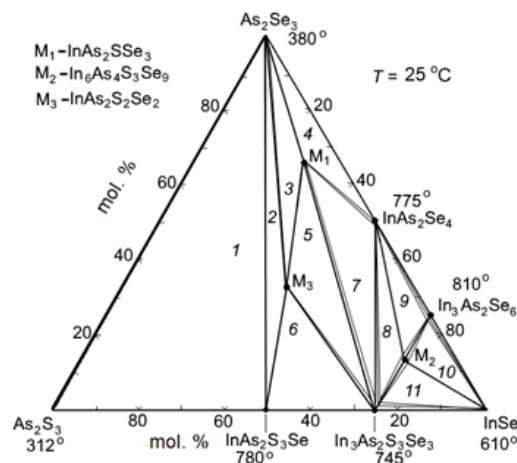


Figure. Isothermal section of the phase diagram of the As₂S₃–As₂Se₃–InSe system at 300 K.

PII-37. Thermodynamic and Transport Properties of Choline Chloride + Urea as a Deep Eutectic Solvent and its Binary Mixtures with Molecular Liquids

*Agieienko V. N.*¹, *Buchner R.*²

¹Aleksander Butlerov Institute of Chemistry, Kazan Federal University, Russia;

²Fakultät für Chemie und Pharmazie, Universität Regensburg, Germany

vira.agieienko@gmail.com

Deep eutectic solvents (DESs) and their mixtures with traditional molecular liquids (MLs) have been recently considered as new green chemistry solvents due to their low cost and eco-friendly properties. When these systems are considered, diversity of possible combinations of the starting materials allows one to develop new media possessing specific characteristics.

In the present contribution, density, ρ , dynamic viscosity, η , and electrical conductivity, κ , of reline (DES composed of choline chloride and urea in 1:2 molar ratio) and its mixtures with MLs covering the entire miscibility range were determined. In particular, mixtures with water were investigated in the temperature range of 293.15 to 338.15 K, whereas mixtures with dimethyl sulfoxide were studied from 308.15 to 363.15 K. Density and viscosity values were used to estimate the corresponding excess properties of the studied systems and to derive excess partial molar volumes of their individual components. The absolute values of the obtained data and their temperature dependence were interpreted in terms of the prevailing interspecies interactions in the studied mixtures. Reline dissolved in MSs shows a conductivity maximum, κ_{\max} , whose location at DES mole fractions of $x_{\text{DES}} \approx 0.067$ for water and ≈ 0.1 for DMSO is somewhat smaller than κ_{\max} commonly found for conventional ionic liquids (ILs) in aqueous and non-aqueous media, $0.1 \leq x_{\text{ILs}} \leq 0.2$. In agreement with the findings of Hammond et al. [1] the conductivity maximum may be interpreted as a transition from a classical electrolyte solution to a solvent-lubricated molten salt [2].

Acknowledgements The present research was funded by the Russian Scientific Foundation (Project No. 18-73-00127).

[1] O. S. Hammond, D. T. Bowron and K. J. Edler, *Angew. Chem Int. Ed.*, 2017, 56, 9782.

[2] T. Sonnleitner, V. Nikitina, A. Nazet and R. Buchner, *Phys. Chem. Chem. Phys.*, 2013, 15, 18445.

PII-38. Termophysical Properties of CoFeSiBNb Alloy in Crystalline and Liquid States

Sidorov V.E.^{1,2}, Rusanov B.A.¹, Mikhailov V.A.¹, Son L.D.^{1,2}

¹Ural State Pedagogical University, Russia;

²Ural Federal University, Russia

rusfive@mail.ru

Bulk metallic glasses (BMG) is a hot topic nowadays. They demonstrate unique combination of mechanical, physical and chemical properties. Co-based alloys are considered to be promising materials for BMG production. However, their physical and chemical properties at high temperature are practically unknown. In the present work we investigated the temperature dependences of density, electrical resistivity and magnetic susceptibility of $\text{Co}_{48}\text{Fe}_{25}\text{Si}_4\text{B}_{19}\text{Nb}_4$ alloy (base composition - BC) and with additions of neodymium (1 and 2 at.%) in crystalline and liquid states.

Density (d) was measured using gamma absorption method; electrical resistivity (ρ) - by a contact-less method in rotating magnetic field. Magnetic susceptibility (χ) was investigated by the Faraday's method. All the experiments were carried out during heating and subsequent cooling in helium atmosphere. Electrical resistivity and magnetic susceptibility in crystalline state were studied above the Curie point (T_c).

The temperature dependences of density are linear both in crystalline and liquid states. Heating of the melt up to 1300 C is accompanied by the appearance of a hysteresis in solid state - the cooling curve is higher than the heating one for all the compositions. Moreover, the melt undercooling for up to 40 C before crystallization was fixed in the experiments. Neodymium additions (1 and 2 at.%) lower the density of the alloys in liquid state significantly (it decreases from 7346 kg/m^3 for base composition to 6692 kg/m^3 for BC + 2% Nd at 1200 C).

Electrical resistivity temperature curves are linear in crystalline and liquid states. The alloys with neodymium have a higher resistivity than BC in liquid state: it increases from 137 $\mu\text{Ohm}\cdot\text{cm}$ for BC to 166 $\mu\text{Ohm}\cdot\text{cm}$ for BC + 2% Nd at 1200 C. The large absolute values of resistivity in liquid state determine its low temperature dependence that agrees well with the Muidji rule. For all the samples a significant (up to 105 C) undercooling was observed before crystallization.

Magnetic susceptibility of the alloys monotonously decreases with increasing temperature. A small change in property was observed at solidus temperature only. It has been found that neodymium additions have a low effect on the absolute values of susceptibility, increasing them from $1.69\cdot 10^{-5}$ emu/g for base composition to $1.81\cdot 10^{-5}$ emu/g for BC + 2% Nd at 1200 °C.

The obtained results can be used in improving regimes of BMGs production.

The reported study was funded by RFBR according to the research project 18-03-00433.

PII-39. On Application of the CP-PC-SAFT Model for Estimation of Sound Speed in Synthetic and Natural Oil-Gas Mixtures

Prikhodko I., Samarov A., Toikka A.

Saint Petersburg State University, Russia

i.prikhodko@spbu.ru

The speed of sound is important thermophysical property which is used, in online measurements, to characterize the heterogeneous or homogeneous mixtures or to estimate the density of reservoir fluids. Besides technological importance of this property, there is also a scientific interest in obtaining the sound speed accurately. From the scientific point of view, as a second-order derivative property, the speed of sound is one of the most demanding tests to check the performance limits for a thermodynamic model.

In this work, capability of application of the CP-PC-SAFT (Critical Point-based Perturbed Chain - Statistical Association Fluid Theory) model for estimation and calculation of sound speed quantities in natural gas is considered. We have applied the approach proposed by Polishuk [1] which requires limited data for the numerical solution of the PC-SAFT parameters, namely, the critical constants and the triple point liquid density. Its implementation has necessitated a careful re-evaluation of part of the original PC-SAFT universal parameters matrix and some additional revisions. Prediction results of density and speed of sound using CP-PC-SAFT equation of state for several multicomponent oil-gas systems containing alkanes, isoalkanes, nitrogen, carbon dioxide in the range of temperatures 250 – 450 K and pressures 0.5 – 60 MPa are presented. Results of modeling for the thermodynamic properties are compared with literature experimental data. The model is shown to reproduce with high accuracy experimental values of density and sound speed (Figure).

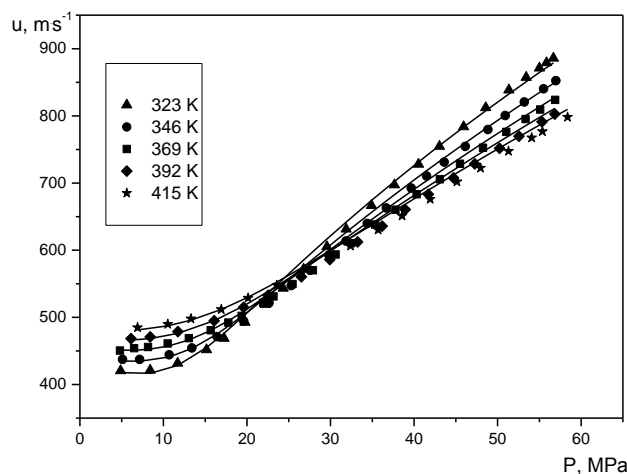


Figure. Speed of sound vs pressure at several temperatures in the natural gas mixture $\text{CH}_4 + \text{C}_2\text{H}_6 + \text{C}_3\text{H}_8 + n\text{-C}_4\text{H}_{10} + i\text{-C}_4\text{H}_{10} + \text{N}_2 + \text{CO}_2$. Symbols are experimental data [2], lines are modeling (prediction) results.

Acknowledgements. The financial support of Russian Foundation for Basic Research (research grant No. 17-58-560018) is gratefully acknowledged. The authors are thankful to prof. I. Polishuk (Ariel University, Israel) for his valuable help in calculations.

[1] I. Polishuk I., *Ind. Eng. Chem. Res.*, 2014, 53, 14127.

[2] P. Ahmadi, A. Chapoy, B. Tohidi, *J. Nat. Gas Sci. Eng.*, 2017, 40, 249.

P11-40. Liquid-Liquid Equilibria for Separation of Alcohols from Esters Using Deep Eutectic Solvents Based on Choline Chloride

Samarov A., Prikhodko I., Liubichev D., Toikka A.

Saint Petersburg State University, Russia

dmitrylyubichev@gmail.com

One of the main and important operations in the chemical industry is the separation, which is implemented through rectification. But in cases where this method fails to work properly (azeotropic mixtures or mixtures with close-boiling components), extractive rectification is exploited. Typical example of azeotropic mixtures is binary alcohol – ester systems. Esters are used as common solvents and have a wide area of application in various chemical engineering issues. Recently, it has been shown in [1,2] that propionic esters can act as components of the second-generation biofuels and be served as fuel additives for gasoline due to their attractive properties. The main problem in the separation of esters in industrial esterification reaction processes is the formation of an azeotrope in the systems with alcohols. Common organic solvents that are currently used to separate such systems have several limitations (high volatility, toxicity and high regeneration costs). That is why in recent years, more attention is paid to the issues of «green chemistry». One of new potentially environment-friendly solvents is deep eutectic solvents (DESs). DES is a mixture consisting of a hydrogen bond donor and a hydrogen bond acceptor. Upon mixing, it forms a liquid with much lower melting point than the individual components.

This contribution is a continuation of a series of works devoted to the study of phase equilibrium and the extraction properties of deep eutectic solvents based on choline chloride and dibasic carboxylic acids in alcohol-ester systems [3,4]. In the present paper, we consider the ability of DESs on the basis of choline chloride and glycerol/urea for the separation of mixtures of alcohols with propionic acids esters: ethyl propionate, *n*-propyl propionate and *n*-butyl propionate. NRTL model was applied to correlate liquid-liquid equilibria (LLE) of these systems.

Choline chloride-based DES was tested for the separation of azeotropic mixtures of ethanol–ethyl propionate, *n*-propanol–*n*-propyl propionate, and *n*-butanol–*n*-butyl propionate via liquid–liquid extraction. The mixtures of choline chloride with glycerol or urea with a molar ratio of 1:2 were used. Experimental LLE data were obtained at temperatures 293.15 and 313.15 K and atmospheric pressure. Liquid–liquid tie-lines for studied systems were determined and analyzed. The extraction performance of DES was characterized with distribution coefficients and values of selectivity respectively to alcohol. NRTL model reproduced experimental binodal curves and tie-lines with high accuracy for the pseudo-ternary systems.

Acknowledgements. The financial support of Russian Foundation for Basic Research (research grant No. 16-33-60128 mol_a_dk) is gratefully acknowledged.

[1] R.W. Jenkins, M. Munro, S. Nash, C.J. Chuck, *Fuel*, 2013, 103, 593.

[2] E.S. Olson, T.R. Aulich, R. Sharma, R.C. Timpe, *Appl. Biochem. Biotechnol.*, 2003, 105, 843.

[3] A. A. Samarov, M.A. Smirnov, A.M. Toikka, I.V.Prikhodko, *J. Chem. Eng. Data*, 2018, 63, 1877.

[4] A. Samarov, N. Shner, E. Mozheeva, A. Toikka, *J. Chem. Thermodyn.*, 2019, 131, 369.

PII-41. Evaluation of Thermal Stability Duration (Useful Life) of Organic Heat-Carriers

Dzhapparov T.A-G.¹, Bazaev A.R.¹, Bazaev E.A.¹, Bagavudinova D.G.², Medzhidova F.Kh.²

¹*Institute for Geothermal Research of the Daghestan Scientific Center of the Russian Academy; of Sciences, Shamil 39A, Makhachkala, Daghestan Republic, 367030, Russia;*

²*Daghestan State University, Gadzhieva 43a, Makhachkala, Daghestan Republic, 367000, Russia*

timur507@mail.ru

Thermal stability is one of the most important property of organic heat carrier. The most general change in properties in the thermal decomposition of organic molecules is an increase in the vapor pressure of the system brought about by cleavage of the molecule into smaller, more volatile fragments. This physical change has the advantage over others such as weight loss, viscosity change, and heat of reaction, of being related to the true rate of thermal decomposition by a simple although usually unknown proportionality constant.

Thermal stability data can be extrapolated by means of equation (1) [1] to estimate the useful life of a compound data given temperature. In equation 1, τ is the time in hours (useful life) for a compound of density d , molecular weight M , decomposition point T_d , K, and x per cent decomposition at a temperature T ' K.

$$\tau = \frac{-0.0285 \cdot T_d}{M} \cdot \log\left[\frac{100-x}{100}\right] \cdot 10^5 \quad (1)$$

In the derivation of this equation the change of density with temperature is neglected, and it is assumed that the mode of decomposition of a compound is unchanged over the temperature range T_d to T , that thermal decomposition is a unimolecular reaction, and that one molecule enters the gas phase per molecule of compound decomposed.

In this work using eq.1 and on the basis of our own experimental data on decomposition temperatures of pure aliphatic alcohols (methanol, ethanol, 1-propanon and 1-butanol) and their water mixtures [2] thermal stability duration (useful life) is evaluated. It is shown that useful life of molecules of alcohol decreases with temperature and concentration of alcohol and increases from methanol to 1-butanol.

[1] E.S. Blake and W.C. Hamma and J.W. Edwards and T.E. Reichard and M.R. Ort. Journal of Chemical and Engineering Data, 1961, 6, 87.

[2] T.A. Dzhapparov and A.R. Bazaev. Teplofizika i aeromechanika, 2012, 19, 793

PII-42. Urea and Tetramethylurea Solutions in Ethylene Glycol: a Comparative Analysis of Temperature-Dependent Volumetric Solvation Characteristics and Interaction Parameters

Ivanov E.V.¹, Lebedeva E.Yu.¹, Kustov A.V.^{1,2}, Ivanova N.G.³

¹Krestov Institute of Solution Chemistry of the RAS, Ivanovo, Russia; ²Ivanovo State University of Chemistry and Technology, Russia; ³Ivanovo State Power Engineering University, Russia

evi@isc-ras.ru

Ethylene glycol (EG) is one of non-aqueous media with the spatial network of molecules, mutually H-bonded. Some physicochemical characteristics of EG such as own isothermal compressibility as well as negative and solvophobic solvation in its solutions resembles those of water [1]. At the same time solvation processes in EG are studied insufficiently full. From a thermodynamic viewpoint, volume-related properties of urea (U) and tetramethylurea (TMU) solutions in EG are proved to be helpful both in understanding the structure-packing transformations of the solvent in the course of solvation and in evaluating the solute – solute (solvent) interactions. Being different in solvation nature, U and TMU were chosen here for studying the interactions associated with the competition between the contributions of hydrophilic and hydrophobic parts of a solute molecule in EG.

Analysis of data on the volume effect of dissolution (Fig. 1), $V_2^{E,0} = V_2^0 - V_2$ where V_2^0 and V_2 are the standard partial and own molar volumes of a solute, showed that a structure-compression effect in (EG + TMU) is enhanced with increasing temperature whereas in (EG + U) it becomes decreasingly less pronounced disappearing nearby $T = 308.15$ K. The volume-related coefficients of the U–U and TMU–TMU pair interactions in EG, v_{22} , have the opposite directions depending on the temperature, too (Fig. 2). Herewith the structuring effect in aqueous TMU is more pronounced than it occurs in (EG + TMU) while the “structure-breaking” effects in both aqueous and glycolic solutions of U play equally important role when the solvation complex of this solute is formed.

Acknowledgements The financial support of the Russian Foundation for Basic Researches (Grant No. 18-03-00016-a) was supplied to carry out the study being presented.

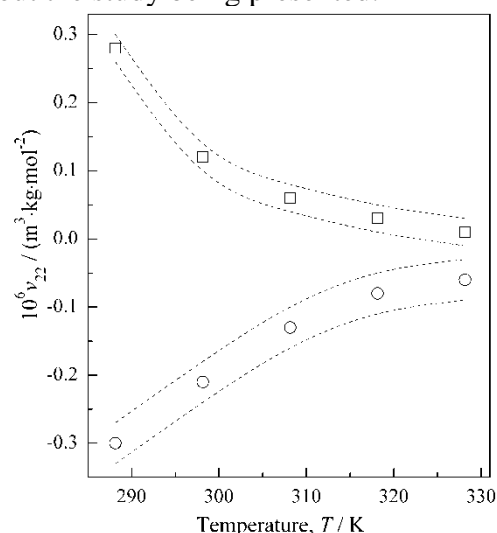
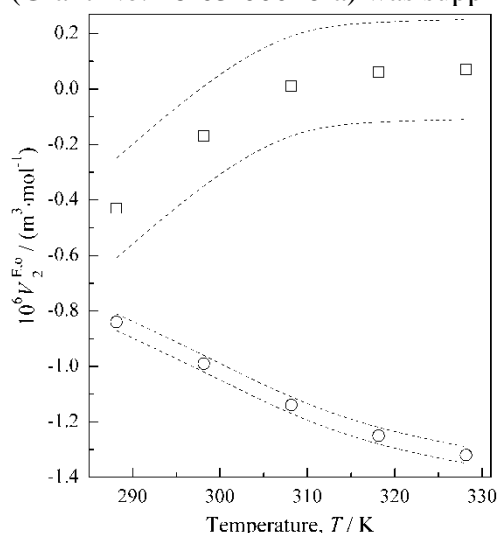


Fig. 1. Standard excess molar volumes of U (\square) and TMU (\circ) in EG as temperature functions. The dashed lines limit the uncertainty interval.

Fig. 2. Volume-related coefficients of solute – solute pairwise interactions for solutions of U (\square) and TMU (\circ) in EG as temperature functions.

[1] M.N. Rodnikova, N.A. Chumaevskii, et al., *Russ. J. Phys. Chem. A*, 2006, 80, 826.

PII-43. Standard Thermodynamic Properties in Water for Equimolecular Co-Crystal of *Cis*- and *Trans*-Coordinated Dimethylglycolurils at Temperatures from 278.15 K to 318.15 K and at the Ambient Pressure

Ivanov E.V.¹, Lebedeva E.Yu.¹, Batov D.V.^{1,2}, Baranov V.V.³, Kravchenko A.N.³, Ivanova N.G.⁴

¹Krestov Institute of Solution Chemistry of the RAS, Ivanovo, Russia; ²Ivanovo State University of Chemistry and Technology, Russia; ³Zelinsky Institute of Organic Chemistry of the RAS, Moscow, Russia; ⁴Ivanovo State Power Engineering University, Russia

evi@isc-ras.ru

In this report, the results of densimetric and calorimetric studies of dissolution process in water for the (1:1) co-crystal [A+B] consisting of *cis*- and *trans*-coordinated dimethylglycolurils (*cis*-DMGU and *trans*-DMGU, see Fig. 1) are presented. The temperature-dependent standard molar volumes of the co-crystal (Fig. 2, where $V_{vdw,x}$ is the solute van-der-Waals volume) as well as standard molar enthalpies (Fig. 3) and isobaric heat capacities (Table 1) of its dissolution in water were discussed. Based on the previously obtained similar results for aqueous *cis*-DMGU, *trans*-DMGU and DMGU (isomer with the unsubstituted and fully methylated rings) [1,2], it was found that the formation of co-crystal [A+B] leads to a peculiar “synergism” in both volume and heat capacity effect of *N,N'*-dimethylglycoluril hydration at all the temperatures studied (see Fig. 2 and Table 1).

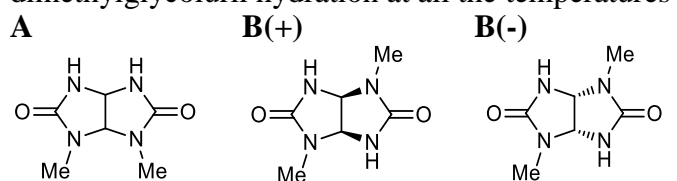


Fig. 1. Molecular structures of the co-crystal [A+B] constituents: (A) *cis*-DMGU and (B) *trans*-DMGU {consisting of 1:1 *R*(+)- and *S*(-)-enantiomers}.

Table 1. Standard molar heat capacities (in $\text{J}\cdot\text{mol}^{-1}\cdot\text{K}^{-1}$) of the dissolution of co-crystal [A+B] and isomeric dimethylglycolurils

[A+B]	(A) <i>cis</i> -DMGU	(B) <i>trans</i> -DMGU	DMGU
106.4 ± 2.3	84.0 ± 1.7	99.5 ± 2.0	90.4 ± 2.2

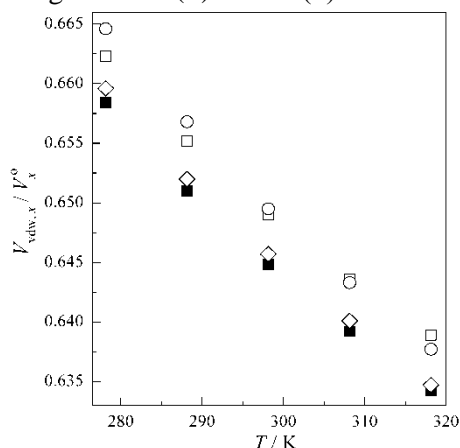


Fig. 2. Packing density parameters for aqueous solutions of co-crystal [A+B] (closed squares) and equimolecular dimethylglycolurils (symbols are depicted in Fig. 3) as temperature functions.

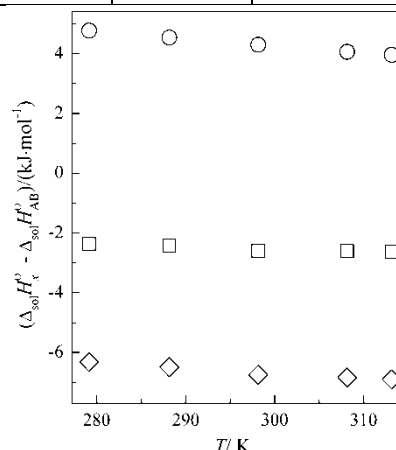


Fig. 3. Differences in standard molar enthalpies of dissolution of co-crystal and equimolecular dimethylglycolurils (x): *cis*-DMGU (circles); *trans*-DMGU (squares); DMGU (rhombuses).

[1] E.V. Ivanov and E.Yu. Lebedeva, *J. Mol. Liq.*, 2016, 222, 1164.

[2] E.V. Ivanov and D.V. Batov, *Thermochim. Acta*, 2016, 625 53.

PII-44. Thermodynamic Properties of Dimethylsulfone-Dimethylsulfoxide-Water Ternary System

Ghazoyan H.H., Markarian S.A.

Department of Chemistry, Yerevan State University, 0025 Yerevan, Armenia

heghine@ysu.am

Fundamental investigation of dimethylsulfone (DMSO₂) - dimethylsulfoxide (DMSO) - water ternary system has a biomedical and environmental significance. It has been established that DMSO₂ also takes part in the global biogeochemical cycle of sulfur.

Earlier, we studied the different physicochemical properties of solutions of DMSO₂ [1]. In this work the volumetric and thermochemical properties of the DMSO₂-DMSO-water ternary system have been studied.

Densities of solutions were measured by using a vibrating-tube densimeter Anton Paar DMA 4500. On the basis of experimental data apparent molar volumes (V_ϕ) and partial molar volumes (V_ϕ^o) of DMSO₂ in DMSO-water mixtures over the 293.15–323.15K temperature range have been calculated.

The results obtained shown that the values of standard partial molar volumes for DMSO₂-water mixture are less compare with those for DMSO₂-DMSO and DMSO₂-DMSO-water mixtures. In the DMSO₂-DMSO-water system the strongest interaction between DMSO and water molecules leads to the increase of partial molar volumes for DMSO₂.

The enthalpies of dissolution ($\Delta_{sol}H$) of DMSO₂ in DMSO and DMSO-water mixture were also calculated. The thermochemical study shows that the dissolution of DMSO₂ in DMSO and DMSO-water is endothermic (Table 1). Therefore, it is reasonable to assume that the endothermal process of sulfone crystalline lattice decomposition predominates during the dissolution of sulfone. Moreover, with the transfer of DMSO₂ from water to DMSO and mixed solvent the endothermic increase of transfer enthalpies ($\Delta_{tr}H^o$) takes place.

Acknowledgements This work was supported by the RA MES State Committee of Science, in the frames of the research project № 18T-1D012.

Table 1. The solution enthalpies, $\Delta_{sol}H$ and standard solution enthalpies, $\Delta_{sol}H^o$ of DMSO₂ in DMSO and DMSO-water equimolar mixture at T=298.15K.

$m/(\text{mol}\cdot\text{kg}^{-1})$	$\Delta_{sol}H$ (kJ mol ⁻¹)	
	DMSO ₂	DMSO-water
0.01	22.96	27.61
0.02	23.47	28.80
0.05	23.24	28.15
0.10	23.70	29.10
0.15	23.00	27.93
$\Delta_{sol}H^o$ (kJ mol ⁻¹)	23.27	28.32

[1] H.H. Ghazoyan, S.A. Markarian, *Journal of Molecular Liquids*, 2013, 183, 85.

PII-45. Thermodynamic Evaluation of Chemical and Electrochemical Oxidation of V – Si System

Nikolaychuk P. A.

Chelyabinsk State University, Russian Federation

npa@csu.ru

Four vanadium silicides, namely V_3Si , V_5Si_3 , V_6Si_5 and VSi_2 , exist in the system; however, the silicide V_6Si_5 is stable only at elevated temperatures [1]. The compounds V_5Si_3 , V_6Si_5 and VSi_2 are stoichiometric, whereas V_3Si has the noticeable homogeneity range at elevated temperatures. However, the broadness of this homogeneity range quickly lowers with the temperature decrease: it is ~5 at. % wide at 1800 °C, and only ~1 at. % wide at 1000 °C. Therefore, in the present study the silicide V_3Si is treated as the stoichiometric compound at 25 °C. The excess Gibbs energy of the bcc-solid solution of silicon in vanadium at 25 °C is expressed [2] as: $G_{298,15, V-Si}^E = -187\,180 \cdot x_{Si} \cdot (1 - x_{Si}) \text{ J mol}^{-1}$. The maximum solid solubility of silicon in vanadium at 25 °C was estimated: $x_{Si} = 1,657 \cdot 10^{-4}$. The activities of the solid solution components were calculated, they are equal to $a_{V(bcc)} = 0,9826$ and $a_{Si(bcc)} = 7,245 \cdot 10^{-35}$.

The phase diagram of V – O system is rich with various oxides. The following ones are thermodynamically stable at 25 °C: VO, V_2O_3 , V_3O_5 , Magnéli phases [3] V_nO_{2n-1} ($4 \leq n \leq 8$), VO_2 , V_6O_{13} , V_3O_7 and V_2O_5 . No vanadium silicates are known at the standard conditions. The standard Gibbs energies of formation of almost all vanadium oxides (except VO_2 , V_3O_7 and V_2O_5) were taken from [4]; the values for these three exceptions were taken from [5].

In aqueous environments vanadium might form four different cations – V^{2+} (aq), V^{3+} (aq), VO^{2+} (aq) and VO_2^+ (aq). Vanadium (V) forms several anions. The simplest vanadate is VO_4^{3-} (aq), however, it tends to polymerise. Several isopolyvanadates, both hydrolysed and unhydrolysed, might exist in a solution, the data on them are often contradictory, and there is still no single opinion about it. Several variations of the potential – pH diagram for vanadium containing different aqueous species exist in the literature. In this study only those species were considered that were presented in each of these publications. The following vanadates were chosen for consideration: VO_4^{3-} (aq), $V_2O_7^{4-}$ (aq), $V_4O_{12}^{4-}$ (aq) and $V_{10}O_{28}^{6-}$ (aq). The standard Gibbs energies of formation of aqueous vanadium species were taken from [6]. No vanadium hydrides are known [7].

The potential – pH diagram of the V – Si – H_2O system at 25 °C, air pressure of 1 bar and the activities of species in a solution of 1 mol l^{-1} is plotted. The upper part of the diagram is a simple superposition of the potential – pH diagrams of vanadium and silicon. The equilibria involving vanadium silicides occur far below the domain of water electrochemical stability. The cross section of the potential – pH diagram in the region of thermodynamic stability of vanadium silicides is also presented. The diagrams show that silicon has a little impact on the corrosion-electrochemical behaviour of the V – Si system. The passivity domain of vanadium is also quite narrow. If the silicon content in the system is enough, H_4SiO_4 would be the only product that could prevent the dissolution of silicides.

[1] J. F. Smith, *Bull. Alloy Phase Diagr.*, 1985, 6(3), 266.

[2] C. Zhang et al., *CALPHAD*, 2008, 32(2), 320.

[3] A. Magnéli, *Pure Appl. Chem.*, 1978, 50(11–12), 1261.

[4] <http://www.chem.msu.ru/cgi-bin/tkv.pl?show=welcom.html>.

[5] M. W. Chase Jr et al., *J. Phys. Chem. Ref. Data*, 1985, Supplement 1.

[6] G. Ketsall, I. Thompson, P. Francis, *J. Appl. Electrochem.*, 1993, 23(5), 417.

[7] R. Griffiths, J. A. Pryde, A. J. Righini-Brand, *J. Chem. Soc. Farad. Trans. 1. Phys. Chem. Condens. Phases*, 1972, 68, 2344.

PII-46. Thermal Conductivity and Thermal Diffusivity of Cerium in the Temperature Range 293 - 1773 K

Savchenko I.V., Samoshkin D.A., Stankus S.V.

Kutateladze Institute of Thermophysics, Siberian Branch of the RAS, Russia

savchenko@itp.nsc.ru

For the first time, the thermal conductivity and thermal diffusivity of cerium were measured by the laser flash method in the temperature range 293 ± 1773 K, including the phase transition regions. The main experiments were performed on the experimental installation LFA - 427 [1]. The samples were cut from a cerium brand CEE-O, purity 99.75% by weight. The results of chemical analysis by atomic emission spectroscopy and mass spectroscopy showed the presence of the following impurities in the initial cerium: Ca - 0.002%, Cr - 0.0004%, Cu - 0.0025%, Eu - 0.0002%, Fe - 0.008%, La - 0.086%, Mo - 0.0082%, Nb - 0.0003%, Nd - 0.078%, Ni - 0.0006%, Pd - 0.0008%, Ta - 0.0004%, Sm - 0.0082%, Pr - 0.043%. Experiments were performed on a sample melted into a tantalum cell. Its design and geometrical dimensions were similar to [2]. The sample was a flat layer about 2 mm thick, which was formed between the bottom of the crucible and the insert. Mechanically pre-cleaned sample of cerium together with the cell details were annealed in a vacuum of $\sim 2 \times 10^{-5}$ mbar at a temperature of 850 K for 4 hours and placed into a glove box with an argon atmosphere. Inside the box, we measured the masses of the sample and parts of the cell, after which the cell was sealed using arc welding. Such an approach made it possible to maximally eliminate the influence of oxides on the results of experiments. To create a contact of the sample with the cell details, the measurements started from the maximum temperature significantly exceeding the melting point (1077 K). To obtain the values of thermal conductivity and thermal diffusivity, the computational model described in detail in [2] was used. The error of measuring thermal conductivity and thermal diffusivity estimated by the method [2] is 4-6%.

A comparison of the results obtained with data available in the literature. It is shown that, within the limits of the total measurement errors, our results agree satisfactorily with the data of earlier works. In the temperature range corresponding to the high-temperature structural phase transition γ - δ , an anomaly is observed more appropriate to the second-order phase transition. We assume that this behavior is due to the cracking of the sample in this area. In the temperature range corresponding to the phase transition β - γ , a change in the nature of the temperature dependence is observed. The thermal conductivity of cerium over the entire temperature range studied is electronic in nature with a positive temperature coefficient.

Acknowledgements The study was supported by the grant of the Russian Science Foundation (Project No. 17-79-10237).

[1] <https://www.netzsch-thermal-analysis.com/en/products-solutions/thermal-diffusivity-%20conductivity/lfa-427/>

[2] S.V. Stankus, I.V. Savchenko, *Thermophysics and Aeromechanics*, 2009, 16, №4, 585-592.

PII-47. Excess Enthalpies of Hydroxy-Containing Esters by Capillary Gas Chromatography

Portnova S.V., Krasnykh E.L.

Samara State Technical University, Russia

kinterm@samgtu.ru

It was shown in [1] that vaporization enthalpy depend linearly on the enthalpy of solution on a nonpolar stationary phase under conditions of gas–liquid chromatography (GLC) for different classes of organic compounds, and the resulting dependences can be used to calculate the enthalpies of vaporization of compounds of similar structure. Also enthalpy of solution and vaporization enthalpy are related by the equation [2]

$$\Delta H^{E,\infty}(T) = \Delta_l^g H_m^0(T) + \Delta_{sol}^g H_m^0(T)$$

where $\Delta H^{E,\infty}(T)$ is the excess enthalpy of mixing (the energy needed or liberated during the transfer of 1 mol of pure liquid solute into 1 mol of infinitely dilute solution).

They were reduced to the standard temperature (298.2 K) using the equation

$$\Delta_{sol}^g H_m^0(T) = \Delta_{sol}^g H_m^0(T_{av}) + (-\Delta_l^g Cp^o) \cdot (T - T_{av})$$

where $\Delta_l^g Cp^o$ is the difference of the isobaric molar heat capacities of the gaseous and the liquid phase were estimated by the QSPR-method [3]

Excess enthalpies $\Delta H^{E,\infty}$ were derived from vaporization enthalpies $\Delta_l^g H_m^0(298,2)$ and enthalpies of solution $\Delta_{sol}^g H_m^0(298,2)$ determinate by gas-liquid chromatography in the temperature range of 363.2-553.2K on DB-1 nonpolar phase for hydroxy-containing esters. In this work we used esters of glycolic, lactic, malic and tartaric acids and alcohols C₁-C₈, mono-, di-, tri- esters of trimethylolpropane esters and carboxylic acids C₂-C₆, mono-, di- esters of neopentylglycol esters and carboxylic acids C₂-C₆, mono-, di-, tri-, tetra- esters of pentaerythritol and carboxylic acids C₂-C₅. These substances are used in the synthesis of lubricants, plasticizers, polymers, solvents.

All these compounds are united by the presence of this or several hydroxyl groups in the molecule. Based on the structure of the compounds, it is possible to assume the presence of intermolecular interactions between the molecules of these substances in the liquid phase. Dilute solutions and a split ratio of 1:80 were used in determining the retention characteristics. We may therefore assume that chromatography was performed under conditions of limiting dilution to exclude the possibility of intermolecular sorbate–sorbate interaction. In the first approximation, $\Delta H^{E,\infty}$ may therefore be considered a value indicating the level of intermolecular interactions between molecules of hydroxy-containing esters in the liquid phase [4].

Acknowledgements The financial support of the Russian Foundation for Basic Research, project no. 17-08-00967_a.

[1] J.S. Chickos, S. Hosseini and D.G. Hesse, *Thermochim. Acta*, 1995, 249, 41.

[2] M. Görgényi and K. Héberger, *Journal of Chromatographic Science*, 1999, 37, 11.

[3] E.L. Krasnykh and S.V. Portnova, *J. Struct. Chem.*, 2017, 58, 4, 753.

[4] S.V. Portnova, Yu.F. Yamshchikova, and E.L. Krasnykh, *Russian Journal of Physical Chemistry A*, 2019, 93, 2, 390.

PII-48. The Determination of the Characteristics of Sorption, Vapor Pressure and Enthalpy of Vaporization of Esters of Neopentylglycol

Lukina O.D., Krasnykh E.L., Portnova S.V.

Samara State Technical University, Russia

kinterm@samgtu.ru

Neopentylglycol (NPG) is diatomic alcohol. Esters of neopentylglycol are used in the synthesis of lubricants with a reduced potential for oxidation or hydrolysis compared to natural esters.

In the work the synthesis of neopentylglycol esters with organic acids C₂-C₆ and determination of the sorption enthalpies, vapor pressures and vaporization enthalpies of the obtained esters was carried out.

The esters of neopentylglycol and organic acids C₂-C₆ were obtained by esterification in the presence of benzene and of phosphoric acid as a catalyst. All samples were purified by a repeated distillation in vacuum. Purities of samples were determined by the gas chromatography. The purity of the samples was more than 98% by weight.

The logarithmic retention indices were determined for the obtained samples by the GLC method on the basis of the gas chromatograph "Crystal-2000M" with a flame ionization detector on a capillary column of 100 m x 0.2 mm x 0.5 μm with a nonpolar phase DB-1. We used isothermal conditions with column temperature 423.2-523.2K, vaporizer temperature 623.2K, detector temperature 573.2K, carrier gas helium with flow splitting 1/100 and sample volume 0.2 μl. Determination of retention indices was carried out according to the standard procedure, using a number of alkanes C₁₀-C₁₈.

The calculation of retention indices were calculated by the Kovacs equation:

$$I = \frac{\lg(t'_x) - \lg(t'_z)}{\lg(t'_{z+1}) - \lg(t'_z)} \cdot 100n + 100N,$$

where t'_x and t'_z are the corrected retention times of the ester and n -alkanes with numbers of carbon atoms Z and $Z + 1$, respectively.

The value of the change in internal energy $\Delta_{sorp}\bar{U}$ (kJ/mol) and sorption enthalpy $\Delta_{sorp}H$ (kJ/mol) at an experimental temperature was determined from the dependencies:

$$\ln(k/T) = C - \frac{\Delta_{cop}\bar{U}}{RT}; \Delta_{sorp}H = \Delta_{sorp}\bar{U} - RT \text{ and } k = \frac{t_R - t_M}{t_M}.$$

where t_R – adjusted retention time of the esters, min; t_M - retention time of nonsorbing substance (benzene), min.

The vapor pressures of NPG esters were determined by the transpiration method. The obtained p-T-dependences were described by the equation of the form:

$$R \cdot \ln\left(\frac{P}{P_{aw}}\right) = A_f - \frac{B_f}{T} + \Delta_{*}^n Cp^0 \cdot \ln\left(\frac{T}{T_{aw}}\right)$$

where P – is the vapor pressure at T ; P_{aw} – is the vapor pressure at the average temperature of the study T_{aw} ; A_f and B_f are empirical coefficients obtained by processing p-T data by the least squares method; $\Delta_{*}^n Cp^0$ – the difference between the molar heat capacities of the gas and liquid phases. [1].

$$\Delta_{vap}H_m^0(298,2) = -B_f + \Delta_{*}^n Cp^0 \cdot 298,2$$

Acknowledgements The financial support of RFBR № 19-08-00928 A

[1]. E. L. Krasnykh and S. V. Portnova. *Journal of Structural Chemistry*. 2017, 58, 4, 706.

PII-49. Vapor Pressure and Enthalpy of Vaporization of Pentaerythritol Esters

Emel' anov V.V., Krasnykh E.L., Levanova S.V.

Samara State Technical University, Russia

kinterm@samgtu.ru

All esters of pentaerythritol were synthesized by the esterification with the monobasic acid C₂-C₅ at the temperature corresponding to the boiling point of acid without the solvent and catalyst. The reaction time was about 25-30 hours for all synthesized compounds. All samples were purified by a distillation in vacuum and by a recrystallization. Purities of samples were determined by the gas chromatography. Five esters were obtained with a purity of at least 98-99%.

The determination of the vapor pressure of the pentaerythritol esters was carried out using the transpiration method [1]. The obtained values of saturated vapor pressure processed by the equation:

$$\ln(p) = A + \frac{B}{T} + C \cdot \ln(T) + D \cdot T$$

Equation coefficients A, B, C, D present in table 1.

Table 1. Equation coefficients A, B, C, D for pentaerythritol esters.

Ester	T-range, K	A	B	C	D
Tetraethanoate	358,7 - 392,7	307.75	-23878.36	-42.48	0.02
Tetrabutanoate	364,7 - 392,7	638.59	-23867.52	-111.45	0.22
Tetra(2-methylpropanoate)	344,7 - 372,7	696.66	-23865.87	-123.25	0.26
Tetrapentanoate	372,7 - 402,7	374.49	-23876.07	-59.05	0.09
Tetra(3-methylbutanoate)	372,7 - 402,7	481.74	-23872.66	-80.04	0.14

Enthalpy of vaporization at 298K for all synthesized esters was calculated by equations

$$R \cdot \ln\left(\frac{P}{P_{aw}}\right) = A_f - \frac{B_f}{T} + \Delta_g^1 Cp^0 \cdot \ln\left(\frac{T}{T_{aw}}\right)$$

$$\Delta_{vap} H_m^0(298,2) = -B_f + \Delta_g^1 Cp^0 \cdot 298,2$$

and present in table 2.

Table 2. Vaporization enthalpies of pentaerythritol esters.

Ester	$\Delta_g^1 Cp^0$ [2] J/(mol·K)	T-range, K	$\Delta_{vap} H_m^0(298,2)$ kJ/mol
Tetraethanoate	-160,6	358,7 - 392,7	106,4±1,1
Tetrabutanoate	-190,3	364,7 - 392,7	129,8±1,6
Tetra(2-methylpropanoate)	-182,3	344,7 - 372,7	122,5±2,0
Tetrapentanoate	-218,9	372,7 - 402,7	144,1±1,7
Tetra(3-methylbutanoate)	-202,2	372,7 - 402,7	137,4±1,6

Acknowledgements The financial support of RFBR № 19-08-00928 A

[1] E. L. Krasnykh, Y.A. Druzhinina, S. V. Portnova, Y.A. Smirnova, *Fluid Phase Equilibria*, 462, 111

[2] E. L. Krasnykh and S. V. Portnova. *Journal of Structural Chemistry*. 2017, 58, 4, 706.

PII-50. Stability of Solid Phases of Ytterbium Oxide and Oxychloride in Molten Alkali Metal Chlorides

Nikolaeva E.V.^{1, 2}, Zakir 'yanova I.D.^{1, 2}, Sosnovtseva T.V.²

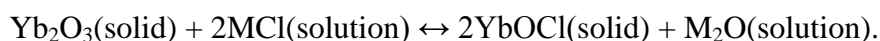
¹Institute of High Temperature Electrochemistry, Yekaterinburg, Russian Federation;

²Ural Federal University, Yekaterinburg, Russian Federation

E.Nikolaeva@ihete.uran.ru

The chloride ionic solvents, among which are alkali and alkali-earth chlorides as well as their mixtures, are characterized by the lack of self-equilibrium of acid-based autodissociation. Nevertheless, some amount of the oxide-ions O^{2-} , forming as a result of interaction with atmospheric oxygen or dissociation of oxygen-containing admixtures, is always presented in such melts. Thermodynamic characteristic of such interaction is the standard chemical potential of the oxygen ion O^{2-} ($\mu^*(O^{2-})$) in corresponding salt media [1]. This parameter can be considered as free Gibbs energy for formation of one mole of oxide in relevant media, discounting the formation energy of an ideal solution

An equilibrium of the Yb_2O_3 and $YbOCl$ solid phases in such salt media can be described by the equation:



The definite value of the oxygen ion concentration corresponds to this equilibrium at certain temperature:

$$pO_{eq} = [2\Delta G^\circ(YbOCl, \text{solid}) - \Delta G^\circ(Yb_2O_3, \text{solid}) + \mu^*(O^{2-})]/2.303RT.$$

The solid oxide phase becomes stable when the melt pO decreases to pO_{eq} . At higher pO values, the oxychloride phase will be stable (Table 1).

The pO_{eq} values increase with rise of the effective radius of the cation of the solvent salt and decrease with temperature growth.

Acknowledgements The study was financial supported by the Russian Foundation for Basic Research (Project No. 18_03_00561a).

Solvent	T, K	$\mu^*(O^{2-})$, kJ/mol [1]	$\Delta G^\circ(YbOCl, \text{solid})$, kJ/mol [2]	$\Delta G^\circ(Yb_2O_3, \text{solid})$, kJ/mol [2]	pO_{eq}
LiCl(0.41)-KCl(0.59)	723	159.6	-1025.538	-1937.281	3.31
CaCl ₂ (0.5)-NaCl(0.5)	823	144.4	-1034.324	-1962.520	2.76
	823	291.6			13.40
NaCl(0.35)-CsCl(0.65)	973	267.4	-1047.504	-2003.315	12.69
	973	254.3			11.75

Таблица 1. The values of pO_{eq} in different chloride solvents (molar units).

[1] E.V. Nikolaeva, A.L. Bovet, A.G. Gavrilov, *Melts*, 2012, **4**, 34.

[2] Barin I. *Thermodynamical data of pure substances*, 1993, VCH Verlags Gesellschaft, Weinheim, Germany.

PII-51. Solubility of Gadolinium Oxide in Molten GdCl₃ - KCl System

Nikolaeva E.V.^{1,2}, Zakir 'yanova I.D.^{1,2}, Korzun I.V.¹

¹Institute of High Temperature Electrochemistry, Yekaterinburg, Russian Federation;

²Ural Federal University, Yekaterinburg, Russian Federation

E.Nikolaeva@ihte.uran.ru

REM chloride melts are often used as electrolytes in high-temperature electrochemical processes. Oxide admixtures in molten REM chlorides essentially affect the properties of electrolytes. The liquidus temperature of the (0.54GdCl₃ - 0.46KCl) - Gd₂O₃ and (0.69GdCl₃ - 0.31KCl) - Gd₂O₃ systems were investigated by the DSC method. On the basis of this data the solubility values of Gd₂O₃ in those melts were found.

Figure 1 illustrates the temperature dependence of Gd₂O₃ solubility in GdCl₃ - KCl molten systems.

The solubility values may be approximated by the (1) in the temperature range under study:

$$\ln S = A + B/T, (1)$$

where *A* and *B* are the empirical coefficients. Table 1 shows the *A* and *B* values for systems under study.

The Gd₂O₃ solubility in molten 0.69GdCl₃-0.31KCl system is larger than that in molten 0.54GdCl₃ - 0.46KCl system at the same temperature. This fact agrees well with the literature data [1]. The Gd₂O₃ solubility in molten chloride melts increases with increasing of GdCl₃ content.

Acknowledgements The study was financial supported by the Russian Foundation for Basic Research (Project No. 18_03_00561a).

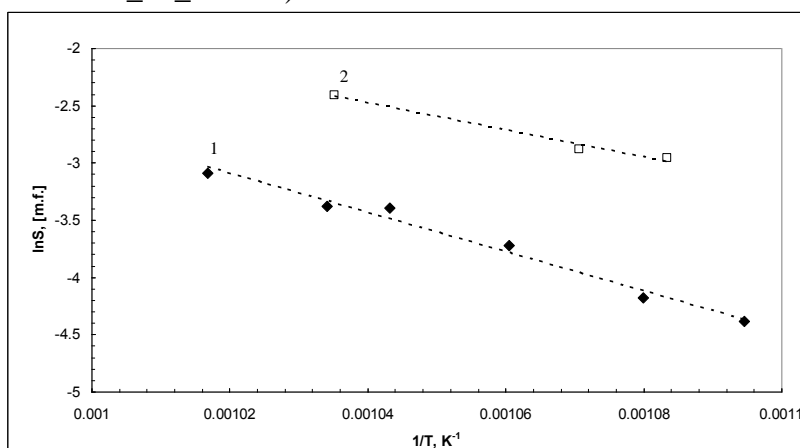


Figure 1. Temperature dependence of Gd₂O₃ solubility in molten chloride systems: 0.54GdCl₃ - 0.46KCl (1); 0.69GdCl₃ - 0.31KCl (2).

Solvent	Temperature interval, K	A	-B·10 ⁴	Δ(lnS)	R ²	S at 950 K, m.f.
0.54GdCl ₃ - 0.46KCl	836 - 984	14.37	1.71	0.08	0.99	0.015
0.69GdCl ₃ - 0.31KCl	923 - 966	9.80	1.18	0.10	0.99	0.050

Table 1. Coefficients of (1) for molten GdCl₃ - KCl systems.

[1] H.Medias, O.Tkatcheva, V.Dracopoulos et al., *Metall and Mat Trans A*, 2000, 31B, 631.

PII-52. Phase Equilibria in Oxide-Chloride Systems $Gd_2O_3 - GdCl_3$ AND $Gd_2O_3 - GdCl_3 - KCl$

Korzun I.V., Nikolaeva E.V. and Zakir'yanova I.D.

Institute of High Temperature Electrochemistry, Yekaterinburg, Russian Federation

korzun@ihte.uran.ru

Using certified samples the new data on phase equilibria in oxide-chloride systems $Gd_2O_3 - GdCl_3$ and $Gd_2O_3 - GdCl_3 - KCl$ have been obtained by the methods of cooling curves and differential scanning calorimetry (DSC).

When measured by the cooling curves method, the melt temperature is recorded as a function of time during the cooling period.

DSC measurements were performed using a synchronous thermal analyzer STA 449C Jupiter® with a heating rate of 5K / min in a high-purity argon atmosphere.

The use of two independent research methods have been allowed obtaining reliable, reproducible and well-consistent data on the liquidus temperatures of the studied oxide-chloride systems with a gadolinium oxide content of up to 9 mol. % (Fig. 1, 2).

Acknowledgements The partial financial support of the Russian Foundation for Basic Research, project № 18-03-00561a.

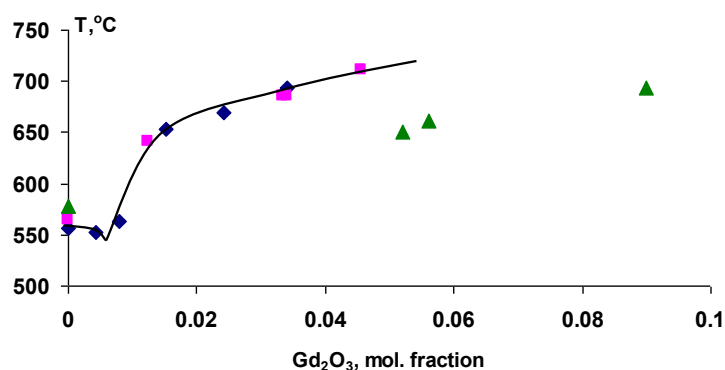


Figure 1. Liquidus temperatures of oxide-chloride systems $Gd_2O_3 - GdCl_3 - KCl$: $0.543GdCl_3 - 0.457KCl - Gd_2O_3$ (squares, ■ - cooling curves method, ■ - DSC); $0.69GdCl_3 - 0.31KCl - Gd_2O_3$ (triangles - DSC method)

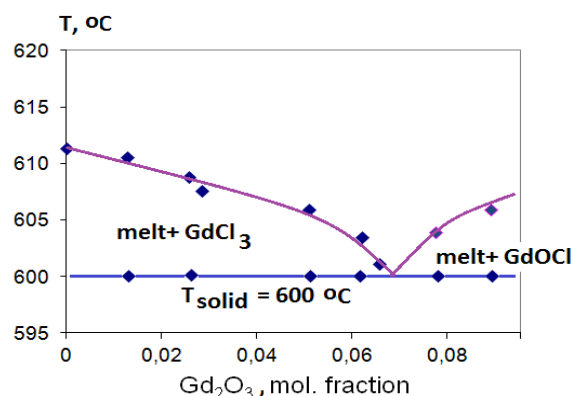


Figure 2. Phase equilibria in the $Gd_2O_3 - GdCl_3$ system

PII-53. Modifications of Ethanol, Toluol and Water at Equilibrium System Liquid - Perfect Gas

Vitvitskiy A.I.

Saint Petersburg, Russia

avitvitskiy@mail.ru

When creating the foundations of chemical thermodynamics, the unified law of ideal gas was not taken into account, according to which, under the same conditions, the same cell of space falls on one molecule of different gaseous substances. The volume of one cell is directly proportional to temperature and inversely proportional to pressure. Taking into account the combined ideal gas law, it was shown [1, 2] that with phase equilibrium in liquid-gas and crystal-gas systems, the equilibrium partial pressure of the substance in the gas phase (P_p , Pa) depends on temperature (T , K) by the equation

$$P_p = (P_m T_m / T) \times \exp(1 - T_m / T),$$

where T_m and P_m are the limiting equilibrium parameters at which the equation becomes an identity. The experimental reference values of P_p and T , presented in $\ln(P_p T) - 1/T$ coordinates, form a straight line relationship that allows you to reliably extrapolate the data to a practically unexplored supercritical region (temperature above critical) and to the supercooled liquid region (temperature below the triple point).

When analyzing the characteristics of the equilibrium state in the liquid-gas system of ethanol and toluene [3], it turned out that they have two modifications of the liquid state (liq.1, liq.2), and the water in the liquid-gas system [4] has three modifications (liq.1, liq.2, liq.3). The table shows the coefficients-parameters of the equation for the description of the equilibrium states of the studied substances and the temperature range of its application; the temperature with index 12 corresponds to the triple system liq.1-gas-liq.2, the temperature with index 23 corresponds to the triple system liq.2-gas-liq.3. The accuracy of the description of the experimental reference material is about $\pm 1\%$ ($\pm 2.6\%$ for $C_6H_5CH_3$, liq.2). The heat of formation of one mole of a gaseous substance (Q_T , J/mol) related to the temperature by $Q_T = R(T_m - T)$, where $R = 8.31447 \text{ J}/(\text{mol} \times \text{K})$. Inside the liquid, the minimum volume of the ideal gas cell ($V_m = RT_m/P_m$, m^3/mol) is commensurate with the own-volume of the molecules of the liquid modification.

Table Modifications of ethanol, toluene and water in liquid state

Substance, system	T_m , K	P_m , MPa	V_m , m^3/mol	Area of implementation
C_2H_5OH : liq.2-gas,	4911.9	3350	12.19×10^{-6}	from 370.5 ₁₂ K to 4911.9 _m K
liq.1-gas.	5429.7	12260	3.68×10^{-6}	from 0 K to 370.5 ₁₂ K
$C_6H_5CH_3$: liq.2-gas,	4527.5	417.8	90.10×10^{-6}	from 332.6 ₁₂ K to 4527.5 _m K
liq.1-gas.	5023.6	1673	24.97×10^{-6}	from 0 K to 332.6 ₁₂ K
H_2O : liq.3-gas,	5199.6	3085	14.01×10^{-6}	from 379.0 ₂₃ K to 5199.6 _m K
liq.2-gas,	5475.8	6071	7.50×10^{-6}	from 296.3 ₁₂ K to 379.0 ₂₃ K
liq.1-gas.	5709.2	12800	3.71×10^{-6}	from 0 K to 296.3 ₁₂ K

[1] Anatoly Vitvitskiy, *Chemicals, Conditions of equilibrium states and conversion* (in Russian), <https://www.lap-publishing.com>. ISBN-13: 978-3-330-08416-2, 64 p. Published 2017.05.12.

[2] A.I. Vitvitskiy, *Russ. J. Appl. Chem.*, 2016, 89, 2, 196-199. DOI: 10.1134/S1070427216020051.

[3] A.M. Moskvina (ed.), *New Handbook of Chemist and Technologist. General Information. Structure of Substance. Physical Properties of the Most Important Substances...* (in Russian), 2006. Professional, St. Petersburg. PP. 158, 178, 225, 226.

[4] A.A. Ravdel, A.M. Ponomareva, (eds), *Concise Handbook of Physicochemical Quantities* (in Russian), 2010. Aris, Moscow. P. 28.

PII-54. The Study of Phase Equilibria in the Fe-Cu-As, Fe-As-S, Cu-As-S Systems

Trofimov E.A.¹, Starykh R.V.², Sineva S.I.², Zaitseva O.V.¹, Galkina D.P.¹

¹South Ural State University, 76, Lenin Ave., Chelyabinsk 454080, Russia;

²Peter the Great St.Petersburg Polytechnic University,
29, Polytechnicheskaya str., St.Petersburg 195251, Russia

tea7510@gmail.com

The high toxicity of arsenic and its compounds significantly increases the cost of a number of metallurgical technologies. During the processing of polymetallic ores, arsenic goes into various metallurgical semi-products and industrial wastes. For example, in lead and zinc production, only about a third of the arsenic of the feedstock turns into waste products, and in the copper industry, about 40% of the arsenic of the feedstock turns into gas emissions and wastewater. Arsenic is also found in converter dusts of copper production, lead mill spares, and copper slips.

Large amount of research work is devoted to the problem of removal arsenic from technological processes and neutralization it into non-toxic forms for further storage. Despite certain scientific and technological results achieved in this area, this task is still far from being solved, and it is relevant to solve this problem using physico-chemical approach. At the same time, the methods of dearsenization, involving the transfer of arsenic into sulphides and arsenides of various metals are the most effective, since they are compact and convenient for transportation, storage and disposal. Thus, it is necessary to develop the effective ways for the conversion of arsenic to sulphide form and/or to As-Fe solution. Both sulfur and iron are essential components of arsenic-containing raw materials of non-ferrous and precious metals. Thus, the bonding of arsenic in compounds or solutions of the As-Fe-Cu-S system is practically justified, and knowledge of the phase equilibria realized in this quaternary system should develop the pyrometallurgical technologies for dearsenizing metallurgical intermediates and subsequent neutralization of arsenic. At the first stage of the project execution it is necessary to study the phase equilibria in the Fe-Cu-As, Fe-As-S, and Cu-As-S ternary systems. This work is devoted to solving of this task.

In the course of the work carried out using a complex of experimental physicochemical research methods, projections of liquidus and solidus surfaces of three-component Fe-Cu-As, Fe-As-S, and Cu-As-S systems were constructed in a wide range of compositions, excluding the area of «sulfur corner».

The thermodynamic description of ternary Fe-Cu-As, Fe-As-S, and Cu-As-S systems is carried out. The database of thermodynamic characteristics have been created, allowing to carry out phase equilibrium calculations in these systems using ThermoCalc and FactSage software.

The information on phase equilibria in the Fe-Cu-As, Fe-As-S, and Cu-As-S systems obtained at this stage makes it possible to estimate the compositional regions of the systems, within whose boundaries arsenic can form intermediates or solid solutions and give primary recommendations to technologists. The results obtained will be the basis for constructing the phase equilibrium diagram of the Fe-Cu-As-S quaternary system. The use of the obtained data gives the possibility for the development of a pyrometallurgical method of dearsenizing ores and concentrates of heavy, non-ferrous and precious metals with the conversion of arsenic to a low-toxic sulfide or arsenide form.

Acknowledgements The reported study was funded by RFBR according to the research project № 18-29-24166.

PII-55. Study of Phase Equilibria at the Fe-As-S Ternary System

Starykh R.¹, Ilatovskaia M.², Kostyanko A.³, Trofimov E.A.⁴, Samoiloa O.⁴, Sineva S.^{1,5}

¹ LLC Gipronickel Institute, Russia; ²TU Bergakademie Freiberg, Germany;

³Peter the Great St.Petersburg Polytechnic University, Russia;

⁴South-Ural State University, Russia; ⁵University of Queensland, Australia;

kafedra-cm@yandex.ru

Arsenic, sulphur and iron are the accompanying elements of any polymetallic ores, treated for exploration of non-ferrous and precious metals. Arsenic is very toxic and harmful element, and should be associated with Fe and S in a form of low toxicity compounds for further removal and storage. For example, formation of arsenic sulphides or arsenides (FeAs, Fe₂As, FeAs₂) can take place during the melting. These compounds are stable at ambient temperature and safe for environment. So, information about phase equilibria at the Fe-As-S ternary system, especially at high temperature range, is very important. Obtained data will allow to provide removal arsenic from metallurgical semiproducts followed by further arsenic neutralization.

The Fe-As-S system is very complex for experimental study due to high toxicity and high partial pressures of arsenic and its compounds. These difficulties determine serious lack of available information regarding phase diagram of the discussed system, as well as absence of liquidus surface projection scheme. Data about phase equilibria are published only at several original issues. So, isothermal section of the Fe-As-S system at 600°C was constructed at [1]. Author of research [2] were the first who established some nonvariant reactions of the system. Following literature reviews of the discussed system [3, 4] refer to mentioned above original works. Consequently, the necessity of detailed experimental investigation of phase equilibria at Fe-As-S system is evident.

With the applying of special experimental techniques, developed by authors or the projects, including high pressure furnace, arsenic sulphides or arsenides were synthesized. Initial sulphides or arsenides as well as high purity iron and arsenic were used for synthesis of ternary compositions. Obtained samples were investigated with the use of spectrum of experimental physico-chemical methods, namely, differential thermal analysis (DTA), scanning electron microscopy (SEM), energy-dispersive microanalysis (EPMA) and X-ray diffraction analysis (XRD). The study of phase equilibria at Fe-As-S ternary system was made from construction of FeS-AsS polythermal section, thus limiting system by sulphur content, as well as FeS-AsFe and FeS-Fe₂As quasibinary sections. Temperatures of phase transitions and nonvariant reactions also compositions of coexisting phases have been defined. Obtained information will be used for construction the liquidus surface projection of the Fe-As-S ternary system.

Acknowledgements The study was funded by RFBR grant No. 18-29-24166.

[1] L.A.Clark, "The Fe-As-S system: Phase Relations and Applications", *Econ. Geol.*, 55, 1345-1381; 1631-1652 (1960).

[2] P. B. Barton; Jr., "Thermochemical Study of the System Fe-As-S", *Geochim. Cosmochim. Acta*, 33, 841-857 (1969).

[3] Raghavan, V., "The As-Fe-S (Arsenic-Iron-Sulphur) System", *Phase Diagrams of ternary Iron alloys*, 2, 35-50 (1988)

[4] O. Kubashewski "Arsenic-Iron-Sulphur", *Ternary Alloys Series*, VCH Verlagsgesellschaft, Weinheim, MSI GmbH, Stuttgart, Germany, 9, 276-296

PII-56. Thermophysical Properties of Ionic Liquids at Wide Range of State Parameters

Safarov J.T.¹, Guluzade A.N.², Hassel E.P.¹

¹Institute of Technical Thermodynamics, University of Rostock, Germany

²Department of Heat Energy, Azerbaijan Technical University, Baku, Azerbaijan

javid.safarov@uni-rostock.de

Investigations of thermophysical properties of typical stable room temperature ionic liquids (ILs) have been increased during the last 20 years. ILs have been suggested as potentially “green” replacements for conventional organic solvents since they are nonvolatile (negligible vapor pressure), nonflammable, thermal stable, and recyclable. They have low melting point, high solvating capacity, high ionic conductivity and high thermal stability, which make them attractive for practical applications. This creates new opportunities for reaction, separation, photochemical and electrochemical processes. ILs has also wide range application as heat transfer fluids and short heat term storage in power plants.

In this case, the study of thermophysical properties of them is very important. This work present our investigations of these properties of 1-alkyl-3-methylimidazolium ionic liquids with trifluoromethanesulfonate anions {[C₂MIM][TFO], [C₄MIM][TFO], [C₆MIM][TFO], [C₈MIM][TFO]} at $T=(273.15$ to $413.15)$ K and pressures up to $p=140$ MPa, which was determined using a high pressure – high temperature Anton-Paar DMA HMP vibrating tube densimeter. The measuring system was calibrated using various standard fluids (double-distilled water, aqueous NaCl solutions, methanol, ethanol, toluene, acetone etc.) with well-known reference density data. The temperature steps were $\Delta T=(5$ to $20)$ K, whereas for pressures, typical steps (for pressures above 5 MPa) were $\Delta p=(5$ to $10)$ MPa. The temperature in the measuring cell, where the U-tube is located, was controlled using a thermostat (F32 - ME Julabo, Germany) within 10 mK and was measured with the (ITS-90) Pt100 thermometer (Type 2141) with an expanded absolute uncertainty of $U(T) = 0.015$ K. Pressure was measured using a pressure transmitters P-10, P-30 (0.25, 2.5, 50, 100 MPa) and HP-1 (160 MPa) with an expanded relative standard uncertainties U of (p, ρ, T) measurements in: $U(p) = 0.00025$ MPa for $p < 0.25$ MPa, $U(p) = 0.0025$ MPa for $p < 2.5$ MPa, $U(p) = 0.01$ MPa for $p < 10$ MPa, $U(p) = 0.1$ MPa for $p < 100$ MPa, $U(p) = 0.25$ MPa for $p > 100$ MPa. The mPDS2000V3 control unit of DMA HMP vibrating tube densimeter measures the vibrating period with an accuracy of $\Delta \tau = \pm 0.001 \mu s$. According to the specifications of Anton-Paar and calibration procedures performed in our laboratory, the observed repeatability of the density measurements at temperatures $T = (263.15$ to $468.55)$ K and pressures up to $p = 140$ MPa is within $\Delta \rho = \pm(0.1$ to $0.3)$ kg·m⁻³ or $\Delta \rho/\rho = \pm(0.01$ to $0.03)\%$. But, the experimental data reported here, attending the high viscosity corrections to vibration tube periods have an expanded uncertainty within $\Delta \rho/\rho = \pm(0.01$ to $0.08)\%$.

An empiric equation of state (EOS) for fitting of the (p, ρ, T) data of ILs has been developed as a function of pressure, temperature and molecular weight of ionic liquids. The heat capacity $c_p(p_0, T)$, speed of sound $u(p_0, T)$ and viscosity $\eta(p_0, T)$ measurements of these ILs at ambient pressure and wide range of temperatures also measured using a differential scanning calorimeters, Anton Paar DSA 5000M, SVM 3000 Stabinger and Rheometer MCR 302 installations. EOS is used for the calculation of the various thermophysical properties, like isothermal compressibility, $\kappa_T(p, T)$, isobaric thermal expansivity, $\alpha_p(p, T)$, thermal pressure coefficient, $\chi(p, T)$, internal pressure, $p_{int}(p, T)$, specific heat capacities, $c_p(p, T)$ and $c_v(p, T)$, speed of sound, $u(p, T)$ and isentropic exponent $\kappa_s(p, T)$ at wide range of temperatures and high pressures. The available literature values of ILs were compared with our calculated values and good agreement was obtained.

PII-57. Vapor Pressure of 1-Butyl-3-Methylimidazolium Trifluoromethanesulfonate and Methanol Solution over Wide Range of Temperature

*Safarov J.T.*¹, *Guluzade A.N.*², *Nocke J.*¹, *Hassel E.P.*¹

¹Institute of Technical Thermodynamics, University of Rostock, Germany

²Department of Heat Energy, Azerbaijan Technical University, Baku, Azerbaijan

javid.safarov@uni-rostock.de

Ionic liquids (ILs) have been suggested as potentially “green” replacements for conventional organic solvents since they have negligible vapor pressure, low melting point, high solvating capacity, high ionic conductivity and high thermal stability, which make them attractive for practical applications. They are nonflammable, thermal stable, and recyclable. ILs and organic substances has also wide range application in various industrial branches. For such application, the vapor-liquid equilibria properties (VLE) of mixtures and activity coefficient of solutions are necessary.

In this work, we present the new VLE measurements of binary 1-butyl-3-methylimidazolium trifluoromethanesulfonate and methanol $\{x\text{CH}_3\text{OH}+(1-x)[\text{BMIM}][\text{TFO}]\}$ solutions at $T=(274.15$ to $413.15)$ K using a two high-accuracy static experimental installations: two different glass cells (absolute or difference measurements) are used for vapor pressures lower than ambient pressure at temperatures $T=(274.15$ to $323.15)$ K using a calibrated high accuracy pressure sensor head (Type 615A, MKS Baratron, USA) with $\Delta P = \pm (10$ to $30)$ Pa experimental uncertainty. The temperature inside the cell is measured by a platinum resistance thermometer PT-100, connected to a signal conditioner Omega PT-104A, with an accuracy of $T = \pm 0.001$ K. All systems are controlled using the LabVIEW program. The stainless steel metal cell for VLE measurements at temperatures $T=(323.15$ to $413.15)$ K) were determined using three various Omega-Keller pressure transmitters ranging from a maximum pressure of 300 kPa with uncertainty $\Delta P=\pm(0.4$ to $1.5)$ kPa, to a pressure of 1000 kPa with uncertainty $\Delta P=\pm(1$ to $5)$ kPa and to a pressure of 1600 kPa with uncertainty $\Delta P=\pm(2$ to $8)$ kPa. The experimental vapor pressure P/Pa results are assessed to be reliable to within $\Delta P=\pm 0.05\%$ average uncertainty according to test measurements and were carried out starting from low temperature ($T=323.15$ K) to high temperature ($T=413.15$ K) and return way with $\Delta T=10$ K intervals. The temperature of the measuring cell and heat transfer reservoir is controlled using a thermostat with an accuracy of $\Delta T=\pm 0.01$ K using two different PT-100 thermometers. One of them is directly connected to the thermostat via PT-100 Libus Modul. This thermometer transfers information from the measuring cell. Using this thermometer, the thermostat sets the desired temperature directly inside of the measuring cell, but not within the thermostat itself. This is a very important point, because it is possible to set, stabilize, and measure the experimental temperature with high accuracy directly in the measured medium. The second PT-100, transfers the measured temperature in the computer via an Omega PT-104A Channel RTD Input Data Acquisition Module for the measuring of temperature, with an accuracy of $\Delta T=\pm 0.001$ K.

The experimental VLE results of investigated $\{x\text{CH}_3\text{OH}+(1-x)[\text{BMIM}][\text{TFO}]\}$ solutions were fit to the various equations. From the vapor pressure data activities of the methanol, osmotic and activity coefficients at $T=(274.15$ to $413.15)$ K have been obtained. The calculated activity coefficients γ_i are described using the NRTL and Clapeyron-Clausius equations. These investigations were carried out at the first time and in this case, no literature comparisons are available.

PII-58. Molecular Models for Phase Equilibria of Alkanes with Air Components and Combustion Products

Vishnyakov A.V.^{1,2}, Chiew Y.², Weathers T.³, Neimark A.V.², Hosangadi A.³*

¹Skolkovo Institute of Science and Technology, Moscow, Russia;

²Rutgers the State university of NJ, Piscataway NJ, USA

³Combustion Research and Flow Technology, Pipersville PA, USA

a.vishnyakov@skoltech.ru

The paper reports simulation study of phase diagram and interfacial properties in mixtures of linear hydrocarbons with oxygen, nitrogen, CO₂ and water. We consider four alkanes: methane, propane, octane and dodecane as characteristic components of natural gas, liquefied natural gas, gasoline and kerosene. Combustion products are presented with common molecular models (three-center models for O₂, N₂, and CO₂, TIP4P-2005 model for water), and hydrocarbons are modelled with united-atom models. The only exception is methane, for which we also use an explicit hydrogen TraPPE forcefield. The parameters for oxygen interactions with CH₂ and CH₃ groups are calculated with Lorentz-Berthelot mixing rules with a single adjustable coefficient for ϵ , which was assumed equal for all temperatures and mixtures. We obtained very reasonable agreement with the experimental data for most binary mixtures and discuss in details the capability of models with unified adjustable parameters.

Keywords: Vapor-liquid equilibria, molecular simulations, interfacial tension, Monte Carlo.

Acknowledgements The studies were supported by US DoD.

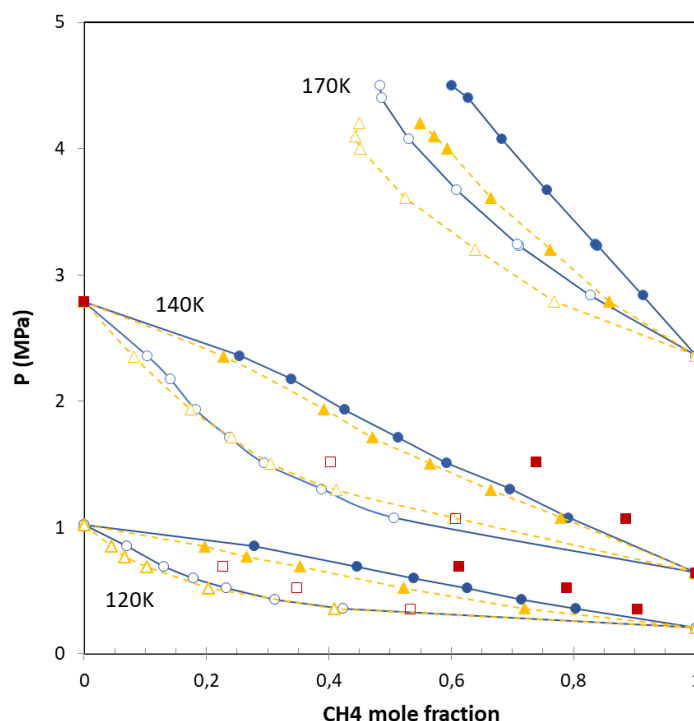


Figure 1. Methane—oxygen VLE phase diagrams obtained with GEMC simulations using TraPPE-EH and VF models for methane and Hansen model for oxygen. Solid symbols – liquid line, open symbols – vapor. Results obtained with the TraPPE-EH forcefield are denoted by circles, the results obtained by the VF model are shown in triangles with $\eta_{\text{CHX-O}} = 1$ and in squares with $\eta_{\text{CHX-O}} = 0.90$

PII-59. Determination of Separatric Manifold Structure of Five-Component System Phase Diagram

Frolkova A.V., Makhnarilova E.G.

MIREA – Russian Technological University, Russian Federation

frolkova_nastya@mail.ru

Analysis of VLE diagrams of multicomponent systems is a rather complex task, primarily due to the multidimensionality of the problem. There is an effective method of studying the structure of the diagram of the four - and five-component systems [1-2], which allows to predict the existence of n -component azeotrope. To determine the type of the latter it is necessary to know the structure of separatric manifold. This paper presents an algorithm for constructing and analyzing the structure of a three-dimensional separatric hypersurface of a VLE diagram of five-component systems. It is based on the analysis of the composition simplex scans of different dimensions (2 and 3). The analysis of two-dimensional scan gives the answer for question whether there is a separatric manifold and if so, how many of them are in the system (the number of saddle azeotropes of 1-st or $(n-2)$ order). Analysis of scans allows selecting a group of singular points, one - and two-dimensional separatric manifolds, which are involved in the formation of three-dimensional separatric hypersurface. After gluing two-dimensional surfaces, the types and indexes of singular points are to be determined with respect to the complete structure of the three-dimensional hypersurface and the balance of indexes of singular points is to be checked (the sum of the indexes must be zero).

The proposed algorithm was illustrated on the example of the system ethanol – water – toluene – butyl acetate – ethyl cellosolve (regeneration of toluene waste solvents). Figure 1 presents qualitatively a two-dimensional scan of pentatope (the yellow highlighted line is one-dimensional boundary of a three-dimensional separatric manifold that separates the distillation region with stable node water), and two three-dimensional hypersurfaces (generated by the two azeotropes of saddle type of the first order: W-EC and BA-EC) built according to the proposed algorithm.

Acknowledgements The financial support of Russian Science Foundation 19-19-00620

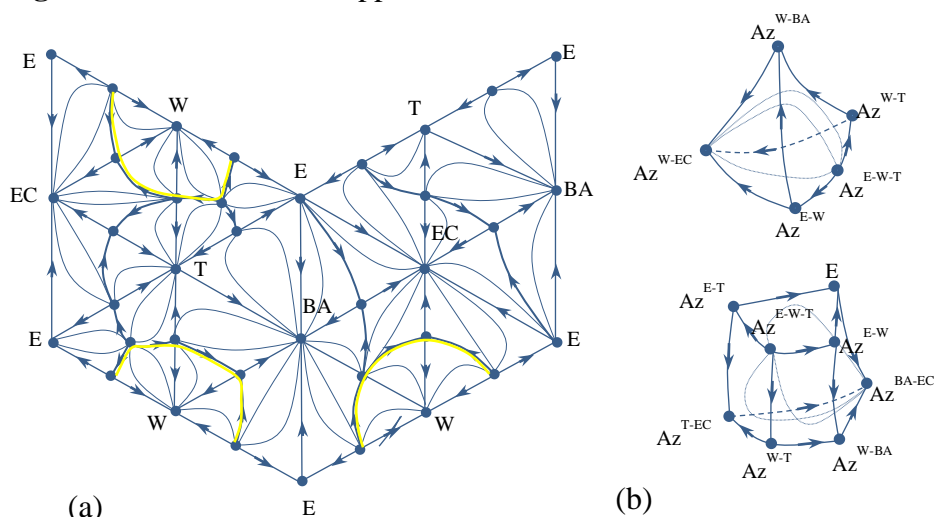


Figure 1. Second dimension scan of composition pentatope (a) and the structure of separatric manifold (b) for ethanol (E) – water (W) – toluene (T) – butyl acetate (BA) – ethyl cellosolve (EC) system

[1] L.A. Serafimov, etc. *Theoretical Foundations of Chemical Engineering*, 2012, 46 (2), 120.

[2] L.A. Serafimov and A.V. Frolkova, *Chemical Papers*, 2016, 70 (12), 1578.

PII-60. The Properties of Separatric Manifold as Poincare Integral Invariant

Frolkova A.K., Frolkova A.V.

MIREA – Russian Technological University, Russian Federation

frolkova_nastya@mail.ru

The composition space of the vapor-liquid equilibrium diagram of n -component system is a simplex of $(n-1)$ dimension. Depending on the presence of special points in the system, in particular of saddle type, the phase diagram can be divided by separatric surfaces of $(n-2)$ dimension into a set of the distillation regions. These varieties have properties of the Poincare integral invariant [1], which is an m -fold integral extended to the surface of the corresponding dimension [2]. In the case of a distillation process, described by a system of nonlinear differential equations, the fold of the integral is determined by the dimension of the separatric manifold (for systems with $n=3$ – one-, $n=4$ – two-, $n=5$ – three-, for n – $(n-2)$ -fold). Properties mentioned above include: the presence of $(m-1)$ -dimensional subspace in the space of m dimension; the insularity with respect to the motion of the phase point (the total variation for the open chemically inert system is $n+2$, for the phase point located on the separatric manifold $n+1$ [2]); the presence of own structure of subspace; the compliance with the normalization condition (the sum of the concentrations is equal to one).

If the phase process is considered with the pressure changes (the analogy with the change of the phase space in time [1]), the displacement of singular points can be observed (without disappearance and appearance of new ones). In this case, for the same separatric manifold $(n-2)$ -fold integral does not change at different pressures (the invariant property). For systems with number of components greater than 3 it is possible to observe the continuous deformation of separatric manifold, the overall structure is preserved (figure 1). For ternary systems, separatric line (the first dimension) is indistinguishable from other distillation lines (does not have its own structure) and when the pressure changes it does not undergo a quantitative deformation, that is, for a one-dimensional separatric manifold a part of the Poincare integral invariant characteristics is not satisfied. This fact puts such systems ($n=3$) on a special "transition" stage between binary ($n=2$) and multicomponent ($n>3$).

Acknowledgements The financial support of Russian Science Foundation 19-19-00620

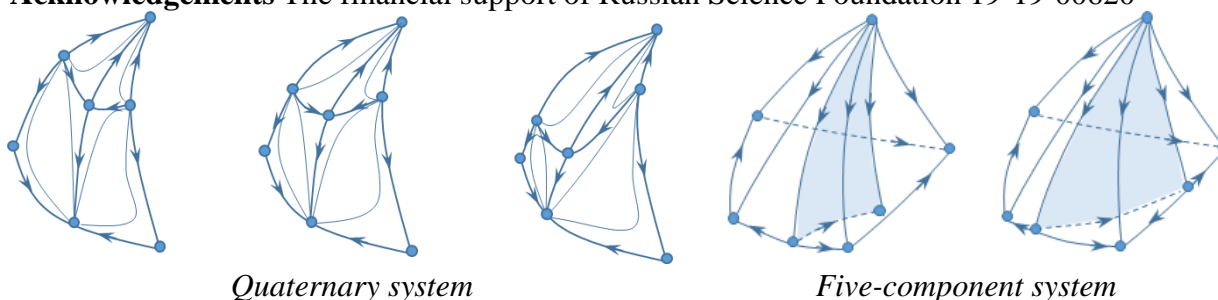


Figure 1. Deformation of separatric manifold structure of quaternary and five-component systems with pressure change

[1] A. Poincaré, *Gauthier-Villars*, V. 3, 1899, **Gauthier-Villars**, Paris, France

[2] L.A. Serafimov, A.K. Frolkova and A.V. Frolkova, *Theoretical Foundations of Chemical Engineering*, 2013, 47 (2), 124.

PII-61. Liquid ⇌ Gas Phase Transitions Water+Aliphatic Alcohol Binary Mixtures

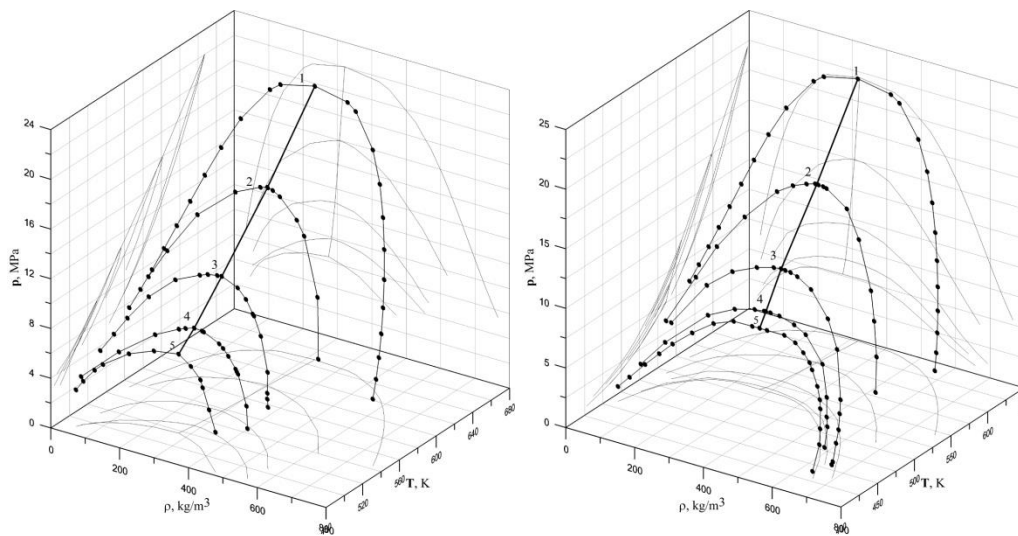
Osmanova B.K, Bazaev A.R., Bazaev E.A.

Institute for Geothermal Research of the Daghestan Scientific Center of the Russian Academy of Sciences, Shamil 39A, Makhachkala, Daghestan Republic, 367030, Russia

badji@mail.ru

By using our experimental data on p, T and p, ρ, T, x – dependences of binary homogeneous water+aliphatic alcohol (methanol, ethanol, 1-propanol) mixtures ($x=0.2, 0.5$ and 0.8 mol.fractions of alcohol) at two-phase, one-phase, nearcritical and supercritical regions of state parameters and using isochoric p - T break points of phase diagram parameters of liquid gas phase transitions are determined.

The equilibrium curves of liquid and gas phases of three researched systems are located between those of pure water and alcohol. The critical curves of water+methanol and water+ethanol systems have smooth and concave form regarding to pressure axis (fig.1a) and the critical curve of water – 1-propanol system has convex form (fig.1b). These facts can be explained by structural features of the mixtures.



a b

Fig.1. p, ρ, T - diagram of phase coexistence curves and their projections of water–ethanol (a) and water–1-propanol binary mixtures (b). Water (1), alcohol (5), $x=0.2$ (2); 0.5 (3); 0.8 (4).

The dependence of pressure of 1-propanol – n-hexane binary mixtures from temperature and composition of mixtures along the phase coexistence curve is described by three-parameter polynomial equation represented by expansion of the compressibility factor $Z = p/RT \rho_m$ into a power series of reduced density $\omega = \rho/\rho_{cr}$, reduced temperature $\tau = T/T_{cr}$ and composition x :

$$Z = p / RT \rho_m = 1 + \sum_{i=1}^m \sum_{j=0}^n \sum_{k=0}^s a_{ijk} \omega^i \cdot x^k / \tau^j \quad \text{and} \quad p = RT \rho_m \left[1 + \sum_{i=1}^m \sum_{j=0}^n \sum_{k=0}^s a_{ijk} \omega^i \cdot x^k / \tau^j \right].$$

The average relative error of calculated values of pressure from experimental ones less than 0.7 %.

PII-62. Liquid-Liquid Equilibrium of Ternary System Cyclohexene + Water + N,N-Dimethylacetamide

Zhuchkov V.I., A. Malyugin A., Frolkova A.V., Frolkova A.K.

MIREA – Russian Technological University, Russian Federation

v-zhuchkov@yandex.ru

N,N-dimethylacetamide can be used for the oxidation of cyclohexene to cyclohexanone in the presence of palladium catalysts [1]. The composition of the mixture supplied to the reactor must belong to the region of homogeneous compositions. In reaction system there are components that are characterized by limited mutual solubility (water and cyclohexene). The liquid-liquid equilibrium (LLE) in this system was studied experimentally to determine the homogeneous region in the phase equilibrium diagram at 295.15 K and atmospheric pressure (close to the reaction condition). The binodal curve was determined by the cloud point titration method under isothermal conditions. A significant difference in the refractive indexes of components makes it possible to use refractometric method to analyze compositions of equilibrium liquid layers with a sufficiently high degree of accuracy. Othmer-Tobias equation was used to check and confirm the reliability of the measured tie-line data (Table 1). LLE diagram of ternary system was built (Fig.1). Binary interaction parameters of the NRTL model were regressed. It was determined that the experimental and calculated (NRTL) data are in good agreement.

Acknowledgements The financial support of Russian Science Foundation 16-19-10632

Table 1. Compositions (W%) of equilibrium liquid layers in cyclohexene + water + N, N-dimethylacetamide ternary system 295 K

Point number	Gross composition		Lower layer composition		$n_D^{295.15}$	Upper layer composition	
	Water	DMAA	Water	DMAA		Water	DMAA
1	44.70	9.26	82.50	17.00	1.3580	traces	0.5
2	38.04	22.17	63.00	36.20	1.3818	0.1	0.9
3	36.44	27.24	56.90	42.20	1.3896	0.1	1.1
4	32.34	39.02	45.30	53.70	1.4045	0.1	3.0
5	25.55	49.47	33.70	64.80	1.4178	0.1	3.6
6	21.43	58.11	26.40	71.00	1.4253	0.1	4.5
7	14.77	69.12	16.00	77.60	1.4320	0.50	9.0

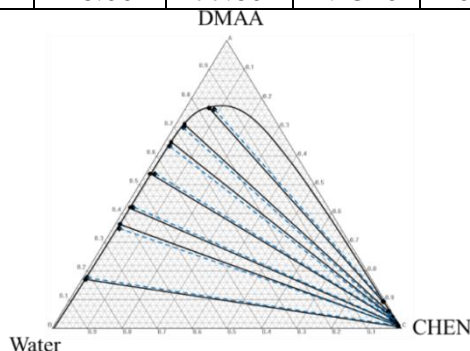


Figure 1. LLE phase diagram for the system cyclohexene (CHEN) + Water (W) + dimethylacetamide (DMAA) at 295 K (experimental data (●); calculated by NRTL model (◆)) [1] Temkin, O.N., etc., *Kinet. Catal.*, 2010, 51 (5), 691.

PII-63. Determination of Critical Parameters of the Mixture $[x\text{H}_2\text{O}+(1-x)\text{C}_7\text{H}_{16}]$ ($x = 0.053$ Molar Fractions) by the Method of Pressure Measurement

Nazarevich D.A., Mirskaya V.A., Ibayov N.V.

Institute of Physics, Dagestan Scientific Center, Russian Academy of Sciences, Russian Federation

naz_77@mail.ru

We have investigated the pressure of the system $[x\text{H}_2\text{O}+(1-x)\text{C}_7\text{H}_{16}]$ with the content of the polar component (water) $x=0.053$ m.f. at the automated installation for the study of Cv and PVT properties of liquids and gases. Studies were conducted on 11 isochores. It is shown how the addition of a small amount of water affects the parameters of the critical point.

We used a digital strain gauge. It is mounted on a valve located on the axis of rotation of the experimental cell and thermostatically controlled. This makes it possible to measure pressure with continuous stirring of the test substance, which in turn creates conditions for thermal equilibrium throughout the entire volume of the experimental cell.

Figure 1 shows the pressure isochores of the mixture $[x\text{H}_2\text{O}+(1-x)\text{C}_7\text{H}_{16}]$ in the density range from 150 kg/m^3 to 501 kg/m^3 and a pressure range from 0.1 MPa to 16 MPa. The n-heptane-water system undergoes two phase transitions during heating: from three-phase (liquid-liquid-vapor) to two-phase (liquid-vapor) and then to single-phase (liquid or vapor). The liquid – liquid phase transition is characterized by an inflection in the course of the $f=P(T)$ curve, while the liquid – vapor phase transition is characterized by a fracture. For vapor isochores, the fracture leads to decrease in the rate of pressure growth, and for liquid isochores - to an increase. For the critical isochore, no fracture is observed.

For a more accurate determination of phase transition parameters, we used the dependence of the derivative of pressure on temperature (dP/dT) of temperature (T) (fig. 2). From this graphs we can see, that for vapor isochores the value of the derivative at the phase transition point to a single-phase state decreases sharply, and for liquid isochores - it increases sharply. For the critical isochore the plot of the $f=dP/dT(T)$ dependence does not have sharp jumps. It only undergoes a fracture. The addition of a small amount of water leads to a shift of the critical point parameters both towards lower temperatures and towards lower densities, but the pressure at the critical point increases.

Acknowledgements This work was financially supported by the Russian Foundation for Basic Research (grant of the Russian Foundation for Basic Research No. 17-08-00800)

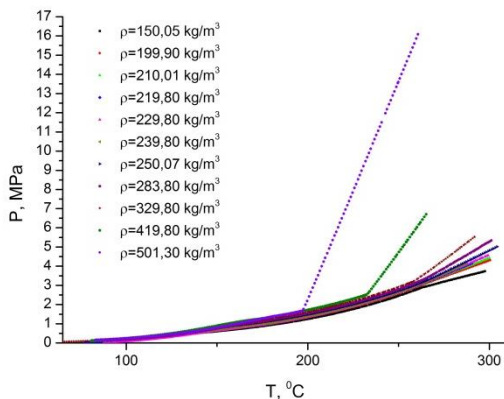


Figure 1. Pressure isochores of mixture.

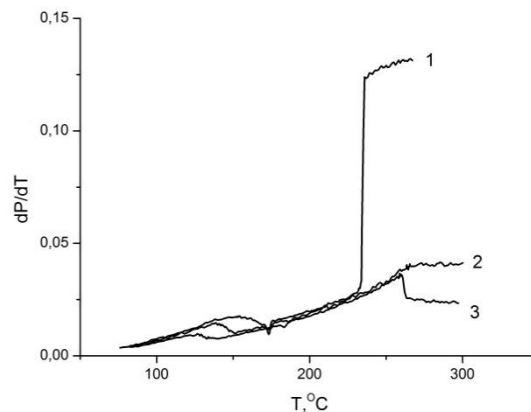


Figure 2. Dependence $f=dP/dT(T)$. 1 - liquid isochore, 2 - critical isochore, 3 - vapor isochore

PII-64. Experimental Assessment of the Ionic Liquids Selectivity for Extractive Distillation of Binary Mixtures

Raeva V.M., Zhuchkov V.I., Ryzhkin D.A.

MIREA – Russian Technological University, Russian Federation

raevalentina1@gmail.com

Currently, considerable attention has been paid to the use of ionic liquids (IL) in reaction systems and separation processes, in particular, as separating agents (SA) in extraction and extractive distillation (ED). The choice of SA for ED can be carried out using gas-liquid chromatography (GLC). The selectivity of tested SA can be determined by retention times of the substances to be

separated by the liquid stationary phase (LSF). Based on the data obtained, the activity coefficients of substances at infinite dilution and the selectivity of tested SA are calculated. We have previously conducted similar studies for traditional SA, their binary combinations [1] and ionic liquids (IL) [2], mixtures of organic substances tested as separating agents, as well as IL, tested in the synthesis of cyclohexanone by oxidation of cyclohexene [3].

This study is devoted to the identification of regularity influence of chemical structure and concentration of IL at their selectivity at ED of binary mono- and azeotropic mixtures, as well as mixtures with a relative volatility close to unity. Eight ionic liquids were tested as SA, including six imidazole IL with different anions [Cl], [PF₆], [BF₄], [CF₃SO₂O], N-butyl-3-methylpyridinium hexafluorophosphate, and triethylammonium trifluoromethanesulfonate. The substances to be separated belong to different classes of compounds (methanol, ethanol, 1-propanol, acetone, methyl ethyl ketone, methyl isobutyl ketone, benzene, cyclohexane, chloroform, perfluorobenzene, tetrahydrofuran, mesityl oxide, water). The selectivity of SA is determined in relation to binary systems composed of the listed substances, the separation of which is of practical importance.

Determination of retention times was carried out under the same conditions GLC. Column temperature is about 343 K; inert sorbent Chromosorb P 60/80 mesh. The carrier gas is helium. LSF - IL (10, 20, 30 % mass. from sorbent's weight), and mixed SA (20 % mass. 1,2-ethandiole from sorbent's weight + IL (5, 10, 20 % mass. from 1,2-ethandiole weight).

The study found that: 1) the considered ionic liquids are ranked by changing the retention time of substances; 2) selectivity of IL are calculated with respect to the considered binary systems; 3) the synergistic effect of mixed SA (1,2-ethandiole + IL) is observed for the cyclohexane - benzene system (triethylammonium trifluoromethanesulfonate) and for the chloroform - acetone system (N-butyl-3-methylpyridinium hexafluorophosphate or 1-butyl-3-methylimidazolium hexafluorophosphate).

Acknowledgements The financial support of Ministry of Education and Science of the Russian Federation (state assignment, project № 10/8454.2017/BP).

[1] Zhuchkov, V.I., Raeva, V.M., and Frolkova, A.K. *Theoretical Foundations of Chemical Engineering*, 2017, 51, 1047.

[2] Frolkova, A.K., Zhuchkov, V.I., Rummyantsev, P.G. *Chem. Eng. Res. Design*, 2015, 99, 215.

[3] Frolkova, A., Zhuchkov, V., Nazansky, S. 45rd International Conference of SSCHE, Tatranske Matliare, Slovakia, 2018, May 21-25. P.113.

P11-65. Experimental Investigation of the Liquidus Surface Projection of The Cu-Pd-Sn Ternary System

Khartsyzov G.¹, Sineva S.², Starykh R.³, Kareva M.⁴, Kuznetsov V.⁴

¹Peter the Great St.Petersburg Polytechnical University, Russia; ²University of Queensland, Australia; ³LLC Gipronickel Institute, Russia; ⁴Lomonosov Moscow State University, Russia

khartsyzov.gs@gmail.com

Palladium, copper and tin are the basic components of many dental alloys and solder grades. For appropriate choice of the compositions of such alloys or solders it is necessary to obtain the information about phase equilibria and components interactions at the Cu-Pd-Sn system at high temperature range. Besides the practical importance, data on phase diagram of the Cu-Pd-Sn ternary system can be used as the basis for thermodynamical modeling of multicomponent systems.

Available literature issues regarding discussed system are scarce and only provide data on solid state equilibria [1-3], however phase diagrams of Cu-Pd, Cu-Sn and Pd-Sn binary systems [4-6] are reliable and investigated quite well. Phase diagrams of mentioned binary systems showed the existence of 14 invariant reactions where liquid phase takes part (5 reactions belong to Cu-Sn system and 9 - to Pd-Sn system). It is evident, that all mentioned reactions will form more complex interactions within the volume of the Cu-Pd-Sn ternary system, but the detailed scheme of phase reactions is absent. Missing information about high-temperature phase interactions in the Cu-Pd-Sn ternary systems volume became the reason for providing the current research.

Preliminary calculations of liquidus surface projection using ThermoCalc software [7], based on thermodynamic data of binary boundary systems, predicted 14 invariant reactions involving liquid phase, but it should be proved with the use of experimental technique. In particular, the temperatures and equilibrium phases of these reactions should be defined experimentally.

As the first step of research, liquidus surface projection of Cu-Pd-Sn ternary system was constructed, limited by 50% at. of Sn. For the purposes of investigation more than 50 samples were synthesized and examined using combination of experimental methods (differential thermal analysis, scanning electron microscopy, electron probe microanalysis and X-Ray diffraction analysis).

Taking into account the results of experimental analysis and well-known binary systems data the liquidus surface projection of the Cu-Pd-Sn ternary system was constructed.

[1] M.A. Kareva, E.G. Kabanova, K.B. Kalmykov, G.P. Zhmurko, and V.N. Kuznetsov, *Journal of Phase Equilibria and Diffusion*, 2014.

[2] M.D. A. Rahman, C. Fan, S. Wang, C. Ho and W.Gierlotka, *Journal of electronic materials*, 2014, 43, 176.

[3] T.L. Evstigneeva, I.Y. Nekrasov, *Ocherki Fiz.-Khim.*, 1980, 9, 20.

[4] S. Furtauer, D. Li, D. Cupid and H.Flandorfer, *Intermetallics*, 2013, 34, 142.

[5] V.V. Romaka et al., *Journal of Alloys and Compounds*, 2010, L7.

[6] P.R. Subramanian, D.E. Laughlin, *Journal of Phase Equilibria*, 1991, 12, 231

[7] H. Lukas, S.G. Fries, B. Sundman, "Computational Thermodynamics: Calphad Method", 2007

PII-66. Fast Methods of Debye-Hückel Limiting Slopes Calculation Based on Iapws Equation of State of Water

Voskov A.L., N.A. Kovalenko N.A.

Department of Chemistry, Lomonosov Moscow State University, Russia

alvoskov@gmail.com

Thermodynamic modeling of aqueous electrolyte solutions is an actual practical task. The most common models used for it are Pitzer, eNRTL and eUNIQUAC models that include Debye-Hückel term containing so called Debye-Hückel limiting slopes, i.e. A_ϕ and its derivatives:

$$G^{\text{DH}}/(\omega_w RT) = -4A_\phi \ln(1+bI^{0.5})/b; A_\phi = (2\pi N_a \rho M_w)^{0.5} e^3 (4\pi \epsilon \epsilon_0 kT)^{-1.5}/3$$

$$A_V = -4RT(\partial A_\phi / \partial p)_T; A_K = (\partial A_\phi / \partial p)_T; A_H/RT = 4T(\partial A_\phi / \partial T)_p; A_C = (\partial A_H / \partial T)_p$$

It requires equations for water density ρ and dielectric constant ϵ . There are several commonly used ones but even minor differences between them have a strong influence on A_ϕ first and especially second derivatives, up to 70% for A_C and A_K . The most recent and consistent to ITS-90 temperature scale are IAPWS equations [1]. They are based on Helmholtz energy equation $F(V,T)$ and calculation of $\rho(p,T)$ requires time-consuming numeric methods. Existing tables of values have large T and p steps [1,2]. The aim of this work is development of new accurate approximations for Debye-Hückel limiting slopes based on IAPWS equations for water density and dielectric constant.

Two approaches were proposed for $T > 273.15$ K. The first one is usage of IAPWS-IF97 equation that is based on Gibbs energy expression $G(p,T)$, valid for $T=273.15-623.15$ K and $p=0-100$ MPa and gives analytical expressions for A_ϕ . It makes A_ϕ and its derivatives computation 100 times faster. Maximal relative deviations are $\epsilon(A_\phi)=5.9 \cdot 10^{-3}\%$, $\epsilon(A_H)=0.33\%$, $\epsilon(A_C)=4.2\%$, $\epsilon(A_V)=0.56\%$, $\epsilon(A_K)=7.0\%$ (see Fig.1). In [3] it is mentioned that they are “low” but no estimations are given. The second are polynomials for A_ϕ that are valid for 273-423 K, 0-5 MPa and with accuracy comparable to the first variant. We also suggest expressions for extrapolation of A_ϕ from 273-373 K to 200-573 K interval. They are required for modeling of concentrated solutions.

All methods and formulas proposed in this work are implemented in open source computer programs that can be used as a library for computation of Debye-Hückel limiting slopes.

Acknowledgements The financial support of RFBR, project no. 18-29-24167.

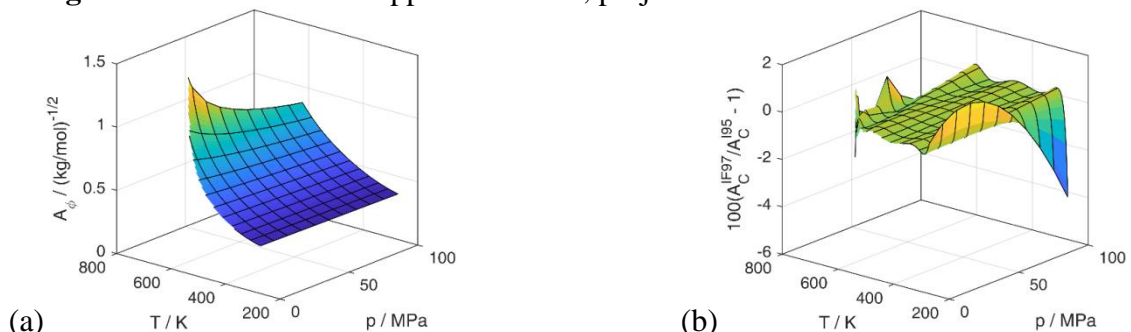


Figure 1. (a) $A_\phi(p,T)$ IAPWS95 function; (b) A_C : difference between IAPWS95 and IAPWS-IF97.

[1] D.P. Fernández, A.R.H. Goodwin et al., *J. Phys. Chem. Ref. Data*, 1997, 26, 1125.

[2] A.A. Aleksandrov, A.B. Matveev, *Teploenergetika, teplofizika: sbornik dokladov yubilejnoj nauchnoi konferencii*, MPEI, Moscow, 1998. P. 87 [in Russian].

[3] A.A. Aleksandrov, *Thermal Engineering*, 2000, 47, 561.

PII-67. Solubility and the Structure of Equilibrium Crystal Solvates in Systems $\text{MX}_2 - \text{S}_1 - \text{S}_2$ ($\text{M} = \text{Cd}, \text{Cu}$; $\text{X} = \text{Cl}, \text{Br}, \text{I}$; $\text{S}_1, \text{S}_2 = \text{Dimethylsulfoxide}, \text{N,N-Dimethylacetamide}, \text{1,4-Dioxane}$) at 298 K

Tolmachev M.V., Bogachev N.A., Skripkin M.Yu.

Saint-Petersburg State University, Russia

makstolm@gmail.com

At present there is no general theoretical model which describes the behavior of such multi-component systems as electrolyte solutions in mixed organic and water-organic solvents and formation of equilibrium solid solid phases in this systems. Therefore, the study of this kind of system is essential for the further development of Solution Chemistry. Moreover, compounds formed in this systems can used as catalysts, precursors for the synthesis of inorganic and metallorganic structures.

The report will present the results of study the solution-solid phase equilibria in ternary systems which contain cadmium and copper halides, mixed aprotic O-donor solvent. The influence of such characteristics as softness of cation and anion, softness and donor ability of molecules of solvents on the structure of solid phase and the areas of crystallization of similar crystal solvates was studied.

All observed phenomena were analyzed with HSAB theory [1], ideas about the structure of individual and mixed solvents, and donor-acceptor interactions in solution [2, 3]. There was observed that solvates with more donor ligand have more extended areas of crystallization. Structural type of solid phase is determined by softness ratio of cation and anion.

The work was done with the assistance of the resource centers of the Scientific Park of St. Petersburg State University "X-ray diffraction research methods", "Optical and laser methods for investigating substances" and "Thermogravimetric and calorimetric research methods", as well as with the support of the RFBR (project 18-33-00636).

1. Y. Marcus, The Journal of Physical Chemistry, 1987, 91 (16), 4422-4428.
2. V. Gutmann, Coord. Chem. Rev., 1976, 18, 225.
3. U. Mayer, V. Gutmann, W. Gerger, Montashefte für Chemie, 1975, 106, 12354.

PII-68. Volumetric Properties of Double-Charged Ions in N-Methylacetamide Solutions over the Temperature Range from 308.15 to 328.15 K at Ambient Pressure

Dyshin A.A., Kiselev M.G.

G.A. Krestov Institute of Solution Chemistry of the Russian Academy of Sciences

aad@isc-ras.ru

Inorganic single- and double-charged ions play an essential role in various cellular processes. Double-charged ions are one of the most important bioactive elements involved in metabolic processes in the human body, located in almost all cells. At the same time N-methylacetamide is a unique solvent. Being a mimetic of the structure of amino acids, NMA attracts the attention of many researchers. This is a good model compound for studying hydrogen bonds between groups of peptides and is widely used as a model of peptides and membranes during computer simulation [1].

Based on these arguments, the study of density and viscosity of salts – N-methylacetamide mixtures in a wide range of concentrations and temperatures is very important. Viscometry and densimetry provide information about the structural changes occurring in solutions. The densities of the N-methylacetamide – electrolyte solutions were measured using an Anton Paar DMA5000M high precision densimeter with an oscillating U-tube. The kinematic viscosity was measured using an automatic Ubbelohde capillary viscometer with a suspended level and optical detection of the liquid flow time.

In this work, the density and viscosity of solutions of $MgCl_2$, $CaCl_2$ and $ZnCl_2$ in N-methylacetamide were measured at atmospheric pressure in temperatures ranges from 308.15 to 328.15 K [2-4]. Partial molar volumes of N-methylacetamide; partial molar volumes, apparent molar volumes of salts and thermal expansion coefficients of solutions have been calculated from the experimental data. The dependences of the volumetric characteristics of solutions on temperature and concentration of components have been analyzed and discussed in the report. An increase in temperature and concentration leads to a decrease in the partial molar volume of salts.

We explain this phenomenon taking into account two factors. First, the increasing temperature destroys the hydrogen bond in N-methylacetamide. Second, the average distance between the cation and NMA in the first solvation shell of ions decreases as a result of their strong charge-dipole interaction.

It is now generally accepted that the ion in a condensed phase creates the electric field, which has an effect on the volume of solvent molecules [5]. The effect of electrostriction, which is observed in solution, has a significant effect on their structure. This leads to changes in the volumetric properties of the solutions.

Acknowledgements This work was performed as part of the government contract (registration number 01201260481). This research was partially supported by the Russian Foundation for Basic Research (RFBR grant no. 17-03-00309 A).

[1] N. Manin, et al., PCCP, 2016, 18, 4191.

[2] A.A. Dyshin, O.V. Eliseeva, M.G. Kiselev, J. Chem. Eng. Data, 2017, 62, 4128.

[3] A.A. Dyshin, O.V. Eliseeva, M.G. Kiselev, J. Chem. Eng. Data, 2018, 63, 3167.

[4] A.A. Dyshin, O.V. Eliseeva, M.G. Kiselev, J. Chem. Eng. Data, 2018, 63, 3130.

[5] Y. Marcus, Chem. Rev., 2011, 111, 2761.

PII-69. Liquid ↔ Gas Phase Transitions of 1-Propanol – n-Hexane Binary and Water – 1-Propanol – n-Hexane Ternary Mixtures

Bazaev A.R., Bazaev E.A., Osmanova B.K., Dzhapparov T.A-G.

Institute for Geothermal Research of the Daghestan Scientific Center of the Russian Academy of Sciences, Shamil 39A, Makhachkala, Daghestan Republic, 367030, Russia

emilbazaev@gmail.com

By using the compressibility method and free ballast constant volume piezometer new accurate values of p, T and p, ρ, T -relations are obtained for 1-propanol – n-hexane binary mixtures ($x=0.2, 0.5, 0.8$ and 0.9 mol fractions of n-hexane) and of water - 1-propanol – n-hexane ternary mixtures ($x=0.333$ mol fractions of each component) in the wide parameters of state including critical locus (fig.1).

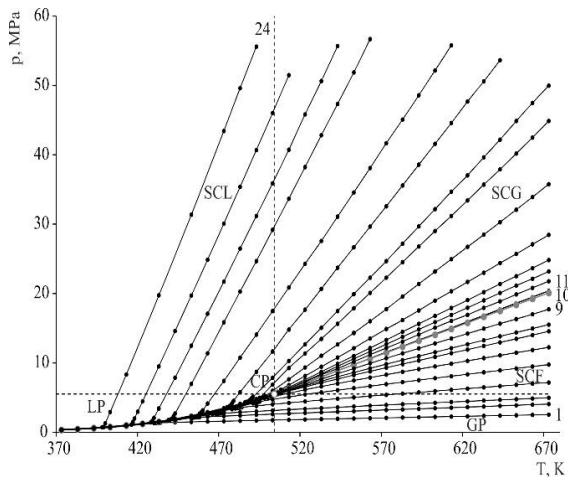


Fig.1. Isochores 25-616 kg/m³ (1-24) of p - T dependences of water - 1-propanol – n-hexane ternary mixtures (The work was supported by RBSF Grant N18-08-00124 A. $x=0.333$ mol fractions of each component). LP–liquid phase, GP–gas phase, SCL – supercritical liquid, SCG – supercritical gas.

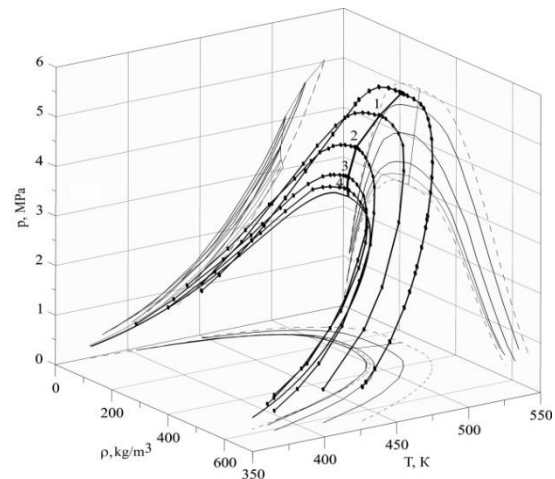


Fig.2. p, T - diagram of phase coexistence curves and their projections of 1-propanol, n-hexane and their mixtures ($x=0.2$ (1), 0.5 (2), 0.8 (3) and 0.9 (4) mol. fractions of n-hexane).

It is experimentally found out that phase diagrams of binary and ternary mixtures are similar to phase diagrams of individual fluid, i.e. researched systems may be considered as homogeneous.

By using isochoric P - T break points the values of the liquid↔gas phase transition (equilibrium) parameters are determined (fig.2).

The dependence of pressure of 1-propanol – n-hexane binary mixtures from temperature and composition of mixtures along the equilibrium phase curve is described by three-parameter polynomial equation represented by expansion of the compressibility factor $Z = p/RT\rho$ into a power series of reduced density $\omega = \rho/\rho_{cr}$, reduced temperature $\tau = T/T_{cr}$ and composition x :

$$Z = p / RT\rho_m = 1 + \sum_{i=1}^m \sum_{j=0}^n \sum_{k=0}^s a_{ijk} \omega^i \cdot x^k / \tau^j \quad \text{and} \quad p = RT\rho_m \left[1 + \sum_{i=1}^m \sum_{j=0}^n \sum_{k=0}^s a_{ijk} \omega^i \cdot x^k / \tau^j \right].$$

The average relative error of calculated values of pressure from experimental ones less than 1.3 %.

The work was supported by RBSF Grant N18-08-00124 A.

PII-70. Experimental Study of Azeotropy in the *n*-Heptane-Water Binary System

Ibavov N.V., Mirskaya V.A., Nazarevich D.A.

Amirkhanov Institute of Physics, Dagestan Scientific Center, Russian Academy of Sciences, Russia

nabi79@mail.ru

The isochoric heat capacity and the pressure of *n*-heptane – water binary layering system were measured using the high-temperature adiabatic calorimeter-piezometer method [1]. Characteristic properties of a change in the temperature dependences of the heat capacity and the pressure along the isochores were revealed in a region of phase transitions. These features allow for fixing the azeotropy state in the system and for estimation of the influence a polar component (water) on a change in the azeotrope state temperature.

The temperature dependences of the isochoric heat capacity and the pressure of the system $[x\text{H}_2\text{O} + (1-x)\text{C}_7\text{H}_{16}]$ with content of polar component (water) x , $0 \leq x \leq 0.420$ mole fractions, in heptane were studied along the isochores for several constant compositions. The measurements were performed in the range of densities of 166.07 kg/m^3 - 415 kg/m^3 and temperatures of 400 K - 553 K.

For *n*-heptane-water system, the pressure on the three-phase equilibrium line is higher than the saturation pressure of both components. This indicates that the system has the heteroazeotropy [2].

The lines of phase equilibria $\rho=f(T)$ liquid-liquid and liquid-gas for mixture studied are plotted in the heat capacity maxima temperatures on isochores and temperatures corresponded to breaks and bends on the $P=f(T)$ dependence Figure 1. As is evident from the figure, the lines of the phase equilibrium, for the considered mixture of constant composition $x=\text{const}$, intersect at one point ($\rho = \rho_{\text{az}}$). This point corresponds to the azeotrope state for the mixture of this composition ($x=\text{const}$).

The character of the heat capacity and pressure dependence on temperature described above allow the determination the parameters of azeotrope formation: (T_{az}) temperature, (P_{az}) pressure and (ρ_{az}) density for the constant composition mixture.

So, in this study we offer new approach for the estimation of the azeotrope state in binary systems with the stratifying area using the results of C_v , x , T , P , ρ measurements. It is shown that the experimental technique of the high-temperature adiabatic calorimeter-piezometer provides a possibility to define the presence of the azeotropy in the system, evaluate the T_{az} , P_{az} , ρ_{az} parameters of its formation, and establish the displacement dynamics of the azeotrope state with a change in the mixture temperature and pressure.

Acknowledgements Work was supported by the Russian Foundation for Basic Research (grant № 17-08-00800-a)

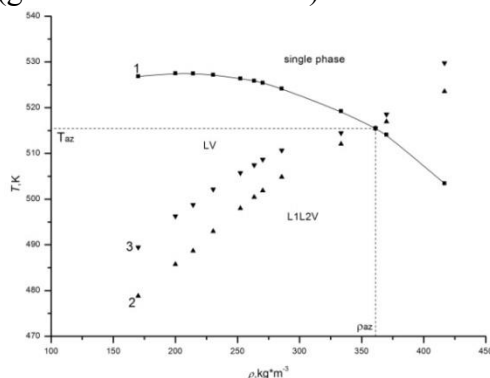


Figure 1. Coexistence curve of mixture $[(1-x)\text{C}_7\text{H}_{16}+\text{H}_2\text{O}]$, $x=0.295$ m.f.: 1– liquid-vapour (TLg), 2– liquid-liquid (TL1), 3 – liquid-liquid (TL2).

[1] V.A. Mirskaya, D.A. Nazarevich, N.V. Ibavov, High Temp., 2016, 54(2), 223

[2] P.J. Smits, C. J. Peters, J. de Swaan Arons, Fluid Phase Equilib., 1998, 150, 745

PII-71. Complex Approach to Acetamide-Water System Investigation

Krestyaninov M.A., Dyshin A.A., Ivlev D.V., Kolker A.M.

G.A. Krestov Institute of Solution Chemistry of the Russian Academy of Sciences

mak1111@bk.ru

Acetamide is one of the most simple molecules among of amides series, which might serve as a mimetic of a protein interface. Acetamide can form the following hydrogen bonds (H-bonds) with itself and with water molecules: OH...O, OH...N, and NH...O, which have been studied by experimental and computer methods. The aim of present work is to study the structure of acetamide–acetamide and acetamide–water complexes using DFT calculations, IR spectroscopy and MD simulations.

The structure of acetamide dimers and hydrogen-bonded complexes of acetamide with water molecules have been studied by quantum chemical method on the base of density functional theory approximation using B3LYP and PBE functionals and aug-CC-pVTZ basis set. The geometrical parameters of hydrogen bonds, binding energies, vibrational bands have been calculated and the Natural Bond Orbital, quantum theory of atoms in molecules analyses has been carried out. A more detailed description of the calculation is given in [1].

MD simulation have been performed in a wide range of temperature, pressures and acetamide concentration from 0 to 0.4 m.f. The calculation of hydrogen-bonded clusters in a water–acetamide mixtures was carried out. There is a decrease in the average number of hydrogen bonds with increasing acetamide concentration. For analysis H-bonds between water and acetamide molecules, detailed analysis was performed.

IR spectroscopy together with chemometric methods were used to study the effect of influences water contents on the structure of hydrogen bonded clusters of a binary water–acetamide mixture in a wide range of concentrations. For model development and facilitate the interpretation of the obtained spectral results, we used the results of quantum-chemical calculations of the structure of hydrogen-bonded clusters of water– acetamide mixtures. The initial spectra were deconvoluted according to the procedure described previously [2, 3]. Based on the analysis, conclusions were made about the change in the number of hydrogen bonds between water molecules and water and acetamide molecules with changes in the concentration of acetamide in solution.

The results of the IR-spectra analysis are fully confirmed by the results of the molecular dynamics simulation (MD).

Acknowledgements

This research was supported by the Russian Foundation for Basic Research (RFBR grant no. 17-03-00309 A).

[1] M.A. Krestyaninov, E.G. Odintsova, A.M. Kolker, M.G. Kiselev, *Journal of Molecular Liquids*, 2018, 264, 343.

[2] A.A. Dyshin, R.D. Oparin, M.G. Kiselev, *Russian Journal of Physical Chemistry B*, 2012, 6, 8, 868.

[3] A.A. Dyshin, O.V. Eliseeva, G.V. Bondarenko, A.M. Kolker, M.G. Kiselev, *Russian Journal of Physical Chemistry A*, 2016, 90, 12, 2434.

PII-72. Quantum-Chemical, Molecular Dynamics and IR Spectroscopic Study of Hydrogen-Bonded Clusters of N-Methylacetamide-Water Mixture

Krestyaninov M.A., Ivlev D.V., Dyshin A.A., Kolker A.M.

G.A. Krestov Institute of Solution Chemistry of the Russian Academy of Sciences

mak1111@bk.ru

N-Methylacetamide (NMA) is a good model compound for studying hydrogen bonds between peptide groups. Quantum chemical calculations, molecular dynamics simulation, and infrared vibrational spectroscopy were used to study the effect of water concentration on the structure of hydrogen-bonded clusters of a binary water–N-methylacetamide mixture in a wide range of state parameters.

The structure of cis- and trans-N-methylacetamide dimers and hydrogen-bonded complexes with water molecules have been studied by DFT approximation using B3LYP and PBE functionals and GD3 dispersion correction and aug-CC-pVTZ basis set. The geometrical parameters of hydrogen bonds, binding energies, vibrational bands have been calculated and the NBO and QTAIM analyses has been carried out. A more detailed description of the calculation is given in [1].

Molecular dynamics simulation of a water–N-methylacetamide mixture was performed in a wide range of temperatures and pressures. The calculation of hydrogen-bonded clusters in a mixture of NMA - water was carried out. With increasing NMA concentration, a decrease in the average number of hydrogen bonds between water molecules is observed. The same trend in the change in the number of hydrogen bonds is observed with increasing temperature. With increasing pressure, the number of hydrogen bonds varies only slightly. The number of hydrogen bonds between NMA molecules and water molecules and between NMA molecules increases with increasing NMA concentration.

The change in the structure of clusters in the system under study was shown from the obtained spectral data using chemometric analysis methods and the previously carried out quantum chemical calculations. In the range of interest, the bands related to oscillations of various types overlap, so for analysis it is necessary to deconvolute it. For this, the bands under study were deconvoluted into profiles according to the procedure described previously [2, 3]. An increase in the half-width of the spectral band related to the N-H...O interactions of N-methylacetamide molecules indicates an increase in the number of N-H...O bonds with increasing its concentration. This fact is also confirmed by the increase in the integral intensity of the contribution we assigned to the N-H...O interactions of N-methylacetamide molecules. The number of hydrogen bonds between water and N-methylacetamide molecules also increases with an increase in the mole fraction of N-methylacetamide in solution.

Acknowledgements

This research was supported by the Russian Foundation for Basic Research (RFBR grant no. 17-03-00309 A).

[1] M.A. Krestyaninov, E.G. Odintsova, A.M. Kolker, M.G. Kiselev, *Journal of Molecular Liquids*, 2018, 264, 343.

[2] A.A. Dyshin, et al., *Russian Journal of Physical Chemistry A*, 2016, 90, 12, 2434.

[3] A.A. Dyshin, R.D. Oparin, M.G. Kiselev, *Russian Journal of Physical Chemistry B*, 2012, 6, 8, 868.

PII-73. Influence of the Initial Composition of the Powders on the Phase Composition of the Surface Layer Formed in the Conditions of Electron Beam Surfacing

Kryukova O.N., Knyazeva A.G.

Institute of Strength Physics and Materials Science
of Siberian Branch Russian Academy of Sciences, Russia

okruk@ispms.tsc.ru

The experimental study of nonequilibrium synthesis of composites faces the complexity of interpretation of the results and the impossibility of direct measurements in dynamics (except for temperature). However, the staging of chemical reactions largely determines the future structure of composites; the limiting stage depends on the conditions of synthesis, properties and structure of the composite is continuously changing, accompanying phenomena of different physical nature, etc are possible. In such situations, mathematical modeling is under interest.

In turn, when modeling the technological processes of synthesis of new materials, taking into account the physical and chemical stages, there is a problem of finding or evaluating the formal kinetic parameters and the dependence of the effective thermal properties on the composition. However, the description of the detailed kinetics of chemical reactions involving solids is a serious problem.

Two basic approaches are common in macrokinetics [1]. The first one is based on the formal description of the transformation kinetics for the total reaction. The kinetic function can take into account the inhibition of the reaction by the product layer with help of braking parameters, which depend on the type of reacting substances [2]. The second approach uses the concept of a reaction cell, the sequence of stages in which is given in accordance with the equilibrium state diagram [3].

This paper presents possible chemical reactions in systems Ti-C, Ti-B, Ti-Si, Ti-C-Al, and gives approximate estimates of formal kinetic parameters for these reactions. The presented set of stages is not complete, and the reaction parameters need to be clarified. However, in the absence of experimental data for most stages, the obtained numerical values can be used to simulate the synthesis of multiphase materials under nonequilibrium conditions. This is demonstrated by the model of controlled synthesis of a multiphase composite on a substrate, taking into account the evolution of the properties and the stage of transformation. Obtained results are consistent and provide detailed information about the interaction of different physical and chemical processes in non-stationary conditions.

Acknowledgements The financial support of Russian Science Foundation (grant No. 17-19-01425).

[1] A.G. Merzhanov, A.S. Mukasyan, *Solid Flame Combustion*, 2007, 336. Torus Press, Moscow.

[2] A.P. Aldushin, T.M. Martem'yanova, A.G. Merzhanov, et al., *Combust Explos Shock Waves*, 1972, 8, 159.

[3] E.A. Nekrasov, V.K. Smolyakov, Y.M. Maksimov, *Combust Explos Shock Waves*, 1981, 17, 513. 6, 8, 868.

POSTER SESSION 3
SATURDAY, 22.06.2019

PIII-1. Electrophysical and Transport Properties of $\text{Me}(\text{La},\text{Sm})_2\text{WO}_7$ (Me=Sr,Ba)

Taimassova Sh.T.¹, Gogol D.B.¹, Bissengaliyeva M.R.¹, Balbekova B.K.²

¹Institute of Problems of Complex Development of Mineral Resources, Kazakhstan;

²Karaganda State Technical University, Kazakhstan

mirabis@ipkon.kz, 160655@mail.ru

Ranges of the properties exhibited by rare-earth compounds can be extended by means of doping with atoms of other lanthanides. Doping with lanthanides has a significant effect on the transport properties of substances, such as conductivity, as well as on dielectric properties. This work studied the ternary oxides of tungsten, alkaline earth elements (barium and strontium) and lanthanum doped with samarium. The synthesis by the solid-phase method was carried out in alundum crucibles in several stages over the temperature interval from 700° C to 1200° C with intermediate abrasion of the samples in an agate mortar. As a result, compounds with the theoretical formulas $\text{Me}(\text{La}_{1-x}\text{Sm}_x)_2\text{WO}_7$ were obtained, where Me - Sr and Ba, x are 1, 3, and 5 mol%.

According to the results of X-ray phase analysis, the samples based on strontium on an average consist of 60% of the target $\text{Sr}(\text{La},\text{Sm})_2\text{WO}_7$ phase and 40% of the phase isostructural to the compound $\text{Sr}_5\text{Re}_2\text{O}_{12}$, i.e., $\text{Sr}_5\text{W}_2\text{O}_{12}$. X-ray phase analysis of barium-based samples are in good agreement with BaLa_2WO_7 compound [1]. There is an impurity of BaWO_4 (about 3-4 vol.%) in the sample with 1% Sm, and there is an impurity of lanthanum oxide La_2O_3 in the sample with 3% Sm. There is no more than 10 vol.% of the target compound BaLa_2WO_7 in the sample with 5% Sm. This sample basically consists of two phases, one of which is $\text{La}_6\text{W}_2\text{O}_{15}$, and the other corresponds to $\text{Ba}_5\text{W}_2\text{O}_{12}$ in approximately equal volume ratios. Thus, the content of 5 mol.% of samarium is critical for crystallization in the space group P112₁/b.

The electrophysical properties of the samples were measured over the range from 25 Hz to 10 MHz with a parallel switching scheme on tablets with a diameter of 1 cm and a thickness of about 2.1 mm, pressed at 5 t/cm². We obtained the data on the capacity C_p , the dielectric permittivity ϵ , the dielectric loss tangent $\text{tg } \delta$, the resistance R_p and the conductivity G_p . The samples are good isolators in the low frequency area/region; the conductivity of the samples increases with increasing frequency, as well as with increasing samarium content. The capacity and dielectric permittivity at low frequencies also increase with increasing samarium share, however, the values of $\text{tg } \delta$ are also high in this frequency range. Therefore, the best values of the quality factor Q (above 50) are observed at frequencies above 100 kHz. The influence of doping can be traced also in the growth of inductance of samples. Thus, for the magnetic moments of the atoms of samarium in the samples, there is not only an ordering observed in the form of peaks of the heat capacity at low temperatures, but also an interaction with the crystalline structure of the compounds up to room temperature.

Acknowledgement The financial support of grant AP05130095 by Science Committee of MES RK.

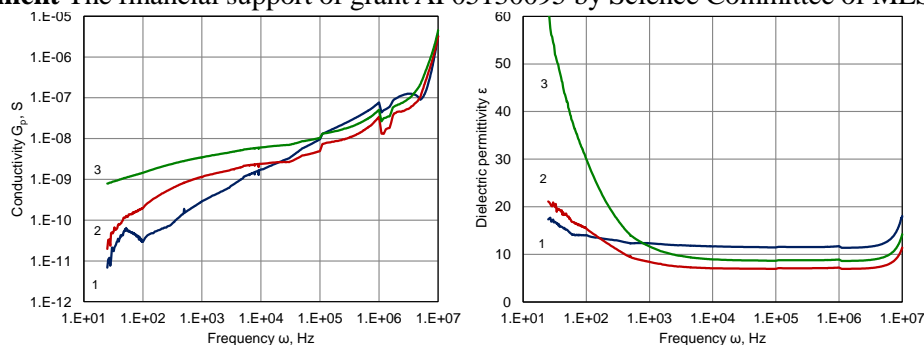


Figure 1. Conductivity (left) and dielectric permittivity (right) of the samples: 1 - BaLa_2WO_7 , 2 - $\text{Ba}(\text{La}_{0.99}\text{Sm}_{0.01})_2\text{WO}_7$, 3 - $\text{Ba}(\text{La}_{0.97}\text{Sm}_{0.03})_2\text{WO}_7$.

[1] W. Fu, D. Ijdo and A. Bontenbal, *J. Solid State Chem.*, 2013, 201, 128.

PIII-2. Effect of the rGO (Reduced Graphene Oxide) Addition on Conductivity and Microstructure of Ceramics ZrO_2 - Y_2O_3 Sintered Using Different Techniques

Glukharev A.G.¹, Temnikova M.S.¹, Glumov O.V.¹ and Konakov V.G.^{1,2}

¹Saint-Petersburg State University, Saint-Petersburg, Russia

²Science and Technical center "Glass and ceramics", Saint-Petersburg, Russia

gluharev1@gmail.com

Nowadays, the development of the novel nanoceramic materials with unique characteristics is one of the major directions in the material science. The use of nanosized precursors for such materials manufacturing makes it possible to design their chemical, physical and mechanical properties. Powder particle properties (i.e. particle size distribution, mean size, agglomeration degree etc) strongly affect on the final microstructure and properties of the ceramics. Here the control of grain growth during ceramics sintering is regarded critical to achieve nanoceramics. In some studies it has been shown that graphene (Gr) and reduced graphene oxide (rGO) addition can act as effective grain growth retarding agent in metal-matrix composites, aluminum, nickel and copper, in particular. However, the state of carbon additive, and, consequently, the properties of the resulting ceramic material strongly depend on the method of compaction and sintering. Thus the aim of the present work was the manufacturing of rGO-zirconia based nanocomposites by three different techniques: in air, in vacuum (10^{-5}) and in closed volume without oxygen access at the same temperature of $1550^{\circ}C$ with the following the investigation of the effect of rGO addition on microstructure, phase composition and conductivity. 9Y2O3-91ZrO2 (mol.%) was chosen for the investigation (Yttria Stabilized Zirconia - YSZ). Reduced graphene oxide was synthesized via Hammers method with following microwave exfoliation. Based on rGO characteristics and particle size distribution the amount of rGO addition was calculated. Precursor powder YSZ was synthesized by the sol-gel synthesis in a variation of reverse co-precipitation of inorganic salts. Via SEM, EDX, XRD, STA and Raman spectroscopy and impedance spectroscopy it was shown that carbon additive burns out during synthesis on air, thus the microstructure and ratio of volume and surface conductivity changes. After sintering in vacuum and in in closed volume the carbon phase and microstructure changes was found but without significant change in conductivity. The research was performed with the support of Research Park of SPSU.

PIII-3. Structure and Conductivity of 9CaO-91ZrO₂ Ceramics, Obtained from Freeze-Dried Powder With Cryoprotectant Addition

Grega M.E., Kurapova O. Yu., Nikiforova K.V., Konakov V.G.

St.Petersburg State University, Russia

demolisher1425@gmail.com

The elimination of the agglomeration degree in the zirconia based precursors during its synthesis and processing is critical for further advanced ceramics manufacturing. So far, to ensure the aggregative stability of nanosystems, the stabilizers, i.e. surfactants are mostly used. However, their removal is complicated and it often leads to drastically conductivity decrease of the final ceramic solid electrolyte. Acetone can play the role of a surfactant, which is easily removed from the system during the dehydration. In case freeze-drying is used for dehydration, it also turns to be a cryoprotectant, diminishing the size of water crystals and preventing the possible change of precursors microstructure. Thus, the aim of this work was to study the effect of the synthesis medium on the phase formation and agglomeration in 9CaO-91ZrO₂ (mol. %) precursors during their thermal evolution as well as structure and conductivity of the ceramics.

Precursor was prepared by sol-gel synthesis in a way of the reverse co-precipitation. Decimolar solution was prepared using the starting salts ZrO(NO₃)₂·5.5H₂O (Acros organics, Belgium), Ca(NO₃)₂·2H₂O (Len.reactiv, Russia). Precipitation of amorphous hydroxides was carried out from water-acetone solution with various acetone content (1M aqueous ammonia was used as a precipitate, T = 1-2 °C, pH = 9-10). The precipitate of hydroxides was dehydrated by freeze drying (Labconco, 11 chamber, USA, 0.018 mm Hg, 24 h). The obtained amorphous samples were calcined at different temperatures (200-1100 °C) for 2 hours to subsequently track the thermal evolution of the system. Based on the data obtained solution containing 7 vol.% acetone was chosen for further ceramics fabrication. Precursor was compacted into the pellets with a diameter of 10.5 and ~4 mm thickness at P ~3.5 kg/cm² and annealed at 1550 °C for 3 hours in air. The samples obtained were comprehensively studied by STA (calorimeter STA 409 C/4/G Jupiter, NETZSCH), BET adsorption-desorption isotherms (ASAP 2020MP, Micromeritics), XRD (SHIMADZU XRD-6000, Cu-K_α radiation, λ= 1,54 Å at room temperature), SEM (Hitachi S-3400N, accelerating voltage 20 eV). Impedance spectroscopy (Autolab PGSTAT 302N Potentiostat/Galvanostat) was used to investigate the electrochemical properties of consolidated calcia stabilized zirconia ceramics. Via SEM and adsorption-desorption it was found that precipitation from a solution containing 7 vol. % of acetone results in flake-like powder having microporous structure and a relatively low specific area of 110.2 m²/g. It was proved that the extended area of a cubic zirconia based solid solution existence, namely 600-1100 °C, is due to high dispersity of the precursor and nanosized crystallites in the entire studied temperature range. It was shown that crystallinity degree of solid solution increases with the increase of temperature. Temperature dependence of the integral conductivity was obtained. Grain and grain boundaries impacts to the internal conductivities, as well as activation energy were established.

Acknowledgements. SEM was performed at the Research park of St. Petersburg State University Center for Geo-Environmental Research and Modeling (GEOMODEL). STA was performed at the Research park of St. Petersburg State University Center for Thermogravimetric and Calorimetric Research. Adsorption-desorption research was performed at the Research park of St. Petersburg State University Center for Innovative Technologies of Composite Nanomaterials.

PIII-4. On the Thermal Behavior of Ammonium Fluorometallates

Laptash N.M.

Institute of Chemistry, Far Eastern Branch of RAS, Vladivostok, Russia

laptash@ich.dvo.ru

Ammonium fluoro (or oxofluoro) metallates are the fluorination products of natural raw materials with ammonium hydrogen difluoride (NH_4HF_2) [1-4]. Thermodynamically possible fluorination reactions with NH_4HF_2 proceed exothermally (even at room temperature) with the entropy reserve and the formation of high symmetry (tetragonal or cubic) complexes. It is accepted that the initial stage of thermal decomposition of ammonium salts is proton transfer [5], and three ways of thermal behavior of ammonium fluorometallates are possible. Most complexes decompose with simultaneous release of NH_3 and HF : $(\text{NH}_4)_3\text{MF}_6 = \text{NH}_4\text{MF}_4 + 2\text{NH}_3 + 2\text{HF}$ ($\text{M}^{3+} = \text{Al, Ga, In, Sc, Ti, V, Cr, Fe}$) [6]. Some of them decompose with the release of ammonia when heated: $2(\text{NH}_4)_3\text{TiOF}_5 = (\text{NH}_4)_2\text{TiF}_6 + (\text{NH}_4)_2\text{TiOF}_4 + 2\text{NH}_3 + \text{H}_2\text{O}$ [7]. A special group is represented by complexes isolating HF , such as NH_4BF_4 , $(\text{NH}_4)_2\text{SiF}_6$, $(\text{NH}_4)_2\text{GeF}_6$, NH_4TiF_5 , NH_4TaF_6 , which sublime incongruently. The process of sublimation proceeds through adducts with ammonia, followed by the formation of dinuclear or even trinuclear complexes, as in the case of silicon, as shown by our tensimetric, mass-spectroscopic, vibrational spectroscopy data and quantum-chemical calculations. This is the first time more than 200 years after Davy [8], we report how $(\text{NH}_4)_2\text{SiF}_6$ actually decomposes.

- [1] N.M. Laptash, E.I. Mel'nichehko, S.A. Polyshchuck, and T.A. Kaidalova, *J. Therm. Anal.* 1992, 38, 2335.
- [2] N.M. Laptash, Yu.M. Nikolenko, L.N. Kurilenko, S.A. Polyshchuk, and T.A. Kalacheva, *J. Fluorine Chem.*, 2000, 105, 53.
- [3] N.M. Laptash, I.G. Maslennikova, L.N. Kurilenko, and N.M. Mishchenko, *Russ. J. Inorg. Chem.*, 2001, 46, 28.
- [4] W. du Plessis, A.D. Pienaar, C.J. Postma, and P.L. Crouse, *Int. J. Mineral Processing*, 2016, 147, 43.
- [5] M.E. Brown, D. Dollimore, and A.K. Galwey, *Reactions in the solid state*, 1980, Elsevier, Amsterdam-Oxford-New York.
- [6] P. Bukovec, N. Bukovec, and A. Demsar, *J. Therm. Anal.*, 1980, 36, 1751.
- [7] N.M. Laptash, E.B. Merkulov, and I.G. Maslennikova, *J. Thermal Anal. Calorim.*, 2001, 63, 197.
- [8] J. Davy, *Phil. Trans., R. Soc. London*, 1812, 102, 352.

PIII-5. Sublimation Thermodynamics of Pyridinedicarboxylic Acids

Drozd K.V., Manin A.N., Perlovich G.L.

G.A. Krestov Institute of solution chemistry of the Russian Academy of Sciences, Ivanovo

ksdrozd@yandex.ru

A heterocyclic molecules, namely, pyridines, bipyridines, quinolones is a center of attention in our laboratory as cocrystal formers. These molecules have a set of donor and acceptors of hydrogen bonds which often found in cocrystals. The most common heterosynthons utilized in cocrystals are acid-pyridine and acid-amide [1]. Pyridinedicarboxylic acids have both acid and pyridine functional groups in their structure. Sufficiently large efforts of scientists are aimed at the development of algorithms for obtaining thermodynamically stable multi-component crystals. The approach to predict the probability of formation of two-component crystals knowing the melting temperatures and sublimation thermodynamic parameters of the individual compounds they are made from was proposed by us earlier. [2] One of the limitations of using this approach is the lack of data on sublimation of individual compounds. To solve this problem, we conducted sublimation experiments for the missing cofomers.

In the present work, we have investigated the thermodynamic functions of sublimation and fusion processes of the pyridine-2,3-dicarboxylic acid (quinolonic acid) and pyridine-2,6-dicarboxylic acid (dipicolinic acid). Sublimation experiments were carried out by the transpiration method. In brief: a stream of an inert gas passes above the sample at a constant temperature and at a known slow constant flow rate in order to achieve saturation of the carrier gas with the vapor of the substance under investigation. The vapor is condensed at some point downstream, and the mass of sublimate and its purity are determined by UV-vis spectrometry and differential scanning calorimetry. The vapor pressure over the sample at this temperature can be calculated by the amount of the sublimated sample and the volume of the inert gas used. Mass-spectrometry analysis of sublimated substances was carried out using a NETZSCH STA 409 CD/7/G + Skimmer DSC/DTA/TG with a Skimmer mass-spectrometric vapor analysis system ($E_{\text{ion}} = 70$ eV) in the argon flow at the rate of 70 mL/min. Figure 1 represents temperature dependencies of vapor pressure for quinolonic acid and dipicolinic acid. The sublimation thermodynamic parameters of the studied compounds were calculated. The sublimation enthalpy of quinolonic acid is 30 kJ/mol higher than dipicolinic acid.

Acknowledgements This work was supported by the Russian Science Foundation (№ 17-73-10351).

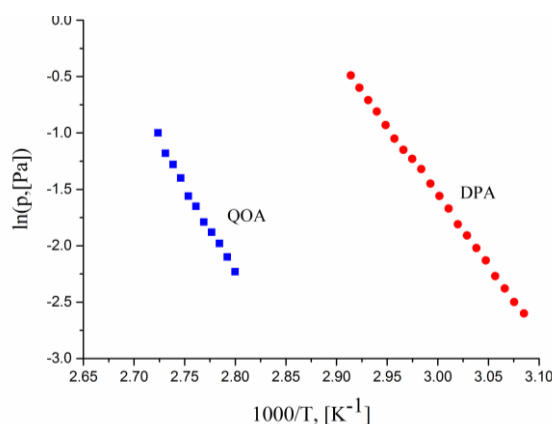


Figure 1. Temperature dependencies of vapor pressure of the quinolonic acid (QOA) and dipicolinic acid (DPA).

[1] N. Qiao, M. Li, et al., *Int. J. Pharm.*, 2011, 419, 1

[2] G. L. Perlovich, *CrystEngComm*, 2017, 19, 2870-2883.

PIII-6. Vapor Pressure and Vaporization Enthalpies of Glycolic Acid Esters

Yamshchikova Y.F., Portnova S.V., Krasnykh E.L.

Samara State Technical University, Russia

kinterm@samgtu.ru

The vapor pressure and vaporization enthalpies of methyl-, ethyl-, *n*-propyl-, *n*-butyl-, *n*-pentyl-, *n*-hexyl-, *n*-octyl esters of glycolic acid were studied in this work. The esters were prepared by esterifying glycolic acid with corresponding alcohols. All samples were purified by a distillation in vacuum. Purities of samples were determined by the gas chromatography. The purity of samples was obtained more than 99.5% mass.

The vapor pressure and vaporization enthalpies of esters of glycolic were obtained by the transpiration method. About 0.5g of the sample was mixed with small glass beads and placed in the thermostatted U-shaped saturator. A helium stream with well-defined flow rate was passed through the saturator at a constant temperature (± 0.1 K), and the transported material was collected in a cold trap. The amount of condensed sample was determined by GC analysis using the *n*-alkane as an external standard. The absolute vapor pressure p at each temperature T_i was calculated from the amount of the material, collected in the cold trap within a definite time:

$$p_i = m_i \cdot R \cdot T_a / V \cdot M_i; V = V_{He} + V_i; V_{He} \gg V_i \quad (1)$$

where $R = 8.314472 \text{ J K}^{-1} \text{ mol}^{-1}$; m_i is the mass of the transported compound, M_i is the molar mass of the compound, and V_i its volume contribution to the gaseous phase. V_{He} is the volume of the carrier gas and T_a is the temperature of the soap bubble meter. The volume of the carrier gas V_{He} was determined from the flow rate and the time measurement.

Temperature dependence of vapor pressures from experimental data was determined by equation:

$$R \times \ln p_i = a + \frac{b}{T} + \Delta_l^g C_p \times \ln \left[\frac{T}{T_0} \right] \quad (2)$$

where a and b are adjustable parameters and is the difference of the isobaric molar heat capacities of the gaseous and the liquid phase respectively. T_0 appearing in Eq. (2) is an arbitrarily chosen reference temperature (which has been chosen to be 298.15 K).

Vaporization enthalpy at temperature T was derived from temperature dependence of vapor pressures using equation (3) :

$$\Delta_l^g H_m(T) = -b + \Delta_l^g C_p \times T \quad (3)$$

The difference of the isobaric molar heat capacities of the gaseous and the liquid phase were estimated by the QSPR-method [1].

The enthalpies of vaporization $\Delta_l^g H_m^0(298,2)$ for alkyl glycolates $\text{HO-CH}_2\text{-COO-C}_n\text{H}_{2n+1}$

n	$\Delta_l^g C_p^0, \text{ kJ} \cdot \text{mol}^{-1} \cdot \text{K}^{-1}$	T-range, K	$\Delta_l^g H_m^0(298,2), \text{ kJ} \cdot \text{mol}^{-1}$
1	-88,1	289,4-328,8	52,19 \pm 0,61
2	-95,2	293,4-333,0	55,09 \pm 0,50
3	-102,4	299,4-343,2	58,21 \pm 0,49
4	-109,5	303,6-343,0	62,26 \pm 0,76
5	-116,6	303,6-343,3	64,64 \pm 0,54
6	-123,6	301,6-343,5	70,73 \pm 0,63
8	-137,9	313,6-353,4	78,30 \pm 1,15

Acknowledgements The financial support of the Russian Foundation for Basic Research, project no. 17-08-00967_a.

[1] E.L. Krasnykh and S.V. Portnova, *J. Struct. Chem.*, 2017, 58, 4, 753.

PIII-7. Thermodynamic Parameters of Formation Reactions for Binary and Ternary Complexes of Zinc(II), Cobalt(II), Nickel(II), Copper(II) Ions with Some Aminocarbonic Ligands

Gridchin S.N.¹, Pyreu D.F.²

¹Ivanovo State University of Chemistry and Technology, Russia;

²Ivanovo State University, Russia

sergei_gridchin@mail.ru

This work presents results of calorimetric, potentiometric and spectrophotometric investigations of acid-base interaction processes and homo- and heteroligand complex formation processes for zinc(II), cobalt(II), nickel(II), copper(II) ions and some amino carbonic acids in aqueous solutions. Among the objects of this investigation were serine, homoserine, threonine, valine, alanine, alanyl-alanine, alanyl-asparagine, glycyl-glycyl-glycine, glycyl-glycine, glycine, glutamine, asparagine, arginine, lysine, ornithine, histidine, aspartic, iminodiacetic, nitrilotriacetic, methyliminodiacetic, and hydroxyethyliminodiacetic acids.

The equilibrium concentration of hydrogen ions was determined by measuring the electromotive force of a glass electrode and a silver – silver chloride reference electrode using a P-363/3 potentiometer with a pH-340 pH-meter-millivoltmeter as the null-instrument. The calorimetric measurements were performed in an isothermal jacket ampoule flow-mixing calorimeter equipped with a thermistor sensor and an automatic recorder of the temperature–time curve. The unit was tested against the heat of solution of crystalline potassium chloride in water. The visible electronic spectra of the solutions investigated were recorded on Specord M-400 IENA and KFK-3 spectrophotometers.

Thermodynamic parameters ($\log K$, ΔG , ΔH , ΔS) of protolytic and coordination equilibria in systems of metal ion + aminocarbonic ligand have been determined at 298.15 K and ionic strength values from 0.1 to 1.5 (KNO_3). The influence of “background” electrolyte concentration on the relevant equilibria was under consideration. The data obtained were extrapolated to the zero ionic strength. The corresponding thermodynamic quantity values have been calculated for the standard solution ($\log K^\circ$, ΔG° , ΔH° , ΔS°).

Thermodynamic parameters for addition of some aminocarbonic ligands to zinc(II), cobalt(II), nickel(II), copper(II) iminodiacetates and nitrilotriacetates have been evaluated at 298.15 K and an ionic strength of 0.5 (KNO_3). The $\log K$, ΔG , ΔH , ΔS values for the mixed complex formation reactions were discussed together with the corresponding thermodynamic parameters of similar formation reactions for the simple binary complexes.

The ESR method and NMR method have been used to study the heteroligand complex formation in the systems of copper(II) complexonate + amino acid and zinc(II) complexonate + amino acid, respectively. ESP spectra were recorded using a Bruker ELEXSYS II-500 spectrometer. ^1H and ^{13}C spectra were recorded on a Bruker AVANCE-500 spectrometer. The relationship between the probable coordination modes of the aminocarboxylate molecules in the mixed-ligand complex and the thermodynamic parameters obtained has been discussed.

The results have been compared with the corresponding data on related compounds (amino acids, complexones, dipeptides and diamines) investigated earlier. A plausible explanation of changes in the thermodynamic quantities has been proposed in view of the metal ion and ligand structures.

This research was specified by the Ministry of Education and Science of the Russian Federation in accordance with a state assignment (basic part), project 4.7104.2017/8.9.

PIII-8. Thermodynamic Study of Ammonium Sulfamate

Tiflova L.A., Druzhinina A.I., Kosova D.A., Uspenskaya I.A., Monayenkova A.S.

Lomonosov Moscow State University, Department of Chemistry, 119992, Moscow, Russia

tiphlova@phys.chem.msu.ru

This work is a part of systematic studies of new functional materials which is carried out at Luginin's Thermochemistry and Chemical Thermodynamics Laboratories. It is devoted to the study of thermodynamical properties of $\text{NH}_4\text{SO}_3\text{NH}_2$. The choice of object of research is caused by its application as components of nitrogen fertilizations, herbicide and reagent for removing vegetation and glaze near airport runways. There are no thermodynamical data for $\text{NH}_4\text{SO}_3\text{NH}_2$ in literature.

In the present study commercial reagent of ammonium sulfamate ("Reahim") was investigated (initial purity 99.0 weight %). Before experiments the substance was recrystallized from water twice and dried at 80°C during several days in air. The sample of $\text{NH}_4\text{SO}_3\text{NH}_2$ was checked by TGA, DSK and HNS elemental analysis (final purity 99.84 ± 0.03 mol %).

The thermodynamical properties of $\text{NH}_4\text{SO}_3\text{NH}_2$ were investigated by methods of solution and adiabatic calorimetry.

The enthalpy of solution of $\text{NH}_4\text{SO}_3\text{NH}_2$ were measured in water at 298.15 K in hermetically sealed swinging calorimeter with an isothermal jacket, similar to that described in [1]. Temperature rise in each run was measured by platinum resistance thermometer. Thermometric sensitivity was $3 \cdot 10^{-5}$ K. The energy equivalent of the calorimeter was determined by electric technique. The enthalpy of formation of $\text{NH}_4\text{SO}_3\text{NH}_2$ at 298.15 K was calculated on the basis of the experimental data and $\text{NH}_4^+(\text{aq})$ and $\text{SO}_3\text{NH}_2^-(\text{aq})$ enthalpies of formation.

The molar low-temperature heat capacity of the $\text{NH}_4\text{SO}_3\text{NH}_2$ was measured with the help of an automated vacuum adiabatic calorimeter in the temperature range from 8 to 330 K. Liquid helium and nitrogen were applied as refrigerants. Detailed description of the device configuration and calorimetric technique were done in [2]. The errors in the determination of heat capacities are on average 0.2 – 0.3 %.

On the curve of temperature dependence of heat capacity of the $\text{NH}_4\text{SO}_3\text{NH}_2$ thermal anomaly at $T = 254.9$ K was observed. Obtained data were approximated by linear combination of Einstein-functions [3]. Heat content and entropy of $\text{NH}_4\text{SO}_3\text{NH}_2$ were calculated from these data for the crystal state in the temperature interval studied.

On the basis of experimental data, the standard entropy, enthalpy and Gibbs energy formation of $\text{NH}_4\text{SO}_3\text{NH}_2$ at 298.15 K were calculated.

Table. Thermodynamic functions of $\text{NH}_4\text{SO}_3\text{NH}_2(\text{cr})$ at $T = 298.15$ K

$C_p^o / \text{J} \cdot \text{K}^{-1} \cdot \text{mol}^{-1}$	$S_m^o / \text{J} \cdot \text{K}^{-1} \cdot \text{mol}^{-1}$	$\Delta_f H_m^o(\text{cr}) / \text{kJ} \cdot \text{mol}^{-1}$	$\Delta_f S_m^o(\text{cr}) / \text{J} \cdot \text{K}^{-1} \cdot \text{mol}^{-1}$	$\Delta_f G_m^o(\text{cr}) / \text{kJ} \cdot \text{mol}^{-1}$
151.49±0.5	173.0±1	-1243.3±6	-750.4±1	-1019.6±6

[1] A.S. Monayenkova, et al., *J. Chem. Thermodynamics*. 2001, 33, 1679.

[2] R.M. Varushchenko, A.I. Druzhinina and E.L. Sorkin. *J. Chem. Thermodynamics*. 1997, 29, 623.

[3] G.F. Voronin and I.B. Kutsenok. *J. Chem. Eng. Data*. 2013, 58, 2083.

PIII-9. Dicyclopropyldinitromethane and Tricyclopropylmethane: Standard Enthalpies of Formation in Condensed and Gas States

Tiflova L.A., Lukyanova V.A., Pimenova S.M., Ilin D.Y., Druzhinina A.I., Dorofeeva O.V.

Department of Chemistry, Lomonosov Moscow State University, 119992, Moscow, Russia

tiphlova@phys.chem.msu.ru

Compounds containing cyclopropane fragments constitute the promising substances for study correlations between energetic parameters and molecular geometry. The study of their thermodynamic properties is of considerable interest for medicine and biology. These compounds perform in syntheses of complex molecules with a specified combination of functional groups, in particular, drugs antitumor and antibacterial.

The samples of dicyclopropyldinitromethane ($C_7H_{10}N_2O_4$ (liq), DCPDNM) and tricyclopropylmethane ($C_{10}H_{16}$ (liq), TCPM) were synthesized in the laboratory of organic synthesis of Chemical Department of Lomonosov Moscow State University and were purified by the distillation and preparative g.l.c. The purity of both samples was 0.9999 ± 0.0002 mass fractions.

The combustion energies of both samples were determined in static-bomb isoperibolic calorimeter at $T=298.15$ K. The temperature rise was measured with a copper resistance thermometer using a bridge circuit. The temperature measurement sensitivity was $5 \cdot 10^{-5}$ K. The combustion products were analyzed for carbon dioxide by the Rossini method [1] and the absence of CO was controlled by indicator tubes. The content of HNO_3 in the solution was determined by titration of washing waters by ~ 0.1 mol·dm⁻³ of NaOH (aq).

The enthalpies of vaporization of DCPDNM and TCPM were estimated on the basis of molecular electrostatic potential model (MEP) [2]. The formation enthalpies of the compounds in gas state were obtained from these data. The gas enthalpies of formation were also calculated by methods of the group additivity (MGA) [3] and isodesmic reactions (MIR). The obtained experimental and calculation values were compared (Table).

Table. Standard energy of combustion, $\Delta_c U_m^o$, and enthalpy of combustion, $\Delta_c H_m^o$, and formation, $\Delta_f H_m^o$, of DCPDNM and TCPM in liquid and gas state at $T=298.15$ K (kJ·mol⁻¹)

substance	$-\Delta_c U_m^o(\text{liq})$	$-\Delta_c H_m^o(\text{liq})$	$\Delta_f H_m^o(\text{liq})$	$\Delta_{\text{liq}}^g H_m^o$	$\Delta_f H_m^o(\text{g})$	$\Delta_f H_m^o(\text{g})$ methods calculation	
						MEP	MGA
DCPDNM	4219.3±2.4	4218.1±2.8	34.4±2.9	66.3±5.0	99.9±5.8	99.8	83.6±7.0
TCPM	6370.9±5.4	6380.8±5.5	159.1±5.6	46.6±5.0	205.7±7.5	207.9	191.9±4.0

The values of the formation enthalpies obtained by the calculation methods indicate that further accumulation of the experimental material is necessary, which will allow more accurate consideration of various interactions in molecules of similar structure and improve the calculation schemes.

This research was supported by the Russian Foundation for Basic Research under Grant No. 17-03-00449.

[1] F.D. Rossini (Ed.), *Experimental Thermochemistry*, 1956, Chapter 4, p. 59; Chapter 3, p. 38; Chapter 5, p. 75. Interscience, New York, USA.

[2] P.Politzer, Y. Ma, P. Lane and M.C. Concha, *Int. J. Quant. Chem.* 2005, 105, 341.

[3] E.S. Domalski and E.D. Hearing, *J. Phys. Chem. Ref. Data* 1993, 22, 805.

PIII-10. Thermodynamic Functions of Lanthanide Orthotantalates at 10-330 K

Gagarin P.G., Guskov V.N., Gavrichev K.S., Sazonov E.G.

Kurnakov Institute of General and Inorganic Chemistry of the Russian Academy of Sciences 31
Leninsky prospect, Moscow 119991, Russia

gagarin@igic.ras.ru

Lanthanide orthotantalates, LnTaO_4 , are refractory compounds with high chemical, electrochemical, and biological inertness. Materials based on these compounds have good prospects in technology due to a wide range of functional properties, such as ionic conductivity, luminescence, photoelectric properties, etc. [1]. Lanthanide orthotantalates are being investigated as potential dopants to zirconia, stabilizing its structure for use as thermal barrier coating materials [2–4].

To obtain lanthanide orthotantalates, a method of reverse sedimentation of components from water-alcohol solutions in ammonia was used, followed by dehydration and stepwise annealing of the obtained samples. For the synthesis, tantalum (V) chloride 99.99% and lanthanide oxides 99.99% were used. Nd-Lu and Y orthotantalates crystallize in the monoclinic syngony of two types of space groups M' ($P2/a$, $Z=2$) and M ($I2/a$, $Z=4$). The first type of structure occurs during crystallization at low temperature in the lanthanides Sm-Lu, the second – at high-temperature treatment of Nd-Dy orthotantalates, and the transformation is irreversible. In this case, single-phase samples can be obtained only as a result of annealing at temperatures of 1200–1500 °C, depending on the lanthanide. For calorimetric measurements we used single-phase compounds annealed at $t = 1500^\circ\text{C}$. Particle sizes of studied orthotantalates were measured by SEM to be sure they are not nanoscale. The adiabatic calorimetry in the range of 10-330 K was used to measure heat capacities of M -NdTaO₄, M -SmTaO₄, M -GdTaO₄, M -DyTaO₄, M' -YbTaO₄, M' -LuTaO₄ and calculate the thermodynamic functions without the contribution of magnetic transition. The extrapolation of the heat capacity to 0 K was performed by the Debye equation. No heat capacity anomalies connected with the structural transitions were observed.

Table. Heat capacity and thermodynamic functions of lanthanide orthotantalates at $T = 298.15$ K

Compound	Structure	$C_p^0(T)$	$S^0(T)$	$\Phi^0(T)$	$H^0(T)-H^0(0)$
		J/(mol·K)			J/mol
NdTaO ₄	M	121.2	136.6	64.80	21390
SmTaO ₄	M	121.2	134.8	63.55	21230
GdTaO ₄	M	113.9	139.0	73.74	19457
DyTaO ₄	M	118.8	139.0	68.26	21080
YbTaO ₄	M'	121.4	130.1	59.99	20910
LuTaO ₄	M'	113.4	119.9	55.59	19170

[1] *Forbes T.Z., et al.*, J. Solid. State Chem. 2010. V. 183. P. 2516.

[2] *Bhattacharya A.K., Shklover V., Steurer W. et.al* // J. Eur. Ceram. Soc. 2011. V.31. P. 249.

[3] *Raghavan S., Wang H., Porter W.D., Dinwiddie R.B* //Acta Mater. 2001. V.49. P.169.

[4] *Shen Y., Leckie R.M., Levi C.G., Clarke D. R.* // Acta Mater. 2010. V. 58. P. 4424.

The study was supported by the Russian Science Foundation (Project No. 18-13-00025)

PIII-11. Low-Temperature Heat Capacity of Pd(C₅HF₆O₂)₂

Bespyatov M.A., Gelfond N.V., Morozova N.B.

Nikolaev Institute of Inorganic Chemistry, Siberian Branch of the Russian Academy of Sciences,
Novosibirsk, Russia

gel@niic.nsc.ru

Beta-diketonates of palladium are perspective complexes for their use as precursors in CVD-technology. Optimization of processes requires detailed information on the various physicochemical properties of precursors, including the thermodynamic properties. The results of experimental research of Pd(C₅HF₆O₂)₂ heat capacity in the temperature range from 6 K to 308 K are presented in this work.

Bis(1,1,1,5,5,5-hexafluoro-2,4-pentanedionato) palladium Pd(C₅HF₆O₂)₂ has been produced by the procedure described in detail in [1]. After synthesis, the product was purified by means of double sublimation in a vacuum gradient furnace. Purity of the final compound is not lower than 99.8%.

The heat capacity $C_{p,m}(T)$ of the sample Pd(C₅HF₆O₂)₂ was measured in the range (6–308) K by the adiabatic method on the installation described in [2]. A sample of 4.962 g was loaded into the calorimetric ampoule. The molar mass used in the calculation of the molar heat capacity was determined from the formula Pd(C₅HF₆O₂)₂ as 520.52 g·mol⁻¹. The smoothed $C_{p,m}(T)$ dependence over the temperature range (6–308) K was used to calculate the thermodynamic functions, including entropy $\Delta_0^T S_m^\circ$, enthalpy $\Delta_0^T H_m^\circ$ and reduced Gibbs energy $\Phi_m^\circ(T)$. An anomaly of heat capacity has been discovered with a maximum at $T_c \sim 237$ K (Fig. 1), which points to the phase transition of the complex. At present, there is insufficient information to separate these contributions. Data on the heat capacity for isostructural compounds, necessary for the calculation of the lattice component, are not presented in the literature. For detailed analysis of the nature of the observed phase transition, one needs to conduct special research.

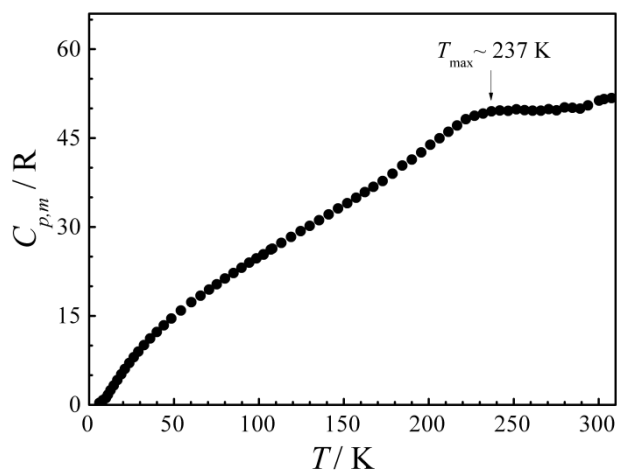


Figure 1. Experimental heat capacity for Pd(C₅HF₆O₂)₂ in the range of 6 K to 308 K.

[1] G.I. Zharkova, P.A. Stabnikov, S.A. Sysoev and I.K. Igumenov, *J. Struct. Chem.*, 2005, 46, 320.

[2] V.N. Naumov and V.V. Nogteva, *Instrum. Exp. Tech.*, 1985, 28, 1194.

PIII-12. Phonon Density of States and Zero-Point Energy of $\text{Eu}(\text{C}_{11}\text{H}_{19}\text{O}_2)_3$

Musikhin A.E., Bespyatov M.A.

Nikolaev Institute of Inorganic Chemistry,
Siberian Branch of the Russian Academy of Sciences, Russia

musikhin@niic.nsc.ru

The beta-diketonates of rare-earth metals are promising materials for the development of OLED technologies. Therefore, interest in these compounds is growing steadily, which leads to a tendency for a comprehensive study of their physicochemical properties [1-5]. Tris(2,2,6,6-tetramethyl-3,5-heptanedionato) europium, $\text{Eu}(\text{C}_{11}\text{H}_{19}\text{O}_2)_3$, belongs to the class of rare-earth metal beta-diketonates. The work presents results of research on a set of important characteristics of the $\text{Eu}(\text{C}_{11}\text{H}_{19}\text{O}_2)_3$ molecular crystal based on low temperature experimental heat capacity data.

Based on the heat capacity data in a wide range of low temperatures, the phonon density of states $g(\omega)$ of $\text{Eu}(\text{C}_{11}\text{H}_{19}\text{O}_2)_3$ was obtained in the framework of the numerical method [6-7]. The method makes it possible to obtain the density of states while identifying three or four peaks and correctly describing their shape and area. Before calculating the density of states $g(\omega)$, we took into account the component of the heat capacity due to stretching vibrations of hydrogen atoms. Our estimation of the anharmonic contribution of the heat capacity up to 320 K is on the level of the experimental uncertainty of the heat capacity measurement. Therefore density of states of $\text{Eu}(\text{C}_{11}\text{H}_{19}\text{O}_2)_3$ was calculated from the experimental heat capacity $C_p(T)$. Obtained spectrum $g(\omega)$ has a few peaks, which include both intramolecular and intermolecular compounds. The low frequency peak is conditioned on vibrational modes in a crystal, which obviously connected with intermolecular interaction.

For obtained phonon density of states with taking into account the stretching vibrations of hydrogen atoms, basic characteristic temperatures related to the moments of $g(\omega)$ were calculated. Using obtained value of characteristic temperature related to the first moments of $g(\omega)$, we calculated molar zero-point energy of $\text{Eu}(\text{C}_{11}\text{H}_{19}\text{O}_2)_3$ with high accuracy.

Using the obtained $\text{Eu}(\text{C}_{11}\text{H}_{19}\text{O}_2)_3$ spectrum reconstruction results, we calculated heat capacity at constant volume up to 464 K. Uncertainty of heat capacity description, as it follows from our calculations, does not exceed 0.3% in the temperature range 300–464 K. The knowledge of the molar zero-point energy of $\text{Eu}(\text{C}_{11}\text{H}_{19}\text{O}_2)_3$ allowed us to calculate the total internal energy and total enthalpy.

Used approach is general and it can be used to obtain the important characteristics of solids based on its experimental low temperature heat capacity.

Acknowledgements The reported study was funded by RFBR according to the research project № 19-03-00385

[1] J. Kido, Y. Okamoto, *Chem. Rev.*, 2002, 102, 2357.

[2] P.P. Lima, et al., *Org. Electron.*, 2014, 15, 798.

[3] J.P. Martins, et al., *Mater. Chem. Phys.*, 2014, 147, 1157.

[4] Z. Ahmed, et al., *Thin Solid Films*, 2016, 620, 34.

[5] Priya, N.K. et al., *ECS J. Solid State Sci. Technol.*, 2016, 5, R166.

[6] V.N. Naumov, A.E. Musikhin, *Phys. B*, 2015, 476, 41.

[7] V.N. Naumov., A.E. Musikhin, *Comput. Mater. Sci.*, 2017, 130, 257.

PIII-13. Thermodynamic Characteristics and Phonon Density of States of Barium Tungstate Based on the Low-Temperature Heat Capacity

Musikhin A.E., Naumov V.N.

Nikolaev Institute of Inorganic Chemistry,
Siberian Branch of the Russian Academy of Sciences, Russia

musikhin@niic.nsc.ru

Currently, the single crystal compounds of molybdate and tungstate are the subject of extensive research due to their unique optical properties, which determine a number of practical applications. Among them, great interest is attracted by barium tungstate, which is the most promising universal Raman-active crystal. It is used, for example, to detect radiation, to create solid-state lasers [1-2]. Many properties of this compound have already been investigated, including experimental low-temperature heat capacity data [3]. Based on the data [3], we present the calculation of the phonon density of states and some thermodynamic characteristics of BaWO₄ single-crystal.

Phonon density of states $g(\omega)$ calculation was carried out using the original numerical method [4-5]. The method allows to obtain the density of states while identifying three or four peaks with the correct description of its shape and correct ratio of the number of vibrational modes in different frequency intervals. The density of states of BaWO₄ has three characteristic peaks and cutoff frequency about 1152 K. Between the second and third peak, there is a region in which there are no phonon modes. Characteristics of the obtained $g(\omega)$ is consistent with the literature data [6-7].

Characteristic temperatures related to the basic moments of the density of states were determined. Using approach [5], the zero-point energy of BaWO₄ was calculated with high accuracy.

To improve the reliability of the result obtained, two different approaches of BaWO₄ heat capacity calculation were used. The first calculation was performed by the effective sum method (ESM) [8], which is based on the high-temperature expansion of heat capacity by even moments of phonon spectrum. The second heat capacity calculation was made on the basis of the obtained phonon density of states. The relative deviation of the heat capacities obtained by the considered methods does not exceed 0.05% and above 410 K systematically decreases with increasing temperature, which is associated with a correct asymptotic description of the function $C_V(T)$ at high temperatures within both approaches.

Using the heat capacity calculation results, thermodynamic functions (entropy, internal energy, and the reduced Helmholtz energy) at a constant volume up to the melting point were obtained. The knowledge of the molar zero-point energy allowed to calculate the total internal energy and enthalpy of BaWO₄.

Acknowledgments The report study was funded by the Ministry of Education and Science of the Russian Federation.

[1] M. Nikl, et al., *J. Lumin.*, 2000, 87–89, 1136.

[2] T.T. Basiev, et al., *RCCT-2017 (June 26-30, 2017, Novosibirsk, Russia)*, 2017, 153.

[4] V.N. Naumov, A.E. Musikhin, *Phys. B*, 2015, 476, 41.

[5] V.N. Naumov., A.E. Musikhin, *Comput. Mater. Sci.*, 2017, 130, 257.

[6] J. Suda, P.G. Zverev, *Vib. Spectrosc.*, 2012, 62, 85.

[7] P. Goel, et al., *Phys. Rev. B*, 2015, 91, 094304.

[8] A.E. Musikhin, V.N. Naumov, M.V. Chislov, I.A. Zvereva, *Thermochim. Acta*, 2018, 661, 160.

PIII-14. Thermodynamics of Evaporation Processes of Yttrium Trichloride and Tribromide

*Osina E.L.*¹, *Gorokhov L.N.*¹, *Osin S.B.*²

¹Joint Institute for High Temperatures of RAS, Russia;

²Lomonosov Moscow State University, Department of Chemistry, Russia

j-osina@yandex.ru

The work on updating and expanding the IVTANTHERMO thermodynamic database for inorganic compounds is in progress now at the Joint Institute for High Temperatures of RAS. The work includes a new assessment of thermodynamic properties for the compounds of Rare-Earth elements including scandium and yttrium. Yttrium trichloride and yttrium tribromide vapors mainly consist of YX_3 monomer molecules and some more low Y_2X_6 dimer content. Experimental information on the structure and spectra necessary for calculation of thermodynamic functions for these molecules, is extremely scarce. The most reliable experimental data for yttrium trichloride are published in [1, 2]. The molecule YBr_3 has not been studied experimentally. The molecular constants of YBr_3 were obtained using the Moller–Plesset perturbation theory MP2 and coupled clusters CCSD(T) method with relativistic pseudopotentials. From these data, we estimated molecular constants for YCl_3 and YBr_3 gaseous species. D_{3h} planar structure was accepted for both molecules. For Y_2Cl_6 and Y_2Br_6 molecules a planar bridged D_{2h} structure was accepted according to results obtained in our *ab initio* computations for Y_2Br_6 and experimental data for Y_2Cl_6 [2]. The vibrational frequencies were selected on the basis of experimental and theoretical data available in the literature. The calculations of the thermodynamic functions were carried out using "rigid rotator - harmonic oscillator" approximation in the temperature range of 298.15K - 6000 K. Yttrium trihalides have a closed electron shell, so the calculation of the thermodynamic functions is carried out without taking into account the excited electronic states.

As was mentioned above, yttrium trichloride and yttrium tribromide vapors mainly consist of YCl_3 and YBr_3 monomer molecules and some small Y_2Cl_6 and Y_2Br_6 dimer molecules content: $P(d)/P(m) = 0.15$ at the temperature 1300 K [2] and $P(d)/P(m) = 0.013$ at the temperature 1062 K [3] respectively. The temperature dependence of these values was calculated from the equilibrium constant values for the reactions $YX_3(cr,l) + YX_3(g) = Y_2X_6(g)$, $K_p = P(d)/P(m)$ ($X = Cl, Br$) with the "Third Law" method. In the first case $P(d)/P(m)$ values over liquid trihalides rise from 0.15 to 0.21 in the temperature range 1300 – 1600 K, in the second case – from 0.04 to 0.12 in the temperature range 1200 – 1500 K. Using these results, $P(d)$ and $P(m)$ values were calculated using the total pressure over liquid yttrium trichloride from the work [4] and over liquid yttrium tribromide from [5]. From the partial pressures so obtained were calculated the enthalpies of sublimation in the form of monomers and dimers (kJ/mole): $\Delta_s H^\circ(YCl_3, cr, 0 K) = 288.9 \pm 5$; $\Delta_s H^\circ(2YCl_3(cr) = Y_2Cl_6(g), 0 K) = 359.9 \pm 8$; $\Delta_s H^\circ(YBr_3, cr, 0 K) = 291 \pm 8$; $\Delta_s H^\circ(2YBr_3(cr) = Y_2Br_6(g), 0 K) = 397 \pm 12$.

Acknowledgements. The financial supported of Russian Foundation for Basic Research under Grant No. 17-03-00449. Authors are indebted to Mr. D. Kovtun for performing quantum-chemical calculations.

[1] R.J.M. Konings, A.S. Booiij, *J. Mol. Struct.*, 1992, 271, 183.

[2] B. Reffy, C.J. Marsden and M. Hargittai, *J. Phys. Chem. A*, 2003, 107, 1840.

[3] S.A. Shlykov, H. Oberhammer, *Austin Symposium on Molecular Structure and Dynamics, Book of abstracts*, 2012, p.163, Dallas, Texas, USA.

[4] G.P. Dudchik, O.G. Polyachenok and G.I. Novikov, *Zh. Neorg. Khim.*, 1969, 14, 3165.

[5] A. Makhmadmurodov, M. Temurova, A. Sharipov, *Izv. Ak. Nauk Tadg.SSR*, 1989, 1, 39.

PIII-15. Study of Thermochemical Properties of Various Porphyrin Ligands

Lazarev N.M., Petrov B.I., Makarov S.G.

G.A. Razuvaev Institute of Organometallic Chemistry of Russian Academy of Sciences

nikolai-lazarev@mail.ru

Porphyrins in solid-state formulations exhibit a wealth of solid-state properties, which render them an important class of functional materials. These compounds have the subject of a large number of applications, due to their unique electronics and molecular structure. In the recent years porphyrins found applications in CD/Rs, as blue and green colors in LCDs, as photoconductor in laser printers and as p-conductor and absorber in organic solar cells.

One of the most significant properties of porphyrins is their volatility and the ability to evaporate without decomposition. One quantitative characteristic of volatility is the pressure of saturated vapor. The thermodynamics parameters of porphyrins sublimation and reflect important physicochemical characteristics of the compound.

In the present work was investigation of thermodynamics parameters of sublimation and vapor phase composition of tetraphenylporphyrin H₂TPP (**1**) and some phenyl-substituted derivatives: H₂TPP(CH₃O)₄ (**2**) and H₂TPP(C₂H₅)₈ (**3**). The compounds were purified by sublimation in vacuum for further experiments.

The temperatures of melting of the **1-3** measured by the DSC method using a differential scanning calorimeter DSC204F1 Phoenix (DSC) (Netzsch Gerätebau, Germany). The endothermic transition was detected for all compounds. This transition was associated with melting. Thermodynamic parameters of melting **1-3** are calculated.

The composition of vapor phase of **1-3** was investigation by mass-spectrometry.

The temperature dependencies of the vapor pressure compounds **1-3** were measured by Knudsen effusion method. Vaporization temperature interval was chosen according to the DSC data (40-550°C). Thermodynamic parameters of sublimation are calculated: for sample **1** Δ_sH=205±7 kJ/mol, for sample **2** Δ_sH=173±5 kJ/mol and for sample **3** Δ_sH=151±6 kJ/mol. The ligands **1-3** are stable according to the mass-spectrometry data, there is not aggregation of molecules in the gas phase. Consequently, the calculation of vapor pressure was performed for the process of sublimation to monomeric vapor.

Acknowledgements The financial support of the Program of the Presidium of Russian Academy of Sciences no35.

PIII-16. Thermodynamic Properties of $\text{Ir}(\text{C}_5\text{H}_7\text{O}_2)(\text{C}_8\text{H}_{12})$

Kuzin T.M., Bespyatov M.A., Pischur D.P., Gelfond N.V.

Nikolaev Institute of Inorganic Chemistry,
Siberian Branch of the Russian Academy of Sciences, Russia

kuzin@niic.nsc.ru

The noble metal iridium great resists oxidation and other types of corrosion even at high temperatures, which makes it a widely known protective coating under extreme conditions. The thermal decomposition of metal-organic compound vapors on heating surfaces (chemical vapor deposition or CVD) is one of the most suitable methods to obtain thin film of refractory metals. Iridium(I)(acetylacetonato)(1,5-cyclooctadiene) (or Ir(aa)(cod)) is one of the most promising precursor for CVD technology. This work presents the results of studies of the thermodynamic properties (heat capacity, entropy, enthalpy, reduced Gibbs energy) of Ir(aa)(cod) in the solid phase.

In this work, we investigated the same sample Ir(aa)(cod) (molar mass is $399.51 \text{ g mol}^{-1}$) as in [1]. The description of synthesis and sample characteristic is provided in [1]. Purity of the final compound is not lower than 99.8%.

Thermodynamic properties of the sample were studied using a differential scanning calorimeter Netzsch DSC 204 FI Phoenix. Two endothermic peaks were found on the DSC profile: at 287 K and at 428 K (standard uncertainty for temperature is 0.5 K). A peak associated with the melting of Ir(aa)(cod) is observed at a temperature of 428 K. Heat capacity of samples was measured by comparison method. The measurements were made from 220 K to 400 K, because at temperatures around 400 K and higher due to the sublimation of the sample increasing systematic error in the measured heat capacity will arise. This result is presented in Fig. 1. The accounting of experimental uncertainty related to the systemic bias for heat capacities obtained by DSC was made by using adiabatic calorimetry data [1]. According to our estimates, the uncertainty of experimental heat capacity measurements was 2%. Within the range (260–300) K, the presence of an anomaly in heat capacity with a maximum at $T_c = 287 \text{ K}$ (Fig. 1) is found. The appearance of the anomaly indicates that the compound exhibits a phase transition. The integral thermodynamic functions (entropy, enthalpy, and reduced Gibbs energy) were calculated in the interval of 0–400 K based on the heat capacity data obtained by adiabatic and scanning methods.

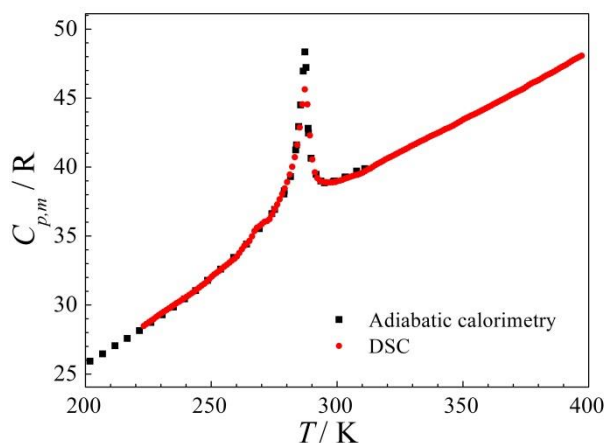


Figure 1. Experimental heat capacity of Ir(aa)(cod)

[1] M.A. Bespyatov, et al., *J. Chem. Thermodyn.*, 2016, 99, 70.

PIII-17. Thermochromism and Anomaly in the Heat Capacity of Dimeric Tris(2,2,6,6-Tetramethyl-3,5-Heptanedionato) Europium

Bespyatov M.A.¹, Cherniaikin I.S.^{1,2}, Kuzin T.M.¹, Stabnikov P.A.¹

¹Nikolaev Institute of Inorganic Chemistry,
Siberian Branch of the Russian Academy of Sciences, Russia

²Novosibirsk State University, Russia

bespyatov@niic.nsc.ru

Currently, immense interest is focused on study of physicochemical properties of lanthanide complexes containing beta-diketonate ligand. Their unique optical properties, such as high luminescence efficiency, long excited-state lifetimes and monochromaticity make them of interest for a wide range of photonic applications.

In this work we report the discovery of two effects for dimeric tris(2,2,6,6-tetramethyl-3,5-heptanedionato) europium ($\text{Eu}_2(\text{thd})_6$): 1) anomaly in the heat capacity looking like peak in the range of (250 – 275) K; 2) reversible change in color of crystals when cooled to $T \sim 240$ K.

The investigated sample $\text{Eu}_2(\text{thd})_6$ is the powder of the grains with average linear size ~ 0.5 mm. The crystals, yellow at the room temperature, become white when cooled to $T \sim 240$ K. The crystals immediately turn yellow when heated back to room temperature.

An additional experiment has demonstrated that (when immersing into liquid nitrogen) the reversible effect of thermochromism occurs in other β -diketonates of Cr(III), Fe(III), Sc(III).

The heat capacity of $\text{Eu}_2(\text{thd})_6$ have been measured by the adiabatic method in the temperature interval (7-312) K. The thermodynamic functions: entropy, enthalpy and reduced Gibbs energy have been calculated. The value of the absolute entropy were used to calculate the entropy of formation of $\text{Eu}_2(\text{thd})_6$ at $T = 298.15$ K. An anomaly of heat capacity has been discovered in the range of (250 – 275) K with a maximum at $T_c \sim 260$ K, which points to the phase transition of the complex. Anomalous contributions to entropy and enthalpy have been revealed.

The questions arise, what is the cause of the observed change in color of the $\text{Eu}_2(\text{thd})_6$ crystals, and what is the relationship between the effect of thermochromism and the anomalies in the heat capacity. Apparently, the decrease of temperature modifies an interaction between the cation Eu(III) and its crystal surrounding, and such a modification gives rise to the observed effects. For ascertaining how discovered effects depend on the type of cation and ligand we further on intend to carry out the measurement of heat capacity for the beta-diketonates of different rare-earth metals with different ligands.

Acknowledgements The reported study was funded by RFBR according to the research project № 19-03-00385.

PIII-18. Influence of N-Methyl Substitution in the Glycine Molecule on its Enthalpic Dissolution Characteristics in Mixed Aqueous - Organic Solvents at T=298.15 K

Smirnov V.I., Badelin V.G.

G.A. Krestov Institute of solution chemistry of the Russian Academy of Sciences, Ivanovo

vis@isc-ras.ru

The dissolution enthalpies of *N*-methylglycine in aqueous solution of acetonitrile (AN), 1,4-dioxane (DO), acetone (AC) and dimethyl sulfoxide (DMSO) with a mole-fraction of organic solvents from $x_2 = (0 \text{ to } 0.25)$ have been measured at $T=298.15 \text{ K}$. The results obtained have been used to calculate the standard enthalpies ($\Delta_{\text{sol}}H^\circ$) and transfer ($\Delta_{\text{tr}}H^\circ$) of *N*-methylglycine from water into mixtures as well as the enthalpy coefficients of pairwise interaction (h_{xy}) of the solute with organic solvents in aqueous solutions.

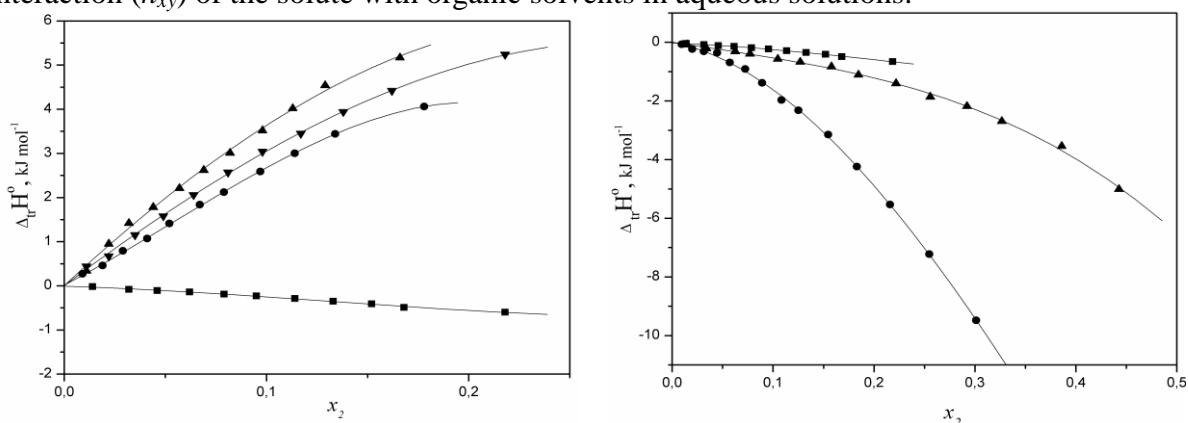


Figure.1. Enthalpies of transfer, $\Delta_{\text{tr}}H^\circ$, of *N*-methylglycine from H_2O into the $\text{H}_2\text{O} + \text{AN}$ (\blacksquare -), $\text{H}_2\text{O} + 1,4\text{-DO}$ (\bullet -), $\text{H}_2\text{O} + \text{DMSO}$ (\blacktriangle -) and $\text{H}_2\text{O} + \text{DMSO}$ (\blacktriangledown -) mixed solvent as a function of the organic solvent mole fraction (x_2) at $T=298.15 \text{ K}$.

Figure.2. Enthalpies of transfer, $\Delta_{\text{tr}}H^\circ$, of *N*-methylglycine (\blacksquare -), glycine (\bullet -) and *DL*- α -alanine (\blacktriangle -) from H_2O into ($\text{H}_2\text{O} + \text{AN}$) mixed solvent as a function of the mole fraction of AN (x_2) at $T=298.15 \text{ K}$.

The endothermic of $\Delta_{\text{tr}}H^\circ$ values for *N*-methylglycine observed for ($\text{H}_2\text{O} + 1,4\text{-DO}$), ($\text{H}_2\text{O} + \text{AC}$) and ($\text{H}_2\text{O} + \text{DMSO}$) mixtures suggest that hydrophobic – hydrophobic, hydrophobic - hydrophilic interactions predominate over the hydrophilic - hydrophilic ones. On the contrary, in ($\text{H}_2\text{O} + \text{AN}$) mixture hydrophilic - hydrophilic interactions between *N*-methylglycine and AN molecules predominate in all studied concentration range of AN (the values of $\Delta_{\text{tr}}H^\circ$ are exothermic). It is associated with low energy of interaction between H_2O and AN molecules in ($\text{H}_2\text{O} + \text{AN}$) mixture. Comparison of the enthalpy coefficients of pairwise interactions *N*-methylglycine with similar coefficients of glycine and *DL*-alanine, in the mixture ($\text{H}_2\text{O} + \text{AN}$) shows that the energy of interparticle interactions depends on the position of the CH_3 - group in the glycine molecule. Replacement of one proton in the CH_2 -group of glycine molecule on the CH_3 -group (alanine) weakens its pairwise interaction with the molecules of AN is weaker than the substitution of one proton in NH_2 - group (*N*-methylglycine). This may be due to weakening of donor-acceptor interactions between the molecules of AN (the donor e-pair) and *N*-methylglycine molecules (in this case, the acceptor of e-pair) because the molecule is missing the one proton in NH_2 -group (in comparison with *DL*-alanine) capable of forming hydrogen bond.

PIII-19. Influence of The Properties of Organic Solvents and the Composition of Water-Organic Mixtures on Thermochemical Characteristics of L-Glutamine Dissolution at T=298.15 K

Smirnov V.I., Badelin V.G.

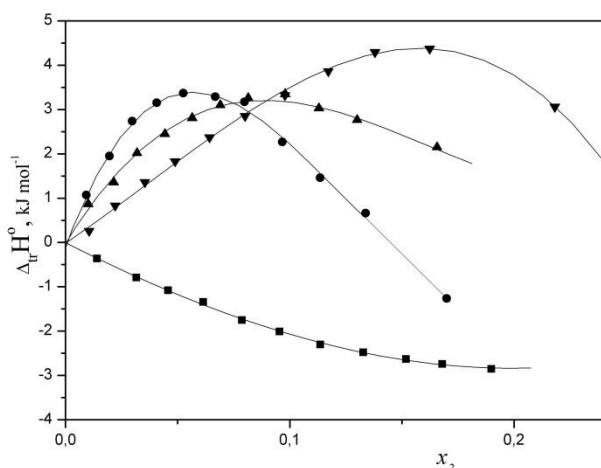
G.A. Krestov Institute of solution chemistry of the Russian Academy of Sciences, Ivanovo

vis@isc-ras.ru

The enthalpies of *L*-glutamine dissolution in aqueous solution of acetonitrile (AN), 1,4-dioxane (DO), acetone (AC) and dimethyl sulfoxide (DMSO), were determined by calorimetric method at $T=298.15$ K and organic solvent mole fractions up to $x_2 \sim 0.25$. The standard enthalpies of solution ($\Delta_{\text{sol}}H^\circ$) and transfer ($\Delta_{\text{tr}}H^\circ$) of *L*-glutamine from water to a mixed solvent (See Figure) as well as the enthalpy coefficients of pairwise interactions (h_{xy}) were calculated. The interrelation between enthalpy characteristics of *L*-glutamine dissolution (transfer) and the composition of water-organic mixtures was determined. Contributions of the organic solvent properties (molar volume, cohesion energy density, polarity/polarizability, acidity and basicity) to the energy of pairwise interactions of *L*-glutamine - organic solvent were estimated quantitatively by means of a modified Kamlet-Taft equation (1).

$$h_{xy} = A_0 + A_1(\delta_1^2/1000)(V_2/100) + A_2(\pi_1^* \pi_2^*) + A_3(\alpha_1\beta_2) + A_4(\beta_1\alpha_2), \quad (1)$$

Figure. Enthalpies of transfer, $\Delta_{\text{tr}}H^\circ$, of *L*-glutamine from H₂O into the H₂O + AN (-■-), H₂O + 1,4-DO (-●-), H₂O + AC (-▲-) and H₂O + DMSO (-▼-) mixed solvent as a function of the organic solvent mole fraction (x_2) at $T=298.15$ K.



From Figure it is seen that the transfer enthalpies of *L*-glutamine are endothermic in character in aqueous solutions of 1,4-DO, AC, DMSO and exothermic in character in aqueous solutions of AN, and depend both on the composition of a mixed solvent and the structure of an organic solvent molecules. Comparison of an enthalpy coefficients of pairwise interactions of organic solvent (y) + H₂O, (h_{H_2O+y}) with the enthalpic coefficients of pairwise interactions (h_{xy}) of *L*-glutamine - organic solvents shows that the strengthening of the pairwise interaction

between organic solvents and H₂O molecules in the mixtures $\{(H_2O + AN) < (H_2O + AC) < (H_2O + DO)\}$ causes endothermic contribution to h_{xy} of *L*-glutamine - solvent to grow.

$$h_{xy} = (1772.29) + (3615.49)(\delta_1^2/1000)(V_2/100) - (3686.91)(\pi_1^* \pi_2^*) - (5436.82)(\alpha_1\beta_2) + (409.43)(\beta_1\alpha_2), \quad R=0.969, N=9, SD=78.46 \quad (2)$$

The analysis of calculated equation (2) taking into account the previously obtained data (h_{xy}) for other mixed solvents shows that the increase in polarity/polarizability and acidity of an organic solvent enhances the energy of pairwise interactions of *L*-glutamine - organic solvent. Increasing of the cohesion energy density, molar volume and basicity of organic solvent decreases the energy of the pairwise interactions of *L*-glutamine -organic solvent.

PIII-20. The Evaluation of Originated Carbon-Paste Electrode Modified by Animal Waste Products Applicability for the Study of Thermodynamic Characteristics of Complex Formation Processes

Amerkhanova Sh.K., Shlyapov R., Uali A.S.

L.N. Gumilyov Eurasian National University, Kazakhstan

amerkhanovashk@gmail.com

The role of complex compounds in medicine, pharmaceutical and analytical chemistry, and metallurgy is enormous, since all medicinal compounds are organic ligands, which are assimilated only as part of complexes with biogenic metals. Chemical methods for the extraction of metals from ores are associated with the formation of highly soluble, low-melting and highly volatile complexes. Consequently, the indicator of the stability of complex compounds is a guideline in the selection of selective-acting reagents in hydrometallurgy and analytical chemistry. Therefore, the development of electrochemical sensors with high selectivity to the detected ion for the potentiometric determination of the stability constants of the complexes is relevant. These conditions correspond to carbon-paste electrodes modified by various substances, in particular, the possibility of using a carbon-paste electrode modified by 2-acetylbenzimidazole benzoyl hydrazone to determine Ag^+ ions [1]. It is established that ionophores A and B that are part of the graphite paste exhibit selectivity with respect to the ions Fe^{3+} , Fe^{2+} , which is used in the analysis of various objects [2]. It is also shown that an electrode based on N-octylpyridine hexafluorophosphate can be used in the determination of gold(III) chlorocomplexes [3].

In this work, animal waste product in a way of wool has been applied as a modifier for the solid electrode membrane. Wool first has been held in ferrous sulfate solution and then burned. Resulting composite material has been studied by electron microscopy, thermal analysis (DTA, TGA) and FT-IR-spectroscopy.

The carbon-paste electrode (CPE) was prepared by mixing 0.2 g of graphite and 0.01 g of modifier, α -Br naphthalene (0.04 mL) was added as a binder. Evaluation of the CPE selectivity with respect to iron(II) ions was studied by potentiometric measurements in solutions with different concentration of Fe(II) 10^{-2} – 10^{-6} mole/L. The selectivity coefficient was determined by the mixed solutions method [4]. The results are shown in table 1.

Table 1 - Analytical characteristics of the carbon-paste electrode

Electrode	S (mV/pFe)	Detection limit (mole/L)	pH range	Response time (min)	$K_{\text{Fe}^{2+}/\text{Cu}^{2+}}^{\text{pot}}$
CPE (bio)	41±3	$5 \cdot 10^{-6}$	3-7	0.5-1.0	$1.35 \cdot 10^{-4}$

From the data in the table it is possible to conclude that modified carbon-paste electrode has a relatively high selectivity for Fe^{2+} ions, which can be used as an indicator electrode in potentiometric studies of complexation processes which involves iron(II) ions.

[1] H.M. Abu-Shawish, S.M. Saadeh, H.M. Dalloul, Najrib B., H.A. Athamna, *Sensors and Actuators B: Chemical*, 2013, 3, 18.

[2] R. F. Aglan, M. S. Rizk, G. G. Mohamed, A. H. El-Wahy, H. A. Mohamed, *American Journal of Analytical Chemistry*, 2014, 5, 140.

[3] G. Absalan, M. Akhond, H. Ershadifar, *J Solid State Electrochem*, 2015, 19, 1113.

H. A. Zamani, M. R. Abedi, *J. Chem. Pharm. Res.*, 2011, 3, 825

PIII-21. Thermodynamic Properties of Crystalline Phosphate $\text{BiFe}_2(\text{PO}_4)_3$ in the Range from $T \rightarrow 0$ to 670 K

Pet'kov V.I., Lavrenov D.A., Smirnova N.N., Markin A.V., Asabina E.A.

G.A. Krestov Institute of solution chemistry of the Russian Academy of Sciences, Ivanovo

Lobachevsky University, Nizhni Novgorod, Russia

elena.asabina@inbox.ru

The thermodynamic properties of the new phosphate $\text{BiFe}_2(\text{PO}_4)_3$ (space group $P6_3/m$, $Z = 6$, $a = 14.3077(5)$, $c = 7.4271(3)$ Å) with the mineral perkovaite $\beta\text{-CaMg}_2(\text{SO}_4)_3$ structure were studied. Its basis is the $\{[\text{Fe}_2(\text{PO}_4)_3]^{3-}\}_{3\infty}$ framework in which the Fe atoms are coordinated by six oxygen atoms from six PO_4 tetrahedra, there are atoms Bi in the voids of the framework.

The research is aimed at calorimetric study of the heat capacity of $\text{BiFe}_2(\text{PO}_4)_3$ phosphate in the range from 5 to 670 K, calculate its standard thermodynamic functions $C_p^\circ(T)$, $[H^\circ(T) - H^\circ(0)]$, $S^\circ(T)$ and $[G^\circ(T) - H^\circ(0)]$ for the temperature range from 0 to 670 K, define the standard entropy of formation at $T = 298.15$ K. The temperature dependence of the heat capacity of the phosphate was studied by methods of precision adiabatic vacuum (over the temperature range from 5 to 346 K with BKT-3.07 thermophysical unit) and differential scanning calorimetry (in the temperature range from 300 to 670 K using DSC 204 F1 Phoenix calorimeter).

The phosphate was synthesized by the method of co-precipitation of salts from aqueous solutions. Annealing at 1223 K led to the formation of a high-crystalline single-phase product. The phase and chemical composition, crystal structure were studied by X-ray diffraction (Shimadzu XRD-6000), electron microscopy (JEOL JSM 7600F) and microprobe analysis, IR spectroscopy (Shimadzu FTIR-8400S). $\text{BiFe}_2(\text{PO}_4)_3$ underwent melting at the temperature of 1273 K.

The phase transition, connected with magnetic contribution of heat capacity, was observed for compound at temperatures 12–32 K ($\Delta H_{\text{tr}} = 87.4 \pm 1.8 \text{ J}\cdot\text{mol}^{-1}$; $\Delta S_{\text{tr}} = 4.00 \pm 0.08 \text{ J}\cdot\text{mol}^{-1}\cdot\text{K}^{-1}$). Except for this temperature range, the heat capacity of the phosphate raised gradually with increasing temperature. According to the experimental data, its standard thermodynamic functions and the standard formation entropy have been calculated.

Acknowledgements The reported study was supported by the Russian Foundation for Basic Research (Project No. 18-29-12063).

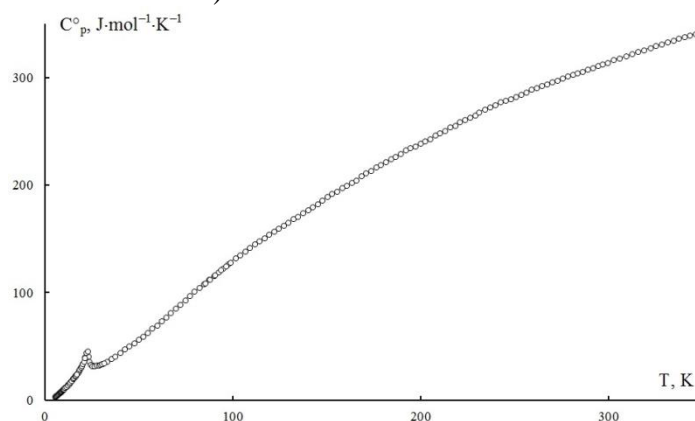


Figure. Plot of heat capacity against temperature dependence for crystalline $\text{BiFe}_2(\text{PO}_4)_3$.

PIII-22. Thermal Stability of Oxychlorides LnOCl (Ln = Gd, Yb)

Zakir 'yanova I.D.^{1,2}, Korzun I.V.¹

¹Institute of High-Temperature Electrochemistry, Ural Branch, Russian Academy of Sciences, Russia;

²Ural Federal University, Russia

optic96@mail.ru

The rare-earth elements form the oxychlorides of the LnOCl composition. The data available in the literature on the thermal stability of these compounds are contradictory [1, 2]. We have synthesized and certified samples GdOCl and YbOCl by XRD, IR and Raman spectroscopy. The thermal decomposition of rare earth oxychlorides in inert atmosphere (Ar) was studied on a thermal analyzer STA 449C Jupiter® allowing simultaneous recording of the TG and DTG curves. It is established that thermal decomposition GdOCl and YbOCl begins at 854 and 630 °C respectively (Figure 1).

The thermal stability of LnOCl (Ln = Gd, Yb) was found to decrease with increasing atomic number of the Ln.

Acknowledgements The partial financial support of the Russian Foundation for Basic Research, project № 18-03-00561a

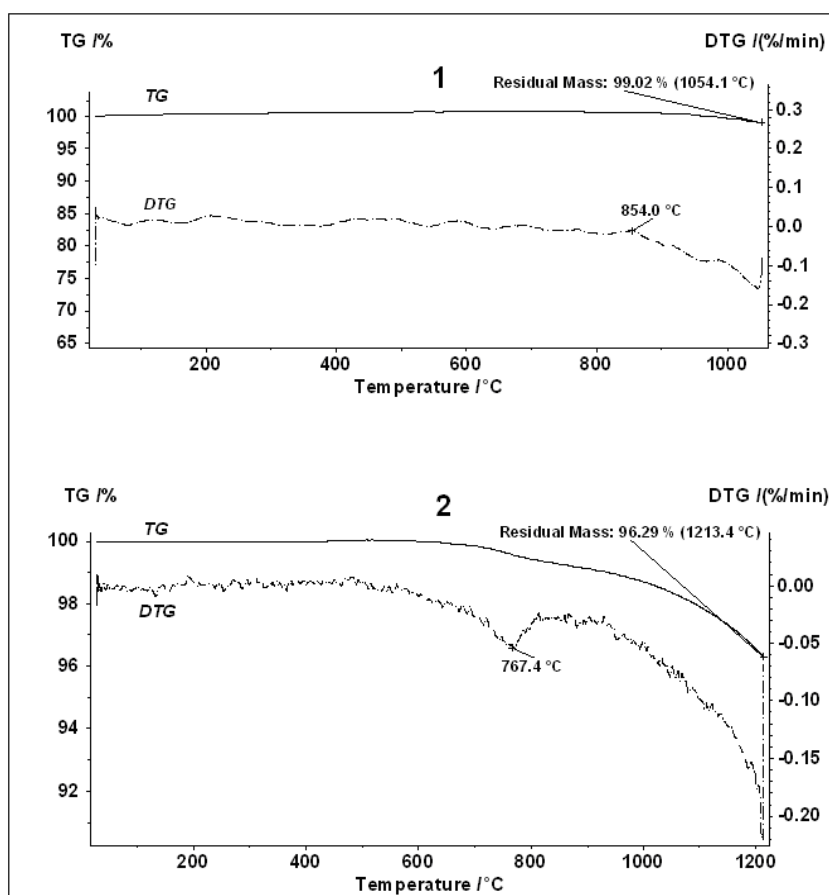


Figure 1. TG and DTG curves of GdOCl (1) and YbOCl (2).

[1] J. Hglsa, M. Leskela and L. Ninistga. *Thermochimica Acta*, 1980, 35, 79.

[2] V.V. Bunda, M.V. Shtilikha, V.M.Golovej. *Zhurnal Neorganicheskoy Khimii*; 1984, 29, 3045.

PIII-23. Thermodynamic Properties of 4'-Cyclohexylacetophenone

Blokhin A.V.¹, Kantsiava V.V.², Kilchytskaya Y.V.¹, Tarazanov S.V.³

¹Belarusian State University, Belarus. 220030 Minsk, Leningradskaya 14;

²Belarusian State Medical University, Minsk, Belarus;

³All-Russian Research Institute of Oil Refining, Moscow, Russia

blokhin@bsu.by

The thermodynamic properties of crystalline and liquid 4'-cyclohexylacetophenone were investigated by combustion bomb calorimetry and low-temperature adiabatic calorimetry. 4'-cyclohexylacetophenone was synthesized by acylation of cyclohexylbenzene with acetic anhydride in a nitrobenzene medium, using aluminum chloride as a catalyst. Purification of the obtained product was carried out by repeated recrystallization from ethyl alcohol. The purity of the sample was more than 99.8 mas. % according to gas-liquid chromatography. The combustion energy of the 4'-cyclohexylacetophenone sample was determined in a combustion calorimeter (B-08-MA) equipped with a stainless-steel bomb of a 326 cm³ volume [1]. The samples were burned in bags made of 80 nm polyethylene film. The standard energy of combustion of the compound

$$\Delta_c U_m^\circ(298.15 \text{ K}) = -(76780 \pm 5.5) \text{ kJ} \cdot \text{mol}^{-1}$$

was determined based on the results of a series from 4 experiments. The standard enthalpy of combustion and enthalpy of formation of crystalline 4'-cyclohexylacetophenone were obtained to be, respectively:

$$\Delta_c H_m^\circ(298.15 \text{ K}) = -(7689.1 \pm 5.5) \text{ kJ} \cdot \text{mol}^{-1},$$

$$\Delta_f H_m^\circ(298.15 \text{ K}) = -(392.6 \pm 5.6) \text{ kJ} \cdot \text{mol}^{-1}.$$

A TAU-10 adiabatic calorimeter (Termis, Moscow) [2] was used between 80 K and 370 K (liquid-nitrogen bath) with the relative expanded uncertainty of the heat capacity measurements determined to be 0.4%. The heat capacities of the compound were measured in 7 independent series. The contribution of the heat capacity of the sample to the total heat capacity of the filled calorimetric ampoule was not less than 45%.

Two anomalous regions due to the solid-phase transition of the λ type (crII \rightarrow crI) in the range of (163 – 179 K) and fusion of the compound (crI \rightarrow liquid) in the interval (313 – 341) K were found on the temperature dependence curve of the heat capacity. The thermodynamic parameters of the phase transitions in the condensed state were determined to be

$$T_{\text{tr}} = (175.1 \pm 0.7) \text{ K}, \Delta_{\text{tr}}H = (29.2 \pm 0.2) \text{ J} \cdot \text{mol}^{-1}, \Delta_{\text{tr}}S = (0.17 \pm 0.01) \text{ J} \cdot \text{mol}^{-1} \cdot \text{K}^{-1};$$

$$T_{\text{fus}} = (341.01 \pm 0.02) \text{ K}, \Delta_{\text{fus}}H = (20742 \pm 18) \text{ J} \cdot \text{mol}^{-1}, \Delta_{\text{fus}}S = (60.83 \pm 0.05) \text{ J} \cdot \text{mol}^{-1} \cdot \text{K}^{-1}.$$

The temperature of fusion and purity of sample $x = (99.58 \pm 0.02) \% \text{ mol}$. were obtained by fractional melting method. The standard thermodynamic functions of the compound in the condensed state in the range (80 to 370) K were calculated.

The method of isodesmic reactions was proposed to calculate the gas-phase enthalpy of formation of 4'-cyclohexylacetophenone. In calculations the density functional theory (DFT) was used at B3LYP/6-311++G(d,p) and B3LYP/6-31++G(d,p) levels of theory. Thermodynamic properties of the compound in the ideal-gas state were calculated in the range (100 – 1000) K

[1] G. J. Kabo, A. V. Blokhin and A. G. Kabo, *Chemical Problems of Creation of New Materials and Technologies*, 2003, 1, 176.

[2] A. V. Blokhin, G. J. Kabo, Y. U. Paulechka, *J. Chem. Eng. Data*, 2006, 51, 1377.

PIII-24. Thermodynamic Parameters of Methyl 3,5-di-tert-Butylbenzoate

Blokhin A.V.¹, Kantsiava V.V.², Neviadzimtsau A.V.¹, Tarazanov S.V.³

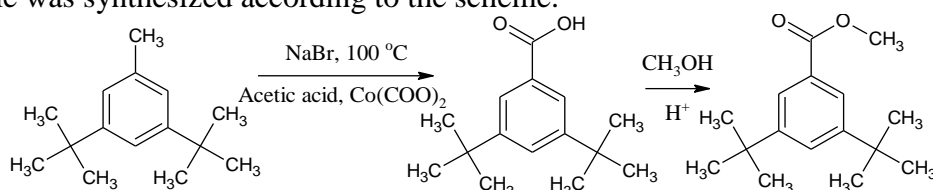
¹Belarusian State University, Belarus. 220030 Minsk, Leningradskaya 14;

²Belarusian State Medical University, Minsk, Belarus;

³All-Russian Research Institute of Oil Refining, Moscow, Russia

blokhin@bsu.by

The thermodynamic properties of crystalline and liquid methyl 3,5-di-tert-butylbenzoate were investigated by combustion bomb calorimetry and low-temperature adiabatic calorimetry. The sample was synthesized according to the scheme:



Purification of the product was carried out by the methods of fractional crystallization and sublimation. The purity of the sample was more than 99.9 mas. % according to gas-liquid chromatography.

The combustion energy of the compound was determined in a combustion calorimeter (B-08-MA) equipped with a stainless-steel bomb of a 326 cm³ volume [1]. The samples were burned in bags made of 80 nm polyethylene film. The standard energy of combustion

$$\Delta_c U_m^\circ(298.15 \text{ K}) = -(8851.4 \pm 5.9) \text{ kJ} \cdot \text{mol}^{-1}$$

was determined based on the series from 4 experiments. The standard enthalpy of combustion and enthalpy of formation of crystalline methyl 3,5-di-tert-butylbenzoate were obtained to be

$$\Delta_c H_m^\circ(298.15 \text{ K}) = -(8863.9 \pm 5.9) \text{ kJ} \cdot \text{mol}^{-1} \text{ and } \Delta_f H_m^\circ(298.15 \text{ K}) = -(874.8 \pm 6.0) \text{ kJ} \cdot \text{mol}^{-1}.$$

A TAU-10 adiabatic calorimeter (Termis, Moscow) [2] was used between 80 K and 370 K with the relative expanded uncertainty of the heat capacity measurements determined to be 0.4 %. The heat capacities of the compound were measured in 6 independent series. The contribution of the heat capacity of the sample to the total heat capacity of the filled calorimetric ampoule was not less than 55 %. The standard heat capacity of the compound at 298.15 K was $(382.3 \pm 1.5) \text{ J} \cdot \text{mol}^{-1} \cdot \text{K}^{-1}$.

Two anomalous regions due to the solid-phase transition (crII \rightarrow crI) in the range of (284 – 298 K) and fusion of the compound (crI \rightarrow liquid) in the interval (307 – 327) K were found on the temperature dependence curve of the heat capacity. The thermodynamic parameters of the phase transitions in the condensed state were determined to be

$$T_{\text{tr}} = (294.36 \pm 0.02) \text{ K}, \Delta_{\text{tr}}H = (1625 \pm 12) \text{ J} \cdot \text{mol}^{-1}, \Delta_{\text{tr}}S = (5.52 \pm 0.04) \text{ J} \cdot \text{mol}^{-1} \cdot \text{K}^{-1};$$

$$T_{\text{fus}} = (325.77 \pm 0.01) \text{ K}, \Delta_{\text{fus}}H = (16315 \pm 21) \text{ J} \cdot \text{mol}^{-1}, \Delta_{\text{fus}}S = (50.08 \pm 0.06) \text{ J} \cdot \text{mol}^{-1} \cdot \text{K}^{-1}.$$

The temperature of fusion and purity of sample $x = (99.86 \pm 0.01) \%$ mol. were obtained by fractional melting method. The standard thermodynamic functions of the compound in the condensed state in the range (80 to 370) K were calculated.

The method of isodesmic reactions was proposed to calculate the gas-phase enthalpy of formation of methyl 3,5-di-tert-butylbenzoate. In calculations the density functional theory (DFT) was used at B3LYP/6-311++G(d,p) and B3LYP/6-31++G(d,p) levels of theory. Thermodynamic properties of the compound in the ideal-gas state were calculated in the range (100 – 1000) K

[1] G. J. Kabo, A. V. Blokhin and A. G. Kabo, *Chemical Problems of Creation of New Materials and Technologies*, 2003, 1, 176.

[2] A. V. Blokhin, G. J. Kabo, Y. U. Paulechka, *J. Chem. Eng. Data*, 2006, 51, 1377.

PIII-25. Thermodynamic Properties of L-Menthol

Yurkshovich Y.N., Blokhin A.V., Neviadzimtsau A.V.

Belarusian State University, Republic of Belarus

yanayurksht@gmail.com

In this work we present the results of experimental and theoretical thermodynamic study of (1R,2S,5R)-2-isopropyl-5-methylcyclohexanol (Natural L-menthol). The test sample was provided by RUE Belpharmatsiya. According to the results of gas chromatography no organic impurities detected.

The heat capacity of L-menthol in the crystalline and liquid states in the range (5 to 370) K and its enthalpy of fusion were determined in TAU-1 and TAU-10 vacuum adiabatic calorimeters [1]. A TAU-1 calorimeter was used between 5 K and 100 K (liquid-helium bath) with the relative expanded uncertainty of the heat capacity measurements estimated to be 2 % near 5 K and 0.4 % above 40 K. A TAU-10 calorimeter was used between 80 K and 370 K (liquid-nitrogen bath) with the relative expanded uncertainty of the heat capacity measurements determined to be 0.4%. The molar heat capacity at 298.15 K is $(250.1 \pm 1.0) \text{ J}\cdot\text{mol}^{-1}\cdot\text{K}^{-1}$. The standard thermodynamic functions of the compounds in the condensed state in the range (5 to 370) K were calculated based on the temperature dependences of heat capacity (Figure) and the parameters of fusion $\Delta_{\text{fus}}H = (13.47 \pm 0.06) \text{ kJ}\cdot\text{mol}^{-1}$ and $\Delta_{\text{fus}}S = (42.68 \pm 0.19) \text{ J}\cdot\text{mol}^{-1}\cdot\text{K}^{-1}$. The melting point $T_{\text{fus}} = (315.60 \pm 0.02) \text{ K}$ and purity of sample $x = (99.73 \pm 0.02) \%$ mol. were determined by fractional melting method.

The standard internal energy of combustion of crystalline L-menthol at 298.15 K was determined to be $\Delta_c U^\circ = -(6303.6 \pm 1.3) \text{ kJ}\cdot\text{mol}^{-1}$ using a static bomb combustion calorimeter. The standard enthalpies of combustion and formation of crystalline L-menthol at 298.15 K were obtained to be $\Delta_c H^\circ = -(6314.7 \pm 1.3) \text{ kJ}\cdot\text{mol}^{-1}$ and $\Delta_f H^\circ = -(478.7 \pm 1.9) \text{ kJ}\cdot\text{mol}^{-1}$. Taking into account the enthalpy of sublimation at 298.15 K $\Delta_{\text{sub}}H^\circ = (84.4 \pm 1.7) \text{ kJ}\cdot\text{mol}^{-1}$ [2] standard enthalpy of formation of L-menthol in gaseous state is $\Delta_f H^\circ = -(394.3 \pm 2.5) \text{ kJ}\cdot\text{mol}^{-1}$. The method of isodesmic reactions was proposed to calculate the gas-phase enthalpies of formation of L-mentol. In calculations the density functional theory (DFT) was used at B3LYP/6-311++G(d,p) and B3LYP/6-31++G(d,p) levels of theory. Experimental results are in a good agreement with results of numerical simulation.

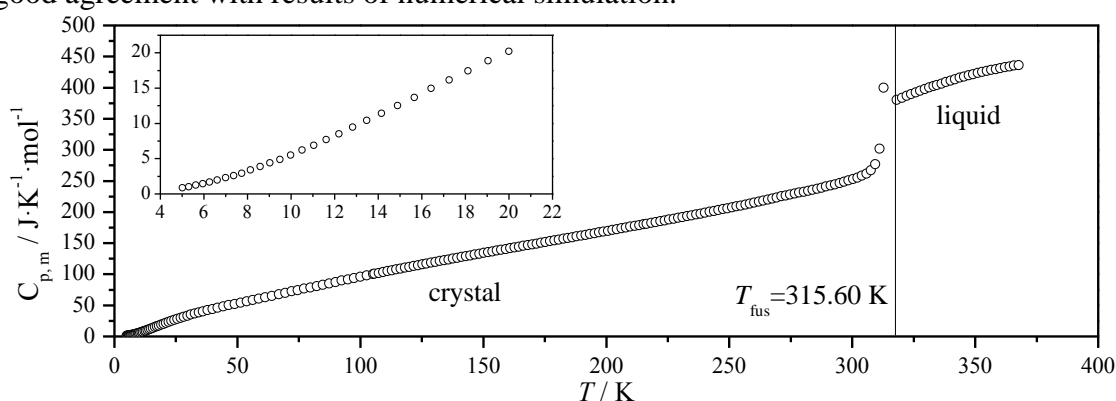


Figure. Condensed-phase heat capacities of L-menthol from adiabatic calorimetry measurements

[1] A. V. Blokhin, G. J. Kabo, Y. U. Paulechka, *J. Chem. Eng. Data*, 2006, 51, 1377.

[2] V. Štejfa, et al., *J. Chem. Thermodynamics*, 2019, 131, 524.

PIII-26. Thermodynamic Characteristics of Energy-Intensive Jet Fuels with Stacked-Cup Multiwall Carbon Nanotubes (MCNTs)

Karpushenkava L.S., Kabo G.J., Blokhin A.V., Seradzenka S.U.

Belarusian State University, Republic of Belarus

karpushenkava@bsu.by

The thermodynamic analysis of the possibility of obtaining model hydrocarbon fuels from toluene and T-1 [1] with MCNTs is carried out. The enthalpy of combustion, heat capacity in the range of 3–350 K, the physical density of multilayer carbon nanotubes (MCNTs) produced by Vision Development (Japan) by gas-phase catalytic pyrolysis of hydrocarbons are measured.

Preparation of MCNTs before measurements consisted of heat treatment at 130 °C and 200 °C in a drying cabinet in the air and at 200 °C in a vacuum ($P \sim 100$ Pa) flask with a volume of 20 cm³ and cooling the samples in a desiccator over P₂O₅. The content in the MCNTs residual catalyst (Ni), not removed by magnetic separation, is 0.69 mass %. According to the results of pycnometric measurements for water and toluene, the physical density of the MCNTs was (2210 ± 22) kg·m⁻³. The combustion energy of the MCNTs sample was determined in a combustion calorimeter (B-08-MA) equipped with a stainless-steel bomb of a volume 326 cm³ [2, 3]. Heat capacities were measured with a TAU-10 adiabatic calorimeter (Termis, Moscow) between 5–370 K [2, 3]. According to the measurement results, the following values of the properties of the technical samples of the MCNTs at 298.15 K were obtained:

$$\Delta_c H^\circ(298.15 \text{ K}) = -(32.336 \pm 0.012) \text{ MJ} \cdot \text{kg}^{-1};$$

$$c_p^\circ(298.15 \text{ K}) = (733.7 \pm 2.9) \text{ J} \cdot \text{kg}^{-1} \cdot \text{K}^{-1};$$

$$S^\circ(298.15 \text{ K}) = (518.1 \pm 2.1) \text{ J} \cdot \text{kg}^{-1} \cdot \text{K}^{-1}.$$

It has been established that mixtures of MCNTs with liquids containing MCNTs of more than mass % sedimentation resistant in a centrifuge at 7000g. The mass and volumetric energy of combustion, adiabatic combustion temperatures, the conditional flight range of the model rockets with the fuel of different compositions are calculated for the model systems “toluene + MCNTs”, “T1 + MCNTs”. It is shown that the volume lower energy of combustion of fuel of combustible “toluene + 50 mass % MCNTs” and “T1 + 50 mass % MCNTs” make up 45.65 and 44.19 MJ kg⁻¹, which is ~ 28% higher than that of hydrocarbon components.

[1] V.N. Bakulin, N.F. Dubovkin, V.N. Kotova, V.A. Sorokin, V.P. Frantskevich, L.S. Yanovsky, *Energy-consuming combustible for aircraft and rocket engines*, 2009, Fizmatlit, Moscow, Russia.

[2] G.J. Kabo, Y.U. Paulechka, A.V. Blokhin, O.V. Voitkevich, T.N. Liavitskaya, A.G. Kabo, *J. Chem. Eng. Data*, 2016, 61, 3849.

[3] G.J. Kabo, A.V. Blokhin, E. Paulechka, G.N. Roganov, M. Frenkel, I.A. Yursha, V.Diky, D. Zaitsau, A. Bazyleva, V.V. Simirsky, L.S. Karpushenkava, V.M. Sevruck, *J. Chem. Thermodyn.*, 2019, 131, 225.

PIII-27. Thermodynamics and Crystal Growth of Lithium Tungstate Doped by Molybdenum

Grigorieva V.D., Shlegel V.N., Matskevich N.I.

Nikolaev Institute of Inorganic Chemistry, SB RAS, 630090 Novosibirsk, Russia

grigorieva @niic.nsc.ru

Molybdates and tungstates of lithium are widely used as scintillation materials, ionic conductors, and also as materials for high energy physics [1-2]. Thus, $\text{Li}_2\text{W}_{1-x}\text{Mo}_x\text{O}_4$ as a material for scintillating cryogenic bolometers has several advantages: an absence of long-lived lithium isotopes, quite high intrinsic radio purity, and an effective ability to distinguish α and β (γ) events, a rather low congruent melting point. It is necessary to perform detailed physical and chemical investigations to develop perspective application of such materials as $\text{Li}_2\text{W}_{1-x}\text{Mo}_x\text{O}_4$.

In present work we carried out thermochemical investigations for single crystals of lithium molybdate and lithium tungstate doped by molybdenum $\text{Li}_2\text{W}_{1-x}\text{Mo}_x\text{O}_4$ ($x = 0.1; 0.15$). A single crystals of Li_2MoO_4 and $\text{Li}_2\text{W}_{1-x}\text{Mo}_x\text{O}_4$ ($x = 0.1; 0.15$) were grown by low temperature gradient Czochralsky method from Li_2CO_3 , MoO_3 and WO_3 [1]. Li_2MoO_4 and $\text{Li}_2\text{W}_{1-x}\text{Mo}_x\text{O}_4$ ($x = 0.1; 0.15$) belong to structural type of phenakite. Phenakite crystallizes in trigonal syngony.

Solution calorimetry was used to study thermochemical properties. The method and measurements procedure were described earlier in paper [3]. 0.4 mol dm^{-3} KOH was chosen as solvent. Thermochemical cycle to determine standard formation enthalpy of Li_2MoO_4 was constructed in such a way that solution enthalpy of lithium molybdate was compared with solution enthalpies of lithium carbonate and molybdenum oxide. To obtain the standard formation enthalpies for $\text{Li}_2\text{W}_{1-x}\text{Mo}_x\text{O}_4$ ($x = 0.1; 0.15$) the schema of thermochemical reactions was following. The solution enthalpies for $\text{Li}_2\text{W}_{1-x}\text{Mo}_x\text{O}_4$ were compared with solution enthalpies of Li_2CO_3 , MoO_3 and K_2WO_4 . On the basis of experimental and literature data the standard formation enthalpies were calculated. It was noted that standard formation enthalpies were increased in absolute values from Li_2MoO_4 up to $\text{Li}_2\text{W}_{1-x}\text{Mo}_x\text{O}_4$. Such behavior can be explained using method of predictive thermodynamics [4]. The lattice enthalpies for Li_2MoO_4 and $\text{Li}_2\text{W}_{1-x}\text{Mo}_x\text{O}_4$ ($x = 0.1; 0.15$) were calculated on the basis of obtained standard formation enthalpies using Born-Haber cycle.

Acknowledgements This research was supported by grant RSF (project 19-19-00095).



Figure 1. Typical form of $\text{Li}_2\text{W}_{1-x}\text{Mo}_x\text{O}_4$ crystals ($x = 0.1$).

[1] V.D. Grigorieva, V.N. Shlegel, Y.V. Vasiliev et al., *Eur. Phys. J.*, 2017, 77, 785.

[2] O.P. Barinova, A. Sadovskiy, I. Ermochenkoy, *J. Cryst. Gr.*, 2017, 468, 365.

[3] N.I. Matskevich, Th. Wolf, C. Greaves, A.N. Bryzgalova, *J. Alloys Comp.*, 2014, 582, 253.

[4] N.I. Matskevich, Th. Wolf, A.N. Semerikova et al., *J. Chem. Thermodyn.*, 2019, 135, 143

PIII-28. Low-Temperature Heat Capacity of $\text{Cu}(\text{C}_{11}\text{H}_{19}\text{O}_2)_2$

Cherniaikin I.S.^{1,2}, Bespyatov M.A.¹, Stabnikov P.A.¹, Dorovskikh S.I.¹, Morozova N.B.¹,
Gelfond N.V.¹

¹Nikolaev Institute of Inorganic Chemistry,
Siberian Branch of the Russian Academy of Sciences, Russia;
²Novosibirsk State University, Russia;

cherny@niic.nsc.ru

Metal-organic compounds are a popular class used as precursors in MOCVD technologies. Metals beta-diketonates also belong to such materials. The bis(2,2,6,6-tetramethyl-3,5-heptanedionato)copper(II) $\text{Cu}(\text{thd})_2$ investigated in this work is used to obtain thin copper films on organic and metallic bases.

The sample of $\text{Cu}(\text{C}_{11}\text{H}_{19}\text{O}_2)_2$ has been produced in aqueous ethanol solution by the procedure described in [1]. After synthesis, the product was additionally purified by means of double sublimation in a vacuum gradient furnace at $p = 7$ Pa and $T = (443\text{--}453)$ K. The elemental analysis for C, H was conducted using Carlo-Erba 1106 (Italy): found, %: C 61.6, H 8.9, for $\text{CuC}_{22}\text{H}_{38}\text{O}_4$ calculated, %: C 61.4, H 8.9. The Cu analysis was performed on atomic absorption spectrometer with Zeeman's correction (Hitachi, Z 8000) with $\lambda=324.8$ nm. The standard sample preparation method described in [2] was used. The average copper content by mass in three parallel probes was found 14.6 ± 0.4 % Cu, for $\text{CuC}_{22}\text{H}_{38}\text{O}_4$ calculated 14.7 %. Purity of the final compound is not lower than 99.8 %. The sample of $\text{Cu}(\text{C}_{11}\text{H}_{19}\text{O}_2)_2$ under Standard Ambient Temperature and Pressure is a dark-blue crystalline powder with a typical crystallite size of 0.2 μm .

The heat capacity $C_{p,m}(T)$ of the $\text{Cu}(\text{thd})_2$ sample was measured on the adiabatic calorimetric installation described in [3]. The mass of the substance loaded into the calorimeter was 5.149 g. The molar mass of $\text{Cu}(\text{C}_{11}\text{H}_{19}\text{O}_2)_2$ which used in the calculation of the molar heat capacity was determined from the formula of the sample as 430.09 $\text{g}\cdot\text{mol}^{-1}$. The heat capacity was measured at 81 points in the range (5–310) K. The resulting dependence of the heat capacity on temperature was smoothed to calculate thermodynamic functions over the entire temperature range under study.

Acknowledgements The reported study was funded by RFBR according to the research project №19-03-00385.

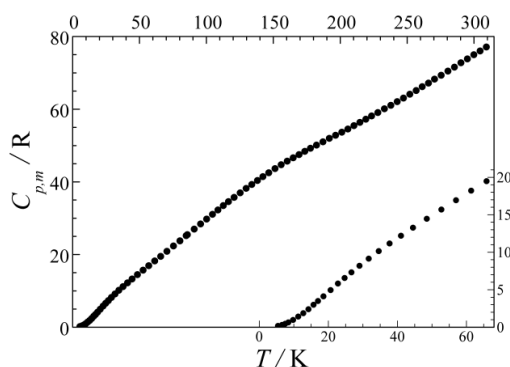


Figure 1. Experimental heat capacity of $\text{Cu}(\text{C}_{11}\text{H}_{19}\text{O}_2)_2$ in the range of (5–310) K.

- [1] P. A. Stabnikov, *Russian Journal of General Chemistry*, 2013, 83, 2009–2017.
[2] A.A. Pupyshev, *Atomic absorption spectral analysis*, 2009, 590-692. Technosphere, Russia.
[3] V.N. Naumov, V.V. Nogteva, *Instrum. Exp. Tech.*, 1985, 28, 1194-1199.

PIII-29. Thermochemistry of Compounds Formed from Guaiacyl Lignin Fragment

Maksimuk Y.V.¹, Krouk V.S.¹, Ponomarev D.A.², Antonava Z.A.¹

¹Research Institute for Physical Chemical Problems of the Belarusian State University, Belarus;

²Saint Petersburg State Forest Technical University, Russia

maksimuk@bsu.by

The thermochemical characteristics of chemical compounds are their energy of combustion and enthalpy of formation, that have a crucial significance in evaluating of thermal effects of chemical reactions involving these compounds or any substances composed of them, for example, lignin. Lignin is a natural aromatic three-dimensional biopolymer with irregular structure. The main way of lignin valorization is thermochemical processing under various conditions: direct combustion, pyrolysis, liquefaction, hydrothermal conversion. Many marketable products, such as fuels, polymers and chemicals could be obtained from lignin.

The values of standard molar enthalpy of formation (in the crystalline state at 298.15 K) for compounds formed from guaiacyl lignin fragment: vanillin, vanillic acid, methyl vanillate and acetovanillone were determined by bomb calorimetry method, and were found to be $-(475.5 \pm 1.5)$, $-(748.5 \pm 1.8)$, $-(715.3 \pm 2.1)$ and $-(526.1 \pm 1.5)$ kJ/mol, respectively [1,2].

The values of standard molar enthalpy of formation (in the gaseous state at 298.15 K) for the following pairs of isomers: vanillin / isovanillin (3-methoxy-4-hydroxybenzaldehyde), 3-methoxy-4-hydroxyacetophenone (acetovanillone, apocynin) / 3-hydroxy-4-methoxyacetophenone, vanillic acid / isovanillic acid and methyl vanillate / methyl isovanillate were calculated by quantum chemical method, were found to be $-(375.8 \pm 2.1)$ / $-(369.0 \pm 2.1)$, $-(420.7 \pm 2.1)$ / $-(415.6 \pm 2.1)$, $-(629.5 \pm 2.3)$ / $-(625.4 \pm 2.3)$ and $-(610.9 \pm 2.5)$ / $-(603.9 \pm 2.5)$ kJ/mol, respectively. The geometry of the molecules was optimized using the PC GAMESS software package (version 8.0) within the framework of the DFT (B3LYP/6-311++G(2df, 2p)). The enthalpies of formation were calculated using G3MP2 with additive corrections for the number of carbon and hydrogen atoms. To test the quantum chemical algorithm used the value for guaiacol was calculated $-(247.9 \pm 1.9)$, which is in excellent agreement with the reliable experimental value $-(247.3 \pm 1.8)$ kJ/mol [3]. The data obtained confirm the preference of the *para*-location of the hydroxyl group in the benzene ring as compared with the methoxyl group in the formation of the aromatic structure of lignin. A basic set of values of standard molar enthalpies of formation for functionally substituted benzene, forming structural fragments of lignin, including more than 100 compounds, has been created.

Methods for the calculation of standard molar enthalpies of formation for benzene derivatives with -OH, -OMe, -COH, -COMe, -COOH, -COOMe substituents in the aromatic ring in crystalline and gaseous states were developed using data for 80 compounds.

[1] Y. Maksimuk, D. Ponomarev, A. Sushkova, *J. Therm. Anal. Calorim.*, 2018, 131, 1721.

[2] Y. Maksimuk, Z. Antonava, D. Ponomarev, *J. Therm. Anal. Calorim.* 2018, V. 134, 2127.

[3] M. Varfolomeev, D. Abaidullina, B. Solomonov, *J. Phys. Chem. B*, 2010, 114, 16503.

PIII-30. The Thermal Decomposition of Lanthanide (III) Chloride Hydrates

Korzun I.V., Zakir 'yanova I.D. and Salulev A.B.

Institute of High-Temperature Electrochemistry, Ural Branch, Russian Academy of Sciences, Russia

korzun@ihite.uran.ru

Processes of the thermal dehydration of $\text{LnCl}_3 \cdot 6\text{H}_2\text{O}$ (Ln - Pr, Nd, Sm, Gd, Dy) crystalline hydrates have been studied using of a synchronous thermal analyzer STA 449C Jupiter®, coupled with the quadrupole mass-spectrometer Aëolos (Germany). This equipment allows for simultaneous measurements using differential scanning calorimetry (DSC) and thermogravimetry (TG) methods with simultaneous analysis of the released gases. The measurements were carried out with a heating rate 5 K/min in an argon atmosphere.

As an example, the results of the synchronous thermal analysis (STA) for $\text{DyCl}_3 \cdot 6\text{H}_2\text{O}$ are shown in Figure 1.

It was found that

- for all the hydrates studied, the gradual removal of water molecules occurs in four stages, with the last stage being accompanied by the hydrolysis of the salt $\text{LnCl}_3 \cdot \text{H}_2\text{O} \rightarrow \text{LnOCl} + \text{HCl}\uparrow$. This leads to the pollution of salts with oxychlorides. To obtain pure salts, additional measures must be taken to prevent these processes.
- the temperature of dehydration increases in the row $\text{La} < \text{Pr} < \text{Nd} < \text{Sm} < \text{Gd} < \text{Dy}$; there is a linear correlation between the atomic number of rare-earth metals and the temperature of removal of the last molecules H_2O .

Acknowledgements The financial support of the Russian Foundation for Basic Research, project № 18-03-00561a.

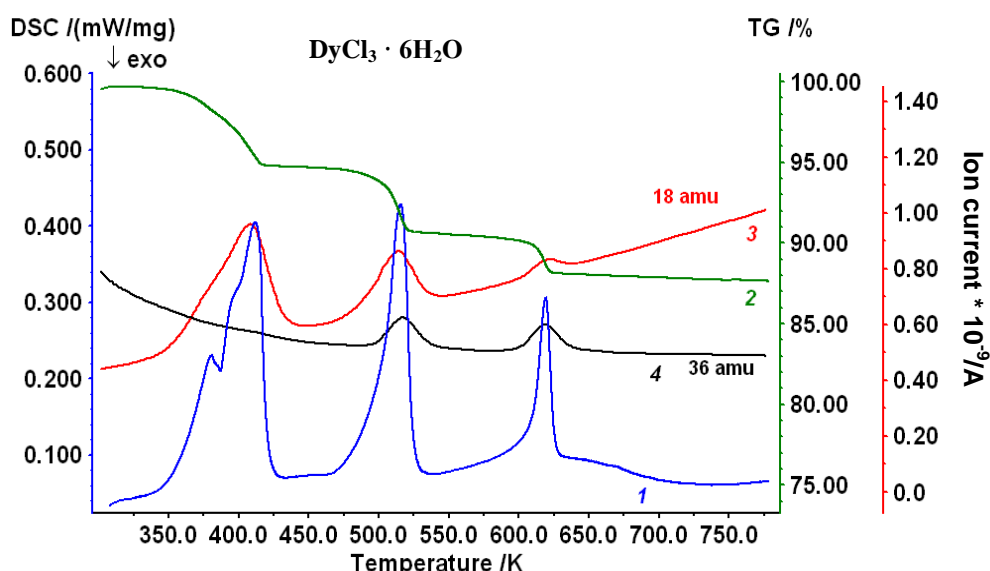


Figure 1. STA results for $\text{DyCl}_3 \cdot 6\text{H}_2\text{O}$ crystalline hydrate: (1) thermal flow (2) sample weight, and ionic current of water (3) and HCl. (4)

PIII-31. High-Temperature Heat Capacity of LnInGe₂O₇ (Ln = Tb - Lu)

Irtugo L.A., Kudashova N.G., Denisov V.M.

Institute of Non-Ferrous Metals and Materials Science, Siberian Federal University

irtugo@rambler.ru

Even though there is unabated interest in the LnMGe₂O₇ (Ln = La–Lu, M = Al, Ga, In) oxides, many of their properties have not yet been studied in sufficient detail. The structures and thermodynamic properties of such germanates are not available in the literature. The goal of this work was to perform the synthesis and experimental study of the structure and high-temperature heat capacity of LnInGe₂O₇ (Ln = Tb - Lu).

The polycrystalline LnInGe₂O₇ (Ln = Tb - Lu) samples have been prepared by solid-state reactions, by sequentially firing stoichiometric mixtures of In₂O₃, Ln₂O₃ (reagent grade), and GeO₂ (99,999%) at temperatures from 1273 to 1473 K, for 200 h, with intermediate grindings and pressing every 20 h.

The phase composition of the compounds was determined by X-ray diffraction (X'Pert Pro MPD diffractometer, PANalytical, the Netherlands, CuK α radiation). The lattice parameters of the samples were determined by profile fitting using derivative difference minimization. The results obtained at room temperature for TbInGe₂O₇ (sp.gr. C2/c, $a = 6,8812(2)$ Å, $b = 8,8774(3)$ Å, $c = 9,7892(4)$ Å, $\beta = 101,401(1)^\circ$, $V = 586,25(4)$ Å³) are in reasonable agreement with data [1]. There are no available data in literature for the others compounds, but our experimental values are closed to the unit cell parameters of TbInGe₂O₇.

The heat capacity C_p was measured in platinum crucibles by differential scanning calorimetry with an STA 449 C Jupiter (NETZSCH) in air atmosphere within the temperature interval 350-1000 K at heating rates of 20 K/min. The samples had the form of pressed polycrystalline powders.

The values of C_p grow regularly with increasing temperature for the all germanates, with no extrema in the $C_p(T)$ curve for the all samples. The heat capacity data are well represented by the Maier-Kelley equation, for example:

$$C_{p,ErInGe_2O_7} = (245.3 \pm 0.4) + (32.4 \pm 0.4) \times 10^{-3} T - (39.4 \pm 0.4) \times 10^5 T^{-2}$$

$$C_{p,TbInGe_2O_7} = (261.1 \pm 0.6) + (9.5 \pm 0.6) \times 10^{-3} T - (41.7 \pm 0.6) \times 10^5 T^{-2}$$

The specific heat of the rare-earth oxides and related mixed oxide compounds are nonlinear functions of the ionic radius of Ln³⁺ in the first to fourth tetrads (tetrad effect). The data presented in Fig. 1 demonstrate in this case too, the plots of C_p^0 Ln₂O₃ vs. $r(\text{Ln}^{3+})$ [2] and C_p^0 LnInGe₂O₇ vs. $r(\text{Ln}^{3+})$ have such a shape in the corresponding tetrads.

Acknowledgements The financial support of the Ministry of Education and Science of the Russian Federation (project no. 4.8083.2017/BCh).

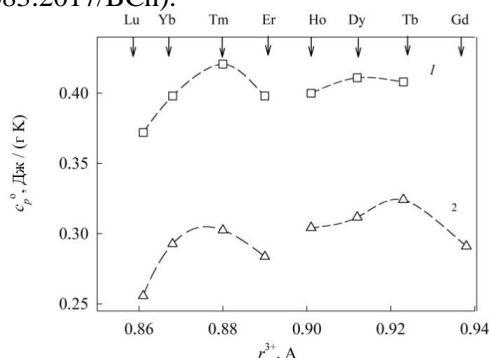


Figure 1. C_p^0 vs. $r(\text{Ln}^{3+})$ ions for the (1) LnInGe₂O₇ and (2) Ln₂O₃ compounds

[1] E.A. Juarez-Arellano, et al. *J. Solid State Chem.*, 2003, 170, 418.

[2] Kawabe, I., *Geochem. J.*, 1992, 26, 309.

PIII-32. Synthesis and Thermodynamic Properties of the Titanates $R_2Ti_2O_7$ ($R = Gd, Lu$)

Golubeva E.O., Chunilina L.G.

Department of Physical and Inorganic Chemistry, Siberian Federal University,
79 Svobodny pr., 660041 Krasnoyarsk, Russia

evg9042@yandex.ru

The titanates $R_2Ti_2O_7$ ($R =$ rare earth element) have interesting catalytic, optical and magnetic properties, therefore these materials are finding a widely application as electrolytes and electrodes in oxide solid fuel cells, oxygen partial-pressure sensors, catalysts and their carrying agents [1]. These compounds crystallizes in pyrochlore structure. Many research papers are devoted to $R_2Ti_2O_7$, but its thermodynamic properties are underexplored. However, thermodynamic investigations are necessary for the development of a theory about the interaction of the components in the substances and to guide the selection of the optimal conditions for their synthesis and application. Thus, the aim of this work were the synthesis of $R_2Ti_2O_7$ ($R = Gd, Lu$) and investigation of the thermodynamic properties.

The titanates $Gd_2Ti_2O_7$ and $Lu_2Ti_2O_7$ were prepared by a solid-phase reaction from TiO_2 and R_2O_3 ($R = Gd, Lu$). Stoichiometric mixtures of the oxides were ground in an agate mortar, pelletized and heated at 1673 - 1773 K temperature range in air for 20 h with five intermediate grindings and pressings. Compositions of the samples were controlled by X-ray phase analysis (PANalytical X'Pert Pro MPD). Influence of rare earth element on oscillation of bonds $R - O$ and $Ti - O$ was investigated by Raman Spectroscopy (Thermo Scientific Nicolet Almega XR Dispersive Raman Spectrometer). The heat capacity was measured by differential scanning calorimetry (NETZSCH STA 449 C Jupiter).

The experimental data $C_p = f(T)$ in the temperature range 320 – 1000 K were described by the classical equation of Mayer–Kelli

- for $Gd_2Ti_2O_7$:

$$C_p = (263,75 \pm 0,49) + (25,6 \pm 0,5) \cdot 10^{-3}T - (33,04 \pm 0,47) \cdot 10^5 T^{-2}; \quad (1)$$

- for $Lu_2Ti_2O_7$:

$$C_p = (257,3 \pm 0,85) + (23,9 \pm 0,9) \cdot 10^{-3}T - (30,19 \pm 0,82) \cdot 10^5 T^{-2} \quad (2)$$

The equations (1), (2) allowed to calculate the thermodynamic properties (the enthalpy change, the entropy change, and the reduced Gibbs energy) of this rare earth titanates.

Acknowledgements This work was supported by the Russian Federation Ministry of Education and Science (state research target for Siberian Federal University in 2017–2019, project no. 4.8083.2017/8.9: Establishing a Database of Thermodynamic Characteristics of Multifunctional Mixed-Oxide Materials Containing Rare and Trace Elements; state research target no. 007-00129-18-00).

[1] M. Farmer, L. A. Boatner, B. C. Chakoumakos, J. of Alloys and Comp., 2014, 605,63.

PIII-33. Vaporization Enthalpies of Mono- and Dibromoalkanes

Samatov A.A., Nagrimanov R.N., Solomonov B.N.

Kazan Federal University, Russian Federation

samatov.aizat@gmail.com

The thermochemical properties are important properties of pure substances used for calculation of technological schemes in chemical production. Nevertheless, thermochemical data on the enthalpies of vaporization/sublimation most of aliphatic compounds are unknown. Study of the enthalpies of vaporization/sublimation of aliphatic compounds with the help of classical techniques: direct calorimetric or methods of vapor pressure determination have rather big limitations. The aliphatic compounds with long alkyl chain possess very low vapor pressure. Due to this fact, the average temperature of determination is shifted to the higher temperatures, what leads to the troubles of low thermal stability. Additionally, the wide range of isomers stems in purification troubles for aliphatic compounds, while purification of the mixture of isomers is a challenging task. At the same time the insufficient purity of the compounds will drastically increase the experimental uncertainties of the enthalpies of phase transitions [1].

At the same time, the dissolution calorimetry method does not have the above disadvantages. In our previous work [1] we have proposed n-heptane as a solvent for aliphatic compounds, because in most cases there is no dependence of solution enthalpy on length of alkyl chain. So, if solute is similar by structure to solvent, the solution enthalpy is close to zero and in this way solvation and vaporization enthalpies are linked by the following equation:

$$-\Delta_{\text{solv}} H_m^{\text{A/S}} = \Delta_l^g H_m^o$$

In this work we have studied vaporization enthalpies of mono- and dibromoalkanes by several methods: transpiration, solution calorimetry, correlation gas chromatography. In most cases, vaporization enthalpies were determined for the first time. All solution enthalpies were measured for the first time. Determined by various methods vaporization enthalpies are in good agreement with each other and in some cases with literature data.

Acknowledgements This work has been performed according to Grant No. 14. Y26.31.0019 from Ministry of Education and Science of Russian Federation.

[1] R.N. Nagrimanov, A.A. Samatov, D.H. Zaitsau, B.N. Solomonov. Improving the method of solution calorimetry for evaluation of the enthalpies of phase transitions and condensed state enthalpies of formation, *The Journal of Chemical Thermodynamics*, 2019, 128, 141-147.

PIII-34. Metal Acetylacetonates: Thermochemistry and Structure-Property Relationships

Makarenko A.M.^{1,2}, Zherikova K.V.²

¹Novosibirsk State University, Russia;

²Nikolaev Institute of Inorganic Chemistry, Siberian Branch of Russian Academy of Science, Russia

alexkot2807@yandex.ru

The most favorable application of volatile metal compounds with organic ligands is as precursors for the metalorganic chemical vapor deposition (MOCVD) of different films and coatings. Knowledge about vapor pressures and sublimation/vaporization thermodynamics of the precursors is indispensable for optimization of practical conditions of the deposition processes. Obviously, for different metals combined with different ligands the experimental conditions of volatilization are significantly different. That is why any understanding of the structure-property relationships in the metalorganic precursors (e.g. metal and ligand dependence, or the ligand branching dependence), which can be utilized for the development of a thermodynamic model able to predict vapor pressures and sublimation/vaporization enthalpies, is highly desired. Unfortunately, those values published are often referred to an arbitrary temperature, and comparing the data requires adjusting them to any common temperature.

Typical representatives of MOCVD precursors are metal β -diketonates. In our work aluminium, chromium(III) and iridium(III) acetylacetonates were considered. These metals were chosen because of their significant difference in molecular weight. The latter apparently can influence on physical-chemical properties of these complexes, so, they can be considered as suitable model compounds to study such structure-property relationships.

According to our previous work [1] devoted to heat capacity estimation of ferrocene we applied some reliable methods for assessment of the difference between the molar isobaric heat capacities of the gaseous $C_{p,m}^o$ (g) and condensed (cr or l) phases, $\Delta_{cr,l}^g C_{p,m}^o$ -values, required for the temperature adjustments of sublimation/vaporization enthalpies of compounds under this study.

Further, we carefully collected sublimation, vaporization and fusion enthalpy data for aluminium(III), chromium(III) and iridium(III) acetylacetonates. We proved the internal consistency of thermodynamic data on sublimation/vaporization enthalpies of aluminium and chromium(III) acetylacetonates by using structure-property analysis and quantum-chemical calculations. Based on these reliable data, the metal centre influence degree was estimated.

[1] K.V. Zherikova, S.P. Verevkin, *Fluid Phase Equilib.*, 2018, 472, 196.

PIII-35. Thermodynamic Properties of CeO₂-ZrO₂ and CeO₂-Y₂O₃ Systems

Lopatin S.I., Shugurov S.M., Vasil'eva E.A., Kurapova O.Yu., Konakov V.G.

Saint Petersburg State University, Russia

s.lopatin@spbu.ru

Study of the vaporization processes and thermodynamic properties of CeO₂-ZrO₂ and CeO₂-Y₂O₃ systems at high temperature were carried out by the high temperature mass spectrometry method. Investigation was done using MS 1301 mass spectrometer at the ionization energy equaled to 30 eV. Vaporization of the samples under consideration was carried out from twin tungsten effusion cell heated by electron bombardment. Temperature was measured by optical pyrometer EOP-66 with the accuracy ± 5 K over the temperature range 1900-2500 K.

The CeO⁺ and CeO₂⁺ ions were detected in mass spectra above CeO₂-ZrO₂ and CeO₂-Y₂O₃ systems in the temperature range 1950-2100 K. The mass spectra analysis and the values of appearance energies of ions show that the vapor over the CeO₂-ZrO₂ and CeO₂-Y₂O₃ systems consists CeO, CeO₂ and O species. YO⁺, ZrO⁺ and ZrO₂⁺ ions appear in the mass spectra at the temperature 2400-2700 K.

The partial pressures of the vapor species were obtained by ion current comparison method. We did not take into account the interaction between the samples and cell material because the products of interaction (WO₂⁺ and WO⁺) were observed at the beginning of vaporization only.

The CeO₂ activities in the CeO₂-ZrO₂ and CeO₂-Y₂O₃ systems at the temperature 2000 K were found by the differential mass spectrometric method using cerium dioxide as the standard of the determination of the activity. The ZrO₂ and Y₂O₃ activities were calculated according to the Gibbs-Duhem equation.

Our study found that the activities of cerium, zirconium and yttrium oxides in concentration range 90-5 mol. % of CeO₂ in the condensed phase have negative deviations from ideal case.

PIII-36. Thermodynamic Analysis of The Possibility of NO₂ to NO Reforming

Nikiforova K.V., Konakov V.G.

St. Petersburg State University, Institute of Chemistry,
Department of Physical Chemistry, St. Petersburg, Russia

kristaliya98@mail.ru

Despite the active introduction of alternative energy sources (solar, wind, tidal stations, etc.), traditional combustion engines remain the most common. Along with CO, CO₂ and SO_x, NO_x, namely NO₂, NO, N₂O₄ are one of the main components of exhaust gases. Their presence in the atmosphere causes acid rain and corrosion of the metal structures. So nowadays their control is of particular importance. Since NO₂ exists in several forms under the same conditions, its detection is associated with a number of difficulties. There is a number works devoted to amperometric and electrochemical NO₂ sensors development, however, their response is unstable and the electrode function does not correspond to the theoretical one. Unlike nitrogen dioxide, nitrogen monoxide is not toxic and its content in the gas phase can be measured precisely. To date, the method of the catalytic reduction of NO₂ to NO is the most promising among the available direct detection methods of NO₂. There are attempts to find an effective catalyst for the NO₂ to NO reduction, but the fundamental thermodynamic base for these studies is lacking. Vanadium, tungsten and molybdenum oxides are known as the most used catalysts for the reduction processes. Thus the aim of this work was a thermodynamic analysis of the possibility of NO₂ to NO transition in the temperature range of 300–1500 K and the search for redox pairs, which would enable conversion. The calculations were carried out using the reliable data [1].

Using the calculations it was found that above 800 K a shift towards NO occurs in the NO + O₂ = NO₂ reaction. By taking into account the intrinsic heat of the reaction it was found that at high partial NO_x pressures the temperature of the system decreases significantly and equilibrium shift towards NO₂ takes place. Among the considered oxide pairs, the V / V₂O₄, W / WO₂ and Mo / MoO₂ pairs showed the highest efficiency in a wide temperature range and in a narrower range, W / WO₃ and Mo / MoO₃ due to WO₃ and MoO₃ phase transitions.

[1] Barin I., Knacke O., Kubaschewski O. Thermochemical properties of inorganic substances: supplement. – Springer Science & Business Media, 2013.

PIII-37. Excess Enthalpies in the Chemically Equilibrium System Ethanol + Acetic Acid + Ethyl Acetate + Water

Golikova A.D.¹, Tsvetov N.S.^{2,3}, Toikka M.A.¹, Toikka A.M.¹

¹Saint-Petersburg State University, Russia;

²Tananaev Institute of Rare Element and Mineral Chemistry and Technology, Kola Research Center
Russian Academy of Sciences, Russia;

³Murmansk Arctic State University, a branch in Apatity, Russia

al.golikova@gmail.com

Ethyl acetate is one of the most important chemicals, due to its widespread use, as a solvent, in various industries for the production of paints, inks, adhesives and fragrances. The development of industrial methods for the synthesis of ethyl acetate requires more accurate data on thermodynamic properties. For the thermodynamic description of systems with a chemical reaction chemical equilibrium data and their thermochemical characteristics are required. In particular interest is the data about excess enthalpies of the system in a state of chemical equilibrium, since these data are used to calculate the heat of chemical reaction.

In this work, data on the heat of mixing in the quadruple system acetic acid + ethyl alcohol + ethyl acetate + water were obtained for the first time. The excess molar enthalpy $H_m(ABCD)^E$ in quaternary system was determined using a C80 (Setaram) calorimeter by mixing two binary subsystems. More than 25 compositions were investigated.

The results were described using NRTL-form equation. It lets to predict excess molar enthalpies for all chemically equilibrium compositions of studied system.

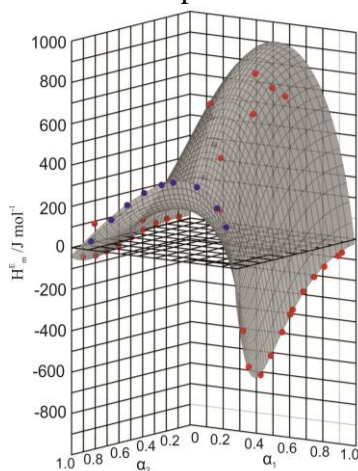


Figure 1. Excess enthalpies of the acetic acid + ethyl alcohol + ethyl acetate + water system at 313.15 K in the space of α -variables.

Acknowledgments

The study was supported by Russian Foundation for Basic Research, N. Tsvetov is grateful for the RFBR grant 18-33-00148. Alexandra Golikova acknowledges for the Scholarships of President of Russian Federation (SP-2680.2018.1). The investigations were carried out using the equipment of the Resource Center of Thermogravimetric and Calorimetric Research (Research Park of St. Petersburg State University).

PIII-38. Thermodynamic Properties of Cation-Ordered Layered Perovskite-Like Oxides $K_2Nd_2Ti_3O_{10}$ and its Protonated Forms

Sankovich A.M.¹, Myshkovskaia T.D.¹, Smirnova N.N.², Markin A.V.², Zvereva I.A.¹

¹St. Petersburg State University, Russian Federation, St. Petersburg

²Lobachevsky State University of Nizhni Novgorod, Russian Federation, Nizhni Novgorod

annasankovich@yandex.ru

Layered perovskite-like oxides are objects of close attention as representatives of one of the most perspective classes of ceramic materials. These compounds exhibit important physical and chemical properties (electric, magnetic, catalytic) due to the peculiarities of their crystal structure and find application in the newest areas of science and technology.

The layered perovskite-like titanate $K_2Nd_2Ti_3O_{10}$ was synthesized by the solid-state reaction at 1100 °C during 6 h. Stable protonated intercalated compounds $H_xK_{2-x}Nd_2Ti_3O_{10} \cdot yH_2O$ were obtained by continuous flushing of $K_2Nd_2Ti_3O_{10}$ with 1 and 5.5 L of water. The results of synthesis and formation of new phases were monitored by XRD (Rigaku “MiniFlex II”). The composition of protonated intercalated forms was determined by TG analysis (“Netzsch TG 209 F1 Libra”).

According to XRD data $K_2Nd_2Ti_3O_{10}$ oxide is described by tetragonal I4/mmm space group and new phases have orthorhombic symmetry C222. Investigation of protonated intercalated compounds $H_xK_{2-x}Nd_2Ti_3O_{10} \cdot yH_2O$ by TG analysis is shown that phases are characterized by the similar amount of intercalated water and differ from the protonation degree: $H_{1,64}K_{0,36}Nd_2Ti_3O_{10} \cdot 0,61H_2O$ and $H_{1,89}K_{0,11}Nd_2Ti_3O_{10} \cdot 0,6H_2O$ that related to a smaller distance between perovskite layers and consistent with XRD results.

The heat capacities of samples are measured in the low-temperature range (6 – 340) K with use of a Termis BCT adiabatic vacuum calorimeter. Heat capacities of all samples rise gradually with temperature increase over the main temperature interval (Fig. 1). At the same time, heat capacities were found to increase with temperature decrease. Thus, the anomalies were observed in the heat capacity curves in the range of (6 – 8.9) K for $K_2Nd_2Ti_3O_{10}$, (6 – 10.7) K for $H_{1,64}K_{0,36}Nd_2Ti_3O_{10} \cdot 0,61H_2O$, and (6 – 9) K for $H_{1,89}K_{0,11}Nd_2Ti_3O_{10} \cdot 0,6H_2O$. Such anomalies are likely to be descending branches for magnetic disorder–order phase transitions, which lie outside the measuring range of the calorimeter.

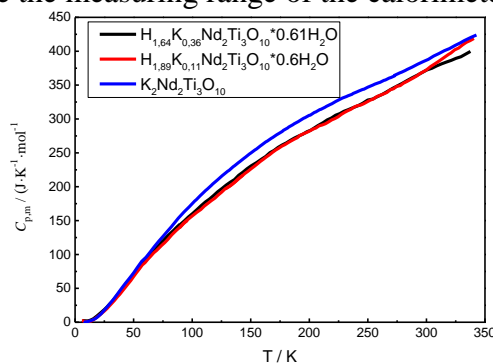


Figure 1. Molar heat capacities of $H_{1,64}K_{0,36}Nd_2Ti_3O_{10} \cdot 0,61H_2O$, $H_{1,89}K_{0,11}Nd_2Ti_3O_{10} \cdot 0,6H_2O$, and $K_2Nd_2Ti_3O_{10}$ as function of temperature.

Standard thermodynamic properties (heat capacity, enthalpy, entropy, and Gibbs energy) of the oxides were evaluated from the experimental heat capacity temperature dependencies.

It will be present the comparison of heat capacity and thermodynamic properties of isostructural compounds from raw $A_2Ln_2Ti_3O_{10}$ $A=H, Na, K$ and $Ln=La, Nd, Gd$. The nature of alkali and rare-earth elements and distortion of structure will take into account to reveal the influence on the heat capacity of layered oxides.

This work was financially supported by Russian Foundation for Basic Research (N 18-03-00915).

PIII-39. Calorimetric Study of Hyperbranched Polyphenylene Pyridine-Containing Polymers in the Range from $T \rightarrow 0$ to 680 K

Smirnova N.N.¹, Markin A.V.¹, Sologubov S.S.¹, Serkova E.S.², Kuchkina N.V.², Shifrina Z.B.²

¹National Research Lobachevsky State University of Nizhni Novgorod, Russia

²Nesmeyanov Institute of Organoelement Compounds, Russian Academy of Sciences, Moscow, Russia

smirnova@ichem.unn.ru

Hyperbranched polymers have a row of unique properties: high solubility, low viscosity solutions and melts, high sorption capacity and thermal stability. In this work, three samples of hyperbranched polyphenylene pyridine-containing polymers of different structure and composition were investigated. The polymer samples were synthesized at the Nesmeyanov Institute of Organoelement Compounds, Russian Academy of Sciences (Moscow) and characterized by gel-permeation chromatography and NMR spectroscopy. The thermal stability of polymer samples was studied by thermogravimetric analysis. It was established that the polymers are stable up to $T \sim 670$ K. The temperature dependence of the heat capacity was studied by adiabatic vacuum calorimetry and differential scanning calorimetry. In Figure 1 as an example the $C_p = f(T)$ curve of one of the studied samples in the range $T = (6-650)$ K is showed. For the other two samples the heat capacity curves are similar (Figure 1, *curve 1*). The heat capacity smoothly increased with rising the temperature up to $T \sim 400$ K, except for the region from 10 to 20 K, where the anomalous change in the C_p resembling the glass transition was observed. Above $T = 400$ K, the decrease in the "apparent" heat capacity was revealed, and the negative values of the apparent C_p were obtained in the temperature range $T = (515-650)$ K, that is lower than the thermal destruction temperature of polymers. The observed change is caused by the exothermic process, most likely related to the cross-linking of macromolecules of the studied polymers. This is also consistent with the repeating measurement of the heat capacity of polymers after their cooling from 650 to 310 K (Figure 1, *curve 2*). The changes in the C_p of the studied samples are identical and similar, but temperatures of the physical transformation depend on the structure and composition of polymers. In the temperature range above $T = 400$ K, the energy release was revealed for all samples, which is probably due to the internal cross-linking of the studied copolymers. Upon cooling to $T = 400$ K and repeating measurement the heat capacity, curves for all studied polymers are not reproduced. The standard thermodynamic functions of polymers were calculated in the interval from $T \rightarrow 0$ to 410 K. The obtained values are reference data and can be used in the calculation of the standard entropy of formation of these polymers.

Acknowledgements This work was financially supported by the Russian Foundation for Basic Research (№№ 18-33-00905, 19-03-00248).

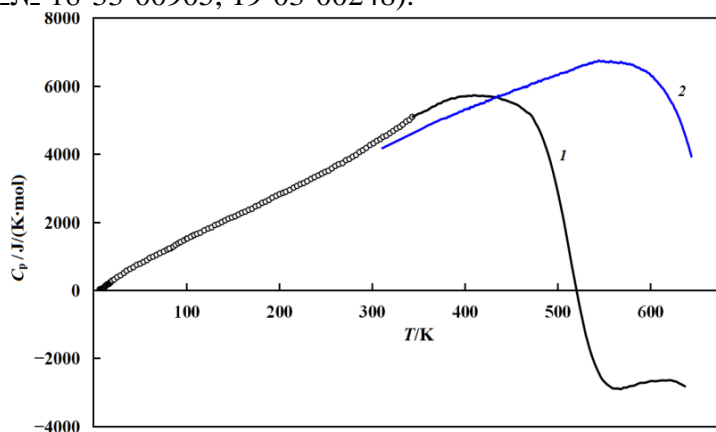


Figure 1. The heat capacity of hyperbranched pyridine-containing polyphenylene.

PIII-40. Benchmark Properties of 2-, 3- and 4-Nitrotoluene: Evaluation of Thermochemical Data with Complementary Experimental and Computational Methods

Bikelyté G.¹, Härtel M.¹, Stierstorfer J.¹, Klapötke T.M.¹, A. Pimerzin A.², Verevkin S.P.³

¹Ludwig-Maximilians-Universität München, Germany;

²Samara State Technical University, Russia;

³University of Rostock, Germany

grbich@cup.uni-muenchen.de

Literature available thermochemical properties of mononitrotoluenes are in disagreement. New molar enthalpies of vaporization of 2-, 3-, and 4-nitrotoluene at the temperature $T = 298.15$ K were determined from the vapour pressure dependence on temperature, measured by the gas-saturation method. Moreover, new standard molar enthalpies of formation at the temperature $T = 298.15$ K of the liquid 3-nitrotoluene and solid 4-nitrotoluene were measured using high-precision combustion calorimetry. Collected literature thermodynamic data on mononitrotoluenes were critically evaluated and compared with own experimental results. This collective set of data has helped to resolve inconsistencies in the available enthalpies of formation data and to recommend vaporization and formation enthalpies for 2-, 3-, and 4-nitrotoluene for further thermochemical calculations.

PIII-41. Recent Developments on The Energetics of Morpholine Derivatives

Ribeiro da Silva M.D.M.C., Silva C.A.O., Freitas V.L.S.

Centro de Investigação em Química, Department of Chemistry and Biochemistry, Faculty of Science, University of Oporto, Porto, Portugal

mdsilva@fc.up.pt

The morpholine presents a hexagonal saturated ring structure with an oxygen and nitrogen in the positions 1 and 4. This structure confers high flexibility, allowing the formation of several conformers. A significant number of morpholine derivatives have relevant applications in the industry, namely as corrosion inhibitors and optical brighteners, as well as in the pharmaceutical area (analgesics, local anaesthetic, and antibiotic agents). The applications of this class of compounds justify the interest by the knowledge of the corresponding thermodynamic properties.

Experimental and computational studies of *N*-(2-hydroxyethyl)morpholine and *N*-(2-aminoethyl)morpholine were performed to evaluate and understand the energetic effect inherent to the substitution of the hydrogen in the amino group of the morpholine scaffold by hydroxyethyl and aminoethyl substituents (Figure 1).

The experimental techniques used were the Calvet microcalorimetry and static bomb combustion calorimetry technique aiming, respectively, the determination of the enthalpy of vaporization and of the massic energy of combustion of the two morpholine derivatives. These data were used to derive the standard enthalpies of formation in the liquid and gaseous phases, at $T=298.15$ K. The computational calculations performed with the composite G3(MP2)//B3LYP approach, enabled the optimization of each structure, computation of their vibrational frequencies and energies at 0 K, as well as their absolute enthalpies at 298.15 K. These quantities were combined with the calculated absolute enthalpies of the compounds in selected working reactions, allowing the computation of the gas-phase standard molar enthalpies of formation, at 298.15 K, of *N*-(2-hydroxyethyl)morpholine and *N*-(2-aminoethyl)morpholine.

The values derived of the gas-phase enthalpies of formation for the two morpholine derivatives are discussed and compared with those already determined for other related derivatives [1, 2].

Acknowledgements: The authors thank the support of the Fundação para a Ciência e Tecnologia (FCT) of Portugal, Project UID/QUI/UI00081/2013 and FEDER Projects POCI-01-0145-FEDER-006980 and NORTE-01-0145-FEDER-000028 (Sustained Advanced Materials, SAM). C.A.O.S. also thanks FCT for the award of a Ph.D. grant (SFRH/BD/137672/2018).

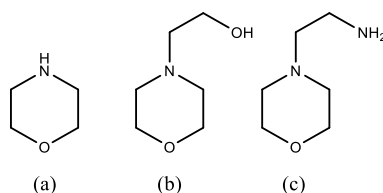


Figure 1. Structural formula of (a) morpholine, (b) *N*-(2-hydroxyethyl)morpholine and (c) *N*-(2-aminoethyl)morpholine

[1] V.L.S. Freitas, J.R.B.Gomes, M.D.M.C. Ribeiro da Silva, *J. Chem. Eng. Data*, 2014, 59, 312.

[2] V.L.S. Freitas, C.A.O. Silva, M.D.M.C. Ribeiro da Silva, *J. Chem. Thermodyn.*, 2018, 122, 95.

PIII-42. Physical Characterization of a Novel Electrolyte Based in Ionic Liquid MPPyrr-TFSI + dMSO + Li-TFSI

Cabeza O.¹, Segade L.¹, García-Garabal S.¹, Domínguez-Pérez M.¹, Ausín D.¹, Rilo E.¹ and Varela L.M.²

¹Universidade da Coruña, E-15071;

²Universidad de Santiago de Compostela, E-15782. Spain

oscar.cabeza@udc.es

In this work we present for the first time the physical characterization of a new electrolyte formed by a ternary mixture of the ionic liquid (IL) 1-methyl-1-propyl pyrrolidinium bis(trifluoromethyl sulfonyl)imide (MPPyrr-TFSI), mixed in different proportions with dimethyl sulfoxide (dMSO) and with (or without) lithium TFSI up to saturation. These ternary mixtures have a great potential as electrolyte due to the characteristics of the IL and solvent used [1]. To perform the study, in addition to the pure compounds, we have measured the physical properties in five different binary mixtures with different dMSO concentrations (10, 20, 25, 50 and 75 wt%). An aliquot of each sample has been saturated with Li-TFSI salt, which gives concentrations of 1260 ppm of the Li⁺ cation for the mixture with the pure IL, up to higher than 5000 ppm for the mixture with the higher solvent contents.

Some of the samples were characterized using FTIR spectroscopy to observe the possible formation of new bonds after the mixing process. Also, for all samples we have measured its density, viscosity and ionic conductivity in a broad range of temperature (ranging from -15 °C up to 95 °C for some of the samples). As it was expected, while density and viscosity decrease with solvent content, ionic conductivity increases with it up to a maximum (obtained for the sample with 54 wt% dMSO), and then decreases to be null for the pure dMSO. In addition, the Li doped samples present a higher density and viscosity than the corresponding undoped ones, while the ionic conductivity decreases. Moreover, in order to relate the three measured magnitudes, we have performed Walden's plot for all the samples, where we can observe the degree of ionicity of each of them [2].

Finally, volumetric and conductivity data are explained through the pseudo-lattice Bahe-Varela model [3], which has been successful explaining the same magnitudes for other IL-solvent mixtures [4,5]. As the ionic conductivity for the most IL saturated samples does not match with the ideal version of that model, we introduce a modification, called random model [6], which perfectly fits the data measured for all the concentration range at all temperatures with only two fitting parameters dependent on temperature which have a physical origin from the theory used. So, these fits allow us to observe the thermal evolution of those parameters.

Acknowledgements The financial support of this work was partially given by MINECO through the projects with Refs. MAT2014-57943-C3-(1,3)-P and MAT2017-89239-C2-(1,2)-P. Also we want to thank to the Xunta de Galicia through the project REGALIs, with Ref. ED431D 2017/06.

References

- [1] S. Indris, R. et al., *J. Electrochem. Soc.*, 2014, 161, A2036.
- [2] S. García-Garabal et al., *Electrochimica Acta*, 2017, 231, 94.
- [3] L.M. Varela et al., *The Journal of Chemical Physics*, 1997, 107, 6415 .
- [4] I.B. Malham et al., *The Journal of Chemical Thermodynamics*, 2007, 39, 1132.
- [5] L.M. Varela et al., *Fluid Phase Equilibria*, 2010, 298, 280.
- [6] H. Montes-Campos, et al., *Phys. Rev. Letters*, 2019. Submitted to publication.

PIII-43. The Influence of Crystalline Structure and Surface Characteristics of Different TiO₂ Nanoforms on Human Serum Albumin Thermal Denaturation: a Differential Scanning Calorimetry Study

Gheorghe D.

„Ilie Murgulescu” Institute of Physical Chemistry of Romanian Academy, 202 Spl. Independentei,
060021, Bucharest, Romania

gheorghedanny2@gmail.com

Titanium dioxide nanoparticles (TiO₂NPs) are used in a wide range of nanotechnology products, biomedical and pharmaceutical applications or agro-food industries. For the safe development and use of commercial nanomaterials, the knowing of their human and environmental toxicity and safety is required. The evaluation of the proteins stability in the presence of nanoparticles is a particular issue allowing to find key findings for nanosafety research.

In the present study we found a strong dependence of protein stability on the crystalline structure and particle surface characteristics of the different nanoforms of the titanium dioxide. The thermal denaturation of human serum albumin (HSA) in sodium buffer phosphate at *pH* 7.4 and adsorbed onto titania nanoparticles (TiO₂NPs) was investigated for three types of nanomaterials (anatase; rutile hydrophobic, Al-coated; rutile-anatase) with various size (< 100 nm) provided by JRC Nanomaterials Repository [1]. The calorimeter Calvet SETARAM C80-3D equipment, with standard vessels made from stainless steel was used to study thermal denaturation behaviour of proteins in solution, in the absence and presence of NPs, in the temperature range of 298 K to 363 K, with a scanning rate of 1 K min⁻¹.

The effect of different titania nanoforms on the protein stability was estimated by means of thermodynamic parameters for the proteins denaturation (peak temperature, heat capacity, enthalpy).

The results of the calorimetric investigation contribute to a better understanding of the changes in structural stability of the protein following adsorption process of nanomaterials.

Acknowledgements Support of the EU (ERDF) and Romanian Government, for the acquisition of the research infrastructure under Project INFRANANOCHEM- No. 19/01.03.2009 is gratefully acknowledged.

Reference

[1] JRC Nanomaterials Repository, List of Representative Nanomaterials, June 2016 and JRC Scientific and Technical Reports (2014)

PIII-44. Thermodynamic Parameters of the Protein Interaction with SiO₂ Nanoparticles

Botea-Petcu A., Precupas A., Gheorghe D., Sandu R., Popa V.T., Tanasescu S.

„Ilie Murgulescu” Institute of Physical Chemistry of Romanian Academy, 202 Spl. Independentei,
060021, Bucharest, Romania

gheorghedanny2@gmail.com

For the assessment of dominant contributions that govern the adsorption processes during the interactions between proteins and nanoparticles (NPs), the evaluation of the binding thermodynamic parameters is crucial. The aim of this work is to explore the thermodynamics of the interactions of SiO₂ NPs (Representative Nanomaterial JRCNM02002a) [1] with three of the most abundant plasma proteins, namely: **BSA** (Bovine serum albumin, fraction V), **BPF type I-S** (Bovine plasma fibrinogen, type I-S) and **IgG** (Bovine Immunoglobulin G).

The main thermodynamic parameters for protein-NPs systems, represented by the binding constant K and stoichiometry n , enthalpy ΔH , Gibbs energy ΔG and entropy ΔS changes were obtained using Isothermal Titration Calorimetry (Microcal iTC200 microcalorimeter). The measurements were performed in water (18.2 M Ω cm, Direct-Q 3UV System, Millipore) and phosphate buffer (KHPO₄; K₂HPO₄) 0.1M pH 7.4.

These results allow for a better understanding of the driving forces controlling the proteins/nanoparticles interaction involved in different biological processes.

Acknowledgements Support of the EU (ERDF) and Romanian Government, for the acquisition of the research infrastructure under Project INFRANANOCHEM- No. 19/01.03.2009 is gratefully acknowledged.

Reference

[1] SiO₂ JRCNM02002a, Synthetic Amorphous Silica, thermal, JRC Nanomaterials Repository, List of Representative Nanomaterials, June 2016

PIII-45. Salting-Out of Isobutyric Acid From Aqueous Solutions with Sodium Chloride

Il'in K.K., Kapustina D.V., and Kurskiy V.F.

Saratov State University named after N.G. Chernyshevsky, Saratov 410012, Russian Federation

ilinkk@info.sgu.ru

The influence of the nature of salts and temperature on the liquid–liquid equilibrium in the ternary system salt + water + isobutyric acid has not almost been studied. This paper is devoted to the study of phase equilibria and critical phenomena in the system sodium chloride + water + isobutyric acid in a temperature range 10.0–60.0°C in order to reveal the salting-out effect of sodium chloride and topological transformation regularities of the phase diagram of the system as temperature changes. The binary liquid system water + isobutyric acid is characterized by delamination with an upper critical solution temperature (UCST = 25.8°C) [1].

Phase equilibria in component mixtures of the ternary system were studied by the visual-polythermal method in glass ampoules over eleven sections of the concentration triangle as described in Ref. [2]. The following phase states were observed in these mixtures: a homogeneous liquid state, a solid phase – a saturated solution, a two-phase liquid state, and a monotectic one. The solid phase of saturated solutions was identified as the individual salt at all temperatures. Phase state polytherms were plotted for all sections.

The temperature dependence of the composition of the mixtures corresponding to the critical solubility points of the liquid–liquid equilibrium in the range of 25.8–61.0°C was determined. The compositions of critical solutions were estimated by the phase-volume ratio method [2]. It was found that the salt introduction into the mixture of the critical composition of the binary system water + isobutyric acid led to an increased UCST of this system.

Phase state polytherms and critical curves were used to plot the isothermal phase diagrams of the ternary system. The isotherms at 60.0 and 40.0°C were similar. The sides of the monotectic triangle $\ell_1+\ell_2+S$ are adjoined by the fields of saturated solutions ℓ_1+S , ℓ_2+S (ℓ_1 means the organic phase, ℓ_2 the aqueous phase, S the solid phase) and the delamination field $\ell_1+\ell_2$ with critical point K. As temperature decreases, the delamination field approaches the side of the $H_2O - i-C_4H_8O_2$ concentration triangle and at 25.8°C its critical point K touches this side at the point corresponding to the composition of the critical solution point of the binary liquid system. The isotherms at 20.0 and 10.0°C correspond to salting-out of a heterogeneous system. The results obtained have fully confirmed a fragment of a variant of our topological transformation scheme of the phase diagrams of ternary systems salt + water + organic solvent with salting-in and salting-out as temperature changes, when the constituent binary liquid system is characterized by delamination with an UCST [3].

The distribution coefficients K_d of isobutyric acid were calculated as the ratio of its concentrations in the organic and aqueous phases of the monotectic state at the indicated temperatures. The effect of salting-out of isobutyric acid from its aqueous solutions with sodium chloride enhances with increasing temperature ($K_d = 57.5$ at 10.0°C, $K_d = 77.4$ at 60.0°C). Thus, sodium chloride can be recommended for effective salting-out of isobutyric acid from its aqueous solutions.

[1] M. Smotrov, *Izv. Saratovsk. Univ., Ser. Khim. Biol. Ekol.*, 2016, 16, 21.

[2] K. Il'in and D. Cherkasov, *Chem.Eng.Commun.*, 2016, 203:5, 642.

[3] D. Cherkasov and K. Il'in, *X Int. Kurnakov meeting on physicochemical analysis*, 2013, 2, 154.

PIII-46. Definition of Subtypes of Three Component System Diagrams, Containing Binary Biazeotropic Constituents and Not Having a Ternary Azeotropes

Chelyuskina T.V., Polkovnichenko A.V., Modurova D.D.

MIREA - Russian Technological University, Russia

cheluskina@mitht.ru

Systematization and expansion of the classification of three component biazeotropic systems [1] by structures of diagrams belonging to different subtypes and having a distinct deformation of distillation lines are an actual scientific task, since the analysis of these structures makes it possible to identify areas of the process of rectification of biazeotropic mixtures, what is necessary to predict the composition of product streams.

The synthesis of structures of equilibrium phase diagrams (SEPD) was carried out in two independent ways: 1) according to the method described in [2], based on the construction of $K=1$ lines (K - component distribution coefficient between vapor and liquid phases); 2) on the basis of an analysis of the transformations of the SEPD with a change of external conditions, based on the principles of the tangential azeotropy theory, described in detail in [3]. In accordance with the first way, an algorithm for synthesis of structures of vapor-liquid equilibrium (VLE) diagrams of three component systems assumes that systems belonging to any class are characterized by a certain set of singular points at the vertices of the triangle (points of pure components), at the boundaries (binary azeotropes) and inside concentration simplex itself (ternary azeotropes). From a given set of singular points, the contour of the Gibbs triangle is formed with the numbering of the components in order of boiling points increasing. To determine the course of distillation lines on a prism scan, at the base of which is a Gibbs triangle, possible variants of the arrangement of K -curves are constructed. Based on the mutual arrangement of $K=1$ lines, the types of boundary and internal singular points in the concentration triangle are determined. The obtained data are compared with a set of singular points characteristic for a given contour, and the qualitative course of distillation lines in the system is determined. Using the second way for synthesis of structures of VLE diagrams based on an analysis of the transformations of SEPD under external conditions change, it was established that all subtypes of diagrams of three component biazeotropic systems according to the method of binary biazeotropy appearance, regardless on which constituent (1-2, 2-3, 1-3) it appears, can be divided into 3 groups. The first group includes subtypes of diagrams that can be obtained only through the stage of formation of an internal tangential azeotrope (ITA). The second group consists of subtypes of diagrams that can be obtained only through the stage of the formation of a boundary tangential azeotrope (BTA). The third group includes subtypes of diagrams in which biazeotropy in binary constituents can appear through both the stage of ITA formation and the stage of BTA formation.

Thus, we obtained all thermodynamically possible subtypes of phase portraits of the process of open equilibrium evaporation of three component systems containing binary biazeotropic constituents and not having ternary azeotropes. A total of 116 subtypes were defined.

Acknowledgements This work was financially supported by the Russian Foundation for Basic Research (project no. 18-03-01224-a).

[1] Serafimov L.A. and Chelyuskina T.V., *Russian Journal of Physical Chemistry*, 2011, 85 (5), 767.

[2] Serafimov L.A., *D.T.S. Thesis*, 1968, MITHT, Moscow, Russia

[3] Zharov V.T. and Serafimov L.A., *Fiziko-khimicheskie osnovy distillyatsii i rektifikatsii* (Physicochemical Foundations of Distillation and Rectification), 1975, Khimia, Leningrad, Russia

PIII-47. Mutual Transformations of $\alpha=1$ Lines Diagrams of Butyl Butyrate - Butyric Acid - γ -Butyrolactone System

Polkovnichenko A.V., Chelyuskina T.V.

MIREA - Russian Technological University, Russia

cheluskina@mitht.ru

Studying of the evolution of $\alpha=1$ lines diagrams (α is the coefficient of relative volatility of components) within the same class of distillation lines diagrams under varying of external conditions, is necessary for a deeper understanding of the rectification separation processes of mixtures with complex physicochemical nature, including biazeotropic ones. The most effective way to separate such mixtures is extractive rectification [1]. The structures of distillation lines diagrams of the 3.[2.0.0].0-2 class according to the classification [2] correspond to systems that forms when the extractive agent is added to binary biazeotropic mixture to be separated. Depending on the physicochemical properties of the mixture, both one and several $\alpha=1$ lines diagrams can correspond to the same structure of liquid-vapor phase equilibrium diagrams. In the latter case, the diagrams of $\alpha=1$ lines transform into each other under varying of external conditions [3].

In this work, the mutual transition between $\alpha=1$ lines diagrams was confirmed by a computational experiment on mathematical modeling of vapor-liquid equilibrium (VLE) in a three component system formed by the butyl butyrate (BB) - butyric acid (BA) biazeotropic constituent and the potential extractive agent γ -butyrolactone (γ -BL), at pressures of 142.5 and 700 mm Hg, using the software package Aspen Plus V. 9.0. The modeling of the liquid-vapor phase equilibrium in the three component system BB - BA - γ -BL was performed using the NRTL-HOC model. The model parameters for the BB - BA system were taken from [4]. For the binary constituents BB - γ -BL and BA - γ -BL, the parameters were estimated using pseudoexperimental VLE data at 142.5 and 700 mm Hg obtained using the model UNIFAC-HOC.

Simulation of vapor-liquid equilibrium in binary systems BB - γ -BL and BA - γ -BL showed that γ -butyrolactone does not form azeotropes with the components of the mixture to be separated. On the basis of complete VLE data at the above mentioned pressures, it has been established that the system BB - BA - γ -BL does not have ternary azeotropes, and the structure of the distillation lines diagram of the system, remains unchanged at two pressures and belongs to 3.[2.0.0].0-2a class according to [5]. At the same time, diagrams corresponding to this system at a pressure of 142.5 and 700 mm Hg illustrate the fundamentally different course of $\alpha=1$ lines, what plays a decisive role in the development of a possible strategy for the separation of such mixtures.

Acknowledgements This work was financially supported by the Russian Foundation for Basic Research (project no. 18-03-01224-a).

[1] Chelyuskina T.V., *D.T.S. Thesis*, 2011, MITHT, Moscow, Russia.

[2] Serafimov L.A. and Chelyuskina T.V., *Russian Journal of Physical Chemistry*, 2011, 85 (5), 767.

[3] Chelyuskina T., Zakhlevniy A. and Modurova D., *Proceedings 45th International Conference of the Slovak Society of Chemical Engineering*, Slovakia, 2018, 139.

[4] Chelyuskina T.V. and Bedretdinov F.N., *Theoretical Foundations of Chemical Engineering*, 2016, 50 (5), 697.

[5] Serafimov L.A., Chelyuskina T.V., Polkovnichenko A.V. and Yakushev R.A., *Theoretical Foundations of Chemical Engineering*, 2018, 52 (6), 963.

PIII-48. Determination of Mean Ionic Activity Coefficients in the $\text{Li}_2\text{CO}_3 - \text{H}_2\text{O}$ System at 25 °C and $P_{\text{CO}_2}=1$ Atm

Gorbachev A.V., Mamontov M.N.

Lomonosov Moscow State University, Department of Chemistry, Russia

toto_neutrino@list.ru

The extraction of lithium from salt brines is one of the developing areas. For the proper selection of salt deposition conditions, experimental data on the thermodynamic properties of the phases and phase equilibria in a particular system are needed in order to build its thermodynamic model.

This work is related to the determination of mean ionic activity coefficient of Li_2CO_3 in the $\text{Li}_2\text{CO}_3 - \text{H}_2\text{O}$ system. While the phase equilibria in this system have been investigated in a number of studies, almost no data on the thermodynamic properties of the solution $\text{Li}_2\text{CO}_3(\text{aq})$ phases. Measurements were carried out using the EMF method with ion-selective electrodes (CO_3^{2-} -ISE | $\text{Li}_2\text{CO}_3 + \text{H}_2\text{O}$ | Li^+ -ISE cell) in the 0.01 – 0.2 mol/kg molality range and $t = 25$ °C . Li^+ , CO_3^{2-} -ISEs were calibrated in aqueous solutions of LiCl and NaHCO_3 , respectively. After calibration, EMF measurements in the $\text{Li}_2\text{CO}_3 - \text{H}_2\text{O}$ system were carried out.

At the first stage of the experiment, the pH values of solutions $\text{Li}_2\text{CO}_3(\text{aq})$ were measured with stirring and bubbling of CO_2 at $p = 1$ atm through the solution until equilibrium in the system was established. The criterion for achieving equilibrium state was considered a constant pH value of solution. At the next stage of the experiment, we measured the EMF between Li^+ -, CO_3^{2-} - ISEs (see fig. 1) while passing CO_2 in the atmosphere above the solution. Further, since the obtained EMF are related with the mean ionic activity coefficient of Li_2CO_3 , experimental values were used to optimize the parameters of the Pitzer [1] model at 25 °C for the solution under investigation.

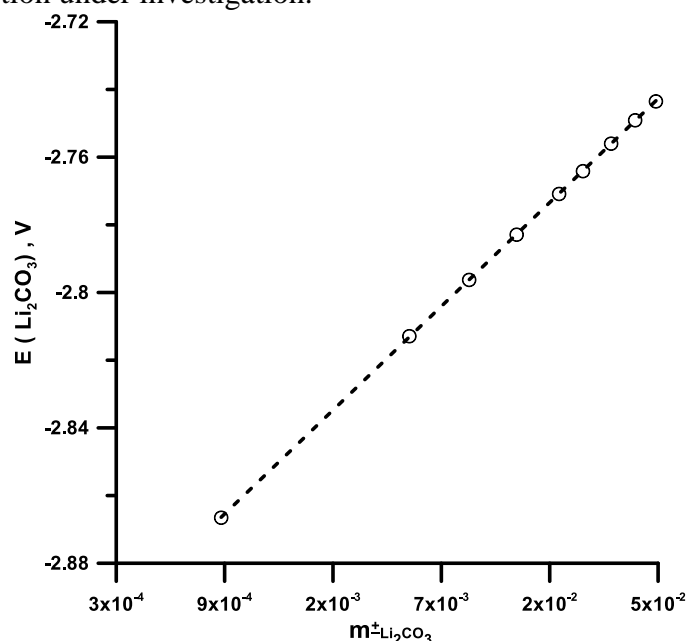


Figure 1. EMF between Li^+ -, CO_3^{2-} - ISEs.

[1] C.E. Harvie, N. Moller, J.H. Weare, *Geochim. Cosmochim. Acta*, 1984, 48, 723.

PIII-49. The Viscosity Predictions for Branched Alkanes at Pressures up to 1 GPa Using Molecular Dynamics

Kondratyuk N.D., Pisarev V.V.

National Research University Higher School of Economics, Russia

nidkond@gmail.com

nidkond@gmail.com

Shear viscosity is one of the key subjects of molecular modeling studies since this quality is used in the development of lubricants¹. In this work, we use molecular dynamics methods to predict viscosity dependence on pressure up to 1 GPa for 2,2,4-trimethylhexane. The COMPASS class II force field is used to determine atomic interactions in the model². The shear viscosity is calculated using Green-Kubo and Muller-Plathe methods. To achieve the convergence of the Green-Kubo integral, the time decomposition method³ is used. The approach is validated by 2,2,4-trimethylpentane for which experimental data are available. The calculated 2,2,4-trimethylhexane viscosity coefficient dependence (shown on Fig. 1) is fit by Tait-like equation and does not show super-Arrhenius behavior⁴. The predicted values of 2,2,4-trimethylhexane viscosity match the experimental data within the accuracy of the methods up to 500 MPa.

Acknowledgements The abstract was prepared within the framework of the Basic Research Program at the National Research University Higher School of Economics (HSE) and supported within the framework of a subsidy by the Russian Academic Excellence Project "5-100".

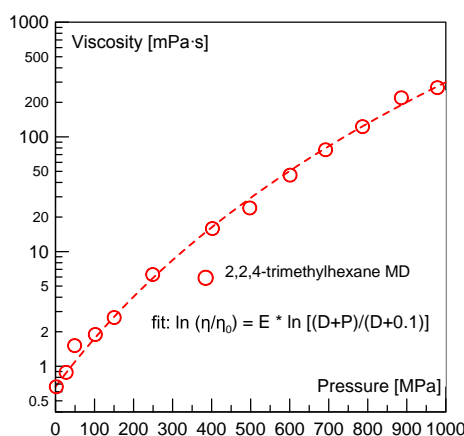


Figure 1. The shear viscosity dependence on pressure for 2,2,4-trimethylhexane liquid.

[1] S. Bair, L. Martinie and P. Vergne, *Tribol. Lett.*, 2016, 63(3), 1–10.

[2] H. Sun, *J. Phys. Chem.*, 1998, 5647(98), 7338–7364.

[3] Y. Zhang, A. Otani, and E. J. Maginn, *J. Chem. Theory Comput.*, 2015, 11(8), 3537–3546.

[4] N. Kondratyuk and V. Pisarev, *Fluid Phase Equilib.*, 2019, accepted.

PIII-50. Thermodynamic Modeling and Experimental Investigations in the System Formed by Water, Nitric Acid, Neodymium Nitrate, o-Xylene and D2EHPA

Kovalenko N.A., Kurdakova S.V., Arkhipin A.S., Maksimov A.I., Uspenskaya I.A.

Lomonosov Moscow State University, Russian Federation

kovalenko@td.chem.msu.ru

Rare-earth elements (REE) are usually extracted from natural raw materials or products of its processing; at present, huge amounts of waste from chemical production in the form of phosphogypsum and red mud are accumulated. Disposal of this waste with the extraction of useful and expensive elements will partially reduce the financial burden on production and solve a number of environmental problems. The purpose of this work is to develop a rigorous thermodynamic model of extraction processes as an alternative to existing traditional approaches, based on the approximation of information about the distribution curves of the target component by a set of real or virtual chemical reactions between the substances of the system under consideration. The main task is to develop sufficiently flexible thermodynamic models that can be easily adapted for modeling of the extraction systems of various types (containing several electrolytes, with a mixed aqueous-organic solvent, with a complexing agent) and can be directly used by technologists when choosing the conditions for carrying out specific extraction processes.

The water – o-xylene – di(2-ethylhexyl)phosphoric acid (D2EHPA or HA) – nitric acid – neodymium nitrate system was chosen as the research object. At the first stage experimental investigations were conducted, the purpose of which was to obtain experimental data that were missing for constructing a thermodynamic model. The method of vapor pressure, isothermal solubility, measurement of bulk properties, liquid-liquid equilibria investigations were chosen as main direction of the research. As a result, the thermodynamic properties of the organic and aqueous phases of the studied system were obtained, and the conditions for the coexistence of phases of the extraction system were studied.

At the second stage, the previously obtained experimental data together with the literature data were used to construct a thermodynamic model, which can be used to select the best conditions for the extraction of neodymium nitrate using D2EHPA. The electrolyte version of the generalized local composition model (eGLCM) was used in the present work for describing the Gibbs energy of the aqueous and organic phases. Different types of experimental data (vapor-liquid equilibria and solid-liquid equilibria data, activities of water) were used to determine parameters of the model for the aqueous $\text{H}_2\text{O} - \text{HNO}_3 - \text{Nd}(\text{NO}_3)_3$ phase. Determination of the parameters of the organic D2EHPA – o-xylene – NdA_3 phase was based on vapor-liquid equilibria data processing. Availability of the information about liquid-liquid equilibria in the water – nitric acid – REE nitrate – o-xylene – D2EHPA system and previously obtained thermodynamic models for aqueous and organic phases made it possible to determine thermodynamic equilibrium constants.

The obtained parameters of the model and equilibrium constants allow to calculate the distribution of neodymium between the phases depending on the pH and the content of REE, D2EHPA, o-xylene.

Acknowledgements This work was funded by RFBR according to the research project No. 18-29-24167

PIII-51. The Conformational Equilibrium of Mefenamic Acid in DMSO: Thermodynamic or Kinetic Origin?

Belov K.V.^{1,2}, *Khodov I.A.*^{2,3}, *Kiselev M.G.*¹, *Efimov S.V.*³, *Batista de Carvalho L.A.E.*⁴

¹G.A. Krestov Institute of Solutions Chemistry, Russian Academy of Sciences, Russia

²Ivanovo State University, Ivanovo, Russia

³Kazan Federal University, Russia

⁴University of Coimbra, Coimbra, Portugal

ilya.khodov@gmail.com

This work presents main results of studies and conformational properties of the mefenamic acid molecule (2-[(2,3-dimethylphenyl)amino]benzoic acid), which is a derivative of N-phenylantranil acid. This compound is used as medicine and belongs to the group of nonsteroidal anti-inflammatory drugs. The aim of this work is determination of the most probable conformers of mefenamic acid dissolved in dimethyl sulfoxide using the methods of NMR spectroscopy and computer simulation. The obtained information can help to determine possible nucleation mechanisms.

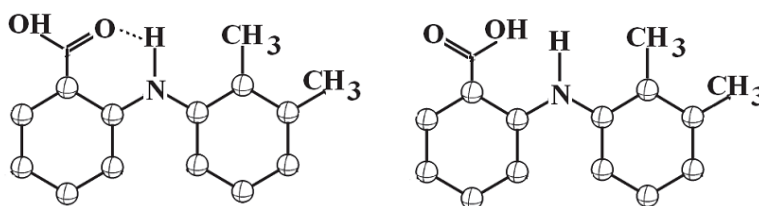


Figure 1. Structure of the mefenamic acid molecule for the polymorph MEF I (left) and MEF II (right).

Studies of mefenamic acid conducted in groups of McConnell and Lee [1], revealed that it can crystallize in two forms, called MEF I and MEF II. They are formed by different conformations of the mefenamic acid molecules (Fig.1), having different orientations of the carboxyl group. The phase transition from MEF I to MEF II in the solid state is observed in the range from 160 to 190°; the transition temperature depends on the heating rate. This transition can also be induced by mechanical compression of solid material. Our hypothesis is that the molecular conformation existing in the saturated solution defines the polymorphic type obtained by evaporation of this solution. Recently we have shown on the example of felodipine [2], that the spatial structure of the molecule changes upon increasing the concentration to the saturated state, and eventually becomes like the configuration found in the crystal. On the other hand, a possibility of complicated, multi-stage mechanism of arising of polymorphic forms is also possible, as it was found during study of ibuprofen [3]. We believe that the multi-stage mechanism is the consequence of competition between processes of solvation (or kinetic) and thermodynamic effects. In this work we try to discuss the influence of the thermodynamic effects on conformation equilibrium of mefenamic acid.

Acknowledgements The work was supported by Russian Foundation for Basic Research (project nos. 18-29-06008, 18-03-00255 and 17-03-00459), by the Ministry of Education and Science of the Russian Federation, project no. RFMEFI61618X0097, by the Basic Research Program of Ministry of Education and Science, project no. 01201260481.

[1] E.H. Lee, S.R. Byrn, and R. Pinal, *J. Pharm. Sci.* 2012 101, 4529.

[2] I.A. Khodov, et al., *J. Pharm. Sci.* 2014, 103.

[3] I.A. Khodov, et al., *J. Mol. Struct.* 2016, 1113.

PIII-52. Thermodynamic Models of the $\text{H}_2\text{O} - \text{HNO}_3 - \text{UO}_2(\text{NO}_3)_2$ and $\text{H}_2\text{O} - \text{HNO}_3 - \text{Th}(\text{NO}_3)_4$ systems

Maliutin A.S., Kovalenko N.A.

Lomonosov Moscow State University, Russian Federation

alex-kla@yandex.ru

The manufacture of the wet-process phosphoric acid produces a large amount of phosphogypsum as a by-product. Although gypsum is a widely used material in the construction industry, phosphogypsum is usually not used mainly because of its weak radioactivity. The long-term storage of phosphogypsum is unfavorable because it requires great capital expenditures and operational costs. Also, phosphogypsum stacks, occupying large territories, are harmful for the environment and for the people's health. All the mentioned makes the problem of removal of the radioactive contaminants from the phosphogypsum very vital.

Several routes of purification of phosphogypsum (i.e. extraction, leaching and sieving) are present, but still these processes are studied relatively poorly. Most of the works concerning them deal with some empiric correlations and often they just state the fact of redistribution of the radioactive species depending on the initial conditions of the processing. To understand these processes better and to have a tool for prediction the behavior of phosphogypsum and its contaminants in a broad range of conditions, a comprehensive thermodynamic model is needed.

Concerning some routes of the phosphogypsum processing, the systems $\text{H}_2\text{O} - \text{HNO}_3 - \text{UO}_2(\text{NO}_3)_2$ and $\text{H}_2\text{O} - \text{HNO}_3 - \text{Th}(\text{NO}_3)_4$ are of prior interest. So, the aim of this work is to introduce thermodynamic models of the systems mentioned.

Pitzer model was used to fit the experimental data including vapor-liquid equilibrium data, osmotic coefficients, and solubilities in a wide range of temperatures at an atmospheric pressure. Modeling was conducted stepwise with the number of components increasing gradually. Parameterization of the model was carried out by the method of least squares. The minimized objective function was the sum of squared residuals of calculated and experimental values.

The results of this work can be useful for the optimization of the complex processing of phosphogypsum.

This work was funded by RFBR according to the research project № 18-29-24167.

[1] R. Goldberg, *Journal of Physical and Chemical Reference Data*, 1979, 8, 1005.

[2] K. Pitzer, *The Journal of Physical Chemistry*, 1973, 77, 268.

PIII-53. Extinction and Saturated Vapor Pressure of Indium Monochloride

Malygina E.N., Zavrazhnov A.Y., Kosyakov A.V., Naumov A.V.

Voronezh State University, Russia

ekaterina.malygina2013@yandex.ru

Equilibria involving indium and gallium halides are important, in particular, for the deep purification of the metallic indium and gallium. At the same time, if gallium can be easily transported during the halide CVT, the similar indium transfer is practically impossible [1 – 3]. In order to approach the identification of the causes of this difficulty we fulfilled the following study. The goal was to carry out the spectrophotometric and vapor-pressure investigation of the two-phase $L_{\text{In}} - V$ and the three-phase $L_{\text{In}} - L_{\text{InCl}} - V$ equilibria and to find the molar extinction coefficients of gaseous indium monochloride. (L_{In} and L_{InCl} are the liquids, based on metallic In and InCl correspondently.)

Electronic absorption spectra of indium monochloride vapor were obtained in the wavelength range of 200 – 400 nm and a temperature range of 225 – 850 °C. The spectrophotometric studies of the $L_{\text{In}} - V$ equilibrium allowed us to show the temperature dependence of the absorption coefficients at wavelengths corresponding to the absorption bands maxima under conditions when the indium monochloride concentration in a vapor (C_{InCl}) remained constant. Indeed, it was shown that in the $L_{\text{In}} - V$ equilibrium $C_{\text{InCl}} = \text{const}$ and the change in the absorption coefficients could only be associated with the temperature dependence of the InCl extinction. The fact is that the characteristic absorption bands of other possible species – In_2Cl_4 and InCl_3 – were not observed. Therefore, we can assume that almost only InCl molecules are present in the vapor in equilibrium $L_{\text{In}} - V$.

The experimental dependences of the absorption coefficient $k(\lambda, T)$ of the InCl saturated vapor (in three-phase equilibrium $L_{\text{In}} - L_{\text{InCl}} - V$) are described by the function of temperature:

$$\ln(T \cdot k(\lambda, T)) = -\frac{A}{T} + B(\lambda).$$

It should be noted that the angular coefficient A is essentially independent of the wavelength and its value is virtually identical to the angular coefficient for the temperature dependence of the saturated vapor pressure:

$$\ln p = -\frac{A}{T} + b.$$

The latter dependency was found in the course of the vapor-pressure experiments for three-phase equilibrium with the use of a quartz membrane null-manometer. We obtained the following parameters: $A = -10255 \pm 69$ K, $b = 10,95 \pm 0.08$ (for the atmospheric pressure as a standard for p). These values correlate well with the literature. Using these results the molar extinction coefficients for the strongest absorption bands of gaseous indium monochloride were calculated. The highest value of the molar extinction coefficient was found for the band at 267.0 nm is $1.17 \cdot 10^8 \text{ cm}^2 \cdot \text{mol}^{-1}$ at the temperature of 327 °C. For other bands in the λ -range of 262 – 280 nm the $\varepsilon(\lambda)$ -values are also very high. Thus the spectrophotometric method is very sensitive for both qualitative and quantitative determination of gaseous indium monochloride.

Acknowledgements. This work was supported by *RFBR*, project 18-33-00900-*mol-a*.

P. I. Fedorov, R. Akchurin, Chemistry of the Indium, 2000. Nauka, Moscow. (In Russian)

2. A. Yu. Zavrazhnov, A. V. Naumov, V. S. Pervov, M. V. Riazhskikh, *Thermochimica Acta*, 2012, 532, 96.

3. A. Yu. Zavrazhnov, A. V. Naumov, A. V. Sergeeva, V. I. Sidei, *Inorganic Materials*, 2007, 43, 1167.

PIII-54. Phase Equilibria in ZrO_2 and $4Y_2O_3-96ZrO_2$ Precursors (mol.%), Obtained by Cryochemical Method

Lomakina T.E., Kurapova O.Yu., Konakov V.G.

St. Petersburg State University, Institute of Chemistry,
Department of Physical Chemistry, St. Petersburg, Russia

st056239@student.spbu.ru

Oxide ceramics based on high-symmetric ZrO_2 modifications is widely used in industry as solid electrolytes in different electrochemical devices in automotive industry and for aerospace, as a functional material for prostheses and bone implants production. The use of new mild chemistry techniques leads to the essential shift of phase equilibrium in oxide systems, crystallization of zirconia polymorphs at lower temperatures, than it is indicated on phase diagrams. Thus the goal of the present work was the investigation of phase equilibriums sequence in the partially stabilized and undoped zirconia precursors, obtained by cryochemical method in the temperature range of 20 – 1100 °C.

For that, cryochemical technique comprising reversed co-precipitation from 0.1 M aqueous solutions of $ZrOCl_2 \cdot 6H_2O$, $ZrO(NO_3)_2 \cdot 6H_2O$ and $Y(NO_3)_3 \cdot 6H_2O$ with the subsequent cryochemical dehydration of gel. As a precipitator 1 M aqueous solution of ammonia was used, solution of salts was added dropwise of 1–2 ml/min, pH = 9–10, T=1–2 °C. The fresh precipitate of hydroxides was placed in Dewar vessel with liquid nitrogen by the small portions, then the frozen granulate was dried in air. The received amorphous powders were annealed for 2 hours at 550, 800, 1000 and 1100 °C. Precursors after synthesis and calcination were investigated by simultaneous thermal analysis (STA, STA 409 of C/4/G Jupiter, NETZSCH), the X-ray diffraction analysis (XRD, Bruker "D2 Phaser", Cu-K α the radiation, $\lambda=1,54\text{\AA}$, with XRD patterns refinement by the Rietveld method), particle size distribution analysis (PSD, Horiba partica LA-950).

It was shown that phase formation in $4Y_2O_3-96ZrO_2$ (4YSZ) powders takes place according to $Y_2O_3-ZrO_2$ diagram. Other situation was observed for undoped zirconia precursors, obtained from various salts, i.e. in all temperature range formation of mixed tetragonal and monoclinic phases takes place with the different ratio. Phase transition from the amorphous to crystalline phase resulted in tetragonal phase content ~87 wt.% and 13 wt% monoclinic phase. The increase of the temperature up to 1100 C leads to tetragonal phase content decrease up to ~ 5 wt. %. The existence of the metastable tetragonal phase ZrO_2 , most likely, is due to high powders dispersity. STA and XRD researches were conducted in the Research Centre for X-ray Diffraction Studies, Research park of Saint Petersburg State University. The work was supported by the President's grant for young scientists # MK-2703.2019.3.

PIII-55. Inverse Solidus Surface Projection of the Cu-Co-Ni Ternary System

Novozhilova O.¹, Sineva S.^{2,3}, Starykh R.³

¹Peter the Great St. Petersburg Polytechnic University, Russia;

²University of Queensland, Australia,

³LLC Gipronickel Institute

olya-novozhilova@inbox.ru

Alloys of the Co-Cu-Ni ternary system are the basis for many functional materials such as catalyst and cutting tools, as well as they can be used as prospective candidates for design of magnet-heterogeneous microstructures and high entropy alloys. Information about phase equilibria in Co-Cu-Ni system is essential for process of directed synthesis of alloys. The current study is devoted to analysis of phase diagram of the Co-Cu-Ni system and, in particular, construction of solidus surface projection.

The analysis of binary boundary systems showed, that solidus line of Co-Cu system has inverse character, which is reached the maximum solubility of copper in cobalt solid solution (19,7% at.Cu at 1367°C) higher of peritectic transformation temperature [1]. So, the phase diagram of the discussed system is characterised of composition area of 12-20% at. Cu having “double” solidus temperature and even crystallisation effect of Co-solid solution at heating. However, discussed exothermal effect of Co-solid solution crystallisation is difficult to register experimentally, as it is overlapped by total endothermic effect of the alloy melting [2]. Moreover, Co-Cu system has a tendency to form metastable liquid miscibility gap [3, 4]. Mentioned peculiarities of this binary system will affect on the topology of the Co-Cu-Ni ternary system. It was discovered that solidus surface projection of the Co-Cu-Ni system hasn't been plotted earlier. Thus, it is necessary to construct it applying the set of experimental methods and to consider the inverse character of solidus surface projection.

The composition of samples, located at the cross-sections of compositional grid at Gibbs triangle with the step of 10% at. change were chosen for study. Additionally the samples were synthesised those compositions are located near miscibility gap in ternary system and also near inverse solidus line of binary Co-Cu system. Obtained samples were examined with the DTA, SEM-EPMA, and XRD methods. DTA-data were used for determination of the solidus temperatures. Area of solid-state miscibility gap and composition of coexisting phases were defined with the use of SEM-EPMA method. To study the behaviour of the inverse solidus with low nickel content the additional equilibrium experiments were done at temperature range 1150-1400 °C aimed at reaching of local equilibrium state among Co-based solid solution and Cu-riched liquid phase. Experimental samples were quenched into the water after long-term holding at equilibrium temperatures. The compositions of coexisting phases were determined on electron probe with wave-length dispersive spectrometer. The solidus surface projection including inverse solidus area was constructed with the use of the mentioned above methods.

The project is supported by RFBR grant № 17-08-00875-a.

[1] Ivanchenko, V., Turchanin, M., Agraval, P. “Co-Cu Binary Phase Diagram Evaluation”. Diagrams as Published in MSIT Workplace, Effenberg, G. (Ed.), MSI; Materials Science International Services GmbH, Stuttgart, (2006)

[2] Curiotto, S., “Undercooling and Phase Transformations in Cu-based Alloys”, Thesis, Universita Degli Studi di Torino, 1-154 (2006)

[3] Cao C., Letzig T., G`orler G. and Herlach D., Journal of Alloys and Compounds, 325, 113–117 (2001).

[4] Sun Z., Song X., Hu Z., Yang S., Liang G. and Sun J., Journal of Alloys and Compounds, 319, 266–270 (2001)

PIII-56. Revisiting the Heat-Capacity Anomaly in Supercooled Water by High-Resolution Adiabatic Calorimetry

Voronov V.P.¹, Podnek V.E.¹, and Anisimov M. A.²

¹Laboratory of Phase transitions & Critical Phenomena, Oil & Gas Research Institute of the Russian Academy of Sciences, Moscow 119333, Russia;

²Department of Chemical & Biomolecular Engineering and Institute for Physical Science & Technology, University of Maryland, College Park, MD 20742, USA

podnek77@gmail.com

Liquid water demonstrates spectacular anomalies upon supercooling. One of the most pronounced anomalies is the seemingly diverging isobaric heat capacity at ambient pressure [1]. A popular hypothesis that explains the anomalies of supercooled water is the existence of a metastable liquid-liquid transition hidden below the line of homogeneous nucleation [2]. The existence of the liquid-liquid transition in real water is still debatable since it is not accessible to direct experiments. There have been three previously reported heat-capacity experiments on supercooled water: the pioneer measurements of Angell et al. in emulsified water [1], differential scanning calorimetry measurements reported by Archer and Carter [3], and adiabatic calorimetry measurements by Tombari et al. [4]. These sets of data significantly deviate from each other. More accurate measurements of the character of the anomaly the heat-capacity may shed additional light on the nature of supercooled water's anomalies. Using a high-resolution slow-scanning adiabatic calorimeter we have measured the temperature dependence of the isobaric heat capacity of supercooled water at 0.1 MPa in sealed 1 ml glass ampoules down to 244 K. The measurements were carried out by quasi-adiabatic heating (with a rate ~ 0.4 K/hour) from the lowest temperature achieved by supercooling. Overall, our data (with a higher resolution and better supercooling achieved) support the results reported by Tombari [4] but significantly deviate from the heat-capacity values for emulsified supercooled water reported by Angell et al. [1] and even more from the DSC measurements by Archer and Carter [3].

Since the existence of the liquid-liquid transition in real water is still an open question, we have checked whether the experimentally observed anomaly would be consistent with a model alternative to the liquid-liquid critical point scenario [2]. Indeed, we show that the new data can be well described by a power-law with an exponent $-3/2$ corresponding to the initial fluctuation regime of Landau-Brazovskii weak-crystallization theory [5]. The apparent temperature of the heat-capacity divergence is 228.8 K. This latter value is just below the temperature of homogenous ice nucleation and is close to the temperature of the projected heat-capacity maximum at ambient pressure in the critical point scenario (below the expected critical pressure of liquid-liquid phase separation) [2]. We note that the nature and analytical shape of the anomaly in these alternative scenarios are fundamentally different even if they both fit well to the experimental data. We observed a sharp increase in the relaxation time in supercooled water with upon supercooling, which did not allow us to conduct the adiabatic measurements at lower temperatures achieved by Angell et al. for emulsified water. A less ambiguous answer on the nature of the anomalies in bulk supercooled water requires further experimental studies closer to the homogeneous nucleation limit, including accurate measurements at both high and negative pressures.

1. C. A. Angell, M. Oguni, W. J. Sichina, *J. Phys. Chem.*, vol. 86, p. 998 (1982).
2. P. Gallo, K. Amann-Winkel, C. A. Angell *et al.*, *Chem. Rev.*, vol. 116, p. 7463 (2016).
3. D. G. Archer and R. W. Carter, *J. Phys. Chem. B*, vol. 104, p. 8563 (2000).
4. E. Tombari, C. Ferrari, G. Salvetti, *Chem. Phys. Lett.*, vol. 300, p. 749 (1999).
5. S. A. Brazovskii, *JETP*, vol. 41, p. 85 (1975).

PIII-57. Prediction of Solubility of Polymers Using Polystyrene-Polysiloxane System as an Example

Poteryaev A.A., Chalykh A.E.

A.N. Frumkin Institute of Physical chemistry and Electrochemistry RAS, Russian Federation

apoteryaev@gmail.com

A method of theoretical assessment of compatibility of thermoplastics with different polysiloxane reagents, based on the using of the Flory-Huggins thermodynamic concept and the group contributions method is proposed in the paper.

According to Flory-Huggins theory, the critical value of the interaction Parameter χ_{cr} depends on the degrees of polymerization of the components of the system and can be calculated using next correlation:

$$\chi_{cr} = \frac{1}{2} \left(\frac{1}{\sqrt{r_1}} + \frac{1}{\sqrt{r_2}} \right)^2 \quad (1),$$

where according to Hildebrand $\chi = V_r(\delta_1 - \delta_2)^2/(2RT)$ (2), δ_1 and δ_2 are solubility parameters of the components, V_r – molar volume, R – gas constant, T – temperature. Solving expressions 1 and 2 an equation for calculating of the values of δ_2 which make up the hypothetical area of complete compatibility of components at a given temperature, can be obtained.

$$\delta_2 = \delta_1 \pm \left(\frac{1}{\sqrt{r_1}} + \frac{1}{\sqrt{r_2}} \right) \sqrt{\frac{RT}{V_r}} \quad (3).$$

The δ_2 region (I) calculated for polystyrene with $M_w = 15000$ g/mol using the equation (3) is shown on diagram (Fig. 1). The values of the solubility parameters of various siloxane oligomers are also shown. It is assumed, that if the figurative point falls into the calculated (shaded on fig. 1) area, that the components of the system are fully compatible one into another.

It should be noted that the information on the mutual solubility of components in the polystyrene-polysiloxane system obtained using the prediction model correlates with the experimental data obtained for the similar systems.

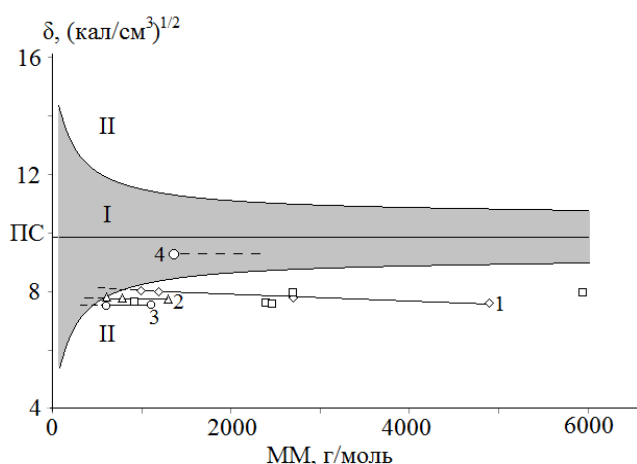


Fig. 1. Dependence of solubility parameters on molecular weight (1) – polydimethylsiloxane with carboxyl ending groups, (2) – polydiethylsiloxane, (3) – polydimethylsiloxane with methyl ending groups, (4) – polyphenylmethylsiloxane.

PIII-58. Melting Scenarios and Unusual Crystal Structures in Two-Dimensional Core-Softened Systems

Ryzhov V.N., Fomin Yu.D., Tareyeva E.E., Tsiok E.N.

Institute for High Pressure Physics, Russian Academy of Sciences, 108840 Troitsk, Moscow, Russia

ryzhov@hppi.troitsk.ru

Recently, there has been growing interest to investigation of behavior of confined fluids, with a special attention to the water. Water plays an important role in many natural processes where it is confined or at contact with substrates, for example, in rocks, in biological cells, at contact with surfaces of proteins, in biological membranes, etc. It is well known, that the qualitative behavior of water, including the water-like anomalies, can be described using the core-softened potentials with two length scales [1,2]. Another example of the core-softened system which also demonstrates complex phase behavior and water-like anomalies is the Hertzian spheres [3,4]. In the talk we present short description of Berezinskii-Kosterlitz-Thouless (BKT) theory, modern melting scenarios of 2D crystals and computer simulation study of phase diagrams of mentioned above 2D systems: core-softened repulsive shoulder potential and Hertzian spheres. It is shown, that in contrast to the case of simple potentials, like soft disks, where the ground state always corresponds to the hexagonal close-packed structure, the various structures are possible including the square, kagome, snub-square lattices and quasicrystalline phase with 12-fold symmetry [5,6]. The possible melting scenarios are discussed and the deviations from the widely accepted Berezinskii-Kosterlitz-Thouless-Halperin-Nelson-Young (BKTHNY) scenario (two BKT transitions with the intermediate hexatic phase) are discussed [5-9]. It is found that depending on the form of the potential, the melting of the systems can occur in accordance with BKTHNY scenario, through one first order transition or through two-stage transition with continuous BKT type solid-hexatic transition and first order hexatic-liquid transition. The influence of the random disorder, which is inevitable in real experiments, on the melting scenario is considered. Random pinning transforms the first order transition into two-stage melting scenario or widens the hexatic phase [7-9]. It gives the possibility to study the behavior of the diffusivity and order parameters in the vicinity of the melting transition and inside the hexatic phase.

Acknowledgements The work was supported by the Russian Foundation for Basic Research (Grant No 17-02-00320). This work was carried out using computing resources of the federal collective usage center «Complex for simulation and data processing for mega-science facilities» at NRC "Kurchatov Institute", <http://ckp.nrcki.ru/> and supercomputers at Joint Supercomputer Center of the Russian Academy of Sciences (JSCC RAS).

[1] Yu. D. Fomin, et al., *J. Chem. Phys.*, 2008, 129, 064512.

[2] S. V. Buldyrev *et al.*, *J. Phys.: Condens. Matter*, 2009, 21, 504106.

[3] J. Pamies, A. Cacciuto and D. Frenkel, *J. Chem. Phys.*, 2009, 131, 044514.

[4] Yu. D. Fomin, V. N. Ryzhov, and N. V. Gribova, *Phys. Rev. E*, 2010, **81**,061201.

[5] N. P. Kryuchkov, et al., *Soft Matter*, 2018, 14, 2152.

[6] Yu. D. Fomin, et al., *Molecular Physics*, 2018, 116, 3258.

[7] V.N. Ryzhov, E.E. Tareyeva, Yu.D. Fomin, E.N. Tsiok, *Physics Uspekhi*, 2017, 60, 857.

[8] E. N. Tsiok, D. E. Dudalov, Yu. D. Fomin, V. N. Ryzhov, *Phys. Rev. E*, 2015, 92, 032110.

[9] E. N. Tsiok, Yu. D. Fomin, and V. N. Ryzhov, *Physica A*, 2018, 490, 819.

PIII-59. Calculation of the Thermodynamic Properties of Natural Gas Using a Limited Number of Experimental Parameters

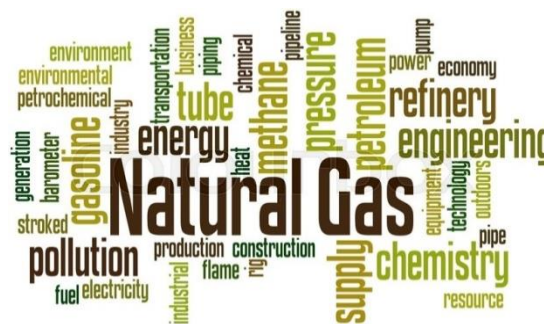
Samarov A.¹, Toikka M.¹, Golikova A.¹, Farzaneh-Gord M.², Toikka A.¹

¹St. Petersburg State University, Russia;

²Technological Institute of Shakhrud, Iran

artemy.samarov@spbu.ru

It is known that the knowledge of the thermodynamic properties of natural gas is necessary in order to investigate its properties in a wide range of pressures, temperatures and concentration of the main components and impurities. There are a lot of traditional methods for determining thermodynamic properties in the laboratory. But the complex aspects of the determination of thermodynamic properties are associated with their practical application in the transport of gas in the pipeline, where we have significant pressure drops. In practice, the solution of such problems is reduced to the simultaneous determination of both the velocity and the density of the gas at gas distribution stations. Gas flow measurement using, for example, turbine or ultrasonic meters does not allow determining the mass flow rate of gas with sufficient accuracy due to changes in its composition, density, temperature dependence or pressure. Such equipment has many drawbacks, with a rather intensive use of this equipment, it is necessary to constantly check the calibration of measuring instruments. Thus, work is continuing on finding new approaches to measuring the properties of natural gas, which will improve the accuracy of determining its density, preferably based on stable, easily determined parameters and minimum measurements [1]. The use of traditional analytical methods such as gas chromatography makes it possible to accurately determine the composition of the gas, but their application in gas distribution stations is difficult and seems to be highly inefficient.



Using the Farzaneh-Gord approach [2], which includes a program for calculating the required thermodynamic properties, an independent assessment was made of the method for determining mass flow and density of natural gas. Considering compounds that simulate various gas fields, empirical molecular weights and densities were calculated. The calculation showed that the average absolute error of the calculated values of the density of natural gas the deviation from the experimentally measured values does not exceed 0.5%. It has been established that the applied method [2] gives optimal results at 250–350 K and pressures from 0.2 to 4 MPa, as well as for a fairly wide range of compositions of mixtures of natural gas. Using this approach, one can determine the mass flow rate with high accuracy without resorting to data on the composition. Note that in order to carry out this, it is necessary to have indirect experimental data on the speed of sound at different temperatures and pressures.

Acknowledgements. This work was supported within a scope of joint project of Russian Foundation for Basic Research and National Foundation of Iran (INSF): contract INSF no. 96004167 and RFBR grant no. 17-58-560018.

[1] Gallagher, J.E., *Natural Gas Measurement Handbook*, Amsterdam: Elsevier, 2013.

[2] Farzaneh-Gord, M., Arabkoohsar, A., Koury, R.N.N., *J. Nat. Gas Sci. Eng.*, 2016, 30, 195–204

PIII-60. Phase Diagram of the Ternary System n-Dodekan-n-Eykozan-Cyclododecane

Shamitov A.A., Garkushin I.K., Kolyado A.V.

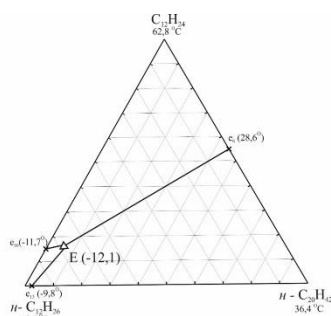
Samara: Samara state technical university, Samara, Russia

sansher@mail.ru

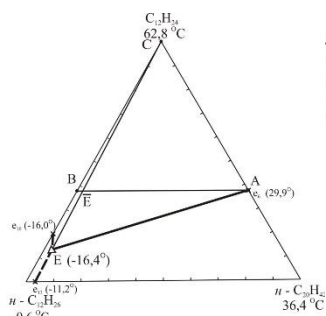
In this work you can see the principle of searching of the new heat carrier which based on a system $n\text{-C}_{12}\text{H}_{26}\text{-}n\text{-C}_{20}\text{H}_{42}\text{-C}_{12}\text{H}_{24}$. Research and determination of the eutectic structure and melting point happens by the method of a differential thermal analysis [1]. At the beginning we made predesign of phase diagrams by the equation of Wilson [1], for the purpose of reduction of a deviation of design data from an experiment, were entered coefficients of activity of components into the system of the equations. The main idea here is that the local structure near a concrete molecule in solution will differ from composition of liquid because of various intermolecular interaction.

Rated coordinates of an eutectic in a system are determined by the solution of the equation of Wilson: 79,64 mas. % of n-dodecane, 2,91 mas. % of n-eykozan and 17,45 mas. % of cyclododecane, melting point of alloy of the eutectic structure of $t_E = -12.1\text{ }^\circ\text{C}$ (pic. 1).

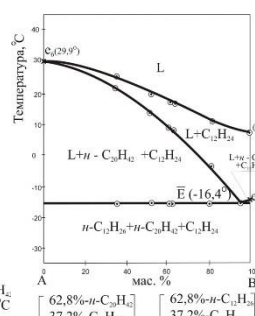
The pilot study of a system is conducted by means of the installation DSK [2] (pic. 2-4) as a result defined the eutectic: 83,0 mas. % of N-dodecane, 3,0 mas. % of N-eykozan and 14,0 mas. % cyclododecane, melting point of alloy of the eutectic structure of $t_E = -16,4\text{ }^\circ\text{C}$. Specific enthalpy of fusion of alloy of the eutectic structure is equal to 192.5 J/g.



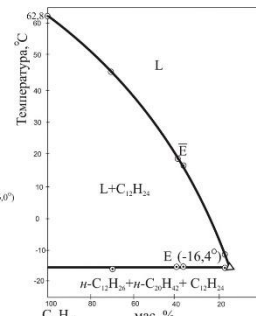
pic. 1 Phase complex
 $n\text{-C}_{12}\text{H}_{26} - n\text{-C}_{20}\text{H}_{42} - \text{C}_{12}\text{H}_{24}$
by the equation of Wilson



pic. 2 Phase complex
 $n\text{-C}_{12}\text{H}_{26} - n\text{-C}_{20}\text{H}_{42} - \text{C}_{12}\text{H}_{24}$



pic. 3 Polythermal section AB



pic. 4 Polythermal section $\text{C}_{12}\text{H}_{24} \rightarrow \bar{E}$
 $\rightarrow \bar{E}$

So the system of N-dodecane – N-eykozan – cyclododecane falls into to the systems of the eutectic type. Alloy of the eutectic structure can be used as a working body of the low-temperature accumulator of heat or as the medium temperature heat carrier of heliopower stations with a temperature of operation from 5 to 240 °C. In the considered system there are deviations from ideality therefore it is necessary to consider an activity coefficient of components of a system when calculating parameters of an eutectic.

[1] Shamitov A.A., etc. Phase diagrams of a ternary system n-decan-n-octadecane-cyclododecane// Magazine of physical chemical – 2018. - T. 92. - №. 9. - page 1421-1425.

[2] Egunov V. P., etc. Thermal analysis and calorimetry. Samara: Samara state technical university, 2013.– page 457.

PIII-61. Calculation of the Thermodynamic Parameters of the Fe-Ni-Co-Cu-Cr-Al-Mn Multicomponent Metallic System

Vladimirov E.S.¹, Starykh R.V.², Sineva S.I.^{2,3}, Vasil'eva A.A.⁴

¹Peter the Great St.Petersburg Polytechnic University, Russia; ²LLC Gipronickel Institute, Russia, ³University of Queensland, Australia; ⁴Saint-Petersburg Mining University

egorvladi@gmail.com

The study is devoted to the calculation of the thermodynamic parameters (ΔS_{av} , ΔH_{av} and ΔG_{av}) of the Fe-Ni-Co-Cu-Cr-Al-Mn multicomponent system. The Calculation was done using the FactSage thermodynamic databases and software version 6.4 [1]. Also boundary systems with lower number of components were considered. Totally, standard thermodynamic properties were calculated for 7 six-component systems, 21 five-component systems, 35 quaternary, 35 ternary and 21 binary systems with the elements listed above.

After calculation of the basic thermodynamic parameters for the given systems, the values of the parameters were averaged for number of components. The results of the calculation are shown, that the main contribution to the energy of the system is attributed to the entropy factor.

It's well-known, that total entropy of the system is sum of three entropy impacts: ideal Boltzmann entropy ($\Delta S_{B.}$), entropy of pure compounds ($\Delta S_{c.c.}$) and nonideal entropy of relationship between components ($\Delta S_{n.i.}$):

$$\Delta S = \Delta S_{c.c.} - \Delta S_{B.} + \Delta S_{n.i.}; [2]$$

Figure 2 illustrates the contribution of each considered thermodynamic parameter to the total change in the entropy of the system, also averaged for each component.

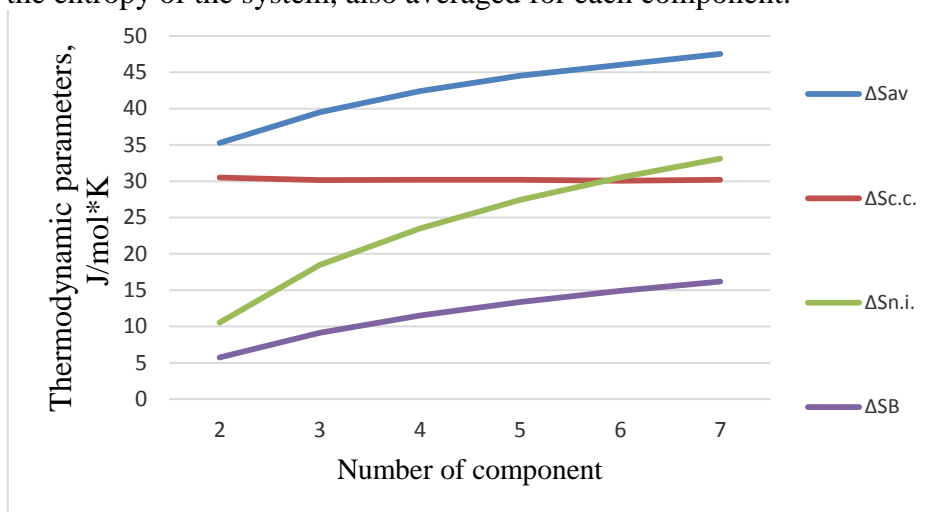


Figure 2. Dependencies of ΔS , $\Delta S_{c.c.}$, ΔS_B , $\Delta S_{n.i.}$ on the number of components

It is shown, that the main factor, effects on the total system entropy, is nonideal entropy of relationship between components of system. Moreover, impact of $\Delta S_{n.i.}$ on the total entropy of system is larger, than the ones for Boltzmann entropy especially for multicomponent systems. Therefore, the impact of the Boltzmann entropy is not dominant, and the assignment of any system to the high-entropy class, based only on this factor, can be considered incorrect.

[1] Bale C.W., Chatrand P., Deckerov S.A., Eriksson G., Hack K., Manfoud R.B., Melanson J., Pelton A.D., Peterson S. CALPHAD; FactSage, Ecole Polytechnique Montreal, 2002 <http://www.factsage.com/>, 2002.

[2] Stepanovskikh E.I., Brysnitsina L.A - Calculation of entropy changes in systems without chemical transformation - Ural Federal University named after the first President of Russia B.N.Yeltsin – 2007.

PIII-62. Thermodynamics of Ion Exchange Process for Titanium(IV) Hydrophosphates

Ivanenko V.I., Maslova M.V.

Tananaev Institute of Chemistry - Subdivision of the Federal Research Centre
“Kola Science Centre of the Russian Academy of Sciences” (ICT KSC RAS), Russia

ivanenko@chemy.kolasc.net.ru

Titanium (IV) hydrated hydrogenphosphates are of great practical interest as promising adsorption materials for uptake of toxic metal cations from complex aqueous solutions and as an attractive precursors for the directed synthesis of electronic materials based on double phosphates. The ion-exchange properties of hydrated titanium (IV) hydrophosphates are caused by the polarization of the acidoligand in the field of the titanium atom. This leads to an increase in the protons mobility and their capability of replacement by metal cations.

In this work we studied the influence of the titanium (IV) hydrophosphates (TiP) composition on the ion-exchange properties with respect to the mono- and divalent cations at different pH and temperature values. For a quantitative description of the ion exchange equilibrium the Nikolsky isotherm equation in the form of the law of the mass action is used. It has been established that at the initial stage of ion-exchange process partial dehydration of the metal cations and TiP matrix occur. This is determined by occurrence of energetically equivalent positions of counter ions with relatively low charge density of exchanging cations on the initially homogeneous monofunctional inorganic ion-exchanger. With increase in the degree of substitution the value of the equilibrium coefficient decreases. This is explained by an increase in the charge density of the guest ions and an increase in the level of crystallinity of the TiP matrix during dehydration. Increasing the ordering of the TiP matrix lead to the formation of energy and special inequivalence exchange sites of the solid phase as it is filled with guest cations.

Influences the TiP hydration degree, the ionic strength of the solution and cations substitution degree on equilibrium coefficient have been investigated and ion exchange constant has been calculated. It was found that the affinity of TiP matrix toward investigated cations depends on their hydration degree and increases in the ionic potential. The selectivity series for the metal ions on TiP were found to be: $\text{Li}^+ < \text{Na}^+ < \text{K}^+ < \text{Rb}^+ < \text{Cs}^+$ and $\text{Mg}^{2+} < \text{Ca}^{2+} < \text{Sr}^{2+} < \text{Ba}^{2+}$

An increase in the temperature of the heterogeneous cationic substitution process leads to an increase in the values of the ion-exchange constant as well as an increase in the selectivity towards of less hydrated cations. From the correlation between the logarithm of the ion-exchange constant and the inverse temperature, the values of the change in enthalpy and entropy of the heterogeneous cationic substitution process were calculated. It is found that the ion-exchange process has an endothermic nature. Positive values of ΔS indicate the increasing randomness in the sorption process. The decrease in the coordinately-bonded water content in TiP matrix leads to decrease in the ion- exchange capacity and an increase in the selectivity of cations adsorption.

The obtained results allowed to substantiated the efficient use of titanium (IV) hydrogen phosphates as an adsorbent for cesium and strontium radonuclides, to produce the highly pure compounds and to develop the synthesis method for functional materials based on titanium (IV) double phosphates and alkali metal with good electrophysical properties.

The research was carried out with the financial support of the Russian science Foundation (Project No 17-19-01522).

PIII-63. Phase Relations in the Fe-Cu-As System

Ilatovskaia M.^{1,2}, Novoghilova O.², Samoiloa O.³, Sineva S.^{2,4}, Starykh R.²

¹TU Bergakademie Freiberg, Germany;

²Peter the Great St. Petersburg Polytechnic University, Russia;

³South Ural State University (National Research University), Russia;

⁴The University of Queensland, Australia

aessone64@mail.ru

Arsenic is one of the major harmful impurities in copper smelting. The recovery of valuable elements and the stabilization of the heavy metals contained as well as the removal of arsenic in the form of stored products with low toxicity are important issues. Thus, knowledge of the phase relations in the Fe-Cu-As system is essential for understanding the behavior of arsenic in copper smelting.

As a part of the ternary system, the Fe₂As-Cu₃As join was described by Kopylov et al. [1] to be a pseudobinary system at temperatures above 700°C. At lower temperatures (300°C [2]), it was found that the solubility of Cu in Fe₂As is up to 20 at.%. On liquidus of the Fe-Cu-As system, based on metallography and DTA [2] three invariant eutectics were estimated at nearly the same temperatures: L ↔ Cu₃As + FeAs + FeAs₂ at about 680°C, L ↔ (Fe,Cu)₂As + Cu₃As + Cu at 680°C, and L ↔ FeAs + (Fe,Cu)₂As + Cu₃As at about 690°C. The temperature of a maximum between (Fe,Cu)₂As and Cu₃As was also reported at 750°C [2] or at 735°C [1]. Despite the presence of different experimental data, only limited area of the ternary system has been studied and the available data are partially contradictory. Thus, the aim of the present work is an experimental study of the Fe-Cu-As system and its Fe₂As-Cu₃As join to resolve existing literature disagreements and to define all phase relations (reported before and unexplored) presented on liquidus and subsolidus. For this, seven different composition related to the Fe₂As-Cu₃As join and some key Fe-Cu-As compositions were prepared through direct melting of metallic iron, copper and arsenic at 1473 K followed by cooling to room temperature under an argon atmosphere. To investigate phase equilibria the samples were annealed at desired temperatures and water-quenched. To minimize evaporation of arsenic during samples preparation and heat treatment (for DTA tests as well), all samples were sealed in vacuum in a quartz ampoule. Key samples were examined by X-ray diffraction. The microstructure characterization was carried out using SEM/EDX. Temperatures of solid phase transformations and melting behavior of the samples were studied by DTA.

Acknowledgements The study was funded by RFBR according to the research No. 18-29-24166.

[1] N.I. Kopylov, S.V. Degtyarev, N.P. Tolkachev, M.Z. Toguzov, and Ya.I. Chirik, (in Russian) *Russ. J. Inorg. Chem.*, 1984, 29, 1086-1088.

[2] U. Hennig, and F. Pawlek, (in German), *Z. Erzbergbau Metallhüttenwesen*, 1965, 18, 293-297.

PIII-64. How are Structures, Properties and Crystallisations Conditions Interrelated? New Solid Forms of Metacetamol as a Case Study

Zemtsova V.M.^{1,2}, Rychkov D.A.^{1,2}, Pulham C.R.³, Boldyreva E.V.^{1,2}

¹Novosibirsk State University, Russia;

²Institute of Solid State Chemistry and Mechanochemistry, Russia;

³The University of Edinburgh, Scotland, UK

vicizemts49@gmail.com

The preparation of new dosage forms and study of their properties play an important role in science and pharmaceutical industry. One of the most popular methods for improving the properties of drugs consists in the use of different polymorphic forms of an active pharmaceutical ingredient (API). In recent decades, other solid forms of APIs also became frequently used for this purpose and, as a result, the first drugs on the basis of hydrates and salts have appeared [1]. However, prediction of the conditions for obtaining such solid forms still remains a big problem since crystallization is a complex process that is controlled by both *kinetic* and *thermodynamic* parameters of a system which are directly related to the crystal structure. This leads to the fact that the establishment of the relationship between the structure of a solid form, its properties and conditions for obtaining remains an important direction in the modern science of pharmaceutical materials.

The drug substances already released to the market are often considered as model systems for scientific investigations. A typical example of such systems is paracetamol, a non-steroidal analgesic and antipyretic agent, for which a large number of different forms (polymorphs, hydrates, salts, *etc.*) have been obtained and studied. At the same time, for a structural analogue of paracetamol, metacetamol, there are little data about possible solid forms, their properties and conditions of obtaining [2].

This work has been devoted to obtaining new forms of metacetamol and studying the relationship between their structure, properties and conditions of formation. As a result of many experimental attempts, two new forms of metacetamol were obtained, namely, the hydrate and the solvate. External thermodynamic parameters (temperature, vapor pressure) of crystallization of these forms were selected based on how the paracetamol hydrate and solvate had been obtained.

Despite the fact that the solvate of metacetamol was prone to rapid desolvation, its structure has been characterized by single-crystal X-ray diffraction as well as the structure of the metacetamol hydrate. Both forms were investigated by IR spectroscopy and X-ray powder diffraction methods to estimate energies of particular interactions in these structures. The crystal structures and intermolecular interactions have been analyzed and compared with various forms of paracetamol and two known polymorphic forms of metacetamol [3]. Based on this analysis, the explanation of mechanisms of desolvation and dehydration was suggested. Besides that, the process of desolvation has been qualitatively studied using IR spectroscopy and X-ray powder diffraction.

[1] A.M. Healy et al., *Adv Drug Deliv Rev*, 2017, 117, 25-46.

[2] V.A. Drebuschak et al., *CrystEngComm*, 2017, 127, 1807-1814.

[3] L. McGregor et al., *CrystEngComm*, 2015, 17, 6183-6192.

PIII-65. The Structure of Ionic and Neutral Liquids of the Similar Molecules

Shelepova E.A.^{1,2}, Paschek D.³, Ludwig R.³, Medvedev N.N.^{1,2}

¹Novosibirsk State University, Novosibirsk, Russia;

²Institute of Chemical Kinetics and Combustion, SB RAS, Novosibirsk, Russia

³Universität Rostock, Institut für Chemie, Physikalische und Theoretische Chemie, Rostock, German

nikmed@kinetics.nsc.ru

The fundamental difference between the structures of the ionic liquid and the neutral liquid consisting of similar molecules (with zero charges) is shown. Electric charges force anions and cations to be located close to each other. This leads to the spatial alternation of the cations and anions. Thus, the structure of an ionic liquid is characterized by some regular motive, which increases the intrinsic homogeneity of both anionic and cationic subsystems. In the absence of charges, there is no preferences in the mutual arrangement of the molecules. Therefore, the motives of the spatial distribution of both subsystems correspond to the usual disordered systems, for which sufficiently large structural fluctuations are typical. It is interesting to note that, in general, the structures of the ionic and neutral liquids look almost the same. They have similar total radial distribution functions of atoms and almost identical distributions of the interstitial spheres radii. Thus, the clear distinction is visible only in the subsystems (anionic and cationic), and not in the structure of the entire system.

The aforementioned conclusions follow from our analysis of molecular dynamic models of ionic and neutral liquids, for which the atomic partial radial distribution functions were calculated, as well as the interstitial spheres inscribed in the voids between the molecules. Coarse-grained molecular dynamics models of 1-butyl-3-methylimidazolium hexafluorophosphate (force fields from [1]) and the model of the neutral liquid consisting of the same molecules, but with zero charges were analyzed. The ionic liquid was simulated at normal pressure and various temperatures, the neutral liquid was modelled at the same temperatures, and the densities as from the ionic liquid. The most distinct result showing the discussed difference between ionic and neutral liquids is that the distributions of the interstitial spheres radii, calculated separately for the anionic and cationic subsystems, turn out to be significantly narrower in the ionic liquid than in the corresponding subsystems of the neutral liquid.

Acknowledgements The financial support of RSF № 19-13-00073 and IChKC SB RAS

[1] D. Roy and M. Maroncelli, J. Phys. Chem. B, 2010, 114 (39), 12629-12631.

PIII-66. Melting Temperature Calculation Through the Simulation of Coexisting Phases

Zakiryarov D.O., Kobelev M.A., Tkachev N.K.

Institute of High-Temperature Electrochemistry Ural Branch of the Russian Academy of Science,
Ekaterinburg, Russia

coulomb76@mail.ru

A methodology is proposed for calculation of melting temperature using molecular dynamic modeling of two coexisting phases.

At the first stage, the solid and liquid phases are prepared separately through NPT modeling at a reasonable temperature near the expected melting point (Figure 1, a, b). In order to provide the compatibility of the cell geometries, the x and y dimensions of liquid cell are fixed at the equilibrium values of these of the solid phase. Thus, the volume of the liquid phase is optimized only by changing the z dimension of the cell. We propose a solid : liquid phase size ratio of 1 : 2. The increased size of the solid phase is due to its partial melting in the subsequent modeling of coexisting phases.

At the second stage, the cells with solid and liquid phases are consolidate along the xy plane and modeling in an NPH ensemble performs at different starting cell energies. The cell energy can be adjusted by setting a nonzero starting temperature (the temperature is not regulated further).

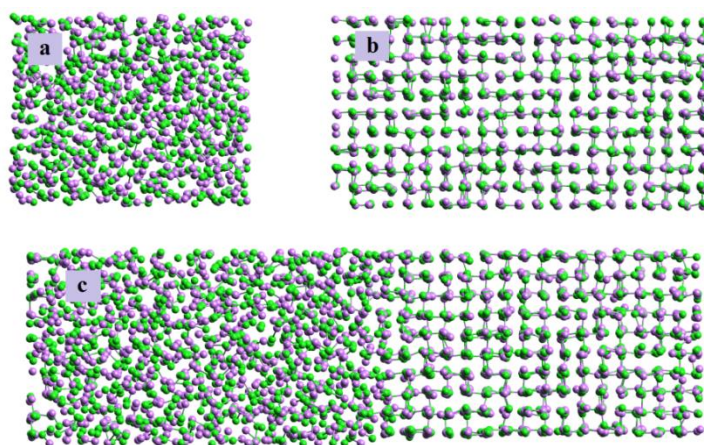


Figure 1. Snapshots while simulating separate phases (a, b) and liquid-solid coexisting (c; the one can see partial melting of solid phase).

Depending on the amount of energy in the system, partial melting or partial crystallization may occur. However, the latter process is much slower. Therefore, it is necessary to set the excess energy, allowing the system equilibrate by partial melting of the solid phase with decreasing temperature (Figure 1, c). It is expected that at different energies more or less of the crystal phase will melt, and the temperature will come to a single value for all cases. This temperature can be considered the temperature of melting.

Our approach is of general applicability and can, in principle, be applied to the study of melting phase transition for any system of a single component.

Acknowledgements The financial support of the Russian Foundation for Basic Research, project № 18-03-00606.

PIII-67. Solubility of hydroxyapatite. New Approaches and Results

Kuranov G., Mikhelson K., Puzyk A.

St. Petersburg State University, Russia

Hydroxyapatite is the main mineral component of teeth, bones and one of the most common minerals in pathologic masses in human body. The solubility of hydroxyapatite has been the subject of extensive studies for several decades. Initially, the interest in this topic was caused by the need for study of the impact of external factors on dental enamel, and for the development of dental materials and means of protecting the enamel. Therefore, the solubility of hydroxyapatite was studied under acid conditions. Biocompatibility of hydroxyapatite allows using this mineral as a material for various artificial implants, and a huge number of works devoted to this issue has been published in recent years. The phenomena of calcification of soft tissues also attract a lot of attention. To date, many works on the solubility of hydroxyapatite in water were published, but the reported data poorly fit together. One of the reasons for this may be the incongruent dissolution of hydroxyapatite. Difficulties of study of hydroxyapatite solubility are also caused by long duration of the setting of chemical and phase equilibria and extremely low solubility. Therefore, until now, no studies of influence of electrolyte and protein composition of body fluids on the solubility of hydroxyapatite have been carried out.

Low solubility of hydroxyapatite complicates the study of phase equilibria, because even a small sampling can shift the equilibrium in the system. In this regard, it is important to provide non-destructive analysis of the composition of a solution that is in contact with hydroxyapatite. This can be done by a direct ionometry with membrane electrode selective to calcium ions. The use of calcium ion-selective electrode (Ca-ISE) allows a continuous measuring the composition of the solution in time, directly in the cell without sampling. This method has an important additional advantage: the signal of the sensor depends on the activity rather than the concentration of calcium ions in solution. Thus, the data obtained by Ca-ISE are more relevant thermodynamically than those obtained by classical “wet chemistry” or by ICP-MS or other modern methods which deliver data on total (free + complexed) calcium concentration.

The main goal of the present work was to get reliable data on the solubility of hydroxyapatite as a function of the solution composition. The results demonstrate that the concentration of calcium ions in solution non-monotonously changes over time: the respective curves contain a maximum. Stabilization of the data (establishing of equilibrium) requires three weeks. The logarithm of activity of calcium ions is directly related to the pH.

The lack of reliable experimental data hampered the development of molecular and thermodynamic modelling in these systems. In this study, we have performed a modelling of the chemical equilibria in solution that served as a prototype of the blood plasma with application to calcification of the tissues. The concentrations of molecular–ionic forms containing calcium and hydrogen cations and phosphate anions in the range of ionized-calcium and total phosphorus concentrations from 0.5 to 3.0 mM, and at the solution pH of 4.0–8.0 were calculated. The activities of the ionized species were related to the respective concentrations via the Debye–Hückel theory. In this way, we have considered the full set of the equilibria taking into account the dissociation of water and of phosphoric acid, as well as formation of both inert and ionic calcium phosphates. All in all, theoretical and experimental results suggest that dissolution of hydroxyapatite is an incongruent process.

PIII-68. Influence of Freezing and Annealing Protocols on Phases Formed in The Tert-Butanol – Water System

Ogienko A.G.^{1,2}, *Stoporev A.S.*^{1,2}, *Ogienko A.A.*^{1,3}, *Yunoshev A.S.*^{2,4}, *Adamova T.P.*^{1,2}, *Manakov A.Yu.*^{1,2}, *Boldyreva E.V.*^{1,5}

¹Nikolaev Institute of Inorganic Chemistry SB RAS, Russia; ²Novosibirsk State University, Russia; ³Institute of Molecular and Cellular Biology SB RAS, Russia; ⁴Lavrentiev Institute of Hydrodynamics SB RAS, Russia; ⁵Boreskov Institute of Catalysis SB RAS, Russia

ogienko@niic.nsc.ru

Employment of the tert-butanol (TBA) – water system is studied intensively to increase efficiency of freeze-drying processes for pharmaceutical industry. Here we report X-ray diffraction and thermal analysis studies which show strong influence of freezing protocols on phases formed in the TBA – water system. We add new data to the TBA-water system phase diagram and show that decahydrate [1] forms only on high cooling rates ($>10^{\circ}/\text{min}$). The decahydrate begin to decompose at temperatures above -40°C to ice *I_h* and heptahydrate. In the “temperature-composition” stability region of heptahydrate the later cannot be obtained by using any cooling rates studied (from 140 to $0.35^{\circ}/\text{min}$); in all cases ice *I_h* and deca-/di- (depending on cooling rates) hydrates crystallizes. X-ray diffraction studies at different temperatures performed on frozen and annealed (at different times of annealing (from 12 hours to 3 months)) samples confirm anomalous stability of dihydrate in the “temperature-composition” stability region of heptahydrate. Annealing leads to “equilibrium” variant phase diagram independently on freezing protocol used.

Acknowledgements The financial support of RFBR (№ 17-03-00784-A).

[1] L. Dobrzycki. *Z. Krist.-Cryst. Mater.* 2018, 233(1), 41.

PIII-69. Quasi-Chemical Approach – Novel Powerful Tool to Study Supramolecular Organization, Macroscopic Equilibrium and Non-Equilibrium Properties of Non-Ideal Liquid Systems. Polyamorphism of Liquid Mixtures

Durov V.A.

Faculty of Chemistry, Moscow Lomonosov State University, Moscow, Russia

durov@phys.chem.msu.ru and vlad_durov@rambler.ru

The recent results on using quasi-chemical approach for studying polyamorphic supramolecular organization, dynamics of molecular thermal motion, and a set of physicochemical properties both equilibrium and non-equilibrium ones, which are based on the concepts of polymorphic supramolecular assemblies and extended quasichemical variable processes in matter are reviewed [1-5]. The concept of polyamorphism introduced by author for liquid mixtures both on structure and/or composition is discussed. The methods for investigating supramolecular ordering in liquids due to non-covalent molecular interactions like H-bonds, and for describing structure and properties of aggregates, those which are polymorphic both on structure and composition, thermodynamics of its formation, and integral and differential parameters of aggregation are discussed for the wide temperature range [1-5].

The models for thermodynamic, dielectric, optic, and relaxation properties of liquid non-ideal systems, which are defined by molecular parameters of different nature, have been constructed on the basis of quasi-chemical approach to describing structure, molecular thermal motion and series of macroscopic properties of liquids and mixtures. For the first time the long-range molecular correlation in liquids in the common parameters of state were revealed. The structure, properties, and thermodynamics of formation of supramolecular forms, consisted from tens of molecules, were studied. Thus the models developed allow us to study structure of disordered condensed systems far more than nearest coordination shells. The comparison of the models developed with diffraction, spectroscopic, simulation methods for studying of liquids are discussed.

The macroscopic manifestations of polymorphic supramolecular ordering in physicochemical properties of liquid mixtures are considered. The molecular models of polyamorphism in liquids are discussed. And finally some prospects on study of next level of structural organization of liquid mixtures named as over supramolecular ordering introduced basically in [6] is briefly outlined.

Acknowledgements This work was supported by the Russian Foundation for Basic Research, project N 10-03-01164 and by the Program of Ministry of Education and Science of the Russian Federation "Development of scientific potential of higher education institutions (2009-2010)", project N 2.1.1/3305.

[1] V.A. Durov. Concentrated and Saturated Mixtures. Monograph in Russian, 2002, P. 170-254.

[2] V.A. Durov. *J. Mol. Liq.*, 2005, 118, 101-110; 41-82.

[3] V.A. Durov. NATO Science Series. II. Mathematics, Physics and Chemistry, Vol. 133. 2004. P. 17-40.

[4] V.A. Durov. *J. Mol. Liquids*, 2003, 103-104(1), 41-82; *ibid* 2004, 113, 81-99. 2005, 118, 101.

[5] V.A. Durov. In: V.A. Durov, E.P. Ageev. Thermodynamic theory of mixtures. Textbook, Chapter.7, URSS. 2-nd ed- 2003 3-rd ed 2010, 4-th ed, 2018.

[6] V.A. Durov. *Russ J. Phys Chem* v.53, 101-105; 50 (9), 2231-2234 *Phys&Phys Chem of Liquids* Iss 3 pp.10-25

AUTHOR INDEX

A

Abdelaziz A.....	19, 20
Abdulagatov A.I.....	56
Abdulagatov I.M.....	56, 98, 206
Abdullaev R.N.....	134
Adamova T.P.....	97, 333
Adolphs J.....	101
Agieienko V. N.....	228
AkentieV A.V.....	219, 220
Akimenko S.S.....	51
Alekseev A.A.....	58
Alekseeva O.M.....	46, 145, 201
Alexandrov A.I.....	209
Aliiev A.....	56, 175
Aliyev E.N.....	226
Almeida A.R.R.P.....	88
Amashaev R.R.....	56
Amerkhanova Sh.K.....	148, 285
Andrianov R.....	25
Androsch R.....	25
Anikeenko A.V.....	195
Anikina E.....	205
Anisimov M.....	6, 44, 321
Antina E.V.....	26, 170
Antina L.A.....	26, 170
Antipov Y.V.....	175
Antonava Z.A.....	294
Antonova O.A.....	138, 139, 140
Aristova N.M.....	69
Arhipin A.S.....	315
Arhipov S.G.....	212, 213
Asabina E.A.....	58, 181, 182, 286
Asadov M.M.....	22, 226, 227
Ashmarin A.A.....	80
Ashurbekova Ka.N.....	56
Ashurbekova Kr.N.....	56
Ausin D.....	307

B

Babanly D.M.....	204
Babanly M.B.....	203, 204
Babenko A.V.....	135
Babkina T.S.....	167
Badelin V.G.....	49, 136, 283, 284
Bagavudinova D.G.....	232
Baidakov V.G.....	53, 106
Bairagya P.....	43
Baklanova N.I.....	82
Balbekova B.K.....	266
Baluja S.....	186
Banerjee T.....	43
Barannikov V.P.....	49, 198
Baranov V.V.....	234
Barbosa G.D.....	102
Barreto Jr. A.G.....	102

Batista de Carvalho L.A.E.....	316
Batov D.V.....	140, 141, 234
Batyrova R.G.....	206
Bauschlicher Jr.C.W.....	120
Bazaev A.R.....	232, 252, 260
Bazaev E.A.....	232, 252, 260
Bazulev A.N.....	124
Belov G.V.....	69, 113, 196
Belov K.V.....	316
Belyaev V.D.....	156
Berezhnaya A.S.....	52
Berezin M.B.....	26, 170
Bespyatov M.A.....	154, 276, 277, 281, 282, 293
Bikelytė G.....	305
Bissengaliyeva M.R.....	266
Blokhin A.V.....	288, 289, 290, 291
Bogachev N.A.....	258
Bogatishcheva N.S.....	8
Boldyrev A.E.....	174
Boldyreva E.V.....	329, 333
Borisenkova A.A.....	220
Botea-Petcu A.....	309
Boycov D.E.....	173
Boytsova A.....	180
Brazhkin V.V.....	93, 94
Brezhnev N.Y.....	83
Brilliantov N.V.....	38
Brodskaya E.N.....	52, 57, 194, 225
Brun E.....	123
Brunetti B.....	77, 112, 193
Bryliakova A.A.....	214
Buchner R.....	228
Budkov Y.A.....	32, 36, 159
Budkov Yu.A.....	101
Budylin N.Y.....	215
<u>Burlakova E.B.</u>	216, 217
Burovaya E.S.....	50
Bykov A.G.....	24

C

Cabeza O.....	307
Casás L.....	127
Castelo S.....	126
Chachkov D.V.....	85
Chalykh A.E.....	137, 177, 215, 322
Chelyuskina T.V.....	311, 312
Cherkasov D.G.....	67, 96, 142
Cherniaikin I.S.....	282, 293
Chernova M.M.....	151
Chernukha A.S.....	152
Chervonova U.V.....	209
Chiew Y.....	249
Chirkov N.S.....	220, 221
Cholach A.R.....	214
Chua Y.Z.....	19
Chuev G.N.....	10, 146

Chunilina L.G.	297
Chusova T.P.	108
Ciach A.	37, 222
Ciccioli A.	77, 112, 193
Corrente N.	122
Coutinho J.A.P.	5
Cuevas C.A.	109

D

Danilina V.V.	142
Dávalos J.Z.	109
Davydov A.G.	14, 149
Denisov V.M.	296
Denisova L.T.	207
Dergal F.	143
Dimitrov O.	143
Dinsdale A.T.	76
Do H.T.	19
Dobrzanski C.D.	122
Domínguez-Pérez M.	307
Dorofeeva O.V.	274
Dorovskikh S.I.	293
Drăgoescu D.	132, 133
Drozd K.V.	147, 270
Druzhinina A.I.	66, 273, 274
Dubovsky I.M.	220
Durov V.A.	334
Dyachkov S.A.	113
Dyshin A.A.	26, 259, 262, 263
Dzhapparov T.A-G.	232, 260
Dzhavadov L.N.	94

E

Efimov S.V.	9, 316
Egorov A.V.	225
Egorov G.I.	130, 131
Egorova E.M.	135
Emel'anov V.V.	240
Emelianova K.A.	27

F

Fabián B.	33
Faizullin M.Z.	8
Falyakhov T.M.	157
Farhadian A.	75
Faria B.F.	223
Farzaneh-Gord M.	324
Fedorov P.P.	163
Fedorova I.V.	161
Fedotova M.V.	10, 146
Flachsmann B.	34
Flämig M.	65
Fomin Yu.D.	93, 94, 104, 323
Freitas V.L.S.	306
Frolkova A.K.	251, 253
Frolkova A.V.	250, 251, 253

Frolov A.M.	157
------------------	-----

G

Gabrielyan L.S.	65, 202
Gagarin P.G.	275
Galiakhmetova N.A.	207
Galkina D.P.	152, 245
Gamov G.A.	199
García-Garabal S.	307
Garkushin I.K.	135, 325
Gavrichev K.S.	80, 169, 176, 275
Gavrilov A.A.	121
Gayol A.	126, 127
Gelfond N.V.	276, 281, 293
Georgi N.	101
Gerasimov A.V.	174
Gerasimov N. Yu.	216, 217
Gerasimov V.K.	137
Ghazoyan H.H.	235
Gheorghe D.	308, 309
Giricheva N.I.	198
Glukharev A.G.	267
Glukhova I.O.	58, 181, 182
Glumov O.V.	267
Gogol D.B.	266
Golikova A.D.	95, 302, 324
Goloshchapov A.N.	216, 217
Golubev V.A.	162
Golubeva E.O.	297
Gómez C.P.	128
Gor G.Y.	122
Gorbachev A.V.	313
Gorbunov V.A.	51
Gorokhov L.N.	279
Grega M.E.	268
Gridchin S.N.	272
Grigorieva V.D.	292
Gromov D.V.	21
Gruzdev M.S.	209
Gudkova S.A.	210
Guichardon P.	143
Guluzade A.N.	247, 248
Gurina D.L.	171
Guseva G.B.	170
Guseynov S.S.	201
Guskov V.N.	80, 275

H

Härtel M.	305
Hassel E.P.	247, 248
Hayes P.C.	41
Held C.	19, 42
Hofmann J.	101
Holubeva N.V.	132, 133
Hosangadi A.	249

I	
Ibavov N.V.	254, 261
Idrissi A.	33, 68
Igumenov I.K.	60
Il'in K.K.	67, 96, 310
Ilatovskaia M.	246, 328
Ilinykh N.I.	178, 179
Imamaliyeva S.Z.	203
Irtyugo L.A.	296
Isaev I.A.	98
Iserovich P.	168
Ivanenko V.I.	327
Ivanov A.	167
Ivanov E.V.	138, 141, 233, 234
Ivanova E.A.	57
Ivanova N.G.	233, 234
Ivlev D.V.	32, 158, 159, 262, 263
J	
Jacobson N.S.	120
Jak E.	41
Janickovic D.	187
Jedlovsky P.	33
Jose J.	143
K	
Kabanova E.G.	29
Kabo G.J.	291
Kadtsyn E.D.	195
Kalikin N.N.	32, 158, 159
Kalyagin A.A.	26
Kantsiava V.V.	288, 289
Kapustina D.V.	310
Karachevtsev F.N.	183
Karakovskaya K.I.	211
Kareva M.	256
Karpushenkava L.S.	291
Kartoshkin A. Yu.	54
Kasparov V.V.	216
Kaverin A.M.	106
Kazakov A.K.	160
Khaibrakhmanova D.R.	153
Khairulin R.A.	134
Khartsyzov G.	256
Khasbiullin R.R.	137
Khodov I.A.	9, 316
Khoroshilov A.V.	80, 176
Khvan A.V.	76
Kilchytskaya Y.V.	288
Kim Yu.A.	46, 145
Kirsanova A.A.	210
Kiselev M.G.9, 32, 36, 68, 158, 159, 162, 259, 316	
Kiss B.	33
Klapötke T.M.	305
Kleiber M.	12
Knyazeva A.G.	264

Kobelev M.A.	197, 331
Kolattukudy P.	166
Kolesnikov A.	32, 36, 101, 159
Kolker A.M.	131, 209, 262, 263
Koltsov S.	90
Kolyado A.V.	325
Kon'kova T.S.	114
Konakov V.G.	84, 267, 268, 300, 301, 319
Kondrasheva N.	180
Kondrat'eva O.N.	169
Kondratyuk N.D.	200, 314
Koneva A.S.	224
Konnova M.E.	150, 151
Konstantinova N.M.	167
Kopanichuk I.V.	50, 52
Korchak P.A.	188
Korzun I.V.	208, 242, 243, 287, 295
Kosova D.A.	273
Kostyanko A.A.	144
Kostyanko A.	246
Kosyakov A.V.	83, 318
Kovalenko N.A.	164, 257, 315, 317
Kovalev L.E.	178
Kovarskii A.L.	216
Kramarenko E.Yu.	121
Krasnykh E.L.	160, 238, 239, 240, 271
Kravchenko A.N.	234
Krementsova A.V.	46, 145
Krest'yaninov M.A.	141
Krestyaninov M.A.	68, 161, 262, 263
Krivandin A.V.	217
Krouk V.S.	294
Kruchin S.O.	138
Kruchinin S.E.	146
Krycki M.M.	100
Kryukova O.N.	264
Ksenofontov A.A.	26, 170, 209
Kuchkina N.V.	304
Kudashova N.G.	296
Kudayrova T.V.	139
Kundu D.	43
Kuranov G.	332
Kurapova O.Yu.	84, 268, 300, 319
Kuratieva N.V.	60
Kurbatova M.S.	49, 198
Kurdakova S.V.	315
Kuritsyna A.A.	136
Kurskiy V.F.	310
Kustov A.V.	138, 139, 140, 141, 233
Kuzin T.M.	281, 282
Kuznetsov V.N.	29, 256

L

Laaksonen A.	225
Laptash N.M.	269
Lasich M.	103
Latini A.	77, 112

Lava D.....	186
Lavrenov D.A.	286
Lavrinenko Ya.....	69
Lazarev N.M.	280
Lebedev V.T.	220
Lebedeva E.Yu.	233, 234
Lebedeva T.S.....	218
Legido J.L.	126, 127, 128
Levanova S.V.	240
Levashov P.R.....	113
Levashova E.Y.	224
Lin S.-Y.	100, 219, 220, 221
Lineva V.I.....	196
Liubichev D.	231
Loglio G.	24
Lomakina T.E.....	319
Lopatin S.I.....	40, 84, 183, 300
Losev E.A.	212
Lozanov V.V.	82
Ludwig R.	330
Lukichev V.F.	227
Lukina O.D.	239
Lukyanova V.A.	274
Lyashchenko A.K.	11

M

Magi M.	193
Makarenko A.M.	299
Makarov D.M.....	130, 131
Makarov S.G.	280
Makarov V.V.	138, 141
Makhnarilova E.G.	250
Maksimov A.I.	315
Maksimuk Y.V.....	294
Maksumova A.M.	56
Maliutin A.S.	317
Maltsev M.A.	184
Malygina E.V.	83, 318
Malyugin A.	253
Mammadov A.N.....	22
Mamontov M.N.....	313
Manakov A.Yu.	97, 333
Manin A.N.....	147, 173, 270
Mansimova Sh.H.....	204
Marczak W.	59
Markarian S.A.	28, 65, 235
Markin A.V.	110, 182, 286, 303, 304
Martynenko E.A.	150
Mashadiyeva L.F.....	204
Maslova M.V.	327
Mato M.M.	126, 127, 128
Matskevich N.I.....	292
Mayorov P.A.	58
Medvedev N.N.....	72, 195, 330
Medzhidova F.Kh.....	232
Mekhdiyeva I.F.	203
Meleshko T.K.....	215

Meshkov A.N.....	199
Mezhevoi I.N.	136
Mikhailov O.V.....	85
Mikhailov V.A.....	229
Mikhelson K.	332
Milevskii N.A.	29
Miller R.	24
Milyaeva O.Y.	24, 30, 100
Minakov D.V.....	113
Miroshnichenko E.A.	66, 114
Mirskaya V.A.	254, 261
Mkhitaryan A.S.	202
Modaressi A.	59
Modurova D.D.	311
Mokbel I.....	143
Möllmer J.	101
Monayenkova A.S.....	273
Monte M.J.S.....	88
Moodley K.	129
Moroz A.I.....	187
Morozov I.V.	69, 113, 184, 196
Morozova E.A.	169
Morozova N.B.	211, 276, 293
Mosyagina S.A.....	60
Mourelle M.L.....	128
Mukhametzyanov T.....	25
Musikhin A.E.	277, 278
Mustafaeva S.N.....	227
Myers D.L.	120
Myshkovskaia T.D.	303

N

Nagrimanov R.N.	17, 298
Narasigadu C.	129
Naumov A.V.....	318
<u>Naumov V.N.</u>	154, 278
Nazarevich D.A.....	254, 261
Neau E.....	143
Neimark A.V.	123, 249
Nekrylov I.N.	83
Neviadzimtsau A.V.....	289, 290
Nevrova O.V.	216, 217
Nguyen T.T.....	212
Nikfarjam S.	44
Nikiforova A.A.	153
Nikiforova G.E.....	176
Nikiforova K.V.....	268, 301
Nikitin E.D.	8
Nikolaeva E.V.	241, 242, 243
Nikolaychuk P. A.	236
Nikulova U.V.	137
Nocke J.	248
Norman G.E.	92
Noskov A.V.	201
Noskov B.A.	24, 100, 219, 220, 221
Notario R.....	109
Novoghilova O.....	328

Novozhilova O.320

O

Ogienko A.A.333
Ogienko A.G.333
Oliva J.M.109
Oparin R.D.68
Opila E.J.120
Orakova S.M.98
Orekhov M.A.92
Osin S.B.279
Osina E.L.184, 279
Osmanova B.K.252, 260

P

Paddubski A.G.132
Panetta R.77
Papanyan Z.K.202
Parmar D.186
Paschek D.330
Pashchenko L.L.66, 114
Pashkova T.V.209
Patterson E.V.77
Perevoshchikov A.V.164
Perlovich G.L.270
Pet'kov V.I.58, 181, 182, 286
Petrov A.62
Petrov B.I.280
Petrova T.F.175
Petukhov S.V.157
Pimenova S.M.274
Pimerzin A.A.64, 111, 150, 151, 305
Pimerzin A.I.150
Pisarev V.V.200, 314
Pischur D.P.281
Podnek V.E.321
Polikhronidi N.G.206
Polishuk I.13, 230
Polkovnichenko A.V.311, 312
Ponomarev D.A.294
Popa V.T.309
Popov A.P.8
Portnova S.V.160, 238, 239, 271
Potemkin D.I.156
Poteryaev A.A.322
Precupas A.309
Prikhodko I.42, 230, 231
Protsenko K.R.53
Pulham C.R.329
Pulyalina A.Yu.95
Puzyk A.332
Pyreu D.F.272

Q

Qasimova A.M.22

R

Raal J.D.129
Rabadanov M.Kh.56
Raeva V.M.255
Ramazanova E.E.226
Rasmussen R.123
Raspo I.143
Rasulov S.M.98
Ribeiro da Silva M.D.M.C.306
Rilo E.307
Rodionova T.V.108
Rogalska E.59
Rogalski M.59
Rosino J.128
Rössler E.A.65
Rubashkin A.A.168
Rumyantsev A.M.121
Rusanov A.I.116
Rusanov B.A.187, 229
Rychkov D.A.45, 212, 213, 329
Ryumin M.A.80, 169, 176
Ryzhkin D.A.255
Ryzhov V.N.93, 94, 104, 323

S

Sadowski G.4, 42
Safarov J.T.247, 248
Safonova E.A.188, 224
Safonova L.P.161
Saiz-Lopez A.109
Salulev A.B.295
Samarov A.42, 230, 231, 324
Samatov A.A.17, 298
Samedzade Q.M.22
Samoilova O.246, 328
Samoshkin D.A.237
Samosudova Ya.S.110
Samsonov V.N.54, 105, 124
Samuilov V.S.132, 133
Sandu R.309
Sankovich A.M.303
Santo K.P.123
Sarmini Yu.A.110
Savchenko I.V.134, 237
Sazonov E.G.275
Schawe J.16, 34
Schick C.19, 20, 25
Sdobnyakov N.Yu.124
Sedov I.A.153
Sedov V.P.220
Segade L.307
Segtovich I.S.V.102
Seradzenka S.U.291
Serkova E.S.304
Sermoud V. de M.102
Shamitov A.A.325

Shapagin A.V.	177
Sharifova U.N.	22
Shchamialiou A.P.	132, 133
Shchekin A.K.	48, 165, 218
Shcherbina A.A.	215
Sheindlin M.A.	157
Shelepova E.A.	330
Shevchenko M.	41
Shichin D.	41
Shifrina Z.B.	304
Shilov I.Yu.	11
Shipilov A.S.	58
Shlegel V.N.	292
Shlyapov R.	148, 285
Shner N.	42
Shokurova N.A.	177
Shugurov S.M.	84, 300
Shukurova G.M.	204
Sidey V.I.	83
Sidorov V.E.	187, 229
Siewert R.	189
Silva C.A.O.	306
Sineva M.A.	69, 196
Sineva S.	41, 61, 144, 245, 246, 256, 320, 326, 328
Sirbu F.	132, 133
Sizov V.V.	52, 57, 194
Sizova A.A.	52, 57, 194
Skorb E.V.	90
Skripkin M.Yu.	258
Skvortsova I.	185
Smirnov V.I.	283, 284
Smirnova I.	89
Smirnova N.L.	138, 139, 140
Smirnova N.N.	110, 182, 286, 303, 304
Smotrov M.P.	67, 96
Snytnikov P.V.	156
Sobyanin V.A.	156
Sologubov S.S.	110, 304
Solomonov B.N.	17, 18, 298
Son L.D.	229
Sorina P.O.	27
Sosnovtseva T.V.	241
Stabnikov P.A.	282, 293
Stankus S.V.	134, 237
Starikov A.Yu.	210
Starykh R.	61, 144, 245, 246, 256, 320, 326, 328
Stepanenko V.Y.	215
Stierstorfer J.	305
Stolyarova V.L.	40, 118, 183
Stoporev A.S.	97, 333
Suh D.	218
Sultanova S.Q.	203
Surov A.O.	172, 173
Surov O.V.	171
Svec P.	187
Svec Sr. P.	187
Sysoev S.V.	211
Szóri M.	33

T

Taherkhani F.	166
Taimassova Sh.T.	266
Talyzin I.V.	54, 105, 124
Tanasescu S.	309
Tarazanov S.V.	288, 289
Tareyeva E.E.	323
Tavares F.W.	102
Temnikova M.S.	267
Testa A.	143
Tiflova L.A.	273, 274
Timoshen K.A.	220
Tkachev N.K.	14, 149, 197, 331
Tobar J.L.	128
Toikka A.M.	21, 42, 117, 230, 231, 302, 324
Toikka M.A.	95, 185, 302, 324
Tolmachev M.V.	258
Trofimov E.A.	210, 245, 246
Tsiok E.N.	93, 94, 104, 323
Tsvetov N.S.	302
Tumba K.	103
Tyrin A.V.	80
Tyunina E.Yu.	136
Tyunina V.V.	136
Tyurin A.V.	176

U

Uali A.S.	148, 285
Ukhov S.A.	74, 192
Uskov S.I.	156
Uspenskaya I.A.	164, 167, 273, 315
Ustinov E.A.	51, 73

V

Vakhitova E.R.	152
Vanin A.A.	50
Varela L.M.	307
Varfolomeev M.A.	75
Vasil'eva A.A.	326
Vasil'eva E.A.	84, 300
Vasileva A.	61
Vasiliev S.A.	54
Vasilyev N.A.	173
Vasilyev S.A.	124
Vasilyeva I.G.	81
Vecchio Cipriotti S.	77, 112, 193
Verbetsky V.	205
Verchovtsev A.Ju.	179
Verevkin S.P.	17, 20, 64, 111, 150, 151, 189, 305
Victorov A.I.	27, 62
Vikulova E.S.	81, 211
Vinnik D.A.	210
Vishnyakov A.V.	123, 166, 223, 249
Vitvitskiy A.I.	155, 244
Vladimirov E.S.	326
Volkov N.A.	165

Volkov V.V.	83
Voronin A.P.	172, 173
Voronov V.P.	321
Voronova M.I.	171
Vorotsov-Velyaminov P.	62
Vorotyntsev M.A.	168
Vorozhtcov V.A.	40, 183
Voskov A.L.	257
Vostrikov S.V.	150, 151
Voznesenskiy M.	62

W

Weathers T.	249
Woehl T.J.	44

Y

Yagofarov M.I.	18
Yakimanskij A.V.	215
Yamshchikova Y.F.	271
Yatsuk O.S.	134

Yunoshev A.S.	333
Yurkshtovich Y.N.	290

Z

Zabuslaev S.V.	81
Zaitsau D.H.	17, 19, 20, 298
Zaitseva O.V.	152, 210, 245
Zakharov A.G.	171
Zakir'yanova I.D.	241, 242, 243, 287, 295
Zakiryaynov D.O.	197, 331
Zakiryaynova I.D.	208
Zavrazhnov A.Y.	83, 318
Zelenina L.N.	108, 211
Zemtsova V.M.	329
Zherebtsov D.A.	210
Zherikova K.V.	60, 81, 299
Zhivulin D.E.	152
Zhivulin V.E.	210
Zhuchkov V.I.	253, 255
Zvereva I.A.	303

